

Department of Civil and Environmental  
Engineering  
University of Strathclyde



**MODELING THE POTENTIAL IMPACTS OF  
CLIMATE CHANGE ON SURFACE AND  
GROUNDWATER RESOURCES IN THE NIGER DELTA  
PART OF NIGERIA**

**IBRAHIM HASSAN**

June 2020

Department of Civil and Environmental Engineering

University of Strathclyde

**MODELING THE POTENTIAL IMPACTS OF  
CLIMATE CHANGE ON SURFACE AND  
GROUNDWATER RESOURCES IN THE NIGER DELTA  
PART OF NIGERIA**

A Thesis submitted in fulfilment of the requirement for the  
Degree of Doctor of Philosophy

By

**IBRAHIM HASSAN**

June 2020

# DECLARATION

This thesis is the result of the author's original research. It has been composed by the author and has not been previously submitted for any examination, which has led to the Award of a degree.

The copyright of this thesis belongs to the author under the terms of the United Kingdom copyrights act as qualified by the University of Strathclyde Regulation 3.50. Therefore, Due acknowledgement must always be made of the use of any material contained in or derived from this thesis.

Signature: .....

Date: .....

## **DEDICATION**

Specially dedicated to my mother Hajiya Zahra, my father Alhaji Hassan, my wife  
Samira, daughter Amina, and Son Abubakar for their love and support



## ACKNOWLEDGEMENT

In the name of Allah, the Most Beneficent the Most Merciful. All praises be to Allah the Lord of the world. Prayers and peace be upon His Prophet and Messenger, Muhammad (S.A.W).

First, I would like to express my sincere gratitude and thanks to ALLAH. I am deeply thankful to my parents, wife, children, sisters and brothers for their continuous support, love and prayers throughout my study.

I undoubtedly owe much to my Supervisor, Prof. Robert M. Kalin, for the guidance, constant motivation and invaluable knowledge given to me during my research study. I also wish to extend my sincere appreciation to my second supervisor, Dr Chris J. White, for his valuable contributions.

I want to express my sincere appreciation to the Petroleum Technology and Development Fund (PTDF) for funding my PhD study under the Overseas PhD scholarship scheme.

Finally, it is difficult to mention everybody. Still, I would like to thank Jamiu Aladejana, Jackson Kawala, Ibrahim Lawan and all my friends and colleagues who have assisted at various occasions generously with their knowledge and expertise in preparing this thesis. Their views and tips are useful, indeed. Unfortunately, it is not possible to list all of them. I am deeply grateful to all my family members.

## PUBLICATIONS RESULTING FROM THIS RESEARCH

1. Hassan, I.; Kalin, R. M.; White, C. J.; and Aladejana, J. A (2020) ‘Evaluation of Daily Gridded Meteorological Datasets over the Niger Delta Region of Nigeria and Implication to Water Resources Management’, *Atmospheric and Climate Sciences* (ACS), SCRIP. doi: 10.4236/acs.2020.101002.
2. Hassan, I.; Kalin, R. M.; White, C. J.; and Aladejana, J. A (2020) ‘Selection of CMIP5 GCM ensemble for the projection of Spatio-temporal changes in precipitation and temperature over the Niger Delta, Nigeria.’ *Water*, MDPI, (Switzerland), 12(385). doi:10.3390/w12020385.
3. Hassan, I.; Kalin, R. M.; White, C. J.; and Aladejana, J. A (2020) ‘Potential Impacts of Climate Change on Extreme Weather Events in the Niger Delta part of Nigeria.’ Submitted to *Hydrology*, MDPI, doi: 10.3390/hydrology7010019.
4. Hassan, I.; Kalin, R. M.; White, C. J.; Aladejana, J. A.; and Kawala, J. (2020) ‘Potential Impact of climate change on hydrological processes of the Niger-South River, Nigeria.’, Submitted to the *Hydrology and Earth System Sciences* (HESS) (EGU).
5. Hassan, I.; Kalin, R. M.; White, C. J.; and Aladejana, J. A. (2019) ‘Hydrostratigraphy and Hydraulic Characterisation of Shallow Coastal Aquifers, Niger Delta Basin: A Strategy for Groundwater Resource Management’, *Geosciences*, MDPI, 9(11), p. 470. doi:10.3390/geosciences9110470.
6. Hassan, I.; Kalin, R. M.; Aladejana, J. A; and White, C. J. (2020) ‘Modelling the Climate Change Impacts on the Shallow Coastal Aquifer of the Niger Delta, Nigeria.’ Submitted to the *Journal of African Earth Sciences* (Elsevier).

## ABSTRACT

Climate change impact studies are challenging in developing countries due to the paucity of climatological datasets resulting from insufficient monitoring stations, and constraint in human and computational resources. The Niger Delta region is one of the most vulnerable and densely populated regions in Nigeria, which presents special challenges for water resource policy and management due to climate change and anthropogenic activities, especially with an increase in water demands. Flooding events are recorded annually in settlements along River Niger and its tributaries, inundating many towns, displacing people from their homes and polluting the surface and groundwater resources. As the surface and groundwater resources are two interconnected components of one single resource, any negative impacts on one will inevitably affect the quantity or quality of the other component. The increase in intense stress on the groundwater from shallow coastal plain sand aquifers as the significant source of water resources for domestic, industrial and agricultural purposes in the area. This study, therefore, presents a novel approach for climate change impact assessment on surface and groundwater resources in developing countries.

The first stage of this study assessed the performance of three widely used daily gridded precipitation (prcp), maximum and minimum temperature (Tmax and Tmin) datasets from the Climatic Research Unit (CRU), Princeton University Global Meteorological Forcing (PGF) and Climate Forecast System Reanalysis (CFSR) datasets available over the Niger Delta part of Nigeria against the observed station datasets to select the best datasets that can serve as a possible replacement to the observed datasets. Symmetrical uncertainty (SU) filter was employed together with the selected hydro-climatological datasets to assess the performance of 26 Coupled

Model Intercomparison Project Phase 5 (CMIP5) general circulation model (GCM) outputs. The selection was made according to their capability to simulate observed daily precipitation (prcp), maximum and minimum temperature (Tmax and Tmin) over the historical period 1980–2005 (Baseline periods) in the Niger Delta region. The selected GCMs were used for climate change predictions and impacts assessment over the period 2020s (2010–2039), 2050s (2040–2069) and 2080s (2070–2099), under Representative Concentration Pathway (RCP) 4.5 and 8.5. Standardized precipitation index (SPI) of 1-month and 12-month time steps were used for extreme event assessment. SWAT (Soil and Water Assessment Tool) model was used to analyse the effects of climate change on the hydrologic processes of the Niger River Basin (NRB) in Nigeria. The hydrostratigraphy of the Niger Delta shallow coastal aquifers was characterised coupled with the simulated aquifer recharge and evapotranspiration deduced from Global Climate Model (GCM) simulations under two Representative concentration pathways (RCP4.5 and RCP8.5) to develop a transient groundwater flow model to investigate the potential impacts of climate change and increased groundwater abstraction on the coastal plain sand aquifer over the periods 2010 to 2099.

Results of the hydro-climatological study revealed that the CRU datasets performed better in most of the statistical assessments conducted. The symmetrical uncertainty filter revealed the four top-ranked GCMs, namely ACCESS1.3, MIROC-ESM, MIROC-ESM-CHM, and NorESM1-M as the best set of GCMs to form an ensemble for the Spatio-temporal climate projection over the study area. The selected GCM ensemble predicted an increase in the mean annual precipitation in the range of 0.26% to 3.57% under RCP4.5, and 0.7% to 4.94% under RCP 8.5 by the end of the century as compared to the base period. The study also revealed an increase in

maximum temperature in the range of 0 to 0.4 °C under RCP4.5 and 1.25–1.79 °C under RCP8.5 during the periods 2080s. Minimum temperature also revealed a significant increase of 0 to 0.52 °C under RCP4.5 and between 1.38–2.02 °C under RCP8.5, which indicates that there might be the occurrence of extreme events in the Niger Delta due to climate change. The 1-month and 12-month SPI under both RCPs predict incidences of extreme wet cycle across all the study locations, especially during the 2080s. The mean annual streamflow was also predicted to increase from 21% to 48% at the Onitsha gauging station under both emission scenarios.

Results of hydrostratigraphic studies revealed that the system was more complicated than previously reported. A unit of silty sand was observed in the western part of the basin, which thins out leaving the eastern part of the basin as an unconfined aquifer underlain by multiple thin beds of the sand aquifer and a layered sand aquifer, which holds freshwater occurring in the northern parts of the basin. Transient groundwater flow model simulations of Port-Harcourt metropolis predicted the maximum change in groundwater budget and levels when abstraction was increased by 50% under RCP 8.5 resulting to a decrease in groundwater levels by 1 m around the coast to 7 m towards the northern part of the study area. This further cause a change in the aquifer storage to decrease by 325,000 m<sup>3</sup>/day and groundwater levels to decrease from a range of 1 to 27 m, respectively. The findings in this study shows that interconnected surface water-groundwater modelling of climate change impacts is critical as predicted change in the surface flow and water levels will affect the regional groundwater budget of the aquifer.

The findings from this study shows that understanding climate changes impacts on both surface and groundwater resources is crucial for the water resources management of any region. Associating climate scenarios, hydrologic modeling and

numerical groundwater modeling of aquifers provides useful insight into the future hydrogeological systems interactions, which can be used to envisage measurements of adaptation and protection of the water resources. For the coastal aquifer of Niger Delta, the study shows that the risk of contamination of this system by rivers is high. It is recommended that end-users should reflect on the results of this study during IWRM planning to preserve the long-term exploitation of this aquifer, and as part of the sustainable management of the local and national water resources.

## TABLE OF CONTENTS

CHAPTER	TITLE	PAGE
	<b>DECLARATION</b>	<b>ii</b>
	<b>DEDICATION</b>	<b>iii</b>
	<b>ACKNOWLEDGEMENT</b>	<b>iv</b>
	<b>PUBLICATIONS RESULTING FROM THIS RESEARCH</b>	<b>v</b>
	<b>ABSTRACT</b>	<b>vi</b>
	<b>TABLE OF CONTENTS</b>	<b>x</b>
	<b>LIST OF FIGURES</b>	<b>xx</b>
	<b>LIST OF ABBREVIATION</b>	<b>xxvii</b>
	<b>LIST OF SYMBOLS</b>	<b>xxviii</b>
<b>CHAPTER 1 - INTRODUCTION</b>		<b>1</b>
1.1	Background of study	1
1.2	Research's Aim	5
1.3	Objectives of the Study	5
1.4	Scope of the study	6
1.5	Limitations of the study	7
1.6	Structure of the thesis	7
<b>CHAPTER 2 - STUDY AREA</b>		<b>9</b>
2.1	Introduction	9
2.2	Description of the Study Area	9
2.3	Climate and Vegetation	9
2.4	Physiography	11
2.5	Geology of the Area	12
	2.5.2 The Deltaic Formations:	14
	2.5.3 Benin Formation:	15
2.6	Hydrogeology	16
	2.6.1 Surface Water Hydrology	16
	2.6.2 Groundwater Hydrology	17
	2.6.3 Characteristics of the Aquifers:	17
	2.6.3.1 Unconfined Groundwater Occurrence:	18
	2.6.3.2 Confined Groundwater Occurrence:	19

<b>CHAPTER 3 - LITERATURE REVIEW</b>	<b>22</b>
3.1 Introduction	22
3.2 Climate Change	22
3.3 Climate Change in Nigeria	24
3.3.1 Precipitation Change in Nigeria	25
3.3.2 Temperature Change in Nigeria	26
3.4 Hydro-Meteorological Data	28
3.5 General Circulation Models (GCMs)	31
3.6 Regional Climate Model	32
3.7 Global Climate Change Scenarios	33
3.7.1 Representative Concentration Pathway 2.6	34
3.7.2 Representative Concentration Pathway 4.5	35
3.7.3 Representative Concentration Pathway 6.0	35
3.7.4 Representative Concentration Pathway 8.5	36
3.8 Downscaling	37
3.8.1 Dynamical downscaling	38
3.8.2 Statistical downscaling	38
3.8.3 Weather generators	39
3.8.4 Transfer functions	39
3.8.5 Weather typing schemes	40
3.9 Bias Correction	40
3.10 GCM Selection	41
3.11 Impacts of Climate Change on hydrological processes	46
3.12 Hydrologic Modeling	48
3.13 Overview of Soil and Water Analysis Tool	51
3.13.1 Precipitation	52
3.13.2 Runoff	53
3.13.3 Evapotranspiration	54
3.13.4 Soil Water	54
3.13.5 Groundwater	55
3.13.6 Flow Routing	56
3.14 SWAT Model calibration and validation (SWAT-CUP)	57
3.15 Groundwater Flow Model	63
3.15.1 Modeling of Groundwater Flow MODFLOW	63



3.15.2	Description of MODFLOW-2005	65
3.15.3	The discretisation of the Subsurface Process (Aquifer system)	67
3.15.4	Model Boundary conditions	69
3.15.5	Groundwater Model Calibration	69
3.16	Impacts of Climate Change on Surface and Groundwater Resources.	70
3.17	Niger Delta's water resource management problems and challenges	74
3.18	Summary	76
<b>CHAPTER 4 - MATERIALS AND METHODS</b>		<b>78</b>
4.1	Introduction	78
4.2	Research Materials	78
4.2.1	Software and Codes	78
4.2.2	Hydro-Meteorological datasets	81
4.2.3	Climate scenario data	82
4.2.4	River Discharge Data	84
4.2.5	Digital elevation Map, Land use and soil data and sources	84
4.2.6	Borehole Datasets	86
4.3	Research Methods	86
4.4	Summary	88
<b>CHAPTER 5 - SELECTION OF DATASETS</b>		<b>90</b>
5.1	Preamble	90
5.2	Paper 1	92
1.0	Introduction	93
2.0	Description of the Study Area	98
3.0	Materials and Methods	100
3.1	Data	100
3.2	Methods	100
3.2.1.	Performance evaluation of the datasets	102
3.2.2.	Analysis of spells characteristics among datasets	103
3.2.3.	Standardised Precipitation Index (SPI)	105
4.0	Results and Discussions	105
4.1	Performance of Gridded Datasets	105
4.2.	Wet spell and Dry spell	108
4.3.	The implication for water resource management	109

5.0. Discussions	112
6.0. Conclusion	114
5.3. Paper 2	123
1.0 Introduction	124
2.0 Materials and Methods	128
2.1. Description of the Study Area	128
2.2. Data and Sources	130
2.2.1. Gridded Dataset	130
2.2.2. CMIP5 GCM Datasets	131
3.0. Methodology	133
3.1. Model Selection Using Symmetrical Uncertainty	134
3.2. Ranking of GCMs Using the Weighting Method	136
3.3. Bias Correction	137
3.4. Performance Assessment	137
4.0. Results and Discussion	139
4.1. Ranking of the GCMs	139
4.2. Spatial Distribution of Top-Ranked GCMs	139
4.3. Selection of GCM Ensemble	141
4.4. Ensemble Model Validation	142
4.5. Spatial Changes in Mean Annual Prcp, Tmax, and Tmin	148
5.0. Conclusions	151
5.4. Concluding Remarks	160
<b>CHAPTER 6 - IMPACTS OF CLIMATE CHANGE ON EXTREME</b>	
<b>WEATHER EVENTS</b>	<b>162</b>
6.1 Preamble	162
6.2 Paper 3	164
1.0 Introduction	165
2.0 Description of the Study Area	168
3.0 Materials and Methods	170
3.1 Meteorological Datasets	170
3.2. CMIP5 GCM Datasets	170
3.3 Bias correction	171
3.4. Meteorological Drought Assessment	172
3.5. Performance Evaluation of the Models	174

4.0 Results and Discussions	175
4.1. Performance assessment of GCM ensemble	175
4.2. Observed and Predicted Rainfall Scenarios	175
4.3. Meteorological Drought Assessment	178
5.0. Discussion	184
6.0. Conclusions	186
<b>CHAPTER 7 - IMPACT OF CLIMATE CHANGE ON THE</b>	
<b>    HYDROLOGICAL PROCESSES</b>	<b>193</b>
7.1 Preamble	193
7.2 Paper 4	195
1.0 Introduction	196
2.0 Description of the study area	199
3.0 Materials and methods	201
3.1 Data and sources	201
3.2 Downscaling Future Climate	204
3.3 Hydrological model: SWAT	205
3.4 Model calibration and validation	207
4.0 Results	209
4.1 Downscaling of climate	209
4.1.2 Observed and Future Climate Scenarios	210
4.2 SWAT model calibration and validation	214
4.3 Climate change analyses	216
4.4 Climate change impact on streamflow	217
4.4.1 Lokoja Mean monthly streamflow	218
4.4.2 Onitsha Mean monthly streamflow	219
4.5 Climate change impact on mean annual Evapotranspiration	220
4.6 Climate change impact on mean annual groundwater recharge	222
5.0 Discussion	223
6.0 Conclusions	225
7.3 Supplementary Data	233
7.3.1 Climate change impact on mean annual surface runoff	233
7.3.2 Lokoja station flow Duration Curve	234
7.3.3 Onitsha station flow Duration Curve	236
7.4 Concluding Remarks	238

<b>CHAPTER 8 - HYDROLOGICAL CONCEPTUAL MODEL</b>	<b>238</b>
8.1 Preamble	239
8.2 Paper 5	241
1.0 Introduction	242
2.0. Materials and Methods	245
2.1 Description of the Study Area	245
2.2 Geology of the Area	246
2.3 Hydrogeology	247
3.0. Methodology	249
4.0. Results and Discussion	251
4.1 Aquifer Characterisation Using Borehole Logs	251
4.2 Cross-Sections from the Selected Boreholes	252
4.3 Hydraulic Characterisation of the Aquifers	258
4.4 Implications for Groundwater Resilience in Shallow Aquifers of the Niger Delta Basin	259
5.0. Conclusions	261
8.3 Supplementary Data	268
8.3.1 Deep aquifers in the Coastal Plain Sands	269
8.3.2 Deep aquifers in Warri-Sambreiro deltaic plain	273
8.3.3 Deep aquifers in Freshwater Swamp	273
8.3.3.1 Deep borehole at Otakeme near Oloibri, Bayelsa state	273
8.3.3.2 Deep borehole at Kaiama, Bayelsa state	274
8.3.3.3 Deep borehole at Gbaran-Ubie	276
8.3.4 Deep aquifers in the saltwater swamp	277
8.3.4.1 Deep borehole at Bille of 400m	278
8.3.4.2 Deep borehole at Bassambiri, Nembe	279
8.3.5 Deep coastal beach aquifers	280
8.3.5.1 Deep boreholes at the Bonny River Terminal.	280
8.3.5.2 Deep boreholes at MPN Life Camp, Bonny	282
8.3.5.3 Deep borehole at Bonny Water Board	284
8.3.5.4 Deep borehole at Oguede, Bonny for NLNG	286
8.3.5.5 Deep borehole at Finima, near Bonny for NLNG	288
8.3.5.6 Deep borehole at Ogidigbenu/Ugborodo, Delta	290
8.4 Concluding Remarks	292

<b>CHAPTER 9 - IMPACT OF CLIMATE CHANGE ON THE GROUNDWATER</b>		
	<b>RESOURCES</b>	<b>294</b>
9.1	Preamble	294
9.2	Paper 6	296
	1.0. Introduction	297
	2.0. Methodology	300
	2.1. Description of the Study Area	300
	2.2. Geologic Setting	302
	2.3. Hydrogeologic Setting	303
	2.4. Data	304
	2.5. Observed and Future Climate Scenarios	305
	3.0. Groundwater Flow Model	307
	3.1. Hydrogeological Conceptual Model	309
	3.2. Numerical Modeling	311
	3.2.1. Steady-State Model Calibration	313
	4.0. Results and Discussions	316
	4.1. Surface water-groundwater interaction	316
	4.2. Base Period.	316
	4.3. Simulation of the potential impact of future climate change scenarios on groundwater resources.	319
	5.0. Implications for groundwater resource management	326
	6.0. Conclusions	328
9.3	Supplementary Data	338
9.4	Concluding Remarks	342
9.5	Filling the Knowledge Gaps	343
<b>CHAPTER 10 - CONCLUSION AND RECOMMENDATIONS</b>		<b>348</b>
10.1	Restatement of Research Aim and Objectives	348
10.2	Conclusion	349
10.3	Overall impact of the Research	352
10.4	Recommendations for Further Studies	354
<b>REFERENCES</b>		<b>356</b>
<b>APPENDIX</b>		<b>413</b>

## LIST OF TABLES

TABLE NO.	TITLE	PAGE
Table 2.1:	Geologic Sequence of the Niger Delta Basins	13
Table 2.2:	Some Selected Boreholes in Rivers State	19
Table 3.1:	Overview of RCP Scenarios	37
Table 3.2:	Summary of climate change studies in Nigeria	44
Table 3.3:	Requirements, Features, strengths and weaknesses of frequently used hydrological models	49
Table 3.4:	Summary of the SWAT Model application in Nigeria.	59
Table 4.1:	Percentage of Soil Texture Compositions	85
Table 5.1:	Characteristics of gridded rainfall data used in this study.	104
Table 5.2:	Comparison of observed gridded climate data.	104
Table 5.1:	General circulation models (GCMs) used in the study at 0.5 ° grid.	132
Table 5.2:	Overall SU weights of GCMs and their ranks according to their ability to simulate the CRU prcp, Tmax, and Tmin datasets. The selected GCMs are shown in bold font.	143
Table 5.3:	Performance assessment of the GCM ensemble at the grid located in Port Harcourt.	146
Table 6.1:	CMIP5 General Circulation Models Used in the Study at 0.5° X 0.5° Grid.	171
Table 6.2:	Categories for standardized precipitation index (SPI) values (Mckee, Doesken and Kleist, 1993; Svoboda, Hayes and Wood, 2012).	173
Table 6.3:	Performance assessment of rainfall in the general circulation model (GCM) ensemble.	175
Table 7.1:	Input data for River Niger Catchment Soil and Water Assessment Tool model	202
Table 7.2:	General Circulation Models used in the Study at 0.5 <sup>0</sup> Grid.	204
Table 7.3:	Percentage changes in future Annual Rainfall, Maximum and Minimum Temperature under RCP4.5 & RCP8.5.	211

Table 7.4: Parameters Sensitivity analysis based on Hydrological stations of Lokoja and Onitsha	215
Table 7.5: SWAT Calibration and Validation Statistics of the River Niger Catchment	215
Table 7.6: Mean Monthly and Percentage Change in Streamflow under RCP4.5 & RCP8.5	218
Table 8.1: Stratigraphic Units of the Niger Delta basin	247
Table 8.2: Borehole locations with strata logs, depths and static water levels.	249
Table 8.3: Hydraulic conductivity values from different authors across the study area.	259
Table 8.4: Distribution of boreholes studied in the geomorphic zones.	269
Table 8.5: lithologic sequence at Onne, Coastal Plain Sands	271
Table 8.6: Lithologic succession in a deep well at NIPP, Omoku	273
Table 8.7: Lithologic succession in a well at Warri Refinery	273
Table 8.8: Lithologic succession in a deep borehole at Otakeme	274
Table 8.9: Lithologic succession in a deep borehole at Kaiama	274
Table 8.10: Lithologic successions in a deep borehole at Gbaran-Ubie	276
Table 8.11: Lithologic succession in a deep borehole at Bille	279
Table 8.12: Lithologic succession in a deep borehole at Bassambiri, Nembe	280
Table 8.13: Lithologic successions in a deep borehole at BRT, Bonny	282
Table 8.14: Lithologic successions in a deep borehole at MPN Life Camp, Bonny	284
Table 8.15: Lithologic successions in a deep borehole at Bonny Water Board	286
Table 8.16: Lithologic successions in a deep borehole at NLNG, Bonny.	288
Table 8.17: Lithologic successions in a deep borehole at NLNG, Finima, Bonny	290
Table 8.18: Lithologic successions in a deep borehole at Ogidigben/Ugborodo, Delta state.	292
Table 9.1: Annual changes in future Rainfall, Maximum and Minimum Temperature under RCP4.5 and RCP8.5	306
Table 9.2: Initial and calibrated model parameters	314
Table 9.3: Summary of the simulated water budget for the modelled area during the observed and future periods under RCP 4.5 and RCP 8.5 emission scenarios.	318

Table 9.4 : Summary of the simulated water budget for the modelled area under Normal and increased pumping conditions during the future periods under RCP 4.5 and RCP 8.5 emission scenarios. 324



## LIST OF FIGURES

FIGURE NO.	TITLE	PAGE
Figure 2.1	Location of the study area in Nigeria.	10
Figure 2.2	Drainage map of the Niger Delta, Nigeria	12
Figure 2.3	Geological map of Niger Delta	14
Figure 3.1	Map of observed surface temperature change from 1901 to 2012	24
Figure 3.2	Maps of observed precipitation change from 1901 to 2010 and from 1951 to 2010	24
Figure 3.3	Average Annual Precipitation	26
Figure 3.4	Average Temperature	27
Figure 3.5	Weather stations in Nigeria	29
Figure 3.6	Regional Climate Model nesting approach.	32
Figure 3.7	A discretised hypothetical aquifer system adopted from 68	
Figure 4.1	Map of the Study Area in Nigeria Showing the Spatial Distribution of 0.50 Grids	82
Figure 4.2	Map of Nigeria showing Study Hydrological Station	83
Figure 4.3	Land-use Map of the Study Area	84
Figure 4.4	Soil Map of the Study area	85
Figure 4.5	Flow chart showing sequence of methods used in the study	88
Figure 5.1	Map of the Study Area in Nigeria Showing the Spatial Distribution of 0.50 Grids	99
Figure 5.2	Seasonal variation of the annual average of observed meteorological station, CRU, PGF and CFRS datasets obtained from the same grid as the station data from 1980-2005 for (a) PH Precipitation (b) Warri Precipitation (c) PH Tmax (d) Warri Tmax (e) PH Tmin and (f) Warri Tmin.	107

Figure 5.3	Comparison of Monthly Rainfall Dry Spell for (a) Port Harcourt (b) Warri and Wet Spell for (c) Port Harcourt (d) Warri observed Meteorological station data, CRU, PGF and CFRS datasets obtained from the same Grid as the station data from 1980-2005.	109
Figure 5.4	Spell length correlation for the observed station, CRU, PGF and CFRS datasets for (a) Port Harcourt (b) Warri station.	110
Figure 5.5	Computed SPI using the observed station, CRU, PGF and CFRS datasets for the periods 1980-2005 for (a) Port Harcourt (b) Warri station.	111
Figure 5.1	Map of the study area showing the spatial distribution of $0.5^{\circ} \times 0.5^{\circ}$ grids.	129
Figure 5.2	The spatial distribution of GCMs ranked best, second-best, and third-best position using a symmetrical uncertainty filter at different grid points for Prcp, Tmax, and Tmin over the Niger Delta.	141
Figure 5.3	Monthly averages of CRU and raw datasets. (a) 26 Prcp, (b) 4 Prcp SU, (c) 26 Tmax, (d) 4 Tmax SU, (e) 26 Tmin, and (f) 4 Tmin SU GCM outputs for the historical period 1980–2005 at the grid point located in Port Harcourt.	144
Figure 5.4	Monthly averages of CRU and bias-corrected datasets. (a) 26 Prcp, (b) 4 Prcp SU, (c) 26 Tmax, (d) 4 Tmax SU, (e) 26 Tmin, and (f) 4 Tmin SU GCM outputs for the historical period 1980–2005 at the grid point located in Port Harcourt.	145
Figure 5.5	Interval plots for the annual averages of CRU datasets with the ensemble of all 26 GCMs and the four SU selected GCMs for (a) Prcp (base period), (b) Prcp (future periods), (c) Tmax (base period), (d) Tmax (future periods), (e) Tmin (base period), and (f) Tmin (future periods) with 95% confidence interval at the grid located in Port Harcourt.	147

Figure 5.6	Spatial distribution of percentage changes in average annual prcp, for periods (a) 2040–2069 and (b) 2070–2099 compared to the base period 1980–2005 for RCP4.5 and RCP8.5.	148
Figure 5.7	Spatial distribution of percentage changes in average annual maximum temperature for periods (a) 2040–2069 and (b) 2070–2099 compared to the base period 1980–2005 for RCP4.5 and RCP8.5.	149
Figure 5.8	Spatial distribution of percentage changes in average annual minimum temperature for periods (a) 2040–2069 and (b) 2070–2099 compared to the base period 1980–2005 for RCP4.5 and RCP8.5.	149
Figure 6.1	Location of the study area in Nigeria;	169
Figure 6.2.	Seasonal Variation of Observed and Predicted Precipitation in (a) Yenagoa-RCP4.5, (b) Yenagoa-RCP8.5, (c) Warri-RCP4.5, (d) Warri-RCP8.5, (e) Port Harcourt-RCP4.5 and (f) Port Harcourt-RCP8.5, during the future periods.	177
Figure 6.3.	Percentage increase in predicted future rainfall in comparison with Observed rainfall across the study areas under RCP 4.5 & RCP 8.5 emission scenarios.	177
Figure 6.4.	Computed standardized precipitation index (SPI) for the base period across the study locations.	180
Figure 6.5.	Computed (a) 1-month RCP4.5 SPI, (b) 12-month RCP4.5 SPI, (c) 1-month RCP8.5 SPI, and (d) 12-month RCP8.5 SPI for the projected periods from 2010 to 2039 across the study locations.	181
Figure 6.6.	Computed (a) 1-month RCP4.5 SPI, (b) 12-month RCP4.5 SPI, (c) 1-month RCP8.5 SPI, and (d) 12-month RCP8.5 SPI for the projected periods from 2040 to 2069 across the study locations.	182
Figure 6.7.	Computed (a) 1-month RCP4.5 SPI, (b) 12-month RCP4.5 SPI, (c) 1-month RCP8.5 SPI, and (d) 12-month RCP8.5	

	SPI for the projected periods from 2070 to 2099 across the study locations.	183
Figure 7.1	Location of the study area in Nigeria	200
Figure 7.2	(a) Land use and (b) Soil Map of River Niger Catchment	203
Figure 7.3	Monthly averages of historical annual Raw (a) Rainfall (c) Tmax (e) Tmin, and Bias-corrected (b) Rainfall (d) Tmax (f) Tmin GCM's for the periods 1980–2005 in Onitsha.	212
Figure 7.4	Monthly averages of Observed and Projected Rainfall at (a) Lokoja (b) Onitsha, Tmax (c) Lokoja (d) Onitsha, and Tmin (e) Lokoja (f) Onitsha Stations under RCP 4.5 and 8.5 scenarios.	213
Figure 7.5	Observed and Predicted Monthly Streamflow for Lokoja Monitoring Stations.	217
Figure 7.6	Observed and Predicted Monthly streamflow for Onitsha Monitoring Stations.	217
Figure 7.7	Mean monthly streamflow for Lokoja Monitoring Stations under RCP4.5 and RCP8.5 emission scenarios.	219
Figure 7.8	Mean monthly streamflow for Onitsha Monitoring Stations under RCP4.5 and RCP8.5 emission scenarios.	220
Figure 7.9	Spatial distribution of Evapotranspiration during the (a) Observed (b) RCP 4.5 (2020s) (c) RCP 4.5 (2050s) (d) RCP 4.5 (2080s) (e) RCP 8.5 (2020s) (f) RCP 8.5 (2050s) (g) RCP 8.5 (2080s) in the Niger river basin.	221
Figure 7.10	Spatial distribution of groundwater recharge during the (a) Observed (b) RCP4.5 (2020s) (c) RCP4.5 (2050s) (d) RCP4.5 (2080s) (e) RCP8.5 (2020s) (f) RCP8.5 (2050s) (g) RCP8.5 (2080s) in the Niger River Basin.	222
Figure 7.11	Spatial distribution of Surface Runoff during the (a) Observed (b) RCP4.5 (2020s) (c) RCP4.5 (2050s) (d) RCP4.5 (2080s) (e) RCP8.5 (2020s) (f) RCP8.5 (2050s) (g) RCP8.5 (2080s) in the Niger River Basin.	233

Figure 7.12	Percentage flow duration curve of Maximum streamflow for each year at Lokoja Monitoring Stations under (a) RCP4.5 and (b) RCP8.5 emission scenarios.	235
Figure 7.13	Percentage flow duration curve of Maximum streamflow for each year at Onitsha Monitoring Stations under (a) RCP4.5 (b) RCP8.5 emission scenarios.	237
Figure 8.1	Digital elevation map showing the location of the study area in Nigeria.	245
Figure 8.2	Geology map (Adopted and Modified from (NGSA, 2012)) of the study area showing cross-section lines along which lithosections are developed.	247
Figure 8.3	Hydrostratigraphic section along profile line AA <sup>I</sup> at various zones within the Niger Delta basin.	254
Figure 8.4	Hydrostratigraphic section along profile line BB <sup>I</sup> at various zones within the Niger Delta basin.	255
Figure 8.5	Hydrostratigraphic section along profile line CC <sup>I</sup> at various zones within the Niger Delta basin.	256
Figure 8.6	Hydrostratigraphic section along profile line DD <sup>I</sup> at various zones within the Niger Delta basin.	257
Figure 8.7	Fence diagram showing hydrostratigraphic section within the Niger Delta basin.	260
Figure 8.8	Down-hole Geophysical log at NAFCON, Onne.	270
Figure 8.9	Down-hole geophysical log of a borehole at Ndoni	272
Figure 8.10	Down-hole geophysical log of a borehole at Otakeme	275
Figure 8.11	Down-hole log of Gbaran-Ubie borehole at SHELL Facility FLB site	277
Figure 8.12	Wireline logs in a deep borehole at Bille	278
Figure 8.13	Wireline logs of a deep borehole at BRT	281
Figure 8.14	Wireline logs of a deep borehole at Mobil Life camp, Bonny Island	283
Figure 8.15	Wireline logs in a deep borehole at Bonny Water Board, Bonny Island	285
Figure 8.16	Wireline logs in a deep water borehole at Oguede, Bonny, NLNG	287

Figure 8.17	Wireline logs in a deep borehole at Finima, NLNG	289
Figure 8.18	Wireline logs of a deep borehole at Ogidigben/Ugborodo,	
Delta state.	291	
Figure 9.1	Map of the study area, Rivers State, Nigeria	301
Figure 9.2	Geological Map of the Rivers State showing the study	
	area	303
Figure 9.3	Observed and Future average annual (a) Precipitation (b)	
	Maximum and (c) Minimum Temperature for Port	
	Harcourt under RCP 4.5 and 8.5 scenarios.	307
Figure 9.4	Map of the study area showing the locations of abstraction	
	wells in the basin and the Model Boundary conditions.	308
Figure 9.5	Map showing Recharge and Evapotranspiration Zones	
	obtained from SWAT hydrologic model.	310
Figure 9.6	(a&b): Simulated observed and future (a) Recharge and	
	(b) Evapotranspiration obtained from SWAT hydrologic	
	model for the five Subbasins housing the study area.	311
Figure 9.7	Spatial variation of calibrated hydraulic conductivity	
	values across the different formations.	315
Figure 9.8	Scatter plot of (a) observed versus simulated heads (b)	
	Residual versus simulated heads for model calibration.	315
Figure 9.9	Spatial variation of simulated steady-state groundwater	
	heads and contours during the observed period.	317
Figure 9.10	Spatial variation of simulated groundwater heads and	
	water table contours for the 2020s (a) RCP4.5 (b) RCP8.5.	
	2050s (c) RCP4.5 (d) RCP8.5, and 2080s (e) RCP4.5 (f)	
	RCP8.5 future periods.	320
Figure 9.11	Spatial variation of change in groundwater heads due to	
	normal pumping condition under (a) RCP4.5 & (b)	
	RCP8.5, 25% increase in pumping under (c) RCP4.5 (d)	
	RCP8.5, and 50% increase in pumping under (c) RCP4.5	
	(d) RCP8.5 for 2010 to 2099 future periods.	322
Figure 9.12	Inflow/Outflow balance of the area from 2010 to 2099	
	under scenario RCP 4.5.	325

Figure 9.13	Inflow/Outflow balance of the area from 2010 to 2099 under scenario RCP 8.5.	325
Figure 9.14	Spatial variation of simulated groundwater heads and water table contours for the base periods (1980-2005).	339
Figure 9.15	Spatial variation of simulated groundwater heads and water table contours under RCP4.5 emission scenario for the years 2010 to 2039 future periods.	339
Figure 9.16	Spatial variation of simulated groundwater heads and water table contours under RCP4.5 emission scenario for the years 2040 to 2069 future periods.	340
Figure 9.17	Spatial variation of simulated groundwater heads and water table contours under RCP4.5 emission scenario for the years 2070 to 2099 future periods.	340
Figure 9.18	Spatial variation of simulated groundwater heads and water table contours under RCP8.5 emission scenario for the years 2010 to 2039 future periods.	341
Figure 9.19	Spatial variation of simulated groundwater heads and water table contours under RCP8.5 emission scenario for the years 2040 to 2069 future periods.	341
Figure 9.20	Spatial variation of simulated groundwater heads and water table contours under RCP8.5 emission scenario for the years 2070 to 2099 future periods.	342

## LIST OF ABBREVIATION

CMIP5	-	Coupled Model Intercomparison Project Phase 5
CRU	-	Climatic Research Unit
CFSR	-	Climate Forecast System Reanalysis
ET	-	Evapotranspiration
Eqn.	-	Equation
GIS	-	Geographic Information System
GCM	-	Global Climate Model
GWT	-	Groundwater Table
GWL	-	Groundwater Level
IDW	-	Inverse Distance Weighted
IWRM	-	Integrated Water Resource Management
MBE	-	Mean Bias Error
NDB	-	Niger Delta Basin
NSB	-	Niger South River Basin
Pcp	-	Precipitation
PET	-	Potential Evapotranspiration
PGF	-	Princeton University Global Meteorological Forcing
RCP	-	Representative Concentration Pathways
RMSE	-	Root Mean Square Error
$R^2$	-	Coefficient of correlation
SDG	-	Sustainable Development Goals
SPI	-	Standardized Precipitation Index
SU	-	Symmetrical Uncertainty
Tmax	-	Maximum Temperature
Tmin	-	Minimum Temperature



## LIST OF SYMBOLS

$\%$	-	Percent
$k^\circ$	-	Kelvin
$^\circ\text{C}$	-	Centigrade
$g$	-	Gram
$m^2$	-	Square meter
$ml$	-	Millilitre
$m$	-	Meter
$min$	-	Minute
$T_m$	-	Daily Mean Air Temperature
$T_{\max}$	-	Daily Maximum Air Temperature
$T_{\min}$	-	Daily Minimum Air Temperature
$R_a$	-	Extra-terrestrial Radiation

# CHAPTER 1

## INTRODUCTION

### 1.1 Background of study

Climate change has recently been a critical issue among researchers due to its severe impacts on the livelihood of human, society and environment (IPCC, 2013a). Climate is defined as the statistical variability of relevant quantities in terms of the mean over a given period ranging from months to millions of years. Climate change is a natural phenomenon which keeps on changing with time but in a languid pace, usually over 100's of years (WMO, 2013). However, due to the increase in anthropogenic activities, the climate is changing at a much faster rate causing various problems.

The fifth assessment report of the IPCC (Intergovernmental Panel on Climate Change) reported an increase of  $0.85^{\circ}\text{C}$  in the global mean temperature from 1880 until 2012 (IPCC, 2014). The mean global temperature for the period 2006–2015 was found to be  $0.86^{\circ}\text{C}$  above the pre-industrial baseline (1850-1900), and the global mean surface temperature for 2018 is estimated to be  $0.99 \pm 0.13^{\circ}\text{C}$  above the pre-industrial baseline (WMO, 2018). The IPCC first assessment also reported that in the 21<sup>st</sup> century, the mean global temperature is predicted to increase by about  $0.3^{\circ}\text{C}$  per decade over the next 100 years. Global sea level is reported to have risen between 10 and 25 cm since the late 19th century and also anticipated to rise in the range of 2 to 4 cm per decade over the next century (IPCC, 1992). This increase in temperatures will hence make the hydrologic cycle to undergo significant changes in the rates of

precipitation, evapotranspiration and soil moisture (Kumar, 2012; Porio, 2014). The significant impacts of these changes are waterlogging, flooding, damage to crops, soil erosion, adverse effects on surface and groundwater quality, water scarcity, water contamination, disease outbreak, loss of properties, disruption of settlements, and different socio-economic challenges (IPCC, 2007a).

These changes in the climate system will have a substantial impact on both regional and local hydrological regimes across the globe (Hu *et al.*, 2013). Impacts of climate change largely depend on the response of the hydrological cycle to global warming (Marvel and Bonfils, 2013). The hydrological cycle through which water moves continuously from ocean to atmosphere constitutes different processes such as precipitation, evapotranspiration, surface runoff, infiltration and percolation (Ye Htut, 2014). As precipitation is generally considered to be the main driver of the cycle, the increase in temperatures increases evapotranspiration which leads to significant changes in the hydrological cycle (Marvel and Bonfils, 2013).

Freshwater is one of the most assailable resources due to climate change. Globally, only 2.5% of the water on earth is freshwater (Spellman, 2014). As the world population is predicted to grow from an estimated 7.7 billion people worldwide in 2019 to around 8.5 billion in 2030, 9.7 billion in 2050 and 10.9 billion in 2100 (UN DESA, 2019), water demand will also rapidly increase. Climate change will enhance the water stress resulting in around 5 billion people living under water stress condition by the year 2025 (Arnell, 1999). By 2030, studies show that about 4 billion people, representing nearly 2 of every three people globally will experience water scarcity in at least one month of the year (Mekonnen and Hoekstra, 2016). Surface and groundwater are the primary sources of natural freshwater resources upon which the sustainability of agriculture, industrialisation and the civilisation of humanity rely.

Unfortunately, these precious resources have been subjected to severe exploitation and contamination due to anthropogenic activities emanating from industrial effluent, solid waste landfills, gas flaring, oil spillage and petroleum refining leading to the release of heavy metals into the atmosphere (Bellos and Sawidis, 2005; Ahmad *et al.*, 2010; Egeonu and Oyanyan, 2018). The increase in groundwater demand for various human activities has globally placed great importance on water science and management (Nouri *et al.*, 2006).

Coastal aquifers have globally been intensely exploited, given the widespread economic and social development of such areas around the world (Mukherjee *et al.*, 2015). In these areas, groundwater tends to be the only source of freshwater of acceptable quality which makes it crucial and unique but under high stress due to very high exploitation given the needs and demands that are continually increasing leading to uncontrolled overexploitation, the consequences of which can be dramatic (Steyl and Dennis, 2010; MacDonald *et al.*, 2012; Mtoni *et al.*, 2013; Dochartaigh *et al.*, 2019). Due to differences in density between freshwater and saltwater, coastal aquifers naturally undergo saltwater intrusion (Bear and Verruijt, 1987; Oteri & Atolagbe, 2003a). This occurs when the water budget of the aquifers becomes unbalanced due to several factors such as over-exploitation, climate change impacts which might lead to a decrease in recharge rate, which aggravates the wedge of seawater intrusion into the inland coastal aquifers and hence, contaminates the exploration wells (Capaccioni *et al.*, 2005; Felisa *et al.*, 2013). In such cases, lack of management can lead to a limitation of the exploitation of these coastal aquifers, which might even lead to the cessation of the exploitation (Razack *et al.*, 2019). For this purpose, numerical modeling of aquifers constitutes a critical tool which permits analysis of the aquifers' reactions to various stresses (Du *et al.*, 2018; Razack *et al.*, 2019).

The Niger Delta is one of the economic hubs of Nigeria due to crude oil exploration. It serves as the operational base of major oil-producing and servicing companies in Nigeria. Petroleum exploration and exploitation has been ongoing in this region for over fifty years and as well, triggered adverse environmental impacts through socio-economic, environmental and physical disasters which accumulated over the years due to negligence, lack of assessment and limited scrutiny (Akpomuvie, 2011; Nnabuenyi, 2012; Oluduro, 2012; Ubani and Onyejekwe, 2013; Amadi, 2014; Mogborukor, 2014). These encourage a high level of rural-urban migration with a resulting surge in population, which puts pressure on the water resources in the area. Lack of public water supply shifts the focus of most household's water resource needs to groundwater from the shallow aquifers to meet their daily demands. The aquifer system in the area is mostly unconfined, highly porous and permeable; hence, the tendency of contaminants infiltrating into the coastal shallow water table is quite apparent with less storativity (Amadi *et al.*, 2014). Drivers such as incessant oil spillage, flooding and gas-flaring have caused near irreversible degradation of groundwater quality in this area leading to a familiar Irony of people "living on the water but thirsty". Lack of a law enabling the control of the abstraction of groundwater in the area worsens the situation (Edet *et al.*, 2014).

An increasing trend in temperature and frequencies of flood following heavy precipitation has been observed over the years, which are some of the indications of climate change impact seen in the Niger Delta. Flooding is recorded annually in all the Niger Delta states located along the River Niger and its tributaries with two-thirds of Bayelsa and Delta State inundated by devastating floods for at least a quarter of each year (Amangabara and Obenade, 2015; Amangabara and Gobo, 2007; Ologunorisa and Adeyemo, 2005; Mmom, 2013; Tawari-fufeyin *et al.*, 2015). Study on the

vulnerability of communities in three Niger Delta states (Rivers, Delta and Bayelsa states) by Amangabara et al., (2015) found out that a total of 1,110 towns are at risk of being inundated and about 7,120,028 people risk displacement. Immense tracts of mangrove forests have been destroyed causing environmental degradation and pollution, which has affected soil fertility, climate variability, surface water, groundwater, aquatic and wildlife (Amadi *et al.*, 2014). It is most likely that the region might be at a higher risk of induced climate variability, which might affect water resources sustainability. This unhealthy situation continues to attract the interest of environmental observers which calls for a comprehensive evaluation of the impact of climate change on both surface and groundwater resources for sustainability in the coastal areas of Nigeria, and these are part of what this research intended to address.

## **1.2 Research's Aim**

The research aims to comprehensively assess the spatial and temporal impacts of climate change on surface and groundwater resources in the Niger-Delta part of Nigeria for sustainable water resource management. The results of this study can be used to formulate necessary adaptation measures to mitigate or reduce the risk in the changing pattern.

## **1.3 Objectives of the Study**

In order to achieve the research aim, the following objectives were adopted:

1. To select an appropriate set of gridded datasets as well as GCM ensemble for climate change impact studies in the scarce data Niger-Delta Basin.

2. To downscale the future climate change of the study area using CIMP5 GCM's under RCP 4.5 and RCP8.5 emission scenarios.
3. To assess the sensitivity and impacts of the different global climate models on the regional hydrologic regime.
4. To develop the hydrogeologic conceptual model of the shallow coastal aquifer of the Niger-Delta Basin; and
5. To develop and calibrate a regional-scale 3-dimensional groundwater flow model to assess the impacts of climate change on groundwater resources of the shallow coastal aquifer of the Niger-Delta Basin.

#### **1.4 Scope of the study**

The scopes of the research are as follows:

1. Suitable gridded hydro metrological Datasets as well as GCM outputs based on available data and its suitability/ performance to mimic observed data were analysed and selected.
2. Data from selected RCM /GCM was further bias corrected.
3. Future climate regimes under RCP 4.5 and 8.6 emission scenarios on three-time windows as 2010-2039, 2040-2069 and 2070-2099 were forecasted.
4. Soil and Water Assessment Tool (SWAT) model was set up, calibrated and validated for modelling the hydrologic processes.
5. The SWAT model was used for the assessment of the climate change impact on the hydrologic processes under the various emission scenarios in the basin.

6. Groundwater flow model using MODFLOW was developed to assess the impact of climate change on groundwater resources under climate change condition for the various emission scenarios.

### **1.5 Limitations of the study**

1. Quality of water may also be influenced by climate change. However, this research only focused on the quantity of water available in the future.
2. Various factors impact the water demand other than population change like change in temperature, water tariff, socio-economic factors etc. which are not taken into consideration while determining the water demand for the future.
3. Land use was considered to be constant in the Niger Delta part of Nigeria.
4. The model cannot be coupled on SWAT due to non-coverage of land use and soil maps in parts of the coastal area.

### **1.6 Structure of the thesis**

This thesis describes a holistic approach for modelling the potential impacts of climate change on surface and groundwater resources in the Niger Delta part of Nigeria for sustainable water resource management. Following the current chapter, eight chapters are developed as follow:

- Chapter 2 presents an overview of the study area's climate, vegetation, physiography, geology, and hydrogeology.
- Chapter 3 presents the review of relevant literature, theoretical background and information related to the impact of climate change on water resources on a global scale as well as in the Niger Delta context. The chapter includes the



summary of RCM/GCM, RCP scenarios, the introduction of the SWAT hydrological model and MODFLOW for groundwater flow modelling, respectively. Climate change impacts on water resources resilience using SWAT and MODFLOW models are also described based on literature review.

- Chapter 4 demonstrates the research datasets and the methodology adopted to address the knowledge gaps and the datasets used in this study.
- Chapter 5 presents the evaluation and selection of daily gridded hydro-meteorological datasets, and a suitable GCM ensemble for climate change impacts assessment in the Niger Delta, Nigeria.
- Chapter 6 outlines the application of the selected gridded datasets and GCMs for the climate investigation into the potential impact of climate change on extreme meteorological events in the Niger-Delta, Nigeria.
- Chapter 7 outlines the application of the selected gridded datasets and GCMs for the climate investigation into the potential impact of climate change on the hydrologic processes in the Niger-South River basin, Nigeria.
- Chapter 8 presents the hydrogeological conceptual model of the Niger-Delta shallow coastal aquifer.
- Chapter 9 presents the application of the hydrologic model outputs and the conceptual model in modelling the impacts of climate change on groundwater resources in the Niger Delta, as well as the limitations of this study and some recommendations for future work; and
- Chapter 10 presents the main conclusions of this research with a list of specific topics suggested for future research.

All references cited are presented at the end of the thesis. This is followed by Appendices referred to within the thesis.

# CHAPTER 2

## 2.1 Introduction

This chapter provides a general overview of the study area, geology, hydrogeology and the datasets used in this study. Detail information is provided in subsequent chapters.

## 2.2 Description of the Study Area

The study area geographically lies within the eastern Niger Delta region of Nigeria between latitude 4.15°N to 5.40° N and longitude 6.01°E to 7.50° E comprising two states in the Niger Delta namely Rivers and Bayelsa state covering an area approximately 29,100 km<sup>2</sup> as shown in Figure 2.1. The topography of the area is under the influence of tides which results in flooding, especially during the rainy season (Mmom, 2013; Amadi, 2014). The area is low lying and drained by Imo, Aba, Kwa-Ibo and Bonny Rivers and their tributaries with a good road network system.

## 2.3 Climate and Vegetation

Climatically, the study area belongs to the tropical rainforest within the wet equatorial climatic region characterised by typical tropical wet and dry climate with a mean annual rainfall decreasing from 4500 mm around the coastal margin to about 2000 mm around the northern fringe of the study area (Adejuwon, 2012). The region is characterised by two seasons, namely dry season (November to March) and the rainy season (April to October) (Etu-Efeotor, 1990; Amadi, 2011). The mean monthly

temperatures are usually higher up to 26.67 °C around March/April and as low as 24.44 °C during July/August giving a small annual range of 2.73 °C. The dry season temperature could be as low as 17 °C, and as high as 34.4 °C.

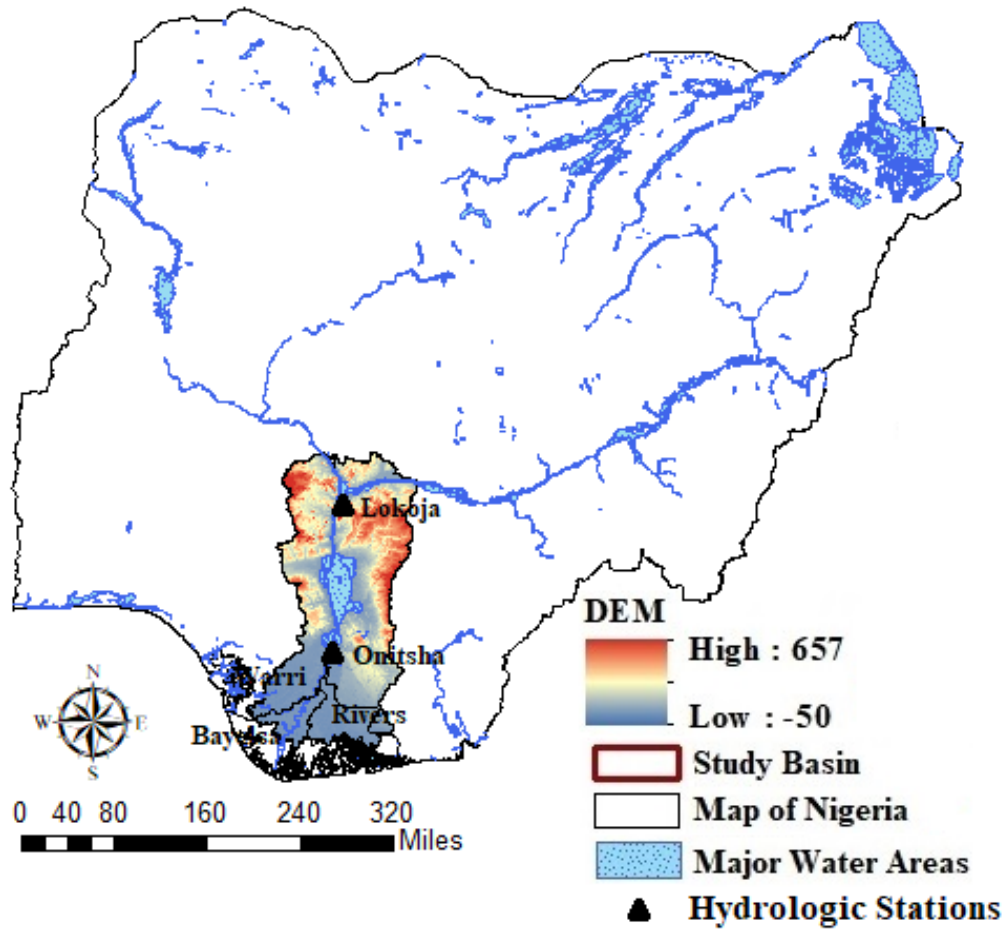


**Figure 2.1** Location of the study area in Nigeria.

The average relative humidity is relatively high, often reaching 90%, at the same time, the warm, wet southwesterly winds blow inland most of the year, and the dust-laden, warm-dry North-easterly winds occasionally reach the coast during small periods of the year (Etim and Alonge, 2009). The mean annual evaporation loss is estimated for the area as 969.5 mm with the highest monthly evaporation loss of 113.8 mm during the dry season and about 89.6 mm in the rainy season. The area has an

average monthly relative humidity that ranged between 50% and 93% over 24 hours during the day and between 66.5% and 86.0% (Etu–Efeotor and Odigi, 1983).

The streams/river channels in these areas are covered with tropical vegetation, which often covers uncultivated farmlands. Grasses are found to have taken over the original tropical forest characteristic of the area due to intense cultivation with abundant sunshine all the year-round (Amadi *et al.*, 2012). The area contains abundant Palm trees, Raffia palms, bananas, plantain, maize, cassava, yams and cocoyams, which are favoured by the high rainfall and high temperature in the area.

## **2.4 Physiography**

The topography of the area is relatively flat, underlain by the Benin Formation, which slopes towards three major rivers namely, Imo, Aba, Kwa-Ibo and Bonny. It has a gentle elevation that is ranging from 40 m – 84 m above sea level (Figure 2.1), which is related to the regional geology of the area. It is characterised by several gully erosion sites, which can be attributed to the friable nature of the dominant coastal plain sand in the area. The slope ranges from 0 to 3% from north to south towards the Atlantic Ocean. The area is characterised by swampy grounds close to the river channels due to the flat topography which drains the area via the four perennial rivers, and their tributaries flowing from north-south joining the Atlantic Ocean (Figure 2.2) (Offodile, 2002; Amadi *et al.*, 2010).

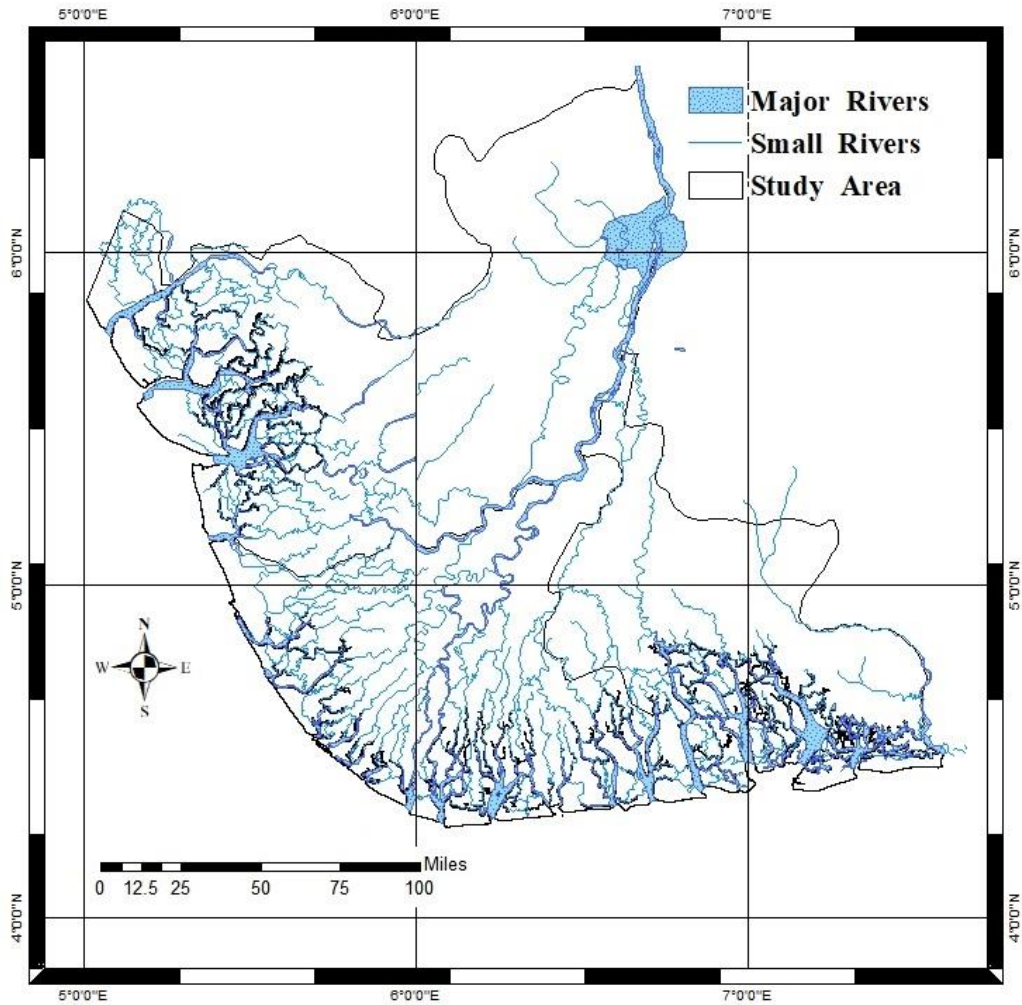


**Figure 2.2** Drainage map of the Niger Delta, Nigeria

## 2.5 Geology of the Area

The Niger Delta Basin is underlain by three formations which are the Benin, Agbada and Akata formation with the Benin and Deltaic Formation as the most critical formations in terms of groundwater aquifer (Adelana *et al.*, 2008; Okeke *et al.*, 2011; Offodile, 2014; Nwankwoala, 2015). The study area is underlain by Pliocene-Pleistocene belonging to the Benin Formation (Figure 2.3) typically found in Port-Harcourt, Aba and Owerri where the formation overlies the older Ogwashi-Asaba Formation (Amadi *et al.*, 2014). The Geological sequence of the Niger Delta is summarised in Table 2.1.

**Table 2.1 : Geologic Sequence of the Niger Delta Basins**

<b>ERA</b>	<b>AGE</b>	<b>FORMATIONS</b>
Quaternary	Late Pleistocene	Upper Deltaic Plains,
	Holocene	Lower Deltaic Plains
	Oligocene	Benin Formation
	Pleistocene	Agbada Formation
	Lower Eocene	Akata Formation
	Palaeocene to Eocene	Ameki Formation

The Deltaic Formation and Benin Formation are the most important aquiferous formations in the Niger Delta (Adelana *et al.*, 2008; Okeke *et al.*, 2011; Offodile, 2014; Nwankwoala, 2015). In the Deltaic Formations, late Pleistocene to Holocene age occupy most of the area of the present delta and stretches narrowly eastwards along the coastline. The Deltaic Plains (upper and lower) consist of coarse to medium-grained unconsolidated sands. These sands form lenticular beds with intercalations of peaty matter and lenses of soft, silty clay and shales (Uko and Emudianughe, 2016). The Benin formation otherwise referred to as coastal plain sand, outcrops in the northeast of the coastal belt and dips at a low angle in the south-west. The sediments consist, generally, of Unconsolidated lenticular and dominantly sandy formations with Massive gravels and pebble beds giving rise to high yielding boreholes, (Ugwu and Nwankwoala, 2008). The geological map of the study area, as shown in Figure 2.3 below, was adopted and Modified from the Nigerian Geological Survey Agency 2006 (NGSA, 2012).

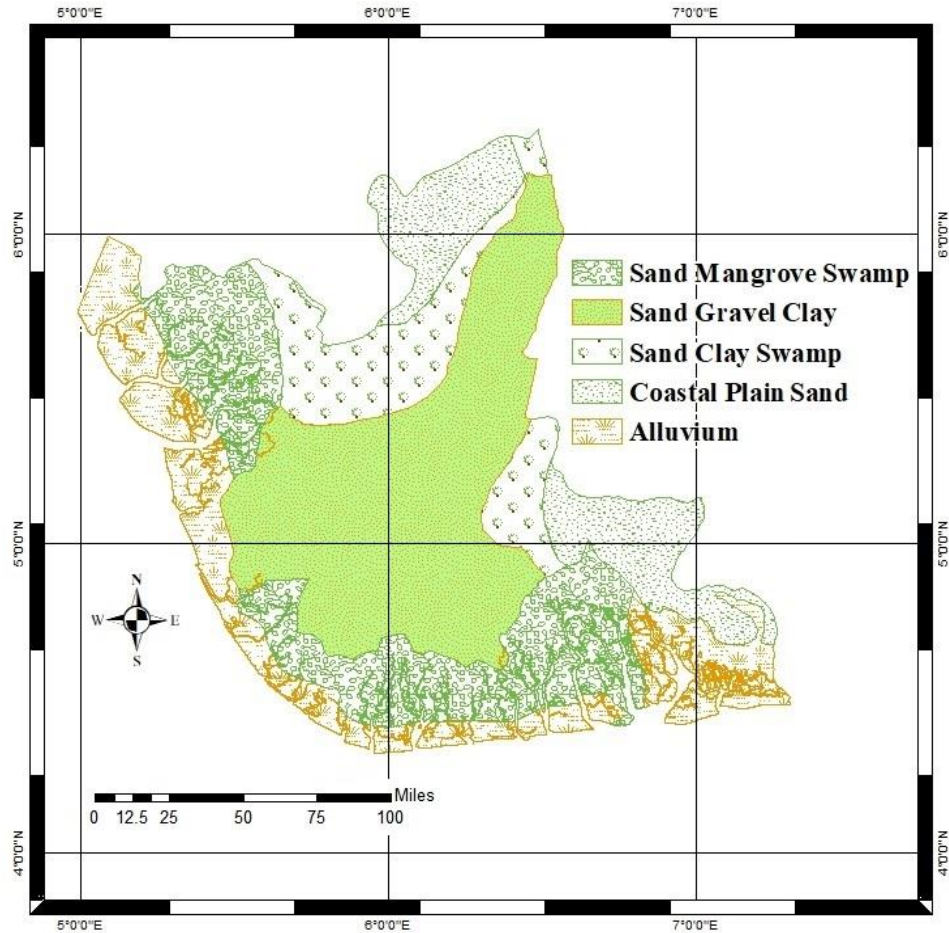


**Figure 2.3** Geological map of Niger Delta, Modified from (NGSA, 2012)

### 2.5.2 The Deltaic Formations:

The Deltaic plains represent the late Pleistocene to Holocene age, which occupies most of the area of the present delta and stretches narrowly eastwards along the coastline, which consists of coarse to medium-grained unconsolidated sands. These sands form lenticular beds with intercalations of peaty matter and lenses of soft, silty clay and shales. Gravelly beds, up to 10m thick, have been reported. These beds dip at varying angles towards the sea, forming units of what represents a series of old Deltas. The sandy beds make prolific aquifers which dip at different angles towards the sea, forming units that represent a series of ancient deltas (Uko and Emudianughe, 2016).

The sediments near the surface dip at low angles and are thought to represent the top set beds of the present phase of development of the delta. In Brass, logs recorded 57m of fine to medium-grained sand followed by 6m of dark grey clay with sand intercalations. This overlies 51m of very coarse to pebbly sands underlain by sandy woody or peaty matter. Below this, a thicker 36m very compact dark clay bed overlies fine to very coarse sand which extends far down from the 150m depth of the clay formation to the bottom of the hole 255m below the ground level (Offodile, 2014). At Bonny, a similar succession was encountered. Thin beds of clay, at the top, precede a 90m column of coarse and pebbly sands overlying dark shale's, 27m thick. This shale is also confined very coarse to pebbly sands below, the 135m depth. In Opobo, the succession changes slightly. The shale bed in this area occurs between 113.4m to 131.4m and also confines an aquifer, which produced pressure water (Offodile, 2014).

### **2.5.3 Benin Formation:**

The Benin Formation is the uppermost unit in Niger Delta which comprises of massive Eocene to Holocene succession characterised by poorly indurated sandstones, thin shales, coals, and gravels of continental to upper delta plain origin (Short and Stauble, 1967). Other accessory minerals include yellowish-brown limonite coatings and lignite. This formation outcrops in the northeast of the Coastal belt and dips at a low angle in the south-west. The sediments consist, generally, of unconsolidated lenticular and dominantly sandy formations (Ugwu and Nwankwoala, 2008). Massive gravels and pebble beds occur in places and have given rise to high yielding boreholes, as in Port Harcourt. Other boreholes in the Benin Formation area (e.g., Azumini and Elele) reveal the same sequence of continuous sandy, pebbly formations. The thickness is estimated at 2300m (Merki, 1970).



Lenticular clays and shales occur mainly in the eastern areas where they confine small but moderately high yielding aquifers. In Uyo, Utapate, Etinan, Oron and Calabar, several confined aquifers were encountered, and most of these gave pressure water. The 90-150m confining clay beds encountered in the Niger Delta area, (Brass, Bonny and Opobo) disappear in the regions, north of the area, and adjacent to the Benin Formation area (Bodo, Okrika and Port Harcourt) (Offodile, 2014). Laterite beds were also encountered in the boreholes in Okrika, Etinan, Oron, Calabar and Port Harcourt and these seem to mark the erosional surfaces of the offset beds of the old Delta.

To complete the stratigraphic sequence, mention was made of the older formations, namely the Agbada and Akata formations. The Agbada Formation consists of interbedded sands and marine shales, reported to range in depth from about 300m to 5000m. At the same time, the Agbada Formation underlines the Akata Formation and has a sequence of similar marine shales and clays of about 700m to 7000m.

## **2.6 Hydrogeology**

### **2.6.1 Surface Water Hydrology**

The Niger Delta has vast flood plains, which run straight on their course and form significant tributaries to the Aba, Imo, Kwa-Ibo and Bonny Rivers. The trends of the river flow is from the northwest-southeast direction (Uma, 1989). The area is characterised with a large percentage of open grasslands with abundant rainfall. These rivers are prone to pollutions along their course due to anthropogenic activities, and so the inhabitants do not rely on them for potable water supply. The continuous rural-urban drift of people in the Niger Delta is further aggravating the pollution of these rivers as they serve as the effluent discharge point for untreated industrial waste due

to the location along the banks of these rivers and lacks functional municipal water supply systems. This makes the people living in those areas depend on private boreholes for their domestic water supply. Stream discharge is from surface runoff and groundwater base-flow with peak stream discharge occurring between September and October (Amangabara, 2006).

### **2.6.2 Groundwater Hydrology**

The study area is characterised by flat terrain with the land structure related to the rock type underlying it. The area is underlain by the Tertiary Benin Formation, which is loose, coarse-grained, friable, and poorly sorted with sub-angular to well-rounded sediments. It consists of over 90% sandstone with minor clay and shale intercalations (Uma, 1984). The Benin Formation extends across the whole of the study area with a variable thickness generally exceeding 1800m (Offodile, 2002).

### **2.6.3 Characteristics of the Aquifers:**

The vast majority of boreholes in the northern parts of the coastal belts tap are unconfined aquifers. In most of these boreholes, the geological sequence consists of continuous sandy formations from top to bottom of the boreholes. However, some aquifers occurred under confined conditions and gave artesian flows (Adelana *et al.*, 2008). The marked distinctions in the groundwater deposition in this area are discussed below.

### **2.6.3.1 Unconfined Groundwater Occurrence:**

#### **(a) Deltaic Formation:**

The water table in the Niger Delta areas is very close to the ground surface, ranging from 0-9 m below ground level. The aquifers found in this area are being recharged directly from steady precipitation. The shallowness of the water table introduces the problem of saline contamination from the sea, and pollution from chemical, petroleum and sewage effluent discharges (Adelana *et al.*, 2008).

Rainfall in the Delta is heavy, varying from an average of 2400 mm a year inland to 4800 mm on the coast. Hazell *et al.*, (1992) estimated the average precipitation in the area at about  $31.4 \times 10^{12}$  litres, based on an average rainfall of 2400 mm per annum. Runoff and evapotranspiration lose some proportion of the rainfall (Hazell *et al.*, 1992). NEDECO 1961 recorded 720 to 960 mm per annum evapotranspiration along the coast, which is mainly thick mangrove swamps, to 1200 mm in the northern parts of the delta which are less thickly vegetated (NEDECO, 1961).

Due to the high amount of precipitation recorded all the year round in these areas, minimal water table fluctuation is recorded. Many studies to determine the storage coefficients of the aquifers in the Niger Delta area were not successful. Pump tests carried out in the areas, at the time of this study only gave results from which specific capacities were obtained (Offodile, 1971).

#### **(b) Benin Formation:**

The sediments of the Benin Formation, as already pointed out, are more permeable than those of the Deltaic Formation areas. However, due to lack of extensive surface drainage network and the presence of reasonably thick vegetation,

runoff is negligible. The depth to water table ranges between 3m to 15m below ground level. However, the Benin Formation, due to the more arenaceous character of their aquifers, is expected to discharge more copiously than the Deltaic sediments. Therefore, with little run-off and minimal losses due to other factors, much of the water will go into storage. The average specific capacity of the area is 10,500 lit/hr/m. The borehole in Port Harcourt is particularly high yielding, with a specific capacity of 58,500 lit/hr/m.

### **2.6.3.2 Confined Groundwater Occurrence:**

Apart from the water table or unconfined conditions described above, confined aquifers are also found to exist within the Deltaic Formation and the areas of Benin Formation. In both areas, moderately to high yielding artesian flow were obtained:

#### **(a) Deltaic Formation (Delta Area):**

Boreholes drilled in the southern parts of the Niger Delta area, especially along the coastline gave pressure water, in the boreholes at Opobo, Bonny and Brass; the aquifers are confined to by a shale or clay bed (Offodile, 2002). The thickening of the shale bed from Opobo in the east to Brass in the South-west, as shown below:

**Table 2.2 :** Some Selected Boreholes in Rivers State (Offodile, 2014)

<b>Location</b>	<b>Depth Range</b>	<b>Thickness(m) Aquiclude</b>
Opobo	113.4 - 131.4 m	19.8 m
Bonny	108 – 135 m	27 m
Brass	114 - 150 m	36 m

The depth at which the confining layer is met in the boreholes is approximately the same, as shown above. This has also been confirmed by the resistivity survey

results obtained in this area by the Geological Survey of Nigeria which revealed the occurrence of a shale bed within the depth range of 114 - 150 m (Offodile, 2014). The total depth of the aquifers below the shale bed has not been determined in any of the boreholes above; hence, it will require deeper test holes. However, at Brass 105m of the aquifer has been proved (Offodile, 2014). There is also the possibility of encountering other confined aquifers lower down the formation since the sands are to remain un-cemented at greater depths.

The section running through Brass, Bonny Opobo, Bodo, Okrika and Port Harcourt shows that the aquifers cannot be said to be entirely confined. It indicates a definite hydrologic connection between the confined aquifers along the coastline and unconfined aquifers along the Benin Formation to the north inland. The aquifers increase in thickness towards the mainland, while the confining clays thin out, exposing the water charged medium to direct recharge, through rainfall in the hinterland (Adelana *et al.*, 2008). It could, therefore, be assumed that closer to the coastline; the confined aquifers are recharged by the groundwater of the Benin Formation and parts of the Deltaic Formation and farther inland of littoral area of the Niger Delta, in its continuous seaward movement. This is confirmed by the reported occurrence of submarine freshwater springs near the coast. As a result, the water from the confined aquifers is free of saline contamination (Adelana *et al.*, 2008).

The lowest specific capacity of 3750 and 4500 lit/hr/m of drawdown was recorded in Bonny and Brass respectively, as against 6480, 13500 and 12,000 lit/hr/m of draw-down recorded in Opobo, Bodo and Okrika respectively, which are shallower in depth (Offodile, 2014). From the evidence, so far available, it would not be prudent to draw any far-reaching conclusions since there is no regular basis for comparison. However, it would appear that the aquifers are either less transmissible with an

increase in depth of the confined aquifer due to its fine texture, denser and less porosity, or that there is not enough water in storage which should be the subject of a more detailed investigation. Hence, the amount of recharge from the hinterland cannot determined the direction of movement assumed to be regionally towards the sea, to the south (Offodile, 1971).

**(b) Benin Formation: (Inland Area)**

In the area underlain by Benin Formation, the confined aquifers occur in the south-eastern parts. Pressure water was proved at Utapate, Etinan, Oron and Calabar. The aquifers were confined by several shale and clay beds, which mainly consist of very coarse to medium-grained sands. The aquifers tapped by these boreholes are mostly unconfined like in the Deltaic Formation. The confined aquifers in this part of the coast are recharged from the immediate inland vicinity. Boreholes in the Benin Formation reported having given rise to free-flowing wells of fairly good yields (Adelana *et al.*, 2008). The sandstone aquifers of the Agbada Formation are too deep, and uneconomical, as a source of groundwater supply in the Niger Delta. Instead, they are more critical as potential hydrocarbon reservoirs (Adelana *et al.*, 2008). Similarly, the underlying Akata Formation, essentially an aquitard, is also much deeper to be of interest.

**Bullet-1**

The geology and hydrogeology of the Niger Delta have extensively been studied. However, no studies characterised the hydrostratigraphy of the Niger Delta shallow coastal aquifers, which is an essential tool for better understanding of the hydraulic characteristics and hydrogeological conceptual model development of the area's groundwater resources.

# CHAPTER 3

## LITERATURE REVIEW

### 3.1 Introduction

This chapter presents the general literature relevant to the research aim and the research gap relating to each chapter is demonstrated. The theoretical background relating to climate change impact on water resources on a global scale as well as in the context of the Niger Delta. The chapter includes the summary of RCM/GCM, RCP scenarios, the introduction of hydrological model SWAT and MODFLOW for surface and groundwater flow modelling, respectively. Climate change impacts on water resources resilience using SWAT and MODFLOW models are also described based on literature review.

### 3.2 Climate Change

Climate change is defined as a change in climate that is attributed directly or indirectly to an anthropogenic activity that alters the composition of the global atmosphere (IPCC, 1996), and that is in addition to natural climate variability over comparable periods (IPCC, 2011). It is also referred to as any change in climate over a period, whether naturally or as a result of human activity happening for thousands of years, and it will continue (IPCC, 2013b).

Multiple climate system indicators such as changes in precipitation pattern, the temperature of oceans, snow cover, sea-level rise, atmosphere and surface, and water

vapour from atmosphere to the oceans show that the entire globe has been experiencing surface warming due to climate change (Hartmann *et al.*, 2013). Climate change constitutes two leading causes, which are the Natural and Anthropogenic causes. The natural causes consist of changes in solar output, volcanic eruption, drifting of the continent, etc., which is a prolonged process. The second cause of climate change due to anthropogenic activities are the emission of greenhouse gases and deforestation, which recently tends to accelerate the depletion of the ozone layer and is of great concern to scientists. IPCC, 1997 reported that increase in the concentration of greenhouse gases resulting from the burning of fossil fuel and deforestation are the main reason for rapid climate change in the 20th century which has very adverse effects, especially on the hydrological process (IPCC, 2007b).

Increase in concentration of greenhouse gases such as CO<sub>2</sub> and other anthropogenic activities are perturbing the global energy balance, heating the atmosphere, and causing global warming (Xu, 1999b). The fourth assessment report of the IPCC reported that the global mean surface temperature has increased by 0.78 °C during the periods (1906–2005), with an increasing rate of about 0.13°C to the 1st decade of 20th century (IPCC, 2007b) (Figure 3.1). This report also predicted a global change in precipitation over the land areas, particularly Northern Hemisphere, after 1951 (Hartmann *et al.*, 2013) (Figure 3.2). As a result of these changes, glaciers have continued to shrink globally, and arctic sea ice and spring snow cover have decreased remarkably in Northern Hemisphere (IPCC, 2013b). Most of the regions in the world have experienced decreased snowfall events where winter temperatures have increased (IPCC, 2007a; Hartmann *et al.*, 2013).



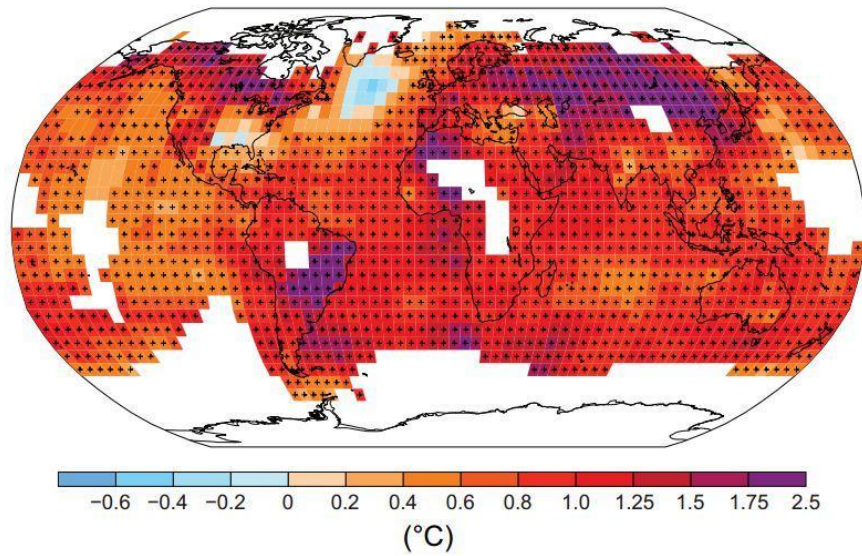


**Figure 3.1** Map of observed surface temperature change from 1901 to 2012 (IPCC, 2013b).

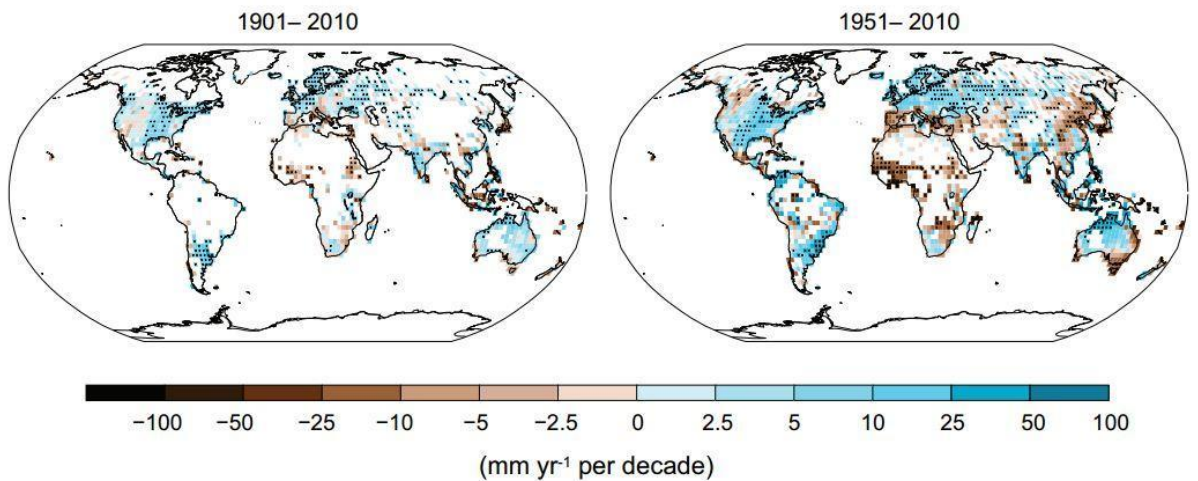


**Figure 3.2** Maps of observed precipitation change from 1901 to 2010 and from 1951 to 2010 (IPCC, 2013b).

### 3.3 Climate Change in Nigeria

Nigeria experiences two seasons, namely; rainy and dry seasons. The recent increases in temperature, rainfall, sea-level rise, flooding, drought, desertification, land degradation and frequent extreme weather events affecting freshwater resources

and loss of biodiversity in Nigeria's is evidence of changing climate (Elisha, and Lawrence, 2017; Haider, 2019). Rainfall intensities and durations have increased, resulting in flooding and large runoffs across the country (Enete, 2014). A rise in sea levels is currently being experienced around the coastal areas in the southern parts of the country exacerbating floods and submersion of coastal lands which is projected to continue with an increase in precipitation (Ebele and Emodi, 2016; Akande *et al.*, 2017). Droughts have also become a recurring incident in the Northern part of Nigeria which is also expected to continue due to the increase in temperature and decrease in precipitation (Oladipo, 2010; Amanchukwu *et al.*, 2015). Studies on climate change projections reveal a significant increase in temperature over all the ecological zones in the coming decades (IPCC, 2007b; Akande *et al.*, 2017).

### **3.3.1 Precipitation Change in Nigeria**

The climate condition in Nigeria mainly comprises of rainy and the dry seasons. In the southern part of the country, the rainy season starts from April to October occurring at over 2000 mm/yr. While in the northernmost parts, the rainy season occurs between June and September, which falls below 500 mm/yr (Shiru *et al.*, 2019). The annual distribution of rainfall between the north and the south of Nigeria is given in Fig. 3.3.

Studies show that rainfall variability is expected to increase by approximately 5-20 %, with an increase in precipitation and subsequent flooding, in some humid areas of the forest regions and savanna areas in southern Nigeria (Oladipo, 2010). Droughts have also been constant phenomena in the Sahelian region around the northern part of Nigerian which recorded about 25% decrease in precipitation on average in the last 30 years often attributable to the effects of climate change (Oladipo, 2010; Amanchukwu

*et al.*, 2015). Climate studies predicted changes in precipitation to vary across the country. Results predicted wetter climate in the south and a drier climate in the northeast. During the 2046-2065 period, reports show an increase of 0.4 mm per day (15 cm annually), in the south, and a decrease of 0.2 mm per day (7.5 cm annually) in the north (Ike and Emaziye, 2012; Haider, 2019; Matemilola *et al.*, 2019). Studies also predicted a rise of 0.1 m and 0.2 m in mean sea levels by 2020 and 2050, respectively, due to climate change (Akande *et al.*, 2017).

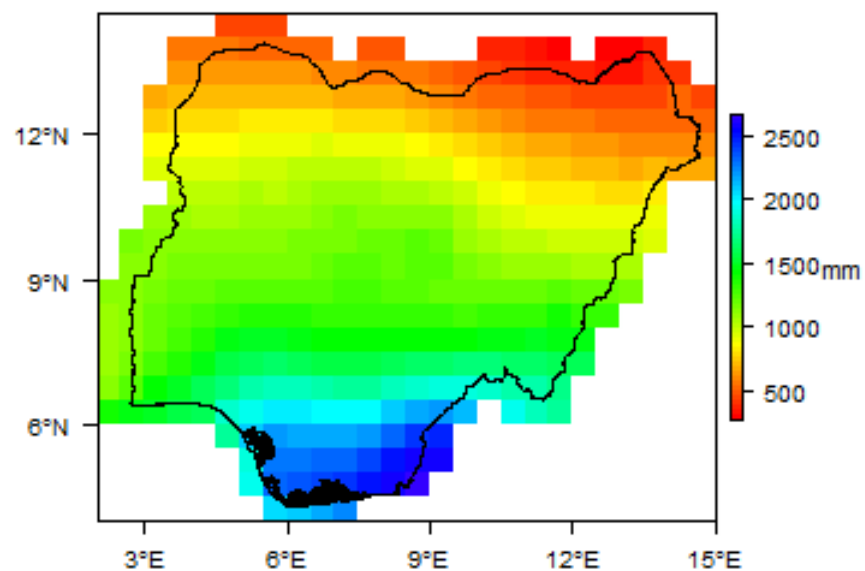


**Figure 3.3** Average Annual Precipitation (BGS, 2019)

### 3.3.2 Temperature Change in Nigeria

Temperatures in the southern parts of Nigeria ranges from 30° to 37 °C, during the dry season while the northern part gets to as high as 45 °C. The lowest temperatures in the country are recorded between December to February during the Harmattan season in all parts of the country. Temperatures during this period are between 17° and 24 °C in the south and reaching 12 °C in the north. Similarly, Climate projections for the coming decades show a significant increase in temperature over all the ecological

zones in the country (Akande *et al.*, 2017). Temperature is projected to increase between 0.4 to 1 °C, over the period 2020-2050 due to climate change, up to 3.2°C by 2050 under a high climate change scenario (Oladipo, 2010; Haider, 2019).

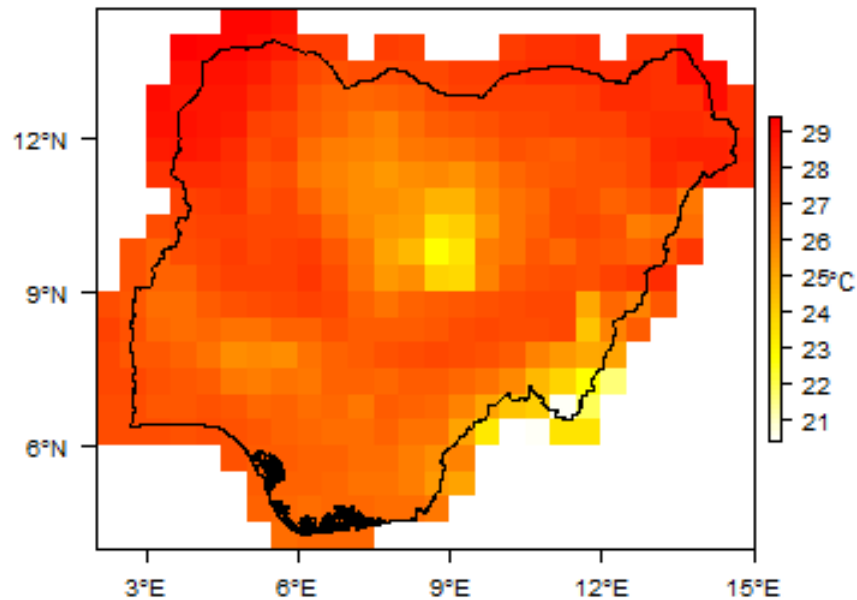


**Figure 3.4** Average Temperature (BGS, 2019)

The Southern part of Nigeria have high vulnerability to climate change stemming from sea level rise, increased precipitation, and intensive industrial activities from oil exploration as compared to other parts of the country, with the South-south (Niger Delta region) as the most vulnerable in the south (Federal Ministry of Environment, 2013; Matemilola *et al.*, 2019). The area belongs to the coastal region, which is densely populated with increasingly urbanised southern coast that is less than twenty feet above sea level (Sayne, 2011). The Niger Delta region is characterised by low topography with an easily flooded network of estuaries, rivers, creeks, and streams, (Sayne, 2011).

Many studies reported an increase in precipitation and rising sea levels, attributable to climate change, are expected to be higher in those areas (IPCC, 2007a;

Ike and Emaziye, 2012; Todd, 2015; Musa *et al.*, 2016; Obroma Agumagu, 2018; Matemilola *et al.*, 2019). This will increase the frequency and intensity of flooding which will, in turn, lead to widespread erosion and disarticulation of coastal wetlands (Federal Ministry of Environment, 2013; Todd, 2015; Obroma Agumagu, 2018). Previous hydrologic modelling studies of the Niger Delta also reported that more than 11,000 square miles of the coastal lands in the area would submerge a 1.5-foot sea level rise (Sayne, 2011; Musa *et al.*, 2016; Matemilola *et al.*, 2019). The summary of climate studies in Nigeria is shown in Table 3.2.

#### **Bullet-2**

The Niger Delta is the most vulnerable region in Nigeria due to the impacts of climate change. Available literature reported an increase in rainfall with devastating floods in cities located along the River Niger and its tributaries, which often inundate the area and pollute the surface and groundwater resources of the shallow coastal aquifer, which is the primary source of freshwater in the basin.

### **3.4 Hydro-Meteorological Data**

The accuracy and reliability of hydroclimatic datasets are crucial for scientific research and hydrologic studies related to climate change impact assessment, and water resources management (Wei *et al.*, 2018). Scarcity of these datasets remains a challenging task especially in developing countries like Nigeria and other parts of the world where rain gauges and radar networks are either not available, sparse or due to the high cost of establishment and maintenance of the infrastructure (Derin and Yilmaz, 2014). In Nigeria, there are 32 weather stations with only two of the stations located within the study area, which poorly represent the area, as shown in Figure 3.5.

Access to climate data at an acceptable spatial resolution is challenging in developing countries, and where available, their quality is either poor or expensive and may poorly represent a study area with large hydroclimatic gradients (Fuka *et al.*, 2014; Wang, *et al.*, 2019). To overcome these challenges, researchers resort to the use of multilayer global gridded meteorological datasets to serve as inputs into climate and hydrological modelling studies (Fuka *et al.*, 2014).



**Figure 3.5** Weather stations in Nigeria

Different organizations have developed different global gridded datasets at different spatial and temporal resolutions. Examples of these are the Climatic Research Unit (CRU) (Harris *et al.*, 2014), Global Historical Climatology Network (GHCN) (Steurer *et al.*, 1992), National Oceanic and Atmospheric Administration (NOAA) (Chen *et al.*, 2002), Climate Forecast System Reanalysis (CFSR) (Saha *et al.*, 2010), Princeton University Global Meteorological Forcing dataset (PGF) (Sheffield *et al.*, 2006) and Global Precipitation Climatology Centre (GPCC) (Schneider *et al.*, 2014). The data assimilation system governs the quality of these datasets, its optimisation and

the quality of observation data used (Bai and Liu, 2018; Wei *et al.*, 2018). The reliability of the gridded datasets varies with time and regional climate (Sun *et al.*, 2018). This makes it necessary to evaluate the capability of gridded data before its application over specific locations.

Several studies (Rahman, Sengupta and Ravichandran, 2009; Derin and Yilmaz, 2014; Singh *et al.*, 2014; Vinnarasi and Dhanya, 2016; Chaudhary, Dhanya and Vinnarasi, 2017; Bai and Liu, 2018; Wei *et al.*, 2018; Ahmed, Shahid, Wang, *et al.*, 2019) compared gridded datasets with station measurements for use as a substitute to the station datasets. However, no study has been conducted in any part of Nigeria to determine the best stable gridded meteorological datasets, which match well with the observed station datasets and thus serve as a substitute to the station datasets in this highly data-scarce region.

### **Bullet-3**

There are 32 weather stations located in Nigeria (Ajetomobia *et al.*, 2011; Eludoyin *et al.*, 2014), with only 2 of the stations located within the study area, which poorly represent the area, as shown in Figure 3.5. To this extent, no study has been conducted in any part of the country to determine the best stable gridded meteorological datasets, which can serve as a substitute to the poorly distributed station datasets.

In this study, different gridded meteorological products for daily precipitation, maximum and minimum temperature available over the Niger Delta will be evaluated and compared with observed station datasets to identify their fundamental differences and identify the datasets can serve as a substitute to the station datasets in the region. The study will also assess the implications of using gridded precipitation products on water resource management. The results will aid water resource managers in selecting

the appropriate gridded precipitation and temperature dataset depending upon the scope and application. This study provides insights into the spatio-temporal behaviour of these three datasets for extreme events estimation, which in turn will benefit hydrological management over un-gauged or sparsely gauged regions.

### **3.5 General Circulation Models (GCMs)**

General Circulation Models, also referred to as Global Climate Models (GCMs), are mathematical representations of the physical processes in the atmosphere, cryosphere, ocean and land surface (IPCC, 2013a, 2013b). GCMs were developed in 1956 to simulate common, synoptic-scale, atmospheric circulation patterns for use to forecast weather conditions, understand the climate and predict future changes of climate (Lupo and Kininmonth, 2013). They are tools that are used to perform climate change experiments from which climate change scenarios can be constructed. GCMs are complex numerical climate models that can simulate the climate variables accurately. The structure and design of an individual GCM determine the climate change analysis that can be performed which are limited by our scientific understanding of the climate system and by the available computing resources (Viner, 2000).

There are two major types of GCMs, namely, atmospheric GCMs and Oceanic GCMs. The combined form of these two GCMs is referred to as atmosphere-ocean coupled general circulation model (AOGCM) developed by the Geophysical Fluid Dynamics Laboratory of NOAA in the 1960s (NOAA, 2015). The GCMs divide the globe into a three-dimensional grid of cells to depict the climate, with a horizontal resolution between 250 to 600 km, with 30 layers in the oceans and up to 10 to 20 vertical layers in the atmosphere (IPCC-TGICA, 2007). GCM outputs are used to simulate a time series of climate variables on a global scale. Accounting for the effects



of physical parameters like GHGs, aerosol concentration, land-use change, technology, population growth and solar constants etc.; they simulate the change in climatic variables like temperatures, precipitation, humidity, wind speed etc. (IPCC, 1990b; Murphy, 1999).

### 3.6 Regional Climate Model

Regional Climate Models (RCMs) are similar to GCMs but with higher resolution. RCMs focus in a small, limited area of interest and mostly cover an area of up to the size of typically 5000 km x 5000 km (Giorgi *et al.*, 2001). RCMs can provide information related to weather and climate at a higher resolution of up to 50 or 25km horizontal and 100 m to 1000 m vertical, as shown in Figure 3.6. The computational time for RCM may vary from weeks to a month, depending on the speed of the computer. The full GCM determines the extensive scale effects of changing greenhouse gas concentrations, volcanic eruptions etc., on a global scale while the 14 climate variables calculated by the GCMs are used as input for the RCMs (Giorgi *et al.*, 2001; Schmidli *et al.*, 2007; Bhuvandas *et al.*, 2014). Various examples of RCM are HadRM3M, Precis RCM, Regional Climatic Model (RegCM), Canadian Regional Climate Model (CRCM) etc. (Murphy, 1999).

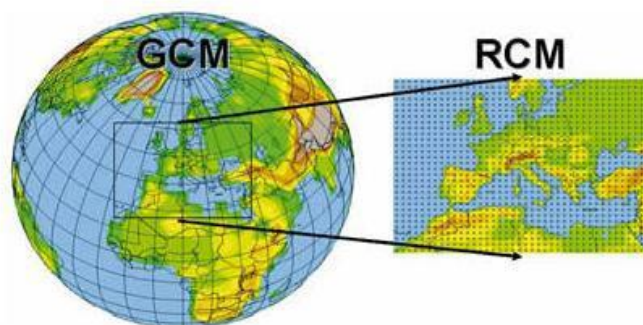


**Figure 3.6** Regional Climate Model nesting approach (IPCC, 2013b).

### 3.7 Global Climate Change Scenarios

The projected impacts of future climate change scenarios are analysed to understand the behaviour or sensitivity of greenhouse gases and other pollutants in the atmosphere to changing climate. The concentration of these gases and other pollutants depends on their emission from either natural or anthropogenic sources. Over time, different scenarios have been developed and used in climate research ranging from SA92 used in IPCC's first assessment report to Special Report on Emissions and Scenarios (SRES) used in the third and fourth assessment report (IPCC, 1990a). Intergovernmental Panel provides four storylines called SRES on Climate Change which provide other predictions to which the world might change in future (Nebojs̃a *et al.*, 2000). These scenarios are based on the assumption of how the population and economic growth, technological development and other factors take place in the future. The emission scenarios describe the future releases of GHGs, aerosols, LULC and other pollutant changes (Nebojs̃a *et al.*, 2000). The climate change scenarios are designed to help policymakers and experts decide for long term consequences of climate change; such scenarios are helpful for planning, mitigation approaches and sustainability of project and cost and benefit analysis of climate policy (IPCC, 2012).

Recently, the IPCC in 2007 developed a set of new emission scenarios used for preparing the fifth assessment report known as the Representative Concentration Pathway (RCP). The RCPs were developed by combined efforts of the researchers from four modeling team working on integrated assessment modeling and analysis of impacts to initiate the climate models for future climate change research (IPCC, 2007c; Meinshausen *et al.*, 2011; van Vuuren *et al.*, 2011). The four RCP pathways, namely RCP 2.6, RCP 4.5, RCP 6.0 and RCP 8.5 were developed based on the radiative

forcing target levels (2.6, 4.5, 6.0 and 8.5 W/m<sup>2</sup>), by the end of the 21st century (Meinshausen *et al.*, 2011; van Vuuren *et al.*, 2011).

RCPs scenarios are based on the pathway of radiative forcing. They rely on the changes in the balance between incoming and outgoing radiation to the atmosphere, which is caused by changes in atmospheric composition (WMO, 2013). The pathway of any single radiative forcing will be based on socioeconomic and technological development in the future. RCP scenarios of climate change have been used as a decision-making and planning tool to analyse the situations which have become an essential element as they allow researchers to understand the long-term consequences (Moss *et al.*, 2010; van Vuuren, Edmonds, *et al.*, 2011). All the four pathways were considered to be the representative of all the literature pertinent to change in climate (Moss *et al.*, 2010; Meinshausen *et al.*, 2011; van Vuuren *et al.*, 2011).

### **3.7.1 Representative Concentration Pathway 2.6**

The RCP 2.6 is a representation of the mitigation scenarios, which aim to limit the increase of global mean temperature to 2°C. This scenario was developed by the IMAGE modeling team of the PBL Netherlands Environmental Assessment Agency (van Vuuren *et al.*, 2011; Graham Wayne, 2013). This pathway indicates that radiative forcing will reach around 3 W/m<sup>2</sup> in the mid-century and decline afterwards to 2.6 W/m<sup>2</sup> by the end of 21<sup>st</sup> century (van Vuuren *et al.*, 2011). In order to achieve this, CO<sub>2</sub> emission would need to be significantly reduced by more than 100 % by 2100 which can only be achieved by replacing the use of fossil fuel with renewable energy, nuclear power, bioenergy and use of carbon capture and storage (CCS). The critical assumption in this scenario is that new energy-efficient technologies can rapidly be

transferred to all over the world for immediate implementation (van Vuuren *et al.*, 2011).

### **3.7.2 Representative Concentration Pathway 4.5**

The RCP 4.5 is a representation of the stabilisation scenario (Graham Wayne, 2013) developed by the Global Change Assessment Model (GCAM) modeling group at the Pacific Northwest National Laboratory's Joint Global Change Research Institute (JGCRI) in the United States (van Vuuren *et al.*, 2011). In RCP 4.5, the radiative forcing stabilises at 4.5 W/m<sup>2</sup> (approximately 650 ppm CO<sub>2</sub>-equivalent) at the end of the year 2100 without ever exceeding that value (Thomson *et al.*, 2011). The stabilisation occurs due to the employment of various technologies and strategies to reduce the GHGs and other pollutant emissions. The major assumptions of this scenario are: 1) that the global population reaches a maximum of more than 9 billion by the year 2065 and then declines to 8.7 billion in the year 2100. 2) That the global GDP grows by orders of magnitude, declines in energy consumption, 3) increase in fossil fuel consumption. 4) a substantial increase in renewable energy and nuclear energy use and 5) a significant increase in forest area as a mitigation strategy (Thomson *et al.*, 2011).

### **3.7.3 Representative Concentration Pathway 6.0**

The RCP 6.0 is a representation of the climate policy intervention scenario developed by the Japan Agency for Marine-Earth Science and Technology (JAMST) and National Institute for Environmental Studies (NIES) in Japan by using Asia-Pacific Integrated Model (AIM). In RCP 6.0, all climate policies are assumed to be implemented to restrain radiative forcing not to exceed 6.0 W/m<sup>2</sup>. The GHG emissions

were also assumed to be the highest in 2060 and then declined after that (Masui *et al.*, 2011; van Vuuren *et al.*, 2011). It is also a stabilisation scenario like RCP 4.5, but here radiative forcing stabilises at 6.0 W/m<sup>2</sup> with 850 ppm concentration of CO<sub>2</sub> by the year 2100 without exceeding that value in prior years (Masui *et al.*, 2011). The primary assumptions of this RCP are: 1) that the increase in energy demand, shift from coal-based to gas-based production technologies. 2) Increase in the use of non-fossil fuel energy type. 3) Increase in the use of carbon capture and storage (CCS) technology. 4) Increase in population and economic growth in the urban area. 5) expansion of cropland and forest area and 6) decrease in grassland (Masui *et al.*, 2011).

#### **3.7.4 Representative Concentration Pathway 8.5**

RCP 8.5 is a representation of high emission scenarios in the literature characterised by the highest increase in GHG emission over time (Riahi *et al.*, 2011). The pathway was developed based on IPCC A2 SRES scenario which was used in IPCC 4th assessment report by the International Institute for Applied System Analysis (IIASA) (van Vuuren *et al.*, 2011; Graham Wayne, 2013). This pathway is also called a baseline scenario consistent with a future that has no change in climate policy to reduce emissions, and without including any mitigation target or without explicit climate policy. In this pathway, the GHG emissions increase significantly over time leading to 8.5 W/m<sup>2</sup> of radiative forcing with CO<sub>2</sub> concentration reaching 1370 ppm by the end of the century (Riahi *et al.*, 2011). The significant assumptions made are: 1) the continuous increase in the global population reaching 12 billion by 2100. 2) Long-term high-energy demand, moving towards coal intensive technologies. 3) slow income growth with modest rates of technological progress, and 4) high emission in the absence of climate change policies (Riahi *et al.*, 2011; van Vuuren *et al.*, 2011).

**Table 3.1** : Overview of RCP Scenarios

RCP	Description	Temp Anomaly	Concentration (ppm)	Pathway
RCP2.6	A peak in radiative forcing at 3 W/m <sup>2</sup> before 2100 and reaches 2.6 W/m <sup>2</sup> by 2100.	1.50°C	490	Peak and decline
RCP4.5	Stabilisation without overshoot pathway to 4.5 W/m <sup>2</sup> at stabilisation before 2100	2.40°C	650	Stabilisation without overshoot
RCP6.0	Stabilising without overshoot pathway to 6.0 W/m <sup>2</sup> at stabilising after 2100	3.00°C	850	Stabilisation without overshoot
RCP8.5	Rising radiative forcing pathway leading to 8.5 W/m <sup>2</sup> in 2100	4.90°C	1370	Rising

The RCP4.5 and RCP8.5 emission scenarios were selected for this study, as these two scenarios are assumed to provide a possible complete range of impact. The RCP4.5 denotes the common pathway scenario depicting a better agreement with the latest lower greenhouse gas emissions policy by the global community. In contrast, RCP8.5 denotes the business-as-usual scenario, consistent with a future with no change in climate policy to reduce emissions (Wang *et al.*, 2016).

### 3.8 Downscaling

Global Circulation Models simulate weather in different layers of the atmosphere, and the resulting output is typically coarse, in the order of 2 to 3 degree. Due to this coarse resolution, it is, therefore, necessary to convert the GCM output at least at the scale of region or watershed before using for impacts studies (Mearns *et al.*, 2009). This process of converting large scale GCM output into a small scale that can be used to study impacts at a local scale is known as downscaling (Chen *et al.*,

2011). It is the process of using information known at larger scales to make predictions at regional or local scales to bridge the spatial scale disparity between the GCMs and the scale required for impacts studies (Mearns *et al.*, 2009). There are two main types of downscaling, namely, dynamical and statistical downscaling.

### **3.8.1 Dynamical downscaling**

Dynamical downscaling is the process of nesting a high-resolution regional climate model (RCM) driven by boundary conditions from a GCM to derive finer-spatial scale information (Schmidli *et al.*, 2007). It uses numerical meteorological modeling to bring global-scale projection down to the regional scale. The disadvantage of using RCM is that they demand more computing resources which are expensive than GCMs whereas the advantage is that they can resolve smaller-scale atmospheric features better than the host GCM (Wilby and Dawson, 2007; Bhuvandas *et al.*, 2014).

### **3.8.2 Statistical downscaling**

Statistical downscaling assumes that the regional or local climate can be determined by two factors which are the large-scale climatic state and regional/local physiographic features (Giorgi *et al.*, 2001). This process is achieved in two stages. The first stage involves developing a statistical relationship between the predictand (local climate variables) and the predictors (large-scale atmospheric variables). In the second stage, the established relationship to the GCM output is then applied to simulate the future climatic data (Murphy, 1999; Gagnon *et al.*, 2005; Shiru *et al.*, 2019). It can, therefore, be said that this technique is highly dependent on the outputs of GCMs, which are used as input data to the downscaling model (Sachindra *et al.*, 2014). The main advantage of this technique is that it is computationally cheaper and can be

applied to provide site-specific information. While the main disadvantage is that it assumes that the statistical relationships derived for the present day are equally valid for the future climate as well, though under changing climatic condition (Giorgi *et al.*, 2001; Wilby *et al.*, 2004).

Statistical downscaling is classified into three broad categories viz; Weather generators, Transfer functions and Weather typing schemes (Giorgi *et al.*, 2001).

### **3.8.3 Weather generators**

Weather generators are statistical models that generate a random number which resembles daily weather data at a particular station to augment the existing climate record where measured data are not available by replicating the statistical attributes of a local climate variable (Dibike and Coulibaly, 2005; Schoof *et al.*, 2005). Two main types of weather generators can be identified for daily precipitation based on the modeling approach, viz; the spell length approach and Markov chain approach (Giorgi *et al.*, 2001; Wilby *et al.*, 2004). Weather generator parameters can be conditioned on large-scale atmospheric predictors, weather states or rainfall properties (Wilby *et al.*, 2004). The efficiency and suitability of the models, however, depend on the characteristics of the study area's climate (Giorgi *et al.*, 2001).

### **3.8.4 Transfer functions**

The transfer function downscaling methods depend on the empirical relationships between the large-scale predictors and the local scale predictand (Wilby and Dawson, 2007). The transfer functions can be derived from multiple regression, linear and non-linear regression, artificial neural network, principal component analysis, redundancy analysis and canonical correlation analysis (Giorgi *et al.*, 2001; Wilby and Dawson, 2007). The main advantage of this approach is that it is easy to



apply, while the main disadvantage is that the downscaling is dependent on the choice of the predictor variables and also the models mostly explain only a fraction of observed climate variability especially for precipitation (Wilby and Dawson, 2007).

### **3.8.5 Weather typing schemes**

This method categorises local meteorological data from a given period into certain weather types or states concerning prevailing patterns of atmospheric circulation and according to their synoptic similarity (Wilby *et al.*, 2004; Wilby and Dawson, 2007). The weather typing schemes method assumes that the weather of a certain period assigned to a particular type is more or less homogenous, and the differences among the types are visible. Climate change scenarios are created by either re-sampling from observed data or creating synthetic sequences of weather patterns and then re-sampling from observed data. The downscaling is then conducted by linking weather at a local scale with the climate on a large scale (Wilby and Dawson, 2007).

### **3.9 Bias Correction**

GCMs and RCMs are very reliable tools used in future climatic variables projections. Their reliability is the only constraint to their use on a larger scale as they might have biases. These biases or errors become less active while performing climate change impact studies which might have a severe impact to the result in a hydrological model (Schmidli *et al.*, 2007; Dosio and Paruolo, 2011; Hempel *et al.*, 2013; Mehrotra and Sharma, 2015). There are various methods of bias correction used in refining the data to make it suitable for basin level analysis viz;

- a) Delta change approach
- b) Linear Scaling method

- c) Multiple linear regression
- d) Analogue method
- e) Local intensity scaling
- f) Quantile mapping.

### **3.10 GCM Selection**

GCMs simulations are essential tools for assessing the impact of climate change for a range of human and natural systems (IPCC, 2007a). The simulated GCMs are associated with different uncertainties due to model assumption, resolution, or calibration processes e.t.c (IPCC, 1990b; Hijmans *et al.*, 2005; Foley, 2010; *et al.*, 2011; Northrop, 2013; Khan *et al.*, 2018; Salman *et al.*, 2018; Sun *et al.*, 2018; Ahmed, *et al.*, 2019). This hinders the GCM outputs from accurately predicting the future climate at a regional or local level. To reduce these uncertainties, a subset of suitable GCMs may be selected for a given study area by eliminating those with limited similarity to the observed climate (Lutz *et al.*, 2016; Lin and Tung, 2017; Khan *et al.*, 2018; Salman *et al.*, 2018; Ahmed *et al.*, 2019). These uncertainties can be minimised by a careful selection of an ensemble model for climate projection (Knutti *et al.*, 2013). It is also not practically feasible to use all the Coupled Model Inter-comparison Project Phase 5 (CMIP5) GCMs for spatio-temporal climate change prediction, and impact assessment studies due to computational and human resources constraint (McSweeney *et al.*, 2015). A small ensemble mean of more appropriate GCMs is selected for any region of interest by excluding those considered unrealistic and in order to reduce the spread of uncertainties associated with GCM (Lutz *et al.*, 2016).

#### **Bullet-4**

Studies reported that GCMs are associated with different uncertainties due to model assumption, resolution, or calibration processes which hinders the GCM outputs from accurately predicting the future climate at a regional or local level.

Several studies have selected a subset of suitable GCMs outputs ensemble by employing various wrappers and filters. This include; clustering hierarchy (Knutti *et al.*, 2013), weighted skill score (Perkins *et al.*, 2007), spectral analysis (Jiang *et al.*, 2015), Bayesian weighting (Min and Hense, 2007), and information entropy (Shukla *et al.*, 2006). Various statistical indicators, such as correlation coefficients (Barfus and Bernhofer, 2015) have also been used for ranking, evaluation, and selection of GCMs. The demerits of using statistical indicators such as correlation coefficients are that their performance matrices are also mostly evaluated based on the mean climatic condition where temporal variability of the climate is not given full attention (Reichler and Kim, 2008).

Several studies have recently used the feature selection methods in selecting the most suitable GCM ensemble subset for climate studies and projection in different study areas. Symmetrical uncertainty (SU) is a feature selection method developed based on the concept of information entropy for similarity or mutual information assessment between GCM outputs and observed datasets to measure the changes in entropy (Shannon, 2001; Singh *et al.*, 2014; Ma and Ma, 2018). Salman *et al.*, (2018) used SU in GCMs selection for the spatiotemporal forecast of changes in temperature of Iraq. Khan *et al.*, (2018); Ahmed *et al.*, (2019) recently used SU in the ranking, selecting and assessing the performance of several GCMs in Pakistan. Shiru *et al.*, (2019) applied a combination of Entropy Gain (EG), Gain Ratio (GR), and

Symmetrical Uncertainty (SU) approach in screening and selection of rainfall GCMs in Nigeria.

**Bullet-5**

To this extent, no study has been conducted in Nigeria to select an ensemble of best-performing CMIP5 GCM outputs for both precipitations, maximum and minimum temperature.

As summarised in table 3.2, several climate studies have been conducted in Nigeria. The table shows that climate studies in Nigeria are still at infancy. Shiru *et al.*, (2019) is the only study that select an ensemble of rainfall GCMs for the projection of spatio-temporal changes in Nigeria using Coupled Model Intercomparison Project Phase 5 (CMIP5) GCMs. However, no study was conducted to select an ensemble of best-performing GCM outputs of both precipitations, maximum and minimum temperature for the prediction of spatio-temporal changes using CMIP5 GCM outputs. This study explores the use of Symmetrical Uncertainty feature in selecting and ranking the most suitable GCMs to form an ensemble GCM for rainfall, the maximum and minimum temperature in the Niger Delta part of Nigeria. The biases in the GCM output will be corrected using the Delta change approach. The Delta change method constitutes the easiest and yet the most common bias correction methods which are the multiplicative method for precipitation and additive method for temperature (Ashraf Vaghefi *et al.*, 2017; Xu, 2018; Beyer *et al.*, 2019).

**Table 3.2 : Summary of climate change studies in Nigeria**

<b>S/N</b>	<b>Author</b>	<b>Research Title</b>	<b>Study Area</b>	<b>Conclusion</b>
1	Akpodiogaga-a and Odjugo, (2010)	General overview of climate change impacts in Nigeria	Nigeria	Results show that temperature increased by 1.1°C, and rainfall decreased by 81 mm over the 105 historical years.
2	Olofintoye and Sule, (2010)	Impact of global warming on the rainfall and temperature in the Niger Delta of Nigeria	Niger Delta Nigeria	Results show that rainfall has significantly increased in the area over the years and that water supply is sustainable under the current climate condition.
3	Ike and Emaziye, (2012)	An assessment of the trend and projected future values of climatic variables in Niger Delta Region, Nigeria	Niger Delta Nigeria	Results show that in the year 2050, the area will witness an increase of about 223.81 to 248.78 mm of rainfall and 31.71 to 32.46°C of temperature, respectively
4	Ebele and Emodi, (2016)	Climate change and its impact in the Nigerian economy	Nigeria	Study shows that many sectors of the Nigerian economy such as the agricultural, health, energy, and water sector appears to be directly vulnerable to the impacts of climate change which will generally affect the growth of the economy
5	Ogbo <i>et al.</i> , (2013)	Risk management and challenges of climate change in Nigeria	Nigeria	Study shows that industrial releases, improper sewage disposals, deforestation are anthropogenic activities responsible for climate change. Secondly, drought, flooding, erosion, are the challenges resulting from climate change, and finally, that government policies do not help to reduce the risk associated with climate change in Nigeria.

<b>S/N</b>	<b>Author</b>	<b>Research Title</b>	<b>Study Area</b>	<b>Conclusion</b>
6	Adeyeri <i>et al.</i> , (2017)	Climate change and coastal floods: The susceptibility of coastal areas of Nigeria	Coastal areas of Nigeria	Results show that areas lying along the coast are highly susceptible to flood hazards with the degree of susceptibility decreasing towards the North and eastern part of the area
7	Odafivwotu Ohwo, (2018)	Climate change impacts, adaptation and vulnerability in the Niger Delta region of Nigeria	Niger Delta Nigeria	Current adaptation strategies are poorly designed and be inadequate in dealing with the current situation because of the reported inadequate adaptive capacity of both ecological and human systems.
8	Matemilola <i>et al.</i> , (2019)	Mainstreaming climate change into the EIA process in Nigeria: Perspectives from projects in the Niger Delta region	Niger Delta Nigeria	Result of this quantitative study shows that there is a weak political will to address climate change issues, as reflected in the absence of climate change requirements in the EIA guidelines of Nigeria
9	Shiru <i>et al.</i> , (2019)	An MCDM-based framework for the selection of general circulation models and projection of Spatio-temporal rainfall changes: A case study of Nigeria	Nigeria	Projected rainfall shows no significant change under RCP 2.6, 4.5 and 6.5, over the century while RCP 8.5 predicted a decrease in rainfall during the last part of the century (2070–2099). The seasonal changes in precipitation showed an increase in rainfall in the range of 0–20% in most parts of the north of Nigeria

### **3.11 Impacts of Climate Change on hydrological processes**

Climate change impacts on hydrology are usually estimated by defining the changes in climate scenarios for hydrological model inputs from the general circulation models (GCMs) outputs. Different climate models have been used globally for climate impact assessment studies (Pandey and Patra, 2014). This is achieved by understanding the linkages between climate change scenarios and hydrologic systems in constructing suitable scenarios for the hydrologic impact assessments. GCMs indicate the likelihood to expect more frequent regional extremes of heavy precipitation events, heat and heatwaves (IPCC, 2007b), which would lead to potentially significant variations in local precipitation.

The problems associated with climate models in impact assessment lies in the spatial and temporal scale mismatch between the GCMs outputs and hydrological models of the catchment. Several downscaling techniques which range from simple interpolation of climate model output to the use of nested regional climate models have been developed and used in hydrological studies (Wilby and Wigley, 1997). These depend on the quality of the global driving model simulation, the relative costs and benefits of each approach. Considerable effort has been made in developing hydrological models for estimating the impacts of climate change on water quality and quantity, with a focus on realistic representation of the physical processes involved (Sun and Caldwell, 2015).

Many researchers have studied the impact of climate change on hydrology over large basins (Apurv *et al.*, 2015; Crosbie *et al.*, 2013; Ouyang *et al.*, 2015; Shen *et al.*, 2018; Z. Wang *et al.*, 2012; Zhang & Zhang, 2012). For example, Ouyang *et al.*, (2015) and Apurv *et al.*, (2015) assessed the climate change impacts on streamflow in the Huangnizhuang catchment under CMIP5 emission scenarios. Wang *et al.*, (2012)

analysed climate change impacts on streamflow of the Shiyang River basin using the output from the Providing Regional Climates for Impacts Studies (PRECIS) regional climate model with the Soil and Water Assessment Tool (SWAT).

Studies on the impacts of climate change using various downscaling techniques for climatic variables projection at a large scale in different parts of the world have recently been carried out. In these studies, predicted future climate scenarios from different global circulation models (GCMs) outputs are the primary meteorological sources for approximating the plausible future climate. These GCMs outputs are spatially too coarse to determine the environmental effects of climate change, and therefore must be transformed into smaller resolutions to be applicable in the local analysis (Wilby and Wigley, 1997; Giorgi *et al.*, 2001; Wilby, 2001; Wilby *et al.*, 2004; Teutschbein and Seibert, 2012). Downscaling approaches depict suitable methods to extract regional-scale meteorological variables from GCM outputs.

Review of different studies carried out at global and basin levels indicates that there is no clear trend on changes in hydrological processes such as stream flow, surface runoff and groundwater recharge. However, changes in the temperature and precipitation were found in comparison with the past, which has altered the stream runoff (Jiang *et al.*, 2007; Wang *et al.*, 2012, 2020; Ouyang *et al.*, 2015). The alteration varies spatially, some having higher discharge, whereas some places having low discharge.

#### **Bullet-6**

To this extent, review of different studies conducted at global and basin level indicates that there is no clear trend on changes in hydrological processes; hence, the impact of climate change should be conducted at basin level to find the change at the local level.



### 3.12 Hydrologic Modeling

Hydrologic models are developed based on mathematical equations using the hydrologic cycle components and taking into account the physical and geomorphological features of the study area (Kharchaf *et al.*, 2013). Mulvany developed the first hydrologic model in 1850, known as the Rational method after which several models have been developed and used tremendously in scientific studies as well as the assessment of climate change impacts on water resources (Xu, 1999a). Unfortunately, none of the models can be classified as the best among the numerous available models as each modeler tends to emphasise on his approaches (Todini, 2007).

Globally, many studies e.g. (Black, 1995; Black and Burns, 2002; Young *et al.*, 2018) used the UK Flood Estimation Handbook (FEH) for economic and social flood risk estimation studies, which serve as a planning tool for decision makers in those areas. Therefore, systematic studies of indices for estimating the risk associated with future extreme weather events in countries that have no such standards such as Nigeria is paramount. The standardized precipitation index (SPI) (Mckee, Doesken and Kleist, 1993, 1995), although developed for drought estimation, can be successfully applied for flood monitoring purposes (Komuscu, 1999; Hayes *et al.*, 2002; Shahid, 2008; Svoboda, Hayes and Wood, 2012).

The choice of every model depends on many factors, such as data availability and the purpose of the study (Jiang *et al.*, 2007). The main features, requirements, strengths and weaknesses of the frequently used hydrological models are summarised in Table 3.3. Here in this study, the Soil and Water Assessment Tool (SWAT) outperformed other models, hence was used for analysing the climate change impacts on hydrological regimes in the Niger Delta. The outputs of the SWAT model will be used for groundwater flow modeling as it meets all the requirements.

**Table 3.3 :** Requirements, Features, strengths and weaknesses of frequently used hydrological models (Modified after Daniel *et al.*, 2011; Devia *et al.*, 2015; Umar *et al.*, 2019)

S/No.	Hydrological models	Main features	Data requirement	Strength	Weakness
1	HEC-1/HECHMS	<ul style="list-style-type: none"> <li>• Lumped-parameter,</li> <li>• Single hydrograph</li> </ul>	<ul style="list-style-type: none"> <li>• Meteorological,</li> <li>• Topographical,</li> <li>• Soils,</li> <li>• Land use,</li> <li>• Streamflow</li> </ul>	<ul style="list-style-type: none"> <li>• It includes a groundwater component to flow,</li> <li>• Variety of hydrologic simulation choices,</li> <li>• Was explicitly developed to simulate floods,</li> <li>• Accommodate many sub-basins, streams, reservoirs, and junction elements.</li> </ul>	<ul style="list-style-type: none"> <li>• Can only model single precipitation event,</li> <li>• Cannot take care of spatial variability of the sub-basins adequately,</li> <li>• It cannot model reservoirs with controlled outflows</li> </ul>
2	PRMS/MMS	<ul style="list-style-type: none"> <li>• Lumped parameter,</li> <li>• Multiple hydrographs</li> </ul>	<ul style="list-style-type: none"> <li>• Meteorological,</li> <li>• Topographical,</li> <li>• Soils,</li> <li>• Land use,</li> <li>• Streamflow</li> </ul>	<ul style="list-style-type: none"> <li>• Continuous simulation models</li> <li>• Simulate the changes in soil moisture between precipitation events</li> <li>• Simulate the effects of climate, precipitation, and land use on watershed response</li> <li>• It has parameter optimisation and sensitivity analysis</li> </ul>	<ul style="list-style-type: none"> <li>• Limited choices in overland and streamflow routing</li> <li>• Challenging to incorporate the lag or attenuating effect due to numerous wetland depressions</li> </ul>

3	HSPF	<ul style="list-style-type: none"> <li>• Lumped parameter,</li> <li>• Multiple hydrographs</li> </ul>	<ul style="list-style-type: none"> <li>• Meteorological,</li> <li>• Topographical,</li> <li>• Soils,</li> <li>• Land use,</li> <li>• Streamflow</li> </ul>	<ul style="list-style-type: none"> <li>• Continuous simulation models</li> <li>• Simulate the changes in soil moisture between precipitation events</li> <li>• Is a general-purpose hydrologic simulation program,</li> <li>• Commonly used for modeling of nonpoint pollutants</li> </ul>	<ul style="list-style-type: none"> <li>• Offer limited choices in overland and streamflow routing</li> <li>• It is challenging to incorporate the lag or attenuating effect that may occur due to numerous wetland depressions</li> </ul>
4	AGNPS	<ul style="list-style-type: none"> <li>• Distributed type,</li> <li>• Single event simulation,</li> <li>• Single hydrographs</li> </ul>	<ul style="list-style-type: none"> <li>• Meteorological,</li> <li>• Topographical,</li> <li>• Land use,</li> <li>• Streamflow</li> </ul>	<ul style="list-style-type: none"> <li>• Captures the spatial variability of the sub-basins</li> <li>• Allows modeling of spatial variations in slope, land use, soil types, and other parameters.</li> </ul>	<ul style="list-style-type: none"> <li>• Can only model single precipitation event</li> <li>• Offers few choices for simulating hydrologic processes</li> <li>• Streamflow routing is limited to a steady-state assumption</li> <li>• Backwater or storage in the stream cannot be modeled</li> <li>• Cannot model flood flows</li> </ul>
5	SWAT	<ul style="list-style-type: none"> <li>• Distributed types,</li> <li>• Continuous simulation,</li> <li>• Multiple hydrographs</li> </ul>	<ul style="list-style-type: none"> <li>• Meteorological,</li> <li>• Topographical,</li> <li>• Soils,</li> <li>• Land use,</li> <li>• Streamflow</li> </ul>	<ul style="list-style-type: none"> <li>• Provides an ample amount of information even outside the boundary</li> <li>• Can be applied for a wide range of situations</li> <li>• Can simulate hydrologic cycle components.</li> <li>• Can be applied for continuous flow, soil erosion, nutrient and sediment transport simulations.</li> </ul>	<ul style="list-style-type: none"> <li>• Require data about the initial state of model and morphology of catchment</li> <li>• Complex model.</li> <li>• Require human expertise and computation capability</li> <li>• Suffer from scale-related problems</li> </ul>

### 3.13 Overview of Soil and Water Analysis Tool

Soil and Water Analysis Tool or SWAT developed by the United States Department of Agriculture–Agricultural Research Service (USDA-ARS) and Texas A & M AgriLife Research is a hydrological/water quality model (Shekhar and Xiong, 2012). The SWAT model is a spatially distributed, physically-based continuous-time model designed to simulate impacts of water, sediment, pesticide, and nutrient transport on a daily time step at a catchment scale (Neitsch *et al.*, 2011).

It uses hydrologic response units (HRUs) which consist of soil type, land use and slope. The HRUs are used to outline the spatial heterogeneity in terms of soil type, land cover, and slope class within a watershed. The SWAT model estimates relevant hydrological components such as surface runoff, evapotranspiration, peak rate of runoff, groundwater recharge, percolation and sediment yield for each HRU (Vilaysane *et al.*, 2015).

The SWAT model has a graphical user interface developed as an extension in either ArcGIS known as ArcSWAT or QGIS known as QSWAT. It can be used in large gauged and ungauged basins to predict the impact of management on water, sediment and agricultural chemical yield. It can also be used for both surface and groundwater simulation. The advantages of this model are:

- a) SWAT is a physically based model and can be used in the basin without any monitoring data (stream gauge).
- b) The SWAT model uses readily available inputs.
- c) The model is computationally efficient to operate on a large basin within a reasonable time scale.
- d) The model is capable of simulating long-term impacts.

The main components of the hydrologic processes in SWAT are precipitation, surface runoff, infiltration, evapotranspiration, groundwater flow and soil water content. The model is developed based on the water balance of a river basin. It analyses the hydrological cycle components such as the volume of water, nutrient and sediment loading to the basin and routes their movement through the channels network of the basin (Neitsch *et al.*, 2005). The water balance equation (3.1) used in the SWAT model is:

$$SW_t = SW_o + \sum_{i=1}^t (R_{day} + Q_{surf} - E_a - w_{sep} - Q_{gw}) \quad (3.1)$$

where  $SW_t$  denotes final soil water content (mm),  $SW_o$  is the initial soil water content on the day  $i$  (mm),  $R_{day}$  is the amount of precipitation on the day  $i$  (mm),  $t$  is the time (days),  $Q_{surf}$  is the quantity of surface runoff on the day  $i$  (mm),  $W_{sep}$  is the amount of water percolating into the vadose zone from the soil profile on the day  $i$  (mm),  $E_a$  is the evapotranspiration amounts on the day  $i$  (mm), and  $Q_{gw}$  is the amount of return flow on the day  $i$  (mm).

### 3.13.1 Precipitation

Precipitation is one of the significant driving components of the hydrological cycle. SWAT model requires daily, sub-daily or monthly precipitation data which might contain missing data or may not be available in some basins around the world. SWAT has an inbuilt feature that can fill these missing data by using precipitation generator (Shekhar and Xiong, 2012). The precipitation generator with skewed distribution model was developed based on equation 3.2;

$$R_{day} = \mu_{month} + 2. \sigma_{month} \left[ \left\{ \left( \frac{SND_{day}}{g_{month}} - \frac{g_{month}}{6} \right) \cdot \frac{g_{month}}{6} + 1 \right\}^3 - 1 \right] / g_{month} \quad (3.2)$$

where,  $R_{day}$  is the amount of precipitation on a given day (mm);  $\mu_{month}$  is the mean daily precipitation (mm) for the month;  $\sigma_{month}$  is the standard deviation of daily

precipitation (mm) for the month;  $SND_{day}$  is the standard normal deviate calculated for the day, and  $gmonth$  is the skew coefficient for daily precipitation in the month.

### 3.13.2 Runoff

Runoff is referred to as the water that remains and flows on the ground surface when the rate of precipitation exceeds the soil infiltration rate and other depression losses. Two methods are used to estimate runoff of a basin in SWAT which are: a) The modified SCS curve number and, b) The Green and Ampt infiltration method (Shekhar and Xiong, 2012).

The SCS curve number depends on soil type, soil cover, land use and the decreases in soil moisture as it approaches wilting point and an increasing to 100 as soil reaches the saturation point. Total runoff is calculated using equation 3.3.

$$Q_{surf} = (R_{day} - I_a)^2 / (R_{day} - I_a + S) \quad (3.3)$$

where  $Q_{surf}$  is the amount of runoff at time  $t$  (mm),  $R_{day}$  is the amount of accumulated rainfall depth at time  $t$ ,  $I_a$  is the initial losses [= 0.2  $S$ ],  $S$  is the potential maximum retention [ $S = \frac{25400 - 254CN}{CN}$ ], and  $CN$  is the Curve number.

The Green Ampt method calculates the surface runoff as infiltration losses by combining unsaturated form of Darcy law and mass conservation. The water that does not infiltrate flows as runoff and the infiltration losses are calculated using equation 3.4.

$$f = K \left[ 1 + \frac{(\Phi - \theta_i)S}{F} \right] \quad (3.4)$$

where  $f$  is the loss during period  $t$  (mm),  $K$  is the saturated hydraulic conductivity,  $\Phi - \theta_i$  is volume moisture deficit,  $F$  is the cumulative loss at time  $t$ ,  $S$  is wetting front suction.

The total runoff in the SWAT model is calculated separately for each of hydrological response unit (HRU) and then routed to obtain runoff for each sub-basin. The runoff of each sub-basin is then routed to find the total runoff of the basin.

### **3.13.3 Evapotranspiration**

Evapotranspiration is the combined effect of evaporation and transpiration by plants, which converts water from the earth surface to the atmospheres. Evaporation can be defined as the movement of water to the atmosphere from water sources, canopy, soil and interception. At the same time, transpiration is the movement of water by plant and loss through the stomata in its leaves (Hargreaves G.H. & Samani Z.A., 1985).

Three methods are used to calculate potential evapotranspiration (PET) in the SWAT model, which are, the Hargreaves method, Penman-Monteith method and the Priestly-Taylor method. Once the PET is calculated, the actual evapotranspiration (AET) is also calculated. AET refers to the actual amount of water removed during the evaporation and transpiration process. The AET is equal to PET if there is enough water in the basin. The SWAT model evaporates rainfall intercepted by plant canopies and then calculates the maximum amount of transpiration and soil evaporation. If snow is present in the basin sublimation process will occur (Neitsch *et al.*, 2011; Shekhar and Xiong, 2012).

### **3.13.4 Soil Water**

When water enters into the soil, part of it evaporates, and part percolates into the soil, which recharges the groundwater or moves laterally through the soil to contribute to the streamflow. The water percolates when the water available is more than the field capacity of the soil, and the lower layer is not saturated (Shekhar and

Xiong, 2012). SWAT model computes the amount of water moving from one layer to another using the Storage routing method developed using equation 3.5.

$$W_{per,ly} = SW_{ly,excess} \mathbf{1} - \exp \left[ -\frac{\Delta t}{TT} \right] \quad (3.5)$$

where  $W_{per,ly}$  is the amount of water percolating to the underlying soil layer on a given day (mm of water);  $SW_{ly,excess}$  is the drainable volume of water in the soil layer on a given day (mm of water);  $TT$  is the travel time for percolation (hrs);  $\Delta t$  is the length of the time step (hrs).

Water starts to pond when it percolates and reaches the impermeable layer, forming a saturated zone, which finally starts the lateral subsurface flow. The SWAT model uses the kinematic storage model to simulate the subsurface flow along the flow path, which was developed based on the mass continuity equation (3.6) given as:

$$Q_{lat} = 0.024 [2 \cdot SW_{ly,excess} \cdot K_{sat} \cdot SLP / \phi_d L_{hill}] \quad (3.6)$$

where  $Q_{lat}$  is lateral flow (mmd-1);  $SW_{ly,excess}$  is the drainable volume of soil water (mm);  $K_{sat}$  is the saturated hydraulic conductivity (mmh-1);  $SLP$  is the slope (m/m);  $\phi_d$  is the drainable porosity (mm/mm); and  $L_{hill}$  is the hill slope length (m).

### 3.13.5 Groundwater

The SWAT model simulates both the shallow unconfined and deep confined aquifers in each sub-basin. The water leaves the groundwater either by capillary rise and discharging to rivers or lakes. The groundwater recharge to unconfined aquifers occurs through percolation of water to the water table. In contrast, in the confined aquifer, groundwater recharge occurs from the upstream end of the confined aquifer, where it is exposed to the earth surface (Shekhar and Xiong, 2012). The equation governing shallow aquifer is shown in equation 3.7, while the equation governing the deep aquifer is shown in equation 3.8:



$$aq_{sh,i} = aq_{sh,i-1} + W_{rchrg,sh} - Q_{gw} - W_{reVap} - W_{pump,sh} \quad (3.7)$$

where  $aq_{sh,i}$  is the amount of water stored in the shallow aquifer on the day  $i$  (mm);  $aq_{sh,i-1}$  is the amount of water stored in the shallow aquifer on day  $i-1$  (mm);  $W_{rchrg,sh}$  is the amount of recharge entering the shallow aquifer on the day  $i$  (mm);  $Q_{gw}$  is the groundwater flow, or baseflow, into the main channel on the day  $i$  (mm);  $W_{reVap}$  is the amount of water moving into the soil zone in response to water deficiencies on the day  $i$  (mm); and  $W_{pump,sh}$  is the amount of water removed from the shallow aquifer by pumping on the day  $i$  (mm).

$$aq_{dp,i} = aq_{dp,i-1} + W_{deep} - Q_{gw} - W_{pump,dp} \quad (3.8)$$

where  $aq_{dp,i}$  is the amount of water stored in the deep aquifer on the day  $i$  (mm);  $aq_{dp,i-1}$  is the amount of water stored in the deep aquifer on day  $i-1$  (mm);  $W_{deep}$  is the amount of recharge percolating from the shallow aquifer into the deep aquifer on the day  $i$  (mm);  $Q_{gw}$  is the groundwater flow, or baseflow, into the main channel on the day  $i$  (mm); and  $W_{pump,dp}$  is the amount of water removed from the deep aquifer by pumping on the day  $i$  (mm).

### 3.13.6 Flow Routing

SWAT model uses the Muskingum and river storage routing methods to route water flow, sediment, nutrients, and pesticides loading into the main channel (Neitsch *et al.*, 2011). Many studies have been conducted to simulate streamflow using the SWAT model, which finds the model to be a suitable tool in various part of the world. For example, Ouyang *et al.*, (2015) and Apurv *et al.*, (2015) used SWAT to assess the climate change impacts on streamflow in the Huangnizhuang catchment in China and five sub-basins of river Brahmaputra in India under CMIP5 emission scenarios. Wang *et al.*, (2012) also use SWAT to analysed climate change impacts on streamflow of the

Shiyang River basin. Other studies conducted using SWAT in Nigeria are summarised in table 3.4 found that the model performed very well in simulating the flow variability.

### **3.14 SWAT Model calibration and validation (SWAT-CUP)**

Model calibration refers to modification or adjustment of model parameters within recommended ranges to optimise model output in comparison with observed datasets which can either be adjusted manually or automatically until the model output best matches the observed data (Vilaysane et al., 2015). SWAT-CUP is a model used for SWAT models calibration, validation, sensitivity and uncertainty analysis. The SWAT-CUP is a computer program for the calibration of SWAT models. It is a public domain program, and as such, can be used and copied freely. It is linked to five different algorithms namely Sequential Uncertainty Fitting (SUFI-2), Generalized Likelihood Uncertainty Estimation (GLUE), Particle Swarm Optimization, (POS), Parameter Solution (ParaSol) and Mark chain Monte Carlo (MCMC) (Vilaysane et al., 2015). SWAT-CUP enables sensitivity analysis, calibration, validation, and uncertainty analysis of SWAT models.

SUFI-2 is an algorithm for calibrating SWAT model. It can provide the broadest marginal parameter uncertainty intervals of model parameters among the five approaches (Gyamfi *et al.*, 2016; Odusanya *et al.*, 2019). The parameter uncertainty is calculated from all the input and output source uncertainties such as the uncertainty in the input rainfall data, the land use and soil type, parameters, and observed data, in SUFI-2. The simulation uncertainty is quantified by the 95% prediction uncertainty (95PPU), which is known as the p-factor (Schuol and Abbaspour, 2006; Khalid *et al.*, 2016). The 95PPU can be simulated at the 2.5 and 97.5% levels of the cumulative distribution of an output variable obtained via Latin hypercube sampling. The strength quantifying the calibration or uncertainty analysis in the SUFI-2 algorithm is the *r*-

*factor* which denotes the average thickness of the 95PPU band divided by the standard deviation of the observed data (Vilaysane *et al.*, 2015; Khalid *et al.*, 2016).

The goodness of fit between the calibration and prediction uncertainty is judged based on the closeness of the *p-factor* to 100% and the *r-factor* to 1 (Santhi *et al.*, 2002; Schuol and Abbaspour, 2006). If the two factors are satisfactory, a uniform distribution in the parameter hypercube is therefore explained as the posterior parameter distribution. The goodness of fit in SUFI-2 is assessed using the  $R^2$ , Percentage Bias (PBIAS), Ratio of Root mean square error to the standard deviation (RSR) and Nash-Sutcliffe (NS) coefficient between the observed data and the best simulation.

In this study, SUFI-2 algorithm was applied for the calibration of the SWAT model because it has the broadest marginal parameter uncertainty intervals among the five approaches. Validation followed as the process through which the model or simulation was tested as an accurate representation of observed datasets.

#### **Bullet-7**

Performance comparison of different hydrologic models in Table 3.3, shows that the SWAT model (Neitsch *et al.*, 2005; 2011) outperformed the other models as it has many novel techniques to generate optimum solutions for integrated water resource management. SWAT model studies conducted in Nigeria as summarized in Table 3.4 finds the model to be a suitable tool in Nigeria and various part of the world. However, no study has been conducted to simulate the impact of climate variability on the hydrological processes in the Niger River Basin and Nigeria at large using the SWAT model.

**Table 3.4 :** Summary of the SWAT Model application in Nigeria.

<b>S/N</b>	<b>Authors</b>	<b>Research Title</b>	<b>Study Area</b>	<b>Conclusion</b>
1.	Schuol and Abbaspour, (2006)	Calibration and uncertainty issues of a hydrological model (SWAT) applied to West Africa	West Africa	Calibrated model results for West Africa show promising results in respect of the freshwater quantification and also described the importance of evaluating the uncertainties in the conceptual models as well as the parameter uncertainty
2.	Schuol <i>et al.</i> , (2008)	Estimation of freshwater availability in the West African sub-continent using the SWAT hydrologic model	West Africa	Results showed that the model SWAT and the selected calibration procedure applies to extensive areas and provides reliable results for west Africa
3.	Schuol <i>et al.</i> , (2008)	Modeling blue and green water availability in Africa	Africa	The results can be used in climate change, water, food security, and virtual water trade studies in Africa. The model results are generally good, albeit with significant prediction uncertainties in some cases.
4.	Xie <i>et al.</i> , (2010)	Evaluation of the Swat Model in Hydrologic Modeling of a Large Watershed in Nigeria	Nigeria	The findings from the hydrologic calibration and uncertainty analysis helped make a robust assessment on the surface runoff and the resulting soil erosion level

5. Adeogun <i>et al.</i> , (2014)	GIS-Based Hydrological Modeling using Swat: Case Study of Upstream Watershed of Jebba Reservoir in Nigeria	Jebba Reservoir Nigeria	Results show a good correlation with the observed data which indicate that SWAT can be an ideal modeling tool for water resources management, policies and decisions at watershed level in the region and other river catchments in Nigeria
6. Adeogun <i>et al.</i> , (2014)	Validation of SWAT Model for Prediction of Water Yield and Water Balance: Case Study of Upstream Catchment of Jebba Dam in Nigeria	Jebba Dam in Nigeria	Results show that the SWAT model could be a promising tool to predict water balance and yield in sustainable water resource management. SWAT could also be applied to other basins in Nigeria as a decision support tool for sustainable water management in Nigeria
7. Adeogun and Sule, (2015)	Simulation of Sediment Yield at the Upstream Watershed of Jebba lake in Nigeria using SWAT model	Jebba Lake, Nigeria	Results show that a properly calibrated SWAT model is suitable for modeling the hydrology and predicting the sediment yield in a watershed. Water engineers and hydrologists can adopt SWAT in Nigeria as a decision support tool to assist policymakers in achieving sustainable sediment and water management at the watershed level
8. Ejieji <i>et al.</i> , (2016)	Prediction of the Streamflow of Hadejia-Jama'are-Komadugu-Yobe River basin, North-Eastern Nigeria using SWAT Model	North-Eastern Nigeria	Results show that SWAT can be useful as a decision support tool for water resources management policies in the basin and other parts of Nigeria

9. Salau <i>et al.</i> , (2017)	SWAT analysis of Ikere Gorge basin for hydrokinetic power estimation in selected rural settlements of Oke Ogun, Nigeria	Oke Ogun, Nigeria	Results show that the average daily discharge and theoretical Hydrokinetic energy of river head in the selected location can be used as a pilot study for the production of hydrokinetic energy in the rural settlements of Oke Ogun, Nigeria.
10. Oladapo <i>et al.</i> , (2018)	Simulation and Forecasting of Soil Moisture Content Variability Over Ogbomoso Agricultural Watershed Using the SWAT Model	Ogbomoso, Nigeria	Results of simulated soil moisture during the 1984 to 2017 and predicted soil moisture during the 2018 to 2037 periods generally shows a decreasing trend, which may have negative implications for crop yield. The variability in both the simulated and predicted soil moistures generally respond to precipitation decreasing and the temperature rising in the region.
11. Daramola <i>et al.</i> , (2019)	Estimating sediment yield at Kaduna watershed, Nigeria using soil and water assessment tool (SWAT) model	Kaduna watershed, Nigeria	The model identified the base flow (ALPHA_BF.gw) and threshold depth of water (GWQMN.gw) as the most sensitive parameters for streamflow and sediment yield estimation in the watershed. Results show that an estimated suspended sediment yield of about 84.1 t/ha/yr was deposited within the period under study.

12. Odusanya <i>et al.</i> , (2019)	Multi-site calibration and validation of SWAT with satellite-based evapotranspiration in a data-sparse catchment in south-western Nigeria	South-western Nigeria	This study demonstrated the potential to use remotely sensed evapotranspiration data for hydrological model calibration and validation in a sparsely gauged large river basin with reasonable accuracy.
13. Adeogun and Sanni, (2019)	Hydrological Modeling of Kangimi Dam Watershed using GIS and SWAT Model	Kangimi Dam, Kaduna, Nigeria	Results show that SWAT can be useful in runoff simulation and to support water management policies in Kangimi Dam watershed efficiently. The model can be used successfully to predict the volume inflow to Kangimi Dam when gauging stations are installed at each subbasin for both climatological and hydrological data collections, to facilitate the storage and efficient water management

### **3.15 Groundwater Flow Model**

A groundwater model supplies a quantitative framework for conceptualising hydrogeologic processes and synthesising field information (Anderson *et al.*, 2015). The application of a model is an exercise in thinking about the way a system works is also referred to as a groundwater model (Anderson, 1983). Groundwater flow models are investigation tools used by hydrologists and hydrogeologists for some applications to describe groundwater flow and transportation processes. They represent mathematical equations, developed based on certain assumptions which involve the geometry of the aquifer, the direction of flow, the contaminant transport mechanisms, chemical reactions and the heterogeneity or anisotropy of sediments or bedrock within the aquifer (Kumar, 2002). MODFLOW model setups are used to simulate groundwater systems and conditions for the present and future years (Kumar, 2016).

#### **3.15.1 Modeling of Groundwater Flow MODFLOW**

Groundwater modeling begins with the conceptual understanding of the sites. The understanding can be translated from physical system into mathematical terms (Kumar, 2002). MODFLOW is a computer program which employs techniques of a finite-difference method to simulate three-dimensional groundwater flow in a porous medium using the partial differential equation governing flow (Harbaugh *et al.*, 2000) shown in equation 3.9. The three-dimensional groundwater flow partial differential equation used in developing MODFLOW when combined with initial and boundary



conditions describes the three-dimensional transient groundwater flow in an anisotropic and heterogeneous medium (Harbaugh *et al.*, 2000):

$$\frac{\partial}{\partial x} \left[ K_{xx} \frac{\partial h}{\partial x} \right] + \frac{\partial}{\partial y} \left[ K_{yy} \frac{\partial h}{\partial y} \right] + \frac{\partial}{\partial z} \left[ K_{zz} \frac{\partial h}{\partial z} \right] + W = S_s \frac{\partial h}{\partial t} \quad (3.9)$$

where;  $K_{xx}$ ,  $K_{yy}$ , and  $K_{zz}$  are hydraulic conductivities along the x, y, and z coordinate axes, which were assumed to be parallel to the principal axes of hydraulic conductivity (L/T).  $h$  is the potentiometric head (L).  $W$  represents the volumetric flux per unit volume which represents sources and sinks of water ( $W < 0.0$  describes flow out of the ground-water system, and  $W > 0.0$  denotes flow in ( $T^{-1}$ )).  $t$  is time (T), and  $SS$  is the specific storage of the porous material ( $L^{-1}$ ).

McDonald and Harbaugh (1984) initially documented MODFLOW, which underwent several overall updates over an extended period as most computer programs do. The second version, which is often called MODFLOW-88, was then recorded in McDonald and Harbaugh (1988) to distinguish it from other versions. MODFLOW-96 was then developed as the third version (Harbaugh *et al.*, 1996a and 1996b). In addition to these updates and enhancements of the program, the U.S. Geological Survey developed two significant extensions to MODFLOW, viz; MODFLOWP (Hill, 1992) and MOC3D (Konikow *et al.*, 1996). MODFLOWP and MOC3D solve equations in addition to the ground-water flow equation (Harbaugh *et al.*, 2000).

MODFLOW-2000 was then developed to accommodate the addition of multiple types of equations and many data input parameters. MODFLOW-2000 also allows definition using parameter values, each of which can be applied to data input for many grid cells which makes it much easier to modify the input values for large parts of a model. Adjustments can be made on defined parameters which can be

calculated to attain associated sensitivities to the nearest possible fit for measuring flows, hydraulic heads, and advective travel. These measurements are accomplished using observation, sensitivity, and parameter-estimation processes of MODFLOW-2000 (Harbaugh *et al.*, 2000). The latest version of MODFLOW developed is the MODFLOW-2005.

### **3.15.2 Description of MODFLOW-2005**

MODFLOW-2005 is a new version of the three-dimensional finite-difference groundwater model. It is used to simulate steady and non-steady flow in an irregularly shaped flow system in which aquifer layers can either be unconfined, confined, or a combination of both. MODFLOW-2005 can be used to simulate steady-state or transient groundwater flow with constant density through porous earth (Harbaugh, Arlen, 2005).

MODFLOW-2005 allows many hydrogeological processes, such as aerial recharge across the water table, subsurface inflows at fixed and variable rates as a function of the head, leakage to aquifers from lakes and streams, discharge to lakes and streams, losses by evapotranspiration from phreatophyte and discharge from pumping wells (Harbaugh, Arlen, 2005). Although MODFLOW-2005 was designed to simulate only the saturated zone beneath the water table, it is, however, still capable of simulating one-dimensional flow through the unsaturated zone above the water table using the unsaturated zone flow package (Niswonger *et al.*, 2006). This package applies the one-dimensional form of Richard's equation in simulating vertical flow through the unsaturated media. MODFLOW-2005 is capable of simulating the effects of groundwater flow barriers such as a fault, and conductance for flow between cells

and the storage terms within each cell (Harbaugh, Arlen, 2005; Harbaugh, 2009). In this study, the USGS version of MODFLOW known as ModelMuse was adopted in this study as it is free and in the public domain (Winston, 2009) and have been used in many areas around the world and found to produce reliable results.

ModelMuse is a graphical user interface (GUI) developed based on GoPhast (Winston, 2009) by the U.S. Geological Survey (USGS) for MODFLOW-2005 (Harbaugh *et al.*, 2005). MODFLOW-LGR (Poeter *et al.*, 2008), MODFLOW-NWT (Niswonger, Panday and Ibaraki, 2011), SUTRA (Voss and Provost, 2002), MODPATH (Pollock, 2016), ZONEBUDGET (Harbaugh, 2009), and PHAST (Parkhurst *et al.*, 2010) models. MODFLOW-NWT provides an alternate method for solving groundwater flow problems relating to drying, rewetting and nonlinearities of the unconfined groundwater-flow equation. MODFLOW-LGR adds local grid refinement to MODFLOW. PHAST simulates three-dimensional saturated groundwater flow systems with multi-component, reactive solute transport (Krčmář and Sracek, 2014).

Many studies (Bear and Verruijt, 1987; Jackson *et al.*, 2004; Du *et al.*, 2018; Montcoudiol *et al.*, 2018; Abdelhalim *et al.*, 2019, 2020) globally developed numerical groundwater flow models to study the interactions between surface and groundwater resources using MODFLOW which were found to produce reliable results. Ophori (2007) developed a numerical regional groundwater flow model to study the link between groundwater movement and petroleum occurrence in the Niger Delta. Edet *et al.*, (2014) also developed a steady-state numerical groundwater flow model for the coastal plain sand aquifer in aqua Ibom state, which concluded that his study forms the basis for future groundwater modeling, simulation and management of the

groundwater resources in the region. However, no study has been conducted in Nigeria to model surface and groundwater resources interactions using MODFLOW.

#### **Bullet-8**

Many researches globally, used MODFLOW to study the interactions between surface and groundwater resources, which were found to produce reliable results. However, to this extent, studies relating to the modeling of surface and groundwater interactions in the context of climate change using MODFLOW is still at infancy.

### **3.15.3 The discretisation of the Subsurface Process (Aquifer system)**

An aquifer refers to regions of permeable porous rocks below the land surface where water is stored and flows (Meinzer, 1923). In most areas, the subsurface comprises regions with low saturated permeability known as confining units (Sun, 1986). A watershed may have multiple aquifers and might be separated by different confining beds that collectively are called an aquifer system. These systems consist of geologic materials that are either partially or fully saturated.

An aquifer system is discretised in MODFLOW-2005 using finite-difference grids representing the computational cells, which are used in calculating groundwater flows and heads. These finite cells are numbered according to the indices  $i$ ,  $j$ , and  $k$ , where  $i$  denotes the row index,  $j$  denotes the column index, and  $k$  denotes the layer index as depicted in Figure 3.7 (Harbaugh *et al.*, 2000; Harbaugh, Arlen, 2005).

There are two methods of discretisation, which are horizontal and vertical discretisation. The horizontal discretisation is defined as a rectangular grid of columns and rows, which the rows are, aligned parallel to the  $x$ -axis. In contrast, layers of cells

define the vertical discretisation, which is aligned parallel to the horizontal plane (Lohman, 1972). In the horizontal discretisation, the increments of the row index,  $i$ , corresponds to a decrease in the  $y$ -direction and the increments in the column index aligns parallel to the  $y$ -axis. Increments of the column index,  $j$ , also correspond to an increase in the  $x$ -direction while the increments of layer index,  $k$ , corresponds to an increase in the  $z$ -direction. The top layer of the model corresponds to  $k=1$ ; the upper-left cell in each layer corresponds to row 1 ( $i=1$ ) and column 1 ( $j=1$ ). The thickness of layers among cells can be uniform or variable. The centre of each cell is called a node and head is computed at the centre of each node (Lohman, 1972; Markstrom *et al.*, 2008).

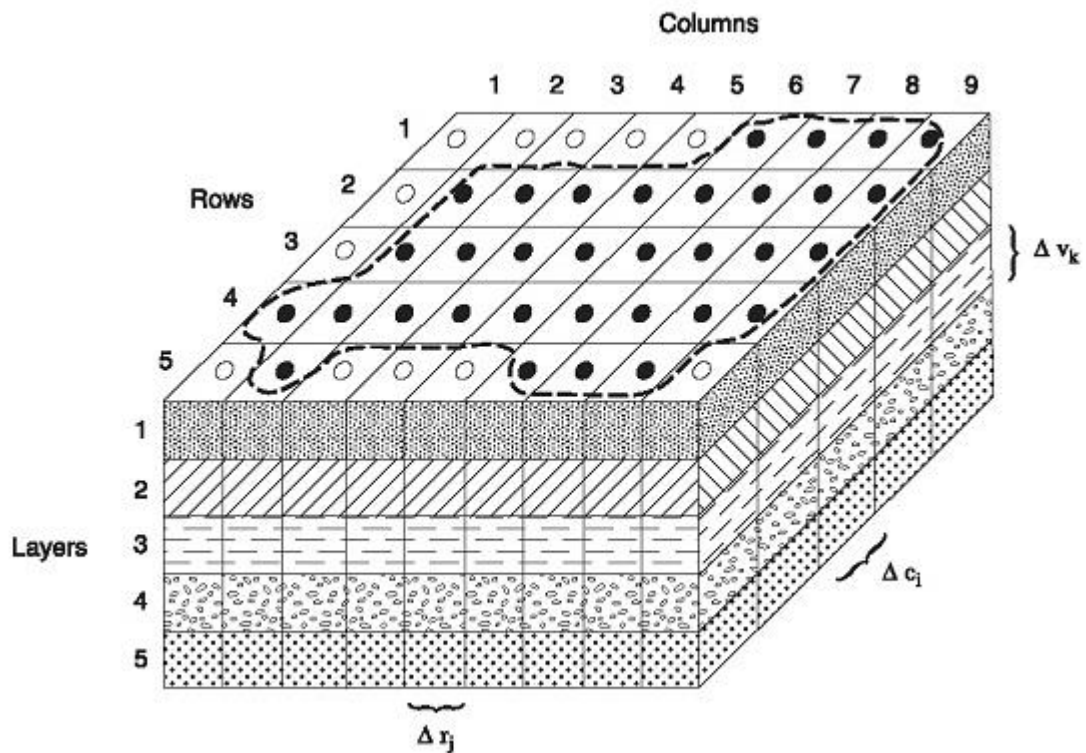


**Figure 3.7** A discretised hypothetical aquifer system adopted from (Harbaugh, Arlen, 2005)

### **3.15.4 Model Boundary conditions**

Boundary conditions are assigned to all the variable head cells using the stress packages in MODFLOW-2005. Specified head or constant head is assigned to cells with certain conditions in which the specified head does not change with time. No-flow boundary condition is assigned to cells where the flows in or out of a cell are not permitted, and there is no groundwater head calculation in those cells. The remaining cells are known as variable head cells. In the variable head cells, groundwater heads are computed, which can vary with time (Harbaugh, Arlen, 2005). An example of a variable head cells boundary condition in MODFLOW-2005 is the head-dependent flow boundary condition, which aids the interaction of groundwater with streams and lakes.

### **3.15.5 Groundwater Model Calibration**

Groundwater Model calibration can be defined as the process of adjusting the model input components and parameters until the simulated values match the values observed in the field. Model calibration in groundwater modeling is necessary due to the complexity of the modeling process. Simulated values of flow and hydraulic head are measured more quickly than the input parameters of hydraulic conductivity, river leakages, recharge, and storage parameters (Hill, 1992). Numerical models cannot represent the subsurface environment correctly. This is because it is hard to capture the full range of heterogeneity in the environment being modeled. To work around this problem, it is more feasible to characterise the environmental system as a model space (Anderson *et al.*, 2015).

The model space represents the range of feasible models and model inputs that are deemed to be appropriate by the groundwater modeler for a specific site. This process further simplifies the conceptual model (a simplified description of the environmental system itself) so that a numerical model that is amenable to computation can be produced (Anderson *et al.*, 2015). To produce an internally consistent groundwater flow model that adequately represents the subsurface system, a process referred to as calibration is employed to reduce the errors between observed and simulated values. This is achieved by solving either a forward problem or inverse problem. In the past, model parameters such as hydraulic conductivities, storativity, and specific storage, are specified, so that predictions can be made. In this case, being heads and fluxes, the problems are solved by history matching, where input parameters are estimated by matching model outputs to field measurements.

In this study, model calibration was performed by varying the aquifer's hydraulic conductivity (K) and aquifer's recharge (R) (Abdelaziz and Bakr, 2012). Parameter values were adjusted for the best fit between field measurements or observed values, and simulated values were achieved.

### **3.16 Impacts of Climate Change on Surface and Groundwater Resources.**

The impacts of climate change on groundwater resources can only be deduced when the hydrodynamic relationships and sensitivity of the groundwater with climate systems are well understood. The components of the hydrologic cycle are vulnerable to changing climate (Barron *et al.*, 1989). The IPCC (2013), reported that climate change has a potential impact on groundwater quantity and quality, which will severely threaten the livelihood of both human and animals. Globally, groundwater resource is

the primary source of potable water for drinking and agriculture. However, many factors affect future groundwater recharge due to changes in precipitation and temperature regimes, urbanisation, land-use changes, coastal flooding and changes in cropping system (Holman, 2006).

Several studies (Priyantha *et al.*, 2006; Herrera-Pantoja and Hiscock, 2008; Jackson, *et al.*, 2011; Kumar, 2012; Ertürk *et al.*, 2014; Chang *et al.*, 2016; Colombani *et al.*, 2016), investigating the potential global impact of climate change on groundwater resources, concluded that the future climate might present a potential decrease in groundwater recharge, which the resultant effect will increase stress on local and regional groundwater resources. However, no study has been conducted to model the potential impacts of climate change on groundwater resources in the Niger Delta and other parts of Nigeria. As climate variability studies on water resources in the Niger Delta (Todd 2015; Obroma Agumagu, 2018) reported an increase in rainfall in the region, this increase, coupled with other anthropogenic factors such as land-use changes would significantly affect groundwater and the rate of groundwater recharge in the basin (Gebremicael *et al.*, 2013).

#### **Bullet-9**

As climate variability, studies on water resources in the Niger Delta reported an increase in rainfall, which will significantly affect the rate of groundwater recharge. Studies on the potential impacts of climate change on surface and groundwater resources may be required to achieve a holistic, integrated water resource management capable of meeting all the regional water demands.

Therefore, the changes in climate and weather conditions in the atmosphere and hydrosphere leads to changes in precipitation patterns, which in turn leads to



changes in groundwater recharge. This will finally lead to changes in groundwater resilience and storage. Groundwater recharge has direct relationships with rainfall. The more the rain falls, the more the water infiltrates through the vadose zone and down to the groundwater, which will lead to more water being stored in the aquifer. Similarly, a decrease in rainfall will reduce available water that recharges the groundwater and hence, less water stored in the aquifer. These possible changes necessitate such studies to develop strategic planning and management of water resources in this vulnerable area.

Coastal aquifers have globally been intensely exploited, given the widespread economic and social development of these areas around the world (Mukherjee *et al.*, 2015). Groundwater tends to be the only source of freshwater of acceptable quality, which makes it crucial and unique, but under risk due to high level exploitation. Given societal needs and economic demands are continually increasing, policy instruments are often ignored, 'watered down' or weak leading to uncontrolled over-exploitation, the consequences of which can be dramatic (Steyl and Dennis, 2010; MacDonald *et al.*, 2012; Mtoni *et al.*, 2013). Coastal aquifers are also naturally at risk from saltwater intrusion (Bear and Verruijt, 1987; Oteri, and Atolagbe, 2003a). This occurs when the water budget of the aquifers becomes unbalanced due to several factors such as over-exploitation, climate change impacts (leading to a decrease in recharge rate) that accelerate seawater intrusion inland contaminating freshwater production wells (Capaccioni *et al.*, 2005; Felisa *et al.*, 2013). Lack of regulation and management can lead to limited future use of coastal aquifers and total loss of the resource (Razack *et al.*, 2019). For this purpose, numerical modelling of aquifers constitutes a critical tool

which is used to test conceptual understanding and analyse the aquifers' reactions to various stresses (Du *et al.*, 2018; Razack *et al.*, 2019).

The shallow coastal plain sand aquifer of the Niger Delta, characterised by high vulnerability to drivers of climate change impacts such as flooding, sea-level rise, gas flaring and oil spillage has over the years caused significant deterioration of groundwater quality in the area (Nnabuenyi, 2012). Lack of public water supply trigger most of the households in the study area to focus on groundwater from shallow aquifers to meet their daily water demand without any law enabling the control of the abstraction of groundwater (Edet *et al.*, 2014). Over the years, more attention has been on groundwater quality studies in this area, while little or no attention is given to the interactions between the surface and groundwater, which has a significant impact on the groundwater resilience.

It is highly likely these shallow aquifers are at high risk due to induced climate variability, which would then affect water resources sustainability. This situation has attracted the interest of environmental activists who called for a comprehensive evaluation of the impact of climate change on groundwater resources for sustainability in the coastal areas of Nigeria. This study is the first attempt to numerically model the impacts of climate change on groundwater flow in the region.

#### **Bullet-10**

Predicting the behaviour of recharge and discharge under future climatic conditions and other changes is of great importance for integrated water management, (Kumar, 2010), references do not indicate any attempt to simulate the impact of climate change and abstraction on groundwater in the Niger Delta.

### 3.17 Niger Delta's water resource management problems and challenges

Based on previous studies, the basic Niger Delta Basin's Water Resource management problems and challenges are:

1. Climate studies predicted an increase in annual precipitation of 0.4mm per day during the 2046-2065 period, (Ike and Emaziye, 2012; Haider, 2019; Matemilola *et al.*, 2019) and an increase in annual temperature between 0.4 to 1°C, over the period 2020-2050 in the Niger Delta due to climate (Oladipo, 2010; Haider, 2019).
2. Studies also predicted a rise of 0.1m and 0.2m in mean sea levels by 2020 and 2050, respectively, due to climate change (Akande *et al.*, 2017).
3. The geographical location of the Niger Delta being a low-lying part of Nigeria make the area to be the most vulnerable region to impacts of climate change causing the area to be easily submerged during heavy rainfall events (Ike and Emaziye, 2012; Todd M, 2015; Musa *et al.*, 2016; Agumagu, 2018; Matemilola *et al.*, 2019).
4. There are 32 weather stations, across the 36 states in Nigeria (Ajetomobia *et al.*, 2011; Eludoyin *et al.*, 2014), with only 2 of the stations located in Port Harcourt and Warri which poorly represent the area.
5. Constraints in human and computational resources limits effective water resource management and climate studies in developing countries like Nigeria, hence the selection of a suitable GCM ensemble is crucial (IPCC, 1990b; Hijmans *et al.*, 2005; Foley, 2010; Chen *et al.*, 2011; Northrop, 2013; Khan *et al.*, 2018; Salman *et al.*, 2018; Sun *et al.*, 2018; Wang *et al.*, 2019).

6. Flooding events are recorded annually in the Niger Delta states located along the River Niger and its tributaries for at least a quarter of each year. This devastating floods often inundate the area and pollute the surface and groundwater resources of the shallow coastal aquifer which is the primary source of fresh water in the area (Ologunorisa and Adeyemo, 2005; Amangabara and Gobo, 2007; Prince Mmom, 2013; Amangabara and Obenade, 2015; Tawari-fufeyin *et al.*, 2015).
7. Review of different studies conducted at global and basin level indicates that there is no clear trend on changes in hydrological processes; hence the impact of climate change should be conducted at basin level to find the change at the local level (Jiang *et al.*, 2007; Wang *et al.*, 2012, 2020; Ouyang *et al.*, 2015).
8. The shallow coastal plain sand aquifer of the Niger Delta have intensely been exploited, and are also naturally at risk to drivers of climate change impacts such as flooding, sea-level rise, gas flaring, oil spillage and saltwater intrusion given the widespread economic and social development due to crude oil exploration activities which has over the years caused significant deterioration of groundwater in the areas (Bear and Verruijt, 1987; Oteri, and Atolagbe, 2003a).
9. Lack of public water supply force most of the Niger Delta households to focus on groundwater from the shallow aquifers to meet their daily water demand without any law enabling the control of the abstraction of groundwater in the area (Edet *et al.*, 2014).
10. It is highly likely these shallow aquifers are at high risk due to induced climate variability, which would then affect water resources sustainability.

### **3.18 Summary**

This study outlines the importance of selecting suitable gridded meteorological datasets and CMIP5 GCM outputs for climate change impact assessment and more accurate predictions, due to the paucity of observed weather stations and constraints in human and computational resources, necessary for effective water resource management and planning in developing countries like Nigeria. Previous studies reported that flooding events are recorded annually in the Niger Delta states located along the River Niger and its tributaries, inundating the area and polluting the surface and groundwater resources of the shallow coastal aquifer in the region often attributed to climate change. Several studies conducted also at global and basin level indicates that there is no clear trend on changes in hydrological processes; hence, hydrological modeling for the assessment of climate change impact on water resources at basin level should be conducted to ascertain the local impacts.

This study, therefore, developed a novel approach for investigating the potential climate change impacts studies on both surface and groundwater resources in developing countries with challenges of scarcity of data, limited access to state of the earth commercial tools, expertise and constraint in computational skills and resources for sustainable water resource management studies. Results of the study will contribute to knowledge on possible climate change impacts on both surface and groundwater resources, especially in coastal aquifers which are subjected to both natural and anthropogenic pressure whose knowledge is globally still at infancy.

As the results might not be entirely certain, due to the uncertainties associated with climate scenarios, such an approach associating climate scenarios, hydrological modeling and numerical groundwater flow modeling of aquifers will provide a useful

insight into the future response of hydrogeological systems that can be used for planning and adaptive strategy for integrated water resources management. The results will also assist end-users in integrated water resource management (IWRM) planning to preserve the long-term exploitation of this aquifer and as part of the sustainable management of the local and national water resources.

# CHAPTER 4

## MATERIALS AND METHODS

### 4.1 Introduction

In the previous chapter, the knowledge gaps and potential problems in water resource management of the Niger Delta Basin are highlighted over ten bullet points (1 to 10). Thus, developing a comprehensive multidisciplinary approach capable of tackling these problems is the main focus of this research. In this chapter, the research methods are presented after the research materials presentation.

### 4.2 Research Materials

#### 4.2.1 Software and Codes

Many softwares are currently available for hydrological analyses and groundwater flow modeling. But in most cases, these software packages are commercial and, hence, very expensive. In this study, attention has been given to the free source softwares where available. This softwares were used for the handling manipulation, and modeling of the climate, hydrological, hydrogeological and groundwater data in this study as presented below:

- **R v.3.6.0** is a free and open-source programming language and environment for graphics and statistical computing. R provides a wide variety of statistical modeling, time-series analysis, classical statistical tests, classification,

clustering, and graphical techniques. In this study, RStudio, which is a graphical user interface of the R package, was used for climate modeling, statistical and graphical analysis.

- **QGIS v.3.12.1** is a free and open-source Geographic Information System software, licensed under the GNU General Public License. It is an official project of the Open Source Geospatial Foundation (OSGeo). QGIS is cross-platform, meaning it can run on different operating systems such as Linux, Unix, Windows and even Android (QGIS, 2015). One of the unique features of QGIS is the ability to enhance its functionality through the use of plugins. The plugins can be programmed by any person or organisation and made freely downloadable from the QGIS official plugins repository. In this study, QGIS was used to visualise maps, manage and edit maps and shapefiles, analyse spatial data, compose printable maps, delineate watersheds, prepare Digital Elevation Models, visualise and plot groundwater-modeling results.
- **ArcGIS v.10.2.2** is a commercial software, licensed to the University of Strathclyde, produced by ESRI company (<https://www.esri.com/en-us/home>) for mapping, spatial analysis, vector and raster processing, etc. In this study, ArcGIS was used to visualise maps, manage and edit maps and shapefiles, analyse spatial data, compose printable maps, delineate watersheds, prepare Digital Elevation Models and run the ArcSWAT model.
- **ArcSWAT v2012.10\_4.19** is a free source graphical user interface for SWAT (Soil and Water Assessment Tool) model tool, available as an ArcGIS-extension. The SWAT Model is a public domain model developed by a group of scientists from the USDA-Agricultural Research Service; USDA-Natural



Resources Conservation Service, and Texas A&M University. It is “a basin-scale sophisticated hydrological model that predicts impacts of weather, land use, and soils management on pollution, water supplies soil erosion, fertility and crop production” (Scopel, 2012).

- **SWAT-CUP v.5.2.1.1** is a free source graphical user interface model used for SWAT models calibration, validation, sensitivity and uncertainty analysis. It is a public domain program, and as such, can be used and copied freely. It is linked to five different algorithms namely Sequential Uncertainty Fitting (SUFI-2), Generalized Likelihood Uncertainty Estimation (GLUE), Particle Swarm Optimization, (POS), Parameter Solution (ParaSol) and Mark chain Monte Carlo (MCMC) (Vilaysane *et al.*, 2015). In this study, the SWAT-CUP was used for the calibration, validation, sensitivity and uncertainty analysis of the SWAT model.
- **GMS v.9.2** is a Groundwater Modelling Software developed by Aquaveo and license to the Department of Civil Engineering, Abubakar Tafawa Balewa University Bauchi, for groundwater flow modelling. The software has many powerful tools like borehole log, fence diagram, 3D solid diagram, 3D analysis and visualization of groundwater flow model, etc. In this study, the GMS software was used to characterise the hydrostratigraphic sections of the aquifer for groundwater conceptual model development.
- **ModelMuse v.4.0** is a free source USGS version of a graphical user interface for MODFLOW-2005, MODFLOW-LGR, MODFLOW-LGR2, MODFLOW-NWT, SUTRA, MT3DMS, MODFLOWCFP, MODFLOW-OWHM, PHAST, MODPATH, and ZONEBUDGET (Winston, 2009). It is supported only for

Microsoft Windows 32 or 64 bit systems. ModelMuse can be used to create the flow and transport input files for PHAST, SUTRA and MODFLOW–2005. In this study, ModelMuse was used for groundwater flow model discretisation, the definition of input parameters and visualisation of MODFLOW results.

#### **4.2.2 Hydro-Meteorological datasets**

The datasets used for this study are observed station datasets located at Warri and Port-Harcourt (PH) international airport, in Delta and Rivers state, which were obtained from the Nigerian Meteorological Agency (NIMET) as shown in Figure 4.1. The observed station data has two observations within the study area with two other contributing stations outside the study area. The gridded datasets used are daily precipitation, maximum and minimum temperature datasets obtained from Climatic Research Unit (CRU), Princeton University Global Meteorological Forcing (PGF) and Climate Forecast System Reanalysis (CFSR) datasets available over the Niger Delta part of Nigeria for the years 1980 to 2005.

The CRU gridded datasets are extracted from the CRU version 4.01 global climate dataset (Harris *et al.*, 2014) and downloaded from <http://www.cru.uea.ac.uk/>. The PGF datasets were developed by the Princeton University Global Meteorological Forcing centre (Sheffield, Goteti and Wood, 2006) and downloaded from <http://hydrology.princeton.edu/data/pgf/>. While the CFSR datasets were developed by the National Centres for Environmental Prediction (NCEP) (Fuka *et al.*, 2014) and downloaded from <http://cfs.ncep.noaa.gov/cfsr/>. These daily datasets were downloaded and extracted at 0.5°X0.5° resulting in an equal number of grids (22 grids) which are spatially distributed across the study area, as shown in Figure 4.1 below.

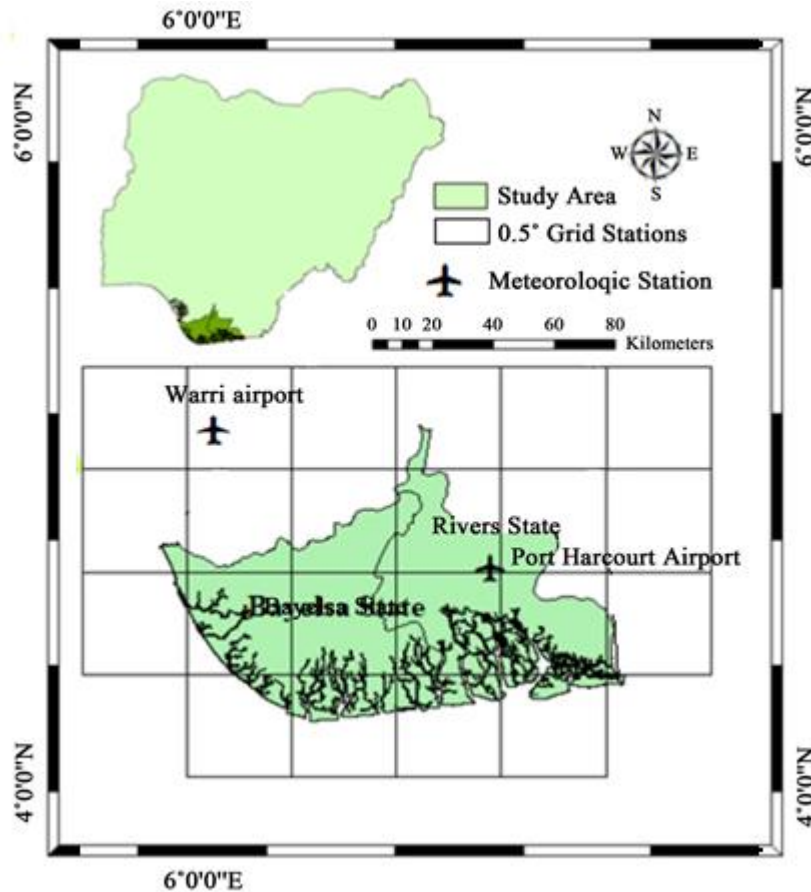


**Figure 4.1** Map of the Study Area in Nigeria Showing the Spatial Distribution of 0.50 Grids

#### 4.2.3 Climate scenario data

The Global Climate Models (GCMs) datasets used in this study consist of 26 GCMs of ISI-MIP (Inter-Sectorial Impact Model Inter-Comparison Project) (Hempel *et al.*, 2013) models (Table 6.1) and two carbon and other greenhouse, aerosols, etc., emission scenarios (RCP4.5 and RCP8.5) for the years (1980–2099) which are downscaled for the basin in order to be consistent with the CRU dataset observations. The GCM data were obtained from the CMIP5 data portal website <http://pcmdi9.llnl.gov/>. The GCMs were selected based on the availability of daily

simulation for two representative concentration pathways (RCP), which were the RCP4.5 and RCP8.5 scenarios.

The RCP4.5 represents an intermediate pathway scenario that shows a good agreement with the latest policy of lower greenhouse gas emissions by the global community, while RCP8.5 is the business-as-usual scenario, which is consistent with a future that has no change in climate policy to reduce emissions (Wang *et al.*, 2016). Therefore, RCP4.5 and RCP8.5 were selected as these two scenarios can provide a possible complete range of impact.

As the GCMs are available in different resolutions, all CMIP5 data were extracted and downscaled uniformly to the same spatial scale ( $0.5^\circ \times 0.5^\circ$ ) to reduce biases introduced by different resolutions for a fair comparison. This technique uses nearby areas to generate point output from each GCM at each grid point, thus providing a smooth interpolation that is widely used for the re-gridding of GCMs (Ashraf Vaghefi *et al.*, 2017). Table 6.1 gives an overview of the GCMs.

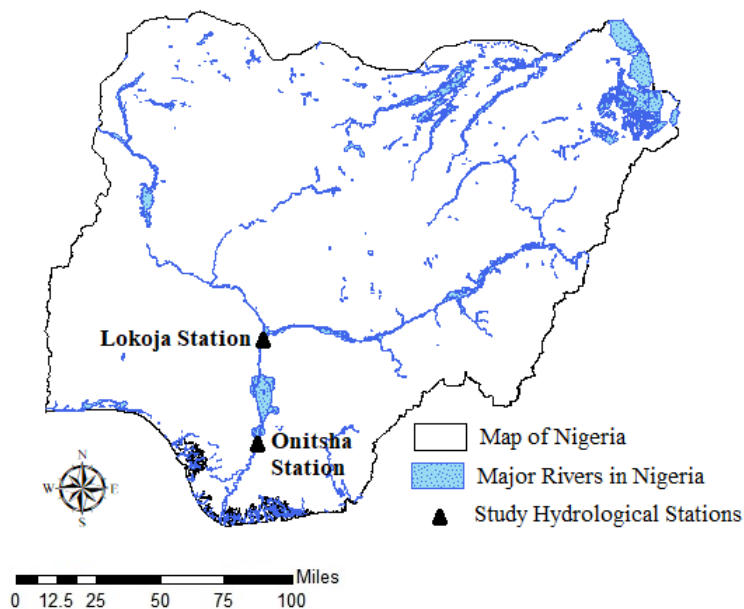


**Figure 4.2** Map of Nigeria showing the Study Hydrological Station

#### 4.2.4 River Discharge Data

Observed daily river discharge data for Lokoja station from 1970 to 2004 was obtained from the Global Runoff data centre (GRDC), while the discharge data for Onitsha station from 1980 to 2005 was obtained from the National Hydrologic service agency (NHISA) in Nigeria as shown in Figure 4.2.

#### 4.2.5 Digital elevation Map, Land use and soil data and sources

The Digital Elevation Map (DEM) used in this study was a 30-m resolution DEM derived from NASA. As Land use distribution and presence and type of vegetation play a vital role in the estimation of water yield in an area, for example, shrubs and grasslands use less water than forests (Zarei *et al.*, 2016). The Nigerian Land use/cover map of the year 2000 developed by the USGS (Tappan *et al.*, 2016) and downloaded from <http://dx.doi.org/10.5066/F73N21JF> was adopted in this study.

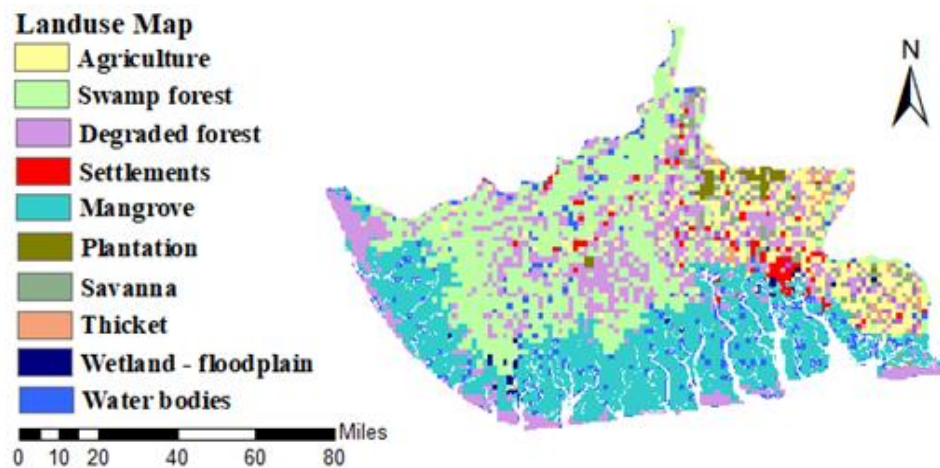


**Figure 4.3** Land-use Map of the Study Area

The Nigerian land use map provides vital information about the extent of groundwater demand and utilisation due to its dense vegetation, which renders it as an excellent site for groundwater exploration. The area located along the coastal part of Nigeria consists of 10 land use classes, as depicted in figure 4.3. This area is characterised by mangroves swamp forests.

**Table 4.1 : Percentage of Soil Texture Compositions**

Units			Sand %		Silt %		Clay %	
Symbol	Name	Texture	Topsoil	Subsoil	Topsoil	Subsoil	Topsoil	Subsoil
G2-2-3a	G-Gleysols Fx-Xanthic	Clay Loam	33	33	37	33	33	35
Fx8-1a	Ferralsols Rd-Dystric	Sandy Loam	65	57	17	15	18	28
Rd8-1a	Regosols Jt-Thionic	Sandy Loam	78	81	13	8	9	11
Jt4-a	Fluvisols	Loam	36	27	37	40	27	34

The soil grid map for the study area was extracted from the Food and Agriculture Organization (FAO) soil map and the soil texture classes are translated into clay loam, sandy loam, and loam soils as indicated on Figure 4.4 and the percentage of texture compositions are summarised in Table 4.1.

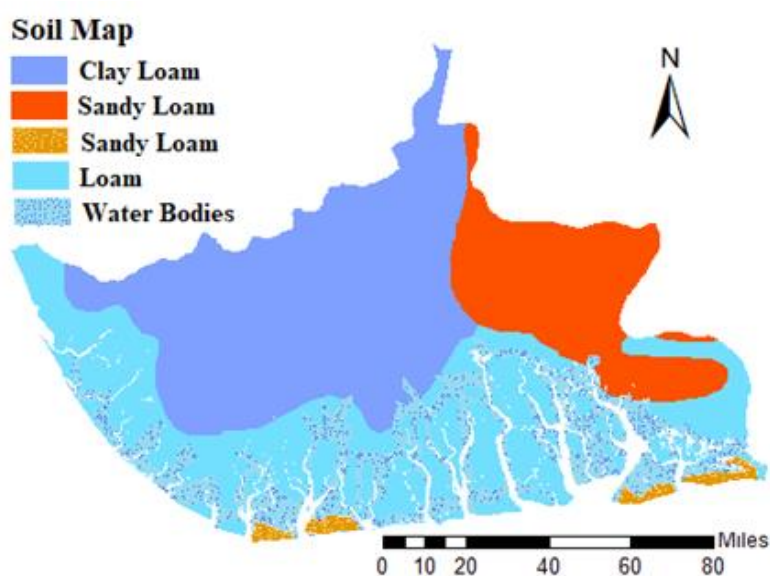


**Figure 4.4** Soil Map of the Study area

#### **4.2.6 Borehole Datasets**

The datasets used in this study consist of 52 Borehole logs, as depicted in Figure 9.2. Furthermore, groundwater level data collected from 130 different observation wells across the study area, as depicted in figure 10.4, respectively. The datasets were obtained from the Nigeria Hydrological Services Agency (NHISA) and MECON Geology and Engineering Services covering a period of 1980 to 2000.

These boreholes were reported to be drilled using the rotary drilling method commonly used in the Niger Delta. Drilling was followed up with down-hole geophysical logging in addition to the pre-drilling surface geophysical survey.

#### **4.3 Research Methods**

In this chapter, after the identification of research materials, the general methodology used in this study are presented and discussed. The process of achieving the objectives involves a series of the procedure, as summarised in Figure 4.5. Specific methods relating to the objectives that arose in the following chapters are discussed within the publications and chapters.

A detailed description of the datasets and methods are described in the research articles written as chapters herein:

1. Chapter 5 presents the selection of appropriate climate datasets, which consist of two parts. The first key step for the research was to evaluate the confidence in daily gridded datasets from the Climatic Research Unit (CRU), Princeton University Global Meteorological Forcing (PGF) and Climate Forecast System Reanalysis (CFSR) datasets available over the Niger Delta part of Nigeria were

analysed against the observed station datasets to select the best datasets that can serve as a possible replacement to the observed rainfall, maximum and minimum temperature datasets (Paper 1). In the second step, the Symmetrical Uncertainty (SU) filter was employed together with the selected gridded datasets to select a subset of a suitable general circulation model (GCM) ensemble from a pool of 26 Coupled Model Intercomparison Project Phase 5 (CMIP5) GCM outputs by excluding those with limited similarity to the observed climate (Paper 2).

2. Chapter 6 used the selected GCMs ensemble in chapter 5 for the prediction of rainfall and the assessment of extreme meteorological event over the period 2010–2039, 2040–2069 and 2070–2099 using the Standardized precipitation index (SPI) with 1-month and 12-month time steps (Paper 3).
3. Chapter 7 also used the selected GCMs ensemble in chapter 4 together with the SWAT hydrologic model to analyse the potential impacts of climate change on the streamflow, runoff, aquifer recharge and evapotranspiration in the Niger River Basin (NRB) of Nigeria over the predicted period 2010–2039, 2040–2069 and 2070–2099 (Paper 4).
4. Chapter 8 presents the hydrostratigraphy and hydraulic characteristics of the Niger Delta shallow coastal aquifers and the assessment of its the resilience to both natural and anthropogenic impacts (Paper 5), and
5. Chapter 9 brings together the hydrostratigraphic characterisations in chapter 8, the simulated aquifer recharge and evapotranspiration deduced from the hydrologic model in chapter 7 under the two Representative concentration pathways (RCP4.5 and RCP8.5) to develop a transient groundwater model



using MODFLOW-2005 to investigate the potential impacts of climate change and increasing groundwater extraction due to increasing population. to predict two scenarios from the year 2010 to 2099 (Paper 6).

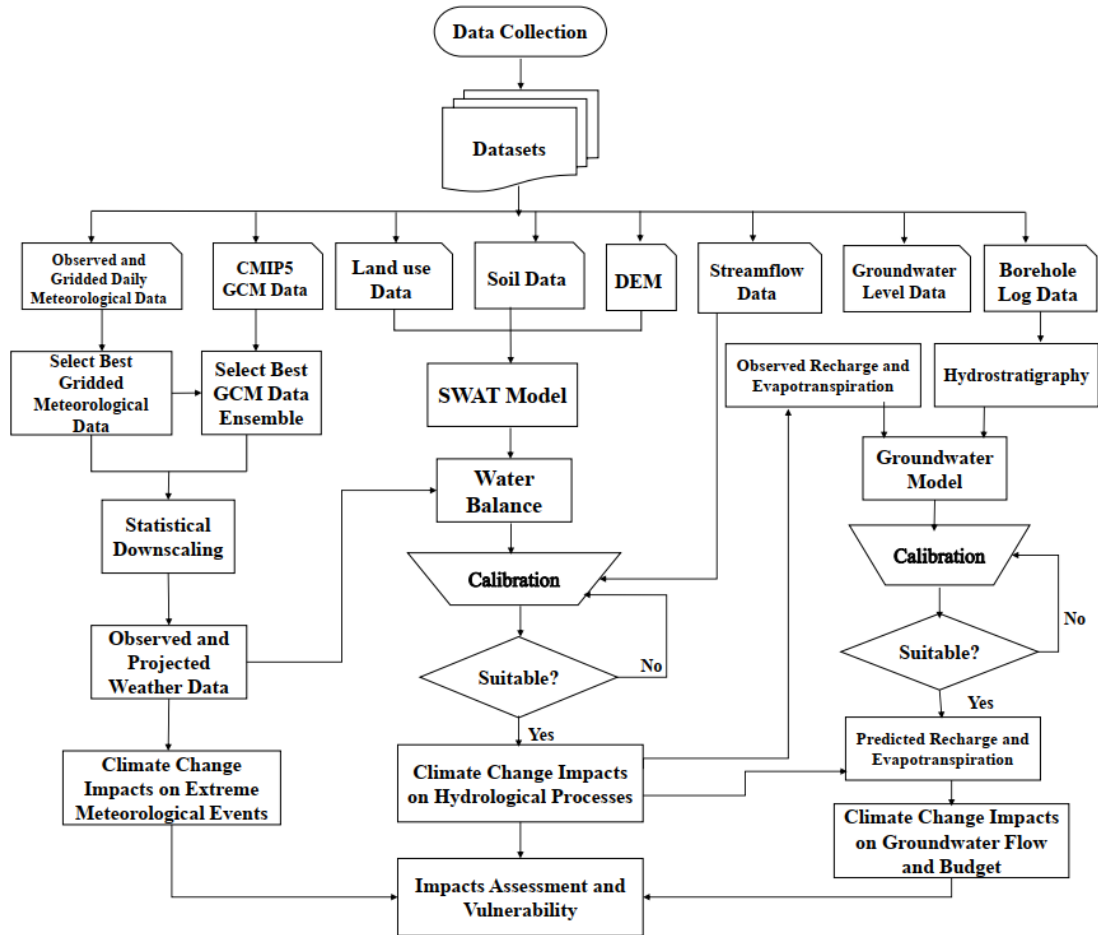


**Figure 4.5** Flow chart showing sequence of methods used in the study

#### 4.4 Summary

The research materials and methods presented in this chapter are to address the ten bullet points highlighted in Chapters two and three. The sources of all codes, maps, database and softwares used in this study were also described. Research methods are presented based on comprehensive IWRM approach, which interconnects between environmental and economic demands in a data-scarce region. The study methods

outline the approach for selecting suitable gridded meteorological datasets and CMIP5 GCM outputs for accurate predictions and climate change impact assessment, which is necessary for effective water resource management planning. The selected gridded datasets and CIMP5 GCM outputs will then be used to project the future rainfall and temperature series up to 2099 and the evaluation of extreme meteorological events under RCP 4.5 and 8.5 emission scenarios, which addressed bullet points 2 to 5 of the literature review. The projected climate variables were used for the development of the SWAT hydrologic model and climate change impact assessment, which addressed bullet points 7.

The borehole logs obtained in this chapter were used to characterise the hydro-stratigraphy, and hydrogeological conceptual model of the Niger Delta shallow coastal aquifers was used to address bullet points 1. The groundwater recharge and evapotranspiration deduced from the SWAT hydrologic model was finally used as input into MODFLOW to model the aquifer response to the climate scenarios and increased abstraction. The 3D groundwater flow model was developed to address groundwater resource management bullets 8 to 10. To this extent, all ten bullet points are addressed to underpin the path to a comprehensive water resource management approach, as illustrated in the subsequent chapters and publications.

# CHAPTER 5

## Selection of Datasets

### 5.1 Preamble

The previous chapters illustrated the need to select and evaluate the confidence in daily gridded meteorological datasets and General Circulation Model (GCM) that will be most applicable to the Niger Delta climate projections. This is due to the lack of adequate observation station datasets, as well as challenges of constraint in human and computational resources in developing countries which makes the use of all the available GCM are not feasible. The area under study houses only two meteorological stations, and the quality of the datasets obtained from these stations are either poor or expensive to purchase, which limits water resource management studies in the area.

To overcome these challenges, gridded representations of meteorological datasets and GCM subsets are selected and used. These GCM subsets are carefully selected by excluding those with limited similarity to the selected observed climate from the existing pool of gridded datasets and GCM outputs. These assessments were accomplished in two research articles published in reputable peer reviewed journals. The first article was published in *Atmospheric and Climate Sciences*, while the second article was published in MDPI Water, as follows:

- Hassan, I.; Kalin, R. M.; White, C. J.; Aladejana, J. A (2020) ‘Evaluation of Daily Gridded Meteorological Datasets over the Niger Delta Region of Nigeria and

Implication to Water Resources Management’, *Atmospheric and Climate Sciences* (ACS), SCRIP. doi:10.4236/acs.2020.101002.

- Hassan, I.; Kalin, R. M.; White, C. J.; Aladejana, J. A (2020) ‘Selection of CMIP5 GCM ensemble for the projection of Spatio-temporal changes in precipitation and temperature over the Niger Delta, Nigeria.’, *Water, MDPI*, (Switzerland), 12(385). doi:10.3390/w12020385.

These articles represent my efforts in conceptualizing, theoretical formulation, development, analytic calculations, numerical simulations, and writing the manuscript. My major supervisor, Prof. Robert M. Kalin, assisted in the research design and gave critical views on the manuscript for further improvement. My second supervisor, Chris J. White, provided technical help and proposed important additions to the models and the manuscript. Finally, my colleague Jamiu A. Aladejana also assisted in giving critical views on the manuscripts and support when required.

## 5.2 Paper 1

Hassan, I.; Kalin, R. M.; White, C. J.; Aladejana, J. A (2020) 'Evaluation of Daily Gridded Meteorological Datasets over the Niger Delta Region of Nigeria and Implication to Water Resources Management', *Atmospheric and Climate Sciences* (ACS), SCRIP. doi: 10.4236/acs.2020.101002.

### **Evaluation of Daily Gridded Meteorological Datasets over the Niger Delta Region of Nigeria and Implication to Water Resources Management.**

Ibrahim Hassan<sup>1,2</sup>, Robert M. Kalin<sup>1</sup>, Christopher J. White<sup>1</sup> and Jamiu A. Aladejana<sup>1,3</sup>

<sup>1</sup>*Department of Civil and Environmental Engineering, University of Strathclyde, Glasgow;*

<sup>2</sup>*Department of Civil Engineering, Abubakar Tafawa Balewa University Bauchi, Nigeria;*

<sup>3</sup>*Department of Geology, University of Ibadan, Nigeria*

*Email: Ibrahim.hassan@strath.ac.uk, ibzara@yahoo.com*

#### **Abstract**

Hydroclimatological study is difficult in most of the developing countries due to the paucity of monitoring stations. Gridded climatological data provides an opportunity to extrapolate climate to areas without monitoring stations based on their ability to replicate the Spatio-temporal distribution and variability of observed datasets. Simple correlation and error analyses are not enough to predict the variability and distribution of precipitation and temperature. In this study, the coefficient of correlation ( $R^2$ ), Root mean square error (RMSE), mean bias error (MBE) and mean wet and dry spell lengths were used to evaluate the performance of three widely used daily gridded precipitation, maximum and minimum temperature datasets from the Climatic Research Unit (CRU), Princeton University Global Meteorological Forcing

(PGF) and Climate Forecast System Reanalysis (CFSR) datasets available over the Niger Delta part of Nigeria. The Standardised Precipitation Index was used to assess the confidence of using gridded precipitation products on water resource management. Results of correlation, error, and spell length analysis revealed that the CRU and PGF datasets performed much better than the CFSR datasets. SPI values also indicate a good association between station and CRU precipitation products. The CFSR datasets in comparison with the other data products in many years overestimated and underestimated the SPI. This indicates weak accuracy in predictability, hence not reliable for water resource management in the study area. However, CRU data products were found to perform much better in most of the statistical assessments conducted. This makes the methods used in this study to be useful for the assessment of various gridded datasets in various hydrological and climatic applications.

**Keywords:** Climate Research Unit (CRU); Princeton University Global Meteorological Forcing dataset (PGF); Climate Forecast System Reanalysis (CFSR); Standardised Precipitation Index (SPI).

## **1.0 Introduction**

The accuracy and reliability of climate datasets are crucial for scientific research and hydrologic studies related to climate change impact assessment, numerical weather prediction, flood forecasting, drought monitoring or water resources management (Wei *et al.*, 2018). Paucity of data remains a challenging task especially in developing countries and in remote parts of the world where ground-based precipitation measurements, such as radar networks and rain gauges are either

sparse or non-existent due to the high cost of establishment and maintenance of the infrastructure (Derin and Yilmaz, 2014).

Recently, climate impact studies have become increasingly detailed as global industrialisation results in an unprecedented increase in greenhouse gases concentrations (GHGs), and associated impact on the changing climate (Worku, 2015). Climate change impact assessment requires climate data at various spatial and temporal scales (IPCC, 1995). Getting data observations at an acceptable spatial resolution is challenging in developing countries, and where available, their quality is either poor or expensive and may poorly represent a study area with large hydroclimatic gradients (Fuka *et al.*, 2014; Ahmed and Shahid, 2019; Wang, *et al.*, 2019). To overcome these challenges, researchers resort to the use of multilayer global gridded representations of meteorological data to serve as inputs into climate and hydrological modelling studies (Fuka *et al.*, 2014).

Climate datasets are typically measured in three ways viz: Gauge-Based observations, Satellite Estimates, and Reanalysis datasets (Sun *et al.*, 2018). Gauge observations provide relatively accurate and trusted measurements at a single point and are subject to limitations, such as reporting time delays, sparse gauge networks, data gaps, unavailable over many sparsely populated and oceanic areas and limited access to available data (Bai and Liu, 2018). Satellite observations provide broad coverage of global atmospheric parameters with adequate spatial and temporal resolution in un-gauged regions, such as the oceans, complex mountain areas, and deserts. They provide information at regular intervals with uniform spatial coverage but contain non-negligible biases and random errors owing to the complicated nature of the relationship between the observations, sampling, and deficiencies in the

algorithms. Reanalysis datasets merge random observations and models that encompass many physical and dynamical processes to generate a synthesised estimate of the state of the system across a regular grid, with spatial homogeneity, temporal continuity, and a multidimensional hierarchy (Sun *et al.*, 2018). These datasets are classified into regional and global datasets. Regional products are explicitly developed for countries or regions, for example, (Lin *et al.*, 2013) and (Yatagai *et al.*, 2009) developed climate datasets for Asia, and (Haylock *et al.*, 2008) developed for Europe, (Herrera *et al.*, 2012) for Spain, and, (Schiemann, Liniger and Frei, 2010) for Switzerland.

Different organizations have developed different global datasets such as the Climatic Research Unit (CRU) (Harris *et al.*, 2014), Global Historical Climatology Network (GHCN) (Steurer *et al.*, 1992), National Oceanic and Atmospheric Administration (NOAA) (Chen *et al.*, 2002), Climate Forecast System Reanalysis (CFSR) (Saha *et al.*, 2010), Princeton University Global Meteorological Forcing dataset (PGF) (Sheffield, Goteti and Wood, 2006) and Global Precipitation Climatology Centre (GPCC) (Schneider *et al.*, 2014). These global gridded datasets have different spatial and temporal resolutions. The quality is governed by the data assimilation system, its optimisation and the quality of observation data used (Bai and Liu, 2018; Wei *et al.*, 2018). The reliability of the gridded datasets varies with time and regional climate (Sun *et al.*, 2018). This makes it necessary to evaluate the capability of gridded data before its application over specific locations.

Recent studies show an increase in the usage of station gauge-based datasets for validating estimates from different interpolated datasets, reanalysis datasets, satellite products and climate models. For example, (Ahmed, Shahid, Wang, *et al.*,



2019) used gauge-based datasets for comparison of four gridded datasets namely Asian Precipitation Highly Resolved Observational Data Integration towards Evaluation (APHRODITE), Global Precipitation Climatology Centre (GPCC), Centre for Climatic Research-University of Delaware (UDel); and Climatic Research Unit (CRU) datasets at stations located in the arid, semi-arid, and hyper-arid regions of Balochistan province of Pakistan. (Chaudhary, Dhanya and Vinnarasi, 2017) used unified rain gauge data with three daily gauge based gridded rainfall datasets, namely the Indian Meteorological Department (IMD), APHRODITE and Climate Prediction centre (CPC) over India. (Rahman, Sengupta and Ravichandran, 2009) used IMD dataset for comparison of two satellite datasets, namely, GPCP and Tropical Rainfall Measurement Mission (TRMM). (Mahe *et al.*, 2008) Compared station datasets with two gridded rainfall datasets, namely Climatic Research Unit (CRU), Hydro-Sciences Montpellier (SIEREM) for Burkina-Faso in West Africa.

Considering such diverse use, it is necessary to carefully examine and compare the characteristics and pattern of the gridded datasets. An inter-comparison should analyse the prominent precipitation spell characteristics such as wet and dry spells among the different gridded datasets and importantly, the implications of using these gridded products on water resource management. Variations in frequency, length and intensity of dry and wet spells within predicted datasets often lead to faulty hydrological and agricultural decisions like extreme events estimation, improper selection of crops, incorrect estimation of sowing and harvesting time (Revadekar and Preethi, 2012). Wet spells are prolonged number of wet days and serve as an indicator of flood conditions while Dry spells are prolonged period of dry days, which also serve as an indicator of drought conditions (Chaudhary *et al.*, 2017). This information is of

prime importance to the hydrologists, agronomist, hydrogeologists and water-resources managers (Ratan and Venugopal, 2013; Vinnarasi and Dhanya, 2016). Standardised Precipitation Index (SPI) is used to identify meteorological wet and drought events from precipitation time series data and serves as a useful tool in water resource management (Mckee, Doesken and Kleist, 1993).

Several studies (Rahman *et al.*, 2009; Derin and Yilmaz, 2014; Singh *et al.*, 2014; Vinnarasi and Dhanya, 2016; Chaudhary, *et al.*, 2017; Bai and Liu, 2018; Wei *et al.*, 2018; Ahmed, *et al.*, 2019) compared gridded datasets with station measurements, however, no study has been conducted in any part of Nigeria to determine which of the best stable gridded climate products matches well with the observed station datasets, and thus serves as a substitute to the station datasets in this highly data-scarce region. Most previous studies use correlation and error analysis to evaluate the performance of gridded products by comparing them with observed station datasets, but performance assessment of the products based on correlation and error analysis alone can be misleading (Ahmed, Shahid, Wang, *et al.*, 2019). This is because the coefficient of correlation is highly sensitive to outliers, hence may not explain the model capabilities fully (Willmott and Matsuura, 2006). The RMSE also varies with the variability in squared errors which reduces its ability to determine the degree to which it reflects average errors and to what extent it reflects variability in the distribution of squared errors (Willmott and Matsuura, 2005, 2006). To overcome these drawbacks, indices like mean bias error (MBE) and spell lengths analysis can be used. MBE is used to analyse the mean in overestimations and underestimations of models. Wet and dry spells analysis are referred to as extended periods of wet and dry days, respectively (Chaudhary, Dhanya and Vinnarasi, 2017) which is used in this

study to compare which of the gridded datasets matches the observed datasets in estimating the wet and dry spells.

This study aims to 1) to evaluate data from three gauge based gridded datasets (CRU, PGF and CFSR) daily precipitation, maximum and minimum temperature datasets available for the Niger Delta and compares it with observed station datasets to identify their fundamental differences. 2) analyse different spell characteristics and identify prominent differences in the spells of the datasets and 3) use the Standardised Precipitation Index (SPI) to assess the implications of using the gridded precipitation products on water resource management in Nigeria. The results will aid water resource management practitioners in selecting the appropriate gridded precipitation and temperature dataset for studying the best-gridded precipitation and temperature products depending upon the scope and application. This study provides insights into the Spatio-temporal behaviour of these three datasets for extreme events estimation, which in turn will benefit hydrological management over un-gauged or sparsely gauged regions.

## **2. Description of the Study Area**

The study area located in the Niger Delta part of Nigeria comprises of Bayelsa and Rivers State is presented in **Figure 5.1**. The area is low lying drained by Rivers Imo, Aba, Kwa-Ibo, Bonny, and their respective tributaries. The topography of the area under the influence of high coastal tides results in flooding mostly during the rainy season (Amadi, 2014). The climatic condition in the region comprises of the wet seasons (March to October) and dry seasons (November to February) characterised by high temperatures and high relative humidity

throughout the year. A short spell of the dry season often referred to as the ‘August break’ caused by the deflection of the moisture-laden current is often experienced in August and sometimes occurs in July or September (Amadi, 2014) due to variations of weather.

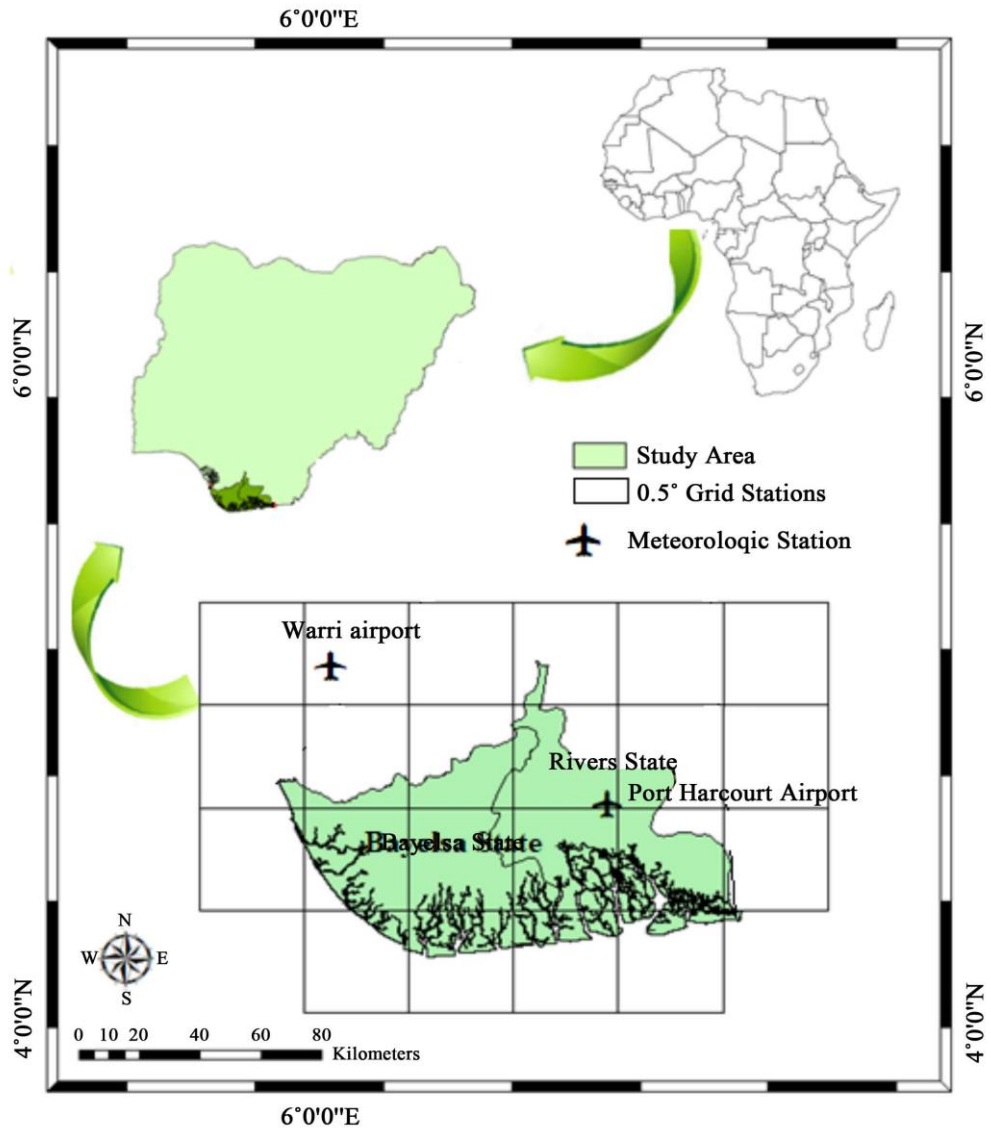


**Figure 5.1** Map of the Study Area in Nigeria Showing the Spatial Distribution of 0.50 Grids

### **3. Materials and Methods**

#### **3.1 Data**

The gridded datasets used in this study are daily precipitation, maximum and minimum temperature datasets obtained from CRU, PGF and CFRS for the years 1980 to 2005. The observed station datasets used for this study are located at Warri and Port-Harcourt (PH) international airport, in Delta and Rivers state, which were obtained from the Nigerian Meteorological Agency (NIMET).

The CRU gridded datasets are extracted from the CRU version 4.01 global climate dataset (Harris *et al.*, 2014) and downloaded from <http://www.cru.uea.ac.uk/>. The PGF datasets were developed by the Princeton University Global Meteorological Forcing centre (Sheffield, Goteti and Wood, 2006) and downloaded from <http://hydrology.princeton.edu/data/pgf/> while the CFRS datasets were developed by the National Centres for Environmental Prediction (NCEP) (Fuka *et al.*, 2014) and downloaded from <http://cfs.ncep.noaa.gov/cfsr/>.

These daily datasets were downloaded as NetCDF files and extracted at  $0.5^{\circ}\times 0.5^{\circ}$  resulting to an equal number of grids (22 grids) which are spatially distributed across the study area as shown in Figure 5.1. The observed station data has two observations within the study area with two other contributing stations outside the study area.

#### **3.2 Methods**

Two ways are generally used to compare gridded datasets with station observations: 1) Computing the average areal precipitation for each grid box from available station data and comparing them grid-to-grid (Yin *et al.*, 2015); 2)

Interpolating the gridded data to station level and comparing the datasets with the observed station data (Hu, *et al.*, 2016). Several methods such as Arithmetic mean, Thiessen polygon, isohyetal method, and gridding or distance weighting are used to estimate areal precipitation from point data. Distance weighting methods are used for gridding of the observed data to the same spatial resolution of the gridded datasets to be compared with the gauges (Prakash *et al.*, 2015). For sparse and unevenly distributed gauges, a simple averaging of all the station data within the grid box is preferred to compute the average areal precipitation (Kursinski and Zeng, 2006; Nkiaka, Nawaz and Lovett, 2017). Previous studies by (Worqlul *et al.*, 2014; Nkiaka, Nawaz and Lovett, 2017; Salman *et al.*, 2019) reported that for evaluation of gridded data with in situ measurements of only one observed station within a grid box, pairwise statistical analyses between the grid point rainfall estimates and rain gauge estimates are carried out assuming that station rainfall is the average observed rainfall for the grid box. This method has been used by Robeson and Ensor, (2006); Worqlul *et al.*, (2014); Hu, (2016); Hu, (2016); Zhang, (2016); Chen, (2016); Li, (2016); and Nkiaka *et al.*, (2017) for the evaluation gridded datasets with observed station measurements. In this study, the performance of the three different gridded precipitation datasets was compared with single-station data located within the grid box. This is because no grid box was found to have more than one observed station.

This study is conducted in three steps. The first involves evaluating the performance of gridded datasets using statistical analysis and visual inspection, and the second involves the analysis of spells among datasets. The third focused on assessing the implication of using each dataset for water resource management.

### 3.2.1. Performance evaluation of the datasets

The performance of gridded datasets was evaluated statistically by comparing the Seasonal variation plots of the observed and gridded datasets for the whole study period. Performance of the datasets was tested using the coefficient of correlation ( $R^2$ ), the Root mean square error (RMSE) and Mean Bias (MB) and summarised in Table 5.1 and 5.2 below. The RMSE measures the global fitness of a predictive model (Willmott, 1981). In these equations,  $o$  and  $y$  are observed and simulated datasets, respectively. The correlation coefficient is measuring the degree of dependence between observations and simulated values. As the  $R^2$  value approaches 1, the accuracy of simulated flows is higher. MAE represents the magnitude of error, and MBE shows bias from the mean. Approach to zero of these two parameters indicates that the method simulates reality well and far from zero shows high deviation and inaccuracy.

$$RMSE = \left( \frac{1}{N} \sum_{i=1}^{N_v} (y_i - o_i)^2 \right)^{1/2} \quad (5.1)$$

where  $y$  and  $o$  represent observed and predicted values respectively; and  $N_v$  is the number of target data used for testing.

$R^2$  measures how the future outcomes are likely to be predicted by the model and are equivalent to the sample cross-correlation between predicted and observed values (Willmott, 1981). In this equation, the overbar denotes average values.

$$R = \frac{\sum_{i=1}^{N_v} (y_i - \bar{y})(o_i - \bar{o})}{\sqrt{\sum_{i=1}^{N_v} (y_i - \bar{y})^2} \sqrt{\sum_{i=1}^{N_v} (o_i - \bar{o})^2}} \quad (5.2)$$

The average model Bias (MB), ranging from  $-\infty$  to 1, measures the model

predictive skill relative to the mean of observations (Willmott and Matsuura, 2006),

$$Mean\ Bias = \frac{1}{n} \sum_{i=1}^n y_i - o_i \quad (5.3)$$

Positive and negative values of MBE represent over or underestimated values respectively;

### 3.2.2. Analysis of spells characteristics among datasets

The analysis of the characteristics of mean dry and wet spells lengths was conducted for the stations, using CRU, PGF and CFSR precipitation datasets to compare their ability to capture the temporal variations in the spell indices of the observed datasets. These indices are computed for the Niger Delta rainfall for a period of 26 years (1980 to 2005). Previous studies defined a day as a wet day or dry day when the amount of daily precipitation falls above or below 1 mm (Sushama *et al.*, 2014). (Dash *et al.*, 2009; Ratan and Venugopal, 2013) also defined spells as the number of consecutive rainy days with rainfall >2.5 mm. A wet day, in general, represents a rainy day while dry day represents a non-rainy day. Wet and dry spells are defined as extended periods of wet and dry days, respectively (Chaudhary *et al.*, 2017).

In this study, the R Multi-Site Rainfall Generator (RMRAINGEN) program `dw.spell` (Cordano, 2016) was used for the spell length analysis. Precipitation thresholds of 1 to 3 mm were selected with a spell length of at least 1 day as recommended in (Sushama *et al.*, 2014) which ensure that no spell with extreme rainfall magnitude is missed out. This is because rainfall of higher magnitude over shorter durations may be disastrous (Vinnarasi and Dhanya, 2016).



**Table 5.1** : Characteristics of gridded rainfall data used in this study.

Datasets		Sum		Maximum		Median		Variance	
		PH	Warri	PH	Warri	PH	Warri	PH	Warri
Precipitation (mm)	Station	2257.5	2236.3	220.4	206.6	9.2	0	459.7	242.4
	CRU	2265.1	2156.2	220.3	223.8	9.8	0	570.8	248.7
	PGF	2243.7	2135.8	263.2	293.5	0	0	546.4	239.3
	CFSR	2854.5	2321	147.6	228.9	8	5.2	81.5	75
Datasets		Mean		Maximum		Median		Variance	
		PH	Warri	PH	Warri	PH	Warri	PH	Warri
Maximum Temperature (°C)	Station	31.1	31.8	44.6	45.5	31.1	32	12.9	14
	CRU	31.1	31.3	44.4	45.5	31.3	31.5	14.1	14.2
	PGF	31.6	31.8	43.8	42	26.5	31.6	4.9	5.4
	CFSR	30.6	31.6	43.8	44.5	30	31.4	22.3	37.2
Minimum Temperature (°C)	Station	22.7	23.2	31.6	31.8	22.9	23.2	4.9	4.6
	CRU	22.6	22.8	32.1	31.8	22.6	22.8	5.5	5.5
	PGF	23	22.3	27.7	27.8	14.2	23.2	1.8	1.8
	CFSR	21.5	23.2	25.4	26.2	21.7	22.5	2.1	15.8

**Table 5.2** : Comparison of observed gridded climate data.

Datasets		R <sup>2</sup>		RMSE		MB	
		PH	Warri	PH	Warri	PH	Warri
Precipitation (mm)	CRU	0.85	0.85	79.36	81.71	-1.58	6.59
	PGF	0.86	0.85	81.33	82.48	2.87	8.24
	CFSR	0.57	0.66	145.58	116.05	-64.94	-6.97
Maximum Temperature (°C)	CRU	0.7	0.9	1.73	1	0.71	0.48
	PGF	0.68	0.9	1.7	0.9	0.33	0.06
	CFSR	0.79	0.8	2.93	2.99	1.03	0.24
Minimum Temperature (°C)	CRU	0.55	0.68	1.15	0.9	0.22	0.35
	PGF	0.48	0.61	1.21	0.92	-0.1	-0.02
	CFSR	0.6	0.37	1.57	2.19	1.17	0.89

### 3.2.3. Standardised Precipitation Index (SPI)

In this study, SPI was used as a water resource management tool to investigate extreme events in the selected stations. This gives an insight into the implication of the wrong choice of datasets for water resource management. SPI was developed for monitoring and defining meteorological drought and wet events from precipitation time series data (McKee, Doesken and Kleist, 1993). SPI computes the precipitation deficit for multiple time steps and therefore facilitates the temporal analysis of drought (Shamsuddin Shahid, 2008). It has also been reported that SPI provides a better spatial standardisation than any other indices. Positive SPI values show higher than median precipitation, while negative values indicate less than median precipitation (Lloyd-Hughes and Saunders, 2002). SPI is calculated taking the difference of the monthly precipitation ( $x_i$ ) from the monthly mean ( $\bar{x}$ ) then dividing by the standard deviation ( $\sigma$ ) (Komuscu, 1999).

$$SPI = \frac{x_i - \bar{x}}{\sigma} \quad (5.4)$$

## 4. Results and Discussions

### 4.1 Performance of Gridded Datasets

The graphs comparing the distribution of the monthly mean for the station, CRU, PGF and CFSR daily precipitation, maximum and minimum temperature datasets of the study area are shown in figure 5.2(a)-(f) respectively. Results of descriptive statistics describing the characteristics of the datasets are also summarised in Table 5.1, and the statistical indicators are summarised in Table 5.2, respectively.

These results and figures show that the CRU and PGF datasets performed

very well in depicting the study areas datasets. The Mean, Maximum, median and Variance for CRU datasets are very similar to that of the station datasets. The PGF datasets depicted the mean, maximum and variance very well in comparison with the observed datasets but highly underestimated the median values. The mean precipitation values in the CFRS datasets tend to be a bit higher while the variance, maximum and median tend to be lower in comparison with the observed precipitation. Statistical indicators in Table 5.2, also suggest that the RMSE values are found to be lower in CRU datasets for precipitation and minimum temperature in both stations. The  $R^2$  values of precipitation for both CRU and PGF are found to be closer to 1, except for the maximum and minimum temperature where the CFRS shows a better performance with an  $R^2$  value of 0.79 and 0.60 in Port-Harcourt station, while the CRU datasets performed better at the Warri station with an  $R^2$  value 0.9 and 0.68 in respectively. However, in all cases, the datasets demonstrated satisfactory statistical performance.

Figure 5.2 shows the relationship between the observed station, CRU, PGF and CFRS datasets. Figure 5.2(a) & (b) shows that the mean monthly distribution of CRU and PGF precipitation matches well with the observed station precipitation. The CFRS datasets consistently overestimate the study areas precipitation from September all through to June and underestimate the mean monthly precipitation from during the peak of the rainy season from June to August. In Figure 5.2(c) & (d), a significant difference exists between the observed station maximum temperature and that of the CFRS in January and February and lower temperatures on the CFRS from March all through to November. In Figure 5.2(e) & (f), the CFRS consistently underestimated the station minimum temperature while the PGF

consistently overestimated the station minimum temperature.

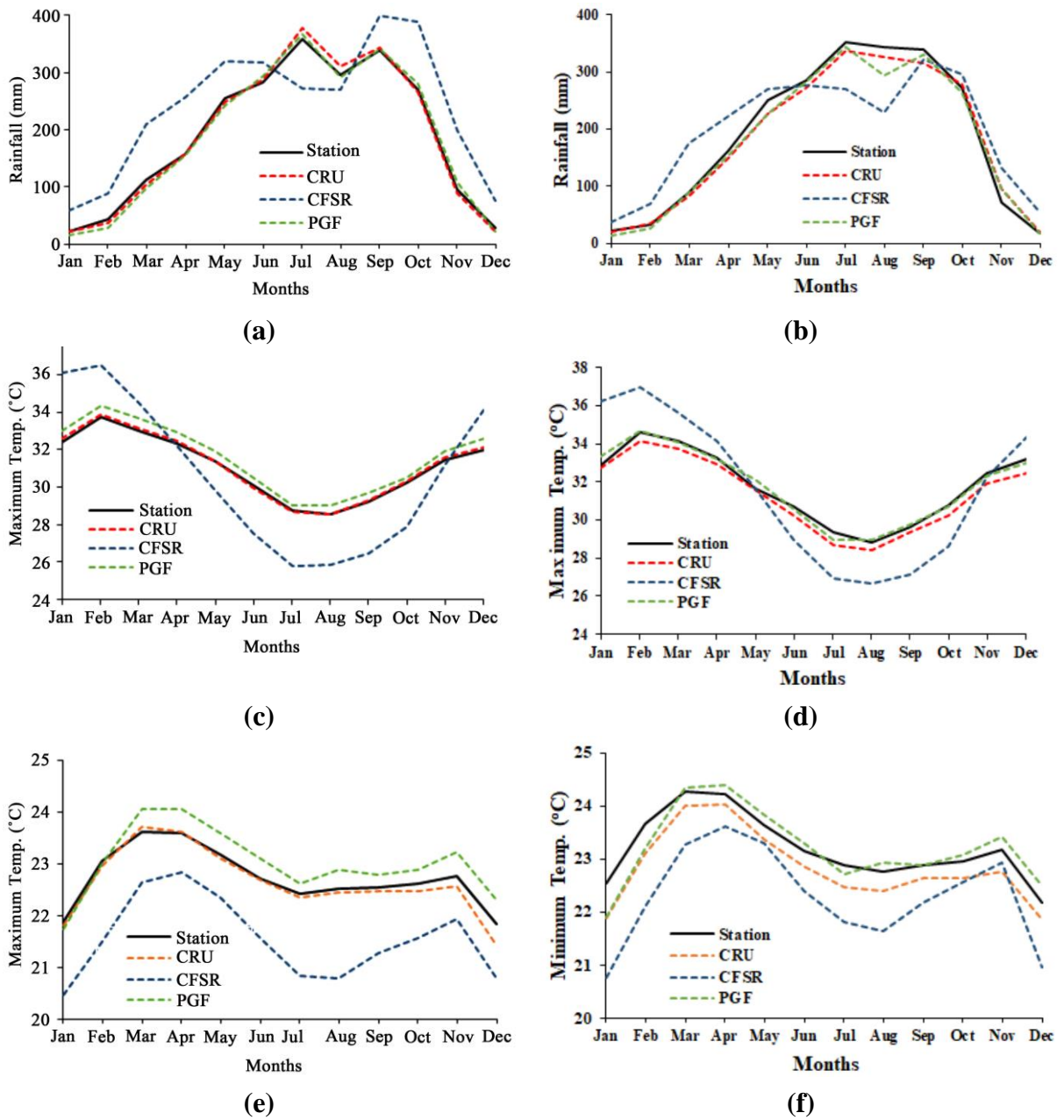


**Figure 5.2** Seasonal variation of the annual average of observed meteorological station, CRU, PGF and CFRS datasets obtained from the same grid as the station data from 1980-2005 for (a) PH Precipitation (b) Warri Precipitation (c) PH Tmax (d) Warri Tmax (e) PH Tmin and (f) Warri Tmin.

Therefore, as shown by statistical performance (Table 5.1 & Table 5.2), and

the graphical visual comparison, there is a better agreement between the monthly means of the observed station datasets and the CRU datasets which shows a better performance to that of PGF and CFRS datasets for both precipitation, maximum temperature (Tmax) and minimum temperature (Tmin) (Figure 5.2) even with the better performance of some of the datasets in correlation and error analysis (Table 5.2). This shows that results of correlation and error analysis can often be misleading in the evaluation of gridded data products as reported by (Ahmed *et al.*, 2019).

#### **4.2. Wet spell and Dry spell**

Results of spell analysis for the distribution of mean monthly Dry and Wet Spell lengths are shown in Figure 5.3 (a) & Figure 5.3 (c) for Port Harcourt, Figure 5.3 (b) & Figure 5.3 (d) for Warri stations respectively. The figures show that the distribution of CRU and PGF rainfall datasets are similar to that of the station rainfall at both study locations.

However, in February and December, the PGF tends to show a much longer dry spell length. The CFRS precipitation datasets consistently overestimated the mean monthly wet-spell length and underestimated the mean monthly dry-spell length. The spell length correlation was then used to assess the annual performance of the spell indices among the datasets. The correlation results summarised in Figure 5.4 (a) & Figure 5.4 (b) for Port Harcourt and Warri stations shows that the CRU datasets correlated better than all the remaining datasets in comparison with the observed station precipitation datasets. Therefore, the CRU can be considered as the most reliable precipitation data in term of temporal characteristics.

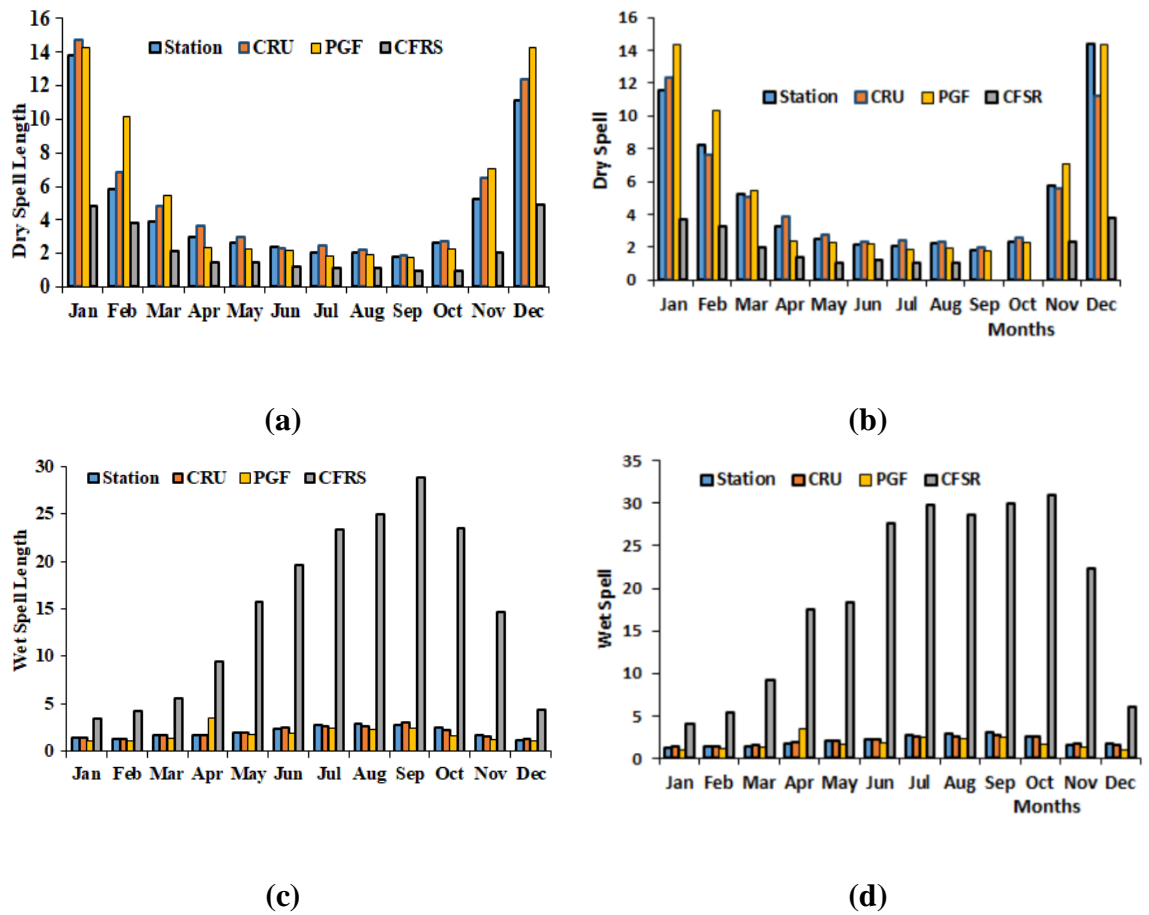
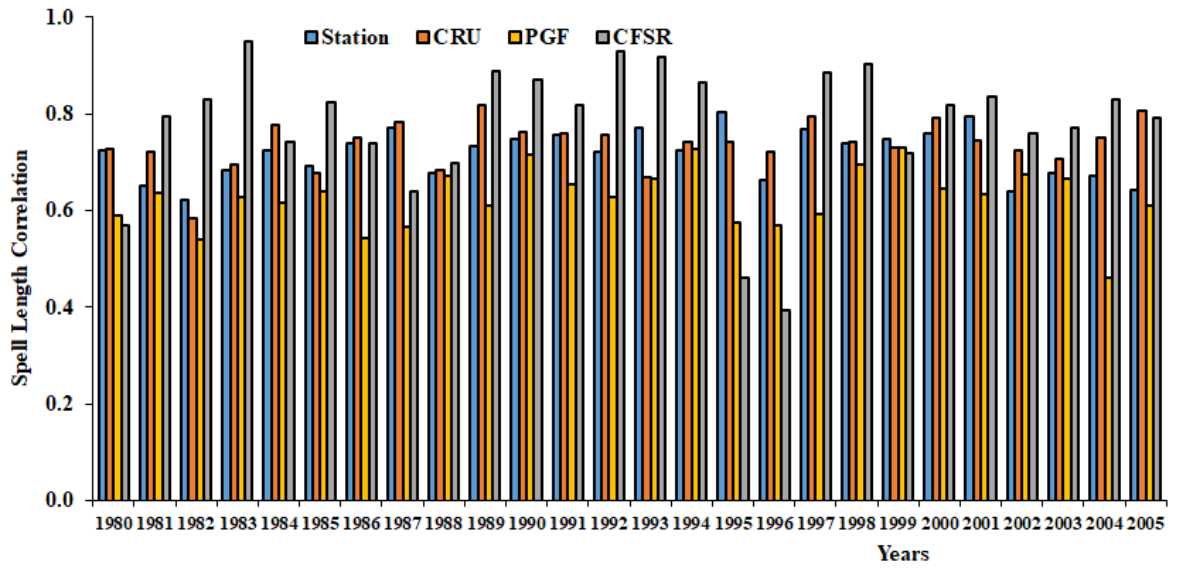


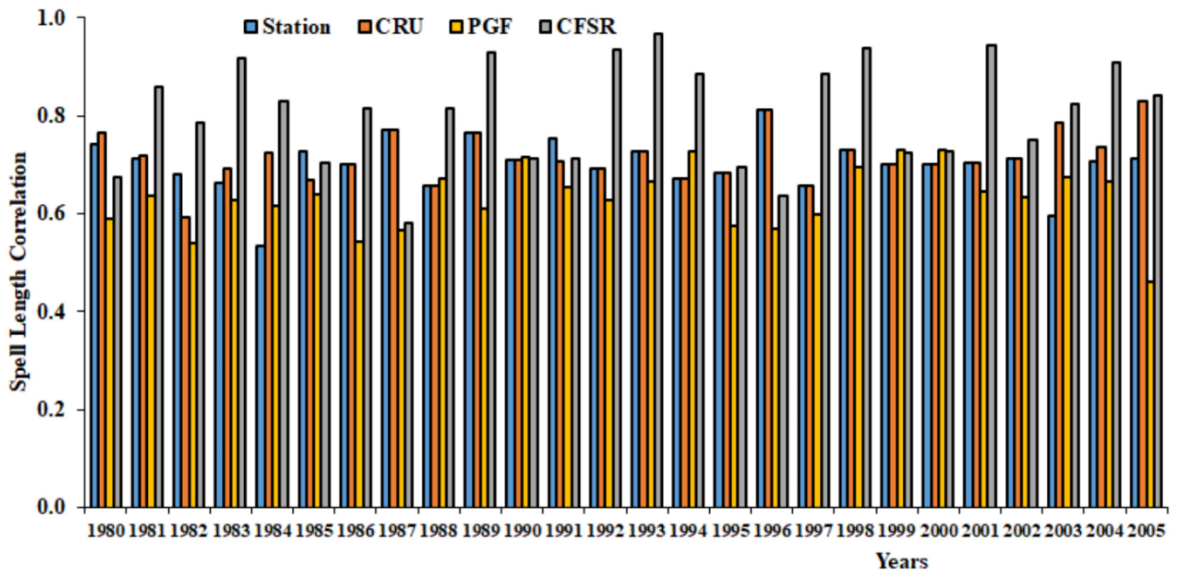
**Figure 5.3** Comparison of Monthly Rainfall Dry Spell for (a) Port Harcourt (b) Warri and Wet Spell for (c) Port Harcourt (d) Warri observed Meteorological station data, CRU, PGF and CFRS datasets obtained from the same Grid as the station data from 1980-2005.

### 4.3. The implication for water resource management

The Standardised precipitation index for 1- year time step is calculated for the period 1980-2005 for all the four datasets (Station, CRU, PGF and CFRS). Result of the comparison of computed SPI for all the datasets is shown in Figure 5.5. The Figure demonstrates a near-perfect relationship between the SPI values (as classified by (Mckee *et al.*, 1993)) computed using the Station, CRU and PGF datasets with most of the peak values falling within the same classification across the years.

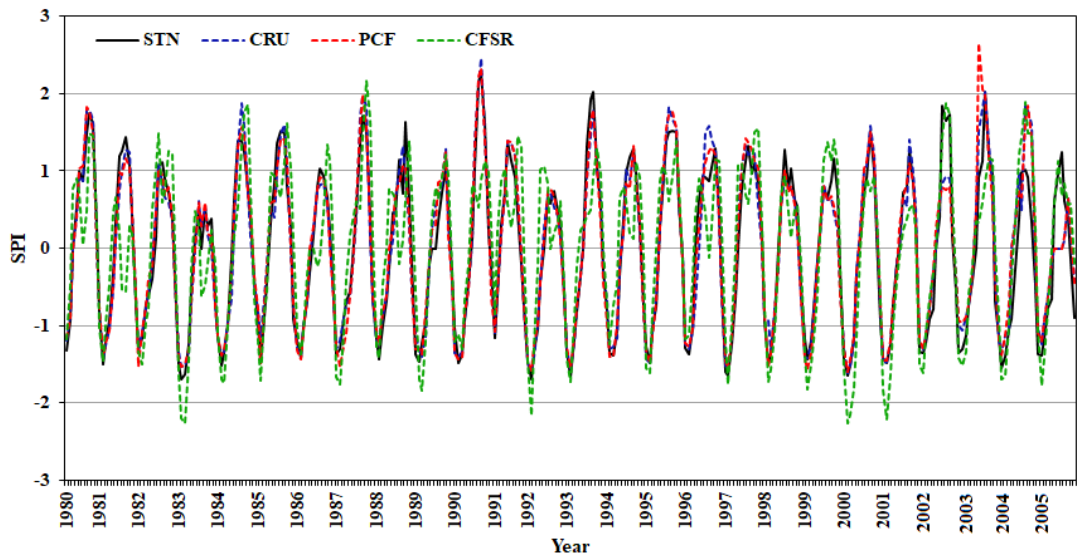


(a)

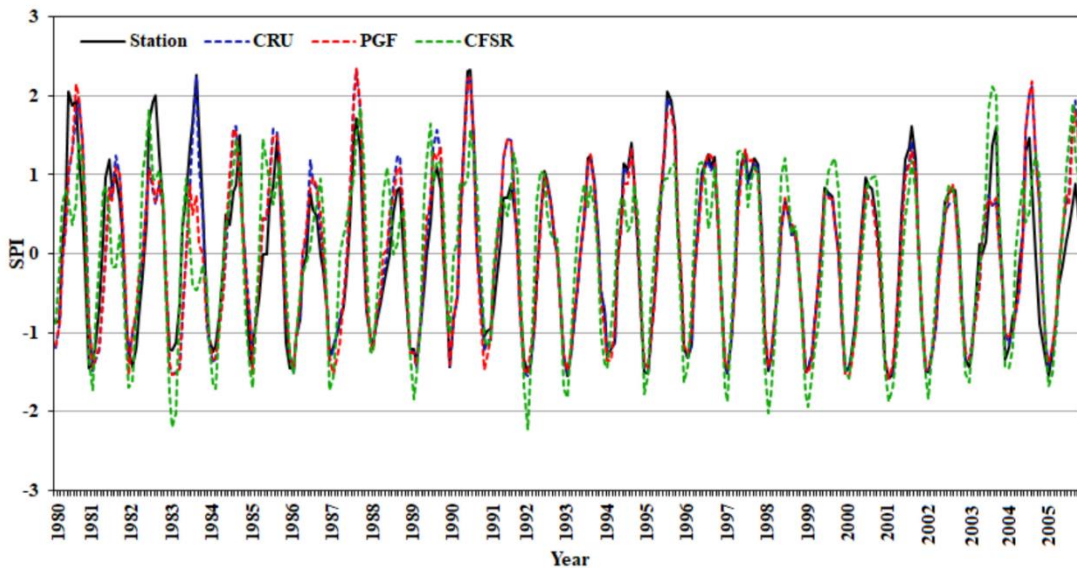


(b)

**Figure 5.4** Spell length correlation for the observed station, CRU, PGF and CFSR datasets for (a) Port Harcourt (b) Warri station.



(a)



(b)

**Figure 5.5** Computed SPI using the observed station, CRU, PGF and CFSR datasets for the periods 1980-2005 for (a) Port Harcourt (b) Warri station.

However, in many years, the CFSR precipitation tends to overestimate or underestimate the SPI. In the years 1983, 1992, 2000 and 2001, the CFSR SPI estimated an extreme drought event for Port Harcourt during the dry season while the



remaining datasets (Station, CRU and PGF) reveals a severe drought event based on (Mckee *et al.*,1993) classification. The CFRS also estimated the near-normal events in the years 1982, 1986 and 1992 to moderate wet events and the very wet event in 1987 to an extremely wet event based on (Mckee, Doesken and Kleist, 1993) classification. In 1991, the extreme wet event that was estimated by the Station, CRU and PGF datasets was also grossly underestimated by the CFRS to a near-normal event.

The evaluation and validation of different gridded datasets are necessary for any region in order to determine the best performing datasets in comparison with the real station datasets of that region before using any of the datasets for any water resource management analysis. Failure to do these results in misleading interpretation that does not depict the realities of the area.

## **5.0. Discussions**

Several statistical techniques have been used in this study to assess the performance of three available daily gridded datasets, commonly used in the Niger Delta part of Nigeria. The study suggests that the CRU datasets replicated the observed station datasets more appropriately when different characteristics of the datasets are considered together. In Nigeria, no study has so far been conducted to assess the performance of daily gridded precipitation and temperature data products that can serve as an alternative to the unavailable station datasets. In west Africa, the only study conducted so far was in Burkina-Faso by Mahe *et al.*, (Mahe *et al.*, 2008). The study evaluated the ability of CRU and SIEREM (HydroSciences Montpellier, France) data to reproduce observed station precipitation characteristics of Burkina-Faso and to analyse the consequences of choosing each one of them on the simulated river flows in the five basins across the country. Mahe *et al.*, (2008) reported the superiority of the

SIEREM precipitation in replicating the station observed precipitation product compared to CRU precipitation. AS SIEREM datasets are developed for largely Francophone African countries (Mahe *et al.*, 2001), hence they are therefore not available for Nigeria. However, comparison of the results from CRU, SIEREM and Burkina-Faso of meteorological station datasets shows that the distribution of annual rainfalls, Mean, standard deviation and minimum values are very similar (Mahe *et al.*, 2008).

Several factors contribute to the performance of gridded data products in a particular area which includes the topography of the area, method of interpolation, the quality of observed stations data, numbers of meteorological stations data and the distribution of the observed meteorological stations used in developing the datasets (Sun *et al.*, 2014; Fu *et al.*, 2016). The availability of quality long-term raw data for use in the construction of the gridded product is very crucial which is in many cases not good enough especially in developing countries where the data are often found to be nonuniform (Salman *et al.*, 2019). Observed meteorological time-series datasets are generally included in gauge-based gridded database preparation after checking its quality (Ahmed *et al.*, 2019). These quality control processes differ for different gridded products. In CRU, all the datasets are passed through a two-stage extensive quality control measures conducted manually and using a semi-automatic approach. The data is checked for the consistency in the first stage followed by the removal of stations or months that gives a large error during the interpolation process in the second stage (New *et al.*, 2002; Harris, 2008). CRU also considers essential factors such as elevation during interpolation, which consequently, enhances its ability for accurate estimation (Harris, 2008). The CRU data was developed from more than 4000 weather

stations distributed around the world (Harris, 2008; Harris *et al.*, 2014). In the southern part of Nigeria alone, more than fifteen station datasets were used as contributing stations, which could be one of the reasons for its better accuracy in the area.

Though PGF was also found to perform very well compared to CFSR in term of various characteristics. It was, however, found to underestimate the mean and median of precipitation, minimum and maximum temperature. This may cause uncertainty in the impact estimated using gridded datasets. It should be noted that no gridded dataset can correctly represent the actual station datasets (Salman *et al.*, 2019). Relevant dataset for a particular study can be selected based on the ability of the dataset to reconstruct specific property of the data required for such study.

## **6.0. Conclusion**

The performances of three gridded daily precipitation and temperature products, namely, CRU, PGF and CFRS available for the study area and widely used as an alternative to observed precipitation and temperature, were evaluated in this paper. The performance of the data was evaluated using statistical indicators, comparison of time-series graphs and spells lengths analysis among datasets. The Standardised Precipitation Index (SPI) was used to determine the implication of using poor gridded precipitation data for water resource management. RMSE and MBE indicate the consistency of the CRU dataset to provide lowest errors in predicted precipitation, and PGF dataset in the prediction of maximum and minimum temperatures.

Results of spell analysis also show a good association between the station datasets, CRU and PGF for estimating the mean monthly distribution of Wet and Dry

Spell lengths. SPI values indicate a good association between observed and CRU and PGF precipitation while the CFRS overestimate and underestimate the SPI in many years. The results revealed a clear superiority of CRU daily precipitation and temperature predictions over the other gridded products for replicating the mean monthly distribution of the station precipitation, maximum and minimum temperature in the Nigeria study area. It can, therefore, be concluded that the CRU datasets are the best performing datasets in this region and hence can confidently be used as observed datasets for further hydrological studies and future climate projection in the study area. The results obtained through the present study can be expanded to other regions in Nigeria, having different climate and topography. It is expected the statistical methods used in the present study can be used in other parts of the world to select better performing data products before application of any gridded product for hydrological and climate studies in study areas with paucity of data.

### **Acknowledgements**

The authors would like to gratefully acknowledge the Petroleum Technology and Development Fund (PTDF) Nigeria under the Overseas PhD scholarship scheme and the Scottish Government under the Climate Justice Fund Water Futures Programme, awarded to the University of Strathclyde (R.M. Kalin) for funding this research.

### **Conflicts of Interest:**

The authors declare no conflict of interest regarding the publication of this paper.

### **References**

Ahmed, K., Shahid, S., Wang, X., Nawaz, N., and Najeebullah, K. (2019). Evaluation of gridded precipitation datasets over arid regions of Pakistan. *Water* (Switzerland),

11(2). <https://doi.org/10.3390/w11020210>

Amadi, A. N. (2014). Impact of Gas-Flaring on the Quality of Rain Water, Groundwater and Surface Water in Parts of Eastern Niger Delta, Nigeria. *Journal of Geosciences and Geomatics*, 2(3), 114–119. <https://doi.org/10.12691/JGG-2-3-6>

Ashouri, H., Nguyen, P., Thorstensen, A., Hsu, K., Sorooshian, S., and Braithwaite, D. (2016). Assessing the Efficacy of High-Resolution Satellite-Based PERSIANN-CDR Precipitation Product in Simulating Streamflow. *Journal of Hydrometeorology*, 17(7), 2061–2076. <https://doi.org/10.1175/JHM-D-15-0192.1>

Bai, P., and Liu, X. (2018). Evaluation of Five Satellite-Based Precipitation Products in Two Gauge-Scarce Basins on the Tibetan Plateau. *Remote Sensing*, 10(8), 1316. <https://doi.org/10.3390/rs10081316>

Chaudhary, S., Dhanya, C. T., and Vinnarasi, R. (2017). Dry and wet spell variability during monsoon in gauge-based gridded daily precipitation datasets over India. *Journal of Hydrology*, 546, 204–218. <https://doi.org/10.1016/j.jhydrol.2017.01.023>

Chaudhuri, A. H., Ponte, R. M., and Nguyen, A. T. (2014). A comparison of atmospheric reanalysis products for the Arctic Ocean and implications for uncertainties in air-sea fluxes. *Journal of Climate*, 27(14), 5411–5421. <https://doi.org/10.1175/JCLI-D-13-00424.1>

Chen, M., Xie, P., Janowiak, J. E., and Arkin, P. A. (2002). Global Land Precipitation: A 50-yr Monthly Analysis Based on Gauge Observations. *Journal of Hydrometeorology*, 3(3), 249–266. [https://doi.org/10.1175/1525-7541\(2002\)003<0249:glpaym>2.0.co;2](https://doi.org/10.1175/1525-7541(2002)003<0249:glpaym>2.0.co;2)

Cordano, E. (2016). Package ‘RMRAINGEN’ (R Multi-site RAINfall GENerator): a package to generate daily time series of rainfall from monthly mean values. *CRAN*. Retrieved from <https://github.com/ecor/RMRAINGEN%0D>

Dash, S. K., Kulkarni, M. A., Mohanty, U. C., and Prasad, K. (2009). Changes in the characteristics of rain events in India. *Journal of Geophysical Research Atmospheres*, 114(10). <https://doi.org/10.1029/2008JD010572>

- Derin, Y., and Yilmaz, K. K. (2014). Evaluation of Multiple Satellite-Based Precipitation Products over Complex Topography. *Journal of Hydrometeorology*, 15(4), 1498–1516. <https://doi.org/10.1175/JHM-D-13-0191.1>
- Fu, Y., Xia, J., Yuan, W., Xu, B., Wu, X., Chen, Y., and Zhang, H. (2016). Assessment of multiple precipitation products over major river basins of China. *Theoretical and Applied Climatology*, 123(1–2), 11–22. <https://doi.org/10.1007/s00704-014-1339-0>
- Fuka, D. R., Walter, M. T., Macalister, C., Degaetano, A. T., Steenhuis, T. S., and Easton, Z. M. (2014). Using the Climate Forecast System Reanalysis as weather input data for watershed models. *Hydrological Processes*, 28(22), 5613–5623. <https://doi.org/10.1002/hyp.10073>
- Harris, I., Jones, P. D., Osborn, T. J., and Lister, D. H. (2014). Updated high-resolution grids of monthly climatic observations - the CRU TS3.10 Dataset. *International Journal of Climatology*, 34(3), 623–642. <https://doi.org/10.1002/joc.3711>
- Haylock, M. R., Hofstra, N., Klein Tank, A. M. G., Klok, E. J., Jones, P. D., and New, M. (2008). A European daily high-resolution gridded data set of surface temperature and precipitation for 1950-2006. *Journal of Geophysical Research Atmospheres*, 113(20). <https://doi.org/10.1029/2008JD010201>
- Herrera, S., Gutiérrez, J. M., Ancell, R., Pons, M. R., Frías, M. D., and Fernández, J. (2012). Development and analysis of a 50-year high-resolution daily gridded precipitation dataset over Spain (Spain02). *International Journal of Climatology*, 32(1), 74–85. <https://doi.org/10.1002/joc.2256>
- Hu, Z.; Hu, Q.; Zhang, C.; Chen, X.; and Li, Q. (2016). Evaluation of reanalysis, spatially interpolated and satellite remotely sensed precipitation data sets in central Asia. *Journal of Geophysical Research Atmospheres*, 121(June), 5648–5663. <https://doi.org/10.1002/2016JD024781>.Received
- IPCC. (1995). Climate Change 1995. The Science of Climate Change. *Journal of Chemical Information and Modeling* (Vol. 53). <https://doi.org/10.1017/CBO9781107415324.004>

Jones, P.D. and Harris, I. C. (2008). Climatic Research Unit (CRU) time-series datasets of variations in climate with variations in other phenomena. *NCAS British Atmospheric Data Centre*.  
<http://catalogue.ceda.ac.uk/uuid/3f8944800cc48e1cbc29a5ee12d8542d>

Komuscu, A. U. (1999). Using the SPI to Analyze Spatial and Temporal Patterns of Drought in Turkey Using the SPI to Analyze Spatial and Temporal Patterns of Drought in Turkey. *Drought Network News*, 11(1), 6–13.

Kursinski, A. L., and Zeng, X. (2006). Areal estimation of intensity and frequency of summertime precipitation over a midlatitude region. *Geophysical Research Letters*, 33(22), 1–5. <https://doi.org/10.1029/2006GL027393>

Lin, C., Maurer, E. P., Andreadis, K. M., Rosenberg, E. A., Livneh, B., Lettenmaier, D. P., and Mishra, V. (2013). A Long-Term Hydrologically Based Dataset of Land Surface Fluxes and States for the Conterminous United States: Update and Extensions. *Journal of Climate*, 26(23), 9384–9392. <https://doi.org/10.1175/jcli-d-12-00508.1>

Lloyd-Hughes, B., and Saunders, M. A. (2002). A drought climatology for Europe. *International Journal of Climatology*, 22(13), 1571–1592. <https://doi.org/10.1002/joc.846>

Mahe, G, New, M., Paturel, J. E., Cres, A., Dezetter, A., Boyer, J. F., and Dezetter, A. (2008). Comparing available rainfall gridded datasets for West Africa and the impact on rainfall-runoff modelling results , the case of Burkina-Faso . *Water SA*, 34(5), 529–536. Retrieved from <http://www.wrc.org.za>

Mahe, Gil, L'Hote, Y., Olivry, J. Claude, and Wotling, G. (2001). Tendances et discontinuités dans des séries de pluies régionales en Afrique de l'Ouest et Centrale: 1951–1989. *Hydrological Sciences Journal*, 46(2), 211–226. <https://doi.org/10.1080/02626660109492817>

Mckee, T. B., Doesken, N. J., and Kleist, J. (1993). The relationship of drought frequency and duration to time scales. *AMS 8th Conference on Applied Climatology*, (January), 179–184. <https://doi.org/citeulike-article-id:10490403>

- New, M., Lister, D., Hulme, M., and Makin, I. (2002). A high-resolution data set of surface climate over global land areas. *Climate Research*, 21(1), 1–25. <https://doi.org/10.3354/cr021001>
- Nkiaka, E., Nawaz, N. R., and Lovett, J. C. (2017). Evaluating global reanalysis precipitation datasets with rain gauge measurements in the Sudano-Sahel region: case study of the Logone catchment, Lake Chad Basin. *Meteorological Applications*, 24(1), 9–18. <https://doi.org/10.1002/met.1600>
- Prakash, S., Gairola, R. M., and Mitra, A. K. (2015). Comparison of large-scale global land precipitation from multisatellite and reanalysis products with gauge-based GPCP data sets. *Theoretical and Applied Climatology*, 121(1–2), 303–317. <https://doi.org/10.1007/s00704-014-1245-5>
- Rahman, S. H., Sengupta, D., and Ravichandran, M. (2009). Variability of Indian summer monsoon rainfall in daily data from gauge and satellite. *Journal of Geophysical Research Atmospheres*, 114(17). <https://doi.org/10.1029/2008JD011694>
- Ratan, R., and Venugopal, V. (2013). Wet and dry spell characteristics of global tropical rainfall. *Water Resources Research*, 49(6), 3830–3841. <https://doi.org/10.1002/wrcr.20275>
- Revadekar, J. V., and Preethi, B. (2012). Statistical analysis of the relationship between summer monsoon precipitation extremes and foodgrain yield over India. *International Journal of Climatology*, 32(3), 419–429. <https://doi.org/10.1002/joc.2282>
- Robeson, S. M., and Ensor, L. A. (2006). Daily precipitation grids for South America. *Bulletin of the American Meteorological Society* (Vol. 87). [https://doi.org/10.1175/1520-0477\(2006\)87\[1095:DPGFSA\]2.0.CO;2](https://doi.org/10.1175/1520-0477(2006)87[1095:DPGFSA]2.0.CO;2)
- Saha, S., Moorthi, S., Pan, H.-L., Wu, X., Wang, J., Nadiga, S., and Goldberg, M. (2010). The NCEP Climate Forecast System Reanalysis. *Bulletin of the American Meteorological Society*, 91(8), 1015–1058. <https://doi.org/10.1175/2010BAMS3001.1>
- Salman, S. A., Shahid, S., Ismail, T., Ahmed, K., and Wang, X. J. (2018). Selection of



climate models for projection of spatiotemporal changes in temperature of Iraq with uncertainties. *Atmospheric Research*, 213(July), 509–522. <https://doi.org/10.1016/j.atmosres.2018.07.008>

Salman, S. A., Shahid, S., Ismail, T., Al-Abadi, A. M., Wang, X. jun, and Chung, E. S. (2019). Selection of gridded precipitation data for Iraq using compromise programming. *Measurement: Journal of the International Measurement Confederation*, 132, 87–98. <https://doi.org/10.1016/j.measurement.2018.09.047>

Schiemann, R., Liniger, M. A., and Frei, C. (2010). Reduced space optimal interpolation of daily rain gauge precipitation in Switzerland. *Journal of Geophysical Research Atmospheres*, 115(14), 1–18. <https://doi.org/10.1029/2009JD013047>

Schneider, U., Becker, A., Finger, P., Meyer-Christoffer, A., Ziese, M., and Rudolf, B. (2014). GPCP's new land surface precipitation climatology based on quality-controlled in situ data and its role in quantifying the global water cycle. *Theoretical and Applied Climatology*, 115(1–2), 15–40. <https://doi.org/10.1007/s00704-013-0860-x>

Shamsuddin Shahid. (2008). Spatial and temporal characteristics of droughts in the western part of Bangladesh. *Hydrological Processes: Wiley InterScience*, 2274(November 2008), 2267–2274. <https://doi.org/10.1002/hyp>

Sheffield, J., Goteti, G., and Wood, E. F. (2006). Development of a 50-year high-resolution global dataset of meteorological forcings for land surface modeling. *Journal of Climate*, 19(13), 3088–3111. <https://doi.org/10.1175/JCLI3790.1>

Singh, D., Tsiang, M., Rajaratnam, B., and Diffenbaugh, N. S. (2014). Observed changes in extreme wet and dry spells during the south Asian summer monsoon season. *Nature Climate Change*, 4(6), 456–461. <https://doi.org/10.1038/nclimate2208>

Singh, N., and Ranade, A. (2010). The wet and dry spells across India during 1951-2007. *Journal of Hydrometeorology*, 11(1), 26–45. <https://doi.org/10.1175/2009JHM1161.1>

Steurer, P. M., Peter, T. C., Heim, R., and Karl, T. R. (1992). The Global Historical

Climatology Network: Long-Term Monthly Temperature, Precipitation, Sea Level Pressure, and Station Pressure Data. Oak Ridge, TN, USA.

Sun, Q., Miao, C., Duan, Q., Ashouri, H., Sorooshian, S., and Hsu, K. L. (2018). A Review of Global Precipitation Data Sets: Data Sources, Estimation, and Intercomparisons. *Reviews of Geophysics*, 56(1), 79–107. <https://doi.org/10.1002/2017RG000574>

Sun, Q., Miao, C., Duan, Q., Kong, D., Ye, A., Di, Z., and Gong, W. (2014). Would the “real” observed dataset stand up? A critical examination of eight observed gridded climate datasets for China. *Environmental Research Letters*, 9(1). <https://doi.org/10.1088/1748-9326/9/1/015001>

Sushama, L., Ben Said, S., Khaliq, M. N., Nagesh Kumar, D., and Laprise, R. (2014). Dry spell characteristics over India based on IMD and APHRODITE datasets. *Climate Dynamics*, 43(12), 3419–3437. <https://doi.org/10.1007/s00382-014-2113-9>

Vinnarasi, R., and Dhanya, C. T. (2016). Changing characteristics of extreme wet and dry spells of Indian monsoon rainfall. *Journal of Geophysical Research: Atmospheres*, 121(5), 2146–2160. <https://doi.org/10.1002/2015JD024310>

Wei, G., Lü, H., Crow, W. T., Zhu, Y., Wang, J., and Su, J. (2018). Evaluation of satellite-based precipitation products from IMERG V04A and V03D, CMORPH and TMPA with gauged rainfall in three climatologic zones in China. *Remote Sensing*, 10(1). <https://doi.org/10.3390/rs10010030>

Willmott, C. J., and Matsuura, K. (2006). On the use of dimensioned measures of error to evaluate the performance of spatial interpolators. *International Journal of Geographical Information Science*, 20(1), 89–102. <https://doi.org/10.1080/13658810500286976>

Willmott, C., and Matsuura, K. (2005). CLIMATE RESEARCH Clim Res. *Climate Research*, 30, 79–82. Retrieved from [www.int-res.com](http://www.int-res.com)

Willmott, Cort J. (1981). On the Validation of Models. *Physical Geography*, 2(2), 184–194. <https://doi.org/10.1080/02723646.1981.10642213>

- Worku, L. Y. (2015). Climate change impact on variability of rainfall intensity in the Upper Blue Nile Basin. *Proceedings of the International Association of Hydrological Sciences*, 366(June 2014), 135–136. <https://doi.org/10.5194/piahs-366-135-2015>
- Worqlul, A. W., Maathuis, B., Adem, A. A., Demissie, S. S., Langan, S., and Steenhuis, T. S. (2014). Comparison of rainfall estimations by TRMM 3B42, MPEG and CFSR with ground-observed data for the Lake Tana basin in Ethiopia. *Hydrology and Earth System Sciences*, 18(12), 4871–4881. <https://doi.org/10.5194/hess-18-4871-2014>
- Yatagai, A., Arakawa, O., Kamiguchi, K., and Kawamoto, H. (2009). A 44-Year Daily Gridded Precipitation Dataset for Asia. *Sola*, 5, 3–6. <https://doi.org/10.2151/sola.2009>
- Yin, H., Donat, M. G., Alexander, L. V., and Sun, Y. (2015). Multi-dataset comparison of gridded observed temperature and precipitation extremes over China. *International Journal of Climatology*, 35(10), 2809–2827. <https://doi.org/10.1002/joc.4174>

### 5.3 Paper 2

Hassan, I.; Kalin, R. M.; White, C. J.; Aladejana, J. A (2020) 'Selection of CMIP5 GCM ensemble for the projection of Spatio-temporal changes in precipitation and temperature over the Niger Delta, Nigeria.', *Water, MDPI, (Switzerland)*, 12(385). doi:10.3390/w12020385.

#### **Selection of CMIP5 GCM Ensemble for the Projection of Spatio-Temporal Changes in Precipitation and Temperature over the Niger Delta, Nigeria**

**Ibrahim Hassan<sup>1,2</sup>, Robert M. Kalin<sup>1</sup>, Christopher J. White<sup>1</sup> and Jamiu A. Aladejana<sup>1,3</sup>**

<sup>1</sup>*Department of Civil and Environmental Engineering, University of Strathclyde, Glasgow;*

<sup>2</sup>*Department of Civil Engineering, Abubakar Tafawa Balewa University Bauchi, Nigeria;*

<sup>3</sup>*Department of Geology, University of Ibadan, Nigeria*

*Email: Ibrahim.hassan@strath.ac.uk*

#### **Abstract**

Selection of a suitable general circulation model (GCM) ensemble is crucial for effective water resource management and reliable climate studies in developing countries with constraint in human and computational resources. A careful selection of a GCM subset by excluding those with limited similarity to the observed climate from the existing pool of GCMs developed by different modeling centers at various resolutions can ease the task and minimize uncertainties. In this study, a feature selection method known as symmetrical uncertainty (SU) was employed to assess the performance of 26 Coupled Model Intercomparison Project Phase 5 (CMIP5) GCM outputs under Representative Concentration Pathway (RCP) 4.5 and 8.5. The selection was made according to their capability to simulate observed daily precipitation (prcp), maximum and minimum temperature (Tmax and Tmin) over the historical period

1980–2005 in the Niger Delta region, which is highly vulnerable to extreme climate events. The ensemble of the four top-ranked GCMs, namely ACCESS1.3, MIROC-ESM, MIROC-ESM-CHM, and NorESM1-M, were selected for the Spatio-temporal projection of prcp, Tmax, and Tmin over the study area. Results from the chosen ensemble predicted an increase in the mean annual prcp between the range of 0.26% to 3.57% under RCP4.5, and 0.7% to 4.94% under RCP 8.5 by the end of the century when compared to the base period. The study also revealed an increase in Tmax in the range of 0 to 0.4 °C under RCP4.5 and 1.25 to 1.79 °C under RCP8.5 during the periods 2070–2099. Tmin also revealed a significant increase of 0 to 0.52 °C under RCP4.5 and between 1.38–2.02 °C under RCP8.5, which shows that extreme events might threaten the Niger Delta due to climate change. Water resource managers in the region can use these findings for effective water resource planning, management, and adaptation measures.

**Keywords:** global climate models; Niger Delta; Coupled Model Intercomparison Project Phase 5; representative concentration pathways; symmetrical uncertainty; temperature; precipitation; gridded dataset

## 1. Introduction

General circulation models (GCMs) are numerical representations of the atmosphere, ocean, and land surface processes developed based on physical laws and physical-based empirical relationships. GCM simulations are essential tools for assessing the impact of climate change for a range of human and natural systems (IPCC, 2007a). The simulated GCM outputs are associated with uncertainties (e.g., due to model resolution, assumption, or calibration processes etc. (IPCC, 1990b;

Hijmans *et al.*, 2005; Foley, 2010; Chen *et al.*, 2011; Northrop, 2013; Khan *et al.*, 2018; Salman *et al.*, 2018; Sun *et al.*, 2018; Ahmed *et al.*, 2019) that hinder GCM outputs from accurately projecting future climate at a regional or local level. To reduce these uncertainties, a subset of GCMs may be selected to caveat a given study area by excluding those with limited similarity to the observed climate (Hijmans *et al.*, 2005; Lutz *et al.*, 2016; Lin and Tung, 2017; Salman *et al.*, 2018; Ahmed *et al.*, 2019). These uncertainties can be minimized by a careful selection of an ensemble model for climate projection (Knutti *et al.*, 2013). It is also practically not feasible to use all of the CMIP5 GCMs for climate change projection and impact assessment due to constraints in human and computational resources (McSweeney *et al.*, 2015). A small ensemble of more appropriate GCMs is selected for any region of interest by excluding those considered unrealistic in order to reduce the spread of uncertainties associated with GCM (Lutz *et al.*, 2016).

The selection of a GCM ensemble subset requires an approach tailored toward the efficacy of the model dependence or performance in climate projection impact analyses (Abramowitz *et al.*, 2019). Existing methods generally follow two approaches: (i) the ‘past performance approach’, which is based on a GCMs’ ability to replicate historical climate but does not take into account the future projection (Srinivasa Raju and Nagesh Kumar, 2015), and (ii) the ‘envelope approach’, which selects GCMs according to their agreement in the future climate projections but does not consider a GCMs’ ability to replicate the past climate (Warszawski *et al.*, 2014). The combination of the past performance approach with the envelope method is referred to as the ‘hybrid approach’. The past performance approach produces better projections when employed for identifying an ensemble from a large pool of GCMs,

suggesting that the past performance evaluation is a suitable approach because the ability of a GCM to simulate the past climatic conditions suggests it may also, therefore, be more likely to predict the future climate with increased accuracy (Lutz *et al.*, 2016; Khan *et al.*, 2018; Salman *et al.*, 2018; Shiru *et al.*, 2019).

A GCM ensemble produced by the past performance approach is usually assessed by comparing historical observed climatic variables with the simulated GCM variables over a baseline period (Shiru *et al.*, 2019). Three algorithms known as ‘filters’, ‘wrappers’, and the ‘hybrid’ of filters and wrappers have been used by the past performance approach in the selection of the GCM subset by ranking the GCMs concerning a climate variable(s) based on their past performance (Chandrashekar and Sahin, 2014; Lutz *et al.*, 2016). These three algorithms are also referred to as ‘feature selection methods’. The filter’s algorithm selects an ensemble of GCMs based on their derived scores from various statistical tests such as correlation coefficient, significance tests, linear discriminant analysis, and information gain (Talavera, 2005; Pierce *et al.*, 2009; Barfus and Bernhofer, 2015; Ruan *et al.*, 2019) while the wrappers algorithm, in contrast, selects an ensemble of GCMs by employing iterative learning algorithms such as forward selection, recursive variable elimination, and greedy search (Dudek, 2010; Ahmed *et al.*, 2019). Hybrids of filters and wrappers are used to identify better performing GCMs from an initially filtered ensemble of GCMs (Hammami *et al.*, 2012; Ahmed, Shahid, Sachindra, *et al.*, 2019). The major drawback of filters is that they ignore inter-dependencies among GCM output for a given variable and therefore, may select inappropriate GCMs for the ensemble. Wrappers are also computationally intensive and are also often found to choose the best set of GCMs due to overfitting of the regression model (Lutz *et al.*, 2016; Ahmed *et al.*, 2019). The hybrids of filters and

wrappers are computationally less intensive when compared to wrappers but were found to perform better when used on a large number of GCMs (McSweeney *et al.*, 2015; Sutha, Tamilselvi, 2015; Lutz *et al.*, 2016).

Many studies have been conducted to determine the performance of GCM outputs by employing various wrappers and filters with respect to gridded data, which include clustering hierarchy (Knutti, Masson and Gettelman, 2013), weighted skill score (Perkins *et al.*, 2007), spectral analysis (Jiang *et al.*, 2015), Bayesian weighting (Min and Hense, 2007), and information entropy (Shukla *et al.*, 2006). Various statistical indicators, such as correlation coefficients (Barfus and Bernhofer, 2015) have also been used for GCM evaluation, ranking, and selection. The disadvantage of using statistical indicators such as correlation coefficients is that their performance matrices are also mostly evaluated based on the mean climatic condition where the temporal variability of the climate is not given full attention (Reichler and Kim, 2008).

Several studies have recently used feature selection methods in selecting the most suitable GCM ensemble subset for climate studies and projections in different areas around the world. Symmetrical uncertainty (SU) is a feature selection method that measures changes in entropy based on the concept of information entropy in order to assess the similarity or mutual information between GCM and the observed datasets (Shannon, 2001; Singh *et al.*, 2014; Ma and Ma, 2018). The authors in (Salman *et al.*, 2018) used SU in the selection of GCMs for the spatiotemporal forecast of changes in temperature of Iraq; (Khan *et al.*, 2018; Ahmed *et al.*, 2019) recently used SU in selecting, ranking, and assessing the performance of several GCMs in Pakistan; and (Shiru *et al.*, 2019) applied a combination of entropy gain (EG), gain ratio (GR), and



a symmetrical uncertainty (SU) approach in screening the past performance and selection of rainfall GCMs in Nigeria.

This study explored the use of symmetrical uncertainty feature selection methods in selecting and ranking the most suitable GCMs to form an ensemble GCM for *prcp*, *Tmax*, and *Tmin* projection in the Niger Delta part of Nigeria. The objective of this study was, therefore, to use symmetrical uncertainty algorithms in identifying the most suitable GCM ensemble from 26 CMIP5 GCMs in reconstructing the *prcp*, *Tmax*, and *Tmin* over the Niger Delta for reliable climate projection. The selected GCM ensemble was then used for the reliable prediction of climate for the Niger Delta, which is highly vulnerable to extreme climate events with large spatial and seasonal variability.

## **2. Materials and Methods**

### **2.1. Description of the Study Area**

The study area is located in the Niger Delta part of Nigeria and comprises Bayelsa and Rivers State (Figure 5.1). The area is a low lying coastal area drained by the Kwa-Ibo, Imo, Bonny, and Aba Rivers and their tributaries. The region has an equatorial climate toward the southern coast and subequatorial climate toward the northern tropical rainforest (Matemilola *et al.*, 2019). The elevation of the area under the influence of high coastal tides results in flooding, especially during the rainy season (Amadi, 2014). The area is characterized by typical tropical wet (March to October) and dry seasons (November to February) with a mean annual rainfall increasing from 2000 mm around the northern fringe to about 4500 mm around the coastal margin (Adejuwon, 2012). A short spell of the dry season, often referred to as the ‘August

break', caused by the deflection of the moisture-laden current, is often experienced in August or September (Amadi, Olasehinde and Nwankwoala, 2014).

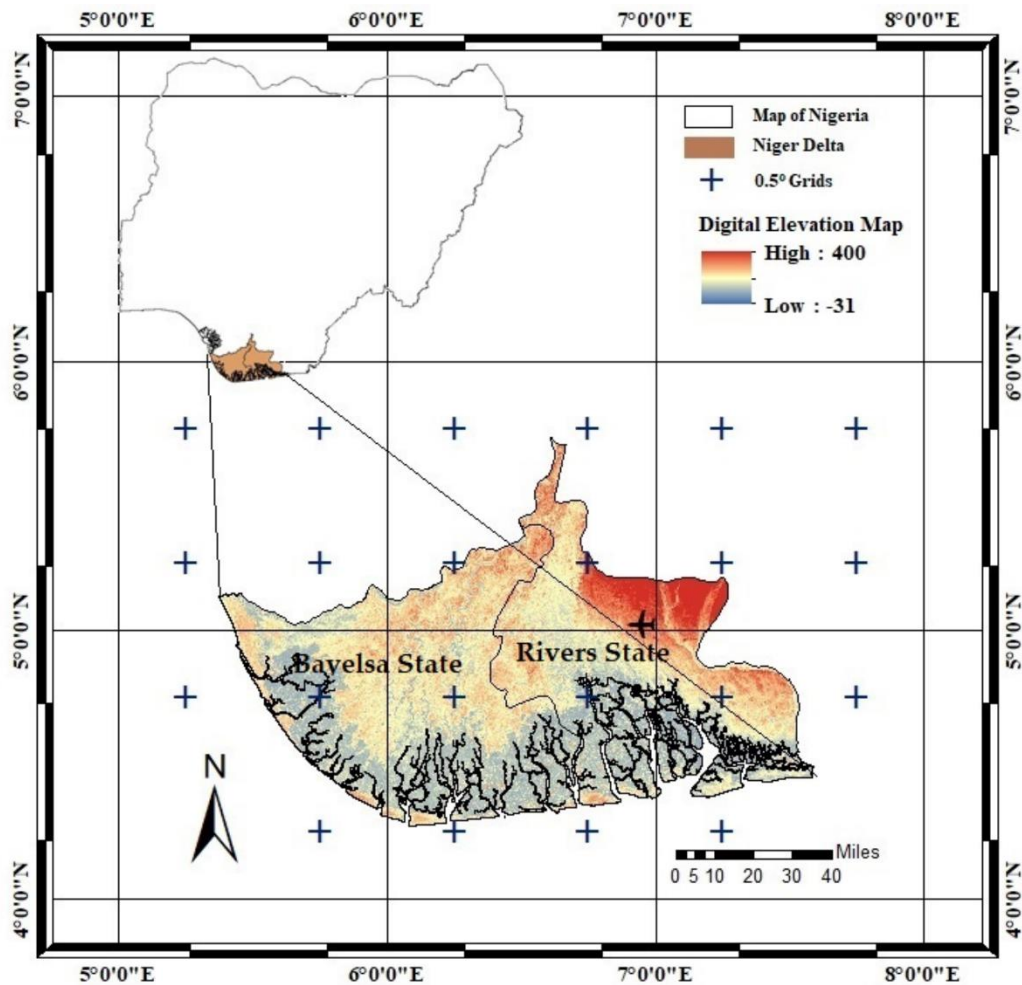


**Figure 5.1** Map of the study area showing the spatial distribution of  $0.5^{\circ} \times 0.5^{\circ}$  grids.

The mean monthly temperatures are higher up to 26.67 °C around March/April and as low as 24.44 °C during July/August giving a small annual range of 2.73 °C. The mean relative humidity of the area is relatively high often reaching 90%, while the warm, wet southwesterly winds blow inland most of the year and the dust-laden, warm-dry northeasterly winds occasionally reach the coast for small periods of the year (Etim U. U Ituen and A Folarin Alonge, 2009). Recent studies have shown that

during the last 20 years (Prince Mmom, 2013), a trend of an increase in prcp, Tmin and Tmax, and flood frequencies observed over the years in the Niger Delta due to global warming depicts a clear sign of climate change with a variable future climate over the region (Ologunorisa and Adeyemo, 2005; Ologunorisa and Tersoo, 2006; Amangabara and Obenade, 2015; Tawari-fufeyin, *et al.*,2015).

## **2.2.Data and Sources**

### **2.2.1. Gridded Dataset**

This study used the climate research unit (CRU) daily prcp, Tmax and Tmin datasets between the historic years of 1980 to 2005 over the Niger Delta part of Nigeria due to the scarcity of reliable long records of hydroclimatological station observations in the area. The CRU datasets are observation-based gridded prcp, Tmin and Tmax datasets, which are widely used because of their extensive spatial and temporal coverage extracted from the CRU version 4.01 global climate dataset (Harris, 2008; Harris *et al.*, 2014; Vaghefi *et al.*, 2017). They were found to be the best-fit datasets that replicated the distribution patterns, spatial, and temporal variability of the Niger Delta's observed datasets (Ashraf Vaghefi *et al.*, 2017). The gridded datasets were re-gridded to a common spatial resolution of  $0.5^{\circ} \times 0.5^{\circ}$  following the agreed resolution of the GCMs. The daily CRU datasets were downloaded from (<http://www.cru.uea.ac.uk>) resulting in an equal number of grids (22 grids), which were spatially distributed across the study area. The observed station data had only one observation within the study area, with two other contributing stations outside the study area. The historic daily climate data (prcp, Tmin and Tmax) within the same grid locations that housed the observed meteorological station were downscaled to the station resolution. These datasets covered a time period of 1980–2005 for the historical

period as the observed climate data; the GCM-simulated dataset covered the periods of 1950–2005 for the historical periods, and 2006–2099 for the future periods.

### **2.2.2. Coupled Model Inter-comparison Project Phase 5 (CMIP5) GCM Datasets**

Twenty-six GCMs of ISI-MIP (Inter-Sectorial Impact Model Inter-Comparison Project) (Hempel *et al.*, 2013) models (Table 1) and two carbon and other greenhouse, aerosols, etc., emission scenarios (RCP4.5 and RCP8.5) for the years (1980–2099) were downscaled for the basin in order to be consistent with the CRU dataset observations. The GCM data were obtained from the CMIP5 data portal website (<http://pcmdi9.llnl.gov/>). The GCMs were selected based on the availability of daily simulation for two representative concentration pathways (RCP), which were the RCP4.5 and RCP8.5 scenarios.

RCP4.5 is an intermediate pathway scenario that shows a good agreement with the latest policy of lower greenhouse gas emissions by the global community, while RCP8.5 is the business-as-usual scenario, which is consistent with a future that has no change in climate policy to reduce emissions (Wang *et al.*, 2016). Therefore, RCP4.5 and RCP8.5 were selected as these two scenarios can provide a possible complete range of impact. As the GCMs are available in different resolutions, all CMIP5 data were extracted and downscaled uniformly to the same spatial scale ( $0.5^\circ \times 0.5^\circ$ ) to reduce biases introduced by different resolutions for a fair comparison. This technique uses nearby areas to generate point output from each GCM at each grid point, thus providing a smooth interpolation that is widely used for the re-gridding of GCMs (Vaghefi *et al.*, 2017). Table 5.1 gives an overview of the GCMs.

**Table 5.1** : General circulation models (GCMs) used in the study at 0.5x0.5° grid.

<b>GCM No</b>	<b>GCM Name</b>	<b>Institute</b>	<b>Resolution</b>
1	ACCESS1.3	Commonwealth Scientific and Industrial Research Organization– Bureau of Meteorology, Australia	1.9 × 1.2
2	CanCM4	Canadian Center for Climate Modelling and Analysis, Canada	2.8 × 2.8
3	CanESM2		
4	CCSM4	National Centre for Atmospheric Research, USA	0.94 × 1.25
5	CMCC.CESM	Centro Euro-Mediterraneo sui Cambiamenti Climatici, Italy	0.7 × 0.7
6	CMCC.CMS		1.9 × 1.9
7	CNRM.CM5	Centre National de Recherches Météorologiques, Centre, France	1.4 × 1.4
8	CSIRO.Mk3.6.0	Commonwealth Scientific and Industrial Research Organization, Australia	1.9 × 1.9
9	CSIRO.Mk3L.1.2		
10	GFDL.CM3	Geophysical Fluid Dynamics Laboratory, USA	2.5 × 2.0
11	GFDL.ESM2M		
12	GISS.E2.H	NASA/GISS (Goddard Institute for Space Studies), USA	2.5 × 2.0
13	HadCM3	Met Office Hadley Centre, UK	1.9 × 1.2
14	HadGEM2.AO		
15	HadGEM2.CC		
16	HadGEM2.ES		
17	INMCM4	Institute of Numerical Mathematics, Russia	2.0 × 1.5
18	IPSL.CM45A.LR	Institut Pierre Simon Laplace, France	2.5 × 1.3
19	IPSL.CM5A.MR		3.7 × 1.9
20	MIROC.ESM	The University of Tokyo, National Institute for Environmental Studies, and Japan Agency for Marine-Earth Science and Technology, Japan	2.8 × 2.8
21	MIROC.ESM.CHM		
22	MIROC5		
23	MPI.ESM.LR	Max Planck Institute for Meteorology, Germany	1.9 × 1.9
24	MPI.ESM.MR		
25	MRI.CGCM3	Meteorological Research Institute, Japan	1.1 × 1.1
26	Noer.ESM1.M	Meteorological Institute, Norway	2.5 × 1.9

### 3. Methodology

The procedure for the identification and ranking of a subset of a GCM ensemble for simulation of the spatial and temporal projection of changes in rainfall and temperature for this study are outlined as follows:

1. Extracting and re-gridding of the selected 26 GCM datasets and CRU gridded datasets to a spatial resolution of  $0.5^{\circ} \times 0.5^{\circ}$  was carried out.
2. SU was then applied to evaluate and assess the association between the 26 GCMs and the CRU gridded observations (prcp, Tmax, and Tmin) at each of the 22 grid points of  $0.5^{\circ} \times 0.5^{\circ}$  resolution covering the study area (Figure 5.1), over the reference period 1980–2005.
3. The GCMs were then ranked based on the computed SU weight obtained at each grid points using the SU weighting technique, where a higher rank was given to GCMs with more weight in most of the grid points. A separate list of rank is prepared for each climatic variable (prcp, Tmax, and Tmin) and each gridded dataset (Table 5.2).
4. The overall GCM ranks were then derived (Equation (5.4)) considering all their ranks and the weights obtained at all 22 grids over the entire study area.
5. The final ranks of all three datasets were determined based on the frequency of occurrence of each GCM to combine the overall ranks in order to obtain a single rank for each GCM valid for the entire study.
6. For simplicity, the easiest and the most common method of bias correction was carried out for correction of the biases in the best-selected future GCM ensemble against the CRU gridded observations. The additive correction method was used for temperature bias correction while the multiplicative correction method was

used to correct the biases in prcp for GCM simulations under the two RCP scenarios for the period 2010–2099.

7. The ensemble of the best four performing GCMs was then used for the prediction of spatial, temporal, and seasonal changes in rainfall for three future periods (2010–2039, 2040–2069, and 2070–2099) against the historical period (1980–2005).

### 3.1. Model Selection Using Symmetrical Uncertainty

Symmetrical uncertainty (*SU*) is an information entropy-based filtering approach that measures the changes in entropy based on the concept of information entropy in order to assess the similarity or mutual information between the GCM and observed datasets (Shannon, 2001; Singh, Kushwaha and Vyas, 2014). The information entropy estimates the amount of information common between the two variables. For example, if  $P(X)$  and  $P(Y)$  are the probability density functions and  $P(X, Y)$  is the joint probability density function of A and B, then the entropy  $H$  between  $X$  and  $Y$  is given in Equation (5.1) below (Singh, Kushwaha and Vyas, 2014; Piao, Piao and Lee, 2019):

$$H(X, Y) = \sum P(X, Y) \log \frac{P(X, Y)}{P(X) \cdot P(Y)} \quad (5.1)$$

The relation of entropy and mutual information can then be used to solve the problem in different ways as follows; if  $H(X)$  denotes the entropy of  $X$ , then:

$$H(X) = - \int P(X) \log(P(X)) dx \quad (5.2)$$

The common information between the two variables is estimated by  $H$  as the difference between the sum of the entropies. The amount by which the entropy of  $X$  decreases reflects additional information about  $X$  provided by  $Y$ , and is called information gain ( $IG$ ), which is given by Equation (5.3) (Adami, 2004). Information gain ( $IG$ ) measures how much one random variable tells about another.

$$IG(X, Y) = H(X) - H(X, Y) \quad (5.3)$$

The  $H$  estimated using Equation (5.1) indicates the amount of mutual information between the observations and GCMs. If the variables are independent of each other, the  $IG$  is 0, while a higher value of  $IG$  indicates that the GCMs have a higher similarity to the gridded observations.

The  $IG$  is biased toward the variable having higher values. These biases are compensated for by dividing the  $IG$  value with the sum of the entropies of the random variables, which is referred to as  $SU$ . Therefore,  $SU$  provides an unbiased estimation of the degree of similarity or dissimilarity of a GCM with the corresponding observations regardless of the shape of the underlying distributions. The  $SU$  uses the following steps for GCM selection:

$$SU(X, Y) = 2 \frac{IG(X, Y)}{H(X) + H(Y)} \quad (5.4)$$

where  $H(X)$  and  $H(Y)$  denotes the conditional entropies of  $X$  and  $Y$ , while  $H(X, Y)$  represents the joint entropy of  $X$  and  $Y$ , respectively,  $SU$  values vary between 0 and 1, where 1 refers to a perfect agreement between the observations and GCMs, while a value of 0 refers to no agreement between the observations and GCMs (Shreem, Abdullah and Nazri, 2016).



### 3.2. Ranking of GCMs Using the Weighting Method

Ranking of GCMs at a single grid point is a relatively simple task. However, assessment and classification of GCMs from multiple grid points become difficult as the exercise may display different degrees of accuracies at different grid points. This becomes more difficult when the underlying preference model, like weights assignable to different attributes for some parameters, are considered. To overcome these challenges, a technique that aggregates and combines information from different sources such as the weighting method (Roszkowska, 2013), frequency of occurrence majority rule (Balinski and Laraki, 2019), and numerical averaging (Lin and Tung, 2017) can be employed. In this study, the ranks of the GCMs relating to each grid point were computed for each climate variable based on the computed SU weights for the 22 grid points, considering all 26 GCMs. These are then ranked based on the frequency of occurrence at different ranks (Kumar, 2015).

Then, the overall weight ( $W_o$ ) for each variable (i.e.,  $P$ ,  $T_{max}$ , and  $T_{min}$ ) and each GCM was determined by multiplying the frequency of occurrence of each GCM at a particular rank with the computed  $SU$  weight corresponding to its rank and summing all the values obtained (Ahmed *et al.*, 2019), as shown in Equation (5.5) below:

$$W_o = X_1(w_1) + X_2(w_2) + X_3(w_3) \dots \dots \dots + X_{26}(w_{26}) \quad (5.5)$$

where  $X$  represents the frequency of occurrence (e.g.,  $X_1$  corresponds to the frequency of occurrence of GCM at rank 1);  $w$  represents the weight corresponding to each rank, and  $W_o$  denotes the overall weight of each GCM. The ensemble of the four top-ranked GCMs was then considered for the simulation of daily prcp,  $T_{max}$ , and  $T_{min}$ .

### 3.3. Bias Correction

Projected raw GCM typically contains biases when compared with observations (Mehrotra and Sharma, 2015). Bias correction was carried out to correct the projected raw GCM output using the differences in the mean and variability between GCM and observed datasets. In this study, the biases in the daily time series of the variables (i.e., prcp, Tmin, and Tmax) from the four top-ranked GCM output were corrected using the easiest and the most common methods, which were the additive method for temperature and multiplicative method for prcp (Ashraf Vaghefi *et al.*, 2017; Xu, 2018; Beyer, Krapp and Manica, 2019). For temperature, the additive correction factor for each month was used, and the adjusted formula for modified daily temperature (Tmax and Tmin) is expressed in Equation (5.6).

$$T_{corrected_{ij}} = T_{GCM_{ij}} + (\bar{T}_{reference_{jk}} - \bar{T}_{GCM_{jk}}) \quad (5.6)$$

where  $T$  is the temperature;  $\bar{T}$  is the long-term average temperature; and  $i, j, k$  are the day, month, and year counters, respectively. For prcp, a multiplicative correction factor for each month is used, and the modified daily rainfall is expressed in Equation (5.7):

$$P_{corrected_{ij}} = P_{GCM_{ij}} * \frac{\bar{P}_{reference_{jk}}}{\bar{P}_{GCM_{jk}}} \quad (5.7)$$

where  $P$  is the precipitation (mm day<sup>-1</sup>), and  $\bar{P}$  is the long-term average precipitation.

### 3.4. Performance Assessment

Performance of the ensemble from all 26 GCMs and 4 SU selected GCMs of prcp, Tmax, and Tmin were examined using the correlation coefficient ( $R^2$ ) (Equation (5.8)), Nash–Sutcliff efficiency (NSE) (Equation (5.9)), and root mean square error

(RMSE) (Equation (5.10)), (Moriassi *et al.*, 2007). The correlation coefficient ( $R^2$ ) is a measure of how the ensemble GCMs are likely to be predicted by the model and is equivalent to the sample cross-correlation between ensemble GCMs and observed datasets, where the overbar denotes mean values.

$$R^2 = \left[ \frac{\sum_{i=1}^n (y_i - \bar{y})(o_i - \bar{o})}{\sqrt{[\sum_{i=1}^n (y_i - \bar{y})^2] [\sum_{i=1}^n (o_i - \bar{o})^2]}} \right] \quad (5.8)$$

where  $y$  and  $o$  are the predicted and observed values, respectively; and  $Nv$  is the number of target data used for testing.

The Nash–Sutcliffe efficiency ( $NSE$ ) indicates the goodness-of-fit of the simulated ensemble GCMs and observed data in line 1:1 and can range from  $-\infty$  to 1.  $NSE$  measures the predictive skill of a model relative to the mean of observations (Moriassi *et al.*, 2007). In this evaluation, the classification suggested by (Motovilov *et al.*, 1999) is described as:  $NSE > 0.75$  (model is appropriate and good);  $0.36 < NSE < 0.75$  (model is satisfactory); and  $NSE < 0.36$  (model is unsatisfactory) was adopted.

$$NSE = 1 - \left[ \frac{\sum_{i=1}^n (Y_i^{obs} - Y_i^{sim})^2}{\sum_{i=1}^n (Y_i^{obs} - Y^{mean})^2} \right] \quad (5.9)$$

where  $Y^{iobs}$  is the  $i$ th observation for the constituent being evaluated;  $Y^{isim}$  is the  $i$ th simulated value for the constituent being evaluated;  $Y^{mean}$  is the mean of observed data for the constituent being evaluated, and  $n$  is the total number of observations.

The root mean square error (RMSE) measures the global fitness of a predictive model.

$$RMSE = \sqrt{\frac{1}{n} \sum_{i=1}^n (y_o - y_i)^2} \quad (5.10)$$

where  $y$  and  $o$  are the observed and predicted values, respectively; and  $N_v$  is the number of target data used for testing.

## **4. Results and Discussion**

### **4.1. Ranking of the GCMs**

Time series GCM and CRU datasets for the period 1980–2005 were used to calculate the SU weights. The GCMs were then ranked according to the weight derived from the SU technique. The SU weights define the advantage of one GCM over the others in simulating the observations. The higher the coefficients, the better performance of the GCM of interest.

The overall scores attained by the GCMs over the entire study area was estimated using Equation (5.4), and the estimated scores for each GCM are shown in Table 5.2. In many cases, small SU weights were observed among the GCMs, mainly in prcp with zero weights, and in some cases observed in both Tmax and Tmin, which have also been reported in previous studies (Srinivasa and Kumar, 2015; Kumar *et al.*, 2017). The smaller difference in SU values among the GCMs indicated that all GCMs performed well with a similar degree of accuracy in replicating observations.

### **4.2. Spatial Distribution of Top-Ranked GCMs**

The SU filter was applied individually to the 26 GCM grid points ( $0.5^\circ \times 0.5^\circ$ ) for prcp, Tmax, and Tmin with CRU data over the study area. The spatial distribution of the GCM ensemble from the SU filter, which ranked as best, second best, and third-best are shown in Figures 5.2a–c. The results obtained shows that ACCESS1.3 was found to be the best GCM in simulating prcp in the first rank, while no single GCM

was found to dominate the study areas with prcp in the second and third rank. The spatial distribution of the SU GCMs shows that CSIRO.Mk3L.1.2 was found to dominate the first rank, IPSL.CM45A.LR was found to dominate the second rank, while GFDL.ESM2M was found to dominate the third rank in simulating both Tmax and Tmin GCMs over the entire study area. However, the distribution of SU GCMs shows that MIROC-ESM simulated both Tmax and Tmin in most of the study area.

Noer.ESM1-M was found to be the best in the western part of the area, while MIROC-ESM was found to be the best in the eastern part of the study area for the Tmax. ACCESS1.3 was also found to dominate the second rank for both Tmax and Tmin. No single GCM was found to dominate the study areas with prcp in the third rank. MIROC-ESM-CHM dominated the Tmin, while the CanESM2 was found to perform best in the western part of the area and MIROC.ESM.CHM was found to be the best in the south-eastern part of the area for Tmax in the third rank.

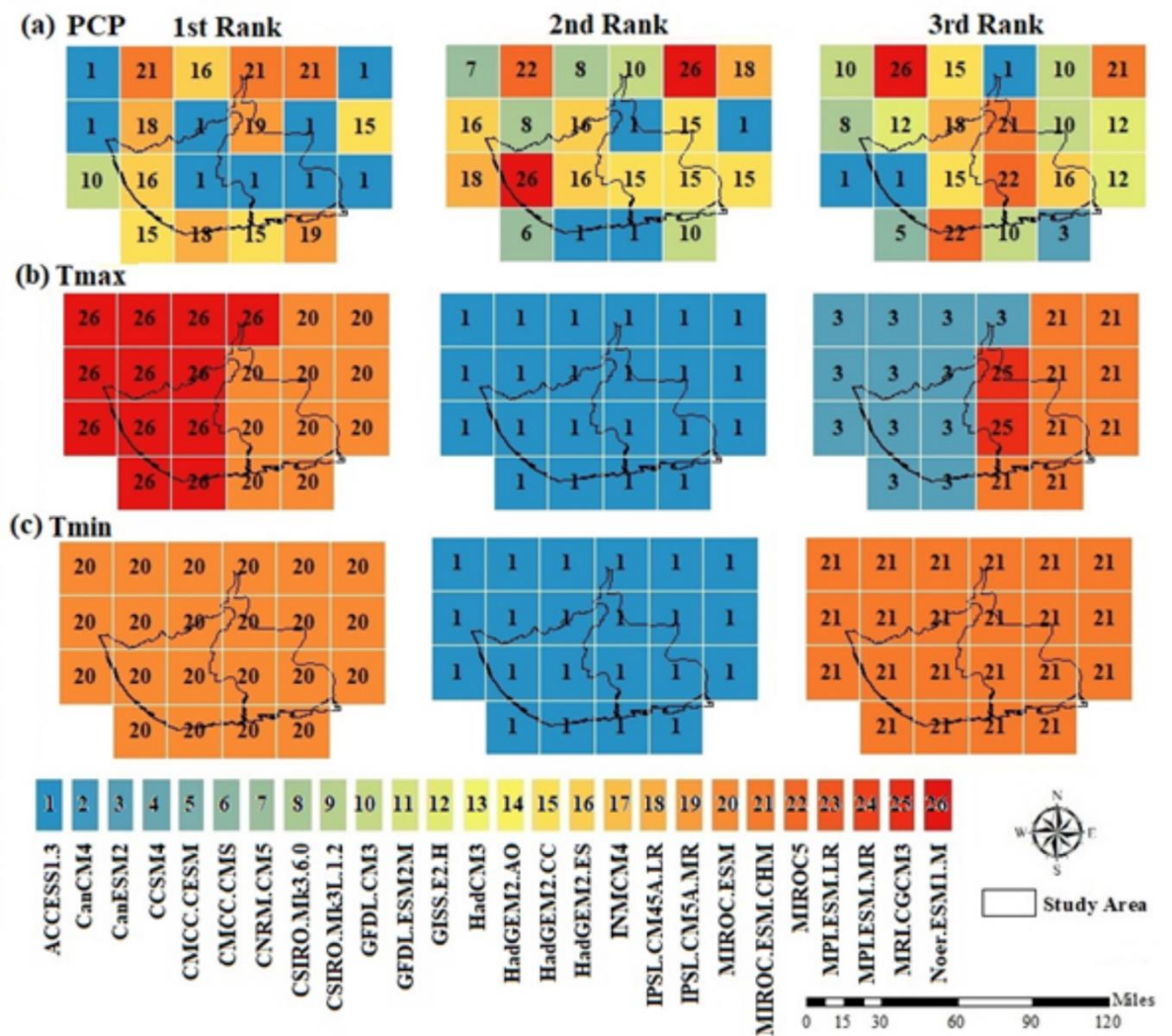


**Figure 5.2** The spatial distribution of GCMs ranked best, second-best, and third-best position using a symmetrical uncertainty filter at different grid points for Precp, Tmax, and Tmin over the Niger Delta.

### 4.3. Selection of GCM Ensemble

GCMs that can simulate both prcp, Tmax, and Tmin are considered more appropriate for climate change impact analysis (Khan *et al.*, 2018; Salman *et al.*, 2018). Twelve GCM outputs (shown in bold) ranking from the best performing to the worst are summarized in Table 6.2; the SU filter shows that the top four performing GCMs were ACCESS1.3, MIROC-ESM, MIROC-ESM-CHM, and NorESM1-M. These

results further verified (Abramowitz *et al.*, 2019), who suggested that GCMs should meet these criteria. The top four GCMs were selected according to their higher SU weight and common performance. Table 5.2 shows the overall GCMs ranks as well as their performances after bias correction in simulating the CRU prep, Tmax, and Tmin obtained from the overall weights derived from SU coefficients. The overall scores can be treated independently as separate data points as each model is a myriad of discrete process representations.

#### **4.4. Ensemble Model Validation**

The performance of the ensemble model at each grid point, for all 26 GCMs, four SU selected GCMs and CRU datasets were assessed by the coefficient of correlation ( $R^2$ ) and Nash–Sutcliff efficiency (NSE). As an example, the results obtained from the grid point in Port Harcourt is presented in Table 6.3. The results indicate that the ranking of GCMs assisted in identifying a better-performing GCM ensemble for the downscaling of simulations/projections and can be a possible way to produce more reliable hydroclimatic information at a finer spatial resolution and with reduced uncertainties.

Comparative plots of the mean monthly raw 26 GCMs and the four SU selected GCMs shown in Figure 5.3 show that the selected GCM outputs better matched the observed CRU datasets, which suggest a better performance after bias correction, as clearly proven in Figure 5.4. Results of the comparative analysis between the ensemble of all GCMs and the ensemble SU selected GCMs over the grid points as depicted in Table 6.3 showed a low RMSE with high NSE and  $R^2$  values, which shows that the SU ensemble performed better in depicting the CRU datasets. The ensemble of all GCMs

underestimated the sum (2166.91 mm) and the mean (5.94 mm) of CRU prcp (2227.95 mm and 6.19 mm), respectively. However, application of the SU filter in ensemble selection improved the results to a sum of 2255.49 mm and a mean of 6.23 mm. This trend was observed in all 22 grid points. A comparison of the mean values obtained at all the grid points for Tmax and Tmin confirmed the better performances of the SU model.

**Table 5.2 :** Overall SU weights of GCMs and their ranks according to their ability to simulate the CRU prcp, Tmax, and Tmin datasets. The selected GCMs are shown in bold font.

Ranks	GCMs	Prcp			Tmax			Tmin		
		SU	NSE	R <sup>2</sup>	SU	NSE	R <sup>2</sup>	SU	NSE	R <sup>2</sup>
1	<b>ACCESS1-3</b>	<b>0.28</b>	<b>0.58</b>	<b>0.81</b>	<b>0.15</b>	<b>0.67</b>	<b>0.84</b>	<b>0.09</b>	<b>0.86</b>	<b>0.55</b>
2	<b>MIROC-ESM</b>	<b>0.14</b>	<b>0.63</b>	<b>0.84</b>	<b>0.10</b>	<b>0.87</b>	<b>0.44</b>	<b>0.12</b>	<b>0.62</b>	<b>0.49</b>
3	<b>MIROC-ESM-CHM</b>	<b>0.15</b>	<b>0.69</b>	<b>0.56</b>	<b>0.11</b>	<b>0.86</b>	<b>0.86</b>	<b>0.02</b>	<b>0.50</b>	<b>0.58</b>
4	<b>Noer-ESM1-M</b>	<b>0.13</b>	<b>0.57</b>	<b>0.82</b>	<b>0.14</b>	<b>0.82</b>	<b>0.89</b>	<b>0.05</b>	<b>0.38</b>	<b>0.48</b>
5	<b>MIROC5</b>	<b>0.08</b>	<b>0.62</b>	<b>0.82</b>	<b>0.15</b>	<b>5.36</b>	<b>0.88</b>	<b>0.06</b>	<b>1.88</b>	<b>0.45</b>
6	<b>HadGEM2-ES</b>	<b>0.19</b>	<b>0.59</b>	<b>0.81</b>	<b>0.03</b>	<b>0.88</b>	<b>0.91</b>	<b>0.02</b>	<b>0.54</b>	<b>0.53</b>
7	<b>CanCM4</b>	<b>0.07</b>	<b>0.49</b>	<b>0.74</b>	<b>0.08</b>	<b>0.91</b>	<b>0.91</b>	<b>0.01</b>	<b>0.65</b>	<b>0.48</b>
8	<b>MRI-CGCM3</b>	<b>0.06</b>	<b>0.55</b>	<b>0.78</b>	<b>0.11</b>	<b>0.70</b>	<b>0.87</b>	<b>0.03</b>	<b>0.48</b>	<b>0.51</b>
9	<b>MPI-ESM-MR</b>	<b>0.06</b>	<b>0.35</b>	<b>0.78</b>	<b>0.05</b>	<b>0.75</b>	<b>0.87</b>	<b>0.02</b>	<b>0.49</b>	<b>0.51</b>
10	<b>CMCC-CMS</b>	<b>0.08</b>	<b>0.55</b>	<b>0.78</b>	<b>0.11</b>	<b>0.63</b>	<b>0.79</b>	<b>0.04</b>	<b>0.31</b>	<b>0.45</b>
11	<b>CNRM-CM5</b>	<b>0.10</b>	<b>0.44</b>	<b>0.73</b>	<b>0.07</b>	<b>0.64</b>	<b>0.81</b>	<b>0.01</b>	<b>0.28</b>	<b>0.51</b>
12	<b>CanESM2</b>	<b>0.10</b>	<b>0.52</b>	<b>0.77</b>	<b>0.12</b>	<b>2.18</b>	<b>0.67</b>	<b>0.01</b>	<b>6.48</b>	<b>0.25</b>
13	IPSL-CM45A-LR	0.15	0.63	0.85	0.03	0.81	0.91	0	0.42	0.57
14	HadGEM2-CC	0.21	0.58	0.82	0	0.90	0.90	0	0.63	0.45
15	HadCM3	0.09	0.58	0.80	0	0.91	0.91	0	0.67	0.51
16	CMCC-CESM	0.08	0.61	0.81	0.00	0.89	0.89	0	0.65	0.48
17	IPSL-CM5A-MR	0.11	0.47	0.74	0	0.84	0.85	0	0.64	0.46
18	GFDL-ESM2M	0.11	0.49	0.74	0.04	0.79	0.85	0	0.40	0.55
19	CSIRO-Mk3L-1-2	0.05	0.31	0.60	0	0.89	0.89	0	0.68	0.53
20	HadGEM2-AO	0.03	0.62	0.83	0	0.84	0.81	0	0.49	0.29
21	GISS-E2-H	0.14	0.32	0.62	0	0.74	0.76	0	0.56	0.37
22	MPI-ESM-LR	0.06	0.55	0.80	0	0.00	0.87	0	0.63	0.56
23	CSIRO-Mk3-6-0	0.13	0.44	0.71	0.02	0.15	0.83	0	0.06	0.57
24	INMCM4	0.05	0.42	0.68	0	0.60	0.69	0	0.54	0.42
25	CCSM4	0.09	0.51	0.76	0	0.70	0.66	0	0.44	0.46
26	GFDL-CM3	0.21	0.35	0.42	0	0.62	0.15	0	0.37	0.20



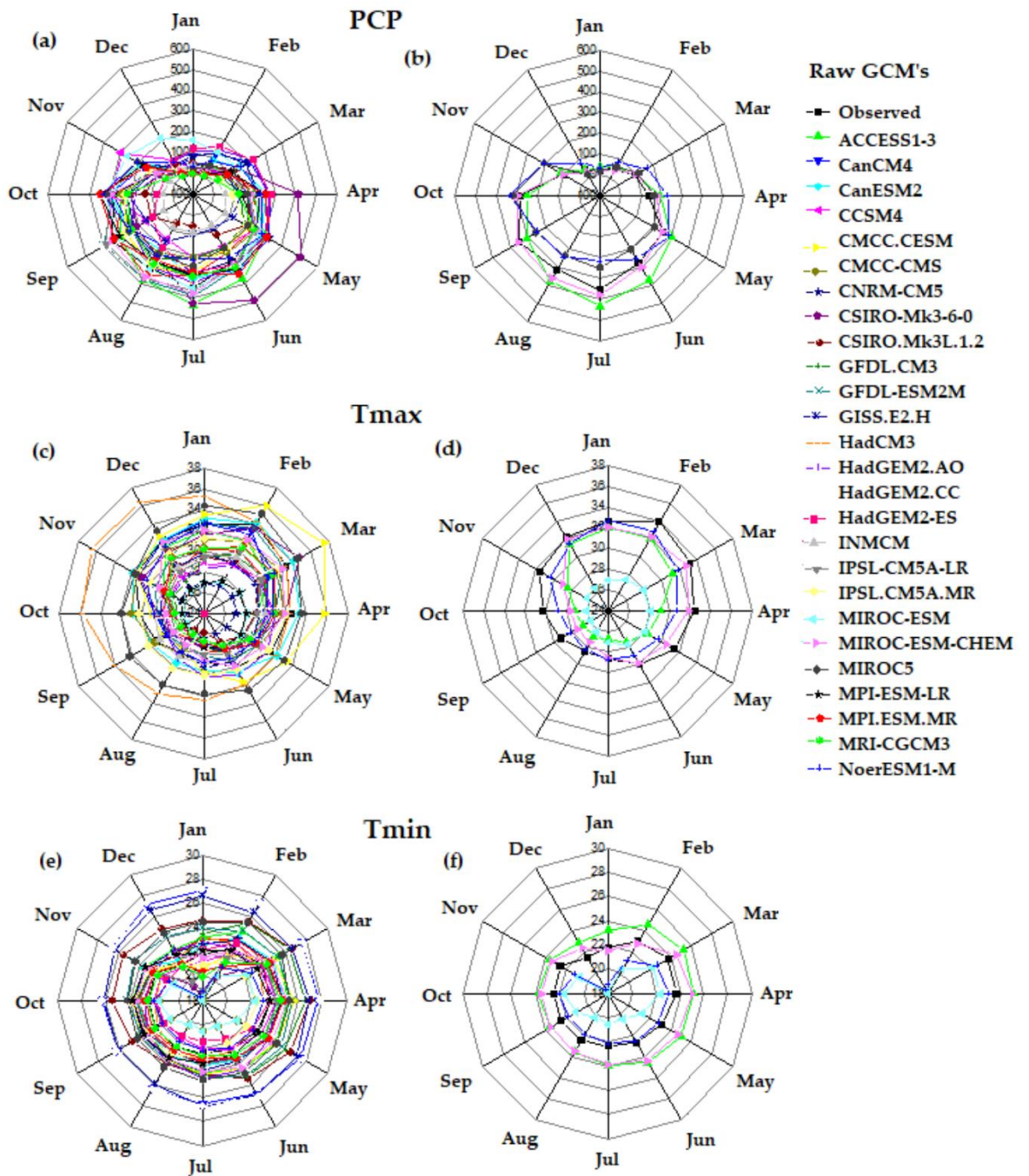


**Figure 5.3** Monthly averages of CRU and raw datasets. (a) 26 Prcp, (b) 4 Prcp SU, (c) 26 Tmax, (d) 4 Tmax SU, (e) 26 Tmin, and (f) 4 Tmin SU GCM outputs for the historical period 1980–2005 at the grid point located in Port Harcourt.

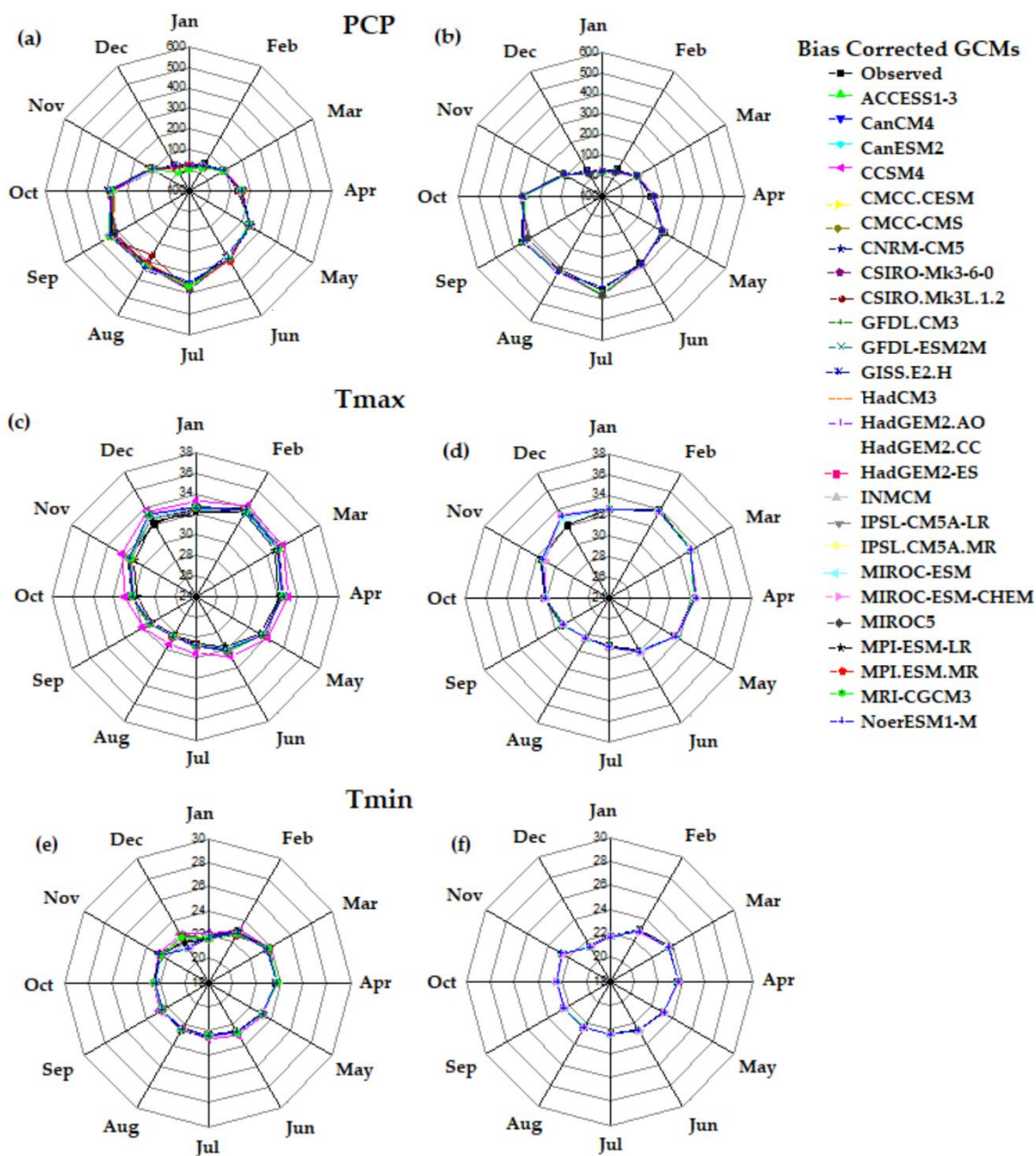


**Figure 5.4** Monthly averages of CRU and bias-corrected datasets. (a) 26 Prcp, (b) 4 Prcp SU, (c) 26 Tmax, (d) 4 Tmax SU, (e) 26 Tmin, and (f) 4 Tmin SU GCM outputs for the historical period 1980–2005 at the grid point located in Port Harcourt.

The seasonal averages of the bias-corrected 26 GCM output and the four selected models were compared to that of the CRU datasets in order to assess the performance of the downscaled model presented in Figure 5.4. The figures show that

the selected GCMs better matched the CRU datasets after correcting the biases, which were assumed to indicate that they produced more realistic projections.

The obtained results were further validated using interval plots of changes in the annual averages of CRU datasets with the ensemble of all 26 GCMs, and the four selected SU GCMs for prcp, Tmax, and Tmin (Figure 5.5). The changes and the levels of uncertainty were estimated using the RMSE, and the 95% confidence band shows the spread of the uncertainties during the future periods. The results obtained indicated the efficiency of the SU ensemble models in GCM selection. Overall, the SU filter was found to perform well in improving GCM ensemble selection for simulating the sum and mean values in the region, as shown in Table 5.3.

**Table 5.3 :** Performance assessment of the GCM ensemble at the grid located in Port Harcourt.

Mean Annual	Observed	GCM Ensemble		
		All	SU	
<b>Prcp (mm)</b>	<b>Sum</b>	2227.95	2166.91	2255.49
	<b>Mean</b>	6.19	5.94	6.23
	<b>RMSE</b>	-	2.42	2.62
	<b>NSE</b>	-	0.58	0.62
	<b>R<sup>2</sup></b>	-	0.86	0.83
<b>Tmax (°C)</b>	<b>Mean</b>	31.13	31.20	31.06
	<b>RMSE</b>	-	0.68	0.71
	<b>NSE</b>	-	1.00	1.00
	<b>R<sup>2</sup></b>	-	0.92	0.92
<b>Tmin (°C)</b>	<b>Mean</b>	22.63	23.12	22.72
	<b>RMSE</b>	-	0.88	1.17
	<b>NSE</b>	-	1.00	1.00
	<b>R<sup>2</sup></b>	-	0.64	0.62

The results showed a reproduction of the CRU observed datasets by the SU ensemble mean for Prcp, Tmax, and Tmin. This indicates that the SU ensemble selection approach can improve the accuracy in the projection by reducing uncertainties associated with individual GCMs.

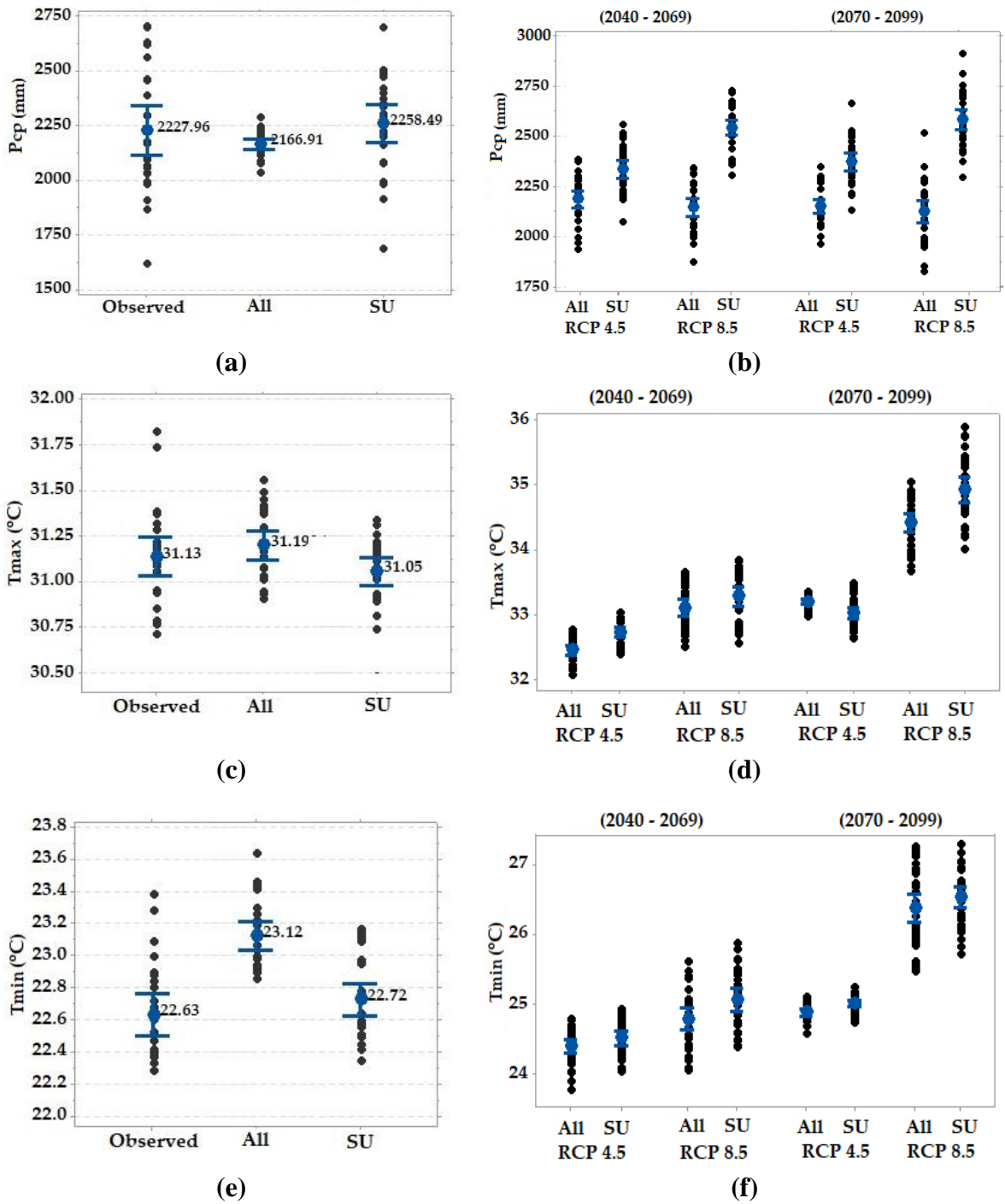


**Figure 5.5** Interval plots for the annual averages of CRU datasets with the ensemble of all 26 GCMs and the four SU selected GCMs for (a) Prcp (base period), (b) Prcp (future periods), (c) Tmax (base period), (d) Tmax (future periods), (e) Tmin (base period), and (f) Tmin (future periods) with 95% confidence interval at the grid located in Port Harcourt.



#### 4.5. Spatial Changes in Mean Annual Prcp, Tmax, and Tmin

The SU selected GCM ensemble was used in this study to map the generated mean changes in Prcp, Tmax, and Tmin in the Niger Delta. To estimate these percentage changes, the averages of the CRU prcp, Tmax, and Tmin for the base period 1980–2005 at all grid points were subtracted from those of the projected prcp, Tmax, and Tmin for the different future periods, 2040–2069, and 2070–2099 as shown in Figures 5.6, 5.7, and 5.8 respectively.

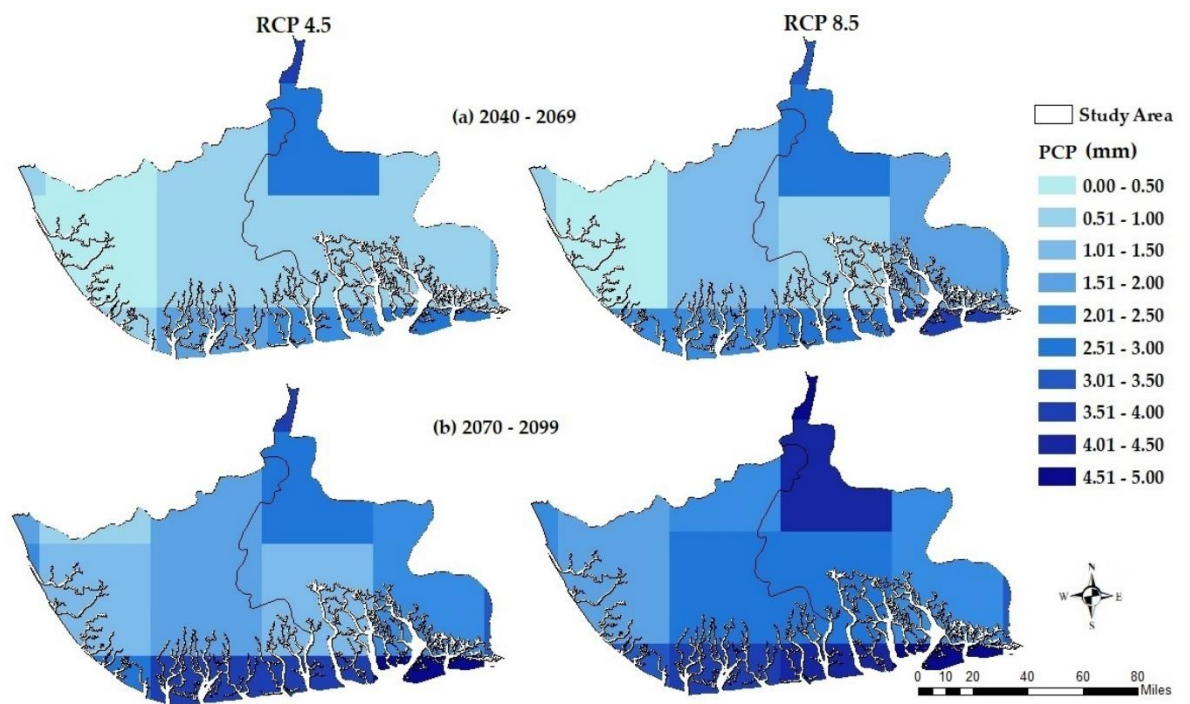


**Figure 5.6** Spatial distribution of percentage changes in average annual prcp, for periods (a) 2040–2069 and (b) 2070–2099 compared to the base period 1980–2005 for RCP4.5 and RCP8.5.

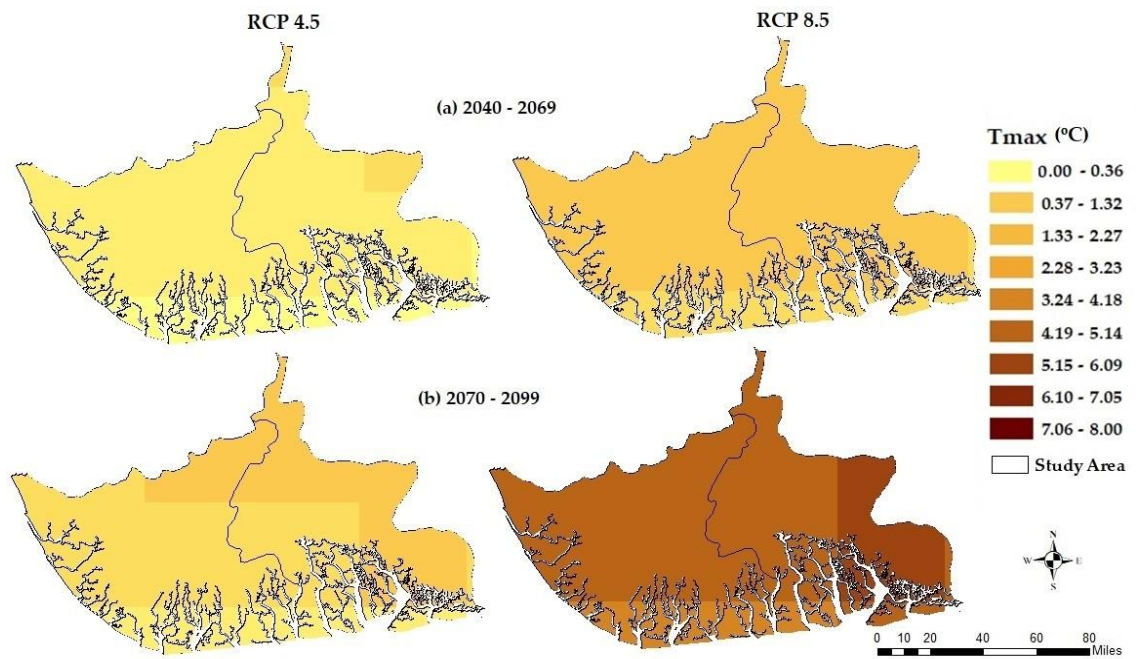


**Figure 5.7** Spatial distribution of percentage changes in average annual maximum temperature for periods (a) 2040–2069 and (b) 2070–2099 compared to the base period 1980–2005 for RCP4.5 and RCP8.5.

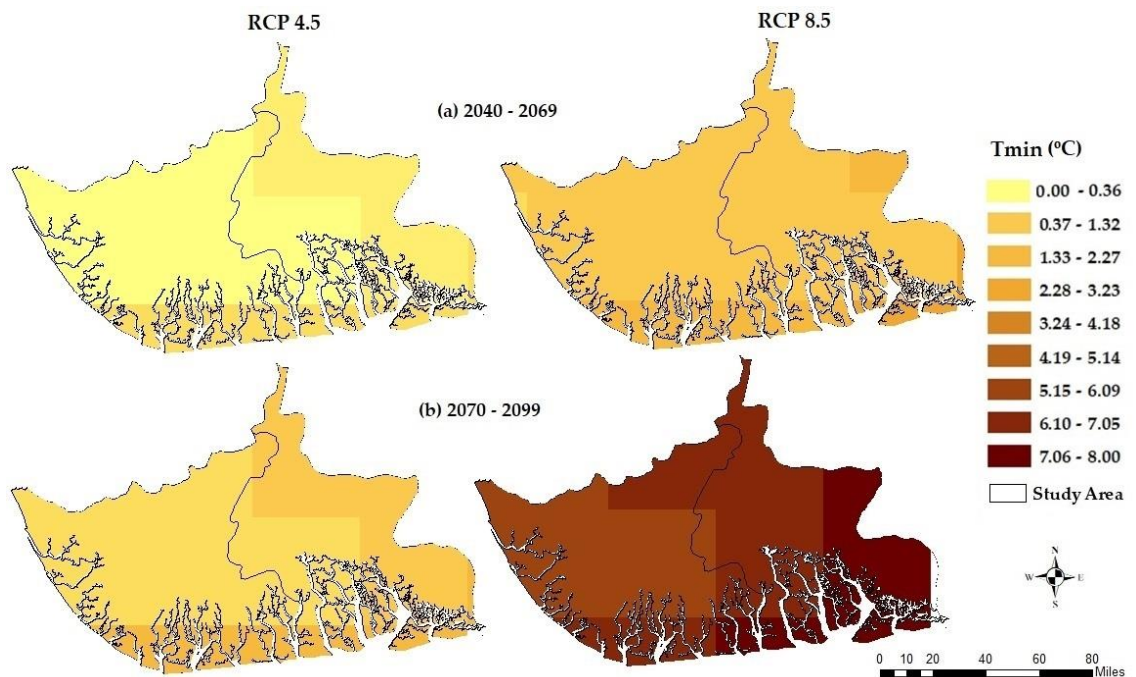


**Figure 5.8** Spatial distribution of percentage changes in average annual minimum temperature for periods (a) 2040–2069 and (b) 2070–2099 compared to the base period 1980–2005 for RCP4.5 and RCP8.5.

Figure 5.6 shows the variation in prcp changes across the area. The coastal areas are generally projected to have the highest percentage of changes in prcp for all RCPs and future periods, while the north-western part showed the lowest percentage changes. The changes in prcp ranged between 0.3% to 3.78% under RCP 4.5, and 1.62% to 4.74% under RCP8.5 for the period 2040–2069. During the period 2070–2099, a change between 0.26% to 3.57% under RCP4.5, and 0.7% to 4.94% under RCP8.5 was also projected across the study area.

The projected changes in annual Tmax and Tmin (Figures 5.7 and 5.8) show an increasing trend across the study area for both future periods and RCPs. Tmax is projected to increase significantly by 3–8% (0.4 °C) under RCP4.5 and between 3.89–5.47% (1.25–1.79 °C) under RCP8.5 during the periods 2070–2099. Tmin is also expected to increase significantly by 0.31–2.52% (0.52 °C) under RCP4.5 and between 5.64–8.22% (1.38–2.02 °C) under RCP8.5 during the periods 2070–2099, as expected in response to greenhouse gases forcing, which is consistent with other parts of the world (Martín, Bethencourt and Cuevas-Agulló, 2012; Rangwala and Miller, 2012; Krinner *et al.*, 2013; Expósito *et al.*, 2015).

Based on the projected values of simulated climatic variables over the study area, the projected increase of this climate variable confirms the report of IPCC (IPCC, 2007a) as well as the studies by Ike and Emaziye, (2012); Todd, (2015); Agumagu, (2018); Matemilola *et al.*, (2019) in this region. These increase will further aggravate the vulnerability of the water quality, water resources, agricultural land, fisheries, and livestock in the Niger Delta coastal zone to climate change. The region might experience more extreme floods, which might threaten the livelihoods and socio-economic growth of the region, which might then also have a significant impact

on Nigeria's GDP as the primary source of the country's revenue is the oil and gas from the study area.

## 5. Conclusions

A suitable set of GCM ensembles for simulating the Spatio-temporal changes in both prcp, Tmin, and Tmax were selected based on their performances in simulating the observed CRU datasets using the symmetrical uncertainty (SU) filter using 26 GCM outputs under RCP4.5 and RCP8.5 emission scenarios. The study identified four GCMs, namely ACCESS1.3, MIROC-ESM, MIROC-ESM-CHM, and NorESM1-M as the most suitable set of GCMs for simulating both prcp, Tmax, and Tmin over the Niger Delta. Though several studies have been conducted to assess future changes in prcp, Tmax, and Tmin at global scales, only limited studies have been conducted in West Africa and Nigeria. This study, therefore, is the first attempt to employ a selection of suitable sets of daily GCMs to simulate both prcp, Tmin, and Tmax together for the spatiotemporal projection changes in the Niger Delta.

The findings of this study predicted an increase in both Tmin, Tmax, and prcp for both periods and RCPs. The predicted increase in future prcp and temperature is useful to inform all stakeholders of the need to regulate anthropogenic activities such as gas flaring, illegal refining of crude oil, and other petrochemical products, which release more CO<sub>2</sub> and other greenhouse gases into the atmosphere in this region. This study will be useful in sustainable environmental management in the extreme weather driven by emerging climate change in the coastal zones of the Niger Delta, Nigeria.

**Author Contributions:** I.H. and R.M.K. designed the research; I.H. wrote the original draft.; R.M.K., C.J.W. and J.A.A reviewed and edited the manuscript and provide



technical help and proposed important additions with the model and to the manuscript.; C.J.W. gave critical views on the manuscript for further improvement.

**Funding:** This research was funded by the Petroleum Technology and Development Fund (PTDF) under the Overseas PhD scholarship scheme and supported by the Scottish Government under the Climate Justice Fund Water Futures Programme, awarded to the University of Strathclyde (R.M. Kalin).

**Conflicts of Interest:** The authors declare no conflicts of interest.

### References:

Abramowitz, G., Herger, N., Gutmann, E., Hammerling, D., Knutti, R., Leduc, M. and Schmidt, G. A. (2019). ESD Reviews: Model dependence in multi-model climate ensembles: Weighting, sub-selection and out-of-sample testing. *Earth System Dynamics*, 10(1), 91–105. <https://doi.org/10.5194/esd-10-91-2019>.

Adami, C. (2004). Information theory in molecular biology. *Physics of Life Reviews*, 1(1), 3–22. <https://doi.org/10.1016/j.plrev.2004.01.002>.

Adejuwon, J. O. (2012). Rainfall seasonality in the Niger Delta Belt, Nigeria. *Journal of Geography and Regional Planning*, 5(2), 51–60. <https://doi.org/10.5897/JGRP11.096>.

Ahmed, K., Shahid, S., Sachindra, D. A., Nawaz, N., and Chung, E. S. (2019). Fidelity assessment of general circulation model simulated precipitation and temperature over Pakistan using a feature selection method. *Journal of Hydrology*, 573 (November 2018), 281–298. <https://doi.org/10.1016/j.jhydrol.2019.03.092>.

Ahmed, K., Shahid, S., Wang, X., Nawaz, N., and Najeebullah, K. (2019). Evaluation of gridded precipitation datasets over arid regions of Pakistan. *Water*, MDPI (Switzerland), 11(2). <https://doi.org/10.3390/w11020210>.

Amadi, A. N, Olasehinde, P. I., & Nwankwoala, H. O. (2014). Hydrogeochemistry

and Statistical Analysis of Benin Formation in Eastern Niger Delta, Nigeria, 4(3), 327–338.

Amadi, Akobundu N. (2014). Impact of Gas-Flaring on the Quality of Rain Water, Groundwater and Surface Water in Parts of Eastern Niger Delta, Nigeria. *Journal of Geosciences and Geomatics*, 2(3), 114–119. <https://doi.org/10.12691/JGG-2-3-6>.

Amangabara, G., and Obenade, M. (2015). Flood Vulnerability Assessment of Niger Delta States Relative to 2012 Flood Disaster in Nigeria. *American Journal of Environmental Protection*, 3(3), 76–83. <https://doi.org/10.12691/env-3-3-3>.

Ashraf Vaghefi, S., Abbaspour, N., Kamali, B., and Abbaspour, K. C. (2017). A toolkit for climate change analysis and pattern recognition for extreme weather conditions – Case study: California-Baja California Peninsula. *Environmental Modelling and Software*, 96(October), 181–198. <https://doi.org/10.1016/j.envsoft.2017.06.033>.

Balinski, M., & Laraki, R. (2019). Majority judgment vs. majority rule. *Social Choice & Welfare*. Springer Berlin Heidelberg. <https://doi.org/10.1007/s00355-019-01200-x>.

Barfus, K., and Bernhofer, C. (2015). Assessment of GCM capabilities to simulate tropospheric stability on the Arabian Peninsula. *International Journal of Climatology*, 35(7), 1682–1696. <https://doi.org/10.1002/joc.4092>.

Beyer, R., Krapp, M., and Manica, A. (2019). A systematic comparison of bias correction methods for paleoclimate simulations. *Climate of the Past Discussions*, (February), 1–23. <https://doi.org/10.5194/cp-2019-11>.

Chandrashekar, G., and Sahin, F. (2014). A survey on feature selection methods. *Computers and Electrical Engineering*, 40(1), 16–28. <https://doi.org/10.1016/j.compeleceng.2013.11.024>.

Chen, J., Brissette, F. P., and Leconte, R. (2011). Uncertainty of downscaling method in quantifying the impact of climate change on hydrology. *Journal of Hydrology*, 401(3–4), 190–202. <https://doi.org/10.1016/j.jhydrol.2011.02.020>.

Dudek, G. (2010). Tournament searching method to feature selection problem. Lecture

Notes in Computer Science (Including Subseries Lecture Notes in Artificial Intelligence and Lecture Notes in Bioinformatics), 6114 LNAI(PART 2), 437–444. [https://doi.org/10.1007/978-3-642-13232-2\\_53](https://doi.org/10.1007/978-3-642-13232-2_53).

Etim U. U. Ituen, and A. Folarin Alonge. (2009). Niger Delta Region of Nigeria, Climate Change and the way Forward. *Bioenergy Engineering*, 11-14 October 2009, Bellevue, Washington, (January 2009). <https://doi.org/10.13031/2013.29162>.

Expósito, F. J., González, A., Pérez, J. C., Díaz, J. P., and Taima, D. (2015). High-resolution future projections of temperature and precipitation in the Canary Islands. *Journal of Climate*, 28(19), 7846–7856. <https://doi.org/10.1175/JCLI-D-15-0030.1>.

Foley, A. M. (2010). Uncertainty in regional climate modelling: A review. *Progress in Physical Geography*, 34(5), 647–670. <https://doi.org/10.1177/0309133310375654>.

Hammami, D., Lee, T. S., Ouarda, T. B. M. J., and Le, J. (2012). Predictor selection for downscaling GCM data with LASSO. *Journal of Geophysical Research Atmospheres*, 117(17), 1–11. <https://doi.org/10.1029/2012JD017864>.

Harris, I., Jones, P. D., Osborn, T. J., and Lister, D. H. (2014). Updated high-resolution grids of monthly climatic observations - the CRU TS3.10 Dataset. *International Journal of Climatology*, 34(3), 623–642. <https://doi.org/10.1002/joc.3711>.

Hassan, I., Kalin, R. M., White, C. J., and Aladejana, J. A. (2020). Evaluation of Daily Gridded Meteorological Datasets over the Niger Delta Region of Nigeria and Implication to Water Resources Management. *Atmospheric and Climate Sciences (ACS), SCRIP*.

Hempel, S., Frieler, K., Warszawski, L., Schewe, J., and Piontek, F. (2013). A trend-preserving bias correction – The ISI-MIP approach. *Earth System Dynamics*, 4(2), 219–236. <https://doi.org/10.5194/esd-4-219-2013>.

Hijmans, R. J., Cameron, S. E., Parra, J. L., Jones, P. G., and Jarvis, A. (2005). Very high resolution interpolated climate surfaces for global land areas. *International Journal of Climatology*, 25(15), 1965–1978. <https://doi.org/10.1002/joc.1276>.

Ike, P. C., and Emaziye, P. O. (2012). An Assessment of the Trend and Projected Future Values of Climatic Variables in Niger Delta Region, Nigeria, 4(2), 165–170.

IPCC. (1990). Climate Change the Intergovernmental Panel on Climate Change (IPCC) Scientific Assessment. <https://doi.org/10.1097/MOP.0b013e3283444c89>.

IPCC. (2007). Climate Change 2007: Impacts, Adaptation and Vulnerability: contribution of Working Group II to the fourth assessment report of the Intergovernmental Panel. Geneva, Suíça. <https://doi.org/10.1256/004316502320517344>.

Jiang, X., Waliser, D. E., Xavier, P. K., Petch, J., Klingaman, N. P., Woolnough, S. J., and Zhu, H. (2015). Vertical structure and physical processes of the Madden-Julian oscillation: Exploring key model physics in climate simulations. *Journal of Geophysical Research: Atmospheres*, 120(10), 4718–4748. <https://doi.org/10.1002/2014JD022375>.

Jones, P.D. and Harris, I. C. (2008). Climatic Research Unit (CRU) time-series datasets of variations in climate with variations in other phenomena. *NCAS British Atmospheric Data Centre*. Retrieved from <http://catalogue.ceda.ac.uk/uuid/3f8944800cc48e1cbc29a5ee12d8542d>.

Khan, N., Shahid, S., Ahmed, K., Ismail, T., Nawaz, N., and Son, M. (2018). Performance Assessment of General Circulation Model in Simulating Daily Precipitation and Temperature Using Multiple Gridded Datasets. *Water*, MDPI, 10(12), 1793. <https://doi.org/10.3390/w10121793>.

Knutti, R., Masson, D., and Gettelman, A. (2013). Climate model genealogy: Generation CMIP5 and how we got there. *Geophysical Research Letters*, 40(6), 1194–1199. <https://doi.org/10.1002/grl.50256>.

Krinner, G., Germany, F., Shongwe, M., Africa, S., France, S. B., Uk, B., and Lucas, C. (2013). Long-term climate change: Projections, commitments and irreversibility. Climate Change 2013 the Physical Science Basis: *Working Group I Contribution to the Fifth Assessment Report of the Intergovernmental Panel on Climate Change*,

9781107057, 1029–1136. <https://doi.org/10.1017/CBO9781107415324.024>.

Lin, C. Y., and Tung, C. P. (2017). Procedure for selecting GCM datasets for climate risk assessment. *Terrestrial, Atmospheric and Oceanic Sciences*, 28(1), 43–55. [https://doi.org/10.3319/TAO.2016.06.14.01\(CCA\)](https://doi.org/10.3319/TAO.2016.06.14.01(CCA)).

Lutz, A. F., Maat, H. W., Biemans, H., Shrestha, A. B., Wester, P., and Immerzeel, W. W. (2016). Selecting representative climate models for climate change impact studies: an advanced envelope-based selection approach. *International Journal of Climatology*, 36(12), 3988–4005. <https://doi.org/10.1002/joc.4608>.

Ma, C.-W., and Ma, Y.-G. (2018). Shannon Information Entropy in Heavy-ion Collisions. <https://doi.org/10.1016/j.pnpnp.2018.01.002>.

Martín, J. L., Bethencourt, J., and Cuevas-Agulló, E. (2012). Assessment of global warming on the island of Tenerife, Canary Islands (Spain). Trends in minimum, maximum and mean temperatures since 1944. *Climatic Change*, 114(2), 343–355. <https://doi.org/10.1007/s10584-012-0407-7>.

Matemilola, S., Adedeji, O. H., Elegbede, I., and Kies, F. (2019). Mainstreaming climate change into the EIA process in Nigeria: Perspectives from projects in the Niger Delta Region. *Climate*, 7(2). <https://doi.org/10.3390/cli7020029>.

McSweeney, C. F., Jones, R. G., Lee, R. W., and Rowell, D. P. (2015). Selecting CMIP5 GCMs for downscaling over multiple regions. *Climate Dynamics*, 44(11–12), 3237–3260. <https://doi.org/10.1007/s00382-014-2418-8>.

Mehrotra, R., and Sharma, A. (2015). Correcting for systematic biases in multiple raw GCM variables across a range of timescales. *Journal of Hydrology*, 520(January), 214–223. <https://doi.org/10.1016/j.jhydrol.2014.11.037>.

Min, S. K., and Hensel, A. (2007). A Bayesian Assessment of Climate Change Using Multimodal Ensembles. Part II: Regional and Seasonal Mean Surface Temperatures. *Journal of Climate*, 20(12), 2769–2790. <https://doi.org/10.1175/jcli4178.1>.

Moriasi, D. N., Arnold, J. G., Liew, M. W. Van, Bingner, R. L., Harmel, R. D., and

- Veith, T. L. (2007). Model Evaluation Guidelines for Systematic Quantification of Accuracy in Watershed Simulations. *American Society of Agricultural and Biological Engineers*, 50(3), 885–900.
- Motovilov, Y. G., Gottschalk, L., Engeland, K., and Rodhe, A. (1999). Validation of a distributed hydrological model against spatial observations, 99.
- Northrop, P. J. (2013). A simple, coherent framework for partitioning uncertainty in climate predictions". *Journal of Climate*, 26(12), 4375–4376. <https://doi.org/10.1175/JCLI-D-12-00527.1>.
- Obroma Agumagu, O. A. (2018). Projected Changes in the Physical Climate of the Niger Delta Region of Nigeria. *SciFed Journal of Global Warming*.
- Ologunorisa, T E, and Tersoo, T. (2006). The changing rainfall pattern and its implication for flood frequency in Makurdi, Northern Nigeria. *Journal of Applied Sciences and Environmental Management*, 10(3), 97–102. Retrieved from <http://www.ajol.info/index.php/jasem/article/view/17327>.
- Ologunorisa, Temi E., and Adeyemo, A. (2005). Public perception of flood hazard in the Niger Delta, Nigeria. *Environmentalist*, 25(1), 39–45. <https://doi.org/10.1007/s10669-005-3095-2>.
- Perkins, S. E., Pitman, A. J., Holbrook, N. J., and McAnarney, J. (2007). Evaluation of the AR4 climate models' simulated daily maximum temperature, minimum temperature, and precipitation over Australia using probability density functions. *Journal of Climate*, 20(17), 4356–4376. <https://doi.org/10.1175/JCLI4253.1>.
- Piao, M., Piao, Y., and Lee, J. Y. (2019). Symmetrical uncertainty-based feature subset generation and ensemble learning for electricity customer classification. *Symmetry*, 11(4), 4–13. <https://doi.org/10.3390/sym11040498>.
- Pierce, D. W., Barnett, T. P., Santer, B. D., and Gleckler, P. J. (2009). Selecting global climate models for regional climate change studies. *Proceedings of the National Academy of Sciences*, 106(21), 8441–8446. <https://doi.org/10.1073/pnas.0900094106>

- Prince C. Mmom, (2013). Vulnerability and Resilience of Niger Delta Coastal Communities to Flooding. *IOSR Journal of Humanities and Social Science*, 10(6), 27–33. <https://doi.org/10.9790/0837-1062733>.
- Rangwala, I., and Miller, J. R. (2012). Climate change in mountains: A review of elevation-dependent warming and its possible causes. *Climatic Change*, 114(3–4), 527–547. <https://doi.org/10.1007/s10584-012-0419-3>.
- Reichler, T., and Kim, J. (2008). How well do coupled models simulate today's climate? *Bulletin of the American Meteorological Society*, 89(3), 303–311. <https://doi.org/10.1175/BAMS-89-3-303>.
- Roszkowska, E. (2013). Rank ordering criteria weighting methods-a comparative overview 2 5. *Optimum Studia Ekonomiczne*, 5(5), 65. Retrieved from <https://pdfs.semanticscholar.org/f983/e8c4eb7d7c30694dd72c5849dd6fee8a5c79.pdf>
- Ruan, Y., Liu, Z., Wang, R., and Yao, Z. (2019). Assessing the Performance of CMIP5 GCMs for Projection of Future Temperature Change over the Lower Mekong Basin. *Atmosphere*, MDPI. 10(2), 93. <https://doi.org/10.3390/atmos10020093>.
- Salman, S. A., Shahid, S., Ismail, T., Ahmed, K., and Wang, X. J. (2018). Selection of climate models for projection of spatiotemporal changes in temperature of Iraq with uncertainties. *Atmospheric Research*, 213(July), 509–522. <https://doi.org/10.1016/j.atmosres.2018.07.008>.
- Shannon, C. E. (2001). A Mathematical Theory of Communication, 5(I), 365–395. [https://doi.org/10.1007/3-540-45488-8\\_15](https://doi.org/10.1007/3-540-45488-8_15).
- Shiru, M. S., Shahid, S., Chung, E.-S., Alias, N., and Scherer, L. (2019). A MCDM-based framework for selection of general circulation models and projection of spatio-temporal rainfall changes: A case study of Nigeria. *Atmospheric Research*, 225(March), 1–16. <https://doi.org/10.1016/j.atmosres.2019.03.033>.
- Shreem, S. S., Abdullah, S., and Nazri, M. Z. A. (2016). Hybrid feature selection algorithm using symmetrical uncertainty and a harmony search algorithm. *International Journal of Systems Science*, 47(6), 1312–1329.

<https://doi.org/10.1080/00207721.2014.924600>.

Shukla, J., DelSole, T., Fennessy, M., Kinter, J., and Paolino, D. (2006). Climate model fidelity and projections of climate change. *Geophysical Research Letters*, 33(7), 3–6. <https://doi.org/10.1029/2005GL025579>.

Singh, B., Kushwaha, N., and Vyas, O. P. (2014). A Feature Subset Selection Technique for High Dimensional Data Using Symmetric Uncertainty. *Journal of Data Analysis and Information Processing*, (November), 95–105.

Srinivasa Raju, K., and Nagesh Kumar, D. (2015). Ranking general circulation models for India using TOPSIS. *Journal of Water and Climate Change*, 6(2), 288–299. <https://doi.org/10.2166/wcc.2014.074>.

Srinivasa Raju, K., Sonali, P., and Nagesh Kumar, D. (2017). Ranking of CMIP5-based global climate models for India using compromise programming. *Theoretical and Applied Climatology*, 128(3–4), 563–574. <https://doi.org/10.1007/s00704-015-17216>.

Sun, Q., Miao, C., Duan, Q., Ashouri, H., Sorooshian, S., and Hsu, K. L. (2018). A Review of Global Precipitation Data Sets: Data Sources, Estimation, and Intercomparisons. *Reviews of Geophysics*, 56(1), 79–107. <https://doi.org/10.1002/2017RG000574>.

Sutha, K., and Tamilselvi, J. (2015). A Review of Feature Selection Algorithms for Data Mining Techniques. *International Journal on Computer Science and Engineering*, 7(6), 63–67. <http://www.enggjournals.com/ijcse/doc/IJCSE15-07-06-010.pdf>

Talavera, L. (2005). An Evaluation of Filter and Wrapper Methods for Feature Selection in Categorical Clustering (pp. 440–451). [https://doi.org/10.1007/11552253\\_40](https://doi.org/10.1007/11552253_40).

Tawari-fufeyin, P., Paul, M., and Godleads, A. O. (2015). Some Aspects of a Historic Flooding in Nigeria and Its Effects on some Niger-Delta Communities. *American Journal of Water Resources*, 3(1), 7–16. <https://doi.org/10.12691/ajwr-3-1-2>.



Todd M, A. O. (2015). Modelling the Climatic Variability in the Niger Delta Region: Influence of Climate Change on Hydrology. *Journal of Earth Science & Climatic Change*, 06(06), 284. <https://doi.org/10.4172/2157-7617.1000284>.

Wang, L., Ranasinghe, R., Maskey, S., van Gelder, P. H. A. J. M., and Vrijling, J. K. (2016). Comparison of empirical statistical methods for downscaling daily climate projections from CMIP5 GCMs: A case study of the Huai River Basin, China. *International Journal of Climatology*, 36(1), 145–164. <https://doi.org/10.1002/joc.4334>.

Warszawski, L., Frieler, K., Huber, V., Piontek, F., Serdeczny, O., and Schewe, J. (2014). The Inter-Sectoral Impact Model Intercomparison Project (ISI-MIP): Project framework. *Proceedings of the National Academy of Sciences*, 111(9), 3228–3232. <https://doi.org/10.1073/pnas.1312330110>.

Xu, Y. (2018). Hydrology and Climate Forecasting R Package for Data Analysis and Visualization.

#### **5.4. Concluding Remarks**

This Chapter demonstrated the selection and evaluation of daily gridded meteorological datasets and GCM ensemble for use in the Niger Delta climate projections. These assessments were accomplished in two published peer-reviewed articles. Gridded products, namely, CRU, PGF and CFRS available over the study area and widely used globally as an alternative to observed rainfall, maximum, and minimum temperature datasets, were evaluated using statistical indicators, comparison of time-series graphs and spells lengths analysis among datasets. The results revealed a clear superiority of daily CRU rainfall, maximum, and minimum temperature over the other gridded products for replicating the datasets from the two observed stations.

The study also used the symmetrical uncertainty (SU) filter to identify four GCMs, namely ACCESS1.3, MIROC-ESM, MIROC-ESM-CHM, and NorESM1-M from a pool of 26 GCM outputs as the most suitable set of ensemble for simulating the Spatio-temporal changes in both rainfall, maximum, and minimum temperature over the Niger Delta. This is achieved based on their performances in simulating the selected observed CRU datasets as none of such studies have been conducted to select gridded datasets and GCMs for both rainfall, maximum, and minimum temperature in Nigeria and West Africa at large. This study, therefore, is the first attempt to employ a selection of suitable sets of daily rainfall, maximum, and minimum temperature together for the spatiotemporal climate projection changes in the Niger Delta. These findings addressed bullet points 3 to 5 of the literature review.

It is expected the statistical methods used in the present study can be used in other parts of the world to select better performing data products before application in any hydrological and climate studies in study areas. The selected datasets and GCMs can also be used for any future climate and hydrologic studies in the Niger Delta. Hence, further assessment and application of the selected gridded datasets and GCM outputs for the potential impacts of climate change on surface and groundwater resources in the Niger Delta are achieved in the next chapters.

## CHAPTER 6

# Impacts of Climate Change on Extreme Weather Events

### 6.1 Preamble

This Chapter presents a risk assessment study concerning flood risk in a developing country such as Nigeria. The findings from the previous chapter show that the Climate Research Unit (CRU) daily rainfall and temperature time series datasets are found to be the best-fit datasets that replicate the distribution patterns, spatial and temporal variability of the Niger Delta's observed datasets. The study also identified four GCMs, namely ACCESS1.3, MIROC-ESM, MIROC-ESM-CHM, and NorESM1-M as the most suitable set of GCMs for simulating both rainfall, maximum, and minimum temperature over the Niger Delta.

As the selected GCMs under RCP4.5 and RCP8.5 emission scenarios suggested an increase in the study areas rainfall during the future periods. These GCMs will be used in this chapter to predict the potential impacts of climate change on extreme meteorological events in the Niger Delta part of Nigeria using the Standardised precipitation indices (SPI) of 1-month and 12-month time steps as the indicator for extreme event assessment. The results of this chapter would inform future policies and investment planning for flood mitigation within the context of climate

change. The findings in this study addressed bullet points 2 and part of 6 of the literature review.

An article was written from the findings in this study and Published in *MDPI, Hydrology* journal (2020) as:

- Hassan, I.; Kalin, R. M.; Aladejana, J. A; and White, C. J. (2020): ‘Potential Impacts of Climate Change on Extreme Weather Events in the Niger Delta part of Nigeria.’, Published in *Hydrology*, MDPI, , doi:10.3390/hydrology7010019.

The article represents my effort in conceptualizing, theoretical formulation, development, analytic calculations, numerical simulations, and writing the manuscript. My primary supervisor, Prof. Robert M. Kalin, assisted in designing the research and gave critical views on the paper for further improvement. My colleague Jamiu A. Aladejana together with my second supervisor, Chris J. White, provided technical help and proposed essential additions to the models and the manuscript.

## 6.2 Paper 3

Hassan, I.; Kalin, R. M.; White, C. J.; Aladejana, J. A (2020) 'Impacts of Climate Change on Extreme Weather Events in the Niger Delta part of Nigeria.', Published in *Hydrology*, MDPI, doi:10.3390/hydrology7010019.

### Potential impacts of climate change on extreme weather events in the Niger Delta part of Nigeria

Ibrahim Hassan<sup>1,2\*</sup>, Robert M. Kalin<sup>1</sup>, Jamiu A. Aladejana<sup>1,3</sup> and Christopher J. White<sup>1</sup>

<sup>1</sup>*Department of Civil and Environmental Engineering, University of Strathclyde, Glasgow,*

<sup>2</sup>*Department of Civil Engineering Abubakar Tafawa Balewa University Bauchi, Nigeria;*

<sup>3</sup>*Department of Geology, University of Ibadan, Nigeria;*

#### Abstract

The Niger Delta is the most climate-vulnerable region in Nigeria. Flooding events are recorded annually in settlements along the River Niger and its tributaries, inundating many towns and displacing people from their homes. In this study, climate change impacts from extreme meteorological events over the period 2010–2099 are predicted and analysed. Four coupled model Intercomparison Project Phase 5 (CMIP5) Global Climate Models (GCMs) under Respectively Concentration Pathways (RCP4.5 and RCP8.5) emission scenarios were used for climate change predictions. Standardized precipitation indices (SPI) of 1-month and 12-month time steps were used for extreme event assessment. Results from the climate change scenarios predict an increase in rainfall across all future periods and under both emission scenarios, with the highest projected increase during the last three decades of the century. Under the RCP8.5 emission scenario, the rainfall at Port Harcourt and Yenagoa Stations is predicted to increase by about 2.47% and 2.62% while the rainfall at Warri Station is

predicted to increase by about 1.39% toward the end of the century. The 12-month SPI under RCP4.5 and RCP8.5 emission scenarios predict an exceedance in the extreme wet threshold (i.e.,  $SPI > 2$ ) during all future periods and across all study locations. These findings suggest an increasing risk of flooding within the projected periods. The finding can be useful to policymakers for the formulation and planning of flood mitigation and adaptation measures.

**Keywords:** Global Climate Model (GCM); Respective Concentration Pathways (RCP); Coupled Model Intercomparison Project Phase 5 (CMIP5); standardized precipitation index (SPI).

## 1.0 Introduction

The industrialization of developed and developing countries increases the concentration of greenhouse gases (GHGs), which enhances climate variability (Worku, 2015). Climate change has become an enormous challenge for developmental planning in many countries, especially for developing countries like Nigeria. The IPCC report (IPCC, 2007c) shows that an increase in the frequency of extreme rainfall is likely to occur in most areas during the 21<sup>st</sup> century with different emissions scenarios. Recent studies by Li *et al.*, (2017) and Chen *et al.*, (2018) reported that human activities played a leading role in increasing climate change impacts. The projected results of these changes include flooding, damage to crops, soil erosion, adverse effects on surface and groundwater quality, water scarcity, water contamination, disease outbreak, loss of properties, disruption of the settlement, and other socio-economic challenges (IPCC, 2007b).

Floods are the result of weather events occurring at variable time frequencies in many areas around the world (Seiler *et al.*, 2002). Many cities are hotspots of risk from extreme weather events, which is growing due to a combination of climate change and anthropogenic activities (Ranger *et al.*, 2011). Different regions in Nigeria are seasonally affected by flood, which significantly alters both the national and regional economic development depending on its severity. Studies in Nigeria (Etuonovbe, 2011; UNOCHA, 2015; Oluwaseyi, 2017; Cirella and Iyalomhe, 2018) reported that flood displaces more people in the country than any other natural disaster, with an estimated 20% of the population at risk. The impacts are recognized more by vulnerable communities, who often build homes along the floodplains, causing millions of people to relocate, destroying their businesses, and polluting water resources, which increase the risk of diseases (Brown and Chikagbum, 2015; Cirella and Iyalomhe, 2018).

The Niger Delta part of Nigeria is the most vulnerable part of the country to impacts of climate change (Prince Mmom, 2013; Musa *et al.*, 2014). Flooding events are recorded annually in the coastal Niger Delta states located along the River Niger and its tributaries (Prince Mmom, 2013). Devastating floods often inundate two-thirds of the coastal communities in the Niger Delta region for at least a quarter of each year (Ologunorisa and Adeyemo, 2005; Amangabara and Gobo, 2007; Mmom, 2013; Amangabara and Obenade, 2015; Tawari-fufeyin *et al.*, 2015). Studies on the vulnerability of communities in three Niger Delta States (Amangabara and Gobo, 2007; Amangabara and Obenade, 2015) reported that a total of 1110 towns are at risk of being inundated and about 7,120,028 people risk displacement. It has, therefore, become very vital to study the impact of climate change on extreme weather events to

predict the possible occurrence of associated risks, which can assist in the planning and management of such incidents. One of the significant effects of climate change is the variation of rainfall. As high rainfall may result in a flood, its deficit may lead to drought. Therefore, the prediction of variation in future rainfall trends is necessary for assessing the impact of climate change.

The cost of climate change adaptation can significantly be reduced through adequate policies and flood control investment plans. There is, therefore, a need for systematic studies of indices that are useful for continuous monitoring of high-risk associated with future extreme weather events. The standardized precipitation index (SPI) (Mckee *et al.*, 1993, 1995), although developed for drought monitoring, can be successfully applied for flood monitoring purposes (Komuscu, 1999; Seiler, Hayes and Bressan, 2002; Shamsuddin Shahid, 2008; Svoboda, Hayes and Wood, 2012). SPI can also serve as an indicator for the development of soil-saturation conditions, leading to flooding potential.

General circulation models (GCMs) are essential tools for assessing the impact of climate change on a range of human and natural systems (IPCC, 1990b). Simulations at these inner scales are of considerable interest to hydrologists in assessing the possible impact of climate change on water resources and extreme weather events (IPCC, 2007a). Different climate models have been used globally for climate impact assessment studies. Climate models, particularly the GCMs, provide an essential source of information for constructing scenarios of climate change and providing such information at a higher spatial resolution. GCMs are based on physical laws and physical-based empirical relationships and are



mathematical representations of the atmosphere, ocean, and land surface processes (IPCC, 1990b).

Though few researchers (Ologunorisa and Adeyemo, 2005; Amangabara and Gobo, 2007; Prince C. Mmom, 2013; Amangabara and Obenade, 2015; Tawari-fufeyin *et al.*, 2015) have studied the vulnerability of the Niger Delta States to flooding, no study has investigated the spatial and temporal variations of future extreme weather events in the context of climate change. In this study, the spatiotemporal variations in rainfall over the Niger Delta, for the observed period (1980 to 2005) and the predicted period (2010 to 2099) under RCP4.5 and RCP8.5 were investigated for extreme events. The results help in the analysis of extreme weather events as part of the strategies in climate change impact mitigation.

## **2.0 Description of the Study Area**

The study area is comprised by three states in the Niger Delta part of Nigeria namely the Delta, Bayelsa, and Rivers States (Figure 1), which are geographically located at a latitude of 4.15°N and a longitude of 6.01°E, and covers an area about 29,100km<sup>2</sup>. It is a low lying coastal area that is drained by the Kwa-Ibo, Imo, Bonny, and Aba Rivers and their tributaries. The study area is classified as an equatorial climate toward the southern coast and subequatorial climate toward the northern tropical rainforest (Matemilola *et al.*, 2019). The altitude of the area under the influence of high coastal tides results in flooding, especially during the rainy season (Amadi, 2014). The area is characterized by typical tropical dry seasons (November to February) and wet season (March to October) with a mean annual rainfall increasing from 2000 mm around the northern fringe to about 4500 mm around the coastal margin

(Adejuwon, 2012). Recent studies reported that during the last 20 years (Prince C. Mmom, 2013), a trend of increase in precipitation, flood frequencies, maximum and minimum temperature were observed over the years in the Niger Delta due to global warming, which show a clear sign of climate change with a variable future climate over the region (Ologunorisa and Adeyemo, 2005; Ologunorisa and Tersoo, 2006; Amangabara and Obenade, 2015; Tawari-fufeyin *et al.*,2015).

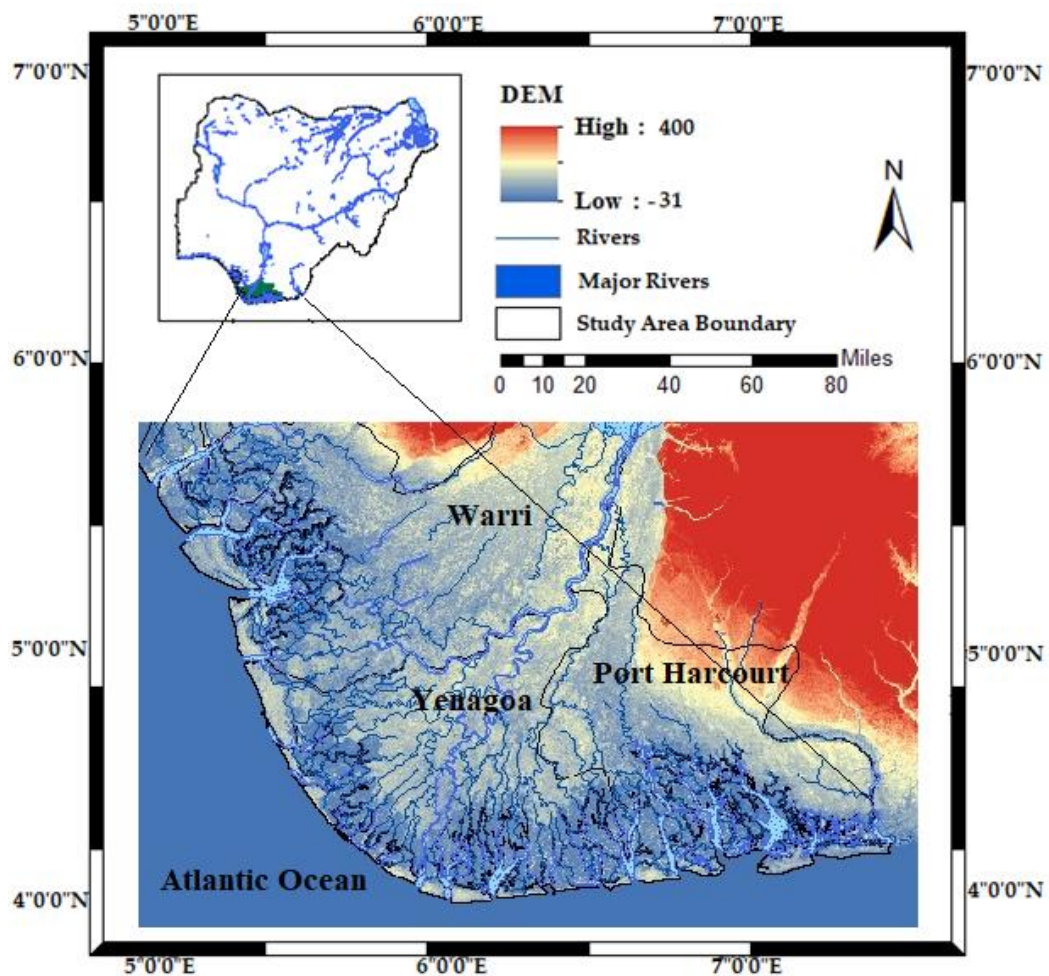


**Figure 6.1** Location of the study area in Nigeria;

The mean monthly temperatures are high up to 26.7 °C around March/April and as low as 24.4 °C during July/August giving a small annual range of 2.7 °C. The relative humidity of the area is relatively high, often reaching 90% and are associated

with warm, wet southwesterly winds blowing inland most of the year whereas dust-laden, warm and dry northeasterly winds occasionally reach the coast for small periods of the year (Etim and Folarin, 2009).

### **3.0 MATERIALS AND METHODS**

#### **3.1 Meteorological Datasets**

The datasets used in this study are daily rainfall time series datasets obtained from the Climate Research Unit (CRU) for the historical periods of 1980 to 2005 over the Niger Delta part of Nigeria due to the scarcity of reliable long time records of hydroclimatological stations in the area. The CRU datasets are observation-based gridded rainfall and temperature datasets, which are widely used globally because of their extensive spatial and temporal coverage (Harris, 2008; Harris *et al.*, 2014; Vaghefi *et al.*, 2017). A study by (Hassan *et al.*, 2020a) found the CRU datasets to be the best-fit datasets that replicate the distribution patterns, spatial, and temporal variability of the Niger Delta's observed hydroclimatological datasets.

#### **3.2. Coupled Model Inter-comparison Project Phase 5 (CMIP5) GCM Datasets**

In this study, four GCMs of the ISI-MIP (Inter-Sectoral Impact Model Inter-comparison Project) (Table 6.1) and two carbon emission and historical scenarios (RCP4.5 and RCP8.5) for the years (2010–2099) were extracted at a grid resolution of 0.5° X 0.5° for the study area coordinates consistent with the observed climate datasets. These GCMs were selected based on their better performance over the Niger Delta in a study conducted by (Hassan *et al.*, 2020b).

The RCP4.5 and RCP8.5 emission scenarios were selected for this study, as these two scenarios are assumed to provide a possible complete range of impact. The RCP4.5 denotes the common pathway scenario depicting good agreement with the latest lower greenhouse gas emissions policy by the global community. In contrast, RCP8.5 denotes the business-as-usual scenario, consistent with a future with no change in climate policy on emissions reduction (Wang *et al.*, 2016). Therefore, as many studies recommend using ensemble results of several climate change models (Teutschbein and Seibert, 2012), the ensemble of the four best performing GCMs (Hassan *et al.*, 2020b) was used in this study.

**Table 6.1** CMIP5 General Circulation Models Used in the Study at 0.5° X 0.5° Grid.

<b>Models</b>	<b>Institute</b>
ACCESS1-3	CSIRO (Commonwealth Scientific & Industrial Research Organisation, Australia), and BOM (Bureau of Meteorology, Australia)
MIROC-ESM	AORI, NIES and JAMSTEC
MIROC-ESM-CHEM	AORI, NIES and JAMSTEC
NoerESM1-M	Norwegian Climate Centre

### **3.3 Bias correction**

Raw GCM outputs typically contain biases when compared with observations (Mehrotra and Sharma, 2015). In this study, the CRU dataset for the periods 1980 to 2005 was used to correct the biases in the historical raw GCMs (1980–2005), which were then used to validate the bias-corrected GCM outputs. The differences in mean and variability between the raw GCM outputs and the observed CRU datasets were later used to correct the biases in the projected raw GCMs (2005–2099). The easiest

and most common bias correction method, which is the multiplicative method, was adopted to correct the biases in the daily time series rainfall from the four GCM outputs (Vaghefi *et al.*, 2017; Xu, 2018; Beyer, Krapp and Manica, 2019). In the multiplicative bias correction method, a multiplicative correction factor for each month is used, and the modified daily rainfall is expressed in Equation (1):

$$P_{corrected_{ij}} = P_{GCM_{ij}} * \frac{\bar{P}_{reference_{jk}}}{\bar{P}_{GCM_{jk}}} \quad (6.1)$$

where P is the rainfall (mm day<sup>-1</sup>);  $\bar{P}$  is the long-term mean rainfall; and *i, j, k* are the day, month, and year counters, respectively.

### 3.4. Meteorological Drought Assessment

The methodology adopted in this study consists of applying the standardized precipitation index (SPI) to investigate the susceptibility of the selected meteorological stations to flooding events. SPI was developed to identify meteorological flood and drought events from precipitation time series data for monitoring and evaluation of extreme events (Mckee *et al.*, 1993, 1995). A wet period for a time scale *i* is defined as the period during which the SPI is continuously positive and reaches a value of +1 or higher (Mckee *et al.*, 1993). SPI is calculated by taking the difference in monthly precipitation ( $x_i$ ) from the monthly mean ( $\bar{x}$ ), then divided by the standard deviation ( $\sigma$ ) (Komuscu, 1999).

$$SPI = \frac{x_i - \bar{x}}{\sigma} \quad (6.2)$$

Positive SPI values show higher precipitation than the mean, while negative values indicate less than mean precipitation (Lloyd-Hughes and Saunders, 2002). In this study, the SPI index was calculated for time scales of 1-month and 12-month rainfall series for each of the selected locations. One-month SPI plots are very similar to a time series plot displaying the percentage of average rainfall for 30 days and reflect short-term conditions. A 12-month SPI indicates long-term rainfall patterns that represent a comparison of the precipitation for 12 consecutive months and that recorded in the same 12 consecutive months during all the previous years of available data (Svoboda *et al.*, 2012). In this study, the SPI package in R (Neves, 2015) was used for the computation analysis. Wet dynamics were graphically analyzed for each scale, each RCP emission scenario, and all the projected durations and each location. The definition of the SPI values in drought characterizations are summarized in Table 2.

**Table 6.2.** Categories for standardized precipitation index (SPI) values (Mckee, Doesken and Kleist, 1993; Svoboda, Hayes and Wood, 2012).

<b>Drought Category</b>	<b>SPI Value</b>
Extremely wet	2.00+
Very wet	1.50 to 1.99
Moderately wet	1.00 to 1.49
Near normal	-0.99 to 0.99
Moderately dry	-1.00 to -1.49
Severely dry	-1.50 to -1.99
Extremely dry	-2.00 and less

### 3.5. Performance Evaluation of the Models

The performance evaluation of the developed models was carried out using three statistical indicators: root mean squared error (RMSE); coefficient of correlation ( $R^2$ ); and the Nash–Sutcliffe efficiency (NSE) (Willmott, 1981). RMSE is considered as a robust measure of accuracy (Moriassi *et al.*, 2007; Moriassi *et al.*, 2013).

$$RMSE = \sqrt{\frac{1}{n} \sum_{i=1}^n (h_{oi} - h_{pi})^2} \quad (6.2)$$

The coefficient of determination ( $R^2$ ) is an indicator of the strength of the relationship between the observed and simulated values, which is considered more accurate if it is approximately equal to one (Willmott, 1981).

$$R^2 = \left[ \frac{\sum_{i=1}^n (h_{pi} - \bar{h}_p) (h_{oi} - \bar{h}_o)}{\sqrt{[(\sum_{i=1}^n (h_{pi} - \bar{h}_p)^2)(\sum_{i=1}^n (h_{oi} - \bar{h}_o)^2)]}} \right] \quad (6.3)$$

The Nash–Sutcliffe efficiency (NSE) is a normalized statistic that determines the relative magnitude of the residual variance compared to the measured data variance. NSE also indicates how well the plot of the observed versus simulated data fits. NSE ranges between  $-\infty$  and 1, with  $NSE = 1$  being the optimum value. Values between 0 to 1 are viewed as an acceptable level of performance, whereas values of 0.0 indicate that the mean observed value is a better predictor than the simulated value, which indicates unacceptable performance (Moriassi *et al.*, 2007).

$$NSE = 1 - \left[ \frac{\sum_{i=1}^N (h_{oi} - h_{pi})^2}{\sum_{i=1}^N (h_{oi} - h_o)^2} \right] \quad (6.4)$$

where  $h_{oi}$  is the observed precipitation at the  $i$ th time;  $h_{pi}$  is the predicted rainfall at the  $i$ th time;  $h_o$  is the mean of the observed rainfall levels;  $h_p$  is the mean of the predicted rainfall, and  $n$  is the total number of observations.

## 4. Results and Discussions

### 4.1. Performance assessment of GCM ensemble

The performance of the four GCM ensemble models during the historical period (1980–2005) was assessed using the root mean square error (RMSE), coefficient of correlation ( $R^2$ ), and Nash–Sutcliffe efficiency (NSE). The results obtained are summarized in Table 3, and the mean monthly distribution of observed and ensemble rainfall in Figures 2a–f shows that the ensemble model performed very well in depicting the observed CRU datasets at each of the three study locations. The statistical indicators showed a low RMSE with high NSE and  $R^2$  values across all of the study locations, which indicate that the model is fit for simulations/ projections of the area’s future rainfall.

**Table 6.3:** Performance assessment of rainfall in the general circulation model (GCM) ensemble.

Location	RMSE	NSE	$R^2$
Port Harcourt	78.49	0.59	0.84
Yenagoa	62.29	0.74	0.92
Warri	75.54	0.64	0.85

### 4.2. Observed and Predicted Rainfall Scenarios

The distribution of mean monthly observed and predicted rainfall scenarios in the study locations are shown in Figures 2a–f, respectively. The projected models were



grouped into three time periods of 2010–2039, 2040–2069, and 2070–2099. The monthly distribution, as presented in Figure 6.2, shows that the projected rainfall, in comparison with the observed rainfall, predicts an increasing trend across all stations and all predicted durations. The highest increase across all three stations was projected to be during the 2070–2099 period. In Port-Harcourt, the rainfall is projected to increase by 1.06% under RCP4.5, and 2.47% under RCP8.5. Yenagoa is also projected to experience an increase of about 1.27% under RCP4.5 and 2.62% under RCP8.5. In comparison, Warri Station is also predicted to experience an increase of about 1.24% under RCP4.5, and 1.39% under RCP8.5 toward the end of the century, as shown in Figure 6.3. This projected increase in rainfall confirms the report of the IPCC (IPCC, 2007a) in response to greenhouse gases forcing, which is consistent with other parts of the world (Martín *et al.*, 2012; Rangwala and Miller, 2012; Krinner *et al.*, 2013; Expósito *et al.*, 2015).

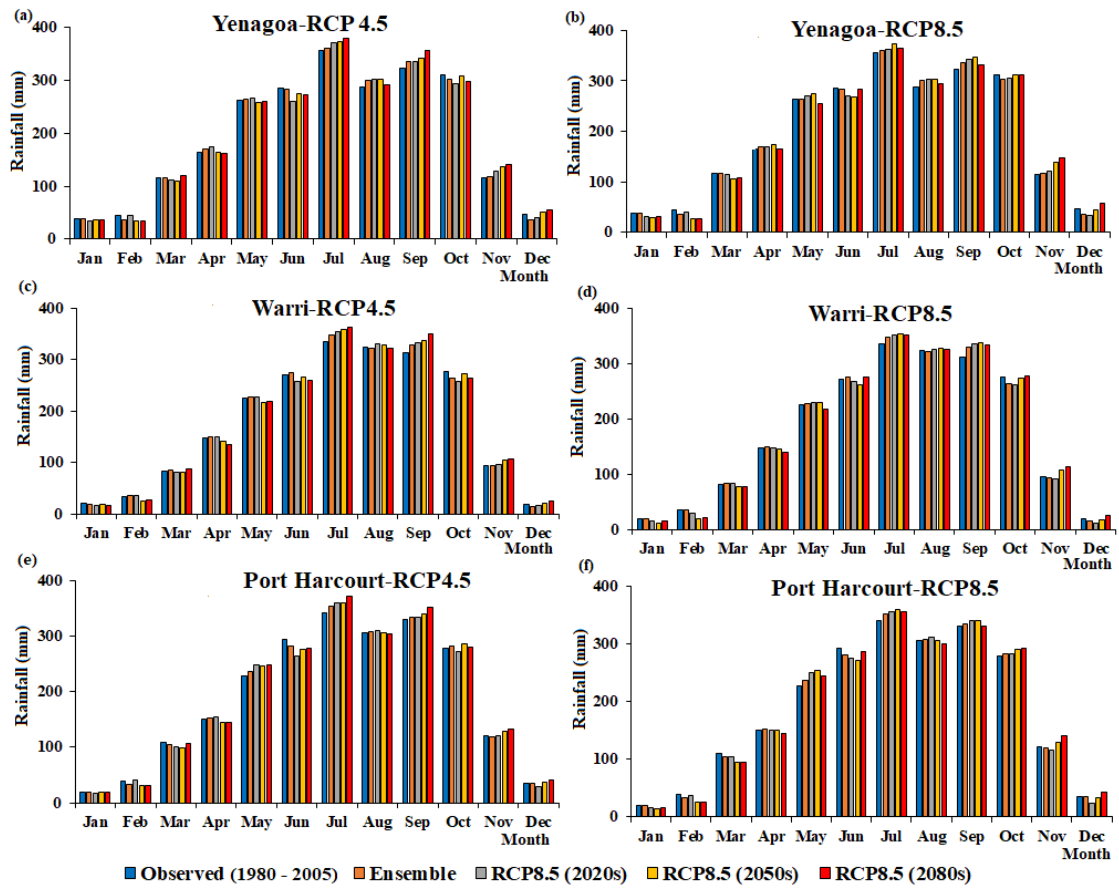


**Figure 6.2.** Seasonal Variation of Observed and Predicted Precipitation in (a) Yenagoa-RCP4.5, (b) Yenagoa-RCP8.5, (c) Warri-RCP4.5, (d) Warri-RCP8.5, (e) Port Harcourt-RCP4.5 and (f) Port Harcourt-RCP8.5, during the future periods.

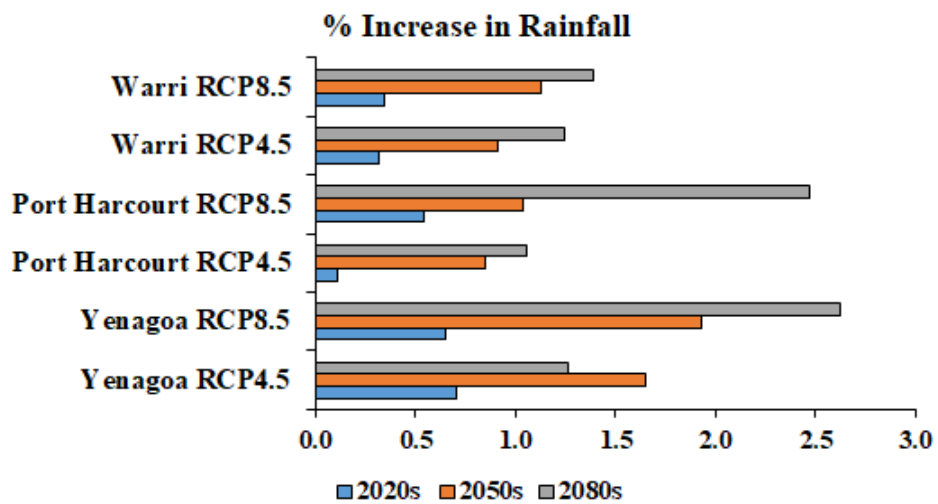


**Figure 6.3.** Percentage increase in predicted future rainfall in comparison with Observed rainfall across the study locations under RCP 4.5 and RCP 8.5 emission scenarios.

### 4.3. Meteorological Drought Assessment

The 1-month and 12-month time-steps in the standardized precipitation index were calculated for the base period (1980–2005) and the predicted duration (2010–2099) across the three study locations. Results of the computed SPI for the base period is shown in Figures 4a, b. In contrast, the results of all the projected periods divided into thirty-year time periods (2010–2039, 2040–2069, and 2070–2099) across all stations, and both emission scenarios are shown in Figures 6.5–6.7. The most striking characteristic is the change in frequency as the time scale changes, as shown in all figures. On the 1-month scale, the wet frequency increases, but its duration decreases while in the 12-month time scale, the wet events become less frequent but last longer. This trend implies that on the shorter time scales, the wet events become more frequent, but last for a short period. The figures show that extremely wet weather (i.e.,  $SPI > 2$ , as classified in Table 6.2) is likely to occur across most of the stations, especially when using the 12-month time steps. However, all the figures show that very wet event weather (i.e.,  $1.5 < SPI < 1.99$ , as classified in Table 6.2) is expected to occur across all the study locations almost on an annual basis and all the predicted durations using all the time steps. Using the 1-month and 12-month SPI, three well-defined extremely wet weather events were identified in all three locations from the base period series analysed, which depicted three major floods associated with three of the weather events (Figures 6.4a, b).

Attention has not been given to flood intensity measurements and records storage in Nigeria. Hence, no historical datasets are available to validate the findings of the historical period. However, the findings of this study match those of the reported extreme flood incidents (Angela, 2011; Oluwaseyi, 2017) in the study area during the

1999 and 2001 rainstorms, which submerged houses, schools, markets, farmlands, and displacement of over 425,839 people in Delta State between March 1999 and April 2001. Additionally, in Bayelsa State, over 273,266 people were displaced by floods in 1999, and 382,000 people in March 2001 (UNOCHA, 2015; Oluwaseyi, 2017). Comparisons of the reported extreme weather events across the study locations with the computed extremely wet events (i.e.,  $SPI > 2$ ) during the historical period in Figure 4 confirm the findings of the base period.

Analysis of SPI variability for the period 2010 to 2039 across the study area shows that the 1-month SPI predicted an exceedance in extreme wet event threshold (i.e.,  $SPI > 2$ ) at Yenagoa Station once under RCP4.5 (Figure 6.5a) and twice under RCP8.5 (Figure 6.5c) during the thirty-year mean. The 12-month SPI under RCP4.5 and RCP8.5 in Figures 6.5b-d also predict an exceedance in extreme wet event threshold (i.e.,  $SPI > 2$ ) twice during the thirty-year mean, similar to the baseline period. No station predicted the risk of severe dryness (i.e.,  $-1.0 < SPI < 1.49$ ) using the 1-month SPI. However, the 12-month SPI suggests that during those periods (2010–2039), the climate at Warri and Port Harcourt Stations exceeds the severely dry threshold (i.e.,  $1.5 < SPI < 1.99$ ) once under RCP4.5 and three times under RCP8.5 (Figure 6.5d) for the thirty-year mean period.

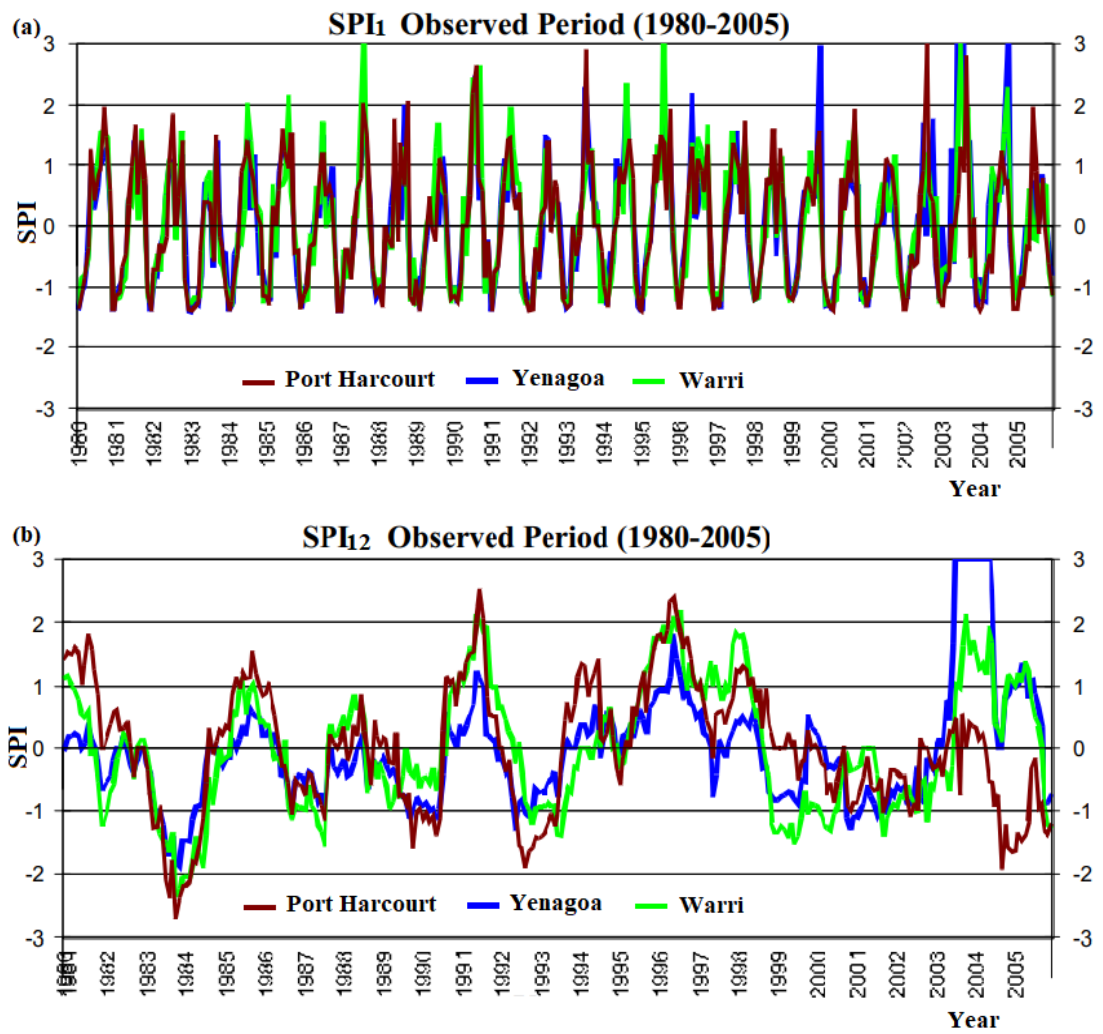


**Figure 6.4.** Computed standardized precipitation index (SPI) for the base period across the study locations.

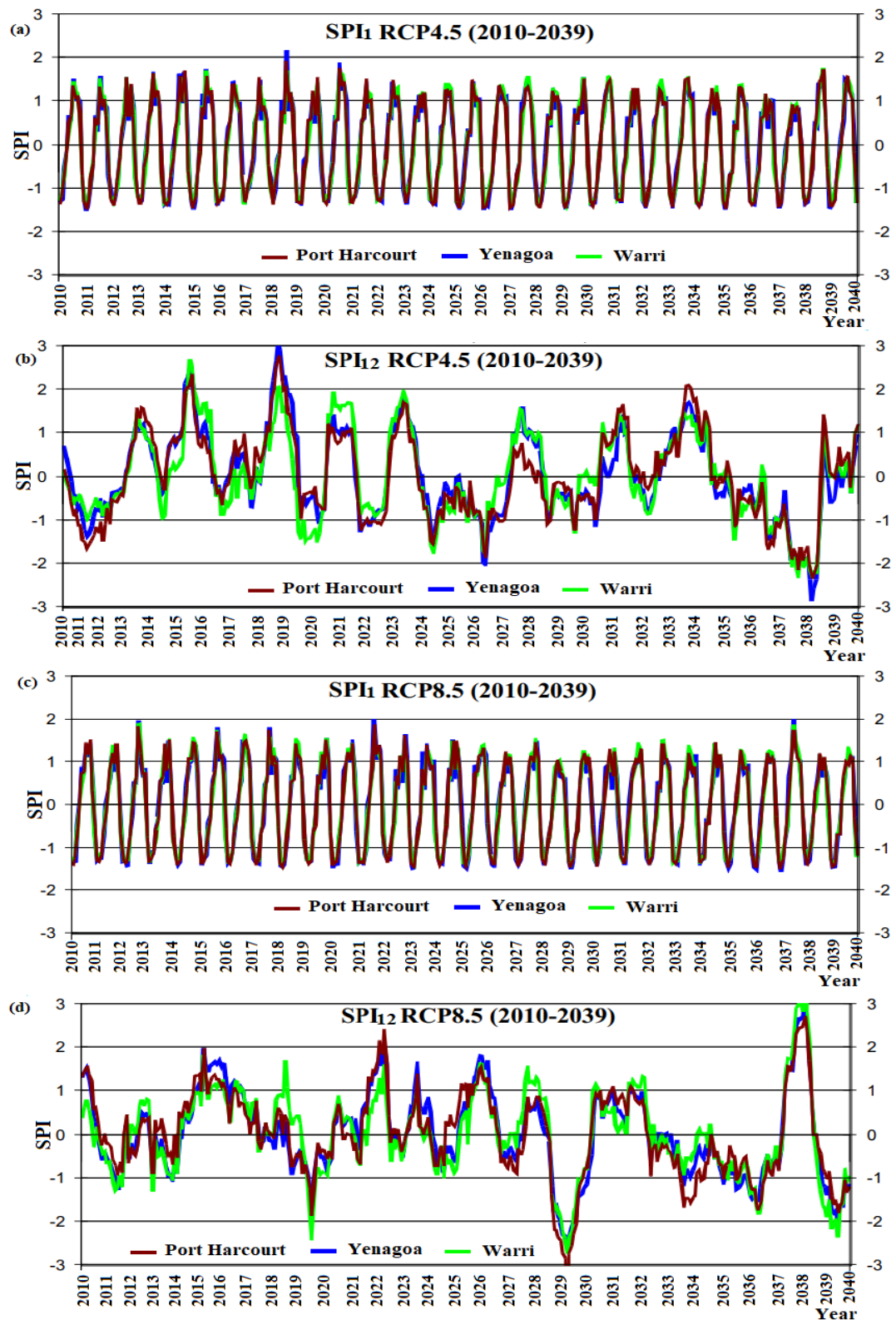


**Figure 6.5.** Computed (a) 1-month RCP4.5 SPI, (b) 12-month RCP4.5 SPI, (c) 1-month RCP8.5 SPI, and (d) 12-month RCP8.5 SPI for the projected periods from 2010 to 2039 across the study locations.

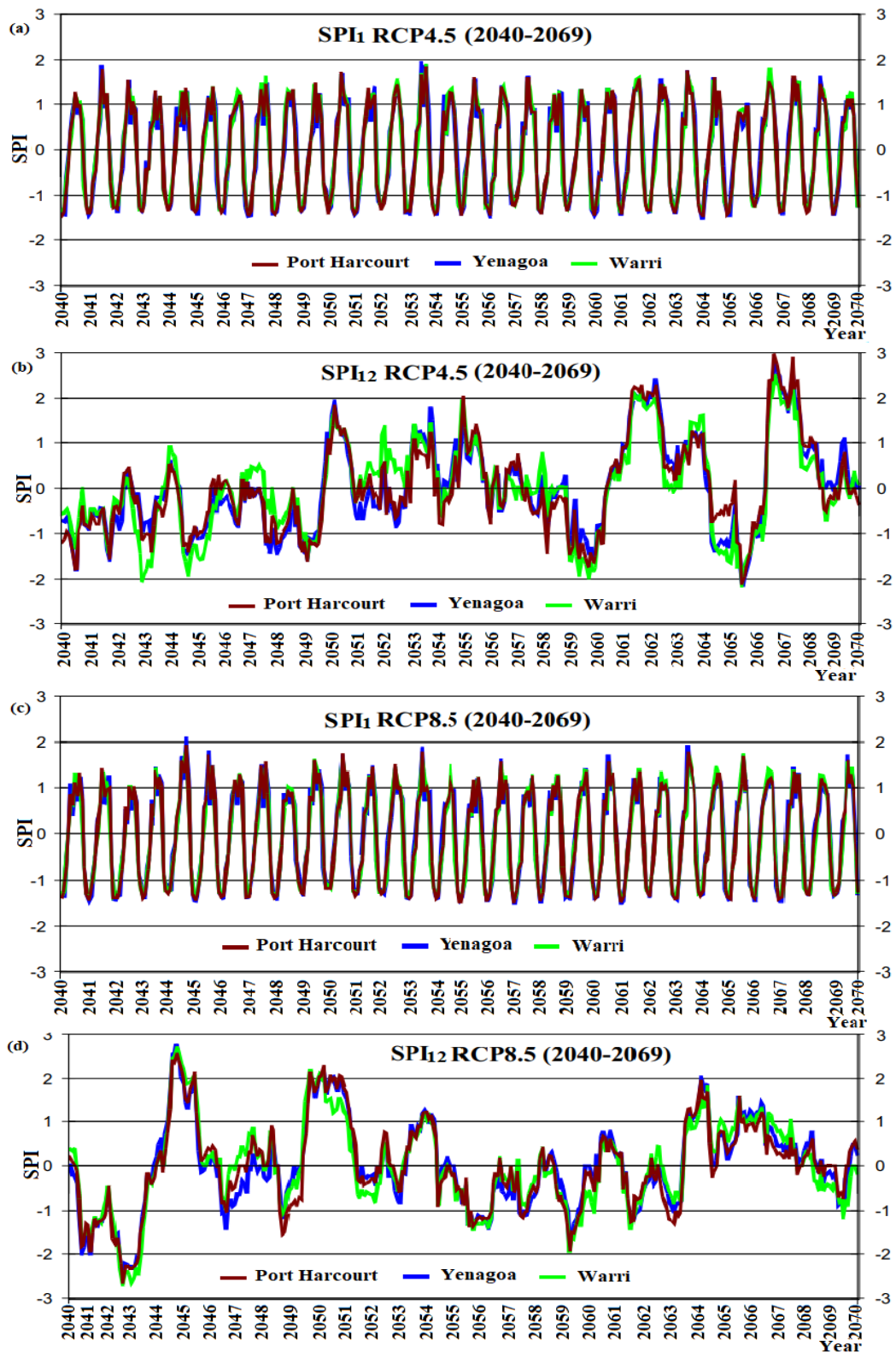


**Figure 6.6.** Computed (a) 1-month RCP4.5 SPI, (b) 12-month RCP4.5 SPI, (c) 1-month RCP8.5 SPI, and (d) 12-month RCP8.5 SPI for the projected periods from 2040 to 2069 across the study locations.

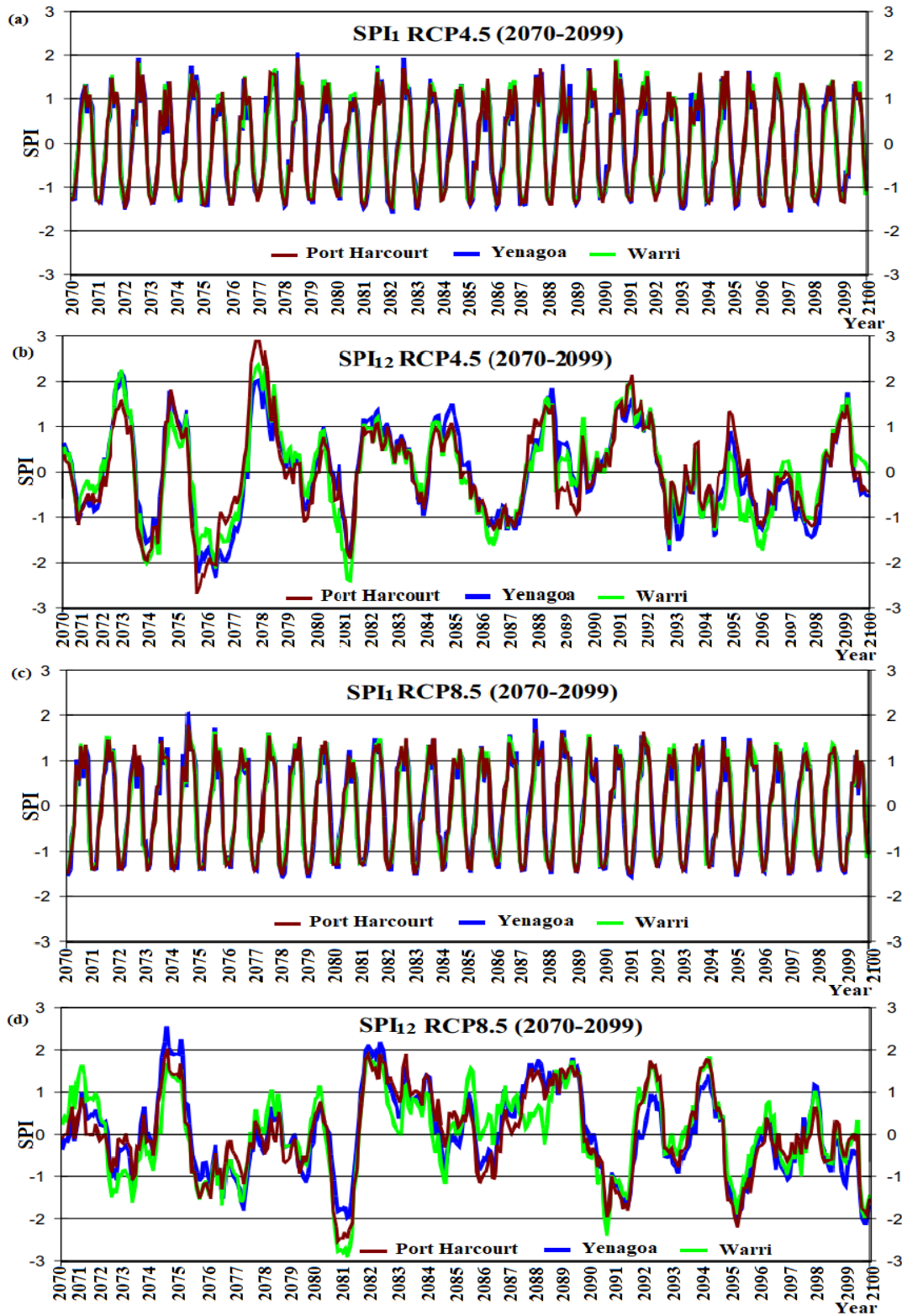


**Figure 6.7.** Computed (a) 1-month RCP4.5 SPI, (b) 12-month RCP4.5 SPI, (c) 1-month RCP8.5 SPI, and (d) 12-month RCP8.5 SPI for the projected periods from 2070 to 2099 across the study locations.



For the periods covering 2040 to 2069, (Figures 6.6a–d), the 12-month SPI under the RCP4.5 and RCP8.5 emission scenarios projected an exceedance in the extreme wet event threshold (i.e.,  $SPI > 2$ ) twice during the thirty-year mean. However, no station showed a risk of severe dryness (i.e.,  $-1.0 < SPI < 1.49$ ) under RCP4.5. The 12-month SPI under the RCP8.5 (Figure 6.6d) emission scenario predicted the risk of a severely dry event (i.e.,  $-1.0 < SPI < 1.49$ ) once during the thirty-year mean and across all study locations. Similarly, during the periods covering 2070 to 2099, the 1-month time step SPI in Figures 6.8a, c under RCP4.5 and RCP8.5 projected an exceedance in the extreme wet threshold (i.e.,  $SPI > 2$ ) once during the thirty-year mean. However, the 12-month SPI predicted the exceedance in the extreme wet threshold (i.e.,  $SPI > 2$ ) twice under RCP4.5 (Figure 6.7b), and three times under RCP8.5 (Figure 6.7d) during the thirty-year mean. The drought magnitude at the Port Harcourt and Warri Stations exceeded the severely dry threshold (i.e.,  $1.5 < SPI < 1.99$ ) once under RCP4.5 and three times under RCP8.5 for the thirty years (2070 to 2099) mean.

## **5. Discussion**

### **Adaptation and planning strategy**

It is evident in several studies (Ologunorisa and Adeyemo, 2005; Amangabara and Gobo, 2007; Mmom, 2013; Amangabara and Obenade, 2015; Tawari-fufeyin, *et al.*, 2015) that the Niger Delta experiences periodic vulnerability in terms of flooding, rendering millions of people homeless by submerging their houses, schools, and markets and destroying their farmlands, which is often attributed to climate change. The geographical location of the study area being a low-lying part of Nigeria exacerbates the situation, causing the area to be easily submerged during heavy rainfall

events. The condition of such areas have forced people to adapt to the frequent seasonal flooding rather than control or mitigating measures. Hence, studies geared toward extreme weather events projections in low-lying areas are necessary. This will create awareness for an urgent collaborative effort between government, stakeholders, and other relevant agencies to support town planning, and in developing strategic plans for mitigating the possible impacts of extreme weather events in the Niger Delta to prevent its long-range consequences. Prevention of common practices such as construction in flood-prone zones should be encouraged to ensure an adequate buffer along the river channels.

The projected increase in rainfall across the three study locations confirmed the IPCC (IPCC, 2007a) report as well as the results in (Ike and Emaziye, 2012; Todd, 2015; Agumagu, 2018; Matemilola *et al.*, 2019; Hassan *et al.*, 2020b) for this region. These findings highlight that the region might be at risk of extreme wet events, which could result in the risk of flooding within the projected periods. These might pose a considerable threat to lives and properties, which might consequently harm the socio-economic growth and livelihood of the region (Ologunorisa and Adeyemo, 2005; Ologunorisa and Tersoo, 2006; Amangabara and Gobo, 2007; Mmom 2013; Amangabara and Obenade, 2015; Tawari-fufeyin *et al.*, 2015). Therefore, routine monitoring and measurement of water levels in rivers, streams, and dams, especially along the Niger River for potential risk of flooding should be enforced to forestall the possible disaster. Sufficient information or warning systems could be put in place across the years predicted by this study to educate the public against the dangers of flooding as well as the government policies for its mitigation adaptation measures.

## 6. Conclusions

In determining the potential impact of climate change on extreme events in the Niger Delta part of Nigeria, rainfall has been projected from 2010 to 2099 using an ensemble of four GCMs under RCP4.5 and 8.5 emission scenarios. The results showed an increase in the projected future rainfall scenarios across all study locations, which suggest a wetter future in the coastal Niger Delta. The extreme weather events at the stations were investigated using the standardized precipitation index (SPI). The SPI index projects an extreme wet event at least once under RCP4.5 and three times under RCP8.5 for the thirty-year mean across the study locations. These findings suggest high rainfall in the future climate of this area across all of the projected duration. Hence, adequate plans for flood mitigation should be put in place. The findings can also be useful to policymakers for the formulation and planning of mitigation and adaptation measures for climate change.

**Author Contributions:** I.H. and R.M.K. designed the research; I.H. wrote the original draft.; R.M.K., C.J.W. and J.A.A reviewed and edited the manuscript and provide technical help and proposed significant additions with the model and to the manuscript.; R.M.K. gave critical views on the manuscript for further improvement.

**Funding:** This research was funded by the Petroleum Technology and Development Fund (PTDF) under the Overseas PhD scholarship scheme and supported by the Scottish Government under the Climate Justice Fund Water Futures Programme, awarded to the University of Strathclyde (R.M. Kalin).

**Conflicts of Interest:** The authors declare no conflict of interest.

## Reference

- Adejuwon, J. O. (2012) 'Rainfall seasonality in the Niger Delta Belt, Nigeria', *Journal of Geography and Regional Planning*, 5(2), pp. 51–60. doi: 10.5897/JGRP11.096.
- Amadi, A. N. (2014) 'Impact of Gas-Flaring on the Quality of Rain Water, Groundwater and Surface Water in Parts of Eastern Niger Delta, Nigeria', *Journal of Geosciences and Geomatics*, 2(3), pp. 114–119. doi: 10.12691/JGG-2-3-6.
- Amangabara, G. and Obenade, M. (2015) 'Flood Vulnerability Assessment of Niger Delta States Relative to 2012 Flood Disaster in Nigeria', *American Journal of Environmental Protection*, 3(3), pp. 76–83. doi: 10.12691/env-3-3-3.
- Amangabara, G. T. and Gobo, A. E. (2007) 'Factors that influence the flooding of the middle and lower Ntamogba stream catchments, Port Harcourt, Nigeria', *Journal of Environmental Hydrology*, 15(November), pp. 1–11.
- Angela Kesiena Etuonovbe (2011) 'The Devastating Effect of Flooding in Nigeria', *TS06J - Hydrography and the Environment*, (May), pp. 18–22. Available at: [http://www.fig.net/pub/fig2011/papers/ts06j/ts06j\\_etuonovbe\\_5002.pdf](http://www.fig.net/pub/fig2011/papers/ts06j/ts06j_etuonovbe_5002.pdf).
- Ashraf Vaghefi, S., Abbaspour, N., Kamali, B., and Abbaspour, K. C. (2017) 'A toolkit for climate change analysis and pattern recognition for extreme weather conditions – Case study: California-Baja California Peninsula', *Environmental Modelling and Software*. Elsevier Ltd, 96(October), pp. 181–198. doi: 10.1016/j.envsoft.2017.06.033.
- Beyer, R., Krapp, M. and Manica, A. (2019) 'A systematic comparison of bias correction methods for paleoclimate simulations', *Climate of the Past Discussions*, (February), pp. 1–23. doi: 10.5194/cp-2019-11.
- Brown, I. and Chikagbum, W. (2015) 'Planning response to water-related disasters in Nigeria the Rivers state experience', *International Journal of Scientific & Engineering Research*, 6(6), pp. 32–44. Available at: <https://www.ijser.org/researchpaper/>.
- Chen, X., Li, X., Yuan, X., Zeng, G., Liang, J., Li, X., Chen, G. (2018) 'Effects of human activities and climate change on the reduction of visibility in Beijing over the

past 36 years’, *Environment International*. Elsevier, 116(April), pp. 92–100. doi: 10.1016/j.envint.2018.04.009.

Cirella, G. T. and Iyalomhe, F. O. (2018) ‘Flooding conceptual review: Sustainability-focalized best practices in Nigeria’, *Applied Sciences (Switzerland)*, 8(9). doi: 10.3390/app8091558.

Etim U. U Ituen and A Folarin Alonge (2009) ‘Niger Delta Region of Nigeria, Climate Change and the way Forward’, *Bioenergy Engineering*, 11-14 October 2009, Bellevue, Washington, (January 2009). doi: 10.13031/2013.29162.

Expósito, F. J., González, A., Pérez, J. C., Díaz, J. P., and Taima, D. (2015) ‘High-resolution future projections of temperature and precipitation in the Canary Islands’, *Journal of Climate*, 28(19), pp. 7846–7856. doi: 10.1175/JCLI-D-15-0030.1.

Harris, I., Jones, P. D., Osborn, T. J., and Lister, D. H. (2014) ‘Updated high-resolution grids of monthly climatic observations - the CRU TS3.10 Dataset’, *International Journal of Climatology*, 34(3), pp. 623–642. doi: 10.1002/joc.3711.

Hassan, I., Kalin, R. M., White, C. J., and Aladejana, J. A. (2020a) ‘Evaluation of Daily Gridded Meteorological Datasets over the Niger Delta Region of Nigeria and Implication to Water Resources Management’, *Atmospheric and Climate Sciences (ACS), SCRIP*.

Hassan, I., Kalin, R. M., White, C. J., and Aladejana, J. A. (2020b) ‘Selection of CMIP5 GCM ensemble for the projection of Spatio-temporal changes in precipitation and temperature over the Niger Delta, Nigeria.’, *Water (Switzerland)*, 12(385). doi: 10.3390/w12020385.

Musa, Z. N., Popescu, I., and Mynett, A. (2014): The Niger Delta's vulnerability to river floods due to sea level rise, *Nat. Hazards Earth Syst. Sci.*, 14, 3317–3329, <https://doi.org/10.5194/nhess-14-3317-2014>, 2014.

Ike, P. C. and Emaziye, P. O. (2012) ‘An Assessment of the Trend and Projected Future Values of Climatic Variables in Niger Delta Region, Nigeria’, 4(2), pp. 165–170.

IPCC (1990) ‘Climate Change The IPCC Scientific Assessment’, *Ipcc*, p. 414. doi: 10.1097/MOP.0b013e3283444c89.

IPCC (2007a) Climate Change 2007: impacts, adaptation and vulnerability: *contribution of Working Group II to the fourth assessment report of the Intergovernmental Panel, Geneva, Suíça*. doi: 10.1256/004316502320517344.

IPCC (2007b) Climate Change 2007 Synthesis Report, Intergovernmental Panel on Climate Change [*Core Writing Team IPCC*]. doi: 10.1256/004316502320517344.

IPCC (2007c) Mitigation of climate change: Contribution of working group III to the fourth assessment report of the Intergovernmental Panel on Climate Change, *Intergovernmental Panel on Climate Change*.

Jones, P.D. and Harris, I. C. (2008) Climatic Research Unit (CRU) time-series datasets of variations in climate with variations in other phenomena. *NCAS British Atmospheric Data Centre*.

Komuscu, A. U. (1999) ‘Using the SPI to Analyze Spatial and Temporal Patterns of Drought in Turkey Using the SPI to Analyze Spatial and Temporal Patterns of Drought in Turkey’, *Drought Network News*, 11(1), pp. 6–13.

Krinner, G., Germany, F., Shongwe, M., Africa, S., France, S. B., Uk, B. and Lucas, C. (2013) ‘Long-term climate change: Projections, commitments and irreversibility’, *Climate Change 2013 the Physical Science Basis: Working Group I Contribution to the Fifth Assessment Report of the Intergovernmental Panel on Climate Change*, 9781107057, pp. 1029–1136. doi: 10.1017/CBO9781107415324.024.

Li, X., Chen, X., Yuan, X., Zeng, G., León, T., Liang, J., and Yuan, X. (2017) ‘Characteristics of particulate pollution (PM<sub>2.5</sub> and PM<sub>10</sub>) and their space scale-dependent relationships with meteorological elements in China’, *Sustainability (Switzerland)*, 9(12), pp. 1–14. doi: 10.3390/su9122330.

Lloyd-Hughes, B. and Saunders, M. A. (2002) ‘A drought climatology for Europe’, *International Journal of Climatology*, 22(13), pp. 1571–1592. doi: 10.1002/joc.846.

- Martín, J. L., Bethencourt, J. and Cuevas-Agulló, E. (2012) ‘Assessment of global warming on the island of Tenerife, Canary Islands (Spain). Trends in minimum, maximum, and mean temperatures since 1944’, *Climatic Change*, 114(2), pp. 343–355. doi: 10.1007/s10584-012-0407-7.
- Matemilola, S., Adedeji, O. H., Elegbede, I., and Kies, F. (2019) ‘Mainstreaming climate change into the EIA process in Nigeria: Perspectives from projects in the Niger Delta Region’, *Climate*, 7(2). doi: 10.3390/cli7020029.
- Mckee, T. B., Doesken, N. J. and Kleist, J. (1993) ‘The relationship of drought frequency and duration to time scales’, *AMS 8th Conference on Applied Climatology*, (January), pp. 179–184. doi: citeulike-article-id:10490403.
- Mckee, T. B., Doesken, N. J. and Kleist, J. (1995) ‘Drought Monitoring with Multiple Time Scales’, in *Proceedings of the 9th Conference on Applied Climatology, 15-20 January 1995, Dallas, TX, American Meteorological Society*, pp. 233–236.
- Mehrotra, R. and Sharma, A. (2015) ‘Correcting for systematic biases in multiple raw GCM variables across a range of timescales’, *Journal of Hydrology*. Elsevier B.V., 520(January), pp. 214–223. doi: 10.1016/j.jhydrol.2014.11.037.
- Moriasi, D., Arnold, J. and Liew, M. W. Van (2013) ‘Model Evaluation Guidelines for Systematic Quantification of Accuracy in Watershed Simulations’, (May 2007). doi: 10.13031/2013.23153.
- Moriasi, D., Arnold, J., and Liew, M. W. Van (2007) ‘Model Evaluation Guidelines for Systematic Quantification of Accuracy in Watershed Simulations’, *American Society of Agricultural and Biological Engineers*, 50(3), pp. 885–900.
- Neves, J. (2015) ‘Package “SPI”: Compute SPI index’.
- Obroma Agumagu, O. A. (2018) ‘Projected Changes in the Physical Climate of the Niger Delta Region of Nigeria’, *SciFed Journal of Global Warming*.
- Ologunorisa, T. E. and Adeyemo, A. (2005) ‘Public perception of flood hazard in the Niger Delta, Nigeria’, *Environmentalist*, 25(1), pp. 39–45. doi: 10.1007/s10669-005-

3095-2.

Ologunorisa, T. E. and Tersoo, T. (2006) 'The changing rainfall pattern and its implication for flood frequency in Makurdi, Northern Nigeria', *Journal of Applied Sciences and Environmental Management*, 10(3), pp. 97–102. Available at: <http://www.ajol.info/index.php/jasem/article/view/17327>.

Oluwaseyi, A. (2017) 'Plant Genetic Resources (PGR) in Nigeria and the Reality of Climate Change - A Review', *Asian Journal of Environment & Ecology*, 2(2), pp. 1–24. doi: 10.9734/ajee/2017/31855.

Prince C. Mmom, (2013) 'Vulnerability and Resilience of Niger Delta Coastal Communities to Flooding.', *IOSR Journal of Humanities and Social Science*, 10(6), pp. 27–33. doi: 10.9790/0837-1062733.

Ranger, N., Hallegatte, S., Bhattacharya, S., Bachu, M., Priya, S., Dhore, K., and Corfee-Morlot, J. (2011) 'An assessment of the potential impact of climate change on flood risk in Mumbai', *Climatic Change*, 104(1), pp. 139–167. doi: 10.1007/s10584-010-9979-2.

Rangwala, I. and Miller, J. R. (2012) 'Climate change in mountains: A review of elevation-dependent warming and its possible causes', *Climatic Change*, 114(3–4), pp. 527–547. doi: 10.1007/s10584-012-0419-3.

Seiler, R. A., Hayes, M. and Bressan, L. (2002) 'Using the standardized precipitation index for flood risk monitoring', *International Journal of Climatology*, 22(11), pp. 1365–1376. doi: 10.1002/joc.799.

Shamsuddin Shahid (2008) 'Spatial and temporal characteristics of droughts in the western part of Bangladesh', *Hydrological Processes: Wiley InterScience*, 2274(November 2008), pp. 2267–2274. doi: 10.1002/hyp.

Svoboda, Hayes, M. and Wood, D. (2012) 'Standardized Precipitation Index User Guide', *World Meteorological Organisation*, 21(6), pp. 1333–1348. doi: 10.1175/2007JCLI1348.1.



Tawari-fufeyin, P., Paul, M., and Godleads, A. O. (2015) 'Some Aspects of a Historic Flooding in Nigeria and Its Effects on some Niger-Delta Communities', *American Journal of Water Resources*, 3(1), pp. 7–16. doi: 10.12691/ajwr-3-1-2.

Teutschbein, C. and Seibert, J. (2012) 'Bias correction of regional climate model simulations for hydrological climate-change impact studies: Review and evaluation of different methods', *Journal of Hydrology*. Elsevier B.V., 456–457, pp. 12–29. doi: 10.1016/j.jhydrol.2012.05.052.

Todd M, A. O. (2015) 'Modelling the Climatic Variability in the Niger Delta Region: Influence of Climate Change on Hydrology', *Journal of Earth Science & Climatic Change*, 06(06), p. 284. doi: 10.4172/2157-7617.1000284.

UNOCHA (2015) Humanitarian Bulletin Nigeria; United Nations Office for the Coordination of Humanitarian Affairs: Abuja, Nigeria. Available at: <https://www.unocha.org/story/niger-heavy-rains-and-floods-force-more-400000-people-their-homes>.

Wang, L., Ranasinghe, R., Maskey, S., van Gelder, P. H. A. J. M., and Vrijling, J. K. (2016) 'Comparison of empirical statistical methods for downscaling daily climate projections from CMIP5 GCMs: A case study of the Huai River Basin, China', *International Journal of Climatology*, 36(1), pp. 145–164. doi: 10.1002/joc.4334.

Willmott, C. J. (1981) 'On the Validation of Models', *Physical Geography*. Taylor & Francis, 2(2), pp. 184–194. doi: 10.1080/02723646.1981.10642213.

Worku, L. Y. (2015) 'Climate change impact on variability of rainfall intensity in the Upper Blue Nile Basin', *Proceedings of the International Association of Hydrological Sciences*, 366(June 2014), pp. 135–136. doi: 10.5194/piahs-366-135-2015.

Xu, Y. (2018) 'Hydrology and Climate Forecasting R Package for Data Analysis and Visualization'.

## CHAPTER 7

# Impact of Climate Change on the Hydrological Processes

### 7.1 Preamble

The findings from the chapter 5 show that the Climate Research Unit (CRU) daily rainfall and temperature time series datasets are found to be the best-fit datasets that replicated the distribution patterns, spatial and temporal variability of the Niger Delta's observed datasets. The study also identified four GCMs, namely ACCESS1.3, MIROC-ESM, MIROC-ESM-CHM, and NorESM1-M as the most suitable set of GCMs for simulating both rainfall, maximum, and minimum temperature over the Niger Delta.

As results of the potential impacts, climate change on extreme weather events assessment in chapter 6 predicted incidences of an extreme wet cycle during the future periods across the Niger Delta and under both RCPs. Several studies (Ologunorisa and Adeyemo, 2005; Amangabara and Obenade, 2015; Tawari-fufeyin, P., Paul, M., Godleads, 2015) also shows that significant amount of the water causing the flood in the study area comes from the upstream part through the Niger River Basin. The findings, therefore, make it very necessary to study the potential impacts of climate change on the hydrological processes in the Niger River Basin.

In the current chapter, the datasets selected in chapter 5 were used in conjunction with a hydrologic model known as surface water assessment tool (SWAT) model was used to analyse the effects of climate change on the observed and future hydrologic processes of the NRB in Nigeria. A research article was developed from this study and under review in the *Hydrology and Earth System Sciences* journal (2020) as:

- Hassan, I.; Kalin, R. M.; White, C. J.; Aladejana; J. A; Kawala, J. (2020) ‘Impact of climate change on hydrological processes of the Niger-South River, Nigeria.’, Submitted to the *Hydrology and Earth System Sciences* (HESS).

The article presents my effort in conceptualising, theoretical formulation, development, analytic calculations, numerical simulations, and writing the manuscript. My supervisors, Prof. Robert M. Kalin, and Chris J. White assisted in designing the research and gave critical views on the paper for further improvement. My colleagues Jamiu A. Aladejana and Kawala, J. provided technical help and proposed essential additions to the models and the manuscript.

## 7.2 Paper 4

Hassan, I.; Kalin, R. M.; White, C. J.; Aladejana; and J. A. Kawala, J. (2020) 'Impact of climate change on streamflow of the Niger-South River, Nigeria.', Submitted to the *Hydrology and Earth System Sciences (HESS)*.

### **Impact of climate change on the hydrological processes of the Niger-South River, Nigeria**

#### **Abstract**

The Niger-South River Basin (NRB) is one of the most densely populated and vulnerable regions in Nigeria. Climate variability significantly affects the hydrology and water resource management in the area with yearly flooding along the coast and drying rivers towards the north. In this paper, four global Coupled Model Intercomparison Project Phase 5 (CMIP5) climate models (GCMs) under Respectively Concentration Pathways (RCP4.5 and RCP8.5) were used in conjunction with the SWAT (Soil and Water Assessment Tool) model to analyse the effects of climate change on hydrologic processes of the NRB in Nigeria. Following SWAT model calibration and validation, the streamflow in the NRB was forecasted using the RCP4.5 and RCP8.5 climate model data. Monthly streamflow and hydrological extremes were compared for the baseline and periods (1980–2005), the 2020s (2010–2039), 2050s (2040–2069) and 2080s (2070–2099). The results indicate that mean annual streamflow will generally decrease in the 2020s, 2050s and 2080s between 28% to 39% at the Lokoja gauging station and increase from 21% to 48% along the coastal area under both emission scenarios. Results of projected future scenarios also show an increase in mean annual evapotranspiration and groundwater recharge over the entire

study period and under both emission scenarios with the highest projected increase during the 2080s. This study provides valuable insight into the NRB future water resources condition for proper management.

### **Keywords**

Soil and Water Assessment Tool (SWAT); Global Climate Models (GCMs); Niger South River Basin (NRB), Coupled Model Intercomparison Project Phase 5 (CMIP5), Respectively Concentration Pathways (RCP).

## **1.0 Introduction**

Climate change has recently been a critical issue due to its severe impacts on the livelihood of society and environment (IPCC, 2013) resulting to changes in seasonal variability of rainfall intensities and increase in temperature, which have a significant impact on both regional and local hydrological cycle across the globe (Hu *et al.*, 2013). The hydrological cycle through which water moves continuously from ocean to atmosphere constitutes different processes such as precipitation, evapotranspiration, surface runoff, infiltration, soil moisture and percolation (Kumar, 2012; Porio, 2014; Htut, 2014). Precipitation is generally considered to be the main driver of the hydrologic processes and the increase in temperatures increases evapotranspiration which leads to significant changes in the hydrological cycle (Marvel & Bonfils, 2013). The significant impacts of these changes are waterlogging, flooding, damage to crops, soil erosion, adverse effects on surface and groundwater quality, water scarcity, water contamination, disease outbreak, loss of properties, disruption of settlements, and different socio-economic challenges (IPCC, 2007a).

Climate change impacts on hydrology are usually estimated by defining the changes in climate scenarios for hydrological model inputs from the general circulation models (GCMs) outputs. Different climate models have been used globally for climate impact assessment studies (Pandey & Patra, 2014). This is achieved by understanding the linkages between climate change scenarios and hydrologic systems in constructing suitable scenarios for the hydrologic impact assessments. GCMs indicate the likelihood to expect more frequent regional extremes of heavy precipitation events, heat and heatwaves (IPCC, 2007b), which would lead to potentially significant variations in local precipitation.

Review of different studies indicates that Many researchers have studied the impact of climate change on hydrology over large basins (Apurv *et al.*, 2015; Crosbie *et al.*, 2013; Ouyang *et al.*, 2015; Shen *et al.*, 2018; Z. Wang *et al.*, 2012; Zhang & Zhang, 2012). For example, Ouyang *et al.*, (2015) and Apurv *et al.*, (2015) assessed the climate change impacts on streamflow in the Huangnizhuang catchment under CMIP5 emission scenarios. Wang *et al.*, (2012) analysed climate change impacts on streamflow of the Shiyang River basin using the output from the Providing Regional Climates for Impacts Studies (PRECIS) regional climate model with the Soil and Water Assessment Tool (SWAT). Results from these studies carried out at global and basin levels shows that, there is no clear trend on changes in hydrological processes such as stream flow, surface runoff and groundwater recharge, hence, the impact of climate change should be conducted at basin level to find the change at the local level. Studies also reported that even small fluctuations in the rainfall probability or intensity can produce significant impacts on streamflow due to the complicated relationship

between streamflow, precipitation and temperature (Jiang *et al.*, 2007; Ouyang *et al.*, 2015; J. Wang *et al.*, 2020; Z. Wang *et al.*, 2012).

Improvement of the regional climate and hydrological simulations, especially of precipitation and streamflow, is a goal for climatologists and hydrologists. Accurate forecasting of climate and hydrologic variables would be key in improving the effectiveness of local water resources management and planning and reduce losses caused by floods and droughts. Hence, future climate change studies are crucial for water resources management and planning for the sustainability of these precious resources. The Niger River Basin (NRB) is located in the lower reaches of the Niger and Benue River basins respectively often categorised as the most vulnerable region in Nigeria to impacts of climate change (Hassan *et al.*, 2020). The NRB is characterised by some significant human activities, making it an ideal catchment to study climate change impacts on hydrology. Uneven distribution of water resources brings floods in the downstream part (Niger Delta) and droughts in the upstream region resulting in economic instability and losses.

One of the effects of climate change in the NRB is the variation of rainfall. High rainfall results in flooding, and its deficit leads to drought. Therefore, the difference in precipitation trend can be used to assess the impact of climate change in a given location. This research is focussed on: (1) considering the effect of climate change independently on water resources over the southern part of River Niger Catchment; (2) assessing the effectiveness of the SWAT model for the study areas streamflow evaluation; (3) understanding how climate change will affect future streamflow; (4) understanding how climate change will affect future evapotranspiration and groundwater recharge.

## 2.0 Description of the study area

The NRB constitutes the Anambra-Imo and Niger Delta Basins downstream of the confluence of the river Niger and river Benue. It is situated in the southern part of Nigeria and drains into the Atlantic Ocean and falls within the Nigerian Hydrological Area V (HA-5) as shown in Figures 7.1. The area is located between 4°14'6.7668"-8°20'47.6628" North Latitude and 6°19'1.7004"-6°53'18.3408" East Longitude, and covers a total area of 609,775 km<sup>2</sup> from Lokoja to the Niger Delta parts of Nigeria. Geographically, the HA-V area begins approximately at the confluence of the Rivers Niger and Benue at Lokoja in Kogi State and extends southward on both sides of the Lower Niger up to and including the Niger Delta. The physiographic features in the area vary from high elevations in the northern parts formed by the Kabba Hills in Kogi State and Ankpa Hills where the topography exceeds 600m in places through the Cuesta formed by the Enugu Escarpment and the Udi Hills formed by the outcrops of the Nsukka/Ajali Formations. The Ubiaja Hills to the west of the Niger and the Ebenebe-Umunze and Awka-Umuduru Ridges follow, where mangrove swamps merge with the coastline at sea level and the Atlantic Ocean.

Lowlands occupy the areas between hills and scarps and numerous rivers drain the area as tributaries to the Niger River until near the coast where its delta subdivides into the multiple distributary channels and creeks. The principal rivers are: the Niger, Anambra, Adada and Mamu Rivers drain the Anambra Basin while the Imo, Orashi, Otamiri and other smaller tributaries drain the low coastal lands. The study area is located within the humid tropics. Mean annual temperatures range between 25° and 27° Celsius in the coastal regions and hinterland respectively. Rainfall ranges from over 4000mm/annum at the coast to about 1000mm/annum in the hinterland. The



relative humidity is generally high and evapotranspiration moderate. The vegetation is dominated by mangroves and tropical rainforest (Etim & Folarin, 2009).

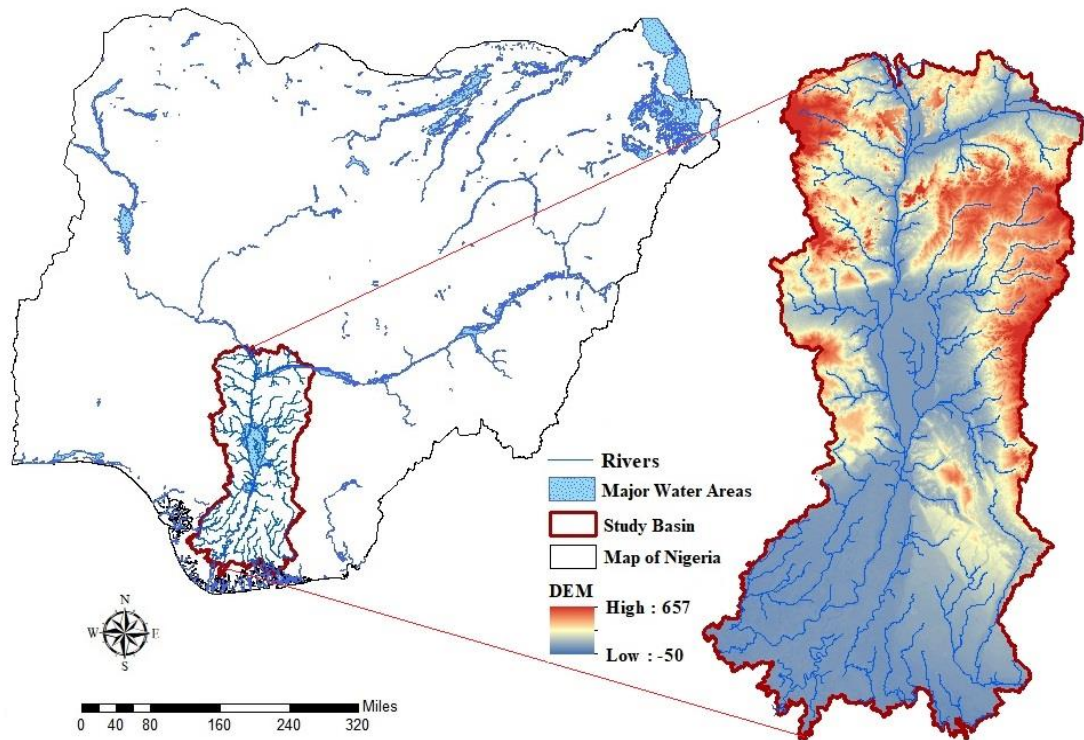


**Figure 7.1** Location of the study area in Nigeria

The basin covers three main agro-ecological zones in Nigerian viz; tall-grass Savanna, rainforest and freshwater swamp, with the more significant part in the rainforest zone. The basin according to 2006 population census houses over 17,000 million people which was projected to grow up to about 25,000 million people by the year 2020 and 31,000 million people by the year 2030 respectively (JICA et al., 2013). Population growth is adding stress to both hydrological cycle and natural ecological processes in the study area, not limited to urbanisation, road constructions and river dredging. The main activities are agriculture, including fish farming with maize and other grain crops being the dominant products (Oloruntade *et al.*, 2017).

### **3.0 Materials and methods**

#### **3.1 Data and sources**

The data required for the ArcSWAT interface include spatially distributed Digital Elevation Model (DEM), land use maps, soil map, and stream network in the form of GIS layers. Weather and river discharge data are used for streamflow prediction, calibration and validation purposes. Daily rainfall time series data of rainfall and temperature recorded from two stations located in around the study area for the period 1980-2010 were collected from the National Meteorological Centre of Nigeria (NIMET). Daily gridded rainfall and temperature datasets between the years 1970 to 2005 were extracted from the CRU version 4.01 global climate dataset (Harris et al., 2014) for the study area in Nigeria. The CRU data is found to replicate available observed data in the study area more accurately compared to other gridded datasets (Hassan *et al.*, 2020a).

Observed daily discharge data for Lokoja station from 1970 to 2004 was obtained from the Global Runoff data centre (GRDC), while the discharge data for Onitsha station from 1980 to 2005 was obtained from the National Hydrologic service agency (NHISA) in Nigeria. The 30-m resolution DEM was derived from NASA, the 400-m land use map shown in Fig. 7.2 (a) was obtained from the Waterbase while the soil type maps shown in Fig. 7.2 (b) were obtained from the FAO. The observed daily discharge data period 1970-2005 used in this model is divided into two periods: model calibration (1973-1997) and validation (1998- 2005). Daily precipitation, Minimum and maximum temperature data are used as the input data for the SWAT model weather generator.

**Table 7.1** : Input data for River Niger Catchment Soil and Water Assessment Tool model

<b>Data Type</b>	<b>Scale</b>	<b>Origin</b>	<b>Data Attribute</b>
Weather Station	1980 - 2005	Nigerian Meteorological Services Agency (NIMET)	Daily Precipitation, Minimum and Maximum Temperature
GCM Datasets	1980 - 2005	CIMP5 Data Portal	Daily Precipitation, Minimum and Maximum Temperature
Gridded Meteorological	1980 - 2005	Climate Research Unit Datasets (CRU)	Daily Precipitation, Minimum and Maximum Temperature
Hydrological Station	1980 - 2005	Nigerian Hydrological Services Agency (NHISA) and Global Runoff Datasets (GRDC)	Streamflow Data
Digital Elevation Model	30m	NASA	Elevation
Land use	400m	Soil Waterbase	Land use
Soil Type	90m	FAO	Soil Physical and Chemical Data

In this study, four state-of-the-art CMIP5 GCMs (ACCESS1.3, MIROC-ESM, MIROC-ESM-CHM, and NorESM1-M) with two RCP scenarios (RCP4.5 and RCP8.5) were used for the projection of temperature and precipitation. These GCMs were selected based on their better performance over the Niger Delta (Hassan *et al.*, 2020b). The GCM data is obtained from the CMIP5 (data portal website <http://pcmdi9.llnl.gov/>). As many studies recommend using ensemble results of several climate change models (Teutschbein and Seibert, 2012), the ensemble of the 4 GCMs are used in this study. For each GCM, many ensembles are available, and these are projections initialised using different initial conditions. In this study, we used multi-ensemble mean for each GCM for projecting future changes in climate. All CMIP5 data were uniformly interpolated to the same spatial scale (0.5° X 0.5°) to

reduce biases introduced by different resolution. Table 7.2 gives an overview of the selected GCMs.

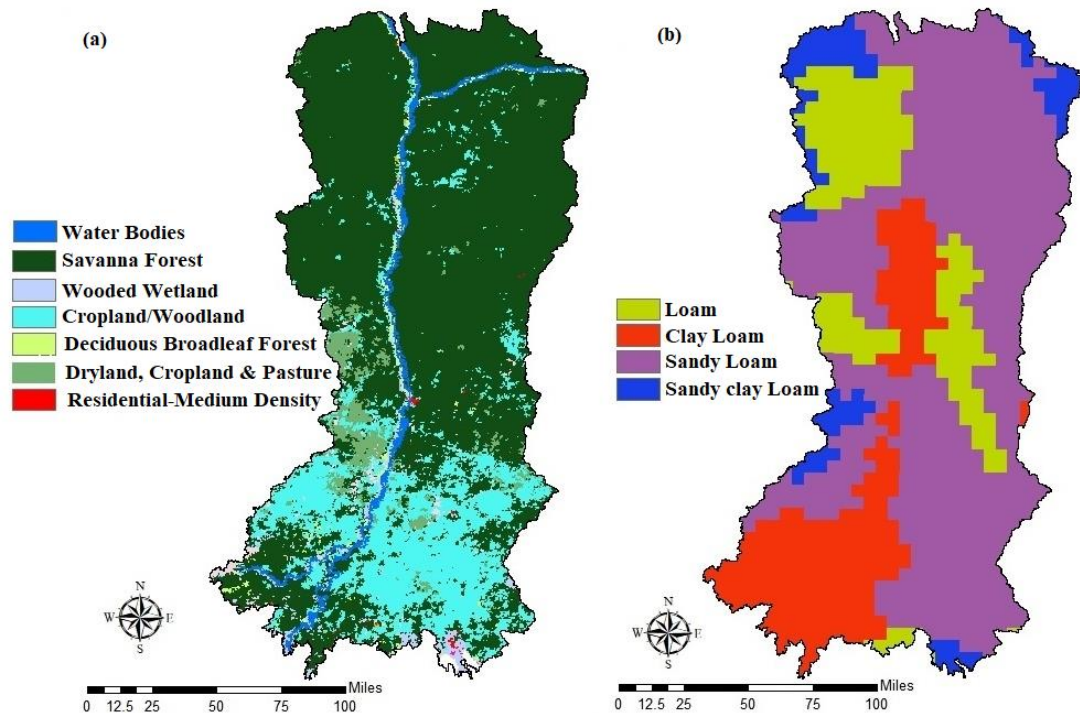


**Figure 7.2** (a) Land use and (b) Soil Map of River Niger Catchment

The study was divided into the following parts.; (1) hydrological simulation of the model involving calibration and validation of the basin with stations at Lokoja and Onitsha. (2) downscaling the study area future climate using CIMP5 GCM's under RCP4.5 and RCP8.5 emission scenarios.; and (3) application of the calibrated model to sections and predicted CIMP5 future climate in assessing the future streamflow of the basin. In the SWAT model version 2012, the basin is divided into sub-basins which are further divided into Hydrological Response Units (HRUs) based on dominant soil type and land use. Thus, the NRB was divided into 354 sub-basins and HRUs (Fig. 7.1) based on soil use (Fig. 7.2a), and soil type (Fig. 7.2b) in the basin.

**Table 7.2** : General Circulation Models (GCMs) Used in the Study at 0.5<sup>0</sup> Grid.

<b>Modeling Centre</b>	<b>Models</b>	<b>Institute</b>
CSIRO-BOM	ACCESS1-3	CSIRO (Commonwealth Scientific & Industrial Research Organisation, Australia), and BOM (Bureau of Meteorology, Australia)
MIROC	MIROC-ESM	AORI, NIES and JAMSTEC
MIROC	MIROC-ESM-CHEM	AORI, NIES and JAMSTEC
NCC	NoerESM1-M	Norwegian Climate Centre

### 3.2 Downscaling Future Climate

Four GCMs of ISI-MIP (Inter-Sectoral Impact Model Inter-comparison Project) (Hempel et al., 2013) models (Table 7.2) and two carbon emission and historical scenarios (RCP4.5 and RCP8.5) for the years (1980-2099) were extracted at a grid resolution of 0.5° X 0.5° for the study areas coordinates consistent with the observed climate datasets. These GCMs were selected based on their better performance over the Niger Delta (Hassan *et al.*, 2020b).

The primary aim of this method was to modify the daily time series of the variables (i.e., precipitation, tasmax, and tasmin) in the future years by adding monthly mean changes of GCM outputs. For simplicity, the easiest and yet the most common method of downscaling was used. For temperature, the additive correction factor for each month was used, and the adjusted formula for modified daily temperature (tasmax and tasmin) is expressed in Eq. (7.1).

$$T_{corrected_{ij}} = T_{GCM_{ij}} + \left( \bar{T}_{reference_{jk}} - \bar{T}_{GCM_{jk}} \right) \quad (7.1)$$

where T is the temperature,  $\bar{T}$  is the long-term average temperature, and i, j, k are respectively day, month, and year counters. For precipitation, a multiplicative correction factor for each month is used, and the modified daily rainfall is expressed in Eq. (7.2):

$$P_{corrected_{ij}} = P_{GCM_{ij}} * \frac{\bar{P}_{reference_{jk}}}{\bar{P}_{GCM_{jk}}} \quad (7.2)$$

where P is the precipitation (mm day<sup>-1</sup>), and  $\bar{P}$  is the long-term average precipitation.

### 3.3 Hydrological model: SWAT

Quantifying hydrologic response caused by anthropogenic activities requires a hydrologic model to link both climatic forcing and human impact on the hydrological response (Zhang *et al.*, 2012). The SWAT model was adopted here as numerous researchers around the world have successfully used it for multiple climate change studies on hydrological regimes (e.g. Ang & Oeurng, 2018; Ertürk *et al.*, 2014; Faramarzi *et al.*, 2013; Luo, *et al.*, 2013; Ouyang *et al.*, 2015; Santhi *et al.*, 2002; Tan *et al.*, 2017; Wang *et al.*, 2018; Wang *et al.*, 2012). SWAT is a physically-based spatially distributed hydrologic model developed by the U.S. Department of Agricultural Research Service (ARS), to simulate water, sediment, nutrient and pesticide transport at a catchment scale over a given period. The Model uses hydrological response units (HRUs) which comprise of land use, soil and slope features used to describe their spatial heterogeneity within a watershed. The SWAT model estimates relevant hydrological components such as evapotranspiration, percolation, surface runoff and peak rate of runoff, groundwater recharge, groundwater

flow and sediment yield for each HRU. In this study, ArcSWAT extension, which is a graphical user interface for the SWAT model in ArcGIS, is adopted (Neitsch *et al.*, 2005). The SWAT simulation hydrologic cycle water balance is based on the following equation:

$$SW_t = SW_0 + \sum_{i=1}^t (R_{day} + Q_{surf} - E_a - w_{seep} - Q_{gw}) \quad (7.3)$$

where  $SW_t$  denotes final soil water content (mm),  $SW_0$  is the initial soil water content on day  $i$  (mm),  $t$  is the time (days),  $R_{day}$  is the precipitation amount on day  $i$  (mm),  $Q_{surf}$  is the quantity of surface runoff on day  $i$  (mm),  $w_{seep}$  is the amount of water percolating into the vadose zone from the soil profile on day  $i$  (mm),  $E_a$  is the evapotranspiration amounts on day  $i$  (mm), and  $Q_{gw}$  is the amount of return flow on day  $i$  (mm).

The components simulated in the SWAT model include evapotranspiration, surface runoff, percolation, subsurface runoff (lateral runoff), underground runoff (base runoff) and groundwater recharge (Pereira *et al.*, 2016). When simulating evapotranspiration, the model separately estimates the evaporation of water in the soil and plant transpiration. The evaporation of soil water is calculated using exponential functions of the depth of water and the soil water content (Neitsch *et al.*, 2005), while transpiration is determined by correcting the potential evapotranspiration for conditions of vapour pressure deficit and soil water content deficit (Neitsch *et al.*, 2005). The model estimates potential evapotranspiration using the Penman-Monteith method, Surface runoff with a change in the retention parameter is estimated using the curve number method (USDA-SCS, 1972), which varies according to the soil's water content (Neitsch *et al.*, 2005). The model also estimates percolation using a combination of a storage propagation technique and a crevice flow model (Arnold *et*

al., 1998). Interflow is determined based on the hydraulic conductivity of the free aquifer; the distance travelled by the runoff to the central canal, and the depth of the water table (Neitsch *et al.*, 2005). The hydrological components were simulated for each HRU and aggregated to the sub-basin.

### **3.4 Model calibration and validation**

Calibration refers to modification or adjustment of model parameters within recommended ranges to optimise model output matched with observed datasets. These parameters can either be adjusted manually or automatically until the model output best matches the observed data (Vilaysane *et al.*, 2015). In this study, the streamflow calibration was done using the SWAT-CUP Model. SWAT-CUP is a model used for the calibration, validation, sensitivity and uncertainty analysis of SWAT models. It is linked to five different algorithms such as Sequential Uncertainty Fitting (SUFI-2), Generalized Likelihood Uncertainty Estimation (GLUE), Particle Swarm Optimization, (POS), Parameter Solution (ParaSol) and Mark chain Monte Carlo (MCMC) (Vilaysane *et al.*, 2015). In this study, SUFI-2 algorithm was applied for the calibration of the SWAT model because it has the broadest marginal parameter uncertainty intervals among the five approaches. Validation followed as the process through which the model or simulation was tested as an accurate representation of observed datasets.

The years from 1970 to 1973 were used in the model calibration as warm-up period to eliminate uncertainties, particularly regarding the soil water conditions. Lokoja station: calibration was performed between 1973 and 1993 and validation was conducted for data from 1994 to 2005; at Onitsha station, calibration was completed



using data between 1980 and 1997 validation on data from 1994 to 2005. The calibration was for average monthly streamflow for both stations examining the setting of minimum and maximum monthly flow rates, shape of the simulated hydrograph, and the values obtained for the correlation coefficient ( $R^2$ ) (Eq. (7.4)), root mean square error observations standard deviation ratio (RSR) (Eq. (7.5)), and Nash-Sutcliff efficiency (NSE) (Eq. (7.6)), (Moriassi *et al.*, 2007), trying to maximise the first and second and minimise the latter.

The correlation coefficient ( $R^2$ ) is a measure of how future outcomes are likely to be predicted by the model and is equivalent to the sample cross-correlation between predicted and observed values, where the overbar denotes mean values.

$$R^2 = \frac{\sum_{i=1}^{N_v} (y_i - \bar{y})(o_i - \bar{o})}{\sqrt{\sum_{i=1}^{N_v} (y_i - \bar{y})^2} \sqrt{\sum_{i=1}^{N_v} (o_i - \bar{o})^2}} \quad (7.4)$$

where  $y$  and  $o$  are predicted and observed values, respectively; and  $N_v$  is the number of target data used for testing.

RMSE-observations standard deviation ratio (RSR), is a model evaluation statistic developed based on the recommendation by Singh *et al.*, (2004). RSR standardises RMSE using the observations standard deviation. It is calculated as the ratio of the RMSE and standard deviation of the measured data, as shown in equation 7.5:

$$RSR = \frac{RMSE}{STDEV_{obs}} = \frac{[\sum_{i=1}^n (Y_i^{obs} - Y_i^{sim})^2]^{1/2}}{[\sum_{i=1}^n (Y_i^{obs} - Y_i^{mean})^2]^{1/2}} \quad (7.5)$$

RSR varies from the optimal value of 0, which indicates zero RMSE or residual variation and therefore, perfect model simulation, to a significant positive value. The

lower the RSR, the lower the RMSE, and the better the model simulation performance (Moriassi et al., 2013).

The Nash-Sutcliff efficiency (NSE) indicate the goodness-of-fit of the simulated and observed data in line 1:1 and can range from  $-\infty$  to 1. NSE measures the predictive skill of a model relative to the mean of observations (Moriassi et al., 2007). The NSE coefficient indicates the model's precision in simulating the flood streamflow. In this evaluation, the classification suggested by Motovilov et al., (1999) described as:  $NSE > 0.75$  (model is appropriate and good);  $0.36 < NSE < 0.75$  (model is satisfactory); and  $NSE < 0.36$  (model is unsatisfactory) was adopted.

$$NSE = 1 - \frac{\sum_{i=1}^n (Y_i^{obs} - Y_i^{sim})^2}{\sum_{i=1}^n (Y_i^{obs} - Y_i^{mean})^2} \quad (7.6)$$

where  $Y_i^{obs}$  is the  $i$ th observation for the constituent being evaluated,  $Y_i^{sim}$  is the  $i$ th simulated value for the constituent being evaluated,  $Y_{mean}$  is the mean of observed data for the constituent being evaluated, and  $n$  is the total number of observations.

The calibration process was finalised when the changes in parameters resulted in little difference in the output of the model. It should be noted that this method was selected for the model calibration to keep the mean physical of the calibration parameters due to a large number of hydrologic response units and subbasins (354) generated for the simulation of the basin.

## 4.0 Results

### 4.1 Downscaling of climate

The Spatial distribution of average annual precipitation, maximum and minimum temperature for the periods 1980 – 2005 are shown in Figure 7.3 & 7.4

respectively. The distribution of the 4 Raw GCMs (Figure 7.3(a, c, e)), shows a high variation in comparison with the distribution of observed CRU climate data. These biases, after correction, match the observed data, and the distribution of the ensemble bias-corrected 4 GCMs are depicted in Figure 7.3(b, d, f). After bias correction, the future climate was predicted for RCP 4.5 and 8.5 scenarios until 2099. The baseline period for the study is from 1970-2005, and the future period was divided into three-time series as 2010-2039, 2040-2069 and 2070-2099.

#### **4.1.2 Observed and Future Climate Scenarios**

Average daily rainfall and temperature during the base period and that projected over the periods 2010-2039, 2040-2069 and 2070-2099 around the study area are shown in Figures 7.4(a), to (f), respectively. Figure 7.4(a) and (b) shows that rainfall in the study area will increase during monsoon and decrease during the dry season. The figures show that the distribution of precipitation in the study area starts from March, reach its maximum between June and August and reduce significantly towards the end of October. The variation between the observed and future mean annual Rainfall is shown in Figure; 7.4 a & b, while the change in mean yearly temperature is depicted in Figure; 7.4 c & d, for Lokoja and Onitsha stations under RCP 4.5 and 8.5 respectively.

Tables 7.3 show changes in the ensemble projected mean annual rainfall, maximum and minimum temperature under RCP4.5 and RCP8.5 emission scenarios. The mean yearly temperature shows a more consistent change trend than precipitation. All the models projected stability increases in the future temperature and decreased in future rainfall under the two emissions scenarios. The expected maximum temperature

increases of the multi-GCMs ensemble for three future periods range from 1.45 °C to 5.54 °C under RCP4.5, and from 1.52 °C to 9.12 °C under RCP8.5 at Lokoja station while the expected minimum temperature increases from 4.43 °C to 20.09 °C under RCP4.5, and from 4.43 °C to 20.09 °C under RCP8.5 at Lokoja station.

**Table 7.3 :** Percentage changes in future Annual Rainfall, Maximum and Minimum Temperature under RCP4.5 & RCP8.5.

Emission Scenario	Periods	% Change in Rainfall (mm)		% Change in Tmax °C		% Change in Tmin °C	
		Lokoja	Onitsha	Lokoja	Onitsha	Lokoja	Onitsha
RCP4.5	2020s	-4.75	3.19	1.45	-3.14	5.74	0.71
	2050s	-10.59	3.80	3.43	-0.71	9.39	4.55
	2080s	-11.77	5.34	5.54	0.71	13.30	6.66
RCP8.5	2020s	-4.79	2.82	1.52	-2.85	4.43	1.17
	2050s	-5.07	3.34	4.93	0.90	11.24	7.13
	2080s	-5.81	3.80	9.12	5.27	20.09	13.74

The multi-GCMs ensemble for the three projected future periods shows a decrease in precipitation at Lokoja station environment ranging from -4.75 mm to -11.77 mm under RCP4.5 and -4.79 mm to -5.81 mm under RCP8.5. The decrease in precipitation coupled with increasing water demand due to the rapid population growth in the region might also result in the continuous drying up of the river if adequate management measures are not put in place for the sustainability of this precious resources. However, the multi-GCMs ensemble projected an increase in precipitation at Onitsha station environment ranging from 3.19 mm to 5.34 mm under RCP4.5 and 2.82 mm to 3.80 mm under RCP8.5. Temperature and rainfall are important factors that affect evapotranspiration and streamflow. The obtained results collaborate with the finding of (Shiru *et al.*, 2019) who reported that rainfall projection showed no significant change in Nigeria over the century under RCP 2.6, 4.5 and 6.5, while RCP 8.5 showed a decrease in the last part of the century (2070–2099).

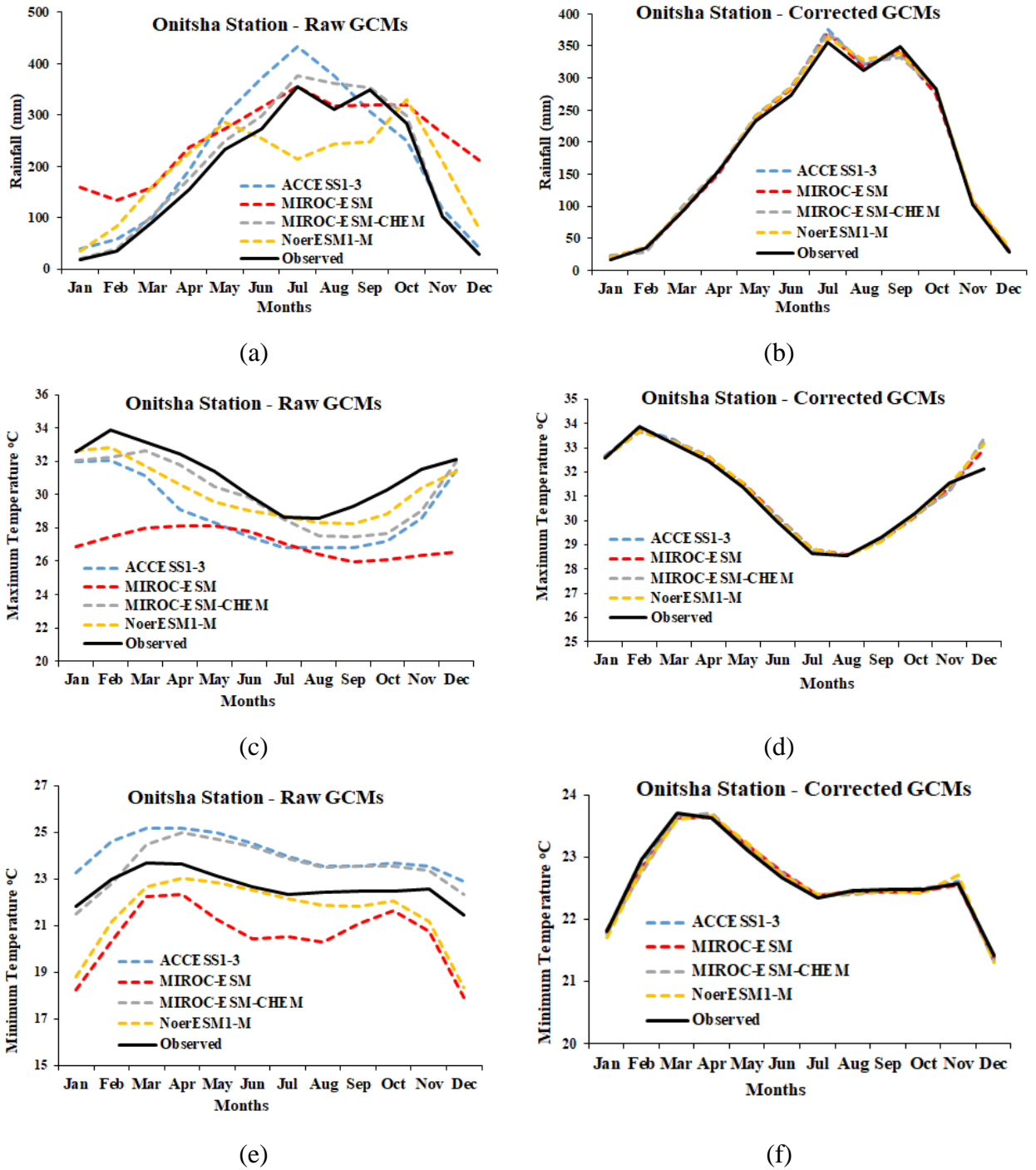
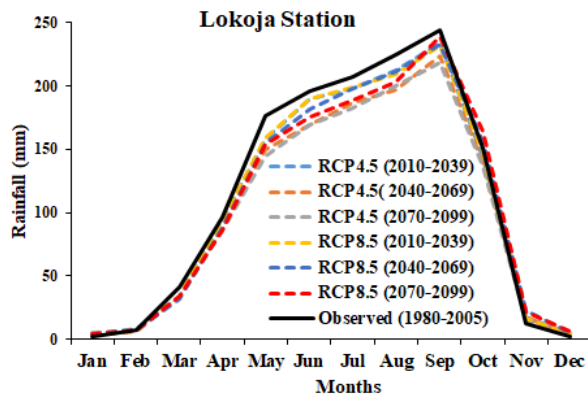
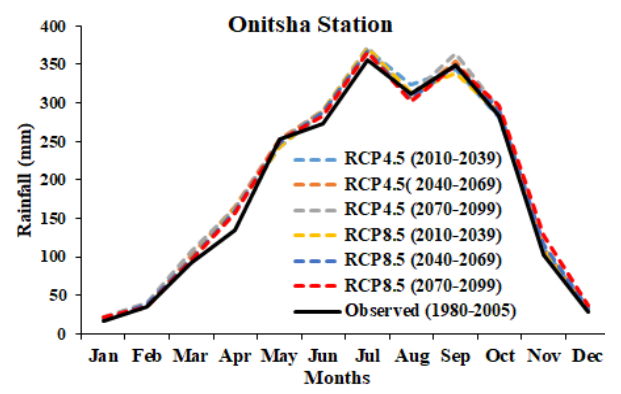


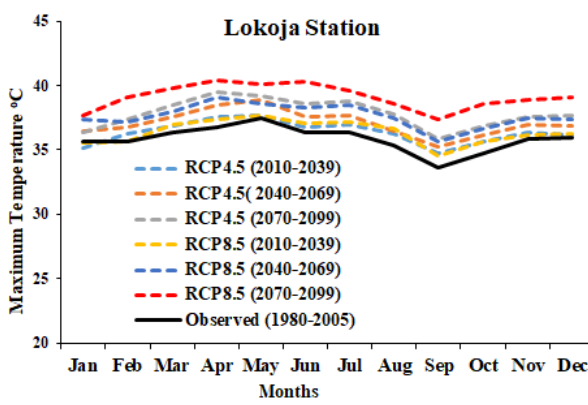
**Figure 7.3** Monthly averages of historical annual Raw (a) Rainfall (c) Tmax (e) Tmin, and Bias-corrected (b) Rainfall (d) Tmax (f) Tmin GCM's for the periods 1980–2005 in Onitsha.



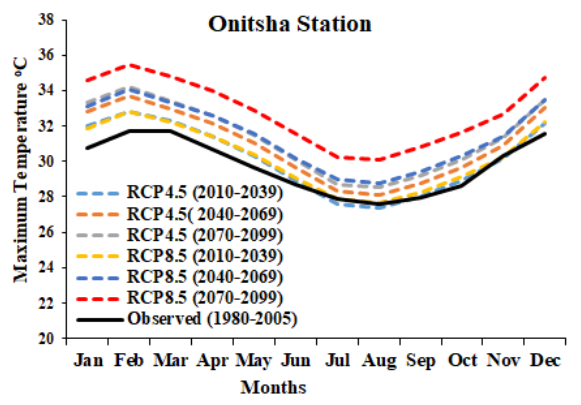
(a) Rainfall



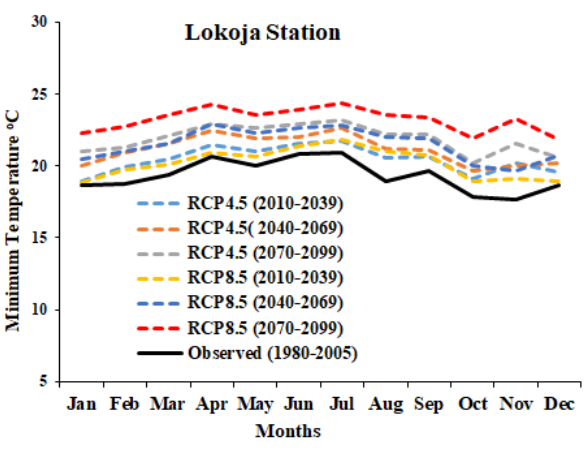
(b) Rainfall



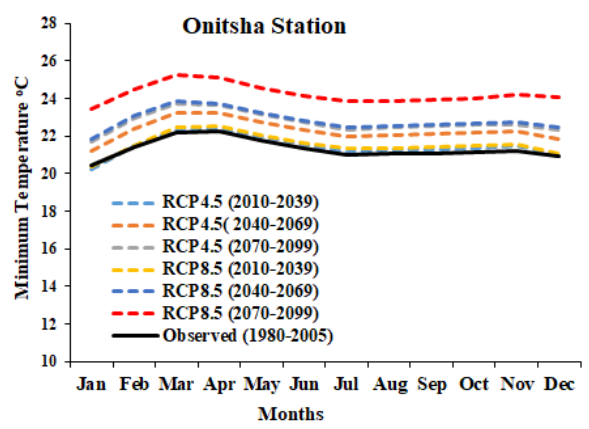
(c) Mean Temperature



(d) Mean Temperature



(e)



(f)

**Figure 7.4** Monthly averages of Observed and Projected Rainfall at (a) Lokoja (b) Onitsha, Tmax (c) Lokoja (d) Onitsha, and Tmin (e) Lokoja (f) Onitsha Stations under RCP 4.5 and 8.5 scenarios.

## 4.2 SWAT model calibration and validation

The relative sensitivity of variables during the parameter estimation process was evaluated. The results of the sensitivity analysis are listed in Table 7.4 based on their sensitivity ranking: Surface runoff lag time (SURLAG), SCS runoff curve number II (CN2), Soil evaporation compensation factor (ESCO), Deep aquifer percolation fraction (RCHRG\_DP), threshold depth of water in the shallow aquifer for return flow to occur (GWQMN), groundwater delay time (GW\_DELAY), base flow alpha-factor (ALPHA\_BF), Effective hydraulic conductivity in main channel alluvium (CH\_K2) and groundwater "revap" coefficient (GW\_REVAP). Details of these parameters and their effect on the hydrological cycle are explained in (Neitsch et al. (2005). A parameter ranked as 1 is considered the most important, and sensitivity decreases as the ranking decrease from 2 to 10. The Surface runoff lag time (SURLAG) shows the highest sensitivity followed by curve number for moisture condition II (CN2) (Table 7.4) for the streamflow simulation.

The results of the area indicate that parameters representing surface streamflow, soil properties, evapotranspiration and groundwater are sensitive and must be accurately estimated for accurate streamflow simulation. These sensitive parameters are considered for the model calibration in SWAT-CUP model. The discharge data were recorded during the years 1970-2004 at Lokoja station and 1980 to 2005 at Onitsha station. The years 1970-1972 were skipped for the model warm-up period, and Monthly discharge from 1973-2005 are used for calibration. The model was calibrated for the period 1973-1994 for Lokoja station, and 1980-1997 for Onitsha station. The model was validated from 1995-2005 for Lokoja station and 1998- 2004 for Onitsha station. Figure 7.5, 7.6 and Table 7.5 shows that SWAT-predicted monthly

streamflow at the Lokoja and Onitsha station very well compared with observed data in addition to the monthly precipitation totals at representative two stations.

**Table 7.4 :** Parameters Sensitivity analysis based on Hydrological stations of Lokoja and Onitsha

Parameter Name	Definition	Sensitivity Rank	Final Parameter	t-Stat	P-Value
SURLAG	Surface runoff lag time	1	18.65	0.16	0.87
CN2	SCS runoff curve number f	2	0.06	-0.17	0.87
ESCO	Soil evaporation compensation factor.	3	0.87	0.36	0.72
RCHRG_DP	Deep aquifer percolation fraction	4	-0.21	-0.43	0.67
REVAPMN	Threshold depth of water in shallow aquifer	5	-99.56	-0.49	0.63
GWQMN	Deep Percolation Loss	6	1.72	0.60	0.55
GW_REVAP	Groundwater "revap" coefficient	7	0.03	-1.22	0.22
CH_K2	Effective hydraulic conductivity	8	128.25	-3.32	0.00
GW_DELAY	Groundwater delay (days)	9	-22.85	-3.65	0.00
ALPHA_BF	Baseflow alpha factor (days)	10	0.10	13.83	0.00

**Table 7.5 :** SWAT Calibration and Validation Statistics of the River Niger Catchment

	Lokoja		Onitsha		Entire Period		Model Performance
	Calibration	Validation	Calibration	Validation	Lokoja	Onitsha	
NSE	0.70	0.56	0.74	0.74	0.65	0.74	Good
R <sup>2</sup>	0.82	0.83	0.84	0.85	0.82	0.85	Very Good
RSR	0.55	0.66	0.51	0.51	0.60	0.51	Good

Comparison between the trend and magnitude of observed and simulated monthly streamflow values (Figure 7.5, 7.6 & Table 7.5) shows that the observed and simulated streamflows measured data quite well. The model evaluation indicators indicate ‘good’ and ‘satisfactory’ simulations of hydrology at the entire watershed level, where the minimum of NSE, R<sup>2</sup> and RSR was 0.70, 0.82 and 0.55 during calibration, and 0.56, 0.83 and 0.66 during validation at Lokoja station and 0.74, 0.84



and 51 during calibration, and 0.74, 0.85 and 0.51 during validation at Onitsha station respectively. Both stations simulations are considered 'good' based on the NSE and RSR criteria developed by Moriasi et al., (2007) where NSE coefficient ( $0.65 \leq \text{NSE} \leq 0.75$ ) and RSR coefficient ( $0.50 \leq \text{RSR} \leq 0.60$ ). The  $R^2$  statistics, where a value close to 1 represents a good streamflow simulation.

### **4.3 Climate change analyses**

The Soil and Water Assessment Tool was used to model climate change impact on streamflow at the Lokoja and Onitsha streamflow monitoring stations located in the NRB of Nigeria (Figure 7.1). Direct input of downscaled precipitation, Maximum and minimum temperature data were used to simulate the hydrological cycle under RCP 4.5 and RCP8.5 emission scenarios. The annual mean monthly streamflow and the corresponding flow duration curves were used as indices for comparison between present-day and future streamflow scenarios at the Lokoja and Onitsha streamflow gauge sites in the Lower NRB. Because of monthly streamflow simulations, we do not distinguish between an increase in 'extreme' hydrological events and an overall increase in streamflow average.

The results were summarised for the periods of 2010–2039, 2040–2069 and 2070–2099, represented as the 2020s, 2050s and 2080s, respectively, and compared with the baseline years of 1980–2005. The baseline period was chosen based on GCM data availability, and the climate change periods were selected to cover all the remaining years in the 21st century as recommended by the IPCC (IPCC, 2007b).

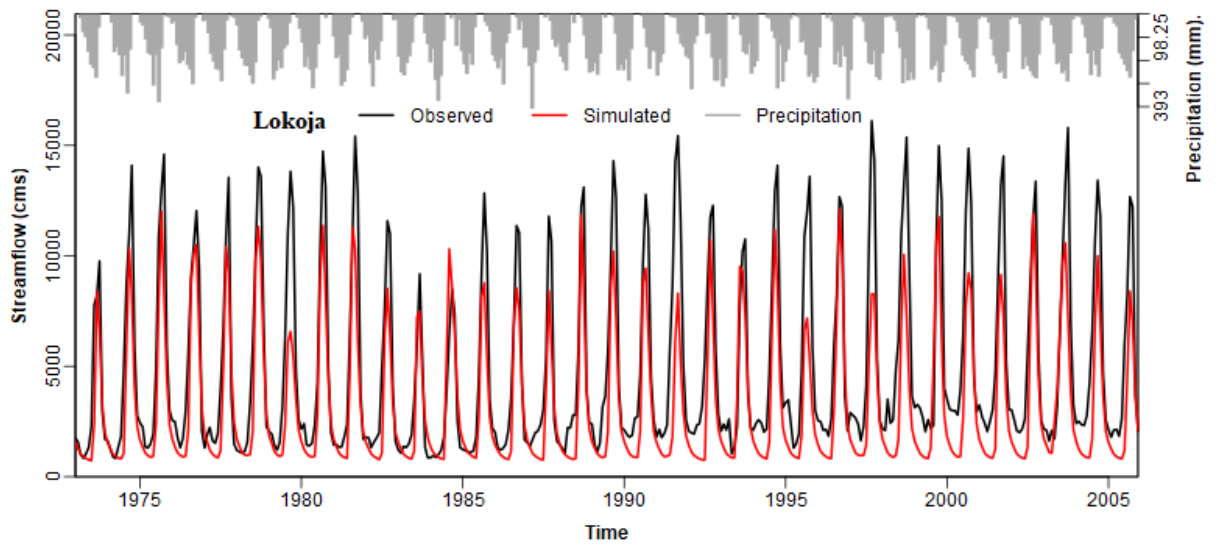


**Figure 7.5** Observed and Predicted Monthly Streamflow for Lokoja Monitoring Stations.

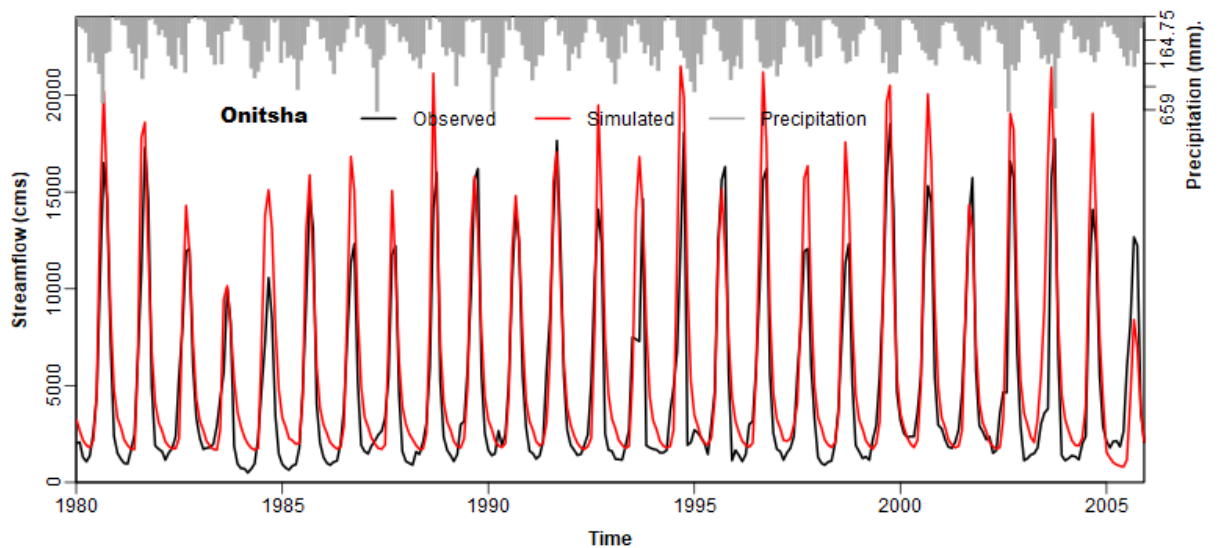


**Figure 7.6** Observed and Predicted Monthly streamflow for Onitsha Monitoring Stations.

#### 4.4 Climate change impact on streamflow

The ensemble of the 4 GCMs used for regional climates impacts studies using precipitation, minimum and maximum temperature output are presented in Table 7.2.

The simulated mean annual temperature for the baseline period is 26.87 °C for the entire basin. Under the RCP4.5 scenario, simulated mean yearly temperature increases by approximately 0.98 °C for the 2020s 1.8 °C for the 2050s and 2.4 °C for the 2080s for both locations.

Under the RCP 8.5 scenario simulated mean annual temperature increases by 0.9 °C for the 2020s for both areas, 2.12 °C for at Lokoja and 2.17 °C at Onitsha for the 2050s and 3.54 °C for Lokoja and 3.65 °C for Onitsha during the 2080s. For the RCP 4.5 scenario, average annual precipitation from the baseline years to the 2080s decreased from 1363.85 to 1203.37 mm for the Lokoja area and 2152.18 to 2018.90 mm for Onitsha station. For the RCP 8.5 scenario, average annual precipitation decreased from the baseline years to the 2080s were 1363.85 to 1203.367 mm for the Lokoja area and 2152.18 to 2033.15 mm for Onitsha station.

**Table 7.6 :** Mean Monthly and Percentage Change in Streamflow under RCP4.5 & RCP8.5

Emission Scenario	Periods	Mean Monthly Streamflow (m <sup>3</sup> /s)		% Change in Streamflow	
		Lokoja	Onitsha	Lokoja	Onitsha
Base Period	1990s	5100	4870		
RCP4.5	2020s	3520	6690	-31	41
	2050s	3435	6700	-33	35
	2080s	3061	5864	-40	18
RCP8.5	2020s	3439	6799	-33	37
	2050s	3025	5888	-41	18
	2080s	2914	5573	-43	12

#### 4.4.1 Lokoja Mean monthly streamflow

The variation in mean monthly streamflow for Lokoja monitoring Stations under RCP4.5 and RCP8.5 emission scenarios is depicted in Figure 7.7. The baseline

mean monthly streamflow at the Lokoja station was 5100 m<sup>3</sup>/s (Table 7.6). All the future scenarios depict a decreasing trend in precipitation. For the RCP 4.5 scenario, the decreases in precipitation for all periods will result to a reduction in mean monthly streamflow, with the most significant monthly streamflow decrease of 2039 m<sup>3</sup>/s occurring in by the end of the century. For the RCP 8.5 scenario, mean monthly streamflow also decreased relative to the baseline scenario by 1660 m<sup>3</sup>/s during the 2020s, 2075 m<sup>3</sup>/s during the 2050s and 2186 m<sup>3</sup>/s by the end of the century. As expected, the mean monthly streamflow for the climate change periods was closer to the mean under the RCP 4.5 scenario than the RCP 8.5 scenario, where a streamflow decrease occurred for every period.

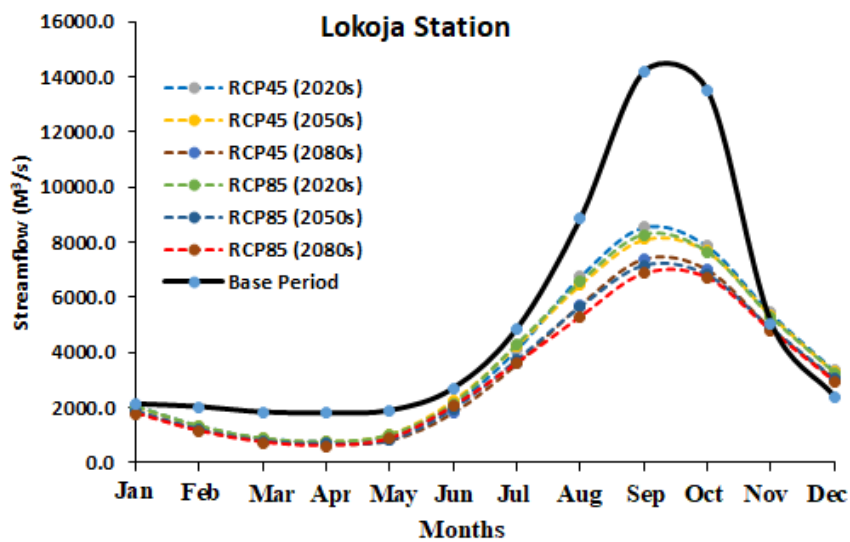


**Figure 7.7** Mean monthly streamflow for Lokoja Monitoring Stations under RCP4.5 and RCP8.5 emission scenarios.

#### 4.4.2 Onitsha Mean monthly streamflow

The mean monthly streamflow at Onitsha stations during the baseline was 4972 m<sup>3</sup>/s (Table 7.6). The RCP 4.5 scenario resulted in a continual streamflow increase for

all periods, with the largest occurring during the 2020s. These increases in streamflow are intuitive as this station receives more precipitation in comparison with the Lokoja station. The highest mean monthly streamflow increased by 41% from the baseline period in the 2020s under RCP 4.5 scenario. During the 2020s, 2050s and 2080s, the mean monthly streamflow was predicted to be all greater than the baseline period under both emission scenarios, respectively. The RCP 4.5 scenario exhibited higher variation under climate change than the RCP 8.5 scenario, as shown in Figure 7.8.

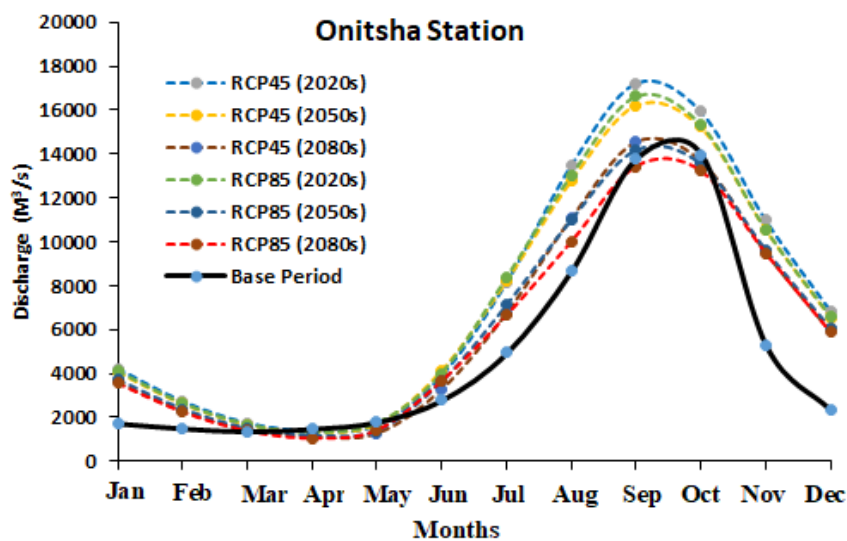


**Figure 7.8** Mean monthly streamflow for Onitsha Monitoring Stations under RCP4.5 and RCP8.5 emission scenarios.

#### 4.5 Climate change impact on mean annual Evapotranspiration

The simulated annual averages of SWAT hydrologic outputs show that the mean annual evapotranspiration of the basin ranges from 227 to 950 mm during the entire study period and under both emission scenarios as depicted in Figure 7.9. The results show that evapotranspiration is one of the major processes by which water is lost in the basin. These results indicate that agricultural areas around the central and northern part of the basin, as well as the degraded forests in the eastern part of the

Niger Delta, have the highest values of evapotranspiration rate while the swamp and mangrove forest in the coastal area has the lowest evapotranspiration rate. Results of projected future scenarios show an increase in mean annual evapotranspiration during the entire study period and under both emission scenarios with the highest projected increase during the 2080s.

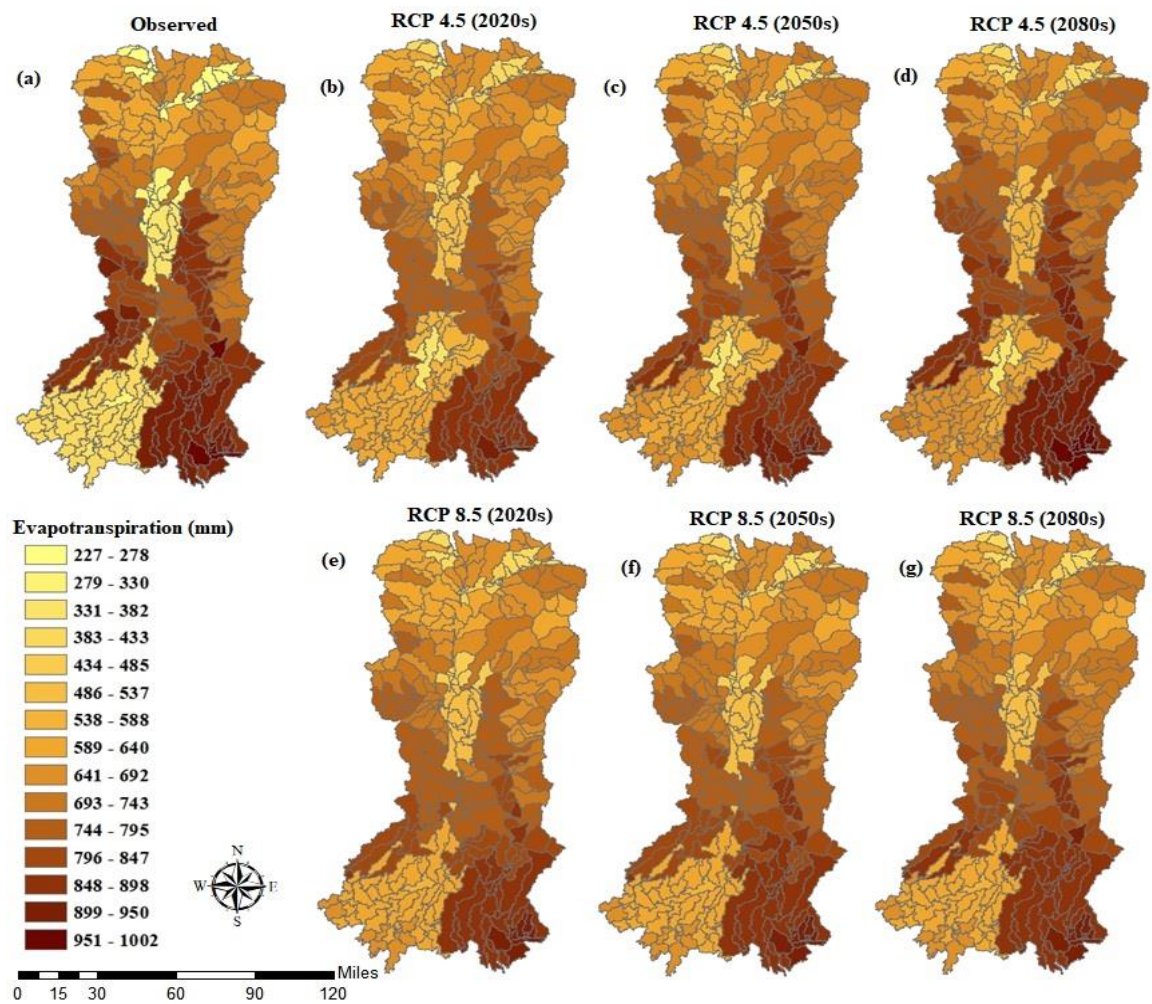


**Figure 7.9** Spatial distribution of Evapotranspiration during the (a) Observed (b) RCP 4.5 (2020s) (c) RCP 4.5 (2050s) (d) RCP 4.5 (2080s) (e) RCP 8.5 (2020s) (f) RCP 8.5 (2050s) (g) RCP 8.5 (2080s) in the Niger river basin.



#### 4.6 Climate change impact on mean annual groundwater recharge

The simulated groundwater recharge to the basin aquifers is presented in Figure 7.10. The average annual recharge in the basin ranges from 270 to 1700 mm as a minimum and maximum values during the entire study period and under both emission scenarios respectively.

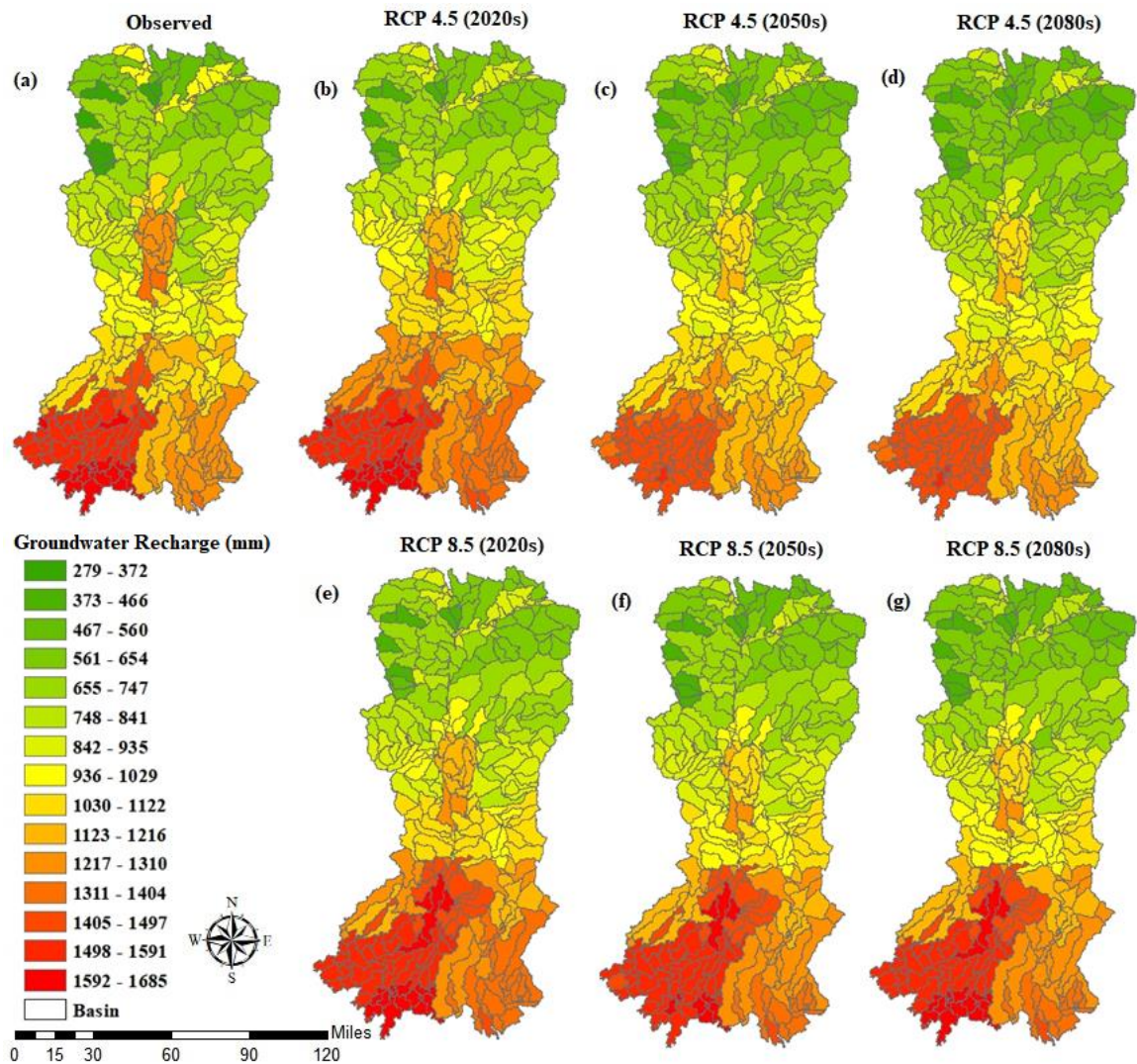


**Figure 7.10** Spatial distribution of groundwater recharge during the (a) Observed (b) RCP4.5 (2020s) (c) RCP4.5 (2050s) (d) RCP4.5 (2080s) (e) RCP8.5 (2020s) (f) RCP8.5 (2050s) (g) RCP8.5 (2080s) in the Niger River Basin.

Higher recharge rates are also projected to occur during the entire study period and under both emission scenarios with the highest projected increase during the 2080s, which might be due to the highest projected increase in precipitation during those periods. Higher recharge rates are expected to occur in the southern part of the basin, which is concentrated on sand plains and sand bars while south-southern part of the coastal area is characterised by marshy, swampy, waterlogged mangrove forest. The sandy soil texture and the plain topography around the south-eastern part of the basin favour surface and groundwater interaction.

## **5.0 Discussion**

Previous studies along the River Niger showed that the basin might be sensitive to changes in climate (Agumagu, & Todd, 2015). Our findings support this work as our results indicate that the southern River Niger Basin may be sensitive to climate change. Presently, Nigerian water resource managers have not had information on which to plan future modifications of the hydrological cycle for this arid region because of a lack of quantitative and qualitative data to determine future policy and management scenarios. In the southern NRB, as well as Nigeria at large, this study is the first of its kind to present the effects of climate change on the hydrological cycle.

For both scenarios and both stations, the mean monthly streamflows, evapotranspiration and recharge exhibited a predicted change from baseline years. The predicted mean monthly streamflow generally decreases for all scenarios at Lokoja station and increased for all scenarios at Onitsha stations, which likely leads to increased runoff out of the watersheds. Analysis of mean annual rainfall indicates that precipitation may decrease with climate change impact in the northern part of the study



area and increase towards the coastal south. This will undoubtedly affect water resource management policy and planning as the river, which is the primary source of drinking water, fishing, and irrigated agriculture. Results showed that the downstream study area would experience an increase in rainfall and average streamflow. This increase is likely a result of the higher number of contributing rivers. Adequate planning measures should be considered to ameliorate extreme flooding events that might, through reservoir management operations to achieve maximum efficiency and flood control. Results of the projected increase in climate variables and streamflow towards the coastal south also correspond with the findings of (Ike and Emaziye, 2012; Todd M, 2015; Obroma Agumagu, 2018; Matemilola *et al.*, 2019; Hassan *et al.*, 2020b) in this region.

The results also confirm the IPCC, (2007a) report on the increasing risks of flooding along the coasts and areas with low elevation due to impacts of climate change. Even minor changes in average monthly streamflow may result in significant differences in the number of water resources for agricultural and human consumption. The consequences of changing flows can be substantial for rivers already at their limits in terms of water resources. In the downstream study area, flooding is recorded every year in all the states along the River Niger and its tributaries, frequently attributed to climate change. Devastating floods inundate two-thirds of Bayelsa State and Delta State for at least a quarter of each year (Amangabara & Obenade, 2015; Amangabara & Gobo, 2007; Ologunorisa & Adeyemo, 2005; Mmom, 2013; Tawari-fufeyin *et al.*, 2015). Study on the vulnerability of communities in three Niger Delta States by Amangabara *et al.*, (2015) found out that over 1,000 towns are at risk of being inundated and about 7 million people risk displacement. Given areas around the

upstream part of the study area have recently been experiencing more frequent violent clashes between herders and farmers, it will be important that decision-makers have information to hand that can allow for policy or management decisions to reduce resource competition, especially in light of climate change that has been highlighted as a concern (Chukwuma & Atelhe, 2014; Marietu & Olarewaju, 2009; Weezel, 2017).

We do note that the analyses performed in this study are too uncertain for detailed (hourly, daily to monthly) water management planning. The results give insight into the sensitivity of this region and other Basins in Nigeria to the effects of climate change. Simulating climate change scenarios with other GCMs and RCPs will yield a broader picture of the impacts of climate change, as the various models may have conflicting precipitation and temperature patterns. We conclude, based on the output of an ensemble of GCMs, that the streamflow projections for this study are realistic. Future NRB climate change studies should include improved future projected land use data, facilitating the assessment of both flow and environmental impacts for current and potential future climate patterns.

## **6.0 Conclusions**

An ensemble of four GCMs was applied to the SWAT model to study the potential impacts of climate change on the hydrologic processes of the NRB over the next century. Using RCP 4.5 and 8.5 climate change scenarios, we showed a range of results aimed to support water resource policy, planning and management in the NRB. The results showed that SWAT is a useful tool for assessing the impacts of climate change on the hydrological cycle in this region. Comparing the climate change simulations of the 2020s, 2050s and 2080s to base year simulations (1980–2005),

several conclusions were drawn. The RCP 8.5 emission scenario leads to more annual precipitation and temperature than the RCP 4.5 emission scenario, resulting in differences in streamflow, groundwater recharge and evapotranspiration. Generally, the mean monthly streamflow in NRB in Nigeria decreased towards the northern part of the study area. It increased towards the coast in the 2020s, 2050s and 2080s compared with the baseline period. As temperatures rise throughout the 21st century, we can expect slightly higher streamflows in the Niger Delta River Basin regardless of the emissions scenario (RCP 4.5 or 8.5). Uncertainties still exist within this study using one RCP to analyse the effects of climate change on streamflow. However, comparable results were obtained after we tested the statistical significance between the four GCMs at both Lokoja and Onitsha stations. Results of projected future scenarios also show an increase in mean annual evapotranspiration and groundwater recharge during the entire study period and under both emission scenarios with the highest projected increase during the 2080s.

These results highlighting the projected change in climate and streamflow for the NRB of Nigeria are highly topical, given frequent clashes between farmers and herders in the study area due to competition for water and grazing lands. The study area was found to be vulnerable to the impacts of the changing climate in the future. There are uncertainties in the SWAT hydrological model calibration, especially around the modeling of future projected land-use change. Our finding should be of value for policy formulation and planning of mitigation and adaptation measures for climate change.

**Acknowledgements:** The authors would like to thank the Petroleum Technology and Development Fund (PTDF) under the Overseas PhD scholarship scheme and the

Scottish Government under the Climate Justice Fund Water Futures Programme, awarded to the University of Strathclyde (R.M. Kalin) for supporting this work.

**Data Availability:** The datasets used to support the findings of this study are available from the corresponding author upon request.

**Conflicts of Interest:** The authors declare no conflict of interest.

## References

Amangabara, G., and Obenade, M. (2015). Flood Vulnerability Assessment of Niger Delta States Relative to 2012 Flood Disaster in Nigeria. *American Journal of Environmental Protection*, 3(3), 76–83. <https://doi.org/10.12691/env-3-3-3>

Amangabara, G. T., and Gobo, A. E. (2007). Factors that influence the flooding of the middle and lower Ntamogba stream catchments, Port Harcourt, Nigeria. *Journal of Environmental Hydrology*, 15(November), 1–11.

Ang, R., and Oeurng, C. (2018). Simulating streamflow in an ungauged catchment of Tonlesap Lake Basin in Cambodia using Soil and Water Assessment Tool (SWAT) model. *Water Science*, 32(1), 89–101. <https://doi.org/10.1016/j.wsj.2017.12.002>

Apurv, T., Mehrotra, R., Sharma, A., Goyal, M. K., and Dutta, S. (2015). Impact of climate change on floods in the Brahmaputra basin using CMIP5 decadal predictions. *Journal of Hydrology*, 527. <https://doi.org/10.1016/j.jhydrol.2015.04.056>

Arnold, J. G., Srinivasan, R., Muttiah, R. S., and Williams, J. R. (1998). Large area hydrologic modeling and assessment part i: Model Development. *Journal of the American Water Resources Association*, 34(1), 73–89.

Chukwuma, A., and George Atelhe, A. (2014). Nomads against Natives: A Political Ecology of Herder/Farmer Conflicts in Nasarawa State, Nigeria. *American International Journal of Contemporary Research*, 4(2), 76–88.

- Crosbie, R. S., Scanlon, B. R., Mpelasoka, F. S., Reedy, R. C., Gates, J. B., and Zhang, L. (2013). Potential climate change effects on groundwater recharge in the High Plains Aquifer, USA. *Water Resources Research*, 49(7). <https://doi.org/10.1002/wrcr.20292>
- Ertürk, A., Ekdal, A., Gürel, M., Karakaya, N., Guzel, C., and Gönenç, E. (2014). Evaluating the impact of climate change on groundwater resources in a small Mediterranean watershed. *Science of the Total Environment*, 499, 437–447. <https://doi.org/10.1016/j.scitotenv.2014.07.001>
- Etim U. U Ituen, and Folarin Alonge. (2009). Niger Delta Region of Nigeria, Climate Change and the way Forward. *Bioenergy Engineering*, 11-14 October 2009, Bellevue, Washington, (January 2009). <https://doi.org/10.13031/2013.29162>
- Faramarzi, M., Abbaspour, K. C., Ashraf Vaghefi, S., Farzaneh, M. R., Zehnder, A. J. B., Srinivasan, R., and Yang, H. (2013). Modeling impacts of climate change on freshwater availability in Africa. *Journal of Hydrology*, 480, 85–101. <https://doi.org/10.1016/j.jhydrol.2012.12.016>
- Harris, I., Jones, P. D., Osborn, T. J., and Lister, D. H. (2014). Updated high-resolution grids of monthly climatic observations - the CRU TS3.10 Dataset. *International Journal of Climatology*, 34(3), 623–642. <https://doi.org/10.1002/joc.3711>
- Hassan, I., Kalin, R. M., White, C. J., and Aladejana, J. A. (2020a). Evaluation of Daily Gridded Meteorological Datasets over the Niger Delta Region of Nigeria and Implication to Water Resources Management. *Atmospheric and Climate Sciences (ACS), SCRIP*.
- Hassan, I., Kalin, R. M., White, C. J., and Aladejana, J. A. (2020b). Selection of CMIP5 GCM ensemble for the projection of Spatio-temporal changes in precipitation and temperature over the Niger Delta, Nigeria. *Water (Switzerland)*, 12(385). <https://doi.org/10.3390/w12020385>
- Ike, P. C., and Emaziye, P. O. (2012). An Assessment of the Trend and Projected Future Values of Climatic Variables in Niger Delta Region, Nigeria, 4(2), 165–170.

- IPCC. (1997). Climate change 1994: Radiative forcing of climate change and an evaluation of the IPCC IS92 emission scenarios. Intergovernmental panel on climate change (IPCC). *Global and Planetary Change* (Vol. 15). [https://doi.org/10.1016/S0921-8181\(96\)00009-4](https://doi.org/10.1016/S0921-8181(96)00009-4)
- IPCC. (2007a). Climate Change 2007: impacts, adaptation and vulnerability: contribution of Working Group II to the fourth assessment report of the Intergovernmental Panel. <https://doi.org/10.1256/004316502320517344>
- IPCC. (2007b). Climate Change 2007 Synthesis Report. Intergovernmental Panel on Climate Change *IPCC*. <https://doi.org/10.1256/004316502320517344>
- IPCC. (2013). Climate Change 2007: The Physical Science Basis. (D. Solomon, Susan & Qin, Ed.), *Journal of Chemical Information and Modeling* (Vol. 53). <https://doi.org/10.1017/CBO9781107415324.004>
- James S. Risbey, D. E. (1996). Observed Sacramento Basin streamflow response to climate impact studies, 184, 209–223.
- JICA (2013). Federal Republic of Nigeria the Project for Review and Update of Nigeria - (National Water Resources Master Plan 2013) Executive Summary - Volume 1. *Japan International Cooperation Agency*.
- Luo, Y. Z., Ficklin, D. L., Liu, X. M., and Zhang, M. H. (2013). Assessment of climate change impacts on hydrology and water quality with a watershed modeling approach. *Science of the Total Environment*, 450, 72–82. <https://doi.org/10.1016/j.scitotenv.2013.02.004>
- Marietu S, T., and Olarewaju O, I. (2009). Resource Conflict among Farmers and Fulani herdsman: Implications for resource sustainability. *African Journal of Political Science and International Relations*, 3(9), 360–364.
- Matemilola, S., Adedeji, O. H., Elegbede, I., and Kies, F. (2019). Mainstreaming climate change into the EIA process in Nigeria: Perspectives from projects in the Niger Delta Region. *Climate*, 7(2). <https://doi.org/10.3390/cli7020029>

- Moriasi, D., Arnold, J., and Liew, M. W. Van. (2013). Model Evaluation Guidelines for Systematic Quantification of Accuracy in Watershed Simulations, (May 2007). <https://doi.org/10.13031/2013.23153>
- Moriasi, D. N., Arnold, J. G., Liew, M. W. Van, Bingner, R. L., Harmel, R. D., and Veith, T. L. (2007). Model Evaluation Guidelines for Systematic Quantification of Accuracy in Watershed Simulations. *American Society of Agricultural and Biological Engineers*, 50(3), 885–900.
- Motovilov, Y. G., Gottschalk, L., Engeland, K., and Rodhe, A. (1999). Validation of a distributed hydrological model against spatial observations, 99.
- Neitsch SL, Arnold JG, Kiniry JR and Williams, J. (2005). Soil and Water Assessment Tool Documentation.
- Obroma Agumagu, (2018). Projected Changes in the Physical Climate of the Niger Delta Region of Nigeria. *SciFed Journal of Global Warming*.
- Ologunorisa, T. E., and Adeyemo, A. (2005). Public perception of flood hazard in the Niger Delta, Nigeria. *Environmentalist*, 25(1), 39–45. <https://doi.org/10.1007/s10669-005-3095-2>
- Oloruntade, A. J., Mohammad, T. A., Ghazali, A. H., and Wayayok, A. (2017). Analysis of meteorological and hydrological droughts in the Niger-South. *Global and Planetary Change*, 155. 225–233. <https://doi.org/10.1016/j.gloplacha.2017.05.002>
- Ouyang, F., Zhu, Y., Fu, G., Lü, H., Zhang, A., Yu, Z., and Chen, X. (2015). Impacts of climate change under CMIP5 RCP scenarios on streamflow in the Huangnizhuang catchment. *Stochastic Environmental Research and Risk Assessment*, 29(7), 1781–1795. <https://doi.org/10.1007/s00477-014-1018-9>
- Pandey, P., and Patra, K. C. (2014). Hydrological Impacts of Climate Change. *International Journal of Engineering Research and Applications (IJERA) ISSN: 2248-9622 National Conference on Advances in Engineering and Technology*, 45–48.
- Pereira, R., Martinez, M. A., Pruski, F. F., and Demetrius, D. (2016). Journal of Hydrology : Regional Studies Hydrological simulation in a basin of typical tropical

- climate and soil using the SWAT model part I: Calibration and validation tests. *Biochemical Pharmacology*, 7, 14–37. <https://doi.org/10.1016/j.ejrh.2016.05.002>
- Prince C. Mmom, (2013). Vulnerability and Resilience of Niger Delta Coastal Communities to Flooding. *IOSR Journal of Humanities and Social Science*, 10(6), 27–33. <https://doi.org/10.9790/0837-1062733>
- Santhi, C., Arnold, J. G., Williams, J. R., Dugas, W. A., Srinivasan, R., and Hauck, L. M. (2002). Validation of the SWAT model on a large river basin with point and nonpoint sources. *Journal of the American Water Resources Association (JAWRA)*, 37(5), 1169–1188. <https://doi.org/10.1111/j.1752-1688.2001.tb03630.x>
- Shen, M., Chen, J., Zhuan, M., Chen, H., Xu, C. Y., and Xiong, L. (2018). Estimating uncertainty and its temporal variation related to global climate models in quantifying climate change impacts on hydrology. *Journal of Hydrology*, 556, 10–24. <https://doi.org/10.1016/j.jhydrol.2017.11.004>
- Shiru, M. S., Shahid, S., Chung, E.-S., Alias, N., and Scherer, L. (2019). A MCDM-based framework for selection of general circulation models and projection of spatio-temporal rainfall changes: A case study of Nigeria. *Atmospheric Research*, 225(March), 1–16. <https://doi.org/10.1016/j.atmosres.2019.03.033>
- Singh, J., Knapp, H. V., Arnold, J. G., and Demissie, M. (2004). Hydrological modeling of the Iroquois River watershed using HSPF and SWAT. *Journal of the American Water Resources Association*, 41(2), 343–360. <https://doi.org/10.1111/j.1752-1688.2005.tb03740.x>
- Tan, M. L., Ibrahim, A. L., Yusop, Z., Chua, V. P., and Chan, N. W. (2017). Climate change impacts under CMIP5 RCP scenarios on water resources of the Kelantan River Basin, *Malaysia. Atmospheric Research*, 189, 1–10. <https://doi.org/10.1016/j.atmosres.2017.01.008>
- Tawari-fufeyin, P., Paul, M., and Godleads, A. O. (2015). Some Aspects of a Historic Flooding in Nigeria and Its Effects on some Niger-Delta Communities. *American Journal of Water Resources*, 3(1), 7–16. <https://doi.org/10.12691/ajwr-3-1-2>



- Teutschbein, C., and Seibert, J. (2012). Bias correction of regional climate model simulations for hydrological climate-change impact studies: Review and evaluation of different methods. *Journal of Hydrology*, 456–457, 12–29. <https://doi.org/10.1016/j.jhydrol.2012.05.052>
- Todd M, A. O. (2015). Modelling the Climatic Variability in the Niger Delta Region: Influence of Climate Change on Hydrology. *Journal of Earth Science & Climatic Change*, 06(06), 284. <https://doi.org/10.4172/2157-7617.1000284>
- USDA-SCS. (1972). (United States Department of Agriculture-Soil Conservation Service). 1985. *National Engineering Handbook, Section 4, Hydrology*. Washington, D.C.: USDA-SCS.
- Vilaysane, B., Takara, K., Luo, P., and Akharath, I. (2015). Hydrological stream flow modelling for calibration and uncertainty analysis using SWAT model in the Xedone river basin, Lao PDR. *Procedia Environmental Sciences*, 28(Sustain 2014), 380–390. <https://doi.org/10.1016/j.proenv.2015.07.047>
- Wang, J., Hu, L., Li, D., and Ren, M. (2020). Potential Impacts of Projected Climate Change under CMIP5 RCP Scenarios on Streamflow in the Wabash River Basin. *Advances in Meteorology*, 2020, 1–18. <https://doi.org/10.1155/2020/9698423>
- Wang, X., Li, Z., and Li, M. (2018). Impacts of climate change on stream flow and water quality in a drinking water source area, Northern China. *Environmental Earth Sciences*, 77(11), 1–14. <https://doi.org/10.1007/s12665-018-7581-5>
- Wang, Z., Ficklin, D. L., Zhang, Y., and Zhang, M. (2012). Impact of climate change on streamflow in the arid Shiyang River Basin of northwest China. *Hydrological Processes*, 26(18), 2733–2744. <https://doi.org/10.1002/hyp.8378>
- Weezel, S. van. (2017). Drought severity and communal conflict in Drought severity and communal conflict in Nigeria.
- World Meteorological Organization WMO. (2018). WMO provisional Statement on the Status of the Global Climate in 2018.
- Zhang, A., and Zhang, C. (2012). Assessments of Impacts of Climate Change and Human Activities on Runoff with SWAT for the Huifa River Basin, Northeast China (April 2014). <https://doi.org/10.1007/s11269-012-0010-8>

### 7.3 Supplementary Data

#### 7.3.1 Climate change impact on mean annual surface runoff

The simulated average annual surface runoff in the basin is presented in Figure 7.11, which ranges from 24 to 360 mm as a minimum and maximum values during the entire study period and under both emission scenarios respectively.

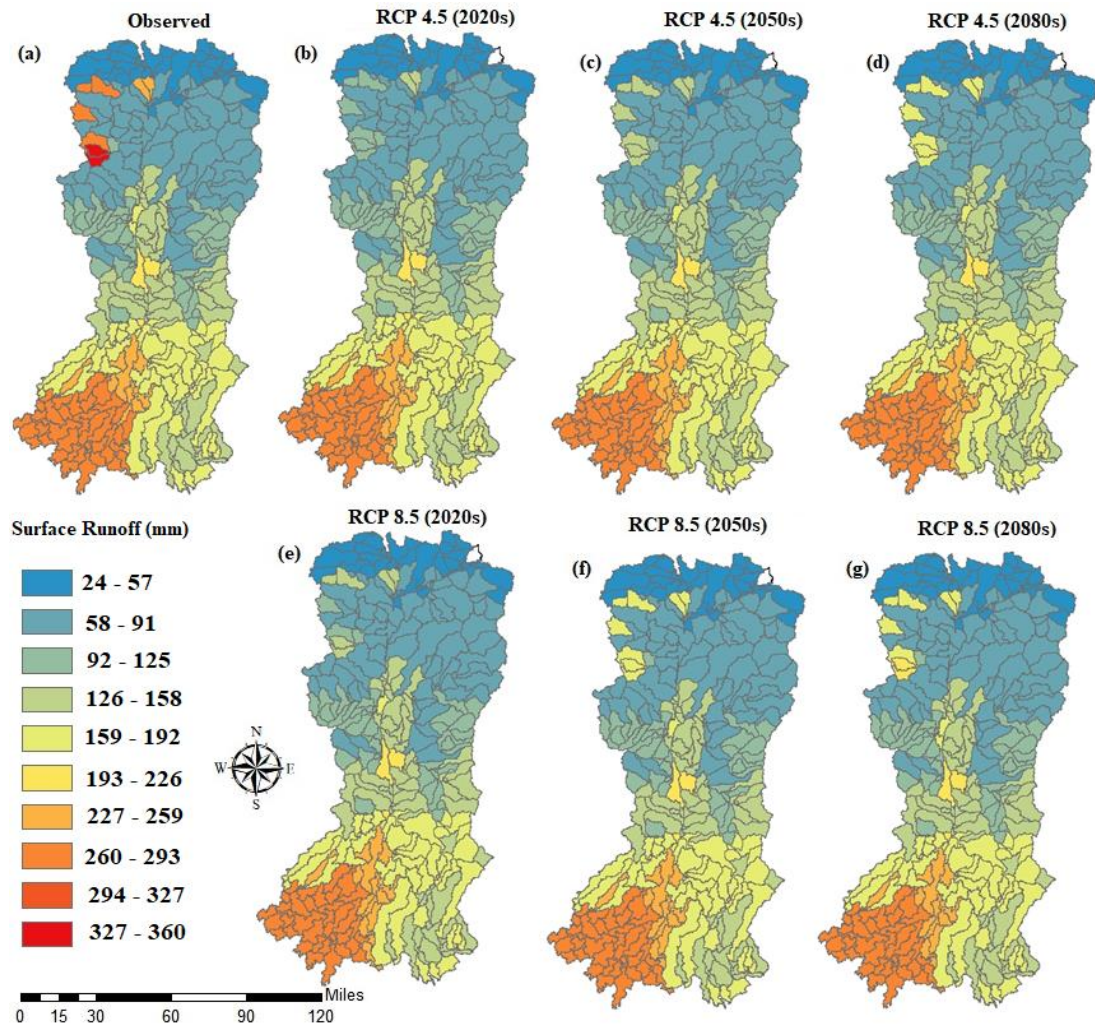


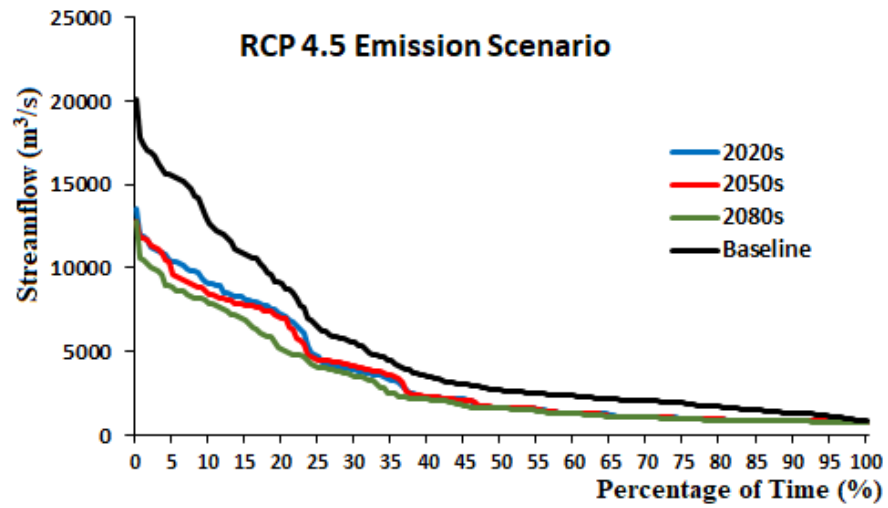
**Figure 7.11** Spatial distribution of Surface Runoff during the (a) Observed (b) RCP4.5 (2020s) (c) RCP4.5 (2050s) (d) RCP4.5 (2080s) (e) RCP8.5 (2020s) (f) RCP8.5 (2050s) (g) RCP8.5 (2080s) in the Niger River Basin.

Higher runoff rates are expected to occur in the southern part of the basin which due to the higher rainfall experienced in those areas. Results of projected future scenarios show an increase in average annual surface runoff during the entire study period and under both emission scenarios with the highest projected increase during the 2080s.

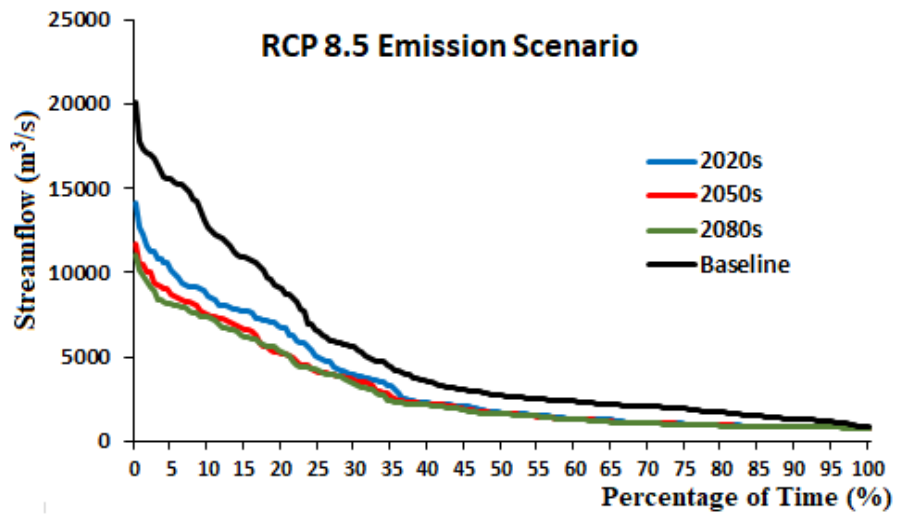
### **7.3.2 Lokoja station flow Duration Curve**

The maximum streamflow duration at the Lokoja station exhibits similar trends as the Onitsha station (Figure 8); however, the differences in streamflow between the climate change and baseline scenarios were more significant in some cases. Mean monthly maximum streamflow for the baseline years at the Lokoja station was higher for streamflow that flowed approximately 40–100% of the time, with a more significant difference for the RCP8.5 scenarios than the RCP4.5 scenario. The difference between climate change and baseline mean monthly maximum streamflows were higher for the RCP8.5 scenario than the RCP4.5 scenario.

The mean monthly maximum streamflows that occurred between 25 and 70% of the time were similar for all scenarios. These results suggest that the extreme streamflows (maximum discharges that occur less than 20% of the time) will increase under climate change. Still, the maximum discharges that occur over 20% will be similar or less than the baseline scenario (Figure 8). In general, the difference between the mean monthly the baseline and climate change scenarios for streamflow had a difference of fewer than 1000 m<sup>3</sup>/s for all streamflow durations. The most significant difference between the baseline and climate change years was for the streamflow that occurred below 38.89% of the time for the RCP8.5 scenarios and 36.56% for the RCP4.5 scenarios.



(a)



(b)

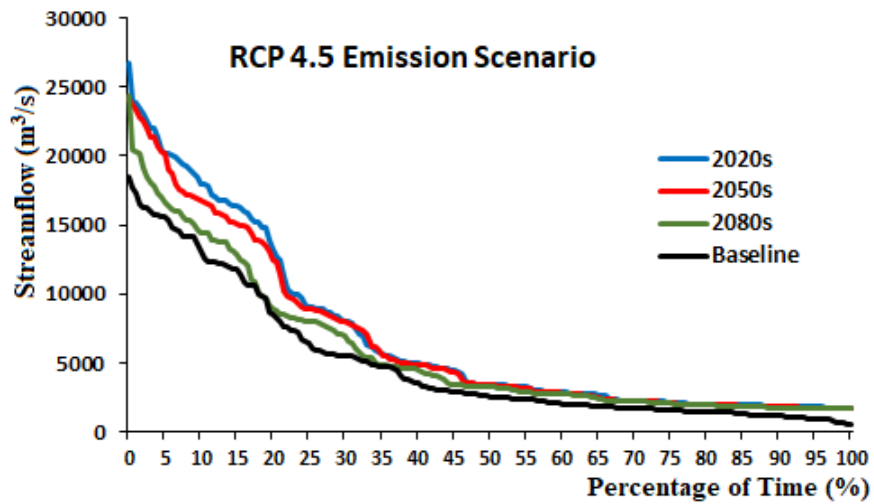
**Figure 7.12** Percentage flow duration curve of Maximum streamflow for each year at Lokoja Monitoring Stations under (a) RCP4.5 and (b) RCP8.5 emission scenarios.

### 7.3.3 Onitsha station flow Duration Curve

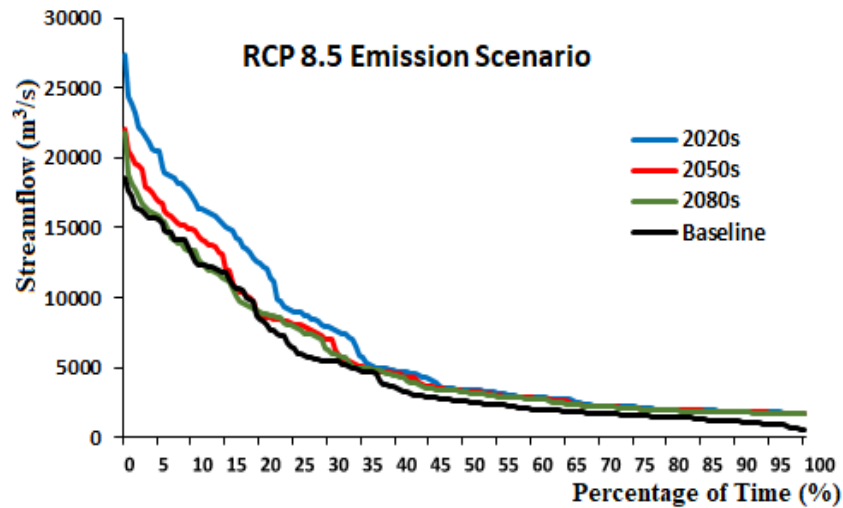
The monthly mean monthly percentage changes in streamflow for RCP4.5 and RCP8.5 scenarios relative to the baseline years than the baseline scenario for every period exhibited similar trends as the Lokoja station with an initial increase during the 2020s followed by decreases during the 2050s and 2080s. Conversely, the mean monthly streamflow that flows 1–20% of the time was higher for both climate change scenarios than the baseline years.

Mean monthly maximum streamflow for the baseline and climate change scenarios that flow 70–100% of the time were approximately equivalent. These corresponding differences in extreme events resulted in a change from baseline of about 50%. These results suggest that overall differences of mean monthly streamflow that flow more than 50% of the time may be highly significant, with the potential for increases in streamflow, which may have significant implications for water resource management. For example, an increase in maximum streamflow may quickly decrease reservoir storage capacity and flood protection. To counter this, water resource managers may need to release more water out of the reservoir during a time when the reservoir inflow needs to be conserved for the upcoming dry season.

The difference between the mean monthly baseline and climate change scenarios for streamflow had a difference of less than 0.1 m<sup>3</sup>/s for all streamflow durations. The most significant difference between the baseline and climate change years was for the streamflow that occurred below 60% of the time for the RCP8.5 scenario and 37% for the RCP4.5 scenario.



(a)



(b)

**Figure 7.13** Percentage flow duration curve of Maximum streamflow for each year at Onitsha Monitoring Stations under (a) RCP4.5 (b) RCP8.5 emission scenarios.

In general, the results indicate that climate change may lead to a gradual increase in mean monthly streamflow. Figure 10 shows that all periods and scenarios exhibited an increase in mean monthly minimum streamflow relative to the baseline years at Onitsha station. Generally, the mean monthly streamflow increases from the

2020s to the 2080s for all percentage time durations. The RCP8.5 scenario shows a much more considerable variation than the RCP4.5 scenario, especially in mean monthly minimum streamflows that occur less than 50% of the time. This accounts for the significant difference in mean monthly streamflow between the two emission scenarios. Substantial changes in minimum streamflow will result in substantial changes for water resource management.

#### **7.4 Concluding Remarks**

This Chapter used the ensemble of the 4 selected GCMs in chapter 5 on the SWAT model to study the potential impacts of climate change on streamflow of the NRB over the next century. The results showed that SWAT is a useful tool for assessing the impacts of climate change on the hydrological cycle in this region and the findings from these study addressed bullet points 6 and 7 of the literature review.

It is expected that the parameters obtained in this study from the Lokoja and Onitsha hydrological stations sensitivity analysis during the SWAT-CUP model calibration can be used in future SWAT studies in the study area and the results of distributed groundwater recharge and evapotranspiration obtained in this study can be used in future studies to analyse the blue and green water footprints of the area. Hence, further assessment and application of the groundwater recharge and evapotranspiration for the potential impacts of climate change on groundwater resources in the Niger Delta is achieved in the next chapters.

# CHAPTER 8

## Hydrological Conceptual Model

### 8.1 Preamble

The findings from the hydrological model in the previous chapter show a significant impact of climate change on groundwater recharge. As surface and groundwater are two interconnected components of one single resource, any negative impacts on one will inevitably affect either the quantity or quality of the other component. The climate change impacts on groundwater recharge serve as a threat to groundwater quality and quantity. It has, therefore, become necessary to develop a hydrogeological conceptual model of the area to understand better the hydrostratigraphy and hydrogeological characteristics of the groundwater aquifers in this area. A research article was written and from this study and published in MDPI, Geosciences journal (2019) as:

- Hassan, I.; Kalin, R. M.; White, C. J.; Aladejana, J. A (2019) ‘Hydrostratigraphy and Hydraulic Characterisation of Shallow Coastal Aquifers, Niger Delta Basin: A Strategy for Groundwater Resource Management’, *Geosciences*, MDPI, 9(11), p. 470. doi:10.3390/geosciences9110470.

The article presents my efforts in conceptualizing, theoretical formulation, development, analytic calculations, numerical simulations, and writing the manuscript. My major supervisor, Prof. Robert M. Kalin, assisted in designing the research and



gave critical views on the manuscript for further improvement. My second supervisor, Chris J. White, provided technical help and proposed important additions to the models and the manuscript. Finally, my colleague Jamiu A. Aladejana also assisted in giving critical views on the manuscripts and support when required.

## 8.2 Paper 5

Hassan, I.; Kalin, R. M.; White, C. J.; Aladejana, J. A. (2019) 'Hydrostratigraphy and Hydraulic Characterisation of Shallow Coastal Aquifers, Niger Delta Basin: A Strategy for Groundwater Resource Management', *Geosciences*, MDPI, 9(11), p. 470. doi:10.3390/geosciences9110470.

### **Hydrostratigraphy and Hydraulic Characterisation of Shallow Coastal Aquifers, Niger Delta Basin: A Strategy for Groundwater Resource Management**

**Ibrahim Hassan<sup>1,2</sup>, Robert M. Kalin<sup>1</sup>, Christopher J. White<sup>1</sup> and Jamiu A. Aladejana<sup>1,3</sup>**

<sup>1</sup>*Department of Civil and Environmental Engineering, University of Strathclyde, Glasgow;*

<sup>2</sup>*Department of Civil Engineering, Abubakar Tafawa Balewa University Bauchi, Nigeria;*

<sup>3</sup>*Department of Geology, University of Ibadan, Nigeria*

*Email: Ibrahim.hassan@strath.ac.uk*

#### **Abstract**

The groundwater from shallow coastal aquifers in Nigeria has been reported to be under intense stress resulting from both natural and anthropogenic impacts ranging from saltwater intrusion, effluent-related contamination and pollution to oil spillage, gas flaring, municipal, industries and agriculture. Here we characterised the hydrostratigraphy and hydraulic characteristics of the shallow coastal aquifers of the Niger Delta basin and assessed the resilience of groundwater to both natural and anthropogenic impacts. Fifty-two borehole logs were analysed from which lithological sections were used to generate cross-sections along with four profiles. The system was more complex than previously reported: a unit of silty sand was observed in the western part of the basin that thins out leaving the eastern part of the basin as an

unconfined aquifer underlain by multiple thin beds of the sand aquifer. A layered sand aquifer occurs in the northern parts of the basin, which holds freshwater in this area, and is interbedded by clay layers, which serve as aquitards. The relatively higher hydraulic conductivity of the Benin Formation units compared to those of the Deltaic Formation leave it with weaker climate change resilience and more vulnerable to pollution and contamination. While groundwater remains the dominant source of fresh water in the northern part of the basin, a strategic approach is needed to access potable water from the southern part where contaminated surface water appears to directly interact with the groundwater of the uppermost-unconfined aquifer. Management of waste and effluent related to oil spillage, municipal, industries and agricultural in this area should be engineered to protect the groundwater resources of this aquifer.

**Keywords:** Coastal aquifers; Groundwater; Characterisation; Borehole logs; Niger Delta.

## **1.0 Introduction**

Safe drinking water is critical to an improved standard of living and is a fundamental goal for sustainable water resources management under water supply sanitation and hygiene (WASH) (Hutton and Chase, 2016). Globally, water resources are facing numerous challenges ranging from quality to quantity (Cosgrove and Loucks, 2015). Groundwater is generally regarded as a source of high-quality freshwater, used not only for drinking purposes but also supporting industrial and agricultural activities (Cox SE, 1999). Groundwater accounts for one-third of all freshwater withdrawals, supplying an estimated 36% of domestic, 42% of agricultural and 27% of industrial water used globally. The ease of exploration to meet the required

water demand with little substantial infrastructure promotes the widespread development of groundwater use (Taylor, 2012).

The Niger Delta in Nigeria is the economic hub of the country due to crude oil exploration around the basin. This has attracted many petroleum and petrochemical industries into the area resulting in rural-urban migration and a surge in the urban population. Increased population has placed pressure on the available water resources in the area (Edet *et al.*, 2014). Data from the National Bureau of Statistics shows that water in the majority of Niger Delta states comes from unsafe supply facilities, such as rivers, lakes, unprotected hand-dug wells and boreholes. Potable water for household consumption used to run in public taps but fell into disrepair 20 years ago; hence people now rely on boreholes, protected wells, unprotected wells, rivers/lakes/ponds, vendor trucks and other water sources. These problems are acute and result in supplies of unsafe water in more than 50% of the cases (UNDP, 2006). These factors have led to a dependence on groundwater from shallow aquifers to meet daily water demands.

Complicating factors, such as oil spillage, flooding and gas-flaring, have caused significant degradation of groundwater quality in this area (Nnabuenyi, 2012), thereby costing the federal government of Nigeria for the remediation of the soil and surface and groundwater resources. Flooding events are recorded every year in all the states along the River Niger, and its tributaries, specifically Delta, Bayelsa and Rivers states, and cause disasters, which are also attributed to climate change (Ologunorisa and Adeyemo, 2005; Amangabara and Gobo, 2007; Prince Mmom, 2013; Amangabara and Obenade, 2015; Tawari-fufeyin *et al.*, 2015). This has resulted in 1110 towns, accommodating over 7 million people, being at risk of inundation by flooding (Amangabara and Obenade, 2015). Floods also serve as a threat to groundwater quality

and quantity. It has, therefore, become imperative to develop a hydrogeological conceptual model of the area to better understand the hydrostratigraphy and hydrogeology of this area. This model will allow for proactive protection policy and strategy, reducing further deterioration in groundwater resources. It also serves as a planning tool for water quantity and quality management models for sustainable water resource management of the vulnerable and critical shallow groundwater aquifers of the Niger Delta basin.

The design and implementation of a conceptual groundwater model requires a thorough understanding of hydrogeological factors that control site-specific flow and transport in the subsurface (Charles *et al.*, 2001). Several hydrogeology methods have been employed in groundwater aquifer characterisation, which range from invasive geophysical methods, such as electrical resistivity and electromagnetic method, and direct methods, such as borehole logging and hydrochemical evaluation (Cox, 1999; Allen and Schuurman, 2008; Sanz *et al.*, 2009; Farid, Jadoon and Akhter, 2013; Asfahani, 2016). Borehole well logging is known for the precise qualitative and quantitative delineation of groundwater aquifers, especially in stratified sedimentary basins (Adepelumi *et al.*, 2009; Oyedele, *et al.*, 2009; Raji *et al.*, 2018), the results of which were used here. Geohydraulic information was extracted from previous studies at different locations across this basin. This study therefore described the shallow coastal aquifers of the Niger Delta basin and assessed its implications on the resilience of groundwater for both natural and anthropogenic impacts. Both borehole logs and hydraulic characterisation were critically assessed to determine the resilience of shallow aquifer groundwater in the study area to pollution and contamination (attenuation) caused by oil exploration activities and waste disposal practices that characterise the study area.

## 2. Materials and Methods

### 2.1 Description of the Study Area

The Niger Delta is an Eocene sedimentary basin that lies between latitude 4°40' N to 5°40' N and longitude 6°50' E to 7°50' E located in the southern part of Nigeria (Figure 8.1) and is situated in the Gulf of Guinea and extends into the central South Atlantic Ocean at the mouths of the Niger Benue and Cross River systems (Aturamu *et al.*, 2015). The basin is divided into three sub-regions, namely, the Western Niger Delta, the Central Niger Delta and the Eastern Niger Delta. The Central Niger Delta consists of the central section of the South-South coast of Nigeria, which includes Bayelsa and Rivers State, and the Eastern Niger Delta consists of Cross River State and Akwa Ibom State. The area has a humid subequatorial climate with a short dry season from November to February and a long wet season from March to October. The annual average temperature is 27 °C, with a small range of 3 °C. The annual rainfall ranges from 2000 mm in the north to more than 4000 mm in the coastal areas, with an average of 3000 mm (Ophori, 2007).

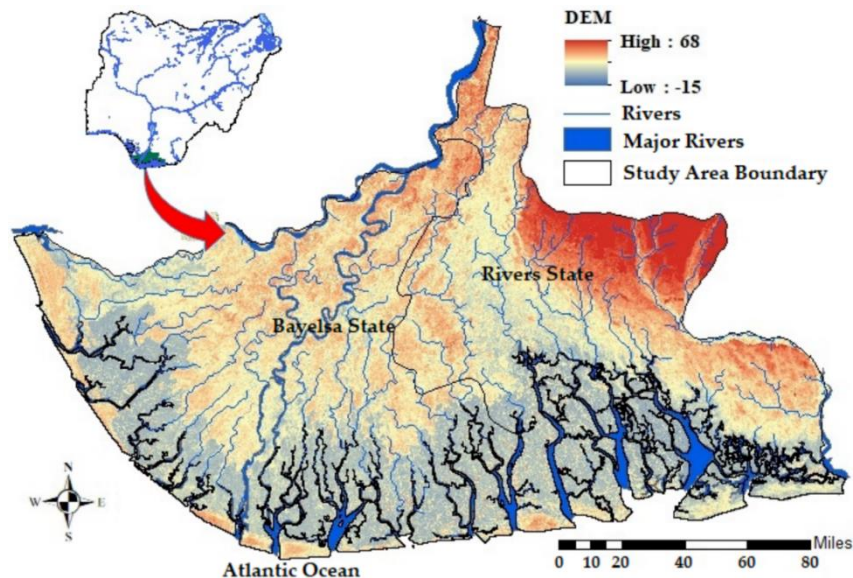


**Figure 8.1** Digital elevation map showing the location of the study area in Nigeria.

## 2.2 Geology of the Area

The Niger Delta is one of the significant regressive deltaic sequences in the world. The delta is over 12 km thick and occupies an area of 75,000 km<sup>2</sup> in the Gulf of Guinea. The Niger Delta basin is underlain by three formations, which include the Benin, Agbada and Akata Formations. The Benin Formation belongs to the Pliocene-Pleistocene age (Owoyemi, 2004).

The Deltaic Formation and Benin Formation are the most critical groundwater aquifer formations in the Niger Delta (Adelana *et al.*, 2008; Okeke *et al.*, 2011; Offodile, 2014; Nwankwoala, 2015). In the Deltaic Formations, late Pleistocene to Holocene age sediments occupy most of the area of the present delta and stretch eastwards along the coastline. The Deltaic Plains (upper and lower) consist of coarse-to-medium-grained unconsolidated sands. These sands form lenticular beds with intercalations of peaty matter and lenses of soft, silty clay and shales. Gravelly beds, up to 10 m thick, have been reported here (Uko E.T. and Emudianughe J.E., 2016). The Benin Formation outcrop is located in the northeast of the coastal belt and dips at a low angle in the south-west. The sediments here consist, generally, of unconsolidated lenticular and predominantly sandy formations with massive gravel and pebble beds giving rise to high-yielding boreholes (Ugwu & Nwankwoala, 2008). The thickness of the outcrop is estimated at 2300 m (Merki, 1970). To complete the stratigraphic sequence, it is important to include the Agbada Formation and the Akata Formation, which are geologically older formations. The Agbada Formation consists of interbedded sands and marine shales, reported to range in depth from about 300 to 5000 m while the Akata Formation underlies the Agbada Formation and has a sequence of similar marine shales and clays with a range in depth of about 700 to 7000 m. Table 8.1 shows the summary of the stratigraphic units of the Niger Delta basin.

**Table 8.1 :** Stratigraphic Units of the Niger Delta basin (Etu-Efeotor J. O & Akpokodje E. G, 1990).

Outcropping Units	Subsurface Units	Present-day Equivalents
Benin Formation	Benin Formation	Continental (fluviatile) deposits, mainly sandstones
Ogwashi–Asaba Formation	Agbada Formation	Mixed continental brackish water and marine deposits, sandstones and clays
Ameki Formation		
Imo Shales	Akata Formation	Marine deposits, mainly clays

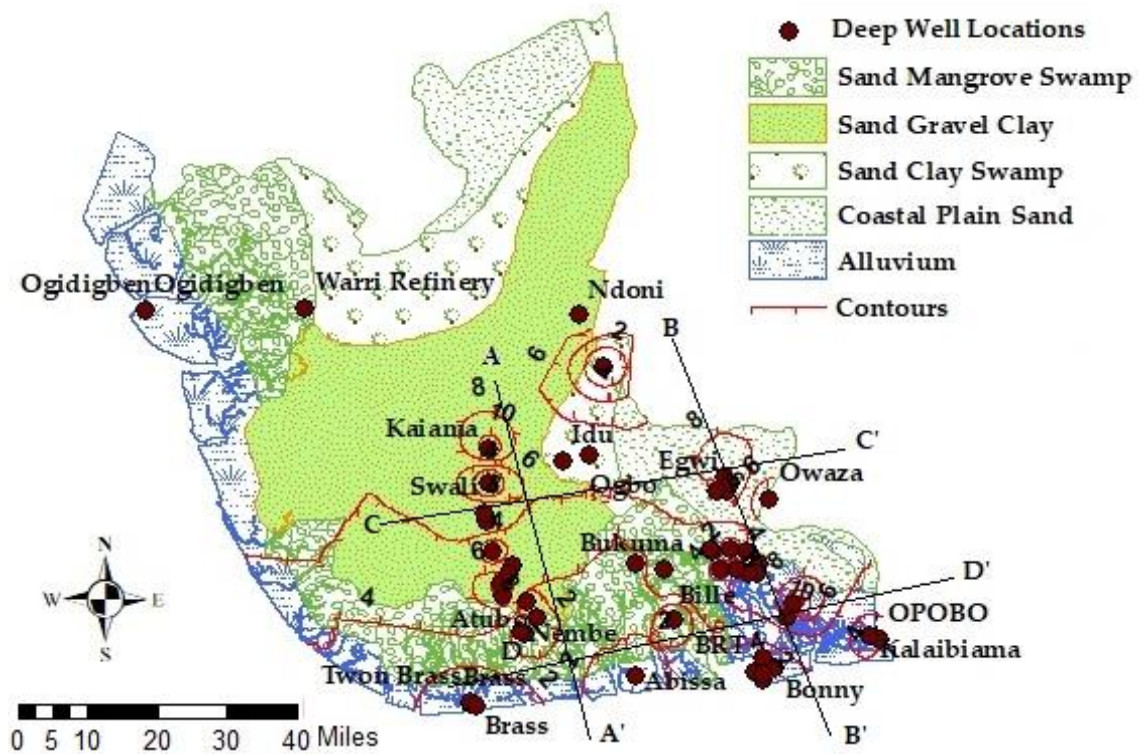


**Figure 8.2** Geology map (Adopted and Modified from (NGSA, 2012)) of the study area showing cross-section lines along which lithosections are developed.

### 2.3 Hydrogeology

The Niger Delta is a sedimentary basin where groundwater recharge is mostly through infiltration and from precipitation and rivers/lagoons at the surface. The most significant aquifers in the Niger Delta are the Deltaic and Benin Formations. Most of



the boreholes in the northern parts of the basin have tapped water from these unconfined aquifers. The geological sequence derived from the existing boreholes through logging revealed deep sandy units at a different part of the area, although some unconfined aquifers with artesian groundwater flow occurred in some locations too (Adelana *et al.*, 2008). The aquifers were, therefore, is classified into unconfined and confined.

**Unconfined aquifers.** The deltaic aquifer is classified as unconfined, which is the first and topmost groundwater unit recharged directly by infiltration from precipitation and baseflow. The water table in the Niger Delta area is very close to the ground surface, ranging from 0 to 9 m below ground level. This area experiences limited water table fluctuation due to heavy rainfall which varies from about 2400 mm a year inland to 4800 mm near the coast although some proportion of the rainfall is lost through runoff and evapotranspiration. As stated in (Offodile, 1992), the Deltaic Plains have specific capacities ranging from 160 to 320 m<sup>3</sup>/d/m.

The Benin Formation is more permeable than the Deltaic Plains due to the nature of the sediments with a specific capacity ranging between 150 and 1400 m<sup>3</sup>/d/m (Offodile, 1992). The depth to the water table ranges between 3 and 15 m below the ground surface. A few values for seasonal fluctuations obtained from the area indicated seasonal differences in static water level fall between 2.1 and 3.6 m.

**Confined aquifers.** This type of aquifer occurs across the Deltaic Formation and the Benin Formation. Moderately high-yielding artesian flows characterise these formations. In some areas, the aquifers are confined by a clay bed up to 36 m thick (Adelana *et al.*, 2008). The depth of the aquifers below this bed is approximately 100 m. Hydrogeological information indicates a hydrological connection between the confined aquifers along the coastline and the unconfined aquifers of the Benin

Formation to the north. The aquifers increase in thickness towards the continent, while the confining clays thin out. The specific capacity for this formation varies from 90 to 320 m<sup>3</sup>/d/m. In the area underlain by the Benin Formation, the confined aquifers occur in the southeastern part of the Niger Delta. Several clay beds confine the aquifers. The confined aquifers consist mainly of very-coarse-to-medium-grained sands. The specific capacity for this formation varies between 140 and 180 m<sup>3</sup>/d/m.

### 3. Methodology

Borehole logs data were collected from 52 wells (Figure 8.2) in strategic locations (Table 8.2) across the Niger Delta basin from the Nigeria Hydrological Services Agency (NHISA). These wells were reported to be drilled using the rotary drilling method commonly used in the Niger Delta. Drilling was followed up with down-hole geophysical logging in addition to the pre-drilling surface geophysical survey. Most of the logging in this study was done using the Mount Sopris Instrument, MGS II Logger that has the ability to run a suite of logs which provide accurate qualitative and quantitative information.

**Table 8.2 :** Borehole locations with strata logs, their depths and static water levels.

S/No.	Borehole Location	Geomorphic Zone	Total Depth Drilled (m)	Static Water Level (m)
1	Ogbo	CPS	186	7.0
2	Edocha	CPS	185	4.26
3	Port Harcourt (Old GRA)	CPS	207	5.5
4	Ndoni	CPS	182	7.55
5	Idu	CPS	185	6.2
6	Ebubu	CPS	92	6.0
7	Azikoro	FWS	335	8.6
8	Swali	FWS	335	8.8
9	Finima (Life camp)	CBR	360	1.3
10	Onne (FOT) *	CPS	190	6.0
11	Finima (BRT)	CBR	360	1.0
12	Bassambiri	CBR	250	0.8

13	Atubo	SWS	193	1.37
14	Nembe	SWS	195	2.1
15	Ogbia	FWS	198	2.5
16	Brass	CBR	192	0.69
17	Twon Brass	CBR	260	1.2
18	NAOC Tank farm	CBR	256	0.8
19	Otegila	FWS	185	4.0
20	Okoroba	FWS	225	0.0
21	Amakalakala	FWS	160	9.14
22	Otugidi	FWS	426	0.91
23	Otuesaga	FWS	102	12.19
24	Owaza	CPS	152	3.6
25	Kolo creek	FWS	102	5.2
26	Onne (NAFCON)	CPS	264	7.49
27	Otakeme	FWS	300	4.2
28	Omoku	SWP	183	0.68
29	Aleto Eleme	CPS	150	7.75
30	Bukuma	SWS	183	1.25
31	Kala Degema	SWS	171	2.8
32	Abissa	SWS	147	0.4
33	Bille	SWS	193	0.6
34	Opiro	SWS	138	13
35	Rumonye	CPS	188	22
36	Chokocho	CPS	132	10
37	Egwi	CPS	201	8.25
38	Umuechem	CPS	132	5.5
39	Okrika	SWS	113	11.4
40	Ibuluya-Dikibo	SWS	180	8.2
41	Bolo 1	SWS	92	5.5
42	Abam Ama	SWS	128	ARTESIAN
43	Okujiagu	SWS	110	0.7
44	George Ama	SWS	200	0.9
45	Kalaibiana	CBR	305	2.4
46	Bonny	CBR	198	3.0
47	Bonny (Water Board)	CBR	450	1.2
48	Bonny (Oguede)	CBR	460	ARTESIAN
49	Okoloma (Afam)	CPS	120	6.3
50	Borokiri *	SWS	190	2.5
51	Gbaran-Ubie	FWS	530	-
52	Ogidigben/Ugorodo	CBR	600	-

CPS = coastal plain sands, FWS = freshwater swamp, SWS = saltwater swamp, CBR = coastal beaches and ridges, SWP = Sambreiro Warri deltaic plain, \* = transitional zone.

The wells studied range in depth from 100 to 600 m and represent the middle and deeper aquifer systems of the Niger Delta. Their completion diameter ranges from 150 to 340 mm. The lining of the wells was mild steel casings adapted, at the intake

region, to a sequence of stainless-steel screens of various diameters and lengths depending on the aquifer thickness and the budget of the water project. All the wells were gravel-packed and developed for optimum yield for domestic and industrial purposes. This data was used to construct cross-sections and fence diagrams from which conceptual aquifer geometry and characterisation was developed.

The lithological information from boreholes was converted into geologically homogeneous hydrogeological units, which might not be isotropic but have unique hydrodynamic properties (Anderson, Woessner and Hunt, 2015). The hydrogeological unit's definition was used to correlate those data points with the lithofacies description and other less precise descriptions. Elevations of the top and the bottom of the units are referred to as meters above sea level (masl).

The top and bottom elevations of the aquifer units were modelled using geographical information systems (GIS) tools (ArcGIS and ArcScene). The information produced by GIS was then exported to other software to perform different hydrogeological analyses and three-dimensional surface mapping. As sub-surface modelling are not free of uncertainty (Heuvelink, 1986; Nilsson *et al.*, 2007; Rojas *et al.*, 2008; Jichun and Xiankui, 2013), both the geological knowledge of the study area and the application of cross-sections to the model allowed for considerable reduction in the degree of uncertainty in this work.

## **4. Results and Discussion**

### **4.1 Aquifer Characterisation Using Borehole Logs**

Aquifer characterisation is critical to groundwater resilience, which is essential to sustainable, groundwater resource management. In this study, borehole logs data

were collected from 52 wells in strategic locations (Table 8.2) across the Niger Delta basin. This data was used to construct cross-sections and fence diagrams from which aquifer geometry and characterisation was derived.

#### **4.2 Cross-Sections from the Selected Boreholes**

Four cross-sections (AA<sup>I</sup>, BB<sup>I</sup>, CC<sup>I</sup> and DD<sup>I</sup>) were generated from the results of the borehole logging. AA<sup>I</sup> and BB<sup>I</sup> are parallel in the SE-NW direction and perpendicular to CC<sup>I</sup> and DD<sup>I</sup>, which are in the SW-SE direction though with a different number of the boreholes in each section depending on the nature of the terrain, land use and settlement. Cross-section AA<sup>I</sup> (Figure 8.3), with orientation SE-NW, contains boreholes from Kaiama, Gbaran-Ubie, Oloibiri, Nembe and Brass with respective depths of 348, 530, 280, 195 and 192 m while their respective static water levels remain at 3, 4.37, 2.4, 2.1 and 0.69 m below the ground level.

Cross-section BB<sup>I</sup> (Figure 8.4), with orientation SE-NW, comprises boreholes from Omoku, Buguma, Bille, Onne, Okrika, Bonny, Bodo Bonny, Opobo and Finima with respective depths of 183, 81, 193, 264, 149, 153, 153, 147 and 450 m while their respective static water levels remain at 0.68, 1.25, 0.6, 7.46, 11.4, 3.0, 6.1, 1.6 and 2.0 m below the ground level. Cross-section CC<sup>I</sup> (Figure 8.5), with orientation SE-NW, comprises boreholes from Gbaran-Ubie, Kaiama and Omoku with the respective depths of 520, 348 and 183 m while their respective static water levels remain at 4.37, 3.0 and 0.68 m below the ground level.

Cross-section DD<sup>I</sup> (Figure 8.6), with orientation SE-NW, comprises boreholes from Brass, Oloibiri, Nembe, Bille, Okrika, Bonny, Bodo, Onne and Opobo with respective depths of 192, 280, 195, 193, 149, 153, 153, 264 and 147 m while their respective static water levels remain at 4.37, 3.0 and 0.68 m below the ground level.

The lithologic logs show that the sand bodies are predominant in the northern part of the study area. These sand bodies begin to give way to distinct clay interbeds at the middle and towards the southeast of the study area. Around Obigbo, through Akpajo and Buguma to Nembe, the number of distinct clay interbeds increases from 3 at Obigbo to 5 at Akpajo and Buguma and 11 at Nembe. While the northern part (Figure 8.3) contains one or two thick aquifers, the increased number of clay layers in the central part has partitioned the aquifers into 3 to 5 thinner units (Figure 8.5). The more frequent alternation of sand and clay layers in the south and towards the coast has resulted in a greater number of aquifers in the southern part (Figure 8.6). However, the greater the number of aquifer lenses, the less their thicknesses tends to be.

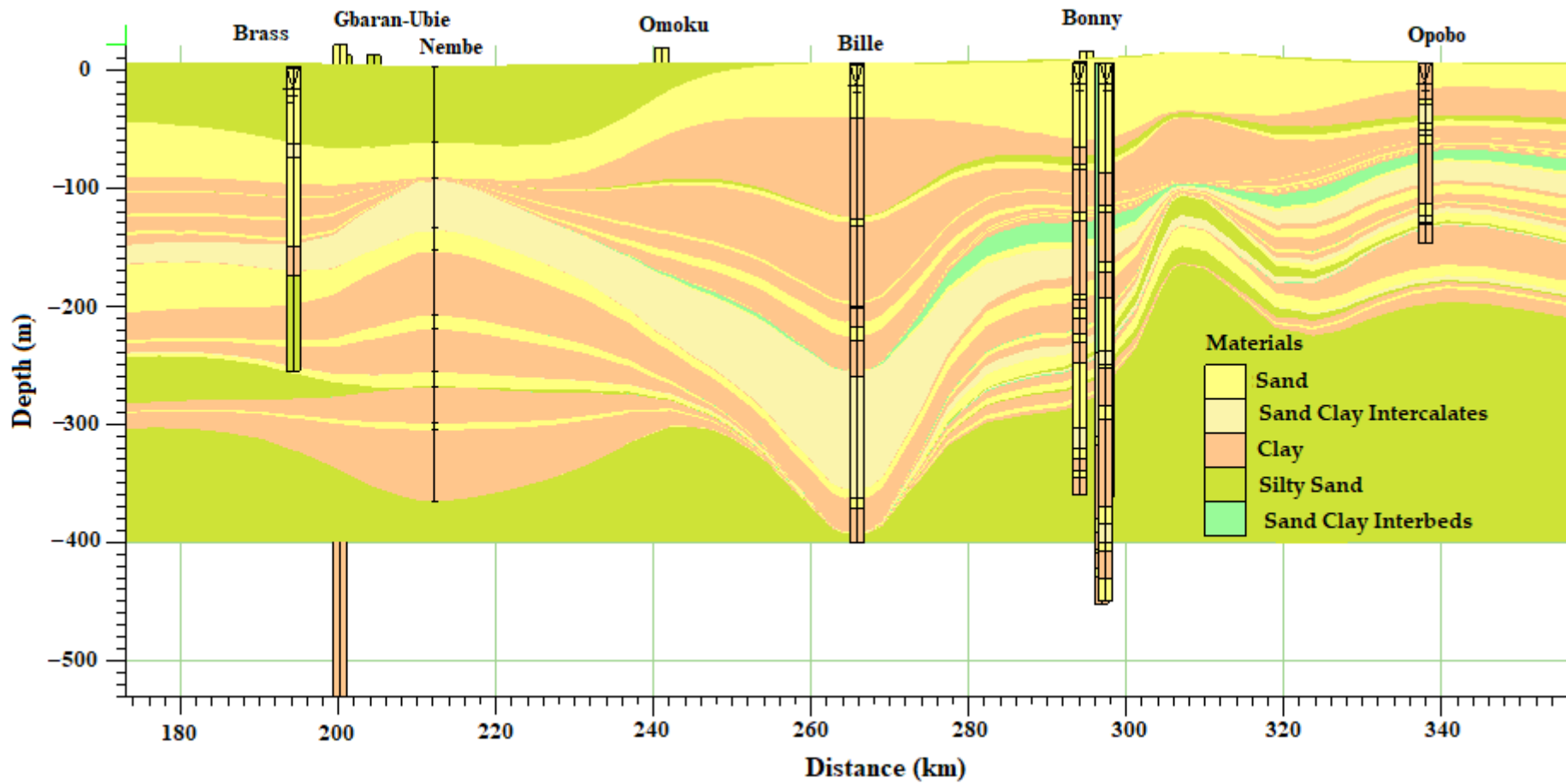


**Figure 8.3** Hydrostratigraphic section along profile line AA<sup>1</sup> at various zones within the Niger Delta basin.

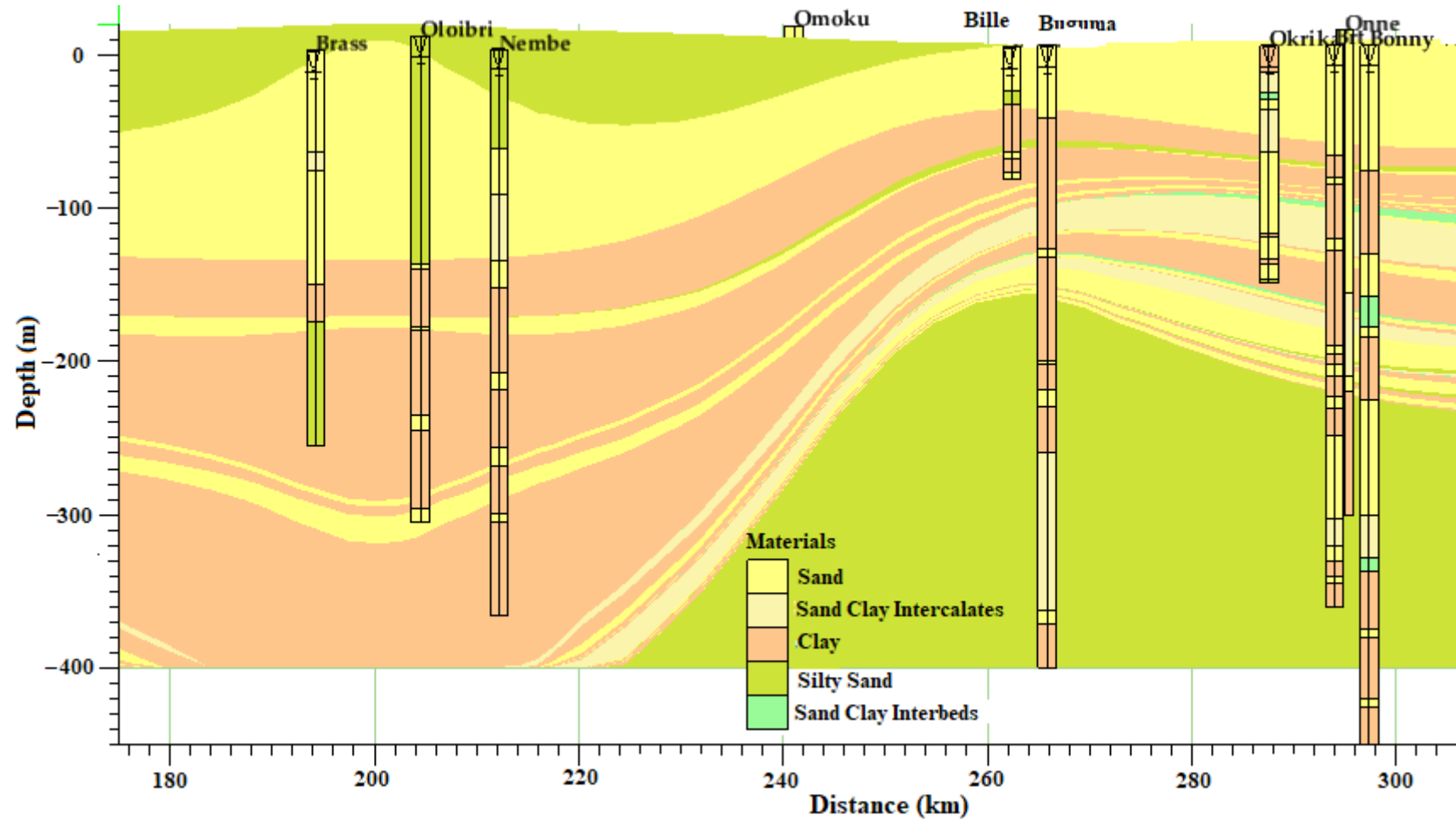


**Figure 8.4** Hydrostratigraphic section along profile line BB<sup>1</sup> at various zones within the Niger Delta basin.



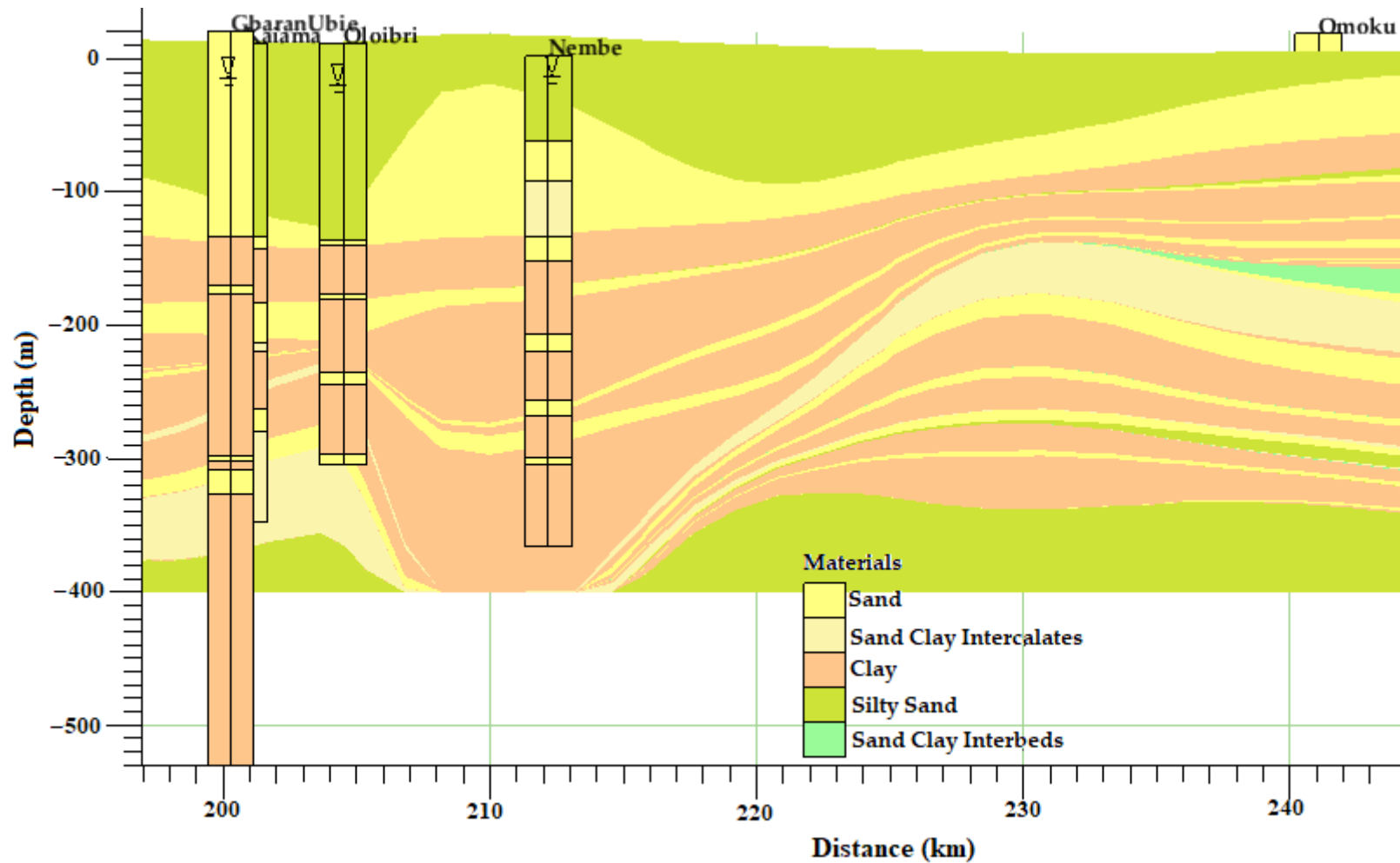


**Figure 8.5** Hydrostratigraphic section along profile line CC<sup>1</sup> at various zones within the Niger Delta basin.

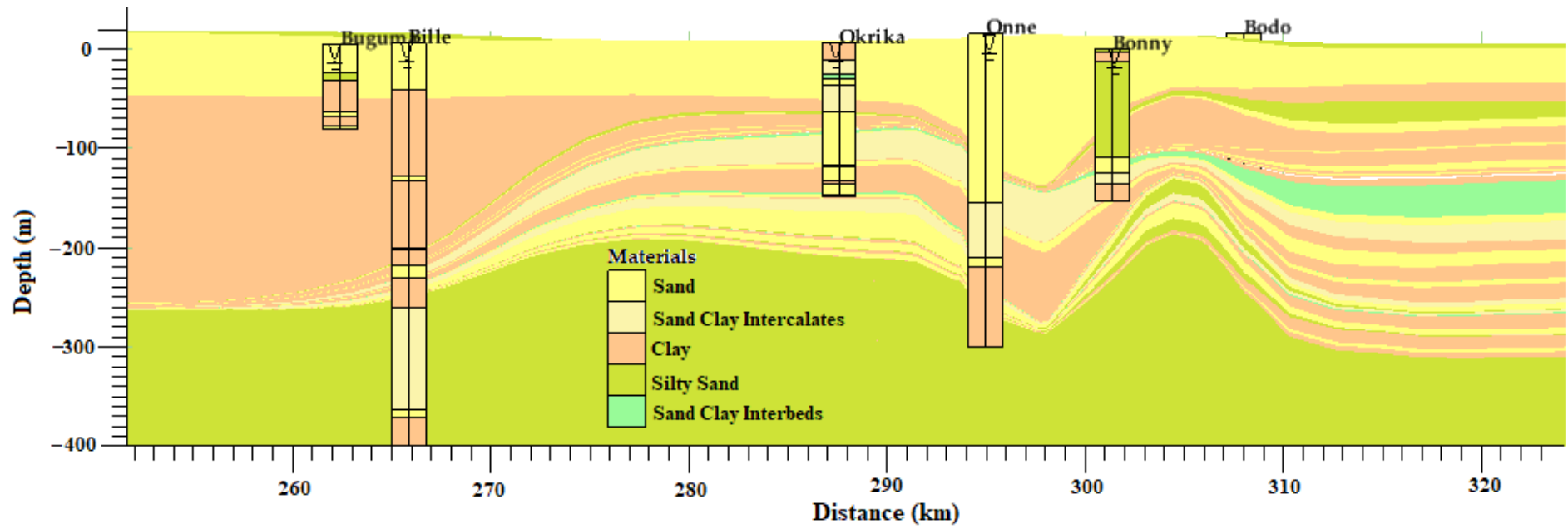


**Figure 8.6** Hydrostratigraphic section along profile line DD<sup>1</sup> at various zones within the Niger Delta basin.

In all these areas, there are unconfined aquifers with unconsolidated fine-to-medium-grain sands with a depth range from 1 to 45 m depending on location. A low permeable aquitard underlies these with clay, shale, peat and some organic materials with a little fraction of sands in some locations and a thickness ranging from 8 to 45 m. The thickness of the second aquifer ranges from 10 to 35 m while the third aquifer is about 10–35 m with a depth ranging from 150 to 240 m thick. The fourth aquifer starts from 200 to 250 m depending on the locations. The groundwater resources are within the alluvium and coastal plain sands of the deltaic formation of the Niger Delta basin. The boreholes around the area tap three main aquifer units. The unconfined aquifer with water levels ranging from 0 to 25 m, and 2–3 confined units ranging from 35 to 48 m, 45 to 65 m and 55 to 102 m. The aquifers are of fine-to-medium-grain sands with clay and shale layers acting as separating layers between them due to their low permeability.

### **4.3 Hydraulic Characterisation of the Aquifers**

Hydraulic conductivity data presented in this report were extracted from previous studies at different periods across the Niger Delta basin (Table 8.3). The value of hydraulic conductivity shows high variability in the alluvium and coastal plain sand formations, which could be a result of an active and complex depositional process of the region.

Hydraulic conductivity (K) data of the study area aquifers was revealed to be  $3.9 \times 10^{-4}$  to  $4.1 \times 10^{-4}$  m/s (Amajor L. C, 1989),  $1.2$  to  $3.53 \times 10^{-4}$  m/s (Uma K. O., 1989),  $2.8 \times 10^{-7}$ – $6.3 \times 10^{-4}$  m/s (Okagbue C. O., 1989) and  $2.8 \times 10^{-7}$ – $6.3 \times 10^{-4}$  m/s (Okagbue C. O., 1989) within the Benin Formation, and  $4.2 \times 10^{-4}$  to  $4.1 \times 10^4$

m/s (Etu-Efeotor J. O & Odigi M. I, 1983),  $7.0 \times 10^{-5}$ – $1.0 \times 10^{-4}$  m/s (Etu-Efeotor J. O & Akpokodje E. G, 1990) and  $2.01 \times 10^{-5}$ – $5.0 \times 10^{-5}$  m/s (Izeze I. A., 1990) within the Deltaic/Alluvium Formation. A recent study (Nwankwoala, 2013) revealed the hydraulic conductivity (K) values for boreholes located in the Port-Harcourt township at Churchill Road ( $3.24 \times 10^{-3}$  cm/sec); Borokiri Sand fill ( $3.62 \times 10^{-3}$  cm/sec); Marine Base ( $9.61 \times 10^{-3}$  cm/sec); Aggrey Road ( $8.41 \times 10^{-3}$  cm/sec); Reclamation Road ( $2.2 \times 10^{-3}$  cm/sec); and Harold Wilson Drive ( $4.0 \times 10^{-3}$  cm/sec). Virtually all the boreholes in these areas terminate within the coastal plain sand of the Benin formation. These layers are depicted in the stratigraphic sections.

**Table 8.3 :** Hydraulic conductivity values from different authors across the study area.

S/N	Author	Hydraulic Conductivity Range	Geology
1	Okagbue et al.(1989)	$7.2 \times 10^{-5}$ – $2.4 \times 10^{-3}$ m/s	Benin Formation
2	Amajor et al. (1989)	$3.91 \times 10^{-4}$ – $4.1 \times 10^{-4}$ m/s	Benin Formation
3	Uma et al. (1989)	1.2 to $3.53 \times 10^{-4}$ m/s	Benin Formation
4	Etu-Efeotor & Odigi (1983)	$4.2 \times 10^{-7}$ – $4.1 \times 10^{-4}$	Deltaic Formation
5	Etu-Efeotor & Akpokodje (1990)	$7.0 \times 10^{-5}$ – $1.0 \times 10^{-4}$ m/s	Deltaic/Alluvium Formation
6	Izeze et al. (1990)	$2.01 \times 10^{-5}$ – $5.0 \times 10^{-5}$ m/s	Deltaic/Alluvium Formation
7	Okagbue et al. (1989)	$2.8 \times 10^{-7}$ – $6.3 \times 10^{-4}$ m/s	Benin Formation (Ajali sandstone)
8	Onuoha & Mbazi (1989)	$4.4 \times 10^{-5}$ – $1.5 \times 10^{-4}$ m/s	Benin Formation (Ajali sandstone)
9	Nwankwoala et al. (2014)	$1.8 \times 10^{-3}$ – $3.2 \times 10^{-3}$ m/s	Deltaic/Alluvium Formation

#### 4.4 Implications for Groundwater Resilience in Shallow Aquifers of the Niger Delta Basin

Hydraulic characterisation shows a thin to a thick layer of silty sand from the Deltaic Formation, which renders little or partial protection for the groundwater stored in the sandy aquifer that is semi-confined at locations in the western part of the study area around Kiama, Gbaran-Ubie, Nembe and Baras (Figure 9.4). This layer thins out towards the middle of the area around Buguma and Bille, towards the

eastern part of the area, leaving the sandy aquifer completely unconfined as presented in Figure 9.7. Results of hydraulic conductivity show higher values in the Benin Formation compared to the Deltaic/Alluvium Formation (Table 9.3), which could be attributed to the nature and types of the dominant sediments. There are more shallow, confined aquifers at the southern part of the basin but most of which are thin, hence a low groundwater potential based on their storage capacity.

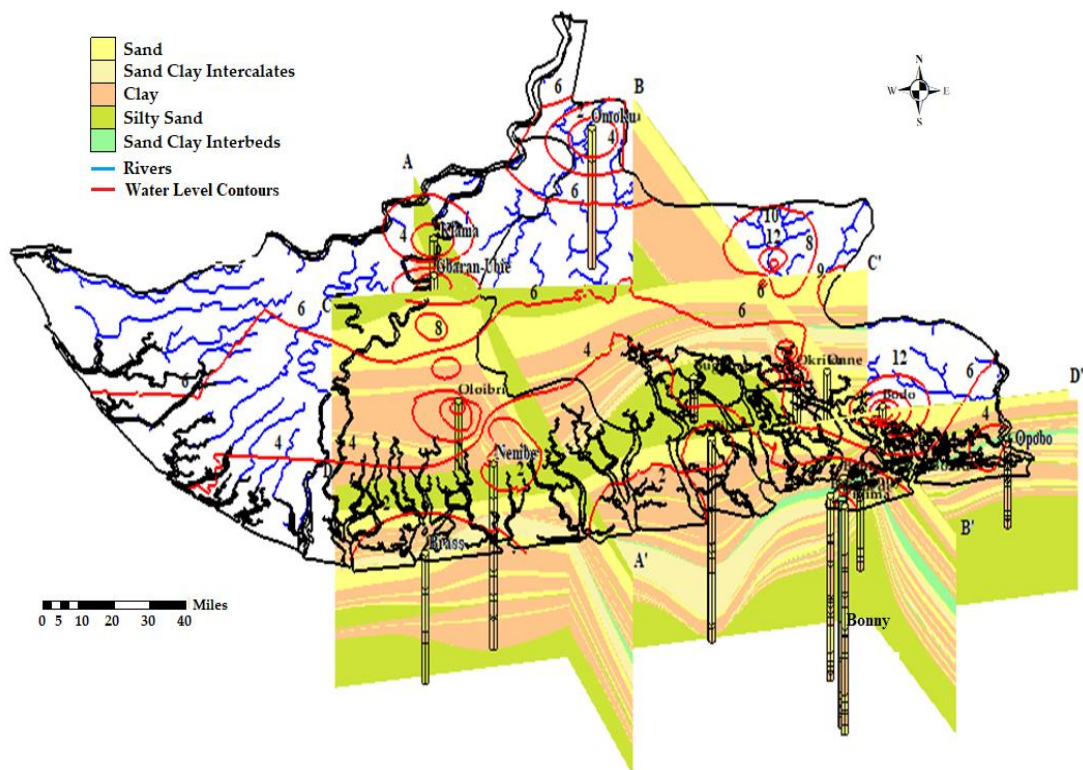


**Figure 8.7** Fence diagram showing hydrostratigraphic section within the Niger Delta basin.

Deeper wells in these areas have been reported by (Oteri, 1984; Oteri, A.U., & Atolagbe, 2003b) to have higher salinity due to saltwater intrusion. The eastern part of this area, which comprises Okrika, Bodo, Bonny, Finima, Opbo and Buguma, has a thick, sandy, unconfined aquifer with higher static water (figure 9.7) which makes it vulnerable to pollution and contamination from the surface water. Deeper

boreholes/wells that are designed to tap multiple thin layers of the sandy aquifer are the source of fresh potable water. Generally, groundwater in the unconfined aquifers of the Niger Delta basin could be described as having low resilience due to the nature of the sediments (hydraulic characteristics) and the number of drivers from natural (climate change, flooding, saltwater intrusion) to anthropogenic (oil spillage, gas flaring, industrial, municipal and agricultural effluents and leachates) pollution sources. There is a need for strategic studies that will include the recharge process of the aquifers, especially the unconfined aquifers in the area, for better assessment of the sustainable management of the groundwater resources of the basin.

## **5. Conclusions**

The study has presented a comprehensive understanding of the hydrostratigraphy and hydraulic behaviour of the Niger Delta basin aquifer system. The study identified 2 to 4 groundwater aquifer layers with some unconfined aquifers with unconsolidated fine-to-medium-grain sands and depth range of 1–45 m based on locations. A low permeable aquitard underlies these with clay, shale, peat and some organic materials with a little fraction of sands in some locations with a thickness ranging from 8 to 45 m. The thickness of the second aquifer ranged from 10 to 35 m while the third aquifer was about 10–35 m with a depth ranging from 150 to 240 m thick. The fourth aquifer started from 200 to 250 m depending on the location. The groundwater resources are within the alluvium and coastal plain sands of the Deltaic Formation of basin. Hence, examination of the borehole depth showed that all of the 52 boreholes terminated in the coastal plain sands with relatively higher hydraulic conductivity values. The higher hydraulic conductivity values coupled with higher static water level indicates

high vulnerability to contaminants and pollution, which are a threat to the groundwater resilience of the Niger Delta basin. The study provided a framework on which numerical model design can be undertaken to form a complete conceptual groundwater flow model of the basin. The study has also provided vital information for water resource managers and other stakeholders in the water industry to make better decisions for the sustainable management of groundwater resources.

**Author Contributions:** I.H. and R.M.K. designed the research; I.H. wrote the original draft.; R.M.K., C.J.W. and J.A.A. reviewed and edited the manuscript and provided technical help and proposed important additions with the model and to the manuscript.; R.M.K. gave critical views on the manuscript for further improvement.

**Funding:** This research was funded by the Petroleum Technology and Development Fund (PTDF) under the Overseas PhD scholarship scheme and supported by the Scottish Government under the Climate Justice Fund Water Futures Programme, awarded to the University of Strathclyde (R.M. Kalin)

**Acknowledgements:** The authors would like to gratefully acknowledge Dr. H.O. Nwankwoala and the Nigerian Hydrological Service Agency (NHISA) for providing the data used in this study.

**Conflicts of Interest:** The authors declare no conflict of interest.

## References

- Adelana, S. M. A., Olasehinde, P. I., Bale, R. B., Vrbka, P., Edet, A. E., and Goni, I. B. (2008) 'An overview of the geology and hydrogeology of Nigeria', *Quarterly Journal of Engineering Geology and Hydrogeology*, 29(May 1994), pp. S1–S12. doi: 10.1144/GSL.QJEGH.1996.029.S1.01.
- Adepelumi, A. A., Ako, B. D., Ajayi, T. R., Afolabi, O., and Omotoso, E. J. (2009) 'Delineation of saltwater intrusion into the freshwater aquifer of Lekki Peninsula, Lagos, Nigeria', *Environmental Geology*, 56(5), pp. 927–933. doi: 10.1007/s00254-008-1194-3.
- Allen, D. M. and Schuurman, Æ. N. (2008) 'Data integration and standardization in cross-border hydrogeological studies : a novel approach to hydrostratigraphic model development', *Environmental Geology*, 53, pp. 1441–1453. doi: 10.1007/s00254-007-0753-3.
- Amajor L. C (1989) 'Geological appraisal of groundwater exploitations in the Eastern Niger Delta. In: C.O Ofoegbu, (Ed.), Groundwater and Mineral Resources of Nigeria.', *Braunschweig/Wiesbaden. Friedr Vieweg and Sohn.*, p. Pp. 85-100.
- Amangabara, G. and Obenade, M. (2015) 'Flood Vulnerability Assessment of Niger Delta States Relative to 2012 Flood Disaster in Nigeria', *American Journal of Environmental Protection*, 3(3), pp. 76–83. doi: 10.12691/env-3-3-3.
- Amangabara, G. T. and Gobo, A. E. (2007) 'Factors that influence the flooding of the middle and lower Ntamogba stream catchments, Port Harcourt, Nigeria', *Journal of Environmental Hydrology*, 15(November), pp. 1–11.
- Anderson, M., Woessner, W. and Hunt, R. (2015) *Applied Groundwater Modeling, Second Edition: Simulation of Flow and Advective Transport*. doi: 10.1016/B978-0-08-091638-5.00001-8.
- Asfahani, J. (2016) 'Hydraulic parameters estimation by using an approach based on vertical electrical soundings (VES) in the semi-arid Khanasser valley region, Syria', *Journal of African Earth Sciences*. Elsevier Ltd, 117, pp. 196–206. doi:



10.1016/j.jafrearsci.2016.01.018.

Aturamu Adeyinka O., Ojo Adebayo O, Adebayo F, A and Olajide. S. A. (2015) 'Palynostratigraphic Analysis of the Agbada Formation (Nep-1 Well) Offshore, Eastern Niger-Delta Basin, Nigeria', *British Journal of Environmental Sciences Centre*, 3(5), pp. 19–31.

B. Nilsson, A. L. Højberg, J. C. Refsgaard, and L. Troldborg (2007) 'Uncertainty in geological and hydrogeological data', *Hydrology and Earth System Sciences*, 3(May 2014), pp. 2675–2706. doi: 10.5194/hessd-3-2675-2006.

Charles, M Noyes Maley, M. P. and Blake, R. G. (2001) 'Defining Hydrostratigraphic Units within the Heterogeneous Alluvial Sediments at Lawrence Livermore National Laboratory', in *American Association of Petroleum Geologists*, p. 39.

Cosgrove, W. J. and Loucks, D. P. (2015) 'Water management: Current and future challenges and research directions', *AGU Publications: Water Resources Research*, pp. 4823–4839. doi: 10.1002/2014WR016869. Received.

Cox SE, K. S. (1999) 'Hydrogeology, ground-water quality, and sources of nitrate in Lowland glacial aquifers of Whatcom County, Washington, and British Columbia, Canada.', *US Geological Survey Water-Resources Investigations Report*, 98-4195.

Edet, A., Abdelaziz, R., Merkel, B., Okereke, C., and Nganje, T. (2014) 'Numerical groundwater flow modeling of the Coastal Plain sand aquifer, Akwa Ibom State, SE Nigeria', *Journal of Water Resource and Protection*, 06(March), pp. 193–201. doi: 10.4236/jwarp.2014.64025.

Etu-Efeotor J. O and Akpokodje E. G (1990) 'Aquifer systems of the Niger Delta', *Journal of Mining Geology*, 26(2), pp. 279–284.

Etu-Efeotor J. O and Odigi M. I (1983) 'Water supply problems in the Eastern Niger Delta', *Journal of Mining Geology*, 20(1+2), pp. 183–193.

Farid, A., Jadoon, K. and Akhter, G. (2013) 'Hydrostratigraphy and hydrogeology of the western part of Maira area, Khyber Pakhtunkhwa, Pakistan : a case study by using

electrical resistivity', *Springer: Environal Monitoring Assessment*, 185:2407–2, pp. 2407–2422. doi: 10.1007/s10661-012-2720-z.

Heuvelink, G. B. M. (1986) 'Propagation of error in spatial modelling with GIS Stochastic Error Model For', pp. 207–218.

Hutton, G. and Chase, C. (2016) 'The Knowledge Base for Achieving the Sustainable Development Goal Targets on Water Supply, Sanitation and Hygiene', *Environmental Research and Public Health (MDPI)*, pp. 1–35. doi: 10.3390/ijerph13060536.

Izeze I. A. (1990) *Aquifer characteristics of the coastal plain sands of southern Nigeria: M.Sc. thesis*. The University of Port Harcourt, Port Harcourt, Nigeria.

Jichun, W. U. and Xiankui, Z. (2013) 'Review of the uncertainty analysis of groundwater', *Chinese Science Bulletin*, 58(25), pp. 3044–3052. doi: 10.1007/s11434-013-5950-8.

Merki, J. P. (1970) 'Structural Geology of the Cenozoic Niger Delta', *African Geology. University of Ibadan Press*, p. pp 251-268.

Nnabuenyi, U. M. (2012) 'Impact of Oil Exploration and Exploitation on the Niger Delta Region: Environmental Perspective', *Nigerian Journal of Science and Environment*, 11(1).

Nwankwoala, H. (2013) 'Aquifer Hydraulic Conductivity Determination from Grain Size Analysis in Parts of Old Port Harcourt Township, Nigeria', *ARPN Journal of Science and Technology*, 3(9), pp. 972–981.

Nwankwoala, H. (2015) 'Hydrogeology And Groundwater Resources Of Nigeria', *New York Science Journal 2015*, 8(1), pp. 89–100.

Nwankwoala, H. O. and Oborie, E., (2014) 'Geotechnical Investigation and Characterization of Sub-soils in Yenagoa, Bayelsa State, Central Niger Delta, Nigeria', 6(7).

Offodile, M. E. (1992) 'An Approach to Groundwater Study and Development in

Nigeria. Mecon Geology and Engineering Services Ltd., Jos.’

Offodile M.E. (2014) *Hydrogeology: Groundwater Study and Development in Nigeria*. Third edit. Jos: Mecon Geology and Engineering Services Ltd.

Okagbue C. O. (1989) ‘Geotechnical And Environmental Problems of the Niger Delta’, *Bulletin of the International Association of Engineering Geology*, pp. 129–138. Available at: <https://link.springer.com/article/10.1007/BF02590349>.

Okeke, O. C., Onyekuru, S. O., Uduehi, G., and Israel, H. O. (2011) ‘Geology and hydrogeology of Northern Ishan district, Edo state, Southwestern Nigeria’, 1(November), pp. 1–11.

Ologunorisa, T. E. and Adeyemo, A. (2005) ‘Public perception of flood hazard in the Niger Delta, Nigeria’, *Environmentalist*, 25(1), pp. 39–45. doi: 10.1007/s10669-005-3095-2.

Onuoha K. M. and Mbazi F. C. (1989) ‘Aquifer transmissivity from electrical sounding data: The case of Ajali sandstone aquifers, southeast of Enugu, Nigeria, in C. O. Ofoegbu, ed., *Groundwater and mineral resources of Nigeria*’, *Braunschweig, Friedr Vieweg & Sohn*, pp. 17–30.

Ophori, D. U. (2007) ‘A simulation of large-scale groundwater flow in the Niger Delta, Niger’, *AAPG Bulletin*, 14(4), pp. 181–195. doi: 10.1306/eg.05240707001.

Oteri, A.U., and Atolagbe, F. P. (2003) ‘Saltwater Intrusion into Coastal Aquifers in Nigeria’, in *The Second International Conference on Saltwater Intrusion and Coastal Aquifers—Monitoring, Modeling, and Management. Mérida, Yucatán, México. Environments and the 1st Arab Water Forum*, pp. 1–15.

Oteri, A. U. (1984) ‘Electric logs for groundwater exploration in the Niger Delta of’, (144).

Owoyemi, A. O. D. (2004) *The Sequence Stratigraphy of Niger Delta, Delta Field, Offshore Nigeria, Texas A&M University*. Texas A&M University.

Oyedele K. F., Ayolabi E. A., Adeoti L., and Adegbola, R. B. (2009) ‘Geophysical

and hydrogeological evaluation of rising groundwater level in the coastal areas of Lagos, Nigeria', *Bulletin of Engineering Geology and the Environment*, 68, pp. 137–143. doi: 10.1007/s10064-008-0182-x.

Prince C. Mmom, (2013) 'Vulnerability and Resilience of Niger Delta Coastal Communities to Flooding.', *IOSR Journal of Humanities and Social Science*, 10(6), pp. 27–33. doi: 10.9790/0837-1062733.

Raji, W. O., Obadare, I. G., Odukoya, M. A., and Johnson, L. M. (2018) 'Electrical resistivity mapping of oil spills in a coastal environment of Lagos, Nigeria', *Arabian Journal of Geosciences*. *Arabian Journal of Geosciences*, 11, p. 144. doi: 10.1007/s12517-018-3470-1.

Rojas, R., Feyen, L. and Dassargues, A. (2008) 'Conceptual model uncertainty in groundwater modeling: Combining generalized likelihood uncertainty estimation and Bayesian model averaging', *Water resources research*, 44, pp. 1–16. doi: 10.1029/2008WR006908.

Sanz, D., Gómez-alday, J. J., Castaño, S., Moratalla, A., Heras, J. De, and Martínez-alfaro, P. E. (2009) 'Hydrostratigraphic framework and hydrogeological behaviour of the Mancha Oriental System (SE Spain)', *Hydrogeology Journal*, 17, pp. 1375–1391. doi: 10.1007/s10040-009-0446-y.

Tawari-fufeyin, P., Paul, M., and Godleads, A. O. (2015) 'Some Aspects of a Historic Flooding in Nigeria and Its Effects on some Niger-Delta Communities', *American Journal of Water Resources*, 3(1), pp. 7–16. doi: 10.12691/ajwr-3-1-2.

Taylor, R. G., Scanlon, B., Döll, P., Rodell, M., van Beek, R., Wada, Y., Longuevergne, L., Leblanc, M., Famiglietti, J. S., Edmunds, M., Konikow, L., Green, T. R., Chen, J., Taniguchi, M., Bierkens, M. F. P., MacDonald, A., Fan, Y., Maxwell, R. M., Yechieli, Y., Gurdak, J. J., Allen, D. M., Shamsudduha, M., Hiscock, K., Yeh, P. J.-F., Holman, I. and Treidel, H. (2013) 'Ground water and climate change, *Nat. Clim. Chang.*, 3(4), 322–329, doi:10.1038/nclimate1744.

Ugwu S A and Nwankwoala H O (2008) 'Application of Seismic Refraction Method in Groundwater', 7(2), pp. 73–80.

Uko E.T. and Emudianughe J.E. (2016) 'Comparison of the Characteristics of Low-Velocity Layer (LVL) in the Mangrove Swamp and the Upper Flood Plain Environments in the Niger Delta, using Seismic Refraction Methods', *Journal of Geology & Geophysics*, 5(4). doi: 10.4172/2381-8719.1000248.

Uma K. O. (1989) 'An appraisal of the groundwater resources of the Imo River Basin, Nigeria', *Journal of Mining and Geology*, Vol. 25 No, p. pp.305-31.

UNDP (2006) *Niger Delta Human Development Report: United Nations Development Programme*.

### **8.3 Supplementary Data**

The distribution of the boreholes with lithologic logs and their geomorphic zones are shown in Table 8.4. It should be observed that the majority of deep boreholes are located in the Coastal Plain Sands. This is due to ease of accessibility and high demand for potable water to match urbanization and serve the increasing population. The strata logs show that the deepest boreholes have depths ranging from 300m in the Coastal Plain Sands (CPS) and Sombreiro-Warri deltaic plain (SWP), through 530m in the freshwater swamp (FWS), 200m in the saltwater swamp (SWS) to 600m in the coastal beaches and ridges (CBR). Examination of the drill cuttings reveals that the subsurface is capped by lateralized soil cover with thicknesses that decrease southward towards the coast.

**Table 8.4 :** Distribution of boreholes studied in the geomorphic zones.

<b>S/No.</b>	<b>Geomorphic Zone</b>	<b>Number of Boreholes</b>
1	Coastal Plain Sands	15
2	Freshwater swamp	10
3	Saltwater/mangrove swamp	14
4	Sambreiro Warri Deltaic plain	1
5	Coastal beaches and ridges	13

### **8.3.1 Deep aquifers in the Coastal Plain Sands**

Due to the prolific nature of the Coastal Plain Sands, boreholes do not usually go too deep to tap freshwater. The 300m deep borehole at Onne, completed in the Coastal Plain Sands aquifer shows the presence of three aquifers between 0 – 300m. These aquifers occur between 0 -80m for the first aquifer, 155 – 210m for second aquifer and 220 – 300m for the lower aquifer. Figure 8.8 is a down-hole geophysical log of the well at NAFCON, Onne and is typical of the upper 0 – 300m of the study area. Six large diameter wells (13<sup>3</sup>/<sub>8</sub>-inch) each to 300m were drilled for the water requirements of the fertilizer complex. Table 8.5 shows the lithologic successions revealed by both gamma logs and driller’s log from the boreholes.

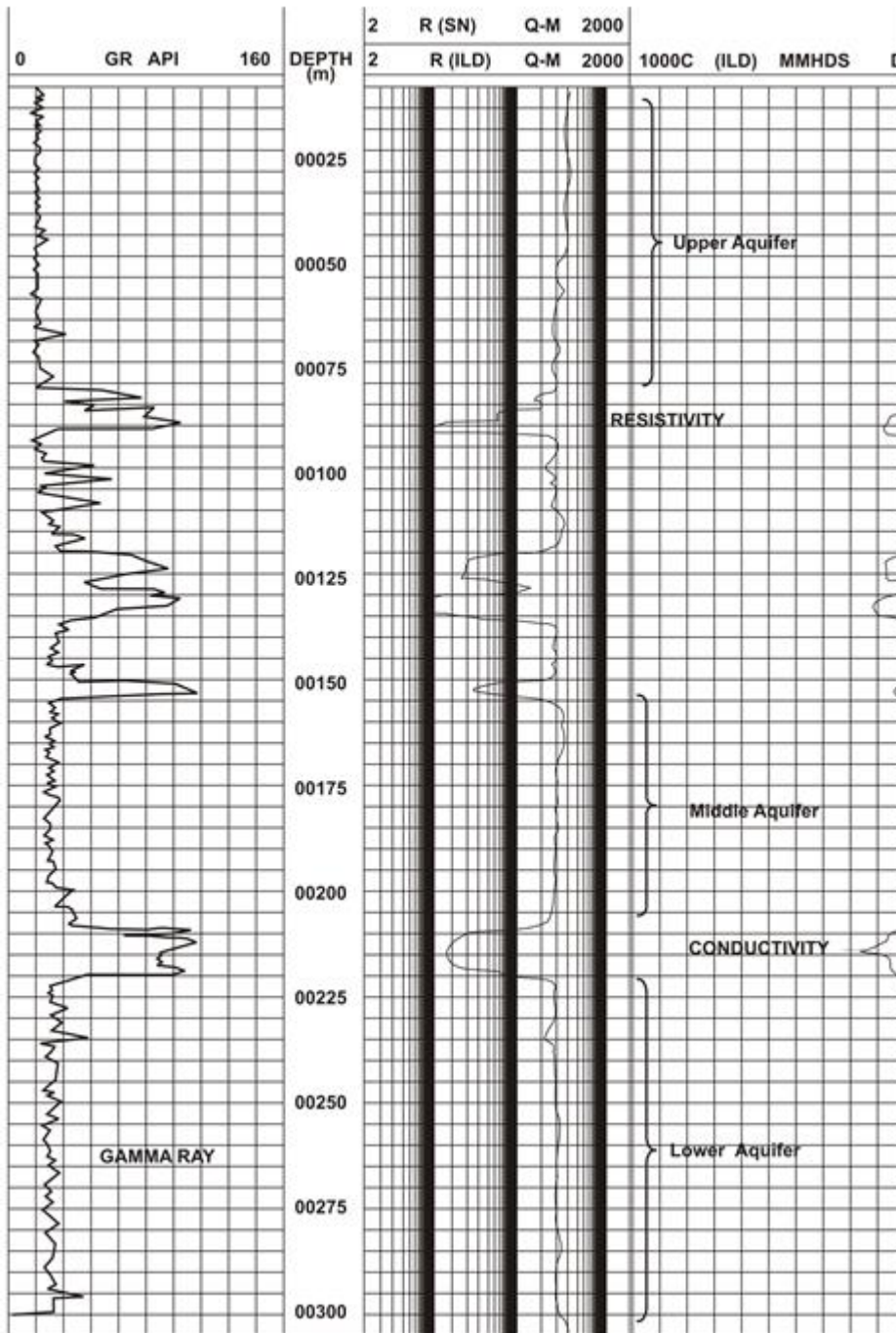


**Figure 8.8** Down-hole Geophysical log at NAFCON, Onne.

**Table 8.5 : Lithologic sequence at Onne, Coastal Plain Sands**

<b>Depth interval (m)</b>	<b>Lithology</b>	<b>Thickness (m)</b>
0 – 80	Sand	80
80 – 155	Clay and sandy clay	75
155 – 210	Sand	55
210 – 220	Clay	10
220 – 300	Sand	80

Only three aquifers are identified at this location to a depth up to 300m. Clay and sandy clay aquifers occur between 80 and 155m in some places within the coastal plain sands.

The deep borehole of 381 m drilled in some parts of the Coastal Plain Sands at Ndoni shown in figure 8.9 reveals that the upper 300m of the coastal plain sands can be taken as one thick aquifer. The borehole logs revealed that two thin layers of clay each about 1m in thickness is found between 20 to 142m below ground surface, and the entire drilled column consists of sands up to the 381m depth.



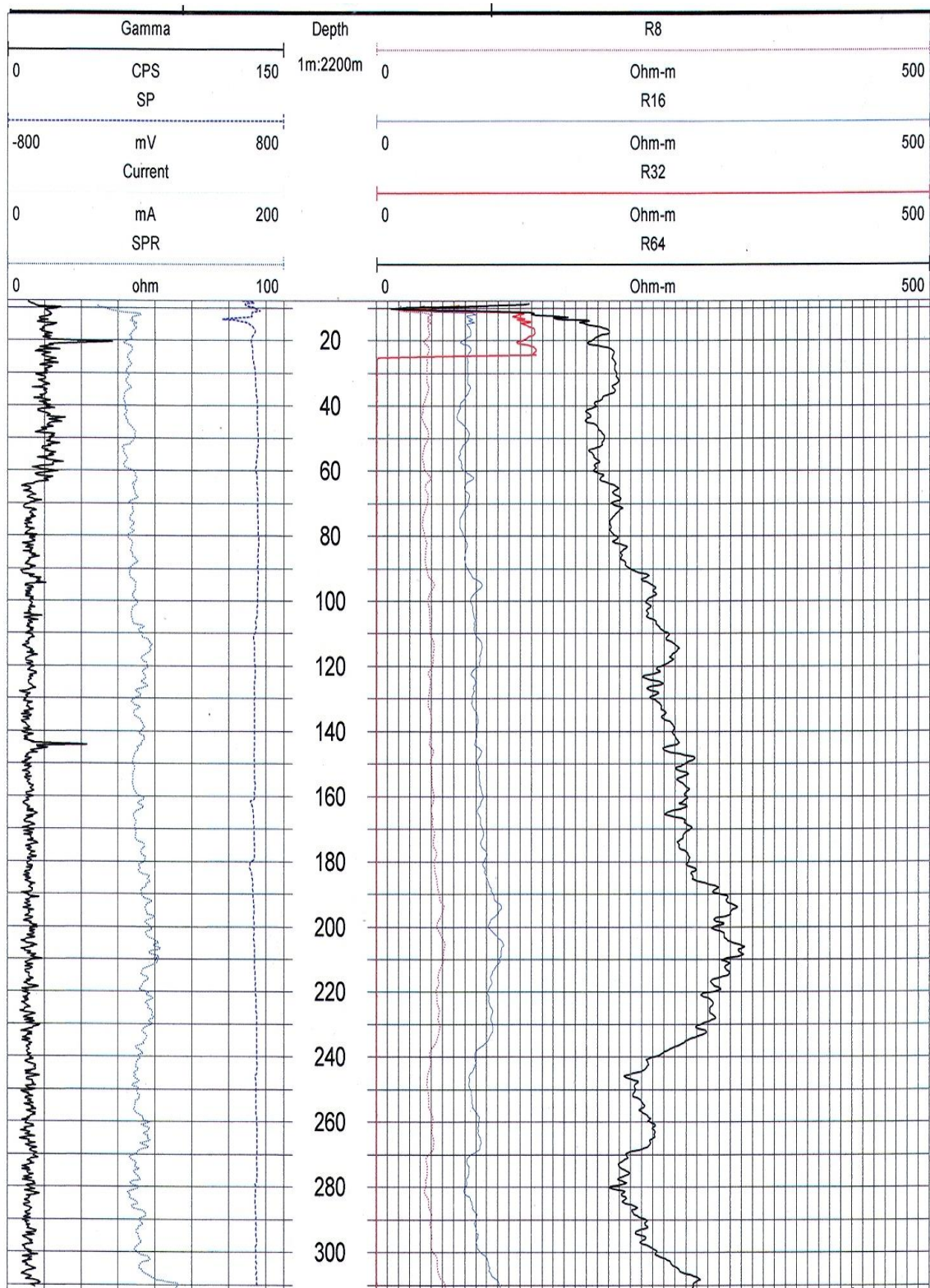


**Figure 8.9** Down-hole geophysical log of a borehole at Ndoni

### 8.3.2 Deep aquifers in Warri-Sambreiro deltaic plain

Table 8.6 summarized the lithological sequence of the two boreholes each to a depth of 260m drilled at the Independent Power Plant Lot 7.

**Table 8.6 :** Lithologic succession in a deep well at NIPP, Omoku

Depth interval (m)	Lithology	Depth (m)
0 – 40	Sand	40
40 – 44	Clay	4
44 – 260	Sand	216

Table 8.7 also summarizes the lithologic sequence of the boreholes at Warri Refinery with a total depth of 160m. The base of the aquifer was not established

**Table 8.7 :** Lithologic succession in a well at Warri Refinery

Depth interval (m)	Lithology	Depth (m)
0 – 23	Sand	23
23 – 29	Clay	6
29 – 160	Sand	131

### 8.3.3 Deep aquifers in Freshwater Swamp

Some of the Deepwater boreholes drilled into the freshwater swamp aquifer regions are illustrated below.

#### 8.3.3.1 Deep borehole at Otakeme near Oloibri, Bayelsa state

The down-hole geophysical logs of a 305m deep borehole drilled at Otakeme as a part of SHELL community water project shows a beautiful alternation of thick sand bodies punctuated at intervals by some clay layers as shown in figure 8.10. and Table 8.8 below.

**Table 8.8 :** Lithologic succession in a deep borehole at Otakeme

<b>Depth interval (m)</b>	<b>Lithology</b>	<b>Thickness (m)</b>
0 – 22	Silty sand	20
22 – 136	Sand	114
136 – 140	Clay	4
140 – 177	Sand	37
177 – 180	Clay	3
180 – 235	Sand	55
235 – 245	Clay	10
245 – 296	Sand	51
296 – 305	Clay	9

### **8.3.3.2 Deep borehole at Kaiama, Bayelsa state**

Table 8.9 shows the subsurface lithologic sequence of another similar deep borehole drilled at Kaiama to a depth of 348m.

**Table 8.9 :** Lithologic succession in a deep borehole at Kaiama

<b>Depth interval (m)</b>	<b>Lithology</b>	<b>Thickness (m)</b>
0- 12	Silty sand	12
12 – 134	Sands	122
134 – 143	Clay	9
143 – 183	Sands	40
183 – 213	Sand/clay intercalates	7
213 – 220	Clay	7
220 – 262	Sands	42
262 – 280	Clay, sandy	18
280 – 348	Sands	68

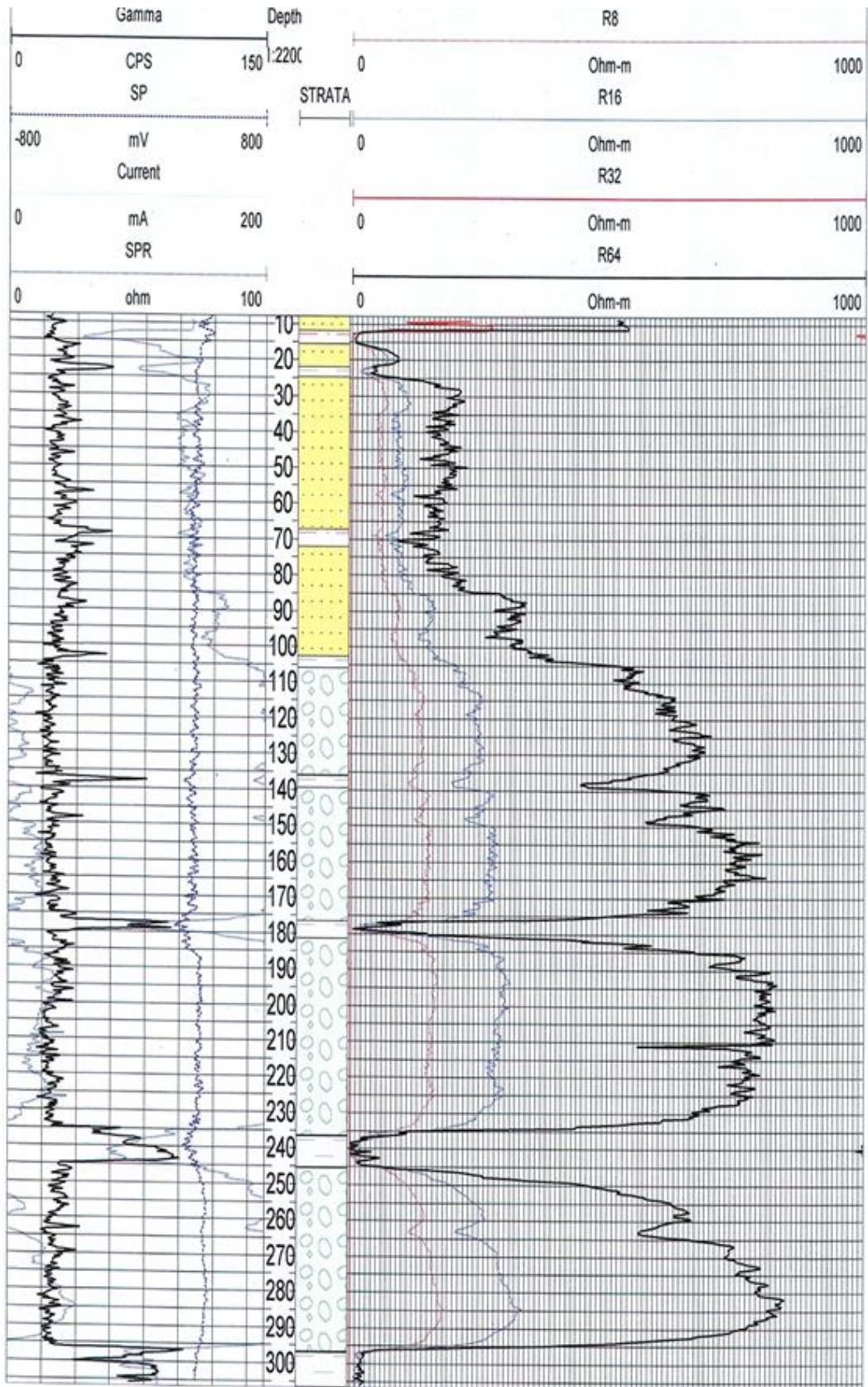


**Figure 8.10** Down-hole geophysical log of a borehole at Otakeme



### 8.3.3.3 Deep borehole at Gbaran-Ubie

The borehole drilled at the SHELL FLP plant located in Gbaran-Ubie represents the deepest known water well in the freshwater geomorphologic zone.

**Table 8.10 :** Lithologic successions in a deep borehole at Gbaran-Ubie

Depth interval (m)	Lithology	Thickness (m)
0 – 124	Sand	124
124 – 133	Clay	9
133 – 170	Sand	37
170 – 176	Clay	6
176 – 298	Sand	122
298 – 302	Clay	4
302 – 308	Sand	6
308 – 327	Clay	19
327 – 530	Sand	203

The lithologic successions of the log is shown in Table 8.10, while Figure 8.11 depicts the down-hole wireline log of the borehole. The log shows that the freshwater swamp geomorphologic zone is underlain by an alternation of sand and clay typical of the Benin Formation. These sands are unconsolidated at shallow depths of varying thicknesses which becomes consolidated at depth due to the weight of the overlying formations. The table reveals the existence of four to five major aquifers in the area up to the 530m below ground surface.

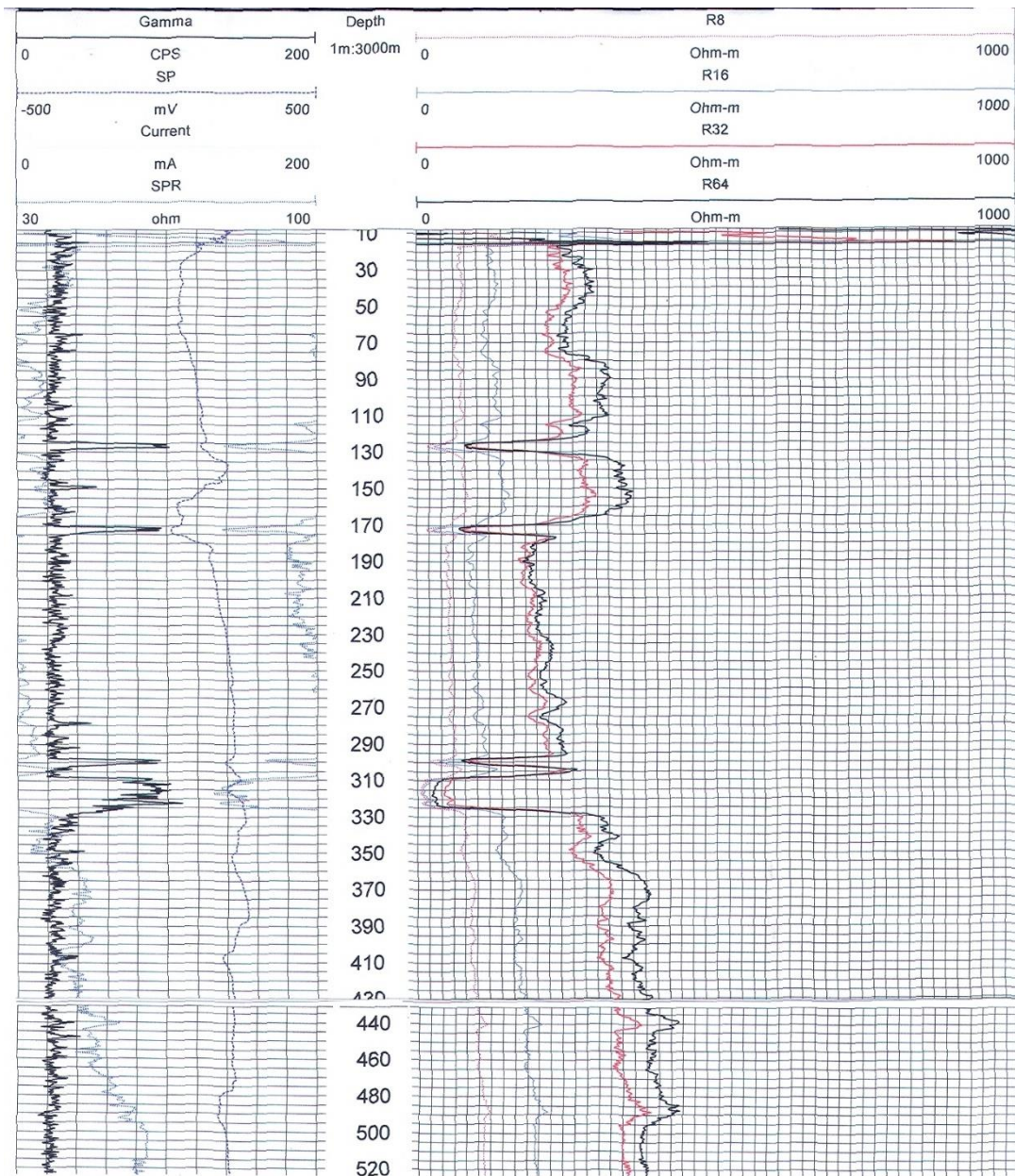


**Figure 8.11** Down-hole log of Gbaran-Ubie borehole at SHELL Facility FLB site

### 8.3.4 Deep aquifers in the saltwater swamp

Records from two deep boreholes drilled in the saltwater swamp geomorphological unit located at Bille and Bassambiri, Nembe are used to characterize the subsurface lithology of the saturating groundwater aquifers in the study area.

### 8.3.4.1 Deep borehole at Bille of 400m

The geophysical and lithologic logs (Figure 8.12) of the deep borehole with a depth of 400m below ground surface drilled in Bille shows the following subsurface sequence as summarised in Table 8.11.

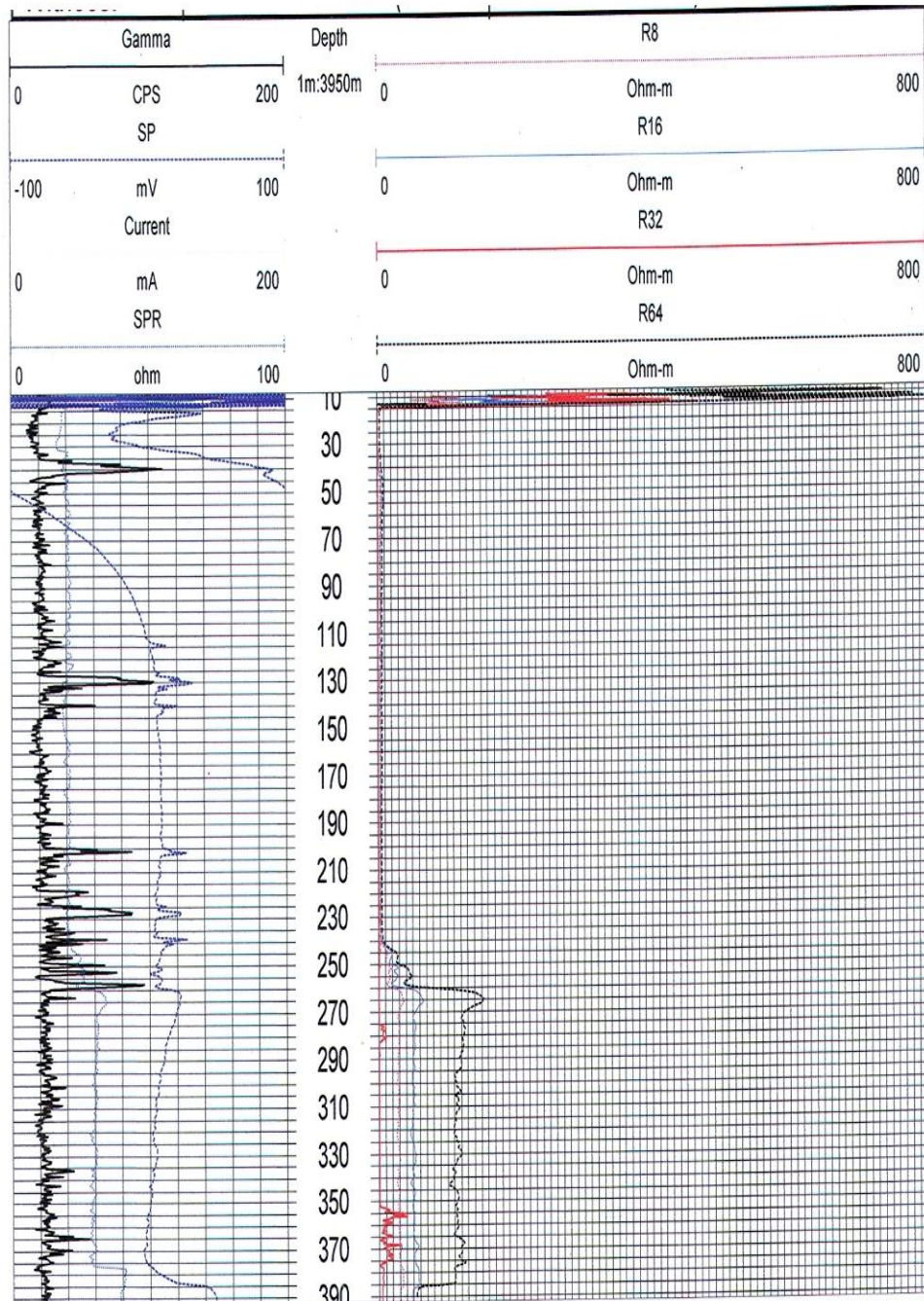


**Figure 8.12** Wireline logs in a deep borehole at Bille

**Table 8.11 :** Lithologic succession in a deep borehole at Bille

<b>Depth interval (m)</b>	<b>Lithology</b>	<b>Thickness (m)</b>
0 – 37	Sand	37
37 – 41	Clay	4
41 – 127	Sand	86
127 – 132	Clay	5
132 – 200	Sand	68
200 – 202	Clay	2
202 – 218	Sand	16
218 – 230	Clay	12
230 – 260	Sand/clay intercalate	30
260 – 363	Sand	103
363 – 371	Clay	8
371 – 400	Sand	29

The log and table show that the area is underlain by six saturated sand bodies. However, the logs revealed that the groundwater in the sand bodies occurring between 0 and 240m is saline while the groundwater in the sand/clay intercalates occurring between 230 to 260m is brackish and all the sand aquifers below the 260m contain freshwater.

#### **8.3.4.2 Deep borehole at Bassambiri, Nembe**

The interpretation of the deep borehole geophysical log of 366m depth drilled in Bassambiri, Nembe is summarised in Table 8.12, which shows the subsurface lithological succession in the area. The resistivity logs revealed six sand bodies with the aquifers located between 0 and 152m contaminated with saltwater. However, the freshwater aquifers occur in the remaining four sand aquifers between 152 and 366m.



**Table 8.12 :** Lithologic succession in a deep borehole at Bassambiri, Nembe

<b>Depth interval (m)</b>	<b>Lithology</b>	<b>Thickness (m)</b>
0 – 12	Silty sand	12
12 – 61	Sand	49
61 – 91	Sand, clayey	30
91 – 134	Sand	43
134 – 152	Clay	18
152 – 207	Sand	55
207 – 219	Clay	12
219 – 256	Sand	37
256 – 268	Clay	12
268 – 299	Sand	31
299 – 305	Clay	6
305 – 366	Sand	61

### **8.3.5 Deep coastal beach aquifers**

The coastal beaches in the Niger Delta are barrier islands and distributary mouth bars fringing the coastline which are laterally separated by the mouths of many rivers splitting them into small islands from 5 to 50km long and less than 15km in width. Presently, the Niger Delta coastal beaches have the highest number of deep-water wells due to the saltwater intrusion in the shallow aquifers. Hence the freshwater wells have to go very deep to harness freshwater. The few deep borehole logs available in the area are presented below.

#### **8.3.5.1 Deep boreholes at the Bonny River Terminal.**

The lithological successions of two closely spaced boreholes drilled at the Bonny River Terminal (BRT) each at a depth of 360m inferred from an integrated

interpretation of geophysical logging and strata logs revealed that the area is underlain by an irregular alternation of sands and clay/shale as shown in Figure 8.13. The logs show that the aquifers within the depth of 0 – 215m contains brackish to saltwater while all the sand bodies below this depth are saturated with freshwater. The increasing number of clay layers which interrupt what would ordinarily have been clean sand bodies has increased the number of aquifers in the coastal ridges.

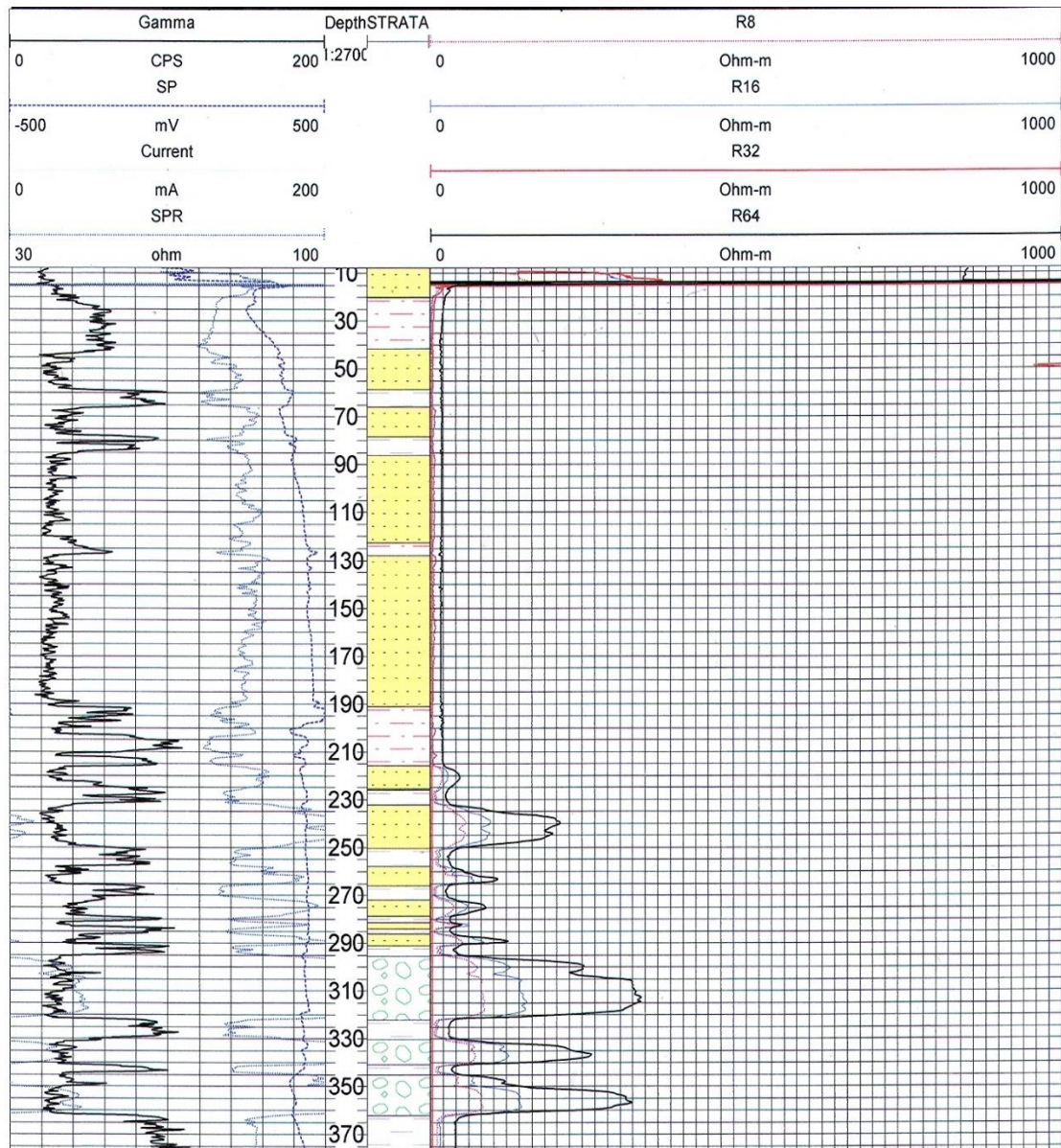


**Figure 8.13** Wireline logs of a deep borehole at Bonny River Terminal

The various lithological units encountered in the area are presented in Table 8.13, which shows ten saturated sand aquifers up to the 360m below ground surface occur in the area.

**Table 8.13 :** Lithologic successions in a deep borehole at BRT, Bonny

<b>Depth interval (m)</b>	<b>Lithology</b>	<b>Thickness (m)</b>
0 – 60	Sand	60
60 – 66	Clay	6
66 – 80	Sand	14
80 – 84	Clay	4
84 – 120	Sand	36
120 – 128	Clay	8
128 – 190	Sand	62
190 – 195	Clay	5
195 – 202	Sand	7
202 – 210	Clay	8
210 – 223	Sand	13
223 – 231	Clay	8
231 – 248	Sand	17
248 – 303	Sand/clay alternation	55
303 – 320	Sand	17
320 – 330	Clay	10
330 – 340	Sand	10
340 – 345	Clay	5
345 – 360	Sand	15

### **8.3.5.2 Deep boreholes at MPN Life Camp, Bonny**

The geophysical log of two closely spaced boreholes drilled to a depth up to 360m at the Mobil Producing Nigeria Unlimited Life camp in Bonny north is presented in the shown Figure 8.14. The lithological successions shown in Table 8.14 revealed distinct sand bodies with thicknesses ranging from 5 to 51m. Nine of these aquifers

occur within 0 – 300m depth bracket while four aquifers occur between 300 and 360m. The frequency of occurrence of the aquifers, therefore, appears to increase both with depth and towards the coast. Resistivity logs show that the aquifers contain brackish/saline water from the surface up to 145m, while the first indication of freshwater was in the 8m thick sand occurring between 146 and 153m. All other aquifers below this level contain freshwater.

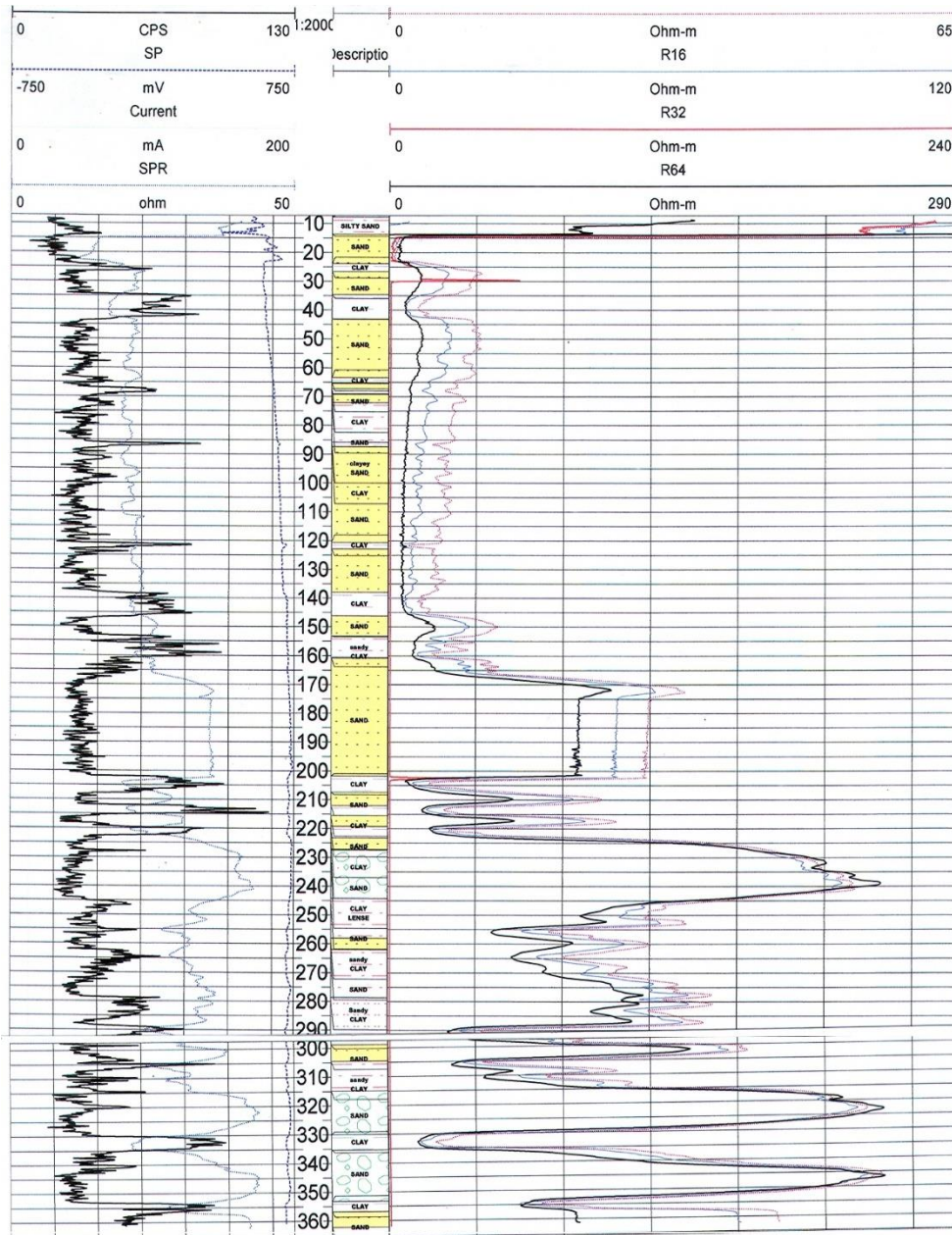


**Figure 8.14** Wireline logs of a deep borehole at Mobil Life camp, Bonny Island

**Table 8.14 :** Lithologic successions in a deep borehole at MPN Life Camp, Bonny

<b>Depth interval (m)</b>	<b>Lithology</b>	<b>Thickness (m)</b>
0 – 14	Silty sand	60
14 – 24	Sand	6
24 – 27	Clay	14
27 – 35	Sand	4
35 – 43	Clay	36
43 – 67	Sand	8
67 – 69	Clay	62
69 – 120	Sand	5
120 – 123	Clay	7
123 – 138	Sand	8
138 – 146	Clay	13
146 – 153	Sand	8
153 – 161	Clay	17
161 – 202	Sand	55
202 – 222	Clay	17
222 – 244	Sand	10
244 – 258	Clay	10
258 – 262	Sand	5
262 – 278	Clay	15
278 – 299	Clay/sand intercalate	21
299 – 305	Sand	6
305 – 315	Clay	10
315 – 330	Sand	15
330 – 335	Clay	5
335 – 353	Sand	18
353 – 357	Clay	4
357 – 362	Sand	5

### 8.3.5.3 Deep borehole at Bonny Water Board

Figure 8.15 shows the down-hole geophysical log of a well drilled at the Water Board premises in Bonny island to a depth of 450m.



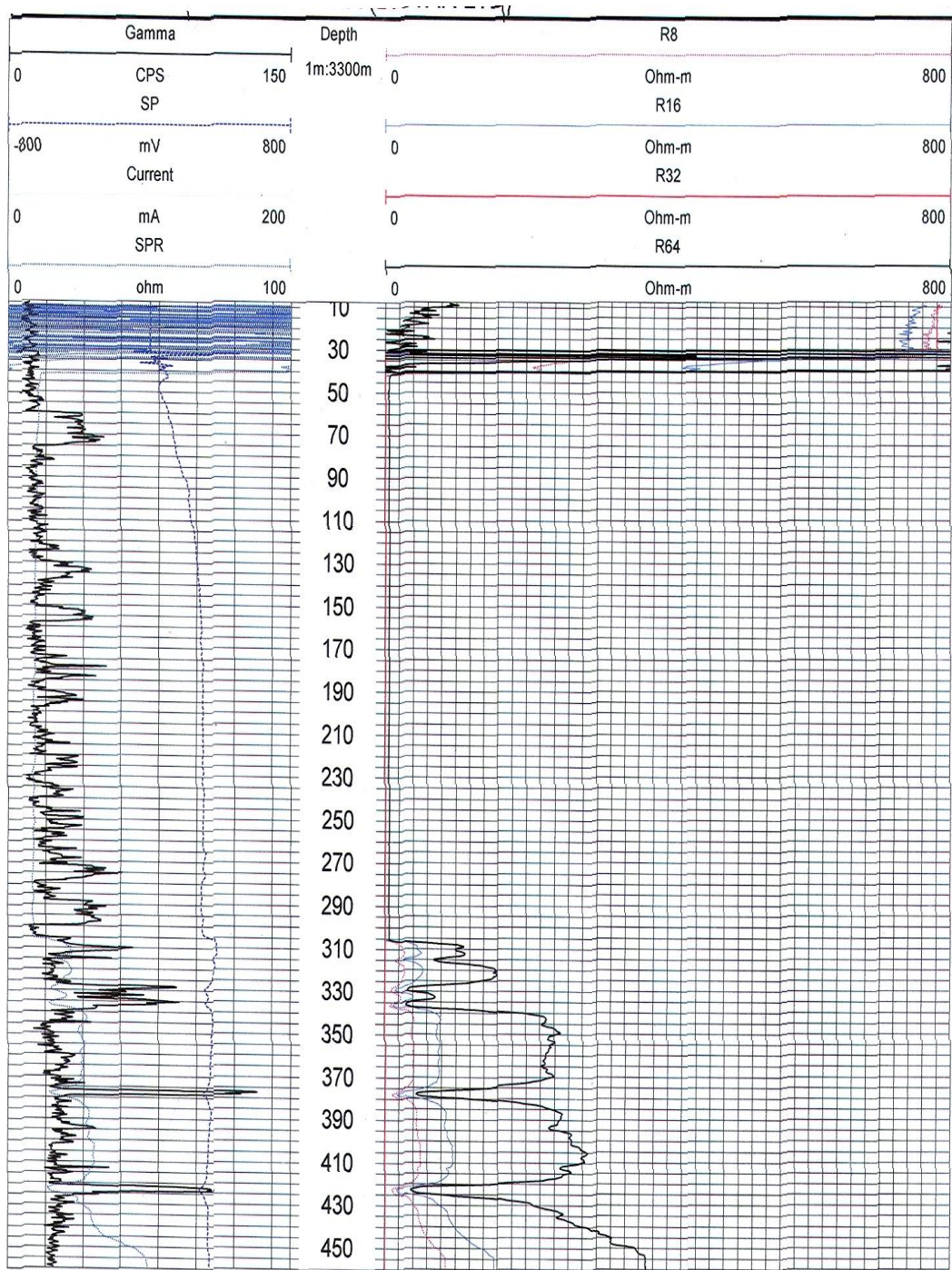


**Figure 8.15** Wireline logs in a deep borehole at Bonny Water Board, Bonny Island

The lithological succession summarised in Table 8.15 reveals that the area is underlain by eight saturated sand bodies up to the depth of 450m. Four of these occur

between 0 - 300m and four between 300 – 450m. The resistivity logs show that the aquifers occurring below 305m contain freshwater.

**Table 8.15 :** Lithologic successions in a deep borehole at Bonny Water Board

<b>Depth interval (m)</b>	<b>Lithology</b>	<b>Thickness of bed (m)</b>
0 – 60	Sand	60
60 – 75	Clay	15
75 – 130	Sand	55
130 – 157	Clay with some sand beds	27
157 – 178	Sand	21
178 – 184	Clay	6
184 – 225	Sand	41
225 – 300	Alternation of thin beds of sand and clay	75
300 – 328	Sand with few clays intercalate	28
328 – 337	Clay	9
337 – 375	Sand	38
375 – 380	Clay	5
380 – 420	Sand	40
420 – 426	Clay	6
426 – 450	Sand	24

#### **8.3.5.4 Deep borehole at Oguede, Bonny for NLNG**

This well was also drilled to a depth of 452m to serve the water requirements of the Nigerian Liquified Natural Gas at Oguede, Bonny. The lithological successions as inferred from the geophysical logs and confirmed by the driller's log is shown in Table 8.16, and the logs presented as Figure 8.16, respectively.



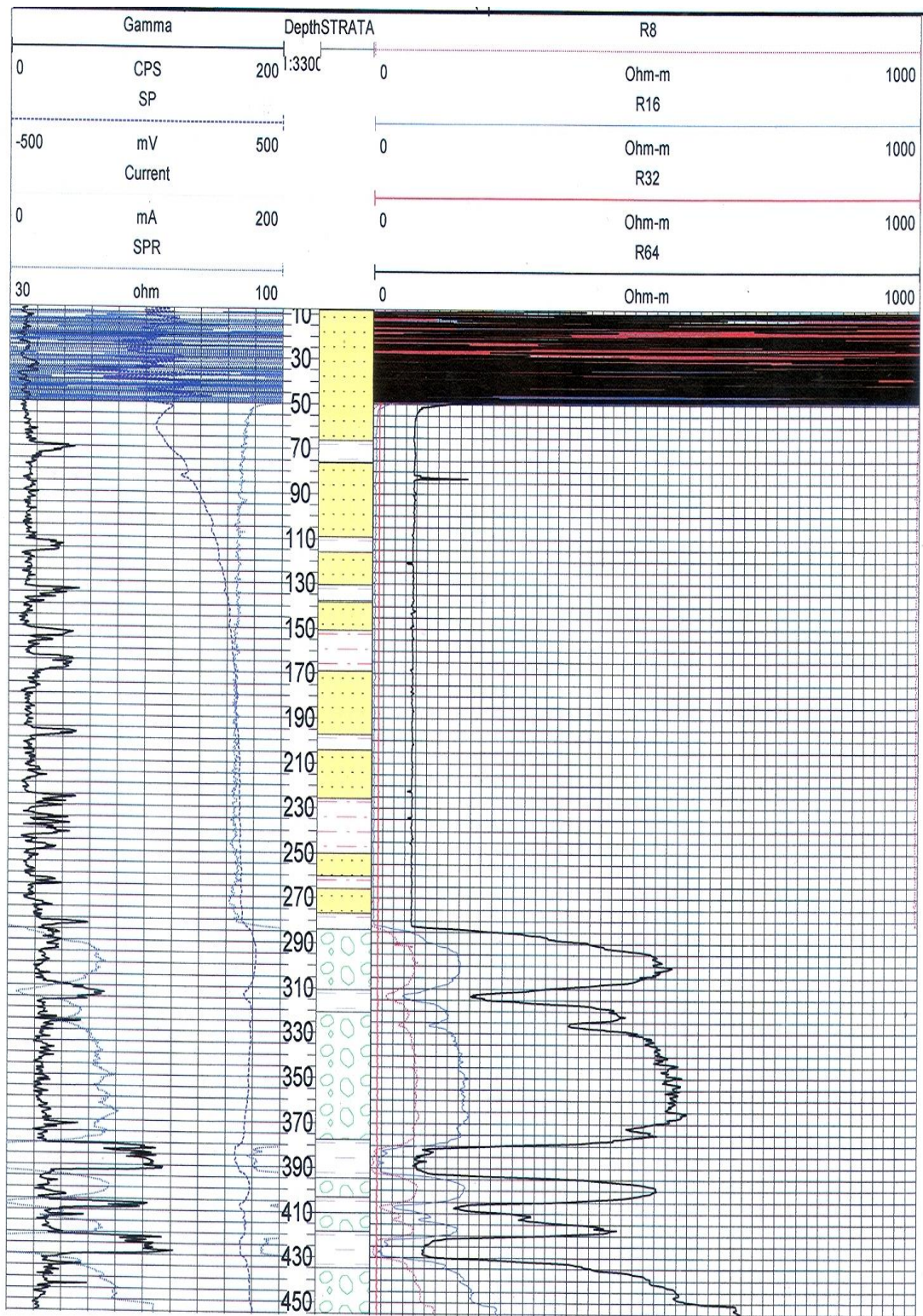


**Figure 8.16** Wireline logs in a deep water borehole at Oguede, Bonny, NLNG



**Table 8.16 :** Lithologic successions in a deep borehole at NLNG, Oguede Bonny.

<b>Depth interval (m)</b>	<b>Lithology</b>	<b>Thickness of bed (m)</b>
0 – 226	Mostly sand with a few clay intercalate	226
226 – 239	Clay, sandy	13
239 – 310	Sand	71
310 – 317	Clay	7
317 – 380	Sand	63
380 – 392	Clay	12
392 – 406	Sand	14
406 – 409	Clay	3
409 – 422	Sand	13
422 – 429	Clay	7
429 – 452	Sand	21

The table reveals that the area is underlain by six saturated sand bodies up to the depth of 452m. The resistivity logs also show that from 0 – 283m, the aquifers are saturated with saline water. In comparison, the lower aquifers contain freshwater until the bottom of the well at 452m below ground surface.

#### **8.3.5.5 Deep borehole at Finima, near Bonny for NLNG**

This well was also drilled to a depth of 452m to serve the water requirements of the Nigerian Liquefied Natural Gas at Finima. The lithological successions as inferred from the geophysical logs and confirmed by the driller's log are shown in Table 5.16, and the wireline logs are shown in Figure 5.13. The table reveals that the area is underlain by nine saturated sand bodies up to the depth of 450m with 6 of the aquifers occurring within the first 300m. The resistivity logs also revealed that the

aquifers are saturated with saline water from 0 – 220m. The lower aquifers contain freshwater until the bottom of the well at 450m below ground surface.

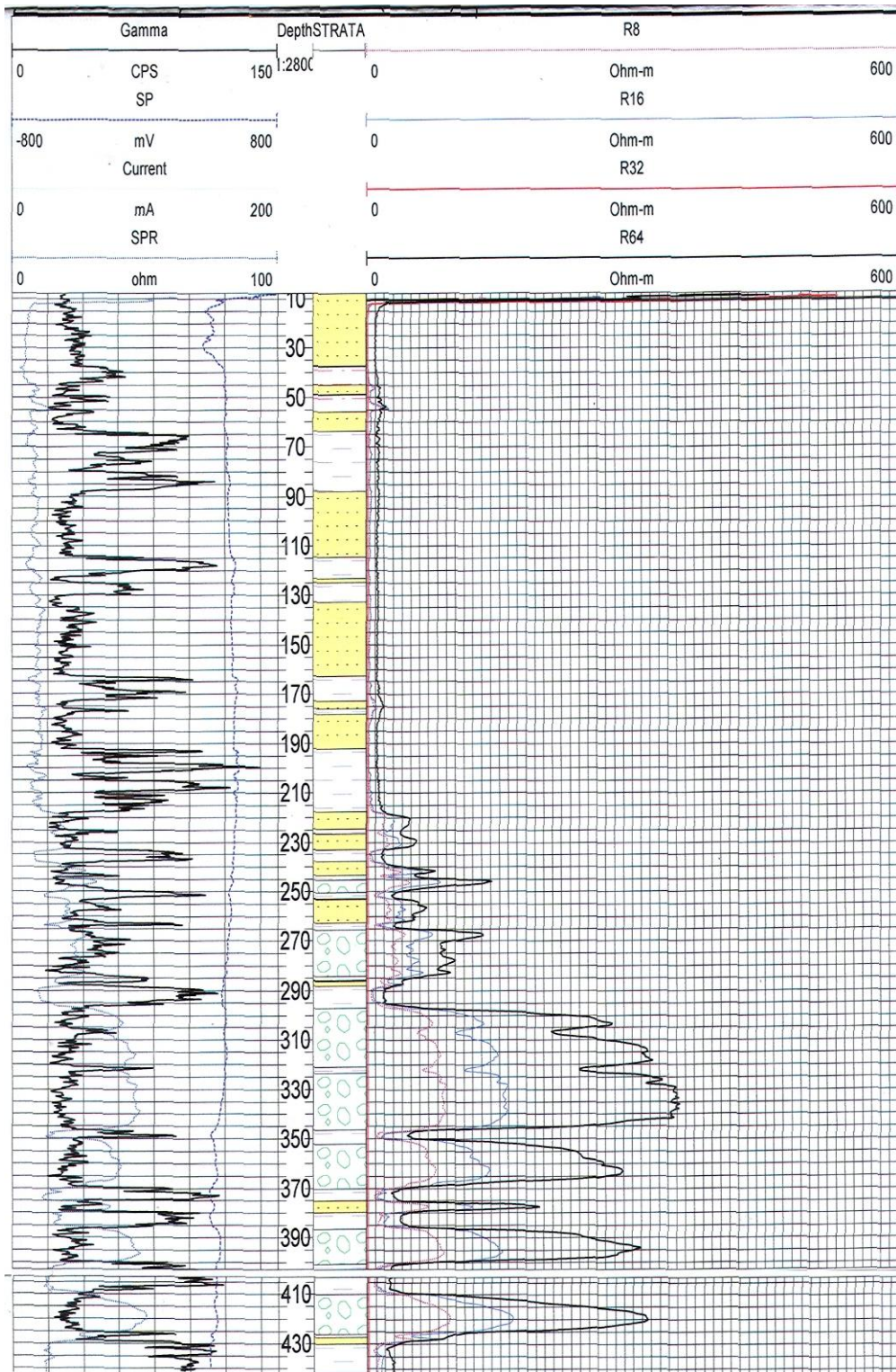


**Figure 8.17** Wireline logs in a deep borehole at Finima, NLNG

**Table 8.17 :** Lithologic successions in a deep borehole at NLNG, Finima, Bonny

<b>Depth interval (m)</b>	<b>Lithology</b>	<b>Thickness of bed (m)</b>
0 – 65	Sand	65
65 – 87	Clay	22
87 – 115	Sand	28
115 – 121	Clay	6
121 – 163	Sand	42
163 – 172	Clay	9
172 – 193	Sand	21
193 – 238	Alternation of thin beds of sands and clay	45
238 – 250	Sand	12
250 – 253	Clay	3
253 – 285	Sand	32
285 – 296	Clay	11
296 – 370	Sand	74
370 – 385	Alternation of sand and clay	15
385 – 400	Sand	15
400 – 407	Clay	7
407 – 430	Sand	27
430 – 450	Clay	20

### **8.3.5.6 Deep borehole at Ogidigbenu/Ugborodo, Delta state**

This well drilled to a depth of 600m for NNPC at Ogidigbenu/ Ugborodo in Delta state is the deepest known water borehole in this study. The lithologic successions shown in Table 8.18 revealed that the area is underlain by ten saturated sand bodies up to the depth of 600m with 6 of the aquifers occurring within the first

300m. The resistivity logs presented in Figure 8.18 reveals that the aquifers are saturated with saline water from 0 – 390, and with brackish water from 390 - 416m while the aquifers occurring between 416 and 600m contain freshwater.

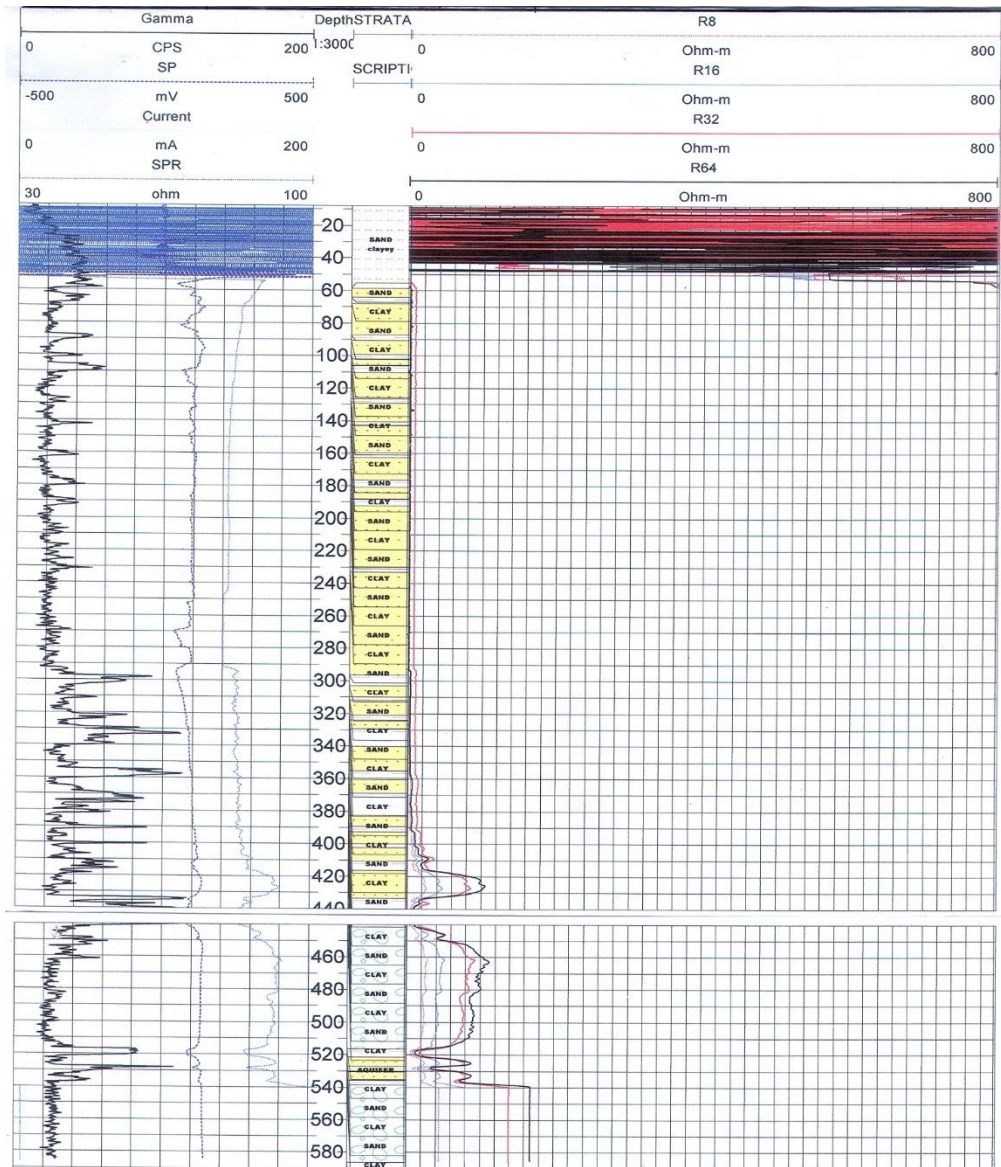


**Figure 8.18** Wireline logs of a deep borehole at Ogidigben/Ugborodo, Delta state.

**Table 8.18 :** Lithologic successions in a deep borehole at Ogidigben/Ugborodo, Delta state.

Depth interval (m)	Lithology	Thickness of bed (m)
0 – 59	Sand, clayey	59
59 – 88	Sand	29
88 – 91	Clay	3
91 – 106	Sand	15
106 – 110	Clay	4
110 – 160	Sand	50
160 – 163	Clay	3
163 – 298	Sand	135
298 – 304	Clay	6
304 – 330	Sand	26
330 – 340	Clay	10
340 – 355	Sand	15
355 – 360	Clay	5
360 – 369	Sand	9
369 – 382	Sand with clay intercalates	13
382 – 434	Sand with few thin clay interbeds	52
434 – 442	Clay	8
442 – 516	Sand	74
516 – 522	Clay	6
522 – 527	Sand	5
527 – 539	Clay, sand	12
539 – 600	Sand	61

#### 8.4 Concluding Remarks

This chapter has presented the conceptual model framework for Hydrogeological studies of the Niger Delta Basins. The results show that the aquifers within the coastal plain sand geomorphic zone and the upper geologic unit Benin



(formation) are so far the most accessible for freshwater within the basins. This is based on the geometry, hydraulic characteristic and depth from the record of drilled boreholes in the area. Three to Four Hydrostratigraphic units had been identified and enumerated based on the results and data from the literature.

The Model has also highlighted some of the critical components within the area that can influence surface and groundwater in term of interaction, occurrence, distribution, and quality. Components which emanated from agriculture, industrialisation, urbanisation, mining, exploration/exploitation and associated poor management of waste from these sources have formed the external environments which interact and interfere with the natural Hydrologic cycle. All these, therefore, determine its status for strategic planning that can enhance sustainable groundwater resources management as part of safe water for all as the basis for the healthy economy.

Combining the findings from chapters 5, 6, 7 and 8 together will, therefore, be used in a numerical groundwater flow model for the evaluation of water resources status and its resilience to the effect of climate change in the next chapter.

## CHAPTER 9

# Impact of Climate Change on the Groundwater Resources

### 9.1 Preamble

This chapter brings together the hydrostratigraphic characterisations and conceptual model developed in chapter 8, the simulated aquifer recharge and evapotranspiration deduced from Global Climate Model (GCM) simulations under two Representative concentration pathways (RCP4.5 and RCP8.5) in chapter 7 to develop a transient groundwater model using MODFLOW-2005 aimed at investigating the potential impacts of climate change and increased groundwater extraction in the coastal plain sand aquifer of the Niger Delta for the periods 2010 to 2099.

A research article was developed from this study and submitted to the *Journal of African Earth Sciences* (2020) as:

- Hassan, I.; Kalin, R. M.; Aladejana, J. A; White, C. J. (2020) ‘Modelling the Climate Change Impacts on the Shallow Coastal Aquifer of the Niger Delta, Nigeria.’, Submitted to the *Journal of African Earth Sciences* (Elsevier). Under review.

The article presents my effort in conceptualising, theoretical formulation, development, analytic calculations, numerical simulations, and writing the manuscript. My supervisors, Prof. Robert M. Kalin, and Chris J. White assisted in designing the

research and gave critical views on the paper for further improvement and my colleague Jamiu A. Aladejana provided technical help and proposed essential additions to the models and the manuscript.



## 9.2 Paper 6

**Hassan, I.; Kalin, R. M.; Aladejana, J. A; White, C. J. (2020) ‘Modelling the Climate Change Impacts on the Shallow Coastal Aquifer of the Niger Delta, Nigeria.’ Submitted to the *Journal of African Earth Sciences* (Elsevier).**

### **Modelling the Climate Change Impacts on the Shallow Coastal Aquifer of the Niger Delta, Nigeria**

Ibrahim Hassan<sup>1,2\*</sup>, Robert M. Kalin<sup>1</sup>, Jamiu A. Aladejana<sup>1,3</sup> and Christopher J. White<sup>1</sup>

<sup>1</sup>*Department of Civil and Environmental Engineering, University of Strathclyde, Glasgow,*

<sup>2</sup>*Department of Civil Engineering Abubakar Tafawa Balewa University Bauchi, Nigeria;*

<sup>3</sup>*Department of Geology, University of Ibadan, Nigeria;*

#### **Abstract**

Surface and groundwater are two interconnected components of one single resource; any negative impacts on one will inevitably affect either the quantity or quality of the other component. The Niger Delta presents special challenges for water resource policy and management due to climate change and anthropogenic activities, especially with an increase in water demands. In this study, a transient groundwater model was developed to investigate the potential impacts of climate change and increasing groundwater extraction due to increasing population. The model used simulated aquifer recharge and evapotranspiration deduced from rainfall series using Global Climate Model (GCM) simulations under two representative concentration pathways (RCP4.5 and RCP8.5) to predict two scenarios from the year 2010 to 2099. The first scenario evaluated only climate change impact on the aquifer, while the second examined the impact of climate change on groundwater budget combined with

25% and 50% increase in groundwater abstraction. Steady-state and transient model simulation of the base period (1980-2005) showed a very good correlation between the simulated and observed groundwater levels. Results show that the maximum change in groundwater budget and levels were found where groundwater extraction was increased by 50% and under RCP 8.5, predicting a decrease in groundwater levels by 1 m around the coast to 7 m towards the northern part of the study area, and with  $\Delta S$  of the aquifer to decrease by 325,000 m<sup>3</sup>/day and groundwater levels to decrease from a range of 1 to 27 m, respectively. This shows that surface water-groundwater modelling of climate change impacts is critical as predicted change in the surface flow and water levels will affect the regional groundwater budget of the aquifer.

**Keywords:** Climate change; Coastal plain sand aquifer; Numerical modeling; Representative Concentration Pathway; Surface water/groundwater interaction.

## 1.0. Introduction

Climate change is highly topical due to its increasing impacts on the livelihood of humans, society and the environment (IPCC, 2013a). Climate change is a natural phenomenon over 100's of years (WMO, 2013). However, due to an increase in anthropogenic activities, the climate is changing at a faster rate. The mean global temperature for the period 2006–2015 is 0.86 °C above the pre-industrial baseline (1850-1900), and the global mean surface temperature for 2018 was  $0.99 \pm 0.13$  °C above the pre-industrial baseline (WMO, 2018). Global sea levels rose between 10 and 25 cm since the late 19th century and are anticipated to rise between 2 to 4 cm per decade over the next century (IPCC, 1992). The increase in temperatures adds energy to the hydrologic cycle resulting in significant changes in the intensity of precipitation,

and impacts on evapotranspiration, soil moisture and groundwater recharge (Kumar, 2012; Porio, 2014). The impacts of these changes are waterlogging, flooding, damage to crops, soil erosion, adverse effects on surface and groundwater quality, water scarcity, water contamination, disease outbreak, loss of properties, disruption of the settlement, and different socio-economic challenges (IPCC, 2007a).

Freshwater resources are vulnerable to climate change. Globally, only 2.5% of the global water budget is freshwater (Spellman, 2014) and of this, approximately 98% of the available freshwater is stored as groundwater (Gleick, 1993; Craig *et al.*, 2010). As the world population is projected to grow from an estimated 7.7 billion people worldwide in 2019 to around 8.5 billion in 2030, 9.7 billion in 2050 and 10.9 billion in 2100 (UN DESA, 2019), water demand will increase. Climate change will enhance the water stress resulting in around 5 billion people living under water stress condition by the year 2025 (Arnell, 1999). Surface and groundwater are the primary sources of natural freshwater upon which the sustainability of agriculture, industrialisation and the civilisation of humanity relies. Unfortunately, these resources have been subjected to exploitation and contamination due to anthropogenic activities emanating from solid waste landfills, industrial effluent, oil spillage, gas flaring and petroleum refining leading to the release of heavy metals into the atmosphere (Bellos and Sawidis, 2005; Ahmad *et al.*, 2010; Egeonu and Oyanyan, 2018). The increase in groundwater demand for various human activities has globally placed great importance on water science-based policy and management (Nouri *et al.*, 2006).

Coastal aquifers have globally been intensely exploited, given the widespread economic and social development of these areas around the world (Mukherjee *et al.*, 2015). Here groundwater tends to be the only source of freshwater of acceptable quality which makes it crucial and unique, but under risk due to high exploitation.

Given societal needs and economic demands are continually increasing, policy instruments are often ignored, ‘watered down’ or weak leading to uncontrolled overexploitation, the consequences of which can be dramatic (Steyl and Dennis, 2010; MacDonald *et al.*, 2012; Mtoni *et al.*, 2013). Coastal aquifers are also naturally at risk from saltwater intrusion (Bear and Verruijt, 1987; Oteri, and Atolagbe, 2003a). This occurs when the water budget of the aquifers becomes unbalanced due to several factors such as over-exploitation, climate change impacts (leading to a decrease in recharge rate) that accelerate seawater intrusion inland contaminating freshwater production wells (Capaccioni *et al.*, 2005; Felisa *et al.*, 2013). Lack of regulation and management can lead to limited future use of coastal aquifers and total loss of the resource (Razack *et al.*, 2019). For this purpose, numerical modelling of aquifers constitutes a critical tool which is used to test conceptual understanding and analyse the aquifers’ reactions to various stresses (Du *et al.*, 2018; Razack *et al.*, 2019).

The Rivers State is one of the economic hubs of Nigeria with a population in 2020 of around 8 million (based on a population of 5,198,716 from census data of 2006 and an estimated annual growth rate of 3.41% (JICA *et al.*, 2013)) making it the sixth-most populous state in Nigeria. Due to crude oil exploration activities, the state serves as the operational base of major oil-producing and servicing companies in Nigeria. Petroleum exploration and exploitation have been going on in this region for over fifty years and has triggered adverse environmental impacts through socio-economic, environmental and physical disasters which accumulated over the years due to negligence, lack of assessment and limited scrutiny (Akpomuvie, 2011; Nnabuenyi, 2012; Oluduro, 2012; Ubani and Onyejekwe, 2013; Amadi, 2014; Mogborukor, 2014). The high level of rural-urban migration resulting surge in population in the area put pressure on the water resources in the area. Lack of public water supply force most of

the households to focus on groundwater from the shallow aquifers to meet their daily water demand. The aquifer system in the area is mostly unconfined, highly porous and permeable; hence, with less storativity, the tendency of contaminants infiltrating into the shallow water table is quite apparent (Amadi *et al.*, 2014; Hassan *et al.*, 2019). Drivers such as incessant oil spillage, flooding and gas flaring have caused near irreversible degradation of shallow groundwater quality in this area leading to a locally ascribed cultural irony “living on the water but thirsty “. Lack of a law enabling the control of the abstraction of groundwater in the area worsens the situation (Edet *et al.*, 2014).

It is highly likely these shallow aquifers are at high risk due to induced climate variability, which would then affect water resources sustainability. This situation has attracted the interest of environmental activists who called for a comprehensive evaluation of the impact of climate change on groundwater resources for sustainability in the coastal areas of Nigeria. This study is the first attempt to numerically model the impacts of climate change on groundwater flow in the region. The main objective was to deduce groundwater recharge based on the simulated CIMP5 GCMs rainfall series up to 2099 under RCP 4.5, and RCP 8.5 climate emission scenarios, and to model the aquifer water budgets using the recharge series as the input to analyse the aquifer reaction to the climate scenarios.

## **2.0.Methodology**

### **2.1.Description of the Study Area**

Rivers State is one of the coastal states of Nigeria (Figure 9.1). It is situated in the Niger Delta region on the oceanward extension of the Benue Trough and covers an area of about 11,077 km<sup>2</sup>. Tropical rainforest characterises the Rivers state inland part

and mangrove swamps towards the coast. The state is bounded the Atlantic Ocean to the south, Imo, Abia and Anambra state to the north, Akwa Ibom state to the east and Bayelsa to the west. The area chosen for this study is the Port Harcourt municipality, which is the capital city of Rivers state. This city houses the highest population growth in the region due to the rapid industrialisation, resulting in a very steep increase in water demand. The area of study is 369 km<sup>2</sup>, which consists of 2 major local governments, namely Port Harcourt and Obio-Akpor local administration areas; therefore, the model has a regional character.

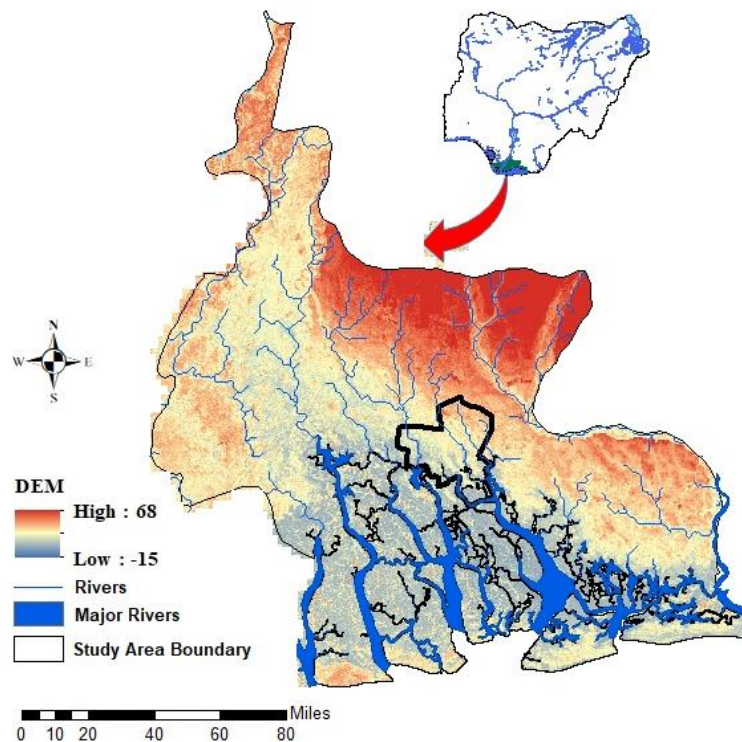


**Figure 9.1** Map of the study area, Rivers State, Nigeria

Climatically, the study area belongs to the wet equatorial climatic region characterised by typical tropical wet and dry climate with a mean annual rainfall decreasing from 4500 mm around the coastal margin to about 2000 mm around the northern fringe of the study area (Adejuwon, 2012). The mean monthly temperatures are up to 26.7°C around March / April and as low as 24.4°C during July/ August giving

a small annual range of 2.7°C. The mean relative humidity of the area is relatively high often reaching 90%, while the warm, wet southwesterly winds blow inland most of the year and the dust-laden, warm-dry North-easterly winds occasionally reach the coast for small periods of the year (Etim and Alonge, 2009). The rainy season starts from March to October, with a short dry spell mostly during August (referred locally as the August break) which occurs when monsoon winds shift and carry moisture from the ocean into the hinterland. The dry season lasts from November to February while harmattan, which is caused by the tropical continental air mass from the north is mostly experienced between December and February (Odafivwotu Ohwo, 2018).

## **2.2.Geologic Setting**

The geology of the Niger Delta was first documented in 1907 and is dominated by the Benin formation (Figure 9.2). The formation consists predominantly of very thick coastal sands, sandstones, and clay and sandy-clay occurring in lenses (Reyment, 1965). The study area located within the Niger Delta Basin (Port-Harcourt) is underlain by Pliocene-Pleistocene (Figure 2.3) belonging to the Benin Formation. The formation is locally found in Port-Harcourt, Aba and Owerri, where it sometimes outcrops in both surface and subsurface in the mode of occurrence (Amadi *et al.*, 2014). The formation was extensively described by (Reyment, 1965) as reddish earth made up of poorly sorted loose sands underlying recent Quaternary sedimentary deposits of southern Nigeria. They consist mainly of sands, sandstone and gravel with clays occurring in lenses (Onyeagocha, 1980). The sands and sandstones are fine to coarse-grained, partly unconsolidated with varying thickness.

The formation is recognised in burrowed pits, river channels, and boreholes in the area. The upper horizon contains reddish-brown clayey sand (Sentelhas *et al.*,

2010) covered by brownish humic soil. The formation is characterised by a thick sequence of sediments about 2100 m thick deposited in the continental phase of the Niger Delta (Short. *et al.*, 1967; Amadi *et al.*, 2014). The thickness of the formation within the study area is estimated at 900m and its maximum thickness of about 1,820 m near the sea. The Benin Formation is also known as the Coastal Plain Sands and alluvial ridges mostly consist of continental sand and gravel with intercalations of clay and shale characterised by a high resistant fresh water-bearing (Amadi *et al.*, 2014).

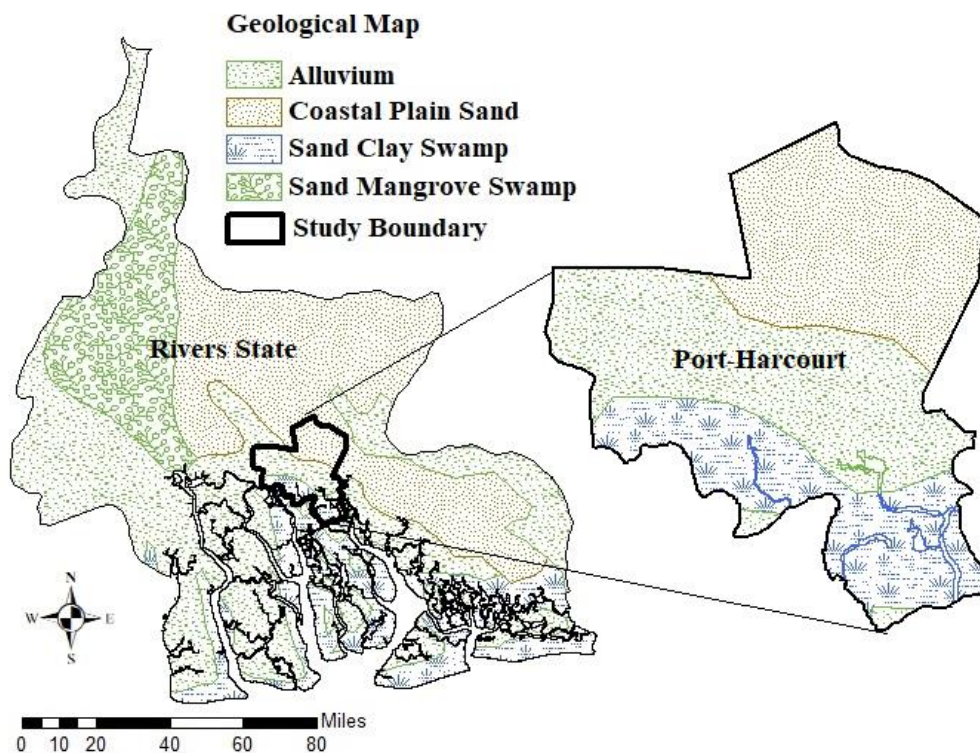


**Figure 9.2** Geological Map of the Rivers State showing the study area (Modified from Nigerian Geological Survey Agency 2006)

### 2.3. Hydrogeologic Setting

The study area has extensive floodplains which incise and form major tributaries to the Aba, Imo, Kwa-Ibo and Bonny Rivers (Figure 9.1). The rivers flow trend is in the northwest-southeast direction (Uma, 1989). There is a large recharge



zone due to the abundant rainfall in the region, a significant percentage of the area being open grasslands. These Rivers are prone to pollution along their course due to anthropogenic activities, and so inhabitants do not rely on them for potable water supply. The continuous rural-urban drift of people to Port-Harcourt further aggravating the pollution of these Rivers as they form the effluent discharge point for untreated industrial waste as the majority of them are sited along the banks of these rivers.

There are three principal drainage rivers in the City of Port Harcourt, which are the Ntamogba Stream, the Nwaja River, and the Rumuogba-Woji Creek, (Amangabara, 2006). Few other significant drainage rivers, e.g. the Nwaja River that drains Rumukalagbor, New GRA Phases IV and V, Elekahia, Presidential Housing Estate and Sun Ray Publications Area of Aba Road. These river systems drain the entire Port Harcourt City dividing the City into three major drainage zones (Amangabara, 2006). The Woji river flows approximately 520.3 km<sup>2</sup>. The New Calabar River located on the eastern flank of the Niger Delta and is one of the most stressed rivers in the region which empties into some creeks and lagoon in the Port-Harcourt area dynamically connected to the Bonny River bordering the Atlantic Ocean (Uzukwu, 2014).

#### **2.4. Data**

The datasets used in this study are groundwater level data collected from 130 different observation wells across the study area, as depicted in Figure 9.4. The datasets covering a period of 1980 to 2000 were provided by the Nigeria Hydrological Services Agency (NHISA) and MECON Geology and Engineering Services. The meteorological datasets used in this study were provided by the Climate Research Unit (CRU) as daily time series data of rainfall, maximum and minimum temperature over

the historic years of 1980 to 2005 (Harris *et al.*, 2014), used as a substitute to the observed station datasets over the study area due to the scarcity of reliable long records of hydro climatological stations observations in the area. They were found to be the best-fit datasets that replicate the distribution patterns, spatial and temporal variability of the Niger Delta's observed datasets (Hassan *et al.*, 2020a).

In a projection study of the changes in rainfall, maximum and minimum temperature over the Niger Delta region by Hassan *et al.*, (2020b), using four Global Climate Models (GCMs) from the IPCC Fifth Assessment Reports (AR5) namely ACCESS1.3, MIROC-ESM, MIROC-ESM-CHM and NorESM1-M and two emission scenarios (RCP 4.5 and 8.5), the results show an overall increasing trend in both precipitation, minimum and maximum temperature over the region as shown in Table 1 and figure 3 respectively. The change in mean annual precipitation was found to range between 16.31 to 109.89 mm under RCP 4.5, and 38.08 to 114.69 mm under RCP8.5 during the 2080s period. The maximum temperature was projected to increase by 0.4 °C under RCP 4.5, and 1.25-1.79 °C under RCP8.5. In comparison, the minimum temperature was also projected to increase in temperature between 0.52 °C under RCP 4.5, and 1.38-2.02 °C under RCP8.5 during the 2080s period. Such a projection in precipitation and temperature represents a warning of for the Niger Delta, consistent with other parts of the world (Martín *et al.*, 2012; Rangwala and Miller, 2012; Krinner *et al.*, 2013; Expósito *et al.*, 2015).

## **2.5. Observed and Future Climate Scenarios**

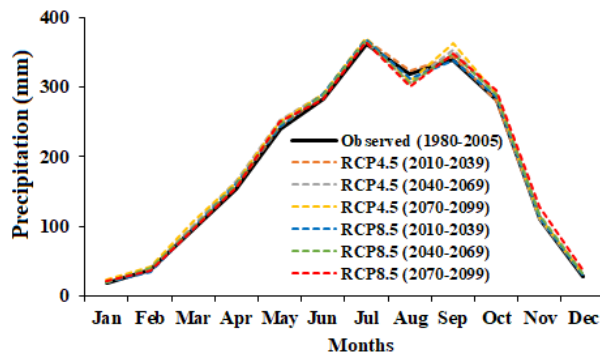
Average daily rainfall and temperature during the base period (1980-2005) projected over the periods 2010-2039, 2040-2069 and 2070-2099 for the study area are shown in Figures 9.3(a, b & c), respectively. Figure 9.3(a) shows an increasing

trend in precipitation during the wet season and decrease during the dry season under both RCP 4.5 and 8.5.

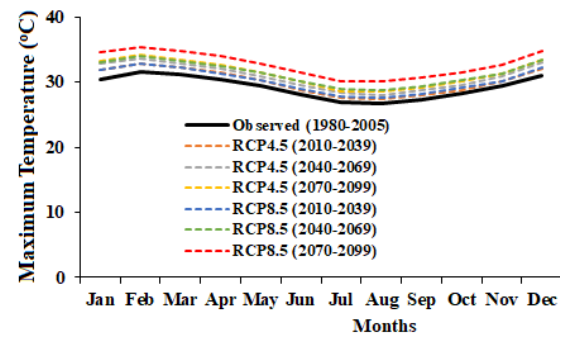
**Table 9.1 :** Annual changes in future Rainfall, Maximum and Minimum Temperature under RCP4.5 and RCP8.5

Emission Scenario	Periods	% Change		
		Precipitation (mm)	Tmax °C	Tmin °C
RCP4.5	2020s	1.65	3.01	0.71
	2050s	2.24	5.59	4.55
	2080s	3.76	7.10	6.66
RCP8.5	2020s	1.28	3.32	1.17
	2050s	1.79	7.31	7.13
	2080s	2.24	11.95	13.74

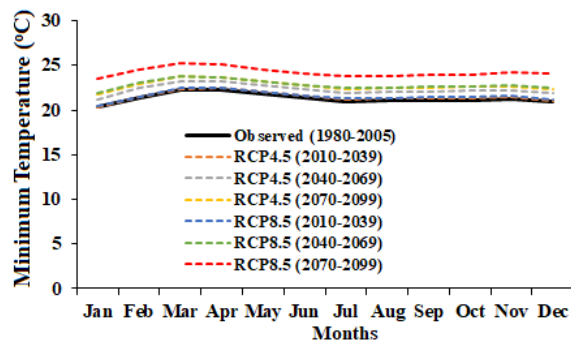
The variation between the observed and future mean annual maximum and minimum temperature depicted in Figures 3b and 3c also shows an increasing trend in the study areas temperature under both RCP's and for all the predicted duration, that will have an impact on the evapotranspiration and recharge of the study areas.



(a) Precipitation



(b) Maximum Temperature



(c) Minimum Temperature

**Figure 9.3** Observed and Future average annual (a) Precipitation (b) Maximum and (c) Minimum Temperature for Port Harcourt under RCP 4.5 and 8.5 scenarios.

### 3.0. Groundwater Flow Model

A transient mathematical model of the coastal plain sand aquifer was developed for Port-Harcourt municipal based on the hydrogeological information of the study area. Climate change scenarios obtained from (Hassan *et al.*, 2020b) and the hydrogeological conditions obtained from (Hassan *et al.*, 2019) were used to conceptualise the hydrogeological model for the area.

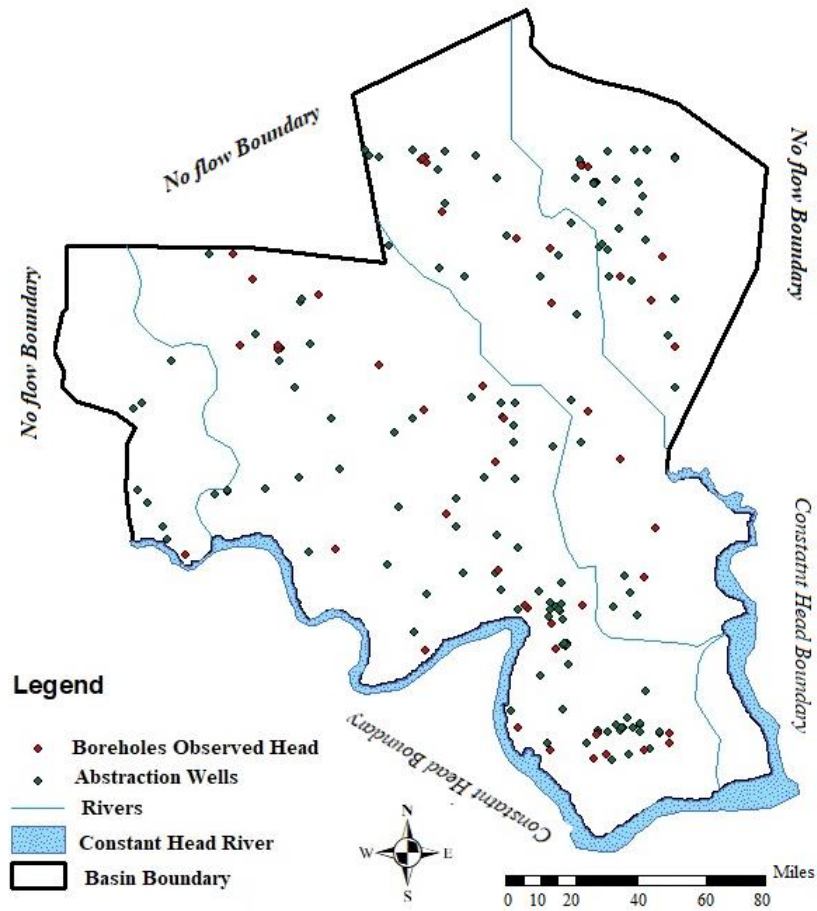


**Figure 9.4** Map of the study area showing the locations of abstraction wells in the basin and the Model Boundary conditions.

The conceptual model was translated into a numerical model, which is manually calibrated under steady-state conditions using ModelMuse. ModelMuse is a graphical user interface (GUI) developed by the U.S. Geological Survey (USGS) for MODFLOW-2005, MODFLOW-LGR, MODFLOW-NWT, MODPATH, ZONEBUDGET, PHAST and MT3DMS models which have been used in many areas around the world and found to produce reliable results.

### 3.1. Hydrogeological Conceptual Model

The study area was conceptualised and lithology grouped into three central units, namely, sand, gravelly sand, and clay (Akinwumiju and Orimoogunje, 2012). Based on the characterisation, it was concluded that the sand/gravelly sand and the clay layers are hydraulically connected (Hassan *et al.*, 2019). The groundwater resources are held within the Alluvium and coastal plain sands of the deltaic formation of the Niger Delta basin. The boreholes around the area are tapping three aquifer units. The unconfined aquifer with water level ranging from 0-25m with 2-3 confined units of depths 35-48 m, 45-65 m and 55-102 m (Hassan *et al.*, 2019). The aquifers are of fine to medium grain sands with Clay and Shale layers acting as separating layers due to their low permeability (Orimoogunje, 2013; Amadi *et al.*, 2014; Hassan *et al.*, 2019). Three hydraulic conductivity zones were demarcated in this study based on the geologic formation, as shown in Figure 9.2.

The boundary conditions for the area are summarised as constant head with the Bonny river/Atlantic Ocean in the south. The southwest and southeast parts of River state were considered as river/constant head boundaries. In contrast, the northern, northwest and northeastern parts of rivers state were taken as no-flow boundaries as presented in Figure 9.4. The topography of the study area for information interchange (ASCII) file was generated using GIS from NASA's Shuttle Radar Topography Mission (SRTM) 1 Arc-Second global dataset DEM. Model-Muse defined the topography via a "fitted surface" interpolation method.

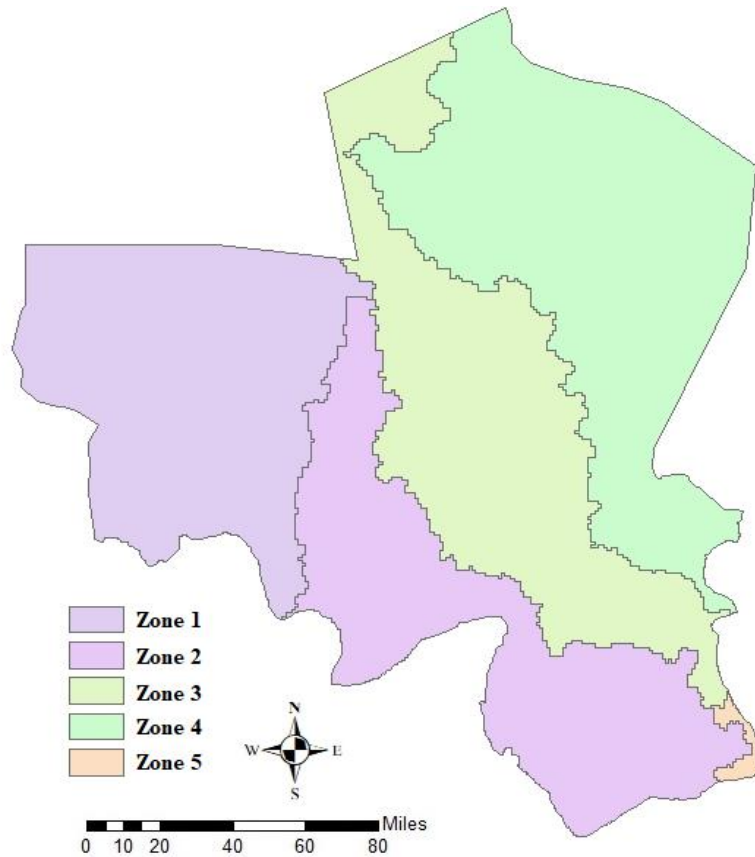
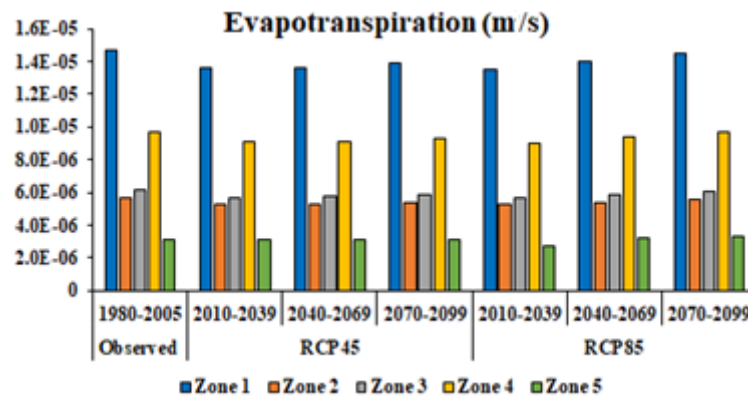


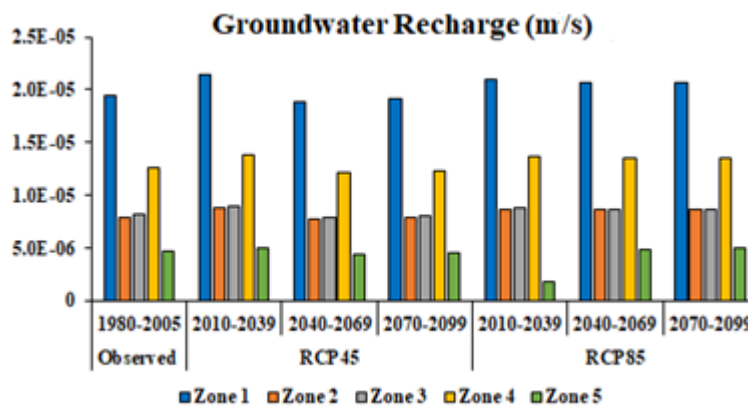
**Figure 9.5** Map showing Recharge and Evapotranspiration Zones obtained from SWAT hydrologic model.

The mean streamflow of the rivers in the modelled area is  $5.85 \text{ m}^3/\text{s}$  for the Woji Basin River (Weli and Ideki, 2014). The average discharge for the middle and lower Ntamogba stream catchments at GRA (from Woji Road down to the Ntawogba Channel) was  $28.04 \text{ m}^3/\text{s}$  for 15 months whereas at Afam – Kaduna Street link Bridge had an average of  $109.35 \text{ m}^3/\text{s}$  between January 2005 and March 2006, (Amangabara and Gobo, 2007). The rate of recharge and evapotranspiration in this study as depicted in Figures 9.6 (a & b), and were obtained from the SWAT hydrologic model extracted from 5 subbasins within the modelled area as shown in figure 9.5. The result shows a significant reduction in recharge and evapotranspiration even with the projected

increase in precipitation which can be attributed to the increase in impervious surfaces due to the rapid urbanisation going on in the area.



(a)



(b)

**Figure 9.6 (a&b):** Simulated observed and future (a) Recharge and (b) Evapotranspiration obtained from SWAT hydrologic model for the five Subbasins housing the study area.

### 3.2. Numerical Modeling

The numerical groundwater model is a mathematical representation of the conceptual understanding of the aquifer system and associated input data for specific problems. They are used to simulate both local and regional settings. Many water resource scenarios require a more sophisticated representation of the groundwater



system, which require increased computing power and new codes that allow the efficient simulation of complicated and broad regional systems (Harbaugh, Arlen, 2005). As mentioned earlier, the USGS ModelMuse version of MODFLOW public domain groundwater flow modelling software package (Winston, 2009) was used to simulate the Coastal Plain Sand aquifer of Port Harcourt Municipal. This model was chosen so that future policy-relevant review in Nigeria can be undertaken without cost implications for expensive or bespoke software. It was applied to construct an equivalent 3-dimensional numerical model of the aquifer under study using all the available climate, hydrological, hydrogeological and pumping data obtained from the extensive investigation.

The basin was discretised with a rectangular grid of 124 rows and 111 columns. The grid cell size was set at 200 x 200 m<sup>2</sup> over the entire grid. A single layer with three hydraulic conductivity zones was defined in the model. The zones are the Sand Mangrove Swamp, Coastal Plain Sand and Alluvial deposits and a lower layer representing the Coastal Plain Sand aquifers, as shown in figure 9.2. These deposits vary in depth across the modelled area from 3 m in the south to a depth of 125m towards the northern part of the area. The main input parameters of the model are hydraulic conductivity (K), Evapotranspiration (ET), recharge (R), well discharge (Q), and river influence and boundary conditions. Based on the data obtained from (Etu-Efeotor & Odigi, 1983; Amajor, 1989; Okagbue, 1989; Onuoha & Mbazi, 1989; Uma, 1989; Etu-Efeotor & Akpokodje, 1990; Izeze, 1990) as summarised by (Hassan *et al.*, 2019), K varies from  $2.8 \times 10^{-7}$  to  $3.2 \times 10^{-3}$  m/s. Hydraulic conductivity (K) values within this range were adjusted manually within the reported range until the model converges with a percentage discrepancy approximately equals 0.

The RIV package in MODFLOW-2005 was used to simulate river-aquifer interaction. To effectively use the RIV Package, parameters such as the riverbed conductance and hydraulic conductivity have to be known with some certainty (Larsen *et al.*, 2000). Since the value of the riverbed hydraulic conductance is unknown, iteration method between 0.001 and 0.0001 was employed for model convergence, as the conductance of the river is one of the most sensitive input parameters in the RIV Package, the return-flow proportion was set at 0.001 for all the rivers. The observed and future scenarios of evapotranspiration and recharge rate in this study are obtained from SWAT hydrologic model following the work of (Hassan *et al.*, 2020) extracted from 5 sub-basins (Figure 9.5) within the modelled area as summarised in Figure 9.6. These are incorporated into the numerical model via the Evapotranspiration Package (EVT) and Recharge Package (RCH) of MODFLOW.

### **3.2.1. Steady-State Model Calibration**

The steady-state model conditions represent a natural balance regime between inputs and outputs from the system. In this study, the steady-state model was developed to calibrate the hydraulic conductivity values of the different zones and formations with known measured data. Recharge and evapotranspiration values in the model were set from the hydrologic model base period of 25 years (1980-2005) obtained from each sub-basin within the aquifer. The model was calibrated in transient-state conditions from 1980 to 2005 using head measurements from 41 observation wells (Figure 9.4) distributed in the study area. Trial and error method based on conceptual model revision was used to calibrate the model in which the hydraulic conductivity (K) values within the reported limit across the three formations as summarises in Table 9.2 to minimise the difference between the observed and

simulated heads, to match field conditions and model convergence with a percentage discrepancy approximately equals to 0. Figure 9.7 shows the spatial variation of the calibrated hydraulic conductivity values across the zones.

**Table 9.2 :** Initial and calibrated model parameters

Hydraulic Conductivity of Materials (m/s)	Initial value	Calibrated value
Upper Layer Alluvium 1	$0.50 \times 10^{-6} - 0.50 \times 10^{-2}$	$7.80 \times 10^{-3}$
Upper Layer Coastal Plain sand	$0.50 \times 10^{-6} - 0.15 \times 10^{-3}$	$5.00 \times 10^{-4}$
Upper Layer Sand Clay Swamp	$0.15 \times 10^{-3} - 0.48 \times 10^{-3}$	$3.50 \times 10^{-3}$
Upper Layer Alluvium 2	$0.36 \times 10^{-3} - 0.51 \times 10^{-3}$	$5.01 \times 10^{-3}$
Upper Layer Alluvium 3	$0.51 \times 10^{-3} - 0.10 \times 10^{-3}$	$5.10 \times 10^{-3}$
Second Layer Coastal Plain sand	$0.50 \times 10^{-5} - 0.10 \times 10^{-2}$	$5.00 \times 10^{-3}$

The variables of the observed hydraulic heads, simulated heads, as well as their residuals, were compared using the scatter plots shown in Figure 9.8 (a & b). The plots show a good match between the observed versus simulated heads and the residual versus simulated heads, respectively. The modelled heads fit satisfactorily with the observed data with an  $R^2$  value of 0.67, root mean square residual of 9.23, the head sum of squared difference of  $3.49 \times 10^{-3}$ , and standard error (SE) of the calculated head is 2.82 m, which is satisfactory (Varni and Usunoff, 1999). The SE of the simulated heads was computed is based on equation 9.1:

$$S.E = \sqrt{\frac{\sum (Sim-Obs)^2}{N}} \quad (9.1)$$

where, the sim is the simulated head, obs the observed head and N the number of cells on the upper layer.

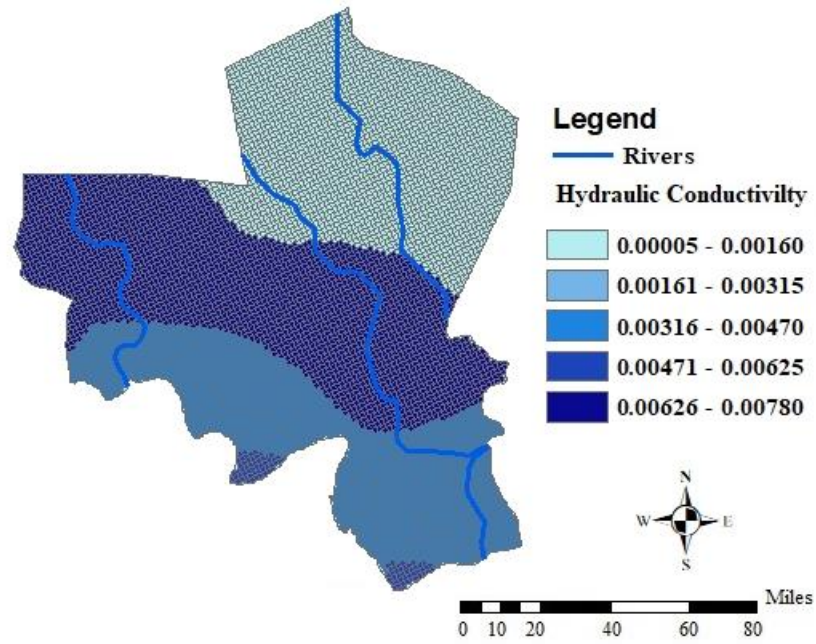


**Figure 9.7** Spatial variation of calibrated hydraulic conductivity values across the different formations.

The plots showing the goodness of fit and the statistical indicators indicate the accuracy of the calibration, which shows that the model is calibrated and ready for prediction.

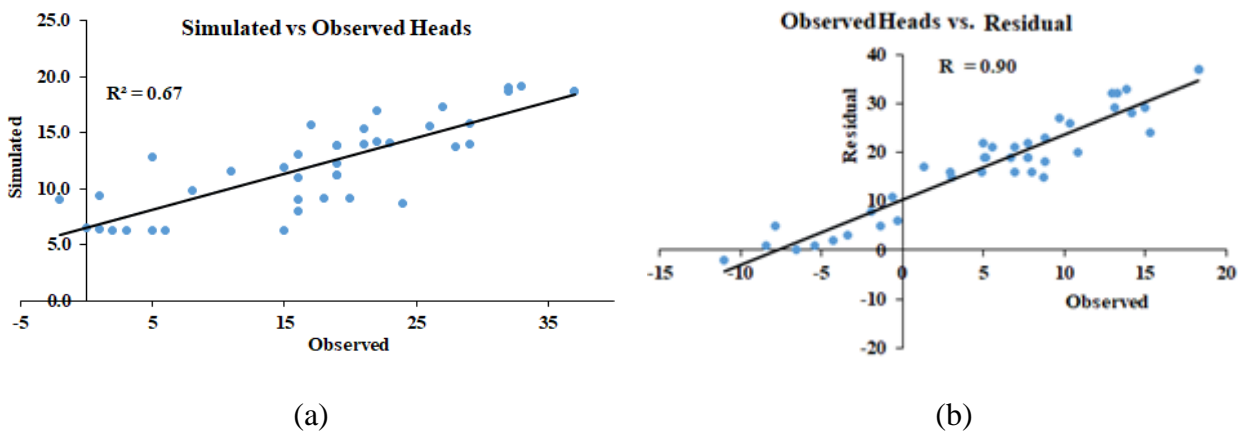


**Figure 9.8** Scatter plot of (a) observed versus simulated heads and (b) Residual versus simulated heads for model calibration.

## **4.0. Results and Discussions**

### **4.1. Surface water-groundwater interaction**

Groundwater represents an essential source of water for different purposes in the area such as irrigation, industry, drinking, and domestic uses. The demand for groundwater is expected to increase throughout the next 80 years. Consequently, two cases were proposed to assess the response of the aquifer due to climate change impacts in this study. In the first scenario, climate change impact was simulated under RCP 4.5 and 8.5 emission scenarios for the three future periods (2020s, 2050s and 2080s). While in the second scenario, pumping scenarios are added to the simulations to represent increasing groundwater extraction in the existing wells by 25% and 50% (response of the aquifer to climate change and increasing population demands).

### **4.2. Base Period.**

During the base period, a steady-state groundwater model was developed for the period 1980 to 2005 using the base period recharge and evapotranspiration values (Figure 9.6) obtained from climate, hydrologic and hydrogeologic model data by Hassan *et al.*, (2019, 2020a, 2020b) as summarised in Table 9.2 and the distribution of groundwater heads and the water table is shown in Figure 9.9. The simulated groundwater budget shows that the primary source of recharge to the aquifer system comes from the surface water recharge, which is  $7.49 \times 10^8$  m<sup>3</sup>/year and river leakage of  $2.76 \times 10^6$  m<sup>3</sup>/year. The total inflow to the aquifer is  $7.51 \times 10^8$  m<sup>3</sup>/year. Evapotranspiration and groundwater pumping represent the main water budget component discharging from the aquifer, respectively  $3.70 \times 10^8$  m<sup>3</sup>/year and  $1.06 \times 10^8$  m<sup>3</sup>/year. Another main outflow component is the outflow from the aquifer to surface

water (baseflow) which is  $3.69 \times 10^7$  m<sup>3</sup>/year. The total outflow from the aquifer is  $7.51 \times 10^8$  m<sup>3</sup>/year. The change in the aquifer storage is positive and equals to  $5.93 \times 10^5$  m<sup>3</sup>/year. It was noted the positive  $\Delta S$  of the groundwater is mainly due to the amount of surface water recharged to the groundwater, an indication that climate change poses a potential threat to the aquifer resilience which confirm the findings of (Edet *et al.*, 2014) for the coastal plain sand aquifer in Akwa Ibom state which is adjacent our study area.

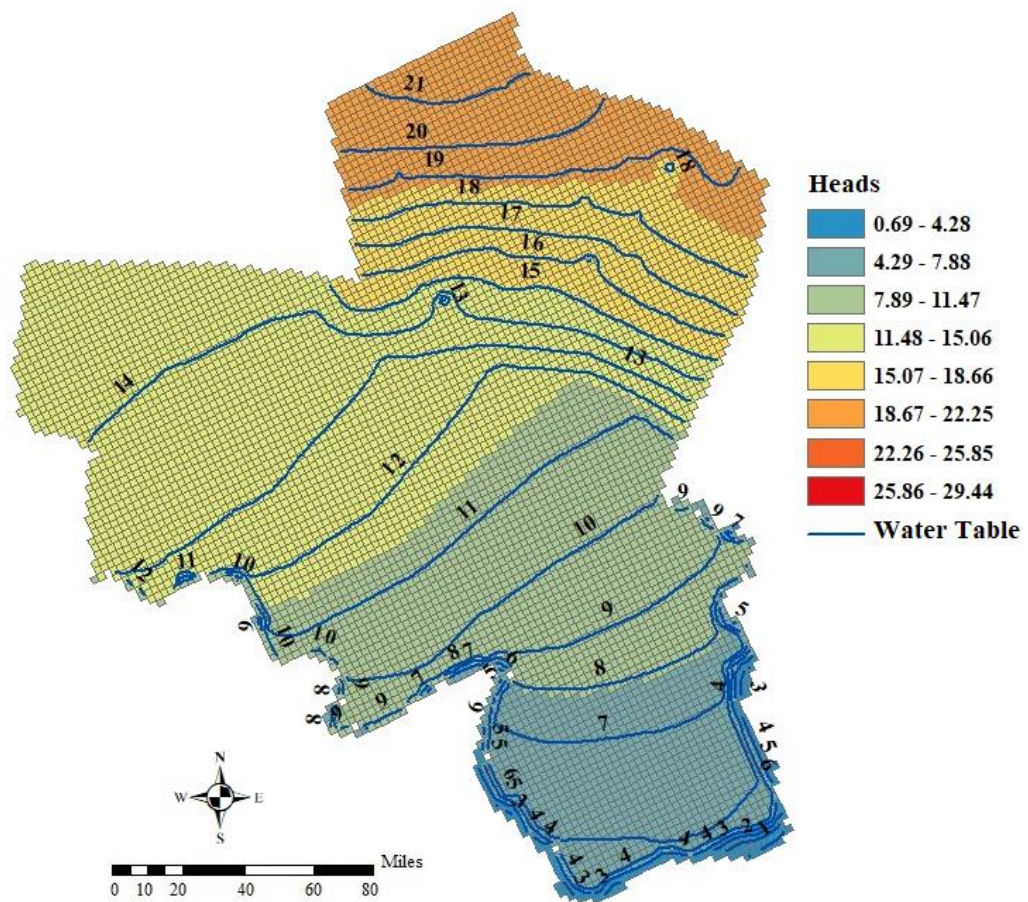


**Figure 9.9** Spatial variation of simulated steady-state groundwater heads and contours during the observed period.

**Table 9.3 :** Summary of the simulated water budget for the modelled area during the observed and future periods under RCP 4.5 and RCP 8.5 emission scenarios.

	<b>Base Period</b>		<b>RCP 4.5</b>		<b>RCP 8.5</b>		
	<b>1980-2005</b>	<b>2010-2039</b>	<b>2040-2069</b>	<b>2070-2099</b>	<b>2010-2039</b>	<b>2040-2069</b>	<b>2070-2099</b>
<b>Inflow (m<sup>3</sup>/year)</b>							
<b>Storage</b>	0	10.5	21.7	30.6	17.9	12.9	2.8
<b>Constant Head</b>	0	0	0	0	0	0	0
<b>Wells</b>	0	0	0	0	0	0	0
<b>River Leakage</b>	2,763,310	117,424	350,144	347,148	262,739	172,032	223763.7
<b>Evapotranspiration</b>	0	0	0	0	0	0	0
<b>Head Dep Boundary</b>	0	0	0	0	0	0	0
<b>Recharge</b>	748,500,652	1,260,891,274	1,119,603,686	1,110,117,658	1,220,957,237	1,234,467,259	1,220,282,366
<b>Total In</b>	751,263,206	1,261,007,957	1,119,953,736	1,110,467,707	1,221,222,139	1,234,640,707	1,220,506,272
<b>Outflow (m<sup>3</sup>/year)</b>							
<b>Storage</b>	0	18.3	45	38.2	46.2	24.6	88.5
<b>Constant Head</b>	0	0	0	0	0	0	0
<b>Wells</b>	106,011,417	106,011,417	106,011,417	106,011,417	106,011,417	106,011,417	106,011,417
<b>River Leakage</b>	36,884,505	102,886,200	76,764,931	77,193,820	86,355,028	97,998,120	90,278,107
<b>Evapotranspiration</b>	369,929,894	754,959,225	681,193,368	670,663,497	755,794,929	740,995,084	745,441,660
<b>Head Dep Boundary</b>	237,844,512	296,775,835	255,618,201	256,255,228	272,508,883	289,153,584	278,346,196
<b>Recharge</b>	0	0	0	0	0	0	0
<b>Total Out</b>	750,670,329	1,260,632,678	1,119,587,918	1,110,123,965	1,220,673,413	1,234,158,206	1,220,077,382
<b>Inflow - Outflow</b>	592,593	376,067	367,268	341,661	548,695	480,230	430,561

### **4.3. Simulation of the potential impact of future climate change scenarios on groundwater resources.**

*Scenario 1: Impacts of future climate change under RCP 4.5 and 8.5 emission scenarios.*

The base period model was simulated for a transient period of 25 years (1980-2005), and the future periods (2020s, 2050s, and 2080s) under RCP4.5 and RCP8.5 emission scenarios using recharge and evapotranspiration values (Figure 9.6) from Hassan *et al.*, (2019, 2020a, 2020b). The water budget results are summarised in Table 9.4, and the distribution of groundwater heads and the water table is shown in figure 9.9, respectively.

The distribution of groundwater heads during the base periods (Figure 9.9) ranges from 0.48 m around the coastal area to 21.67 m towards the North. The distribution and the patterns of the groundwater level contour lines during the base period show that high hydraulic gradient around Obio-Akpor area in the northern part of the study area, which becomes gentle towards the coastal area. During the three future periods, the simulated groundwater heads were found to be ranging from 0.8 to 29.4 m based on RCP 4.5 and from 0.77 to 28.82 m for RCP8.5 during the 2020s as shown in Figure 9.10 (a & b). During the 2050s, the simulated groundwater heads were found to be ranging from 0.69 to 26.31 m based on RCP4.5 and 0.75 to 27.76 m for RCP8.5 as shown in Figure 9.10 (c & d) while during the 2080s, the simulated groundwater heads were found to be ranging from 0.69 to 26.22 m based on RCP 4.5



and 0.73 to 27.24 m for RCP8.5 emission scenario as depicted in Figure 9.10 (e & f) respectively.

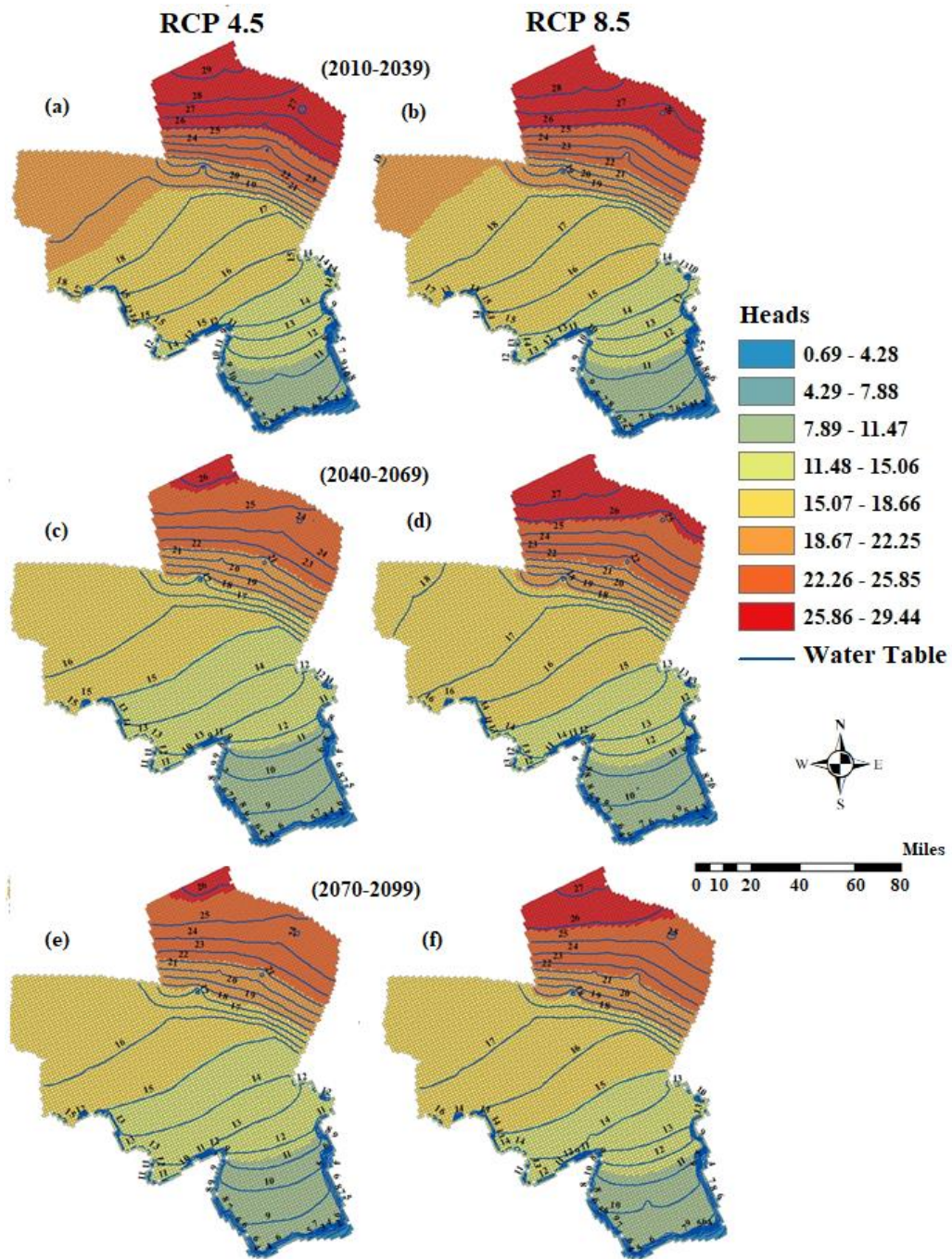


**Figure 9.10** Spatial variation of simulated groundwater heads and water table contours for the 2020s (a) RCP4.5 (b) RCP8.5, 2050s (c) RCP4.5 (d) RCP8.5, and 2080s (e) RCP4.5 (f) RCP8.5 future periods.

*Scenario 2: Impact of climate change combined with population-driven additional pumping*

To study the impact of climate change combined with the response of the hydrologic system to additional stress from growing population and industrialisation in the area, groundwater abstraction in the existing wells were modelling as increasing by 25% and 50%. There are no official records of groundwater abstraction for agriculture, domestic and industrial use in the study area and the present abstraction rates may already be higher due to a large number of boreholes that are unregulated and improperly monitored.

Based on the RCP 4.5 emission scenario, the simulated groundwater heads were found to range between 1.03 to 26.98 m during normal pumping condition, and from 1.02 to 26.7 m with 25% increase in abstraction. Increasing groundwater abstraction by 50%, the simulated groundwater heads were found to be range between from 1.11 to 26.46 m. Similarly, based on RCP8.5, the simulated groundwater heads were found to be range from 1.02 to 27.86 m during normal pumping condition, from 1.04 to 27.46 m with 25% increase in groundwater abstraction and from 1.01 to 27.13 m with 50% increase in groundwater abstraction. The water budget results between the model components for the periods 2010 to 2099 is summarised in Table 9.5.

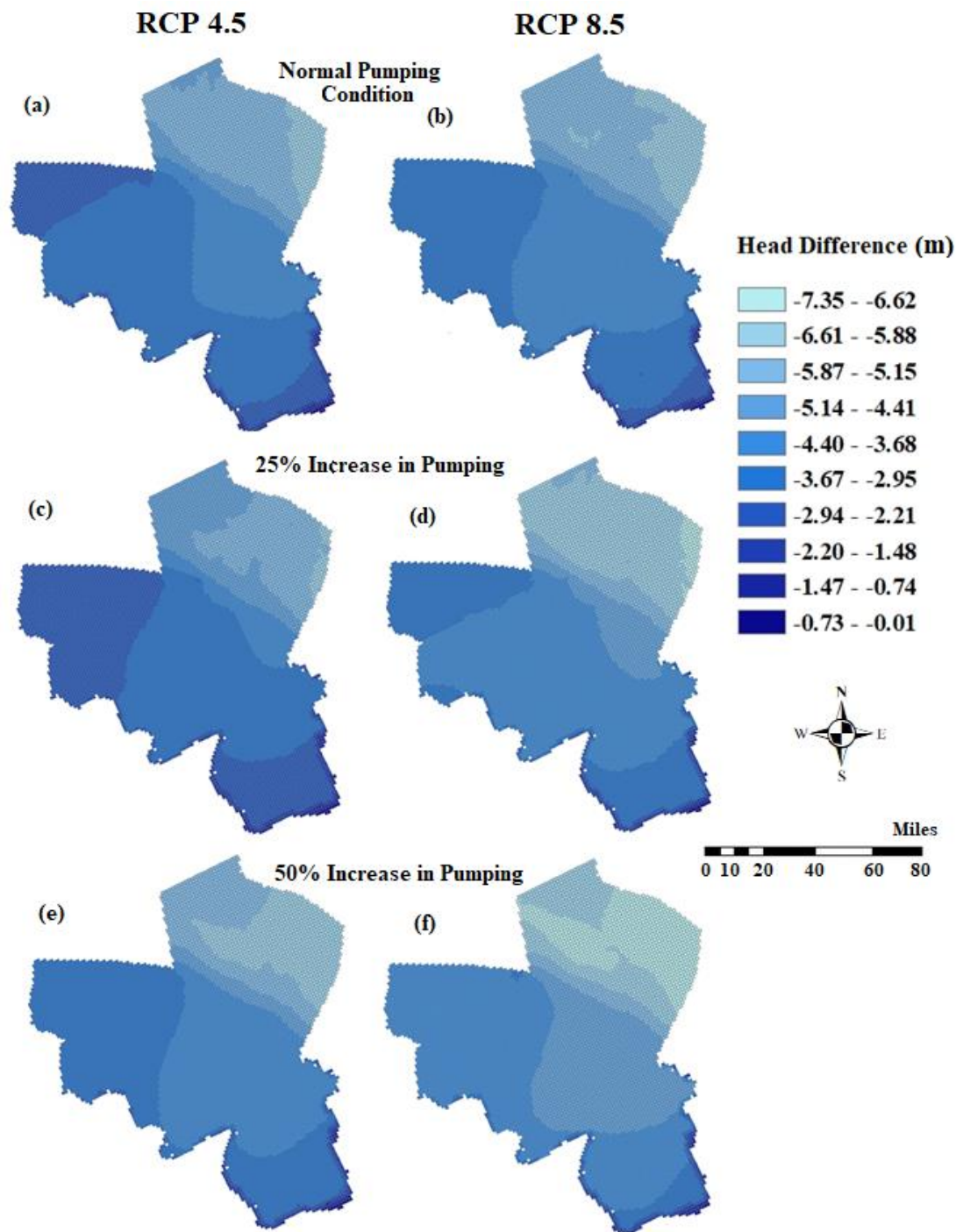


**Figure 9.11** Spatial variation of change in groundwater heads due to normal pumping condition under (a) RCP4.5 & (b) RCP8.5, 25% increase in pumping under (c) RCP4.5 (d) RCP8.5, and 50% increase in pumping under (e) RCP4.5 (f) RCP8.5 for 2010 to 2099 future periods.

Results of head difference between the normal pumping and increased pumping scenarios show that as groundwater extraction increases by 25%, the groundwater level decreased by 1 to 5 m under RCP 4.5 and 1 to 6 m under RCP 8.5 emission scenarios as shown in Figure 9.11 (a, c & e). With the 50% increase in pumping, the groundwater level was projected to decrease by 1 to 6 m under RCP 4.5 and 1 to 7 m under RCP 8.5 emission scenarios as depicted in Figure 9.11 (b, d & f) respectively.

The results show that as groundwater extraction is increased by 25 and 50% coupled with the variation in groundwater recharge, the groundwater level was found to decrease between 1 to 7 m in most of the area with the highest impact on 50% pumping increase. Under RCP 4.5,  $\Delta S$  of the aquifer is expected to decrease by -19,620 m<sup>3</sup>/year with 25% increase in pumping and -28,290 m<sup>3</sup>/year with 50% increase in pumping. However, under RCP 8.5,  $\Delta S$  of the aquifer is expected to decrease by -70,960 m<sup>3</sup>/year with 25% increase in pumping and -182,500 m<sup>3</sup>/year with 50% increase in pumping respectively. The  $\Delta S$  of the aquifer presented in Figures 9.12 and 9.13 for both RCP 4.5 and RCP 8.5 during the future periods shows a decreasing trend in aquifer storage under both scenarios with more impact under the RCP 8.5 emission scenario.

**Table 9.4 :** Summary of the simulated water budget for the modelled area under Normal and increased pumping conditions during the future periods under RCP 4.5 and RCP 8.5 emission scenarios.

	RCP 4.5			RCP 8.5		
	Normal Pumping	25% Pumping	50% Pumping	Normal Pumping	25% Pumping	50% Pumping
<b>Inflow (m<sup>3</sup>/year)</b>						
Storage	6.4	38.4	17.7	7.5	8.0	17.7
Constant Head	0	0	0	0	0	0
Wells	0	0	0	0	0	0
River Leakage	322,897	356,641	288,264	294,594	252,774	216,485
Evapotranspiration	0	0	0	0	0	0
Head Dep Boundary	0	0	0	0	0	0
Recharge	1,163,536,488	1,163,536,488	1,163,536,488	1,225,236,672	1,225,236,672	1,225,236,672
<b>Total In</b>	<b>1,163,861,308</b>	<b>1,163,895,998</b>	<b>1,163,826,619</b>	<b>1,225,529,956</b>	<b>1,225,488,960</b>	<b>1,225,451,116</b>
<b>Outflow (m<sup>3</sup>/year)</b>						
Storage	34.7	36.5	26.5	85.5	72.1	23.9
Constant Head	0	0	0	0	0	0
Wells	132,514,272	159,017,126	106,011,417	159,017,126	132,514,272	106,011,417
River Leakage	80,397,878	76,982,529	83,961,446	83,355,955	87,036,206	91,091,736
Evapotranspiration	689,695,473	673,675,185	705,558,081	717,686,827	733,420,137	748,513,267
Head Dep Boundary	260,856,331	253,845,878	267,926,702	264,965,472	272,083,147	279,513,028
Recharge	0	0	0	0	0	0
<b>Total Out</b>	<b>1,163,463,955</b>	<b>1,163,517,566</b>	<b>1,163,457,648</b>	<b>1,225,022,227</b>	<b>1,225,053,763</b>	<b>1,225,126,296</b>
<b>Inflow - Outflow</b>	<b>395,556</b>	<b>375,940</b>	<b>367,268</b>	<b>507,540</b>	<b>436,584</b>	<b>325,041</b>

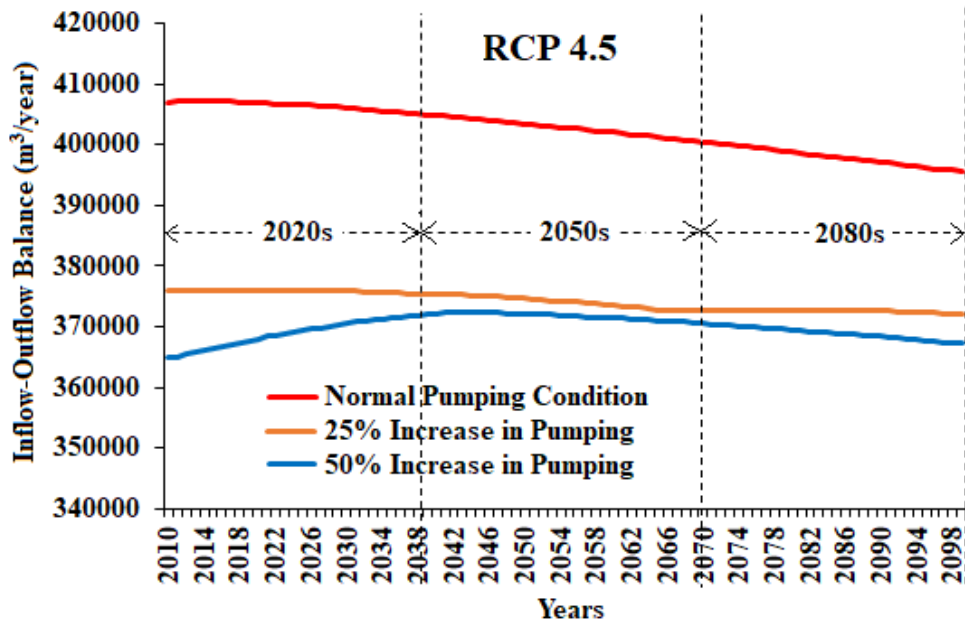


**Figure 9.12** Inflow/Outflow balance of the area from 2010 to 2099 under scenario RCP 4.5.

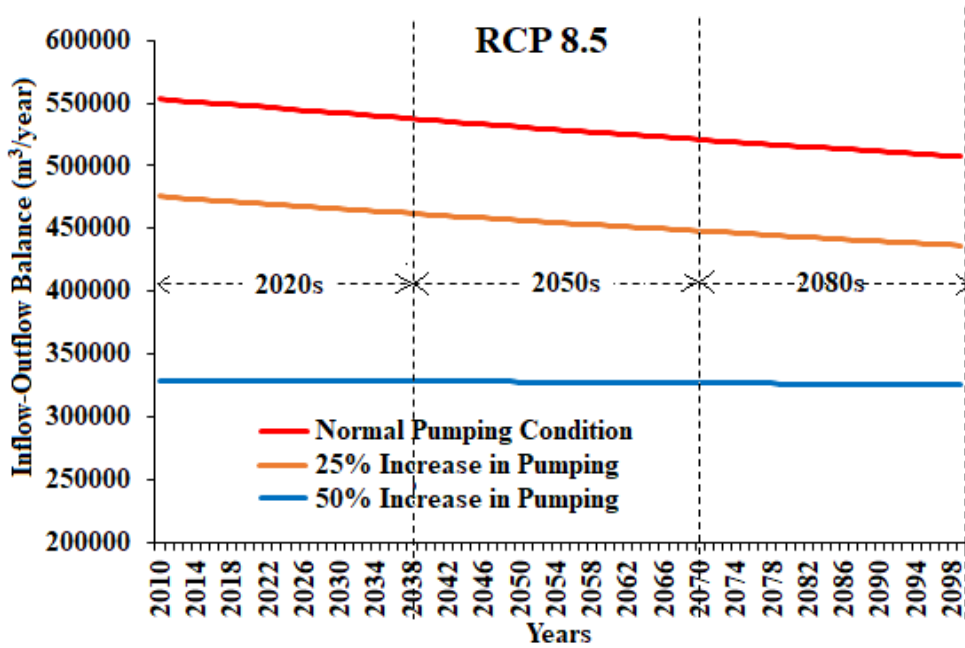


**Figure 9.13** Inflow/Outflow balance of the area from 2010 to 2099 under scenario RCP 8.5.

## 5.0. Implications for groundwater resource management

The potential impacts of climate change on groundwater resources occur locally from precipitation through surface water bodies to groundwater recharge (Döll and Fiedler, 2008). Results from this study show that precipitation has a significant impact on the study areas groundwater resources through recharge as the primary climatic driver. As precipitation was projected to increase by 1 to 3%, the groundwater level was projected to decrease by less than 1 m along the coastal area and up to 6 m under RCP 4.5 and 7 m under RCP 8.5 emission scenarios with 50% increase in pumping in the northern part of the study area. This shows that an increase in population and water usage will have a significant impact on groundwater resources in the area.

Recharge is not only influenced by the magnitude of precipitation, but also by its seasonality, intensity, frequency, changes in soil properties, land use, water use, and the geological setting of the area (Craig *et al.*, 2010). Groundwater storage is the difference between recharge and discharge over a period largely influenced by aquifer hydraulic properties, size and type (Döll and Fiedler, 2008). This makes shallow groundwater systems mostly of the unconfined aquifers under study more responsive to smaller-scale climate variability (Döll & Fiedler, 2008; Petra Döll, 2009; Hassan *et al.*, 2019; Kundzewicz & Döll, 2009). Flooding, Sea level rise and storm surges have been reported to lead seawater intrusion and causing higher salinity of freshwater in the coastal part of the study area (Abel *et al.*, 2012; Hassan *et al.*, 2019; Odafivwotu Ohwo, 2018; Oke, 2015; Omosuyi, & Olorunfemi, 2008). This, therefore, necessitates the need for reviewing the existing water resources policy and formulate a new planning and investment strategy for water resources sustainability.

The current water resources policy and Master Plan 2013 of Nigeria was first formulated in the year 2004 following the National Water Resources Master Plan studies in 1984 and 1993, based on the philosophy and principles of Integrated Water Resource Management (IWRM). However, Nigeria's score is still low towards achieving the SDG 2030 goals implementation of the IWRM (Sokolov, 2011). Sectoral approaches to water resources management dominated the past and are still prevailing, which leads to fragmented and uncoordinated development and management of the resource (FMWR, 2016). The "top-down and supply-side approach" water services in Nigeria has failed due to poor stakeholders' participation and management of the infrastructure and inadequate financial resources.

The findings of this study provide vital information about groundwater potential in the northern part of the study area. The results show aquifer storage decreases as a result of climate change and population growth stress, however in the northern part of the aquifer greater recharge somewhat compensates population growth demands through increased precipitation, with the effect that groundwater may be more resilient in this part of the aquifer even with an increase in abstraction (Hassan *et al.*, 2019). However, to take advantage of these predictions, monitoring to verify, and policy that supports coherent regulation is needed to ensure investment planning that supports Integrated Water Resources Management implementation. One example might be an investment in well fields in the northern part of the study area, managed through distributions systems, to provide clean water to other parts of the basin especially the coastal areas where the water table is polluted due to flooding and saltwater intrusion. Ultimately, a policy that supports good decision making within regulatory boundaries should be encouraged to water service providers as they can promote water as an economic good to attract revenue, rather than the current practice



of unregulated sinking of boreholes. Policy revision may also enhance public awareness about water conservation and management. In addition, enforcement regulations around waste, wastewater, sanitation and hygiene is necessary to protect further contamination of the groundwater of the shallow aquifers to prevent an unwanted outbreak of water-borne diseases.

## **6.0. Conclusions**

This study analysed the response of the Niger Delta coastal plain sand aquifer to climate change under RCP 4.5 and RCP 8.5 over the period 2010–2099 and predicted its potential to meet freshwater demands. The aquifer is mainly used for domestic and industrial water supply through abstraction in the city of Port Harcourt. Given the future development of the urban population and the economic activities of this region, water needs will increase.

Results of steady-state and transient model simulation of the years 1980-2005 show a very good correlation between the simulated and observed groundwater levels. Due to the hydraulic contact between surface water bodies and the coastal plain sand aquifer, surface water-groundwater interaction plays an important role in the study area, and any change in the flow and water levels will affect the regional groundwater budget of the aquifer. Therefore, understanding this interaction and the nature of this complex flow system represents a great challenge for water resources management in the study area.

Results of predictive model simulations revealed a decrease in groundwater level in the coastal regions. Groundwater pumping scenarios confirmed that surface water represents a primary source of recharge to the aquifer, especially when there is increased groundwater abstraction. The results show that groundwater levels are

decreased with increased groundwater abstraction from the aquifer and increasing groundwater abstraction for more than 50% of the current state will decrease the storage of the aquifer, which can present a challenge for water management in the study area.

The results of this study show that understanding climate changes impacts on groundwater resources, especially in coastal aquifers, is crucial for water resources management. Although these results may not be entirely certain, given the uncertainties associated with climate scenarios, such an approach associating climate scenarios and numerical modeling of aquifers provides useful insight into the future reactions of hydrogeological systems that can be used to envisage measurements of adaptation and protection of the water resources. For the coastal aquifer of Niger Delta, the study shows that the risk of contamination of this system by rivers is high. It is recommended that end-users should reflect on the results of this study during IWRM planning to preserve the long-term exploitation of this aquifer, and as part of the sustainable management of the local and national water resources.

**Author Contributions:** I.H. and R.M.K. designed the research; I.H. wrote the original draft; R.M.K., C.J.W. and J.A.A. reviewed and edited the manuscript and provided technical help and proposed important additions with the model and to the manuscript; R.M.K. gave critical views on the manuscript for further improvement.

**Funding:** This research was funded by the Petroleum Technology and Development Fund (PTDF) under the Overseas PhD scholarship scheme and supported by the Scottish Government under the Climate Justice Fund Water Futures Programme, awarded to the University of Strathclyde (R.M. Kalin)

**Acknowledgements:** The authors would like to gratefully acknowledge Dr. H.O. Nwankwoala and the Nigerian Hydrological Service Agency (NHISA) for providing the data used in this study.

**Conflicts of Interest:** The authors declare no conflict of interest.

## References

- Abel O., T. (2012) ‘Geostatistical Assessment of Groundwater Quality from coastal aquifers of Igbokoda, Southwestern Nigeria’, *IOSR Journal of Environmental Science, Toxicology and Food Technology*, 2(2), pp. 18–24. doi: 10.9790/2402-0221824.
- Adejuwon, J. O. (2012) ‘Rainfall seasonality in the Niger Delta Belt, Nigeria’, *Journal of Geography and Regional Planning*, 5(2), pp. 51–60. doi: 10.5897/JGRP11.096.
- Ahmad, M. K., Islam, S., Rahman, S., Haque, M. R. and Islam, M. M. (2010) ‘Heavy Metals in Water, Sediment and Some Fishes of Buriganga River, Bangladesh.’, *International Journal of Environmental Resources*, 4(2), pp. 321–332.
- Akinwumiju A. S and Orimoogunje O. I (2012) ‘Determining the Occurrence of Freshwater in the Aquifers of the Deltaic Formation, Niger Delta Nigeria’, *Journal of Environmental & Analytical Toxicology*, 03(01), pp. 1–4. doi: 10.4172/2161-0525.1000162.
- Amadi, A. N., Nwankwoala, H. O., Olasehinde, P. I., Okoye, N. O., Okunlola, I. A. and Alkali, Y. B. (2012) ‘Investigation of Aquifer Quality in Bonny Island, Eastern Niger Delta, Nigeria using Geophysical and Geochemical Techniques Department of Geology, Federal University of Technology’, *Journal of Emerging Trends in Engineering and Applied Sciences (JETEAS)*, 3(1), pp. 183–187.
- Amadi, A. N., Olasehinde, P. I., Nwankwoala, H. O., Dan-Hassan, M. A. and Okoye, N. O. (2014) ‘Aquifer Vulnerability Studies using DRASTIC Model’, *International Journal of Engineering Science Invention*, 3(3), pp. 1–10.
- Amadi, A. N. (2014) ‘Impact of Gas-Flaring on the Quality of Rain Water, Groundwater and Surface Water in Parts of Eastern Niger Delta, Nigeria’, *Journal of*

*Geosciences and Geomatics*, 2(3), pp. 114–119. doi: 10.12691/JGG-2-3-6.

Amadi A.N., Olasehinde P.I., Dan-Hassan, M. A, Okoye, N. O., and E. G. (2014) ‘Hydrochemical Facies Classification and Groundwater Quality Studies in Eastern Niger Delta, Nigeria’, *International Journal of Engineering Research and Development*, 10(3), pp. 1–9.

Amajor L. C (1989) ‘Geological appraisal of groundwater exploitations in the Eastern Niger Delta. In: C.O Ofoegbu, (Ed.), *Groundwater and Mineral Resources of Nigeria.*’, *Braunschweig/Wiesbaden. Friedr Vieweg and Sohn.*, p. Pp. 85-100.

Amangabara, G. T. (2006) ‘Factors of Stream Instability in Urban Centres of Southern Nigeria: Case Study of Port Harcourt City River Systems.’, in *American Geophysical Union, Fall Meeting 2007, abstract #H23D-23*. American Geophysical Union.

Amangabara, G. T. and Gobo, A. E. (2007) ‘Factors that influence the flooding of the middle and lower Ntamogba stream catchments, Port Harcourt, Nigeria’, *Journal of Environmental Hydrology*, 15(November), pp. 1–11.

Arnell, N. (1999) ‘Climate change and global water resources’, *Global Environmental Change*, 9, pp. S31–S49. doi: 10.1016/S0959-3780(99)00017-5.

Bear, J. and Verruijt, A. (1987) *Modeling groundwater flow and pollution.*, D. Reidel Publishing Company: Dordrecht, The Netherlands. doi: 10.1139/t88-098.

Bellos, D. and Sawidis, T. (2005) ‘Chemical pollution monitoring of the River Pinios (Thessalia - Greece)’, *Journal of Environmental Management*, 76(4), pp. 282–292. doi: 10.1016/j.jenvman.2005.01.027.

Benedict, Akpomuvie, O. (2011) ‘Tragedy of Commons: Analysis of Oil Spillage, Gas Flaring and Sustainable Development of the Niger Delta of Nigeria’, *Journal of Sustainable Development*, 4(2), p. 200. doi: 10.5539/jsd.v4n2p200.

Capaccioni, B., Didero, M., Paletta, C., and Didero, L., (2005) ‘Saline intrusion and refreshing in a multilayer coastal aquifer in the Catania Plain (Sicily, Southern Italy): Dynamics of degradation processes according to the hydrochemical characteristics of groundwaters’, *Journal of Hydrology*, 307(1–4), pp. 1–16. doi:

10.1016/j.jhydrol.2004.08.037.

Craig Clifton, Rick Evans, Susan Hayes, Rafik Hirji, and Gabrielle Puz, C. P. (2010) 'Water Working Notes adaptation options', *Managing*, (25).

Döll, P. (2009) 'Vulnerability to the impact of climate change on renewable groundwater resources: a global-scale assessment', *Environmental Research Letters*, 4(3), p. 035006. doi: 10.1088/1748-9326/4/3/035006.

Döll, P. and Fiedler, K. (2008) 'Global-scale modeling of groundwater recharge', *Hydrology and Earth System Sciences*, 12(3), pp. 863–885. doi: 10.5194/hess-12-863-2008.

Du, X., Lu, X., Hou, J., and Ye, X., (2018) 'Improving the reliability of numerical groundwater modeling in a data-sparse region', *Water (Switzerland)*, 10(3), pp. 1–15. doi: 10.3390/w10030289.

Edet, A., Abdelaziz, R., Merkel, B., Okereke, C., and Nganje, T., (2014) 'Numerical groundwater flow modeling of the Coastal Plain sand aquifer, Akwa Ibom State, SE Nigeria', *Journal of Water Resource and Protection*, 06(March), pp. 193–201. doi: 10.4236/jwarp.2014.64025.

Egeonu, N. C. and Oyanyan, R. O. (2018) 'Hydrochemistry of Groundwater in Obiga-Asa and its Environs, Abia State, Nigeria', *International Journal of Scientific & Engineering Research*, 9(3), pp. 311–323.

Etim U. U Ituen and A Folarin Alonge (2009) 'Niger Delta Region of Nigeria, Climate Change and the way Forward', *Bioenergy Engineering*, 11-14 October 2009, Bellevue, Washington, (January 2009). doi: 10.13031/2013.29162.

Etu-Efeotor J. O and Akpokodje E. G (1990) 'Aquifer systems of the Niger Delta', *Journal of Mining Geology*, 26(2), pp. 279–284.

Etu–Efeotor, J. O. and Odigi, M. I. (1983) 'Water supply problems in the Eastern Niger Delta', *Journal of Mining and Geology*, 20(1), pp. 182–192.

Expósito, F.J., González, A., Pérez, J.C., Díaz, J.P., and Taima, D., (2015) 'High-resolution future projections of temperature and precipitation in the Canary Islands',

*Journal of Climate*, 28(19), pp. 7846–7856. doi: 10.1175/JCLI-D-15-0030.1.

Felisa, G., Ciriello, V. and Di Federico, V. (2013) ‘Saltwater intrusion in coastal aquifers: A primary case study along the Adriatic coast investigated within a probabilistic framework’, *Water (Switzerland)*, 5(4), pp. 1830–1847. doi: 10.3390/w5041830.

FMWR (2016) ‘National Water Resources Policy’, (July).

Gleick, P. H. (1993) *Water in crisis: a guide to the world’s freshwater resources*, Pacific Institute for Studies in Development and Security, Environment Institute, Stockholm Environment. New York: Oxford University Press.

Harbaugh, Arlen, W. (2005) ‘MODFLOW-2005, The U. S. Geological Survey Modular Ground-Water Model — the Ground-Water Flow Process’, *U.S. Geological Survey Techniques and Methods*, p. 253. doi: U.S. Geological Survey Techniques and Methods 6-A16.

Harris, I., Jones, P.D., Osborn, T.J., and Lister, D.H., (2014) ‘Updated high-resolution grids of monthly climatic observations - the CRU TS3.10 Dataset’, *International Journal of Climatology*, 34(3), pp. 623–642. doi: 10.1002/joc.3711.

Hassan, I., Kalin, R.M., White, C.J., and Aladejana, J.A., (2019) ‘Hydrostratigraphy and Hydraulic Characterisation of Shallow Coastal Aquifers, Niger Delta Basin: A Strategy for Groundwater Resource Management’, *Geosciences*, 9(11), p. 470. doi: 10.3390/geosciences9110470.

Hassan, I., Kalin, R.M., White, C.J., and Aladejana, J.A., (2020a) ‘Evaluation of Daily Gridded Meteorological Datasets over the Niger Delta Region of Nigeria and Implication to Water Resources Management’, *Atmospheric and Climate Sciences (ACS), SCRIP*.

Hassan, I., Kalin, R.M., White, C.J., and Aladejana, J.A., (2020b) ‘Selection of CMIP5 GCM ensemble for the projection of Spatio-temporal changes in precipitation and temperature over the Niger Delta, Nigeria.’, *Water (Switzerland)*, 12(385). doi: 10.3390/w12020385.

IPCC (1992) *Climate Change 1992 - The Supplementary Report to the IPCC Scientific Assessment*.

IPCC (2007) *Climate Change 2007: impacts, adaptation and vulnerability: contribution of Working Group II to the fourth assessment report of the Intergovernmental Panel, Geneva, Suíça*. doi: 10.1256/004316502320517344.

IPCC (2013) *Climate Change 2007: The Physical Science Basis, Journal of Chemical Information and Modeling*. Edited by D. Solomon, Susan & Qin. doi: 10.1017/CBO9781107415324.004.

Izeze I. A. (1990) *Aquifer characteristics of the coastal plain sands of southern Nigeria: M.Sc. thesis*. University of Port Harcourt, Port Harcourt, Nigeria.

JICA. (2013) *Federal Republic of Nigeria the Project for Review and Update of Nigeria - (National Water Resources Master Plan 2013) Executive Summary - Volume I, Japan International Cooperation Agency*.

Krinner, G., Germany, F., Shongwe, M., Africa, S., France, S.B., Uk, B., Germany, V.B., Uk, O.B., France, C.B., Uk, R.C., Canada, M.E., Erich, M., Uk, R.W.L., Uk, S.L., and Lucas, C., (2013) ‘Long-term climate change: Projections, commitments and irreversibility’, *Climate Change 2013 the Physical Science Basis: Working Group I Contribution to the Fifth Assessment Report of the Intergovernmental Panel on Climate Change*, 9781107057, pp. 1029–1136. doi: 10.1017/CBO9781107415324.024.

Kumar, C. P. (2012) ‘Assessing the impact of climate change on groundwater resources’, *India Water Week*, (April), pp. 10–14.

Kundzewicz, Z. W. and Döll, P. (2009) ‘Will groundwater ease freshwater stress under climate change?’, *Hydrological Sciences Journal*, 54(4), pp. 665–675. doi: 10.1623/hysj.54.4.665.

Larsen, E. H., Sørensen, J. B. and Sørensen, J. N. (2000) ‘A mathematical model of solute coupled water transport in toad intestine incorporating recirculation of the actively transported solute.’, *The Journal of general physiology*, 116(2), pp. 101–124. doi: 10.1085/jgp.116.2.101.

MacDonald, A.M., Bonsor, H.C., Dochartaigh, B.É.Ó., and Taylor, R.G., (2012) ‘Quantitative maps of groundwater resources in Africa’, *Environmental Research Letters*, 7(2). doi: 10.1088/1748-9326/7/2/024009.

Martín, J. L., Bethencourt, J. and Cuevas-Agulló, E. (2012) ‘Assessment of global warming on the island of Tenerife, Canary Islands (Spain). Trends in minimum, maximum, and mean temperatures since 1944’, *Climatic Change*, 114(2), pp. 343–355. doi: 10.1007/s10584-012-0407-7.

Mogborukor, J. O. A. (2014) ‘The Impact of Oil Exploration and Exploitation on Water Quality and Vegetal Resources in a Rain Forest Ecosystem of Nigeria’, *Mediterranean Journal of Social Sciences*, 5(27), pp. 2039–9340. doi: 10.5901/mjss.2014.v5n27p1678.

Mtoni, Y., Mjemah, I.C., Bakundukize, C., Van Camp, M., Martens, K., and Walraevens, K., (2013) ‘Saltwater intrusion and nitrate pollution in the coastal aquifer of Dar es Salaam, Tanzania’, *Environmental Earth Sciences*, 70(3), pp. 1091–1111. doi: 10.1007/s12665-012-2197-7.

Mukherjee, A., Saha, D., Harvey, C.F., Taylor, R.G., Ahmed, K.M., and Bhanja, S.N., (2015) ‘Groundwater systems of the Indian Sub-Continent’, *Journal of Hydrology: Regional Studies*, 4, pp. 1–14. doi: 10.1016/j.ejrh.2015.03.005.

Nnabuanyi, U. M. (2012) ‘Impact of Oil Exploration and Exploitation on the Niger Delta Region: Environmental Perspective’, *Nigerian Journal of Science and Environment*, 11(1).

Nouri, J., Mahvi, A.H., Babaei, A., and Ahmadpour, E., (2006) ‘Regional pattern distribution of groundwater fluoride in the Shush aquifer of Khuzestan County, Iran’, *Fluoride*, 39(4), pp. 321–325.

Odafivwotu Ohwo (2018) ‘Climate Change Impacts, Adaptation and Vulnerability in the Niger Delta Region of Nigeria’, *Journal of Environment and Earth Science*, 8(6), pp. 171–179.

Okagbue C. O. (1989) ‘Geotechnical And Environmental Problems of the Niger Delta’, *Bulletin of the International Association of Engineering Geology*, pp. 129–138.



Available at: <https://link.springer.com/article/10.1007/BF02590349>.

Oke, S. A. (2015) 'Evaluation of the Vulnerability of Selected Aquifer Systems in the Eastern Dahomey Basin, South Western Nigeria', (January).

Oluduro, O. (2012) 'Oil exploration and ecological damage: The compensation policy in Nigeria', *Canadian Journal of Development Studies*, 33(2), pp. 164–179. doi: 10.1080/02255189.2012.693049.

Omosuyi, G. O., Ojo, J. S. and Olorunfemi, M. O. (2008) 'Geoelectric Sounding to Delineate Shallow Aquifers in the Coastal Plain Sands of', *The Pacific Journal of Science and Technology*, 9(2), pp. 62–77.

Onuoha K. M. & Mbazi F. C. (1989) 'Aquifer transmissivity from electrical sounding data: The case of Ajali sandstone aquifers, southeast of Enugu, Nigeria, in C. O. Ofoegbu, ed., Groundwater and mineral resources of Nigeria', *Braunschweig, Friedr Vieweg & Sohn*, pp. 17–30.

Onyeagocha, A. C. (1980) 'Petrography and depositional environment of the Benin Formation, Nigeria.', *Journal of Mining and Geology*, 17, pp. 147–151.

Orimoogunje, A. A. (2013) 'Predicting the Yields of Deep Wells of the Deltaic Formation, Niger Delta Nigeria', *Journal of Waste Water Treatment & Analysis*, 04(01), pp. 1–5. doi: 10.4172/2157-7587.1000145.

Oteri, A.U., and Atolagbe, F. P. (2003) 'Saltwater Intrusion into Coastal Aquifers in Nigeria', in *The Second International Conference on Saltwater Intrusion and Coastal Aquifers — Monitoring, Modeling, and Management. Mérida, Yucatán, México, March 30 - April 2, 2003*, pp. 1–15.

P.U. Uzukwu, T. G. L. and N. A. J. (2014) 'Seasonal Variations in Some Physico-chemical Parameters of the Upper Reach of the New Calabar River', *International Journal of Fisheries and Aquatic Sciences*, 3(1), pp. 8–11.

Porio (2014) Climate Change Vulnerability and Adaptation in Groundwater-dependent Irrigation System in Asia-Pacific Region (Metro Manila), *Asian Journal of Social Science*. doi: 10.1163/15685314-04201006.

Rangwala, I. and Miller, J. R. (2012) 'Climate change in mountains: A review of elevation-dependent warming and its possible causes', *Climatic Change*, 114(3–4), pp. 527–547. doi: 10.1007/s10584-012-0419-3.

Razack, M., Jalludin, M. and Houmed-Gaba, A. (2019) 'Simulation of Climate Change Impact on A Coastal Aquifer under Arid Climate. The Tadjourah Aquifer (the Republic of Djibouti, Horn of Africa)', *Water*, 11(11), p. 2347. doi: 10.3390/w11112347.

Reyment R. A. (1965) 'Aspects of Geology of Nigeria', *Ibadan University Press*, p. 145pp.

Sentelhas, P. C., Gillespie, T. J. and Santos, E. A. (2010) 'Evaluation of FAO Penman-Monteith and alternative methods for estimating reference evapotranspiration with missing data in Southern Ontario, Canada', *Agricultural Water Management*. Elsevier B.V., 97(5), pp. 635–644. doi: 10.1016/j.agwat.2009.12.001.

Short. K. C. and Stauble, A. J. (1967) 'Outline geology of the Niger Delta, Nigeria', *American Association of Petroleum Geologist*, 5, pp. 761–779.

Sokolov, V. (2011) 'Integrated Water Resources Management', in *NATO Science for Peace and Security Series C: Environmental Security*, pp. 37–52. doi: 10.1007/978-90-481-9974-7\_3.

Spellman, F. (2014) 'All about Water', *The Science of Water*, pp. 9–42. doi: 10.1201/b17484-3.

Steyl, G. and Dennis, I. (2010) 'Review of coastal-area aquifers in Africa', *Hydrogeology Journal*, 18(1), pp. 217–225. doi: 10.1007/s10040-009-0545-9.

Ubani, E. C. and Onyejekwe, I. M. (2013) 'Environmental impact analyses of gas flaring in the Niger Delta region of Nigeria', *American Journal of Scientific and Industrial Research*, 4(2), pp. 246–252. doi: 10.5251/ajsir.2013.4.2.246.252.

Uma K. O. (1989) 'An appraisal of the groundwater resources of the Imo River Basin, Nigeria', *Journal of Mining and Geology*, Vol. 25 No, p. pp.305-31.

UN DESA (2019) World population prospects 2019, United Nations. Department of

Economic and Social Affairs. *World Population Prospects 2019*. Available at: <http://www.ncbi.nlm.nih.gov/pubmed/12283219>.

Varni, M. R. and Usunoff, E. J. (1999) ‘Simulation of regional-scale groundwater flow in the Azul River basin, Buenos Aires Province, Argentina’, *Hydrogeology Journal*, Springer-Verlag, 7(October 1998), pp. 180–187.

Weli, V. E. and Ideki, O. (2014) ‘The Effect of Urbanization on Channel Adjustment and Flood Vulnerability of Woiy Basin, River State, Nigeria’, *Journal of Natural Sciences Research*, 4(10), pp. 86–94.

Winston, R. B. (2009) ‘ModelMuse: A Graphical User Interface for MODFLOW-2005 and PHAST’, *U.S. Geological Survey Techniques and Methods 6-A29*, p. 52 p. Available at: <http://pubs.usgs.gov/tm/tm6A29/tm6A29.pdf>.

WMO (2013) The global climate 2001 – 2010, *World Meteorological Organization*. Available at: [https://library.wmo.int/doc\\_num.php?explnum\\_id=7829](https://library.wmo.int/doc_num.php?explnum_id=7829).

WMO (2018) World Meteorological Organization (WMO) provisional Statement on the Status of the Global Climate in 2018.

### **9.3 Supplementary Data**

The 3-D view of the spatial variation in simulated groundwater heads and the water-table contours for the base period and future periods are presented in the figures below. The model base period was simulated for a transient period of 25 years (1980-2005) as depicted in figure 9.14, while the future periods under RCP4.5 are depicted in figures 9.15 to 9.17 and under RCP8.5 emission scenarios are depicted in figures 9.18 to 9.20.

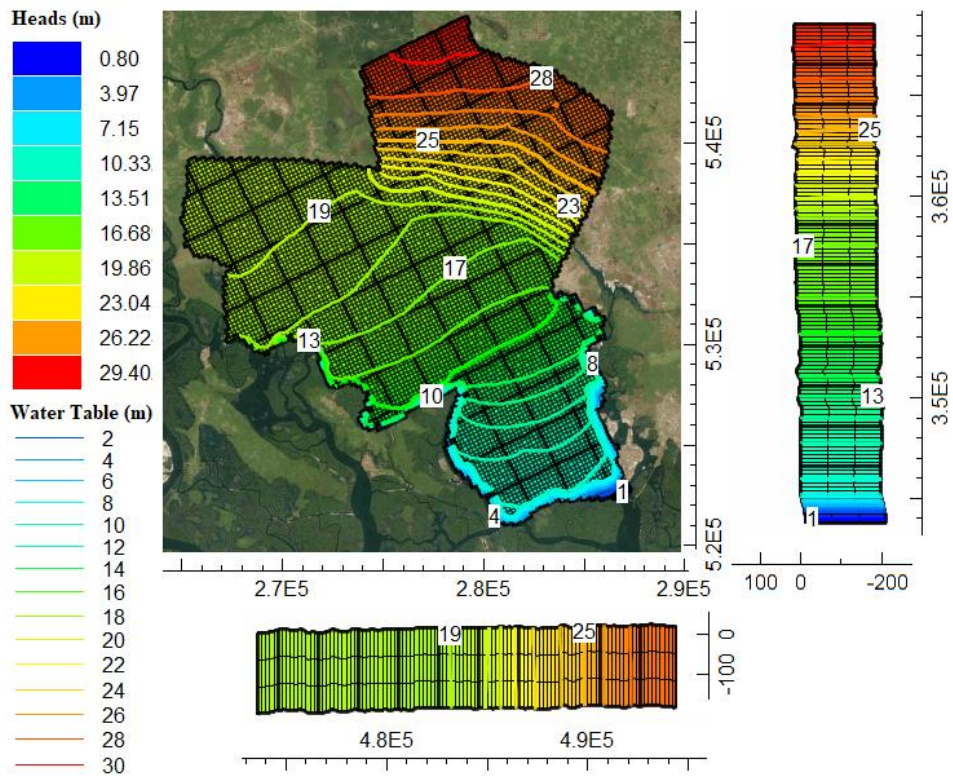


**Figure 9.14** Spatial variation of simulated groundwater heads and water table contours for the base periods (1980-2005).

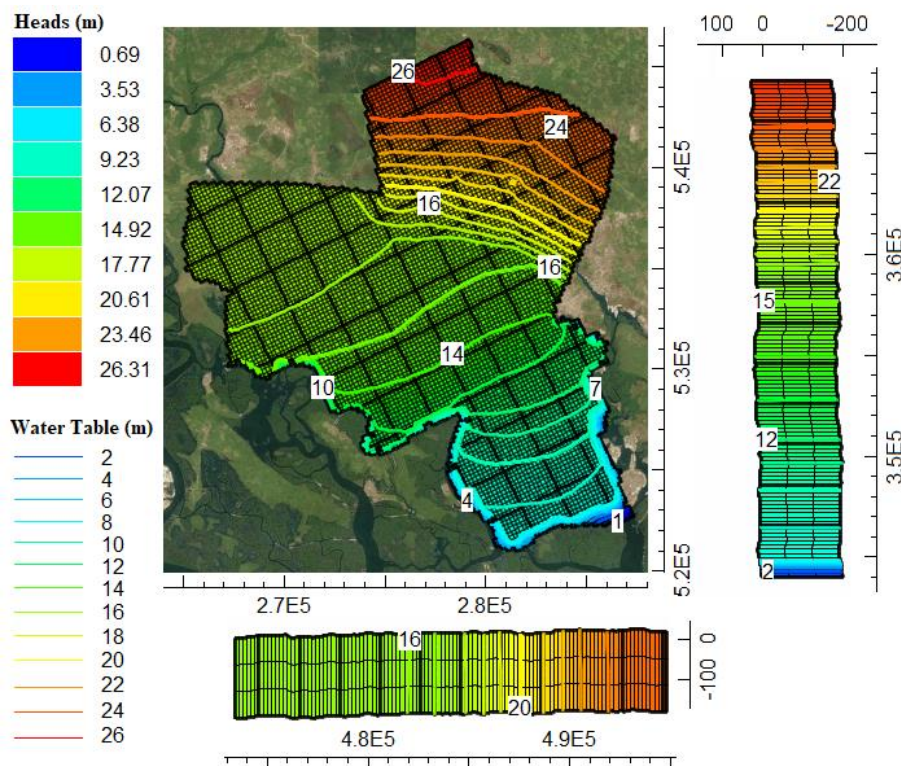


**Figure 9.15** Spatial variation of simulated groundwater heads and water table contours under RCP4.5 emission scenario for the years 2010 to 2039 future periods.



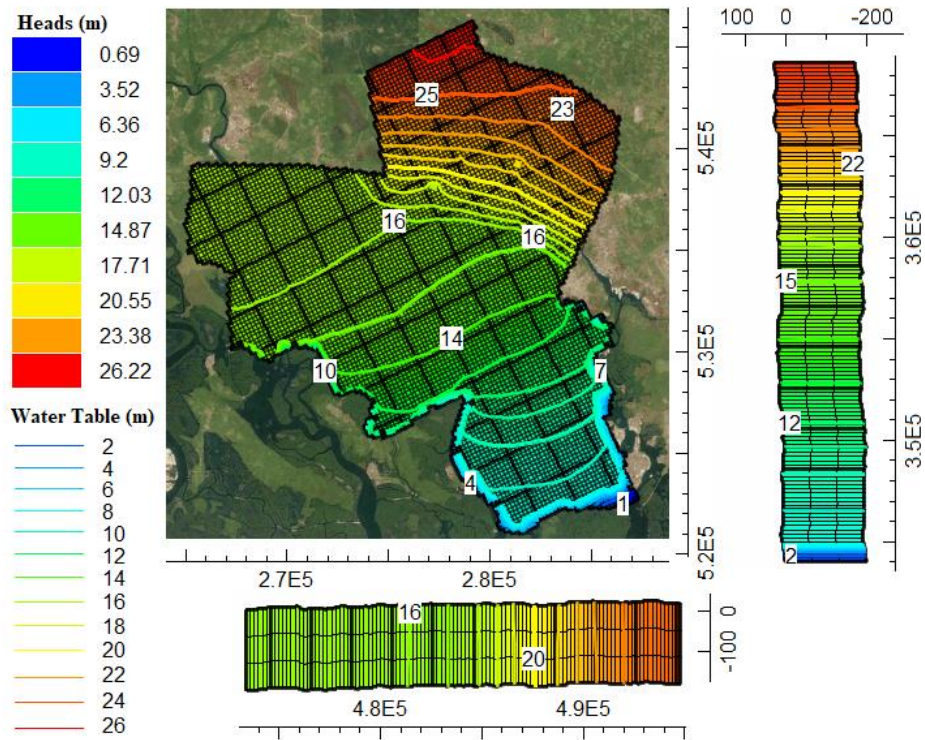


**Figure 9.16** Spatial variation of simulated groundwater heads and water table contours under RCP4.5 emission scenario for the years 2040 to 2069 future periods.

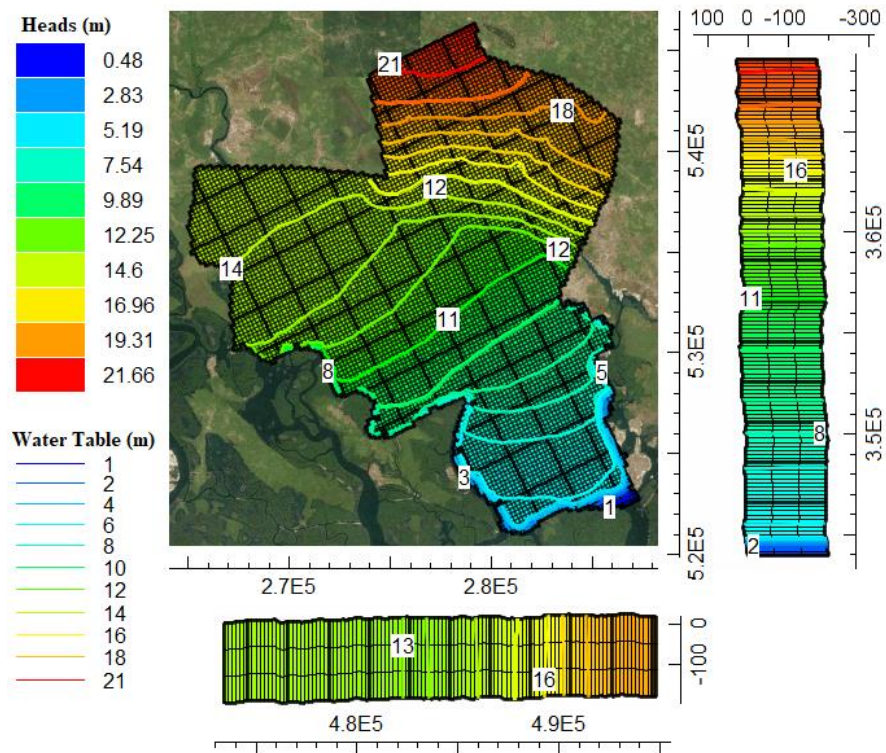


**Figure 9.17** Spatial variation of simulated groundwater heads and water table contours under RCP4.5 emission scenario for the years 2070 to 2099 future periods.

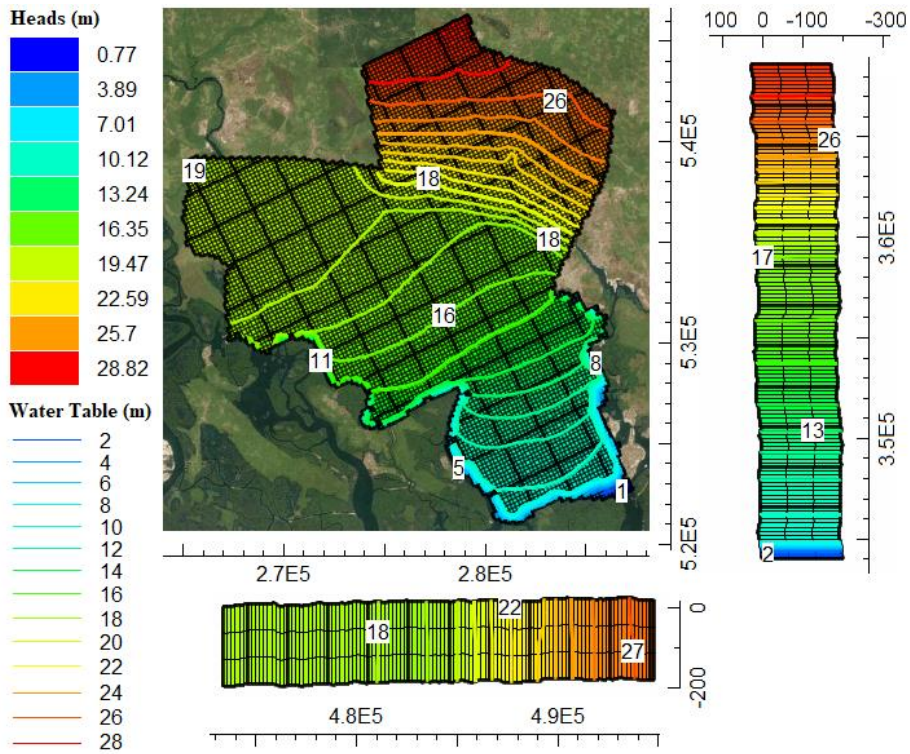


**Figure 9.18** Spatial variation of simulated groundwater heads and water table contours under RCP8.5 emission scenario for the years 2010 to 2039 future periods.

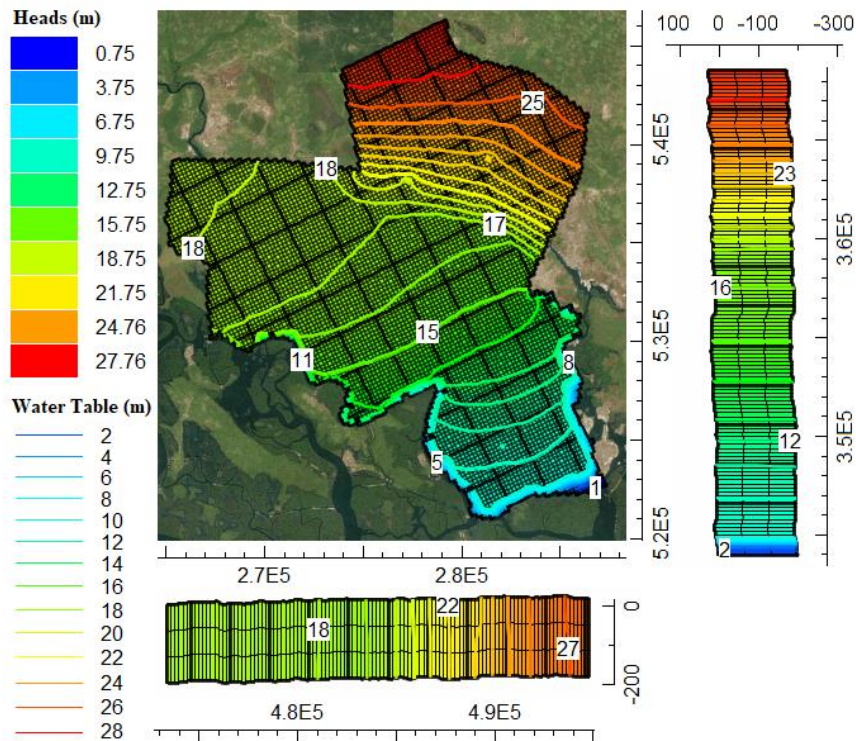


**Figure 9.19** Spatial variation of simulated groundwater heads and water table contours under RCP8.5 emission scenario for the years 2040 to 2069 future periods.



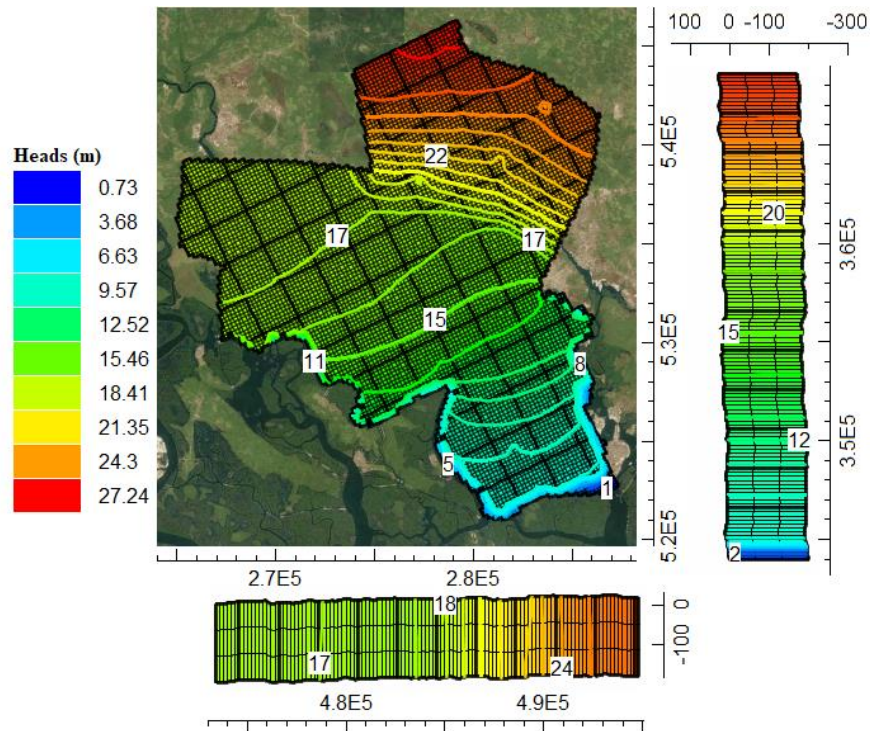


**Figure 9.20** Spatial variation of simulated groundwater heads and water table contours under RCP8.5 emission scenario for the years 2070 to 2099 future periods.

#### 9.4 Concluding Remarks

This Chapter has presented the potential impacts of climate change on the groundwater resources of the Niger Delta coastal plain sand aquifer under RCP 4.5 and RCP 8.5 over the period 2010–2099. The potentials of the aquifer to meet freshwater the growing water demands of Rivers state, which is mainly used for domestic and industrial water supply was also predicted.

Results of predictive model simulations revealed a decrease in groundwater level in the coastal regions in comparison with the base periods. Groundwater pumping scenarios confirmed that surface water represents a primary source of recharge to the aquifer, especially when there is increased groundwater abstraction. It can, therefore, be concluded that the aim of the study has been achieved as the results of model

simulation show a very good interaction between surface water bodies and the coastal plain sand aquifer, which plays an important role in IWRM, as any change in the flow and water levels will affect the regional groundwater budget of the aquifer. The study revealed a very good potential of the coastal plain sand aquifer in meeting the freshwater demand of the study area.

## 9.5 Filling the Knowledge Gaps

The summary of the identified knowledge gaps from literature and how they are addressed in the above Chapters are itemised below:

1. The geology and hydrogeology of the Niger Delta have extensively been studied. However, no studies characterised the hydrostratigraphy of the Niger Delta shallow coastal aquifers, which is an essential tool for better understanding of the hydraulic characteristics and hydrogeological conceptual model development of the area's groundwater resources.
  - To address this gap, the hydrostratigraphy and hydraulic characteristics of the Niger Delta shallow coastal aquifer was characterised and published in Hassan *et al.*, 2019 which forms the chapter 8 of this thesis.
2. There are 32 weather stations located in Nigeria (Ajetomobia et al., 2011; Eludoyin et al., 2014), with only 2 of the stations located within the study area, which poorly represent the area, as shown in Figure 3.5. To this extent, no study has been conducted in any part of the country to determine the best stable gridded meteorological datasets, which can serve as a substitute to the poorly distributed station datasets.
  - To address this gap, the confidence in commonly used daily gridded datasets which are Climatic Research Unit (CRU), Princeton University



Global Meteorological Forcing (PGF) and Climate Forecast System Reanalysis (CFSR) available over the Niger Delta part of Nigeria were evaluated and analysed against the observed station datasets to select the best datasets that can serve as a possible replacement to the observed rainfall, maximum and minimum temperature datasets for use in the study. The finding from this study was published in Hassan, *et al.*, 2020 which forms part 1 of chapter 5 in this thesis.

3. Studies reported that GCMs are associated with different uncertainties due to model assumption, resolution, or calibration processes which hinders the GCM outputs from accurately predicting the future climate at a regional or local level.
  - To address this gap, the Symmetrical uncertainty (SU) filter was employed together with the selected gridded datasets to obtain a subset of a suitable general circulation model (GCM) ensemble from a pool of 26 Coupled Model Intercomparison Project Phase 5 (CMIP5) GCM outputs by excluding those with limited similarity to the observed climate. The finding from this study was published in Hassan, *et al.*, 2020 which forms the second part of chapter 5 in this thesis.
4. To this extent, no study has been conducted in Nigeria to select an ensemble of best-performing CMIP5 GCM outputs for both precipitations, maximum and minimum temperature.
  - As stated in bullet point 4, the Symmetrical uncertainty (SU) filter was employed ensemble of best-performing CMIP5 GCM outputs for both precipitations, maximum and minimum temperature over the Niger Delta.

The finding from this study was published in Hassan, *et al.*, 2020 which forms the second part of chapter 5 in this thesis.

5. To this extent, review of different studies conducted at global and basin level indicates that there is no clear trend on changes in hydrological processes; hence, the impact of climate change should be conducted at basin level to find the change at the local level.
  - To address this gap, a combination of climate scenarios and hydrologic model were employed at the Niger River Basin level, housing the Niger Delta part of Nigeria to demonstrate a good understanding of potential impacts of climate changes on hydrological processes over the Niger River Basin, which forms the chapter 7 of this thesis.
6. Performance comparison of different hydrologic models in Table 3.3, shows that the SWAT model (Neitsch et al., 2005; 2011) outperformed the other models as it has many novel techniques to generate optimum solutions for integrated water resource management. SWAT model studies conducted in Nigeria as summarized in Table 3.4 finds the model to be a suitable tool in Nigeria and various part of the world. However, no study has been conducted to simulate the impact of climate variability on the hydrological processes in the Niger River Basin and Nigeria at large using the SWAT model.
  - To address this gap, the SWAT hydrologic model was employed together with climate variables under RCP 4.5 and RCP 8.5 emission scenarios to study the variability and potential impacts of climate changes on hydrological processes over the Niger River Basin, which forms the chapter 7 of this thesis.

7. Many researches globally, used MODFLOW to study the interactions between surface and groundwater resources, which were found to produce reliable results. However, to this extent, studies relating to the modeling of surface and groundwater interactions in the context of climate change using MODFLOW is still at infancy.
  - To address this gap, a groundwater flow model was developed using MODFLOW for the coastal plain sand aquifer in Port-Harcourt municipal to model the aquifer response to the climate scenarios using groundwater recharge and evapotranspiration deduced from the hydrologic model as inputs, which forms the chapter 9 of this thesis.
  
8. As climate variability, studies on water resources in the Niger Delta reported an increase in rainfall over the Niger Delta, which will significantly affect groundwater and recharge rate. Studies on the potential impacts of climate change on surface and groundwater resources may be required to achieve a holistic, integrated water resource management capable of meeting all the regional water demands.
  - To address this gap as stated in bullet point 8 above, the hydrostratigraphy developed from bullet point 1, and the groundwater recharge and evapotranspiration deduced from the SWAT hydrologic model under RCP 4.5 and RCP 8.5 emission scenarios were used as input into MODFLOW, to model the aquifer response to the climate scenarios and increased abstraction in Port-Harcourt municipal which houses the highest concentration of settlements and population in the region which forms the chapter 9 of this thesis.

9. Predicting the behaviour of recharge and discharge under future climatic conditions and other changes is of great importance for integrated water management, (Kumar, 2010), references do not indicate any attempt to simulate the impact of climate change and abstraction on groundwater in the Niger Delta.

➤ To address this gap, the behaviour of recharge, discharge and other hydrologic as well as hydrogeologic processes were predicted using the SWAT hydrologic model and MODFLOW, for the future periods 2010 to 2099, and under RCP 4.5 and RCP 8.5 emission scenarios and the findings are reported in chapters 7 and 9 of this thesis.

# CHAPTER 10

## Conclusion and Recommendations

### 10.1 Restatement of Research Aim and Objectives

This research aimed to comprehensively assess the potential impacts of climate change on surface and groundwater resources in the Niger-Delta part of Nigeria for sustainable water resource management. A combination of climate, hydrologic and groundwater flow models were employed to generate long-term flow regime strategy under a sustainable development framework. Hence, the approach integrates both environmental and economic impacts on the water resources (e.g., surface water and groundwater) in the Niger-Delta. Hence, the following objectives were achieved in the study to address the research's aim in a concise form:

- Review of climate, hydrological, groundwater flow models, and their potential drawbacks.
- Performance assessment of gridded datasets as well as GCM outputs for climate change impact studies in the data-scarce Niger-Delta Basin.
- Analysis of the potential impacts and vulnerability of climate change on extreme weather events in the Niger Delta within the period 2010–2099 under RCP 4.5 and RCP 8.5 emission scenarios.
- Assessment of the sensitivity and potential impacts of climate change on the regional hydrologic regime in the Niger Delta, for the periods 2010–2099 under RCP 4.5 and RCP 8.5 emission scenarios.

- Development of a hydrogeologic conceptual model of the shallow coastal aquifer of the Niger-Delta Basin.
- Development of a groundwater flow models of the shallow coastal plain sand aquifer of the Niger-Delta Basin to evaluate sustainable use of aquifer storage in the context of climate change.

## **10.2 Conclusion**

This study combined different models to formulate a novel approach for the evaluation of the potential impacts of climate change on surface and groundwater resources. This approach could be adopted for the climate impact assessment on water resources resilience in developing countries, necessary for strategic planning and sustainable water resources management. Hence, the following conclusions can be drawn from the study:

1. From Chapter 5, it was concluded that in most of the statistical assessments conducted, the CRU datasets performed better in replicating the observed station datasets, which suggest that the CRU datasets can serve as a possible replacement to the observed station datasets in the region. Results of GCM selection also identified four top-ranked GCMs, namely ACCESS1.3, MIROC-ESM, MIROC-ESM-CHM, and NorESM1-M, as the most suitable set of GCMs for simulating precipitation, maximum and minimum temperature over the Niger Delta. The findings of the study predicted an increase in both rainfall, maximum and minimum temperature during the future periods and under both RCP4.5 and 8.5 emission scenarios, which indicates the likelihood of extreme weather events in the Niger Delta due to climate change. Hence, further studies should be conducted to ascertain the potential impacts of climate change on

extreme weather events and hydrological processes in the region is recommended.

2. From Chapter 6, based on the recommendation in chapter 5, the selected CRU datasets and GCMs were used for the Spatio-temporal climate projection and extreme weather events assessment over the study area. The model revealed that the 12-month time standardised precipitation index (SPI) under RCP4.5 and RCP8.5 emission scenarios predicted an exceedance in the extreme wet threshold (i.e.,  $SPI > 2$ ) during all future periods and across all study locations which suggest an increased risk of flooding within the projected periods. Hence, studies on the potential impacts of climate change on the hydrologic variables such as the streamflow of the Niger River Basin is recommended to ascertain the volume of water flowing into the basin from the upstream part of the study area.
3. From Chapter 7, based on the recommendation from chapter 6, the selected CRU datasets and GCMs were used for climate change impact studies on the hydrologic processes in the Niger River Basin (NRB) using the SWAT (Soil and Water Assessment Tool) model. The results from this study also predicted an increase of about 21% – 48% in the mean annual streamflow at the Onitsha gauging station during the future periods (2010-2099) under both emission scenarios. Results also projected an increase in mean annual evapotranspiration and groundwater recharge over the entire study period and under both emission scenarios with the highest projected increase during the 2080s (2070-2099) which could have a significant impact on the intensely exploited shallow coastal aquifer. Hence studies into the potential impacts of climate change on the groundwater resources is recommended.

4. From Chapter 8, based on the recommendation to model, the potential impacts of climate change on groundwater resources in chapter 7, the hydrostratigraphy and hydrogeological conceptual model of the study area was developed. The result from the model identified 2 to 4 groundwater aquifer units. The first aquifer units are the unconfined aquifers with unconsolidated fine to medium grain sands and depth range of 1-45 m based on locations. The thickness of the second aquifer ranges from 10–35 m while the third aquifer is about 10-35 m with a depth ranging from 150-240 m thick. The fourth aquifer starts from 200 m to 250 m depending on the locations. The study found the groundwater resources to be within the alluvium and coastal plain sands of the deltaic formation in the basin. The deduced aquifer geometry from the hydrostratigraphic analysis shows that the upper unconfined aquifers at the southern parts of the study area will be more vulnerable to climate drivers.
5. From Chapter 9, based on the recommendation of chapter 7 and 8, the potential impacts of climate change on the shallow coastal aquifer, the hydrogeological conceptual model, coupled with the simulated aquifer recharge and evapotranspiration obtained from chapter seven were used in MODFLOW-2005 to develop a steady-state and transient groundwater flow model. The groundwater model simulations predicted the significant changes in groundwater budget and levels especially when the abstraction rate was increased by 50% under RCP 8.5, which results to a decrease in groundwater levels by 1 m around the coast to 7 m towards the northern part of the study area. The results, therefore, show that the aquifer storage decreases as a result of climate change and population growth stress. However, in the northern part of the aquifer higher recharge somewhat compensates population growth



demands through increased precipitation, with the effect that groundwater may be more resilient in this part of the aquifer even with an increase in abstraction.

### **10.3 Overall impact of the Research**

The Niger Delta is the major economic hub of Nigeria and the operational base of crude oil exploration and production companies in the country, which has been going on for over fifty years in this region. This has encouraged a high level of rural-urban migration from all parts of the country with a resulting surge in population and adding more pressure on the regions water resources. Pollution of water bodies due to incessant flooding, oil spillage, industrial and municipal solid waste has over the years hindered public water supply in the region forcing most of the households to focus on groundwater from the shallow aquifers to meet their daily water demand. Over the years, more attention was given to studies on water quality in the region with no attention given to the resilience of these precious resources, which is what this study addressed. The study associated climate scenarios, hydrologic and groundwater models to demonstrate a good understanding of climate changes impacts on both surface and groundwater resources, which is crucial for water resources management. The knowledge gaps from the literature review were itemised in 10 bullet points, which were addressed in Chapters five to nine, respectively.

The selection of suitable gridded meteorological datasets and GCM ensemble were successfully conducted and used for the projection of future rainfall and temperature series and for the periods 2010 to 2099 under RCP 4.5 and 8.5 emission scenarios which predicted an increase in future rainfall and temperature across the study area. Extreme meteorological events assessment projected instances of extreme wet events during the future periods and under both emission scenarios, which

addressed gaps in bullet points 2 to 5 of the knowledge gaps. The projected increase in future rainfall and temperature coupled with the hydrological model predicted an increase in streamflow at the downstream of the Niger River Basin which might pose a considerable threat to lives and properties, and consequently harm the socio-economic growth and livelihood of the region. Results also projected an increase in evapotranspiration and groundwater recharge in areas with a low settlement concentration and decreased in groundwater recharge in areas with a higher settlements concentration across the watershed. These findings addressed the gaps in bullet points number 6 and 7.

The aquifers characterisation was used to address the gap in bullet points 1. The groundwater recharge and evapotranspiration deduced from the SWAT hydrologic model were then used as input into MODFLOW to model the aquifer response to the climate scenarios and increased abstraction in Port-Harcourt municipal, which houses the highest concentration of settlements, and population in the region. The results show aquifer storage decreases as a result of climate change and population growth stress. However, in the northern part of the aquifer, results show greater recharge somewhat compensates population growth demands through increased precipitation, with an effect that groundwater may be more resilient in this part of the aquifer even with an increase in abstraction. These findings addressed the gaps in bullet points 8 to 10 of the knowledge gaps. To this extent, all 10-bullet points are addressed to underpin the path to a comprehensive water resource management approach, as illustrated in the result chapters and publications.

The findings of this study, therefore, indicate that the Niger Delta Basin is sensitive to climate change. Presently, Nigerian water resource managers have not had information on which to plan for the future modifications of the hydrological cycle for

this region due to lack of sufficient quantitative and qualitative data to determine future policy and management scenarios. In the Niger Delta Basin, as well as Nigeria at large, this study is the first of its kind to present the effects of climate change on both surface and groundwater resources. These findings will, therefore, be useful to government, policymakers and water resource managers in the formulation and enforcement of policies that support coherent regulation aimed at ensuring investment planning that supports Integrated Water Resources Management implementation.

Adequate planning measures should be considered to ameliorate extreme flooding events that might occur to achieve flood control. Routine monitoring and measurement of water levels in rivers, streams, and dams, especially along the Niger River for potential risk of flooding should be enforced to forestall the possible disaster. Regulatory bodies and water service providers should be encouraged to promote water as an economic good to attract revenue, rather than the current practice of unregulated sinking of boreholes. Policy revision may also enhance public awareness about water conservation and management. Furthermore, enforcement of regulations around waste, wastewater, sanitation and hygiene are necessary to protect further contamination of the groundwater resources in the coastal plain sand aquifer to prevent an unwanted outbreak of water-borne diseases.

#### **10.4 Recommendations for Further Studies**

The findings from this study provides a useful insight into the future climate, hydrologic and hydrogeological systems interactions, which can be used as a vital information or tool for the sustainability, adaptation and protection of the water resources. However, these results may not be entirely certain, given the uncertainties

associated with associating climate scenarios and numerical modelling; hence, the following recommendations for future studies can be made:

1. As the simulations of the future hydrologic regime was conducted based on the future changes in precipitation, maximum, and minimum temperature. Incorporating other hydroclimatic parameters such as projected relative humidity, wind speed and solar radiation into the hydrological modeling is therefore recommended.
2. Simulations of the future hydrologic regime were conducted using a constant land use map and land use and land cover change, which might have an impact in the study areas hydrology. A study on the potential impacts of future land-use changes on the hydrological regime of the study areas is therefore recommended.
3. It is also recommended to incorporate the projected climate change and land-use changes in the future studies to understand more approximate future projection of change in the climatic condition and hydrological regimes of the region.
4. Due to the time limitation, only two emission scenarios (RCP4.5 and RCP8.5) were used in this study. It is, therefore, recommended to use the two emission scenarios (RCP2.5 and RCP6.0) together with the newer Shared Socio-Economic Pathways (SSPs) for studying hydrological impacts of climate change to enhance the plausibility of the results.

## REFERENCES

- Amadi A.N., Nwankwoala H.O., Jimoh M. O., Dan-Hassan M. A., and Aminu Tukur. (2014) 'Modeling the Groundwater Quality in parts of Eastern Niger-Delta, Nigeria using Multivariate Statistical Techniques', *American Journal of Water Resources*, 2(5), pp. 118–125. doi: 10.12691/ajwr-2-5-3.
- Abdelaziz, R. and Bakr, M. I. (2012) 'Inverse Modeling of Groundwater Flow of Delta Wadi', 2012(July), pp. 432–438.
- Abdelhalim, A., Sefelnasr, A. and Ismail, E. (2019) 'Numerical modeling technique for groundwater management in Samalut city, Minia Governorate, Egypt', *Arabian Journal of Geosciences*. *Arabian Journal of Geosciences*, 12(4). doi: 10.1007/s12517-019-4230-6.
- Abdelhalim, A., Sefelnasr, A. and Ismail, E. (2020) 'Response of the interaction between surface water and groundwater to climate change and proposed megastructure', *Journal of African Earth Sciences*. Elsevier, 162(June 2019), p. 103723. doi: 10.1016/j.jafrearsci.2019.103723.
- Abel O., T. (2012) 'Geostatistical Assessment of Groundwater Quality from coastal aquifers of Igbokoda, Southwestern Nigeria', *IOSR Journal of Environmental Science, Toxicology and Food Technology*, 2(2), pp. 18–24. doi: 10.9790/2402-0221824.
- Abramowitz, G., Herger, N., Gutmann, E., Hammerling, D., Knutti, R., Leduc, M., and Schmidt, G. A. (2019) 'ESD Reviews: Model dependence in multi-model climate ensembles: Weighting, sub-selection and out-of-sample testing', *Earth System Dynamics*, 10(1), pp. 91–105. doi: 10.5194/esd-10-91-2019.

- Adami, C. (2004) 'Information theory in molecular biology', *Physics of Life Reviews*, 1(1), pp. 3–22. doi: 10.1016/j.plrev.2004.01.002.
- Adejuwon, J. O. (2012) 'Rainfall seasonality in the Niger Delta Belt , Nigeria', *Journal of Geography and regional Planning*, 5(2), pp. 51–60. doi: 10.5897/JGRP11.096.
- Abramowitz, G., Herger, N., Gutmann, E., Hammerling, D., Knutti, R., Leduc, M., and Schmidt, G. A. (2008) 'An overview of the geology and hydrogeology of Nigeria', *Quarterly Journal of Engineering Geology and Hydrogeology*, 29(May 1994), pp. S1–S12. doi: 10.1144/GSL.QJEGH.1996.029.S1.01.
- Adeogun, A., Sule, B., Salami, A., and Okeola, O. (2014) 'GIS-Based Hydrological Modelling Using Swat: Case Study of Upstream Watershed of Jebba Reservoir in Nigeria', *Nigerian Journal of Technology*, 33(3), p. 351. doi: 10.4314/njt.v33i3.13.
- Adeogun, Adeniyi G, Sule, B. F., Salami, A. W., and Daramola, M. O. (2014) 'Validation of SWAT Model for Prediction of Water Yield and Water Balance : Case Study of Upstream Catchment of Jebba Dam in Nigeria', *International Journal of Physical, Nuclear Science and Engineering*, 8(2), pp. 1–7.
- Adeogun, A. G. and Sule, B. F. (2015) 'Simulation of Sediment Yield at the Upstream Watershed of Jebba Lake in Nigeria Using Swat Model', 27(1), pp. 25–40. doi: 10.11113/mjce.v27n1.356.
- Adeogun, B. K. and Sanni, I. M. (2019) 'Hydrological Modelling of Kangimi Dam Watershed using GIS and SWAT Model', *International Journal of Engineering*, (2007), pp. 165–171.
- Adepelumi, A. A., Ako, B. D., Ajayi, T. R., Afolabi, O., and Omotoso, E. J. (2009)

‘Delineation of saltwater intrusion into the freshwater aquifer of Lekki Peninsula, Lagos, Nigeria’, *Environmental Geology*, 56(5), pp. 927–933. doi: 10.1007/s00254-008-1194-3.

Adeyeri, O., Ishola, K. and Okogbue, E. (2017) ‘Climate Change and Coastal Floods: The Susceptibility of Coastal Areas of Nigeria’, *Journal of Coastal Zone Management*, 20(2). doi: 10.4172/2473-3350.1000443.

Ahmad, M. K., Islam, S., Rahman, S., Haque, M. R. and Islam, M. M. (2010) ‘Heavy Metals in Water, Sediment and Some Fishes of Buriganga River, Bangladesh.’, *International Journal of Environmental Resources*, 4(2), pp. 321–332.

Ahmed, K., Shahid, S., Sachindra, D. A., Nawaz, N., and Chung, E. S. (2019) ‘Evaluation of gridded precipitation datasets over arid regions of Pakistan’, *Water (Switzerland)*, 11(2). doi: 10.3390/w11020210.

Ahmed, K., Shahid, S., Wang, X., Nawaz, N., and Najeebullah, K. (2019) ‘Fidelity assessment of general circulation model simulated precipitation and temperature over Pakistan using a feature selection method’, *Journal of Hydrology*. Elsevier, 573(November 2018), pp. 281–298. doi: 10.1016/j.jhydrol.2019.03.092.

Ajetomobia, J., Abiodunb, A. and Hassan, R. (2011) ‘Impacts of climate change on rice agriculture in Nigeria’, *Tropical and Subtropical Agroecosystems*, 14(2), pp. 613–622.

Akande, A., Costa, A. C., Mateu, J., and Henriques, R. (2017) ‘Geospatial Analysis of Extreme Weather Events in Nigeria (1985-2015) Using Self-Organizing Maps’, *Advances in Meteorology*, 2017. doi: 10.1155/2017/8576150.

Akinwumiju A. S and Orimoogunje O. I (2012) ‘Determining the Occurrence of Freshwater in the Aquifers of the Deltaic Formation, Niger Delta Nigeria’, *Journal of Environmental & Analytical Toxicology*, 03(01), pp. 1–4. doi: 10.4172/2161-0525.1000162.

Akpodigaga-a, P. and Odjugo, O. (2010) ‘General Overview of Climate Change Impacts in Nigeria’, *Journal of Human Ecology*. Routledge, 29(1), pp. 47–55. doi: 10.1080/09709274.2010.11906248.

Allen, D. M. and Schuurman, Æ. N. (2008) ‘Data integration and standardization in cross-border hydrogeological studies : a novel approach to hydrostratigraphic model development’, *Environmental Geology*, 53, pp. 1441–1453. doi: 10.1007/s00254-007-0753-3.

Amadi, A. N., Nwankwoala, H. O., Olasehinde, P. I., Okoye, N. O., Okunlola, I. A. and Alkali, Y. B. (2012) ‘Investigation of Aquifer Quality in Bonny Island , Eastern Niger Delta , Nigeria using Geophysical and Geochemical Techniques Department of Geology, Federal University of Technology’, *Journal of Emerging Trends in Engineering and Applied Sciences (JETEAS)*, 3(1), pp. 183–187.

Amadi, A. N., Olasehinde, P. I., Nwankwoala, H. O., Dan-Hassan, M. A. and Okoye, N. O. (2014) ‘Aquifer Vulnerability Studies using DRASTICA Model’, *International Journal of Engineering Science Invention*, 3(3), pp. 1–10.

Amadi, A. N. (2011) ‘Assessing the Effects of Aladimma Dumpsite on Soil and Groundwater Using Water Quality Index and Factor Analysis’, *Australian Journal of Basic and Applied Sciences*, 5(11), pp. 763–770. doi: 10.5539/eer.v3n1p125.

Amadi, A. N. (2014) ‘Impact of Gas-Flaring on the Quality of Rain Water,



Groundwater and Surface Water in Parts of Eastern Niger Delta, Nigeria', *Journal of Geosciences and Geomatics*, 2(3), pp. 114–119. doi: 10.12691/JGG-2-3-6.

Amadi, A. N., Olasehinde, P. I. and Nwankwoala, H. O. (2014) 'Hydrogeochemistry and Statistical Analysis of Benin Formation in Eastern Niger Delta , Nigeria', 4(3), pp. 327–338.

Amadi, A. N., Olasehinde, P. I. and Yisa, J. (2010) 'Characterization of groundwater chemistry in the coastal plain-sand aquifer of Owerri using factor analysis', *International Journal*, 5(8), pp. 1306–1314.

Amadi A.N., Olasehinde P.I., Dan-Hassan, M. A, Okoye, N. O., and Ezeagu G. (2014) 'Hydrochemical Facies Classification and Groundwater Quality Studies in Eastern Niger Delta, Nigeria', *International Journal of Engineering Research and Development*, 10(3), pp. 1–9.

Amadi A.N., Olasehinde P.I., Yisa J., Okosun E.A., Nwankwoala H. O., and Alkali Y.B. (2012) 'Geostatistical Assessment of Groundwater Quality from Coastal Aquifers of Eastern Niger Delta, Nigeria', *Journal of Geo-sciences*, 2(3), pp. 51–59. doi: 10.5923/j.geo.20120203.03.

Amajor L. C (1989) 'Geological appraisal of groundwater exploitations in the Eastern Niger Delta. In: C.O Ofoegbu, (Ed.), *Groundwater and Mineral Resources of Nigeria.*', *Braunschweig/weisbaden. Friedr vieweg and Sohn.*, p. Pp. 85-100.

Amanchukwu, R. N., Amadi-ali, T. G. and Ololube, N. P. (2015) 'Climate change education in Nigeria : The role of Curriculum Review', *Education*, 5(3), pp. 71–79. doi: 10.5923/j.edu.20150503.01.

Amangabara, G. and Obenade, M. (2015) 'Flood Vulnerability Assessment of Niger Delta States Relative to 2012 Flood Disaster in Nigeria', *American Journal of Environmental Protection*, 3(3), pp. 76–83. doi: 10.12691/env-3-3-3.

Amangabara, G. T. (2006) 'Factors of Stream Instability in Urban Centres of Southern Nigeria: Case Study of Port Harcourt City River Systems.', in *American Geophysical Union, Fall Meeting 2007, abstract H23D-23*. American Geophysical Union.

Amangabara, G. T. and Gobo, A. E. (2007) 'Factors that influence the flooding of the middle and lower Ntamogba stream catchments, Port Harcourt, Nigeria', *Journal of Environmental Hydrology*, 15(November), pp. 1–11.

Anderson, M. P. (1983) 'Ground water modeling: The emperor has no clothes.', *Groundwater*, 21(6), pp. 666–669.

Anderson, M., Woessner, W. W. and Hunt, R. (2015) *Applied Groundwater Modeling, Second Edition: Simulation of Flow and Advective Transport*. doi: 10.1016/B978-0-08-091638-5.00001-8.

Ang, R. and Oeurng, C. (2018) 'Simulating streamflow in an ungauged catchment of Tonlesap Lake Basin in Cambodia using Soil and Water Assessment Tool ( SWAT ) model', *Water Science*. COPYRIGHT.TEXT=National Water Research Center, 32(1), pp. 89–101. doi: 10.1016/j.wsj.2017.12.002.

Angela Kesiena Etuonovbe (2011) 'The Devastating Effect of Flooding in Nigeria', *TS06J - Hydrography and the Environment*, (May), pp. 18–22. Available at: [http://www.fig.net/pub/fig2011/papers/ts06j/ts06j\\_etuonovbe\\_5002.pdf](http://www.fig.net/pub/fig2011/papers/ts06j/ts06j_etuonovbe_5002.pdf).

Apurv, T., Mehrotra, R., Sharma, A., Goyal, M. K., and Dutta, S. (2015) 'Impact of

climate change on floods in the Brahmaputra basin using CMIP5 decadal predictions’, *Journal of Hydrology*, 527. doi: 10.1016/j.jhydrol.2015.04.056.

Arnell, N. (1999) ‘Climate change and global water resources’, *Global Environmental Change*, 9, pp. S31–S49. doi: 10.1016/S0959-3780(99)00017-5.

Arnold, J. G., Srinivasan, R., Muttiah, R. S., and Williams, J. R. (1998) ‘Large area hydrologic modeling and assessment part i: Model Development’, *Journal of the American Water Resources Association*, 34(1), pp. 73–89.

Asfahani, J. (2016) ‘Hydraulic parameters estimation by using an approach based on vertical electrical soundings ( VES ) in the semi-arid Khanasser valley region , Syria’, *Journal of African Earth Sciences*. Elsevier Ltd, 117, pp. 196–206. doi: 10.1016/j.jafrearsci.2016.01.018.

Ashraf Vaghefi, S., Abbaspour, N., Kamali, B., and Abbaspour, K. C. (2017) ‘A toolkit for climate change analysis and pattern recognition for extreme weather conditions – Case study: California-Baja California Peninsula’, *Environmental Modelling and Software*. Elsevier Ltd, 96(October), pp. 181–198. doi: 10.1016/j.envsoft.2017.06.033.

Aturamu Adeyinka O, Ojo Adebayo O, Adebayo Olajide F. and Akinyemi Segun A (2015) ‘Palynostratigraphic Analysis of the Agbada Formation (Nep-1 Well) Offshore, Eastern Niger-Delta Basin, Nigeria’, *British Journal of Environmental Sciences Centre*, 3(5), pp. 19–31.

Nilsson, B., Højberg, A. L., Refsgaard, J. C., and Trolldborg, L. (2007) ‘Uncertainty in geological and hydrogeological data’, *Hydrology and Earth System Sciences*, 3(May 2014), pp. 2675–2706. doi: 10.5194/hessd-3-2675-2006.

- Bai, P. and Liu, X. (2018) 'Evaluation of Five Satellite-Based Precipitation Products in Two Gauge-Scarce Basins on the Tibetan Plateau', *Remote Sensing*, 10(8), p. 1316. doi: 10.3390/rs10081316.
- Balinski, M. and Laraki, R. (2019) *Majority judgment vs. majority rule*, *Social Choice and Welfare*. Springer Berlin Heidelberg. doi: 10.1007/s00355-019-01200-x.
- Barfus, K. and Bernhofer, C. (2015) 'Assessment of GCM capabilities to simulate tropospheric stability on the Arabian Peninsula', *International Journal of Climatology*, 35(7), pp. 1682–1696. doi: 10.1002/joc.4092.
- Barron, E. J., Hay, W. W. and Thompson, S. (1989) 'The hydrologic cycle: A major variable during earth history', *Palaeogeography, Palaeoclimatology, Palaeoecology*, 75(3), pp. 157–174. doi: 10.1016/0031-0182(89)90175-2.
- Bear, J. and Verruijt, A. (1987) *Modeling groundwater flow and pollution.*, D. Reidel Publishing Company: Dordrecht, The Netherlands. doi: 10.1139/t88-098.
- Bellos, D. and Sawidis, T. (2005) 'Chemical pollution monitoring of the River Pinios (Thessalia - Greece)', *Journal of Environmental Management*, 76(4), pp. 282–292. doi: 10.1016/j.jenvman.2005.01.027.
- Benedict, Akpomuvie, O. (2011) 'Tragedy of Commons: Analysis of Oil Spillage, Gas Flaring and Sustainable Development of the Niger Delta of Nigeria', *Journal of Sustainable Development*, 4(2), p. 200. doi: 10.5539/jsd.v4n2p200.
- Beyer, R., Krapp, M. and Manica, A. (2019) 'A systematic comparison of bias correction methods for paleoclimate simulations', *Climate of the Past Discussions*, (February), pp. 1–23. doi: 10.5194/cp-2019-11.

BGS (2019) Hydrogeology of Nigeria - *Earthwise, British Geological Survey*. Available at: [http://earthwise.bgs.ac.uk/index.php/Hydrogeology\\_of\\_Nigeria](http://earthwise.bgs.ac.uk/index.php/Hydrogeology_of_Nigeria).

Bhuvandas, N., Timbadiya, P. V, Patel, L., and Porey, D. (2014) 'Review of downscaling methods in climate change and their role in hydrological studies', *International Journal of Environmental, Ecological, Geological and Marine Engineering*, 8(10), pp. 648–653.

Black, A. R. (1995) 'Flood seasonality and physical controls in flood risk estimation', *Scottish Geographical Magazine*, 111(3), pp. 187–190. doi: 10.1080/00369229518736965.

Black, A. R. and Burns, J. C. (2002) 'Re-assessing the flood risk in Scotland', *Science of the Total Environment*, 294(1–3), pp. 169–184. doi: 10.1016/S0048-9697(02)00062-1.

Brown, I. and Chikagbum, W. (2015) 'Planning response to water related disasters in Nigeria the Rivers state experience', *International Journal of Scientific & Engineering Research*, 6(6), pp. 32–44.

Capaccioni, B., Didero, M., Paletta, C., and Didero, L. (2005) 'Saline intrusion and refreshing in a multilayer coastal aquifer in the Catania Plain (Sicily, Southern Italy): Dynamics of degradation processes according to the hydrochemical characteristics of groundwaters', *Journal of Hydrology*, 307(1–4), pp. 1–16. doi: 10.1016/j.jhydrol.2004.08.037.

Chandrashekar, G. and Sahin, F. (2014) 'A survey on feature selection methods', *Computers and Electrical Engineering*. Elsevier Ltd, 40(1), pp. 16–28. doi: 10.1016/j.compeleceng.2013.11.024.

Chang, S. W., Nemecek, K., Kalin, L., and Clement, T. P. (2016) 'Impacts of Climate Change and Urbanization on Groundwater Resources in a Barrier Island', *Journal of Environmental Engineering*, 142(12), p. D4016001. doi: 10.1061/(asce)ee.1943-7870.0001123.

Charles, M Noyes Maley, M. P. and Blake, R. G. (2001) 'Defining Hydrostratigraphic Units within the Heterogeneous Alluvial Sediments at Lawrence Livermore National Laboratory', in *American Association of Petroleum Geologists*, p. 39.

Chaudhary, S., Dhanya, C. T. and Vinnarasi, R. (2017) 'Dry and wet spell variability during monsoon in gauge-based gridded daily precipitation datasets over India', *Journal of Hydrology*. Elsevier B.V., 546, pp. 204–218. doi: 10.1016/j.jhydrol.2017.01.023.

Chen, J., Brissette, F. P. and Leconte, R. (2011) 'Uncertainty of downscaling method in quantifying the impact of climate change on hydrology', *Journal of Hydrology*. Elsevier B.V., 401(3–4), pp. 190–202. doi: 10.1016/j.jhydrol.2011.02.020.

Chen, M., Xie, P., Janowiak, J. E., and Arkin, P. A. (2002) 'Global Land Precipitation: A 50-yr Monthly Analysis Based on Gauge Observations', *Journal of Hydrometeorology*, 3(3), pp. 249–266. doi: 10.1175/1525-7541(2002)003<0249:glpaym>2.0.co;2.

Chen, X., Li, X., Yuan, X., Zeng, G., Liang, J., Li, X., and Chen, G. (2018) 'Effects of human activities and climate change on the reduction of visibility in Beijing over the past 36 years', *Environment International*. Elsevier, 116(April), pp. 92–100. doi: 10.1016/j.envint.2018.04.009.

Chukwuma, A. and George Atelhe, A. (2014) 'Nomads against Natives: A Political

Ecology of Herder/Farmer Conflicts in Nasarawa State, Nigeria’, *American International Journal of Contemporary Research*, 4(2), pp. 76–88. Available at: [www.ajcernet.com](http://www.ajcernet.com).

Cirella, G. T. and Iyalomhe, F. O. (2018) ‘Flooding conceptual review: Sustainability-focalized best practices in Nigeria’, *Applied Sciences (Switzerland)*, 8(9). doi: 10.3390/app8091558.

Colombani, N., Osti, A., Volta, G., and Mastrocicco, M. (2016) ‘Impact of Climate Change on Salinization of Coastal Water Resources’, *Water Resources Management*. *Water Resources Management*, 30(7), pp. 2483–2496. doi:10.1007/s11269-016-1292-z.

Cordano, E. (2016) ‘Package “ RMRAINGEN ” (R Multi-site RAINfall GENerator): a package to generate daily time series of rainfall from monthly mean values’. CRAN, p. 23. Available at: <https://github.com/ecor/RMRAINGEN%0D>.

Cosgrove, W. J. and Loucks, D. P. (2015) ‘Water management: Current and future challenges and research directions’, *AGU Publications: Water Resources Research*, pp. 4823–4839. doi: 10.1002/2014WR016869.Received.

Cox SE, K. S. (1999) ‘Hydrogeology, ground-water quality, and sources of nitrate in Lowland glacial aquifers of Whatcom County, Washington, and British Columbia, Canada.’, *US Geological Survey Water-Resources Investigations Report*, 98-4195.

Craig Clifton, Rick Evans, Susan Hayes, Rafik Hirji, and Gabrielle Puz, C. P. (2010) ‘Water Working Notes adaptation options’, *Managing*, (25).

Colombani, N., Osti, A., Volta, G., and Mastrocicco, M. (2013) ‘An assessment of the

climate change impacts on groundwater recharge at a continental scale using a probabilistic approach with an ensemble of GCMs’, *Climatic Change*, 117(1–2), pp. 41–53. doi: 10.1007/s10584-012-0558-6.

Daramola, J., Ekhwan, T. M., Mokhtar, J., Lam, K. C., and Adeogun, G. A. (2019) ‘Estimating sediment yield at Kaduna watershed, Nigeria using soil and water assessment tool (SWAT) model’, *Heliyon*. Elsevier Ltd, 5(7), p. e02106. doi: 10.1016/j.heliyon.2019.e02106.

Dash, S. K., Kulkarni, M. A., Mohanty, U. C., and Prasad, K. (2009) ‘Changes in the characteristics of rain events in India’, *Journal of Geophysical Research Atmospheres*, 114(10). doi: 10.1029/2008JD010572.

Derin, Y. and Yilmaz, K. K. (2014) ‘Evaluation of Multiple Satellite-Based Precipitation Products over Complex Topography’, *Journal of Hydrometeorology*, 15(4), pp. 1498–1516. doi: 10.1175/JHM-D-13-0191.1.

Devia, G. K., Ganasri, B. P. and Dwarakish, G. S. (2015) ‘A Review on Hydrological Models’, *Aquatic Procedia*, 4(Icwrcoe), pp. 1001–1007. doi: 10.1016/j.aqpro.2015.02.126.

Dibike, Y. B. and Coulibaly, P. (2005) ‘Hydrologic impact of climate change in the Saguenay watershed: Comparison of downscaling methods and hydrologic models’, *Journal of Hydrology*, 307(1–4), pp. 145–163. doi: 10.1016/j.jhydrol.2004.10.012.

Döll, P. (2009) ‘Vulnerability to the impact of climate change on renewable groundwater resources: a global-scale assessment’, *Environmental Research Letters*, 4(3), p. 035006. doi: 10.1088/1748-9326/4/3/035006.



Döll, P. and Fiedler, K. (2008) ‘Global-scale modeling of groundwater recharge’, *Hydrology and Earth System Sciences*, 12(3), pp. 863–885. doi: 10.5194/hess-12-863-2008.

Dosio, A. and Paruolo, P. (2011) ‘Bias correction of the ENSEMBLES high-resolution climate change projections for use by impact models: Evaluation on the present climate’, *Journal of Geophysical Research Atmospheres*, 116(16), pp. 1–22. doi: 10.1029/2011JD015934.

Du, X., Lu, X., Hou, J., and Ye, X. (2018) ‘Improving the reliability of numerical groundwater modeling in a data-sparse region’, *Water (Switzerland)*, 10(3), pp. 1–15. doi: 10.3390/w10030289.

Dudek, G. (2010) ‘Tournament searching method to feature selection problem’, *Lecture Notes in Computer Science (including subseries Lecture Notes in Artificial Intelligence and Lecture Notes in Bioinformatics)*, 6114 LNAI(PART 2), pp. 437–444. doi: 10.1007/978-3-642-13232-2\_53.

Ebele, N. and Emodi, N. (2016) ‘Climate Change and Its Impact in Nigerian Economy’, *Journal of Scientific Research and Reports*, 10(6), pp. 1–13. doi: 10.9734/jsrr/2016/25162.

Edet, A., Abdelaziz, R., Merkel, B., Okereke, C., and Nganje, T. (2014) ‘Numerical groundwater flow modeling of the Coastal Plain sand aquifer, Akwa Ibom State, SE Nigeria’, *Journal of Water Resource and Protection*, 06(March), pp. 193–201. doi: 10.4236/jwarp.2014.64025.

Edsel B. Daniel, Janey V. Camp, Eugene J. LeBoeuf, Jessica R. Penrod, James P. Dobbins, and Mark D. Abkowitz (2011) ‘Watershed Modeling and its Applications: A

State of the Art Review’, *The Open Hydrology Journal*, 5, pp. 26–50.

Egeonu, N. C. and Oyanyan, R. O. (2018) ‘Hydrochemistry of Groundwater in Obiga-Asa and its Environs, Abia State, Nigeria’, *International Journal of Scientific & Engineering Research*, 9(3), pp. 311–323.

Ejeji, C., Amodu, M. and Adeogun, A. (2016) ‘Prediction of the streamflow of Hadejia-Jama’are-Komadugu-Yobe-River Basin, North Eastern Nigeria, using swat model’, *Ethiopian Journal of Environmental Studies and Management*, 9(2), p. 209. doi: 10.4314/ejesm.v9i2.8.

Elisha, I., B. A, S. and Lawrence, E. U. (2017) ‘Evidence of Climate Change and Adaptation Strategies among Grain Farmers in Sokoto State, Nigeria’, *IOSR Journal of Environmental Science, Toxicology and Food Technology*, 11(03), pp. 01–07. doi: 10.9790/2402-1103020107.

Eludoyin, O. M., Adelekan, I. O., Webster, R., and Eludoyin, A. O. (2014) ‘Air temperature, relative humidity, climate regionalization and thermal comfort of Nigeria’, *International Journal of Climatology*, 34(6), pp. 2000–2018. doi: 10.1002/joc.3817.

Enete, I. (2014) ‘Impacts of Climate Change on Agricultural Production in Enugu State, Nigeria’, *Journal of Earth Science & Climatic Change*, 05(09), pp. 9–11. doi: 10.4172/2157-7617.1000234.

Ertürk, A., Ekdal, A., Gürel, M., Karakaya, N., Guzel, C., and Gönenç, E. (2014) ‘Evaluating the impact of climate change on groundwater resources in a small Mediterranean watershed’, *Science of the Total Environment*. Elsevier B.V., 499, pp. 437–447. doi: 10.1016/j.scitotenv.2014.07.001.

Etim U. U Ituen and Folarin Alonge (2009) ‘Niger Delta Region of Nigeria, Climate Change and the way Forward’, *Bioenergy Engineering*, 11-14 October 2009, Bellevue, Washington, (January 2009). doi: 10.13031/2013.29162.

Etu-Efeotor J. O and Akpokodje E. G (1990) ‘Aquifer systems of the Niger Delta’, *Journal of Mining Geology*, 26(2), pp. 279–284.

Etu–Efeotor, J. O. and Odigi, M. I. (1983) ‘Water supply problems in the Eastern Niger Delta’, *Journal of Mining and Geology*, 20(1), pp. 182–192.

Expósito, F. J., González, A., Pérez, J. C., Díaz, J. P., and Taima, D. (2015) ‘High-resolution future projections of temperature and precipitation in the Canary Islands’, *Journal of Climate*, 28(19), pp. 7846–7856. doi: 10.1175/JCLI-D-15-0030.1.

Faramarzi, M., Abbaspour, K. C., Ashraf Vaghefi, S., Farzaneh, M. R., Zehnder, A. J. B., Srinivasan, R., and Yang, H. (2013) ‘Modeling impacts of climate change on freshwater availability in Africa’, *Journal of Hydrology*. Elsevier B.V., 480, pp. 85–101. doi: 10.1016/j.jhydrol.2012.12.016.

Farid, A., Jadoon, K. and Akhter, G. (2013) ‘Hydrostratigraphy and hydrogeology of the western part of Maira area , Khyber Pakhtunkhwa , Pakistan : a case study by using electrical resistivity’, *Springer: Environal Monitoring Assessment*, 185:2407–2, pp. 2407–2422. doi: 10.1007/s10661-012-2720-z.

Federal Ministry of Environment (2013) ‘Nigeria Post-Disaster Needs Assessment ( PDNA ) 2012 Floods’, *Federal Government of Nigeria*, (June), pp. 1–188. Available at:[www.gfdr.org/sites/gfdr/files/NIGERIA\\_PDNA\\_PRINT\\_05\\_29\\_2013\\_WEB.pdf](http://www.gfdr.org/sites/gfdr/files/NIGERIA_PDNA_PRINT_05_29_2013_WEB.pdf)

Felisa, G., Ciriello, V. and Di Federico, V. (2013) ‘Saltwater intrusion in coastal

aquifers: A primary case study along the adriatic coast investigated within a probabilistic framework’, *Water (Switzerland)*, 5(4), pp. 1830–1847. doi: 10.3390/w5041830.

FMWR (2016) ‘National Water Resources Policy’, (July).

Foley, A. M. (2010) ‘Uncertainty in regional climate modelling: A review’, *Progress in Physical Geography*, 34(5), pp. 647–670. doi: 10.1177/0309133310375654.

Fu, Y., Xia, J., Yuan, W., Xu, B., Wu, X., Chen, Y., and Zhang, H. (2016) ‘Assessment of multiple precipitation products over major river basins of China’, *Theoretical and Applied Climatology*, 123(1–2), pp. 11–22. doi: 10.1007/s00704-014-1339-0.

Fuka, D. R., Walter, M. T., Macalister, C., Degaetano, A. T., Steenhuis, T. S., and Easton, Z. M. (2014) ‘Using the Climate Forecast System Reanalysis as weather input data for watershed models’, *Hydrological Processes*, 28(22), pp. 5613–5623. doi: 10.1002/hyp.10073.

Gagnon, S., Singh, B., Rousselle, J., and Roy, L. (2005) ‘An Application of the statistical downscaling model (SDSM) to simulate climatic data for streamflow modelling in Québec’, *Canadian Water Resources Journal*, 30(4), pp. 297–314. doi: 10.4296/cwrj3004297.

Gebremicael, T. G., Mohamed, Y. A., Betrie, G. D., van der Zaag, P., and Teferi, E. (2013) ‘Trend analysis of runoff and sediment fluxes in the Upper Blue Nile basin: A combined analysis of statistical tests, physically-based models and landuse maps’, *Journal of Hydrology*, 482(May), pp. 57–68. doi: 10.1016/j.jhydrol.2012.12.023.

Giorgi, F., Hewitson, B., Christensen, J., Hulme, M., Von Storch, H., Whetton, P., and

Fu, C. (2001) 'Regional Climate Information Evaluation and Projections', *Climate Change 2001: The Scientific Basis. Contribution of Working Group I to the Third Assessment Report of the Intergovernmental Panel on Climate Change*.

Gleick, P. H. (1993) *Water in crisis : a guide to the world's fresh water resources*, Pacific Institute for Studies in Development and Security, Environment Institute, Stockholm Environment. New York: Oxford University Press.

Graham Wayne (2013) *The Beginner's Guide to Representative Concentration Pathways*, *Skeptical Science*. doi: 10.1063/1.478923.

Gyamfi, C., Ndambuki, J. M. and Salim, R. W. (2016) 'Application of SWAT Model to the Olifants Basin: Calibration, Validation and Uncertainty Analysis', *Journal of Water Resource and Protection*, 08(03), pp. 397–410. doi: 10.4236/jwarp.2016.83033.

Haider, H. (2019) Climate change in Nigeria: impacts and responses, *K4D Helpdesk Report*. Available at: [https://assets.publishing.service.gov.uk/media/5dcd7a1aed915d0719bf4542/675\\_Climate\\_Change\\_in\\_Nigeria.pdf](https://assets.publishing.service.gov.uk/media/5dcd7a1aed915d0719bf4542/675_Climate_Change_in_Nigeria.pdf).

Hammami, D., Lee, T. S., Ouarda, T. B. M. J., and Le, J. (2012) 'Predictor selection for downscaling GCM data with LASSO', *Journal of Geophysical Research Atmospheres*, 117(17), pp. 1–11. doi: 10.1029/2012JD017864.

Harbaugh, A.W., and McDonald, M. G. (1996) User's documentation for MODFLOW-96, an update to the U.S. Geological Survey modular finite-difference ground-water flow model and Programmer's documentation for MODFLOW-96, *an update to the U.S. Geological Survey modular finitedifference ground-water flow*.

Harbaugh, Arlen, W. (2005) 'MODFLOW-2005', The U . S . Geological Survey

Modular Ground-Water Model — the Ground-Water Flow Process’, *U.S. Geological Survey Techniques and Methods*, p. 253. doi: U.S. Geological Survey Techniques and Methods 6-A16.

Harbaugh, A. W. (2009) ‘Zonebudget Version 3’, *U.S. Geological Survey Software Release*, pp. 1–10.

Harbaugh, B. A. W., Banta, E. R., Hill, M. C., and McDonald, M. G. (2000) ‘MODFLOW-2000 , The U .S . Geological Survey modular ground-water model — User guide to modularization concepts and the ground-water flow process’, *U.S. Geological Survey*, p. 130. Available at: <http://www.gama-geo.hu/kb/download/ofr00-92.pdf>.

Hargreaves G.H. and Samani Z.A. (1985) ‘Reference Crop Evapotranspiration from Temperatures’, *American society of Agricultural Engineers; Applied Engineering in Agriculture*, 1(2), pp. 96–99. doi: 0883-8542/85/0102-0096.

Harris, I., Jones, P. D., Osborn, T. J., and Lister, D. H. (2014) ‘Updated high-resolution grids of monthly climatic observations - the CRU TS3.10 Dataset’, *International Journal of Climatology*, 34(3), pp. 623–642. doi: 10.1002/joc.3711.

Hartmann, D. L., Tank, A. M. G. K., Rusticucci, M., Alexander, L., Brönnimann, S., Charabi, Y., and Zhai, P. M.. (2013) ‘Observations: Atmosphere and Surface Supplementary Material’, *Climate Change 2013 the Physical Science Basis: Working Group I Contribution to the Fifth Assessment Report of the Intergovernmental Panel on Climate Change*, pp. 2SM-1-2SM – 30. Available at: [www.climatechange2013.org%0Awww.ipcc.ch](http://www.climatechange2013.org%0Awww.ipcc.ch).

Hassan, I., Kalin, R. M., White, C. J., and Aladejana, J. A. (2019) ‘Hydrostratigraphy

and Hydraulic Characterisation of Shallow Coastal Aquifers, Niger Delta Basin: A Strategy for Groundwater Resource Management’, *Geosciences*, 9(11), p. 470. doi: 10.3390/geosciences9110470.

Hassan, I., Kalin, R. M., White, C. J., and Aladejana, J. A. (2020) ‘Selection of CMIP5 GCM Ensemble for the Projection of Spatio-Temporal Changes in Precipitation and Temperature over the Niger Delta, Nigeria’, *Water*, 12(2), p. 385. doi: 10.3390/w12020385.

Hassan, I., Kalin, R. M., White, C. J., and Aladejana, J. A. (2020) ‘Evaluation of Daily Gridded Meteorological Datasets over the Niger Delta Region of Nigeria and Implication to Water Resources Management’, *Atmospheric and Climate Sciences (ACS)*, *SCRIP*.

Hassan, I., Kalin, R. M., White, C. J., and Aladejana, J. A. (2020) ‘Potential Impacts of Climate Change on Extreme Weather Events in the Niger Delta Part of Nigeria’, *Hydrology*, 7(1), p. 19. doi: 10.3390/hydrology7010019.

Haylock, M. R., Hofstra, N., Klein Tank, A. M. G., Klok, E. J., Jones, P. D., and New, M. (2008) ‘A European daily high-resolution gridded data set of surface temperature and precipitation for 1950-2006’, *Journal of Geophysical Research Atmospheres*, 113(20). doi: 10.1029/2008JD010201.

Musa, Z. N., Popescu, I., and Mynett, A. (2014) The Niger Delta's vulnerability to river floods due to sea level rise, *Nat. Hazards Earth Syst. Sci.*, 14, 3317–3329, <https://doi.org/10.5194/nhess-14-3317-2014>,

Hazell, J. R. T., Cratchley, C. R. and Jones, C. R. C. (1992) ‘The hydrogeology of crystalline aquifers in northern Nigeria and geophysical techniques used in their

exploration’, *Geological Society, London, Special Publications*, 66(1), pp. 155–182.  
doi: 10.1144/GSL.SP.1992.066.01.08.

Hempel, S., Frieler, K., Warszawski, L., Schewe, J., and Piontek, F. (2013) ‘A trend-preserving bias correction – The ISI-MIP approach’, *Earth System Dynamics*, 4(2), pp. 219–236. doi: 10.5194/esd-4-219-2013.

Herrera-Pantoja, M. and Hiscock, K. M. (2008) ‘The effects of climate change on potential groundwater recharge in Great Britain’, *Hydrological Processes*, 22(1), pp. 73–86. doi: 10.1002/hyp.6620.

Hempel, S., Frieler, K., Warszawski, L., Schewe, J., and Piontek, F. (2012) ‘Development and analysis of a 50-year high-resolution daily gridded precipitation dataset over Spain (Spain02)’, *International Journal of Climatology*, 32(1), pp. 74–85. doi: 10.1002/joc.2256.

Heuvelink, G. B. M. (1986) ‘Propagation of error in spatial modelling with GIS STOCHASTIC ERROR MODEL FOR’, pp. 207–218.

Hijmans, R. J., Cameron, S. E., Parra, J. L., Jones, P. G., and Jarvis, A. (2005) ‘Very high resolution interpolated climate surfaces for global land areas’, *International Journal of Climatology*, 25(15), pp. 1965–1978. doi: 10.1002/joc.1276.

Hill, M. C. (1992) A computer program (MODFLOW) for estimating parameters of a transient, three-dimensional, ground-water flow model using nonlinear regression: *U.S. Geological Survey Open-File Report 91-484*.

Holman, I. P. (2006) ‘Climate change impacts on groundwater recharge-uncertainty, shortcomings, and the way forward?’, *Hydrogeology Journal*, 14(5), pp. 637–647. doi:



10.1007/s10040-005-0467-0.

Hu, Z.; Hu, Q.; Zhang, C.; Chen, X.; and Li, Q. (2016) ‘Evaluation of reanalysis, spatially interpolated and satellite remotely sensed precipitation data sets in central Asia’, *Journal of Geophysical Research Atmospheres*, 121(June), pp. 5648–5663. doi: 10.1002/2016JD024781.

Hu, Y., Maskey, S. and Uhlenbrook, S. (2013) ‘Downscaling daily precipitation over the Yellow River source region in China: A comparison of three statistical downscaling methods’, *Theoretical and Applied Climatology*, 112(3–4), pp. 447–460. doi: 10.1007/s00704-012-0745-4.

Hutton, G. and Chase, C. (2016) ‘The Knowledge Base for Achieving the Sustainable Development Goal Targets on Water Supply , Sanitation and Hygiene’, *Environmental Research and Public Health (MDPI)*, pp. 1–35. doi: 10.3390/ijerph13060536.

Ike, P. C. and Emaziye, P. O. (2012) ‘An Assessment of the Trend and Projected Future Values of Climatic Variables in Niger Delta Region , Nigeria’, 4(2), pp. 165–170.

IPCC-TGICA (2007) ‘General Guidelines on the Use of Scenario Data for climate impact and adaptation assessment’, *Finnish Environment Institute*, 312(June), p. 66. doi: 10.1144/SP312.4.

IPCC (1990a) Climate Change 1990: The IPCC Impacts Assessment. Contribution of Working Group II to the First Assessment Report of the Intergovernmental Panel on Climate Change, *Climate change*. doi: 10.2307/3298564.

IPCC (1990b) ‘Climate Change The IPCC Scientific Assessment’, *Ipcc*, p. 414. doi: 10.1097/MOP.0b013e3283444c89.

IPCC (1992) *CLIMATE CHANGE 1992 - The Supplementary Report to the IPCC Scientific Assessment.*

IPCC (1995) *Climate Change 1995. The Science of Climate Change, Journal of Chemical Information and Modeling.* doi: 10.1017/CBO9781107415324.004.

IPCC (1996) *Climate Change 1995: Economic and Social Dimensions of Climate Change - Contribution of Working Group III to the Second Assessment Report of the Intergovernmental Panel on Climate Change, Published for the Intergovernmental Panel on Climate Change - CAMBRIDGE UNIVERSITY PRESS.* Edited by J. T. Houghton. doi: 10.1016/S0959-3780(97)82915-9.

IPCC (1997) *Climate change 1994: Radiative forcing of climate change and an evaluation of the IPCC IS92 emission scenarios.* Intergovernmental panel on climate change (IPCC), *Global and Planetary Change.* doi:10.1016/S0921-8181(96)00009-4.

IPCC (2007a) *Climate Change 2007: impacts, adaptation and vulnerability: contribution of Working Group II to the fourth assessment report of the Intergovernmental Panel, Geneva, Suíça.* doi: 10.1256/004316502320517344.

IPCC (2007b) *Climate Change 2007 Synthesis Report, Intergovernmental Panel on Climate Change [Core Writing Team IPCC.* doi: 10.1256/004316502320517344.

IPCC (2007c) *Mitigation of climate change: Contribution of working group III to the fourth assessment report of the Intergovernmental Panel on Climate Change, Intergovernmental Panel on Climate Change.*

IPCC (2011) 'Climate change science - the status of climate change science today', *United Nations Framework Convention on Climate Change*, (February 2011), pp. 1–

7. doi: 10.1111/j.1467-9388.1992.tb00046.x.

IPCC (2012) Managing the risks of extreme events and disasters to advance climate change adaptation, *IPCC*. doi: 10.1596/978-0-8213-8845-7.

IPCC (2013a) Climate Change 2007: The Physical Science Basis, Journal of Chemical Information and Modeling. Edited by D. Solomon, Susan & Qin. doi: 10.1017/CBO9781107415324.004.

IPCC (2013b) The Physical Science Basis. Contribution of Working Group I to the Fifth Assessment Report of the Intergovernmental Panel on Climate Change., Cambridge, United Kingdom and New York, NY, USA: Cambridge University Press, Cambridge. *Cambridge, United Kingdom and New York, NY, USA: Cambridge University Press, Cambridge*. Available at: [https://www.ipcc.ch/site/assets/uploads/2018/03/WG1AR5\\_SummaryVolume\\_FINAL.pdf](https://www.ipcc.ch/site/assets/uploads/2018/03/WG1AR5_SummaryVolume_FINAL.pdf).

IPCC (2014) *Climate Change 2013 - The Physical Science Basis*. Edited by Intergovernmental Panel on Climate Change. Cambridge: Cambridge University Press. doi: 10.1017/CBO9781107415324.

Izeze I. A. (1990) Aquifer characteristics of the coastal plain sands of the southern Nigeria: *M.Sc. thesis*. University of Port Harcourt, Port Harcourt, Nigeria.

Jackson, C. R., Hughes, A. G. and O Dochartaigh, B. E. (2004) 'Preliminary numerical modelling of groundwater flow in the Dumfries basin', *British Geological Survey Report*, (IR/04/053). Available at: <http://nora.nerc.ac.uk/12618/>.

Jackson, C. R., Meister, R. and Prudhomme, C. (2011) 'Modelling the effects of climate change and its uncertainty on UK Chalk groundwater resources from an

ensemble of global climate model projections’, *Journal of Hydrology*. Elsevier B.V., 399(1–2), pp. 12–28. doi: 10.1016/j.jhydrol.2010.12.028.

James S. and Risbey, D. E. (1996) ‘Observed Sacramento Basin streamflow response to climate impact studies’, 184, pp. 209–223.

Jiang, T., Chen, Y. D., Xu, C. yu, Chen, X., Chen, X., and Singh, V. P. (2007) ‘Comparison of hydrological impacts of climate change simulated by six hydrological models in the Dongjiang Basin, South China’, *Journal of Hydrology*, 336(3–4), pp. 316–333. doi: 10.1016/j.jhydrol.2007.01.010.

Jiang, X., Waliser, D. E., Xavier, P. K., Petch, J., Klingaman, N. P., Woolnough, S. J., and Zhu, H. (2015) ‘Vertical structure and physical processes of the Madden-Julian oscillation: Exploring key model physics in climate simulations’, *Journal of Geophysical Research: Atmospheres*, 120(10), pp. 4718–4748. doi: 10.1002/2014JD022375.

JICA (2013) 'Federal Republic of Nigeria the Project for Review and Update of Nigeria - (National Water Resources Master Plan 2013) *Executive Summary - Volume 1, Japan International Cooperation Agency*.

Jichun, W. U. and Xiankui, Z. (2013) ‘Review of the uncertainty analysis of groundwater’, *Chinese Science Bulletin*, 58(25), pp. 3044–3052. doi: 10.1007/s11434-013-5950-8.

Jones, P.D., and Harris, I. C. (2008) Climatic Research Unit (CRU) time-series datasets of variations in climate with variations in other phenomena. NCAS British Atmospheric Data Centre. Available at: <http://catalogue.ceda.ac.uk/uuid/3f8944800cc48e1cbc29a5ee12d8542d>.

Khalid, K., Ali, M. F., Rahman, N. F. A., Mispan, M. R., Haron, S. H., Othman, Z., and Bachok, M. F. (2016) ‘Sensitivity Analysis in Watershed Model Using SUFI-2 Algorithm’, *Procedia Engineering*. The Author(s), 162, pp. 441–447. doi: 10.1016/j.proeng.2016.11.086.

Khan, N., Shahid, S., Ahmed, K., Ismail, T., Nawaz, N., and Son, M. (2018) ‘Performance Assessment of General Circulation Model in Simulating Daily Precipitation and Temperature Using Multiple Gridded Datasets’, *Water*, 10(12), p. 1793. doi: 10.3390/w10121793.

Kharchaf, Y., Rhinane, H., Kaoukaya, A., and Fadil, A. (2013) ‘The Contribution of the Geospatial Information to the Hydrological Modelling of a Watershed with Reservoirs: Case of Low Oum Er Rbiaa Basin (Morocco)’, *Journal of Geographic Information System*, 05(03), pp. 258–268. doi: 10.4236/jgis.2013.53025.

Knutti, R., Masson, D. and Gettelman, A. (2013) ‘Climate model genealogy: Generation CMIP5 and how we got there’, *Geophysical Research Letters*, 40(6), pp. 1194–1199. doi: 10.1002/grl.50256.

Komuscu, A. U. (1999) ‘Using the SPI to Analyze Spatial and Temporal Patterns of Drought in Turkey Using the SPI to Analyze Spatial and Temporal Patterns of Drought in Turkey’, *Drought Network News*, 11(1), pp. 6–13.

Konikow, L.F., Goode, D.J., and Hornberger, G. Z. (1996) A three-dimensional method-of-characteristics solute-transport model (MOC3D): *U.S. Geological Survey Water-Resources Investigations Report 96-4267*.

Krčmář, D. and Sracek, O. (2014) ‘MODFLOW-USG: the New Possibilities in Mine Hydrogeology Modelling (or What is Not Written in the Manuals)’, (April). doi:

10.1007/s10230-014-0273-9.

Krinner, G., Germany, F., Shongwe, M., Africa, S., France, S. B., Uk, B., and Lucas, C. (2013) 'Long-term climate change: Projections, commitments and irreversibility', *Climate Change 2013 the Physical Science Basis: Working Group I Contribution to the Fifth Assessment Report of the Intergovernmental Panel on Climate Change*, 9781107057, pp. 1029–1136. doi: 10.1017/CBO9781107415324.024.

Kumar, C. P. (2002) 'Groundwater Flow Models', *Scientist 'EI' National Institute of Hydrology Roorkee*, 247667, pp. 1–27.

Kumar, C. P. (2016) 'Assessing the Impact of Climate Change on Groundwater Resources', *National Institute of Hydrology, India*, 5(no.1), pp. 163–167.

Kumar, C. P. (2012) 'Assessing the impact of climate change on groundwater resources', *India Water Week*, (April), pp. 10–14.

Kundzewicz, Z. W. and Döll, P. (2009) 'Will groundwater ease freshwater stress under climate change?', *Hydrological Sciences Journal*, 54(4), pp. 665–675. doi: 10.1623/hysj.54.4.665.

Kursinski, A. L. and Zeng, X. (2006) 'Areal estimation of intensity and frequency of summertime precipitation over a midlatitude region', *Geophysical Research Letters*, 33(22), pp. 1–5. doi: 10.1029/2006GL027393.

Larsen, E. H., Sørensen, J. B. and Sørensen, J. N. (2000) 'A mathematical model of solute coupled water transport in toad intestine incorporating recirculation of the actively transported solute.', *The Journal of general physiology*, 116(2), pp. 101–124. doi: 10.1085/jgp.116.2.101.

- Li, X., Chen, X., Yuan, X., Zeng, G., León, T., Liang, J., and Yuan, X. (2017) 'Characteristics of particulate pollution (PM<sub>2.5</sub> and PM<sub>10</sub>) and their spacescale-dependent relationships with meteorological elements in China', *Sustainability (Switzerland)*, 9(12), pp. 1–14. doi: 10.3390/su9122330.
- Lin, C., Maurer, E. P., Andreadis, K. M., Rosenberg, E. A., Livneh, B., Lettenmaier, D. P., and Mishra, V. (2013) 'A Long-Term Hydrologically Based Dataset of Land Surface Fluxes and States for the Conterminous United States: Update and Extensions', *Journal of Climate*, 26(23), pp. 9384–9392. doi:10.1175/jcli-d-12-00508.1.
- Lin, C. Y. and Tung, C. P. (2017) 'Procedure for selecting GCM datasets for climate risk assessment', *Terrestrial, Atmospheric and Oceanic Sciences*, 28(1), pp. 43–55. doi: 10.3319/TAO.2016.06.14.01(CCA).
- Lloyd-Hughes, B. and Saunders, M. A. (2002) 'A drought climatology for Europe', *International Journal of Climatology*, 22(13), pp. 1571–1592. doi: 10.1002/joc.846.
- Lohman, S. W. (1972) *Definitions of selected ground-water terms, revisions and conceptual refinements, Water Supply Paper*. Washington, D.C. doi: 10.3133/wsp1988.
- Luo, Y. Z., Ficklin, D. L., Liu, X. M., and Zhang, M. H. (2013) 'Assessment of climate change impacts on hydrology and water quality with a watershed modeling approach', *Science of the Total Environment*, 450, pp. 72–82. doi: 10.1016/j.scitotenv.2013.02.004.
- Lupo, A. and Kininmonth, W. (2013) 'Global Climate Models and Their Limitations', *Climate Change Reconsidered II: Physical Science.*, pp. 7–148. doi:

10.1038/ncomms2656.

Luo, Y. Z., Ficklin, D. L., Liu, X. M., and Zhang, M. H. (2016) ‘Selecting representative climate models for climate change impact studies: an advanced envelope-based selection approach’, *International Journal of Climatology*, 36(12), pp. 3988–4005. doi: 10.1002/joc.4608.

Ma, C. W. and Ma, Y. G. (2018) ‘Shannon Information Entropy in Heavy-ion Collisions’. doi: 10.1016/j.ppnp.2018.01.002.

MacDonald, A. M., Bonsor, H. C., Dochartaigh, B. É. Ó., and Taylor, R. G. (2012) ‘Quantitative maps of groundwater resources in Africa’, *Environmental Research Letters*, 7(2). doi: 10.1088/1748-9326/7/2/024009.

Mahe, Gil, L’Hote, Y., Olivry, J. Claude, and Wotling, G. (2001) ‘Tendances et discontinuités dans des séries de pluies régionales en Afrique de l’Ouest et Centrale: 1951–1989’, *Hydrological Sciences Journal*, 46(2), pp. 211–226. doi: 10.1080/02626660109492817.

Mahe, G, New, M., Paturel, J. E., Cres, A., Dezetter, A., Boyer, J. F., and Dezetter, A. (2008) ‘Comparing available rainfall gridded datasets for West Africa and the impact on rainfall-runoff modelling results , the case of Burkina-Faso .’, *Water SA*, 34(5), pp. 529–536. Available at: <http://www.wrc.org.za>.

Marietu S, T. and Olarewaju O, I. (2009) ‘Resource Conflict among Farmers and Fulani herdsmen: Implications for Implications for resource sustainability’, *African Journal of Political Science and International Relations*, 3(9), pp. 360–364.

Markstrom, S. L., Niswonger, R. G., Regan, R. S., Prudic, D. E., and Barlow, P. M.



(2008) 'GSFLOW Coupled Ground-Water and Surface-Water Flow Model Based on the Integration of the Precipitation-Runoff Modeling System (PRMS) and the Modular Ground-Water Flow Model (MODFLOW-2005), *U.S. Geological Survey*. Available at: <http://pubs.er.usgs.gov/publication/tm6D1>.

Martín, J. L., Bethencourt, J. and Cuevas-Agulló, E. (2012) 'Assessment of global warming on the island of Tenerife, Canary Islands (Spain). Trends in minimum, maximum and mean temperatures since 1944', *Climatic Change*, 114(2), pp. 343–355. doi: 10.1007/s10584-012-0407-7.

Marvel, K. and Bonfils, C. (2013) 'Identifying external influences on global precipitation', in *Proceedings of the National Academy of Sciences of the United States of America*, pp. 19301–19306. doi: 10.1073/pnas.1314382110.

Masui, T., Matsumoto, K., Hijioka, Y., Kinoshita, T., Nozawa, T., Ishiwatari, S., and Kainuma, M. (2011) 'An emission pathway for stabilization at 6 Wm<sup>-2</sup> radiative forcing', *Climatic Change*, 109(1), pp. 59–76. doi: 10.1007/s10584-011-0150-5.

Matemilola, S., Adedeji, O. H., Elegbede, I., and Kies, F. (2019) 'Mainstreaming climate change into the EIA process in Nigeria: Perspectives from projects in the Niger Delta Region', *Climate*, 7(2). doi: 10.3390/cli7020029.

Mckee, T. B., Doesken, N. J. and Kleist, J. (1993) 'The relationship of drought frequency and duration to time scales', *AMS 8th Conference on Applied Climatology*, (January), pp. 179–184. doi: citeulike-article-id:10490403.

Mckee, T. B., Doesken, N. J. and Kleist, J. (1995) 'Drought Monitoring with Multiple Time Scales', in *Proceedings of the 9th Conference on Applied Climatology, 15-20 January 1995, Dallas, TX, American Meteorological Society*, pp. 233–236.

McSweeney, C. F., Jones, R. G., Lee, R. W., and Rowell, D. P. (2015) 'Selecting CMIP5 GCMs for downscaling over multiple regions', *Climate Dynamics*. Springer Berlin Heidelberg, 44(11–12), pp. 3237–3260. doi: 10.1007/s00382-014-2418-8.

Mearns, L. O., Gutowski, W., Jones, R., Leung, R., Mcginnis, S., Nunes, A., and Qian, Y. (2009) 'A regional climate change assessment program for North America', *Eos*, 90(36), p. 311. doi: 10.1029/2009EO360002.

Mehrotra, R. and Sharma, A. (2015) 'Correcting for systematic biases in multiple raw GCM variables across a range of timescales', *Journal of Hydrology*. Elsevier B.V., 520(January), pp. 214–223. doi: 10.1016/j.jhydrol.2014.11.037.

Meinshausen, M., Smith, S. J., Calvin, K., Daniel, J. S., Kainuma, M. L. T., Lamarque, J., and Van Vuuren, D. P. (2011) 'The RCP greenhouse gas concentrations and their extensions from 1765 to 2300', *Climatic Change*, 109(1), pp. 213–241. doi: 10.1007/s10584-011-0156-z.

Meinzer, O. E. (1923) *Outline of ground-water hydrology, with definitions, US Geology Survey Water Supply*. Available at: [http://aquadoc.typepad.com/files/usgs\\_publication\\_meinzer\\_1923\\_cover\\_and\\_page\\_9.pdf](http://aquadoc.typepad.com/files/usgs_publication_meinzer_1923_cover_and_page_9.pdf).

Mekonnen, M. M. and Hoekstra, A. Y. (2016) 'Sustainability: Four billion people facing severe water scarcity', *Science Advances*, 2(2), pp. 1–7. doi: 10.1126/sciadv.1500323.

Merki, J. P. (1970) 'Structural Geology of the Cenozoic Niger Delta', *African Geology*. University of Ibadan Press, p. pp 251-268.

Min, S.-K. and Hense, A. (2007) 'A Bayesian Assessment of Climate Change Using

Multimodel Ensembles. Part II: Regional and Seasonal Mean Surface Temperatures’, *Journal of Climate*, 20(12), pp. 2769–2790. doi: 10.1175/jcli4178.1.

Mogborukor, J. O. A. (2014) ‘The Impact of Oil Exploration and Exploitation on Water Quality and Vegetal Resources in a Rain Forest Ecosystem of Nigeria’, *Mediterranean Journal of Social Sciences*, 5(27), pp. 2039–9340. doi: 10.5901/mjss.2014.v5n27p1678.

Montcoudiol, N., Molson, J. and Lemieux, J. M. (2018) ‘Numerical modelling in support of a conceptual model for groundwater flow and geochemical evolution in the southern Outaouais Region, Quebec, Canada’, *Canadian Water Resources Journal*, 43(2), pp. 240–261. doi: 10.1080/07011784.2017.1323560.

Moriasi, D., Arnold, J. and Liew, M. W. Van (2013) ‘Model Evaluation Guidelines for Systematic Quantification of Accuracy in Watershed Simulations’, (May 2007). doi: 10.13031/2013.23153.

Moriasi, D. N., Arnold, J. G., Liew, M. W. Van, Bingner, R. L., Harmel, R. D., and Veith, T. L (2007) ‘Model Evaluation Guidelines for Systematic Quantification of Accuracy in Watershed Simulations’, *American Society of Agricultural and Biological Engineers*, 50(3), pp. 885–900.

Moss, R. H., Edmonds, J. A., Hibbard, K. A., Manning, M. R., Rose, S. K., Van Vuuren, D. P., and Wilbanks, T. J. (2010) ‘The next generation of scenarios for climate change research and assessment’, *Nature*. Nature Publishing Group, 463(7282), pp. 747–756. doi: 10.1038/nature08823.

Motovilov, Y. G., Gottschalk, L., Engeland, K., and Rodhe, A. (1999) ‘Validation of a distributed hydrological model against spatial observations’, 99.

Mtoni, Y., Mjemah, I. C., Bakundukize, C., Van Camp, M., Martens, K., and Walraevens, K. (2013) 'Saltwater intrusion and nitrate pollution in the coastal aquifer of Dar es Salaam, Tanzania', *Environmental Earth Sciences*, 70(3), pp. 1091–1111. doi: 10.1007/s12665-012-2197-7.

Mukherjee, A., Saha, D., Harvey, C. F., Taylor, R. G., Ahmed, K. M., and Bhanja, S. N. (2015) 'Groundwater systems of the Indian Sub-Continent', *Journal of Hydrology: Regional Studies*, 4, pp. 1–14. doi: 10.1016/j.ejrh.2015.03.005.

Murphy, J. (1999) 'An evaluation of statistical and dynamical techniques for downscaling local climate', *Journal of Climate*, 12(8 PART 1), pp. 2256–2284. doi: 10.1175/1520-0442(1999)012<2256:aeosad>2.0.co;2.

Musa, Z. N., Popescu, I. I. and Mynett, A. (2016) 'Approach on modeling complex deltas in data scarce areas: a case study of the lower Niger delta', *Procedia Engineering*. Elsevier B.V., 154, pp. 656–664. doi: 10.1016/j.proeng.2016.07.566.

Musa, Z. N., Popescu, I. and Mynett, A. (2016) 'Assessing the sustainability of local resilience practices against sea level rise impacts on the lower Niger delta', *Ocean and Coastal Management*. Elsevier Ltd, 130(June), pp. 221–228. doi: 10.1016/j.ocecoaman.2016.06.016.

Nebojs̃a Nakic'enovic', Ogunlade Davidson, Gerald Davis, Arnulf Gr̃ubler, Tom Kram, Emilio Lebre La Rovere, Bert Metz, Tsuneyuki Morita, William Pepper, Hugh Pitcher, Alexei Sankovski, Priyadarshi Shukla, Robert Swart, and Robert Watson, Z. D. (2000) *IPCC Special Report Emissions Scenarios; Summary for Policymakers*, *International Panel on Climate Change*. doi: 10.1017/CBO9781107415416.005.

NEDECO (1961) 'The Waters of the Niger Delta.', *The Hague, Netherlands*.revised

edition (Netherland Engineering Consultant), p. 317pp.

Neitsch S. L., Arnold J. G., Kiniry J. R., and Williams, J. (2005) *Soil and Water Assessment Tool Documentation*.

Neitsch, S., Arnold, J., Kiniry, J., and Williams, J. (2011) 'Soil & Water Assessment Tool Theoretical Documentation Version 2009', *Texas Water Resources Institute*, pp. 1–647. doi: 10.1016/j.scitotenv.2015.11.063.

Neves, J. (2015) 'Package "spi": Compute SPI index'.

New, M., Lister, D., Hulme, M., and Makin, I. (2002) 'A high-resolution data set of surface climate over global land areas', *Climate Research*, 21(1), pp. 1–25. doi: 10.3354/cr021001.

NGSA (2012) *Geological Maps of Nigeria - Nigerian Geological survey Agency*. Available at: <https://ngsa.gov.ng/GeoMaps>.

Niswonger, R. G., Panday, S. and Ibaraki, M. (2011) MODFLOW-NWT, A Newton Formulation for MODFLOW-2005: U.S. Geological Survey Techniques and Methods 6–A37, *Groundwater Book 6, Section A, Modeling Techniques*.

Niswonger, R. G., Prudic, D. E. and Regan, S. R. (2006) 'Documentation of the Unsaturated-Zone Flow (UZF1) Package for Modeling Unsaturated Flow Between the Land Surface and the Water Table with MODFLOW-2005', *U.S. Geological Survey Techniques and Methods*, p. 71.

Nkiaka, E., Nawaz, N. R. and Lovett, J. C. (2017) 'Evaluating global reanalysis precipitation datasets with rain gauge measurements in the Sudano-Sahel region: case study of the Logone catchment, Lake Chad Basin', *Meteorological Applications*,

24(1), pp. 9–18. doi: 10.1002/met.1600.

Nnabuenyi, U. M. (2012) ‘Impact of Oil Exploration and Exploitation on the Niger Delta Region: Environmental Perspective’, *Nigerian Journal of Science and Environment*, 11(1).

NOAA (2015) *Global Climate Report, National Oceanic and Atmospheric Administration*.

Northrop, P. J. (2013) ‘A simple, coherent framework for partitioning uncertainty in climate predictions’’, *Journal of Climate*, 26(12), pp. 4375–4376. doi: 10.1175/JCLI-D-12-00527.1.

Nouri, J., Mahvi, A. H., Babaei, A., and Ahmadpour, E. (2006) ‘Regional pattern distribution of groundwater fluoride in the Shush aquifer of Khuzestan County, Iran’, *Fluoride*, 39(4), pp. 321–325.

Nwankwoala, H. (2013) ‘Aquifer Hydraulic Conductivity Determination from Grain Size Analysis in Parts of Old Port Harcourt Township, Nigeria’, *ARPN Journal of Science and Technology*, 3(9), pp. 972–981.

Nwankwoala, H. (2015) ‘Hydrogeology And Groundwater Resources Of Nigeria’, *New York Science Journal 2015*, 8(1), pp. 89–100.

Nwankwoala, H. O., Oborie, E., Island, W., and State, B. (2014) ‘Geo-technical Investigation and Characterization of Sub-soils in Yenagoa , Bayelsa State , Central Niger Delta , Nigeria’, 6(7).

Brighid É Ó Dochartaigh, Alan M. MacDonald, Andrew R. Black, Jez Everest, Paul Wilson, W. George Darling, Lee Jones, and Mike Raines (2019) ‘Groundwater /

meltwater interaction in proglacial aquifers’, *Hydrology and Earth System Sciences*, pp. 1–19. doi: 10.5194/hess-2019-120.

Obroma Agumagu, (2018) ‘Projected Changes in the Physical Climate of the Niger Delta Region of Nigeria’, *SciFed Journal of Global Warming*.

Odafivwotu Ohwo (2018) ‘Climate Change Impacts, Adaptation and Vulnerability in the Niger Delta Region of Nigeria’, *Journal of Environment and Earth Science*, 8(6), pp. 171–179. Available at: <https://www.iiste.org/Journals/index.php/JEES/article/view/43170/44473>.

Odusanya, A. E., Mehdi, B., Schürz, C., Oke, A. O., Awokola, O. S., Awomeso, J. A., and Schulz, K. (2019) ‘Multi-site calibration and validation of SWAT with satellite-based evapotranspiration in a data-sparse catchment in southwestern Nigeria’, *Hydrology and Earth System Sciences*, 23(2), pp. 1113–1144. doi: 10.5194/hess-23-1113-2019.

Offodile, M. E. (1971) *The Hydrogeology of Coastal Areas of Southeastern states of Nigeria.*, *Unpublished Geological survey of Nigeria Report*.

Offodile, M. E. (1992) ‘An Approach to Groundwater Study and Development in Nigeria. Mecon Geology and Engineering Services Ltd., Jos.’

Offodile M.E. (2014) *Hydrogeology: Groundwater Study and Development in Nigeria*. Third edit. Jos: Mecon Geology and Engineering Services Ltd.

Offodile ME. (2002) ‘Groundwater study and development in Nigeria’, *Mecon Services Ltd, Jos, Nigeria*.

Ogbo, A., Lauretta, N. E. and Ukpere, W. (2013) ‘Risk Management and Challenges

of Climate Change in Nigeria’, *Journal of Human Ecology*. Routledge, 41(3), pp. 221–235. doi: 10.1080/09709274.2013.11906570.

Okagbue C. O. (1989) ‘Geotechnical And Environmental Problems of the Niger Delta’, *Bulletin of the International Association of ENGINEERING GEOLOGY*, pp. 129–138. Available at: <https://link.springer.com/article/10.1007/BF02590349>.

Oke, S. A. (2015) ‘Evaluation of the Vulnerability of Selected Aquifer Systems in the Eastern Dahomey Basin , South Western Nigeria’, (January).

Okeke, O. C., Onyekuru, S. O., Uduehi, G., and Israel, H. O. (2011) ‘Geology and hydrogeology of Northern Ishan district , Edo state , Southwestern Nigeria’, 1(November), pp. 1–11.

Oladapo, O.O. Amekudzi, L.K. Oni, O.M., Aremu, A.A., and Osei, M. A. (2018) ‘Simulation and Forecasting of Soil Moisture Content Variability Over Ogbomoso Agricultural Watershed Using the SWAT Model’, in *The European Conference on Sustainability, Energy & the Environment 2018 Official Conference Proceedings*.

Oladipo, E. (2010) *Towards enhancing the adaptive capacity of Nigeria: a review of the country’s state of preparedness for climate change adaptation, Heinrich Böll Foundation Nigeria*.

Olofintoye, O. O. and Sule, B. F. (2010) ‘Impact of Global Warming on the Rainfall and Temperature in the Niger Delta of Nigeria’, *Journal of Research Information in Civil Engineering*, 7(2), pp. 33–48.

Ologunorisa, T. E. and Adeyemo, A. (2005) ‘Public perception of flood hazard in the Niger Delta, Nigeria’, *Environmentalist*, 25(1), pp. 39–45. doi: 10.1007/s10669-005-



3095-2.

Ologunorisa, T. E. and Tersoo, T. (2006) 'The changing rainfall pattern and its implication for flood frequency in Makurdi, Northern Nigeria', *Journal of Applied Sciences and Environmental Management*, 10(3), pp. 97–102. Available at: <http://www.ajol.info/index.php/jasem/article/view/17327>.

Oloruntade, A. J., Mohammad, T. A., Ghazali, A. H., and Wayayok, A. (2017) 'Analysis of meteorological and hydrological droughts in the Niger-South', *Global and Planetary Change*. Elsevier, 155(September 2016), pp. 225–233. doi: 10.1016/j.gloplacha.2017.05.002.

Oluduro, O. (2012) 'Oil exploration and ecological damage: The compensation policy in Nigeria', *Canadian Journal of Development Studies*, 33(2), pp. 164–179. doi: 10.1080/02255189.2012.693049.

Oluwaseyi, A. (2017) 'Plant Genetic Resources (PGR) in Nigeria and the Reality of Climate Change - A Review', *Asian Journal of Environment & Ecology*, 2(2), pp. 1–24. doi: 10.9734/ajee/2017/31855.

Omosuyi, G. O., Ojo, J. S. and Olorunfemi, M. O. (2008) 'Geoelectric Sounding to Delineate Shallow Aquifers in the Coastal Plain Sands of', *The Pacific Journal of Science and Technology*, 9(2), pp. 62–77.

Onuoha K. M. and Mbazi F. C. (1989) 'Aquifer transmissivity from electrical sounding data: The case of Ajali sandstone aquifers, southeast of Enugu, Nigeria, in C. O. Ofoegbu, ed., Groundwater and mineral resources of Nigeria', *Braunschweig, Friedr Vieweg & Sohn*, pp. 17–30.

Onyeagocha, A. C. (1980) 'Petrography and depositional environment of the Benin Formation, Nigeria.', *Journal of Mining and Geology*, 17, pp. 147–151.

Ophori, D. U. (2007) 'A simulation of large-scale groundwater flow in the Niger Delta, Niger', *AAPG Bulletin*, 14(4), pp. 181–195. doi: 10.1306/eg.05240707001.

Orimoogunje I, A. (2013) 'Predicting the Yields of Deep Wells of the Deltaic Formation, Niger Delta Nigeria', *Journal of Waste Water Treatment & Analysis*, 04(01), pp. 1–5. doi: 10.4172/2157-7587.1000145.

Oteri, A.U., and Atolagbe, F. P. (2003) 'Saltwater Intrusion into Coastal Aquifers in Nigeria', in *The Second International Conference on Saltwater Intrusion and Coastal Aquifers—Monitoring, Modeling, and Management. Mérida, Yucatán, México. Environments and the 1st Arab Water Forum*, pp. 1–15.

Oteri, A. U. (1984) 'Electric logs for groundwater exploration in the Niger Delta of', (144).

Ouyang, F., Zhu, Y., Fu, G., Lü, H., Zhang, A., Yu, Z., and Chen, X. (2015) 'Impacts of climate change under CMIP5 RCP scenarios on streamflow in the Huangnizhuang catchment', *Stochastic Environmental Research and Risk Assessment*. Springer Berlin Heidelberg, 29(7), pp. 1781–1795. doi: 10.1007/s00477-014-1018-9.

Owoyemi, A. O. D. (2004) *The Sequence Stratigraphy of Niger Delta, Delta Field, Offshore Nigeria, Texas A&M University*. Texas A&M University.

Oyedele K. F., Ayolabi E. A., Adeoti L., and Adegbola, R. B. (2009) 'Geophysical and hydrogeological evaluation of rising groundwater level in the coastal areas of Lagos , Nigeria', *Bulletin of Engineering Geology and the Environment*, 68, pp. 137–

143. doi: 10.1007/s10064-008-0182-x.

P.U. Uzukwu, T. G. L. and N. A. J. (2014) ‘Seasonal Variations in Some Physico-chemical Parameters of the Upper Reach of the New Calaber River’, *International Journal of Fisheries and Aquatic Sciences*, 3(1), pp. 8–11.

Pandey, P. and Patra, K. C. (2014) ‘Hydrological Impacts of Climate Change’, *International Journal of Engineering Research and Applications (IJERA) ISSN: 2248-9622 National Conference on Advances in Engineering and Technology*, (March), pp. 45–48.

Parkhurst, D., Kipp, K. and Charlton, S. (2010) ‘PHAST Version 2 - A program for simulating groundwater flow, solute transport, and multicomponent geochemical reactions’, *Modeling Techniques, Book 6*, pp. 1–181. Available at: <http://pubs.usgs.gov/tm/06A35/>.

Pereira, R., Martinez, M. A., Pruski, F. F., and Demetrius, D. (2016) ‘Journal of Hydrology : Regional Studies Hydrological simulation in a basin of typical tropical climate and soil using the SWAT model part I: Calibration and validation tests’, *Biochemical Pharmacology*. Elsevier B.V., 7, pp. 14–37. doi: 10.1016/j.ejrh.2016.05.002.

Perkins, S. E., Pitman, A. J., Holbrook, N. J., and McAneney, J. (2007) ‘Evaluation of the AR4 climate models’ simulated daily maximum temperature, minimum temperature, and precipitation over Australia using probability density functions’, *Journal of Climate*, 20(17), pp. 4356–4376. doi: 10.1175/JCLI4253.1.

Piao, M., Piao, Y. and Lee, J. Y. (2019) ‘Symmetrical uncertainty-based feature subset generation and ensemble learning for electricity customer classification’, *Symmetry*,

11(4), pp. 4–13. doi: 10.3390/sym11040498.

Pierce, D. W., Barnett, T. P., Santer, B. D., and Gleckler, P. J. (2009) ‘Selecting global climate models for regional climate change studies’, *Proceedings of the National Academy of Sciences*, 106(21), pp. 8441–8446. doi: 10.1073/pnas.0900094106.

Poeter, E., Hill, M., Banta, E., Mehl, S., and Christensen, S. (2008) ‘UCODE 2005 and Six Other Computer Codes for Universal Sensitivity Analysis , Calibration , and Uncertainty Evaluation’, *Environmental Protection*, p. 299. doi: Cited By (since 1996) 28\rExport Date 4 April 2012.

Pollock, D. W. (2016) ‘User guide for MODPATH Version 7 -- A particle-tracking model for MODFLOW: U.S. Geological Survey Open-File Report’, *USGS: Open File Report 2016-1086*, p. 35. doi: <http://dx.doi.org/10.3133/ofr20161086>.

Porio (2014) *Climate Change Vulnerability and Adaptation in Groundwater-dependent Irrigation System in Asia-Pacific Region (Metro Manila)*, *Asian Journal of Social Science*. doi: 10.1163/15685314-04201006.

Prakash, S., Gairola, R. M. and Mitra, A. K. (2015) ‘Comparison of large-scale global land precipitation from multisatellite and reanalysis products with gauge-based GPCC data sets’, *Theoretical and Applied Climatology*, 121(1–2), pp. 303–317. doi: 10.1007/s00704-014-1245-5.

Prince C. Mmom, (2013) ‘Vulnerability and Resilience of Niger Delta Coastal Communities to Flooding.’, *IOSR Journal of Humanities and Social Science*, 10(6), pp. 27–33. doi: 10.9790/0837-1062733.

Priyantha Ranjan, S., Kazama, S. and Sawamoto, M. (2006) ‘Effects of climate and

land use changes on groundwater resources in coastal aquifers’, *Journal of Environmental Management*, 80(1), pp. 25–35. doi: 10.1016/j.jenvman.2005.08.008.

QGIS (2015) *Open source geographic information system. available on <http://www.qgis.org/en/site>.*

Rahman, S. H., Sengupta, D. and Ravichandran, M. (2009) ‘Variability of Indian summer monsoon rainfall in daily data from gauge and satellite’, *Journal of Geophysical Research Atmospheres*, 114(17). doi: 10.1029/2008JD011694.

Raji, W. O., Obadare, I. G., Odukoya, M. A., and Johnson, L. M. (2018) ‘Electrical resistivity mapping of oil spills in a coastal environment of Lagos , Nigeria’, *Arabian Journal of Geosciences*. *Arabian Journal of Geosciences*, 11, p. 144. doi: 10.1007/s12517-018-3470-1.

Ranger, N., Hallegatte, S., Bhattacharya, S., Bachu, M., Priya, S., Dhore, K., and Corfee-Morlot, J. (2011) ‘An assessment of the potential impact of climate change on flood risk in Mumbai’, *Climatic Change*, 104(1), pp. 139–167. doi: 10.1007/s10584-010-9979-2.

Rangwala, I. and Miller, J. R. (2012) ‘Climate change in mountains: A review of elevation-dependent warming and its possible causes’, *Climatic Change*, 114(3–4), pp. 527–547. doi: 10.1007/s10584-012-0419-3.

Ratan, R. and Venugopal, V. (2013) ‘Wet and dry spell characteristics of global tropical rainfall’, *Water Resources Research*, 49(6), pp. 3830–3841. doi: 10.1002/wrcr.20275.

Razack, M., Jalludin, M. and Houmed-Gaba, A. (2019) ‘Simulation of Climate Change

Impact on A Coastal Aquifer under Arid Climate. The Tadjourah Aquifer (Republic of Djibouti, Horn of Africa)', *Water*, 11(11), p. 2347. doi: 10.3390/w11112347.

Reichler, T. and Kim, J. (2008) 'How well do coupled models simulate today's climate?', *Bulletin of the American Meteorological Society*, 89(3), pp. 303–311. doi: 10.1175/BAMS-89-3-303.

Revadekar, J. V. and Preethi, B. (2012) 'Statistical analysis of the relationship between summer monsoon precipitation extremes and foodgrain yield over India', *International Journal of Climatology*, 32(3), pp. 419–429. doi: 10.1002/joc.2282.

Reyment R. A. (1965) 'Aspects of Geology of Nigeria', *Ibadan University Press*, p. 145pp.

Riahi, K., Rao, S., Krey, V., Cho, C., Chirkov, V., Fischer, G., and Rafaj, P. (2011) 'RCP 8.5-A scenario of comparatively high greenhouse gas emissions', *Climatic Change*, 109(1), pp. 33–57. doi: 10.1007/s10584-011-0149-y.

Robeson, S. M. and Ensor, L. A. (2006) *Daily precipitation grids for South America*, *Bulletin of the American Meteorological Society*. doi: 10.1175/1520-0477(2006)87[1095:DPGFSA]2.0.CO;2.

Rojas, R., Feyen, L. and Dassargues, A. (2008) 'Conceptual model uncertainty in groundwater modeling : Combining generalized likelihood uncertainty estimation and Bayesian model averaging', *Water resources research*, 44, pp. 1–16. doi: 10.1029/2008WR006908.

Roszkowska, E. (2013) 'Rank ordering criteria weighting methods-a comparative overview 2 5.', *Optimum. Studia Ekonomiczne*, 5(5), p. 65. Available at:

<https://pdfs.semanticscholar.org/f983/e8c4eb7d7c30694dd72c5849dd6fee8a5c79.pdf>

Ruan, Y., Liu, Z., Wang, R., and Yao, Z. (2019) ‘Assessing the Performance of CMIP5 GCMs for Projection of Future Temperature Change over the Lower Mekong Basin’, *Atmosphere*, 10(2), p. 93. doi: 10.3390/atmos10020093.

Sachindra, D. A., Huang, F., Barton, A., and Perera, B. J. C. (2014) ‘Statistical downscaling of general circulation model outputs to precipitation-part 1: calibration and validation’, *International Journal of Climatology*, 34(11), pp. 3264–3281. doi: 10.1002/joc.3914.

Saha, S., Moorthi, S., Pan, H.-L., Wu, X., Wang, J., Nadiga, S., and Goldberg, M. (2010) ‘The NCEP Climate Forecast System Reanalysis’, *Bulletin of the American Meteorological Society*, 91(8), pp. 1015–1058. doi: 10.1175/2010BAMS3001.1.

Salau, W., Paul, I. I. and Ganiyu, A. A. (2017) ‘SWAT analysis of Ikere Gorge basin for hydrokinetic power estimation in selected rural settlements of Oke Ogun, Nigeria’, *Ruhuna Journal of Science*, 8(1), p. 24. doi: 10.4038/rjs.v8i1.24.

Salman, S. A., Shahid, S., Ismail, T., Ahmed, K., and Wang, X. J. (2018) ‘Selection of climate models for projection of spatiotemporal changes in temperature of Iraq with uncertainties’, *Atmospheric Research*. Elsevier, 213(July), pp. 509–522. doi: 10.1016/j.atmosres.2018.07.008.

Salman, S. A., Shahid, S., Ismail, T., Al-Abadi, A. M., Wang, X. Jun, and Chung, E. S. (2019) ‘Selection of gridded precipitation data for Iraq using compromise programming’, *Measurement: Journal of the International Measurement Confederation*. Elsevier Ltd, 132, pp. 87–98. doi: 10.1016/j.measurement.2018.09.047.

Santhi, C., Arnold, J. G., Williams, J. R., Dugas, W. A., Srinivasan, R., and Hauck, L. M. (2002) 'Validation of the SWAT model on a large river basin with point and nonpoint sources', *Journal of the American Water Resources Association (JAWRA)*, 37(5), pp. 1169–1188. doi: 10.1111/j.1752-1688.2001.tb03630.x.

Sanz, D., Gómez-alday, J. J., Castaño, S., Moratalla, A., Heras, J. De, and Martínez-alfaro, P. E. (2009) 'Hydrostratigraphic framework and hydrogeological behaviour of the Mancha Oriental System (SE Spain)', *Hydrogeology Journal*, 17, pp. 1375–1391. doi: 10.1007/s10040-009-0446-y.

Sayne, A. (2011) *Climate Change Adaptation and Conflict in Nigeria, United States Institute of Peace*. doi: 10.2307/j.ctt211qx0v.8.

Schiemann, R., Liniger, M. A. and Frei, C. (2010) 'Reduced space optimal interpolation of daily rain gauge precipitation in Switzerland', *Journal of Geophysical Research Atmospheres*, 115(14), pp. 1–18. doi: 10.1029/2009JD013047.

Schmidli, J., Goodess, C. M., Frei, C., Haylock, M. R., Hundscha, Y., Ribalaygua, J., and Schmith, T. (2007) 'Statistical and dynamical downscaling of precipitation: An evaluation and comparison of scenarios for the European Alps', *Journal of Geophysical Research Atmospheres*, 112(4), pp. 1–20. doi: 10.1029/2005JD007026.

Schneider, U., Becker, A., Finger, P., Meyer-Christoffer, A., Ziese, M., and Rudolf, B. (2014) 'GPCP's new land surface precipitation climatology based on quality-controlled in situ data and its role in quantifying the global water cycle', *Theoretical and Applied Climatology*, 115(1–2), pp. 15–40. doi: 10.1007/s00704-013-0860-x.

Schoof, J. T., Arguez, A., Brolley, J., and O'Brien, J. J. (2005) 'A new weather generator based on spectral properties of surface air temperatures', *Agricultural and*



*Forest Meteorology*, 135(1–4), pp. 241–251. doi: 10.1016/j.agrformet.2005.12.004.

Schuol, Jürgen, Abbaspour, K. C., Srinivasan, R., and Yang, H. (2008) ‘Estimation of freshwater availability in the West African sub-continent using the SWAT hydrologic model’, *Journal of Hydrology*, 352(1–2), pp. 30–49. doi: 10.1016/j.jhydrol.2007.12.025.

Schuol, Jürgen, Abbaspour, K. C., Yang, H., Srinivasan, R., and Zehnder, A. J. B. (2008) ‘Modeling blue and green water availability in Africa’, *Water Resources Research*, 44(7), pp. 1–18. doi: 10.1029/2007WR006609.

Schuol, J. and Abbaspour, K. C. (2006) ‘Calibration and uncertainty issues of a hydrological model (SWAT) applied to West Africa’, *Advances in Geosciences*, 9, pp. 137–143. doi: 10.5194/adgeo-9-137-2006.

Scopel, C. (2012) *SWAT: Soil & Water Assessment Tool*.

Seiler, R. A., Hayes, M. and Bressan, L. (2002) ‘Using the standardized precipitation index for flood risk monitoring’, *International Journal of Climatology*, 22(11), pp. 1365–1376. doi: 10.1002/joc.799.

Sentelhas, P. C., Gillespie, T. J. and Santos, E. A. (2010) ‘Evaluation of FAO Penman-Monteith and alternative methods for estimating reference evapotranspiration with missing data in Southern Ontario, Canada’, *Agricultural Water Management*. Elsevier B.V., 97(5), pp. 635–644. doi: 10.1016/j.agwat.2009.12.001.

Shamsuddin Shahid (2008) ‘Spatial and temporal characteristics of droughts in the western part of Bangladesh’, *Hydrological Processes: Wiley InterScience*, 2274(November 2008), pp. 2267–2274. doi: 10.1002/hyp.

Shannon, C. E. (2001) 'A Mathematical Theory of Communication', 5(I), pp. 365–395. doi: 10.1007/3-540-45488-8\_15.

Sheffield, J., Goteti, G. and Wood, E. F. (2006) 'Development of a 50-year high-resolution global dataset of meteorological forcings for land surface modeling', *Journal of Climate*, 19(13), pp. 3088–3111. doi: 10.1175/JCLI3790.1.

Shekhar, S. and Xiong, H. (2012) *Soil and Water Assessment Tool "SWAT", Input/Output Documentation*. doi: 10.1007/978-0-387-35973-1\_1231.

Shen, M., Chen, J., Zhuan, M., Chen, H., Xu, C. Y., and Xiong, L. (2018) 'Estimating uncertainty and its temporal variation related to global climate models in quantifying climate change impacts on hydrology', *Journal of Hydrology*. Elsevier B.V., 556, pp. 10–24. doi: 10.1016/j.jhydrol.2017.11.004.

Shiru, M. S., Shahid, S., Chung, E. S., Alias, N., and Scherer, L. (2019) 'A MCDM-based framework for selection of general circulation models and projection of spatio-temporal rainfall changes: A case study of Nigeria', *Atmospheric Research*. Elsevier, 225(March), pp. 1–16. doi: 10.1016/j.atmosres.2019.03.033.

Short, K. C. and Stauble, A. J. (1967) 'Outline geology of the Niger Delta, Nigeria', *American Association of Petroleum Geologist*, 5, pp. 761–779.

Shreem, S. S., Abdullah, S. and Nazri, M. Z. A. (2016) 'Hybrid feature selection algorithm using symmetrical uncertainty and a harmony search algorithm', *International Journal of Systems Science*. Taylor & Francis, 47(6), pp. 1312–1329. doi: 10.1080/00207721.2014.924600.

Shukla, J., DelSole, T., Fennessy, M., Kinter, J., and Paolino, D. (2006) 'Climate

model fidelity and projections of climate change', *Geophysical Research Letters*, 33(7), pp. 3–6. doi: 10.1029/2005GL025579.

Singh, R. D. and Kumar, C. P. (2010) 'Impact of Climate Change on Groundwater Resources', 247667, pp. 1–14. doi: 10.4018/978-1-4666-8814-8.ch010.

Singh, B., Kushwaha, N. and Vyas, O. P. (2014) 'A Feature Subset Selection Technique for High Dimensional Data Using Symmetric Uncertainty', *Journal of Data Analysis and Information Processing*, (November), pp. 95–105.

Singh, B., Kushwaha, N., and Vyas, O. P. (2014) 'Observed changes in extreme wet and dry spells during the south Asian summer monsoon season', *Nature Climate Change*, 4(6), pp. 456–461. doi: 10.1038/nclimate2208.

Singh, J., Knapp, H. V., Arnold, J. G., and Demissie, M. (2004) 'Hydrological modeling of the Iroquois River watershed using HSPF and SWAT', *Journal of the American Water Resources Association*, 41(2), pp. 343–360. doi: 10.1111/j.1752-1688.2005.tb03740.x.

Sokolov, V. (2011) 'Integrated Water Resources Management', in *NATO Science for Peace and Security Series C: Environmental Security*, pp. 37–52. doi: 10.1007/978-90-481-9974-7\_3.

Spellman, F. (2014) 'All about Water', *The Science of Water*, pp. 9–42. doi: 10.1201/b17484-3.

Srinivasa Raju, K. and Nagesh Kumar, D. (2015) 'Ranking general circulation models for India using TOPSIS', *Journal of Water and Climate Change*, 6(2), pp. 288–299. doi: 10.2166/wcc.2014.074.

Srinivasa Raju, K., Sonali, P. and Nagesh Kumar, D. (2017) 'Ranking of CMIP5-based global climate models for India using compromise programming', *Theoretical and Applied Climatology*. *Theoretical and Applied Climatology*, 128(3–4), pp. 563–574. doi: 10.1007/s00704-015-1721-6.

Steurer, P. M., Peter, T. C., Heim, R., & Karl, T. R. (1992) *The Global Historical Climatology Network: Long-Term Monthly Temperature, Precipitation, Sea Level Pressure, and Station Pressure Data*. Oak Ridge, TN, USA.

Steyl, G. and Dennis, I. (2010) 'Review of coastal-area aquifers in Africa', *Hydrogeology Journal*, 18(1), pp. 217–225. doi: 10.1007/s10040-009-0545-9.

Sun, G. and Caldwell, P. (2015) 'Impacts of Urbanization on Stream Water Quantity and Quality in the United States', *Water Resources Impact*, Volume 17(1), pp. 17–20.

Sun, Q., Miao, C., Duan, Q., Kong, D., Ye, A., Di, Z., and Gong, W. (2014) 'Would the “real” observed dataset stand up? A critical examination of eight observed gridded climate datasets for China', *Environmental Research Letters*, 9(1). doi: 10.1088/1748-9326/9/1/015001.

Sun, Q., Miao, C., Duan, Q., Ashouri, H., Sorooshian, S., and Hsu, K. L. (2018) 'A Review of Global Precipitation Data Sets: Data Sources, Estimation, and Intercomparisons', *Reviews of Geophysics*, 56(1), pp. 79–107. doi: 10.1002/2017RG000574.

Sun, R. J. (1986) Regional Aquifer-System Analysis Program of the U.S. Geological Survey: *Summary of projects, 1978-84, Circular*. Washington, D.C. doi: 10.3133/cir1002.

Sushama, L., Ben Said, S., Khaliq, M. N., Nagesh Kumar, D., and Laprise, R. (2014) 'Dry spell characteristics over India based on IMD and APHRODITE datasets', *Climate Dynamics*, 43(12), pp. 3419–3437. doi: 10.1007/s00382-014-2113-9.

Sutha, K., and Tamilselvi, J. (2015) 'A Review of Feature Selection Algorithms for Data Mining Techniques', *International Journal on Computer Science and Engineering*, 7(6), pp. 63–67. Available at: <http://www.enggjournals.com/ijcse/doc/IJCSE15-07-06-010.pdf>.

Svoboda, Hayes, M. and Wood, D. (2012) 'Standardized Precipitation Index User Guide', *World Meteorological Organisation*, 21(6), pp. 1333–1348. doi: 10.1175/2007JCLI1348.1.

Talavera, L. (2005) 'An Evaluation of Filter and Wrapper Methods for Feature Selection in Categorical Clustering', in, pp. 440–451. doi: 10.1007/11552253\_40.

Tan, M. L., Ibrahim, A. L., Yusop, Z., Chua, V. P., and Chan, N. W. (2017) 'Climate change impacts under CMIP5 RCP scenarios on water resources of the Kelantan River Basin, Malaysia', *Atmospheric Research*, 189, pp. 1–10. doi: 10.1016/j.atmosres.2017.01.008.

Tappan, G. G., Cushing, W.M., Cotillon, S.E., Mathis, M.L., Hutchinson, J.A., and Dalsted, K. (2016) *West Africa Land Use Land Cover Time Series: U.S. Geological Survey data release*. doi: <http://dx.doi.org/10.5066/F73N21JF>.

Tawari-fufeyin, P., Paul, M., and Godleads, A. O. (2015) 'Some Aspects of a Historic Flooding in Nigeria and Its Effects on some Niger-Delta Communities', *American Journal of Water Resources*, 3(1), pp. 7–16. doi: 10.12691/ajwr-3-1-2.

Taylor, R. G. (2012) 'Ground water and climate change', *Nature Climate Change*, (November). doi: 10.1038/NCLIMATE1744.

Teutschbein, C. and Seibert, J. (2012) 'Bias correction of regional climate model simulations for hydrological climate-change impact studies: Review and evaluation of different methods', *Journal of Hydrology*. Elsevier B.V., 456–457, pp. 12–29. doi: 10.1016/j.jhydrol.2012.05.052.

Thomson, A. M., Calvin, K. V., Smith, S. J., Kyle, G. P., Volke, A., Patel, P., and Edmonds, J. A. (2011) 'RCP4.5: A pathway for stabilization of radiative forcing by 2100', *Climatic Change*, 109(1), pp. 77–94. doi: 10.1007/s10584-011-0151-4.

Todd M, A. O. (2015) 'Modelling the Climatic Variability in the Niger Delta Region: Influence of Climate Change on Hydrology', *Journal of Earth Science & Climatic Change*, 06(06), p. 284. doi: 10.4172/2157-7617.1000284.

Todini, E. (2007) 'Hydrological catchment modelling: Past, present and future', *Hydrology and Earth System Sciences*, 11(1), pp. 468–482. doi: 10.5194/hess-11-468-2007.

Ubani, E. C. and Onyejekwe, I. M. (2013) 'Environmental impact analyses of gas flaring in the Niger delta region of Nigeria', *American Journal of Scientific and Industrial Research*, 4(2), pp. 246–252. doi: 10.5251/ajsir.2013.4.2.246.252.

Ugwu S. A. and Nwankwoala H. O. (2008) 'Application of Seismic Refraction Method in Groundwater', 7(2), pp. 73–80.

Uko E.T. and Emudianughe J.E. (2016) 'Comparison of the Characteristics of Low Velocity Layer (LVL) in the Mangrove Swamp and in the Upper Flood Plain

Environments in the Niger Delta, using Seismic Refraction Methods', *Journal of Geology & Geophysics*, 5(4). doi: 10.4172/2381-8719.1000248.

Uma K. O. (1989) 'An appraisal of the groundwater resources of the Imo River Basin, Nigeria', *Journal of Mining and Geology*, Vol. 25 No, p. pp.305-31.

Umar, D. A., Ramli, M. F., Aris, A. Z., Sulaiman, W. N. A., Zaudi, M. A., and Tukur, A. I. (2019) 'An overview of climate change and variability impact studies in Nigeria', *Arabian Journal of Geosciences*. *Arabian Journal of Geosciences*, 12(20). doi: 10.1007/s12517-019-4773-6.

UN DESA (2019) World population prospects 2019, United Nations. Department of Economic and Social Affairs. *World Population Prospects 2019*. Available at: <http://www.ncbi.nlm.nih.gov/pubmed/12283219>.

UNDP (2006) Niger Delta Human Development Report: *United Nations Development Programme*.

UNOCHA (2015) Humanitarian Bulletin Nigeria; United Nations Office for the Coordination of Humanitarian Affairs: Abuja, Nigeria. Available at: <https://www.unocha.org/story/niger-heavy-rains-and-floods-force-more-400000-people-their-homes>.

USDA-SCS (1972) United States Department of Agriculture-Soil Conservation Service 1985. *National Engineering Handbook, Section 4, Hydrology.*, Washington, D.C.: USDA-SCS.

Varni, M. R. and Usunoff, E. J. (1999) 'Simulation of regional-scale groundwater flow in the Azul River basin , Buenos Aires Province , Argentina', *Hydrogeology Journal*,

*Springer-Verlag*, 7(October 1998), pp. 180–187.

Vilaysane, B., Takara, K., Luo, P., and Akkharath, I. (2015) ‘Hydrological stream flow modelling for calibration and uncertainty analysis using SWAT model in the Xedone river basin , Lao PDR’, *Procedia Environmental Sciences*. Elsevier B.V., 28(Sustain 2014), pp. 380–390. doi: 10.1016/j.proenv.2015.07.047.

Viner, D. (2000) ‘Modelling Climate Change: A conceptual structure of a coupled ocean-atmosphere GCM’, p. 3. Available at: [www.cru.uea.ac.uk/modelling-climate-change](http://www.cru.uea.ac.uk/modelling-climate-change).

Vinnarasi, R. and Dhanya, C. T. (2016) ‘Changing characteristics of extreme wet and dry spells of Indian monsoon rainfall’, *Journal of Geophysical Research: Atmospheres*, 121(5), pp. 2146–2160. doi: 10.1002/2015JD024310.

Voss, C. I. and Provost, A. M. (2002) *SUTRA: A model for 2D or 3D saturated-unsaturated, variable-density ground-water flow with solute or energy transport*. Version 2D, *Water-Resources Investigations Report*. Version 2D. doi: 10.3133/wri024231.

Van Vuuren, D. P., Stehfest, E., den Elzen, M. G. J., Kram, T., van Vliet, J., Deetman, S., and van Ruijven, B. (2011) ‘RCP2.6: Exploring the possibility to keep global mean temperature increase below 2°C’, *Climatic Change*, 109(1), pp. 95–116. doi: 10.1007/s10584-011-0152-3.

Van Vuuren, D. P., Edmonds, J., Kainuma, M., Riahi, K., Thomson, A., Hibbard, K., and Rose, S. K. (2011) ‘The representative concentration pathways: An overview’, *Climatic Change*, 109(1), pp. 5–31. doi: 10.1007/s10584-011-0148-z.



Wang, J., Hu, L., Li, D., and Ren, M. (2020) 'Potential Impacts of Projected Climate Change under CMIP5 RCP Scenarios on Streamflow in the Wabash River Basin', *Advances in Meteorology*, 2020, pp. 1–18. doi: 10.1155/2020/9698423.

Wang, L., Ranasinghe, R., Maskey, S., van Gelder, P. H. A. J. M., and Vrijling, J. K. (2016) 'Comparison of empirical statistical methods for downscaling daily climate projections from CMIP5 GCMs: A case study of the Huai River Basin, China', *International Journal of Climatology*, 36(1), pp. 145–164. doi: 10.1002/joc.4334.

Wang, X., Li, Z. and Li, M. (2018) 'Impacts of climate change on stream flow and water quality in a drinking water source area , Northern China', *Environmental Earth Sciences*. Springer Berlin Heidelberg, 77(11), pp. 1–14. doi: 10.1007/s12665-018-7581-5.

Wang, Z., Ficklin, D. L., Zhang, Y., and Zhang, M. (2012) 'Impact of climate change on streamflow in the arid Shiyang River Basin of northwest China', *Hydrological Processes*, 26(18), pp. 2733–2744. doi: 10.1002/hyp.8378.

Warszawski, L., Frieler, K., Huber, V., Piontek, F., Serdeczny, O., and Schewe, J. (2014) 'The Inter-Sectoral Impact Model Intercomparison Project (ISI-MIP): Project framework', *Proceedings of the National Academy of Sciences*, 111(9), pp. 3228–3232. doi: 10.1073/pnas.1312330110.

Weezel, S. van (2017) 'Drought severity and communal conflict in Drought severity and communal conflict in Nigeria', (July). Available at: [https://www.researchgate.net/publication/320374674\\_Drought\\_severity\\_%0Aand\\_communal\\_conflict\\_in\\_Nigeria](https://www.researchgate.net/publication/320374674_Drought_severity_%0Aand_communal_conflict_in_Nigeria).

Wei, G., Lü, H., Crow, W. T., Zhu, Y., Wang, J., and Su, J. (2018) 'Evaluation of

satellite-based precipitation products from IMERG V04A and V03D, CMORPH and TMPA with gauged rainfall in three climatologic zones in China’, *Remote Sensing*, 10(1). doi: 10.3390/rs10010030.

Weli, V. E. and Ideki, O. (2014) ‘The Effect of Urbanization on Channel Adjustment and Flood Vulnerability of Woiy Basin, River State, Nigeria’, *Journal of Natural Sciences Research*, 4(10), pp. 86–94.

Wilby, R. L. (2001) ‘Sdsm — a Decision Support Tool for the Assessment of Regional Climate Change Impacts’, 2, pp. 147–159.

Wilby, R. L., Charles, S. P., Zorita, E., Timbal, B., Whetton, P., and Mearns, L. O. (2004) ‘Guidelines for Use of Climate Scenarios Developed from Statistical Downscaling Methods’, *Analysis*, 27(August), pp. 1–27. doi: citeulike-article-id:8861447.

Wilby, R. L. and Dawson, C. W. (2007) ‘SDSM 4.2-A decision support tool for the assessment of regional climate change impacts, Version 4.2 User Manual’, *Lancaster University: Lancaster/Environment Agency of England and Wales*, (August), pp. 1–94.

Wilby R.L. and Wigley T.M.L. (1997) ‘model output : a review of methods and limitations Downscaling general b’, *Progress in Physical Geography*, 21(4), pp. 530–548.

Willmott, C. J. (1981) ‘On the Validation of Models’, *Physical Geography*. Taylor & Francis, 2(2), pp. 184–194. doi: 10.1080/02723646.1981.10642213.

Willmott, C. J. and Matsuura, K. (2006) ‘On the use of dimensioned measures of error

to evaluate the performance of spatial interpolators’, *International Journal of Geographical Information Science*, 20(1), pp. 89–102. doi: 10.1080/13658810500286976.

Willmott, C. and Matsuura, K. (2005) ‘CLIMATE RESEARCH Clim Res’, *Climate Research*, 30, pp. 79–82. Available at: [www.int-res.com](http://www.int-res.com).

Winston, R. B. (2009) ‘ModelMuse: A Graphical User Interface for MODFLOW-2005 and PHAST’, *U.S. Geological Survey Techniques and Methods 6-A29*, p. 52 p. Available at: <http://pubs.usgs.gov/tm/tm6A29/tm6A29.pdf>.

WMO (2013) *The global climate 2001 – 2010*, World Meteorological Organization. Available at: [https://library.wmo.int/doc\\_num.php?explnum\\_id=7829](https://library.wmo.int/doc_num.php?explnum_id=7829).

Worku, L. Y. (2015) ‘Climate change impact on variability of rainfall intensity in the Upper Blue Nile Basin’, *Proceedings of the International Association of Hydrological Sciences*, 366(June 2014), pp. 135–136. doi: 10.5194/piahs-366-135-2015.

WMO (2018) ‘World Meteorological Organization (WMO) provisional Statement on the Status of the Global Climate in 2018. Available at: [https://library.wmo.int/doc\\_num.php?explnum\\_id=5789%0Ahttp://ane4bf-datap1.s3-eu-west-1.amazonaws.com/wmocms/s3fs-public/2016\\_WMO\\_Statement\\_on\\_the\\_Status\\_of\\_the\\_Global\\_Climate-14-11-16-ver2.pdf?ZmIaubFZknHEGDBpyxTBpTcrNotiDpDo](https://library.wmo.int/doc_num.php?explnum_id=5789%0Ahttp://ane4bf-datap1.s3-eu-west-1.amazonaws.com/wmocms/s3fs-public/2016_WMO_Statement_on_the_Status_of_the_Global_Climate-14-11-16-ver2.pdf?ZmIaubFZknHEGDBpyxTBpTcrNotiDpDo).

Worqlul, A. W., Maathuis, B., Adem, A. A., Demissie, S. S., Langan, S., and Steenhuis, T. S. (2014) ‘Comparison of rainfall estimations by TRMM 3B42, MPEG and CFSR with ground-observed data for the Lake Tana basin in Ethiopia’, *Hydrology and Earth System Sciences*, 18(12), pp. 4871–4881. doi: 10.5194/hess-18-4871-2014.

- Xie, H., Nkonya, E. and Wielgosz, B. (2010) 'Evaluation of the swat model in hydrologic modeling of a large watershed in Nigeria', *Proceedings of the 3rd IASTED African Conference on Water Resource Management, AfricaWRM 2010*, 1(AfricaWRM), pp. 71–76. doi: 10.2316/p.2010.686-055.
- Xu, C. Y. (1999a) 'Climate change and hydrologic models: A review of existing gaps and recent research developments', *Water Resources Management*, 13(5), pp. 369–382. doi: 10.1023/A:1008190900459.
- Xu, C. Y. (1999b) 'From GCMs to river flow: A review of downscaling methods and hydrologic modelling approaches', *Progress in Physical Geography*, 23(2), pp. 229–249. doi: 10.1191/030913399667424608.
- Xu, Y. (2018) 'Hydrology and Climate Forecasting R Package for Data Analysis and Visualization'.
- Yatagai, A., Arakawa, O., Kamiguchi, K., and Kawamoto, H. (2009) 'A 44-Year Daily Gridded Precipitation Dataset for Asia', *Sola*, 5, pp. 3–6. doi: 10.2151/sola.2009.
- Ye Htut, A. (2014) 'Forecasting Climate Change Scenarios in the Bago River Basin, Myanmar', *Journal of Earth Science & Climatic Change*, 05(09). doi: 10.4172/2157-7617.1000228.
- Yin, H., Donat, M. G., Alexander, L. V., and Sun, Y. (2015) 'Multi-dataset comparison of gridded observed temperature and precipitation extremes over China', *International Journal of Climatology*, 35(10), pp. 2809–2827. doi: 10.1002/joc.4174.
- Young A., Black A., Haxton T., and Formetta G., (2018) 'Understanding and estimating the influence of urbanisation on the flood and low flow regimes of heavily

urbanised catchments’, *20th EGU General Assembly, EGU2018, Proceedings from the conference held 4-13 April, 2018 in Vienna, Austria, p.10513*, 20, p. 10513. Available at: <http://adsabs.harvard.edu/abs/2018EGUGA..2010513Y>.

Zarei, M., Ghazavi, R., Vli, A., and Abdollahi, K. (2016) ‘Estimating Groundwater Recharge , Evapotranspiration and Surface Runoff using Land-use data : A Case Study in Northeast Iran’, 8(2), pp. 196–202.

Zhang, A. and Zhang, C. (2012) ‘Assessments of Impacts of Climate Change and Human Activities on Runoff with SWAT for the Huifa River Basin , Northeast China Assessments of Impacts of Climate Change and Human Activities on Runoff with SWAT for the Huifa River Basin , Northeast China’, (April 2014). doi: 10.1007/s11269-012-0010-8.

# APPENDIX

## Precipitation NetCDF extraction code

```
# Load libraries
library(raster)
library(tidyverse)
library(data.table)

# Set working Directory
setwd("H:/Final_Models/Climate/PGF datasets/NetCDF")

# Read coordinates file
coords <- read_csv("pcp.txt")

# Read netcdf file as rasterbrick
file <- brick("prcp_daily_2005-2005.nc")

# Get coordinates from coordinates file
lon <- coords$LONG
lat <- coords$LAT

# Extract values at coordinates
pr <- raster::extract(file, cbind(lon,lat))

# Convert matrix to dataframe
pr <- as.data.frame(pr)
pr <- pr*86400
pr <- round(pr, digits = 2)
pr <- data.frame(coords$NAME,pr)

# Transpose dataframe
maxtemp <- data.table::transpose(pr)

# Assign column and row names
colnames(maxtemp) <- rownames(pr)
rownames(maxtemp) <- colnames(pr)

# Write csv file
write_csv(maxtemp,"prcp_daily_2005-20052.csv")
```

## Maximum Temperature NetCDF extraction code

```
# Load libraries
library(raster)
library(tidyverse)
library(data.table)

# Set working Directory
setwd("H:/Final_Models/Climate/PGF datasets")

# Read coordinates file
coords <- read_csv("pcp.txt")

# Read netcdf file as rasterbrick
file <- brick("tmax_daily_2005-2005.nc")

# Get coordinates from coordinates file
lon <- coords$LONG
lat <- coords$LAT

# Extract values at coordinates
tasmax <- raster::extract(file, cbind(lon,lat))

# Convert matrix to dataframe
tasmax <- as.data.frame(tasmax)
tasmax <- tasmax - 273
tasmax <- data.frame(coords$NAME,tasmax)

# Transpose dataframe
maxtemp <- data.table::transpose(tasmax)

# Assign column and row names
colnames(maxtemp) <- rownames(tasmax)
rownames(maxtemp) <- colnames(tasmax)

# Write csv file
write_csv(maxtemp,"tmax_daily_2005-2005.csv")
```

## Minimum Temperature NetCDF extraction code

```
# Load libraries
library(raster)
library(tidyverse)
library(data.table)

# Set working Directory
setwd("H:/Final_Models/Climate/PGF datasets")

# Read coordinates file
coords <- read_csv("pcp.txt")

# Read netcdf file as rasterbrick
file <- brick("tmin_daily_2005-2005.nc")

# Get coordinates from coordinates file
lon <- coords$LONG
lat <- coords$LAT

# Extract values at coordinates
tasmin <- raster::extract(file, cbind(lon,lat))

# Convert matrix to dataframe
tasmin <- as.data.frame(tasmin)
tasmin <- tasmin - 273
tasmin <- data.frame(coords$NAME,tasmin)

# Transpose dataframe
mintemp <- data.table::transpose(tasmin)

# Assign column and row names
colnames(mintemp) <- rownames(tasmin)
rownames(mintemp) <- colnames(tasmin)

# Write csv file
write_csv(mintemp,"tmin_daily_2005-2005.csv")
```



### **Code to write columns as separate csv files**

```
library(readxl)
library(plyr)
setwd('C:/Users/User/Documents/ibrahim')

df <- read_excel("Rainfall.xlsx")
df <- as.data.frame(df)
#df
l_ply(names(df), function(x) write.table(df[[x]], paste(x, ".csv", sep = ""),
                                          sep = ",", col.names = F, row.names = F))
```

### **Code for Spell Length Analysis**

```
library(RMRAINGEN)
data(trentino) year_min <- 1961 year_max <- 1990
period <- PRECIPITATION$year >= year_min &
PRECIPITATION$year <= year_max station <-
names(PRECIPITATION)[!(names(PRECIPITATION) %in%
c("day", "month", "year"))] prec_mes <- PRECIPITATION[period, station]
## removing nonworking stations (e.g. time series with NA) accepted <-
array(TRUE, length(names(prec_mes))) names(accepted) <- names(prec_mes) for (it
in names(prec_mes)) { accepted[it] <-
(length(which(!is.na(prec_mes[, it]))) == length(prec_mes[, it]))}
prec_mes <- prec_mes[, accepted] ## the dataset is reduced!!!
prec_mes <- prec_mes[, 1:3]
origin <- paste(year_min, 1, 1, sep = "-") dw.spell <- dw.spell(prec_mes, origin = origin)
dw.spell.dry <- dw.spell(prec_mes, origin = origin, extract = "dry")
hist(dw.spell.dry$T0001$spell_length)
```

### **Code to Ensemble Precipitation GCM**

```
# Set working directory
setwd("H:/Research Models/Final_Climate/Data/Ensamble")

# Import libraries
library(tidyverse)
```

```

# Create a function to read all the sheets in the excel file as a list
read_excel_allsheets <- function (filename, tibble = FALSE) { sheets <-
readxl::excel_sheets(filename)
  x <- lapply(sheets, function(X) readxl::read_excel(filename, sheet = X, col_names
= FALSE))
  if(!tibble) x <- lapply(x, as.data.frame)
  names(x) <- sheets x }

# Read sheets in a list
X <- read_excel_allsheets("Rain-Historical-Rworksheet.xlsx")
# Coonvert sheets to matrices
X <- lapply(X, as.matrix)

# Combine the matrices into an array
Y <- do.call(cbind, X)
Y <- array(Y, dim=c(dim(X[[1]]), length(X)))

# Calculate ensemble means
Ensemble_mean <- apply(Y, c(1, 2), mean, na.rm = TRUE)
Ensemble_mean <- as.data.frame(Ensemble_mean)
Date <- seq(from = as.Date('2006-01-01'), length.out = 34698, by = 1)
Ensemble_mean <- data.frame(Date,Ensemble_mean)

# Write excel file
write_csv(x = Ensemble_mean, path =
"TempSC4_Ensemble_Tmean.csv",col_names = T)

```

### **Code to Ensemble Temperature GCM**

```

library(data.table)
# Set directories
mainDir <- "H:/Research Models/Final_Climate/Temp"
tmaxDir <- "tmax"
tminDir <- "tmin"
mergedDir <- "merged"
setwd(mainDir)

```

```

# Read files
tmax <- readxl::read_excel("Maximum_Temperature.xlsx")
tmin <- readxl::read_excel("Minimum_Temperature.xlsx")
tmax <- as.data.frame(tmax)
tmin <- as.data.frame(tmin)

# Create tmax directory
if (file.exists(tmaxDir)){
  setwd(file.path(mainDir, tmaxDir))
} else {
  dir.create(file.path(mainDir, tmaxDir))
  setwd(file.path(mainDir, tmaxDir))}

# Split tmax columns
plyr::l_ply(names(tmax), function(x) write.table(tmax[[x]], paste(x, ".csv", sep = ""),
                                                  sep = ",", col.names = F, row.names = F))

# Create tmin directory
if (file.exists(tminDir)){
  setwd(file.path(mainDir, tminDir))
} else {
  dir.create(file.path(mainDir, tminDir))
  setwd(file.path(mainDir, tminDir))}

# Split tmin columns
plyr::l_ply(names(tmin), function(x) write.table(tmin[[x]], paste(x, ".csv", sep = ""),
                                                  sep = ",", col.names = F, row.names = F))

# Read files from tmax directory
setwd(file.path(mainDir, tmaxDir))
files <- list.files(pattern = "\\*.csv$")
tmaxfiles <- lapply(files, fread)
names(tmaxfiles) <- gsub("\\*.csv$", "", files)

# Read files from tmin directory
setwd(file.path(mainDir, tminDir))
files1 <- list.files(pattern = "\\*.csv$")

```

```

tminfiles <- lapply(files, fread)
names(tminfiles) <- gsub("\\.csv$", "", files1)

# Create merged directory
if (file.exists(mergedDir)){
  setwd(file.path(mainDir, mergedDir))
} else {
  dir.create(file.path(mainDir, mergedDir))
  setwd(file.path(mainDir, mergedDir))}

# merge and write files
for(i in seq_along(tmaxfiles)) {
  write.table(round(cbind(tmaxfiles[[i]],tminfiles[[i]]), digits = 2),
paste(names(tmaxfiles)[i], ".txt", sep = ""),
           col.names = F, row.names = F, sep = ",", quote = F)}

```

### **Code for Symmetrical Uncertainty for Precipitation GCM Ensemble**

```

# Import libraries
library(readr)
library(FSelector)

# Set working directory
setwd("H:/Final_Models/Symmetrical Uncertainty/SU Rscript")

# Read data
prcp <- read_csv('prcp.csv')

# Convert data into categories i.e dry and wet
df <- as.data.frame(lapply(prcp, function(x) ifelse(x > 0 & x < 2, "dry", "wet"))) #
Threshold here is set to 2mm

# Compute Information Gain
weights <- information.gain(Observed~., df)
print(weights)
subset <- cutoff.k(weights, 28)

```

```

f <- as.simple.formula(subset, "Observed")
print(f)

# Compute Gain Ratio
weights <- gain.ratio(Observed~., df)
print(weights)
subset <- cutoff.k(weights, 5)
f <- as.simple.formula(subset, "Observed")
print(f)

# Compute symmetrical uncertainty
weights <- symmetrical.uncertainty(Observed~., df)
print(weights)
subset <- cutoff.k(weights, 5)
f <- as.simple.formula(subset, "Observed")
print(f)

```

### **Code for Symmetrical Uncertainty for Temperature Ensemble GCM**

```

# Import libraries
library(readr)
library(FSelector)

# Set working directory
setwd("C:/Users/xsb16197/Desktop/Climate/SU")

# Read data
Temp <- read_csv('Temp.csv')
df <- as.data.frame(ifelse(Temp > 38, 'hot', ifelse(Temp < 17, 'cold', 'medium')))

# Compute symmetrical uncertainty
weights <- symmetrical.uncertainty(Observed~., Temp) # with factors
weights1 <- symmetrical.uncertainty(Observed~., df) # without factors
print(weights) # with factors
print(weights1) # without factors
subset <- cutoff.k(weights, 5) # with factors

```

```

subset1 <- cutoff.k(weights1, 5) # without factors
print(subset) # with factors
print(subset1) # without factors

```

### **Code for GCM Bias Correction**

```

# Import libraries
library(hyfo)
library(hydroTSM)
library(zoo)
library(tidyverse)
setwd("H:/Climate Modeling/ND_Data")
# Load the data and assign dates
dates <- as.Date("1980-01-01") + 1:9861
dates1 <- as.Date("1980-01-01") + 1:9496
obs <- data.frame(as.Date(dates),Obs200_10p)
names(obs) <- c("Date","prcp")
hindcast <- data.frame(as.Date(dates1),X200_10p)
names(hindcast) <- c("Date","prcp")
frc <- hindcast
# Trim obs to match hindcast
obs <- obs[1:9496,]
# assign min and max temp
temperature <- X200_10t
names(temperature) <- c("tmax","tmin")
tmin <- temperature$tmin
tmax <- temperature$tmax
tmin <- data.frame(as.Date(dates),tmin)
tmax <- data.frame(as.Date(dates),tmax)
tmin <- tmin[1:9496,]
tmax <- tmax[1:9496,]
# Convert to zoo object
pcp <- read.zoo(obs, format="%Y-%m-%d")
tmx <- read.zoo(tmax, format="%Y-%m-%d")
tmn <- read.zoo(tmin, format="%Y-%m-%d")

```

```
# Bias correction
bias_correct_precip <- biasCorrect(frc, hindcast, obs, preci = TRUE)
write_csv(bias_correct_precip,"corrected_precip.csv")
write_csv(obs,"obs.csv")
```

### **Code for SPI Calculation**

```
##load data data(spi_data) ##write to file
write.table(spi_data,file="spi.txt",quote=FALSE,row.names=TRUE) ## Standard
format with the output in the text format spi(3,"spi.txt",1963,2010) ## A full output
in graphical format spi(7,"spi.txt",1963,2010,"Standardized Precipitation Index - Rio
Grande do Norte State",1,"years","months")
```